

https://dspace.org/

Nanocrystalline Cellulose – Attapulgite/ Sepiolite as water-based drilling fluids and their impacts on the oil drilling penetration rate

Lotanga, K D G

2021
https://hdl.handle.net/10539/32953

Downloaded from a DSpace repository. https://dspace.org/

UNIVERSITY OF THE
WITWATERSRAND,
JOHANNESBURG

Nanocrystalline Cellulose – Attapulgite / Sepiolite as water-based drilling fluids and their impacts on the oil drilling penetration rate.

ERA00: MSc RESEARCH REPORT

Prepared by

MR K.D.G LOTANGA (Student Number: 1731859)

Submitted to:

School of Chemical and Metallurgical Engineering,
Faculty of Engineering and the Built Environment of the University of the Witwatersrand, Johannesburg, South Africa.

Supervisor: Prof. Diakanua Nkazi
Co supervisor: Prof. Geofrey Simate

April 2021.

DECLARATION

I hereby declare that the MSc project presented in this thesis was carried out by myself at University of Witwatersrand, Johannesburg, except where due acknowledgement is made, and has not been submitted for any other degree.

……  …….

Lotanga kondoma doudou-gilbert (Candidate)

Professor Diakanua Nkazi (Supervisor)

Professor Geoffrey Simate (Co-supervisor)

30 April 2021.

ABSTRACT

Production of oil and gas from deep well that operate under high pressure and high temperature (HPHT) conditions require the use of smart or advanced drilling fluid with improved rheological and filtration properties that are cheaper, eco-environmentally friendly, biodegradable and applicable for reducing the drilling cost. Due to the limitation of the use of Bentonite (BT) in harsh conditions of HPHT, Attapulgite (ATT) and Sepiolite (SEP) are used through unconventional hydrocarbon resources, such as shale gas, shale oil, deep water, and artic reservoirs. Nanotechnology demonstrated promising solutions to address such issues in the oil and gas industry. As many researchers investigated the improvement of the drilling fluids through the application of nanotechnology, success brought hope. In this study, the effect of the incorporation of cellulose nanocrystals (CNCs) at different concentrations into ATT and SEP water-based drilling fluids (ATT/SEP-WDFs) and the variation of temperature were investigated to evaluate the improvement on the rheological and filtration properties of cellulose nanocrystals into attapulgite water-based drilling fluids (CNC/ATT-WDFs) and cellulose nanocrystals into sepiolite water-based drilling fluids (CNC/SEP-WDFs) in fresh-water (FW) and sea-water (SW). Herschel-Bulkley's (HB) rheological model was applied to analyze quantitatively the fluid properties. Results showed that the incorporation of CNC at various concentrations into ATT/SEP-WDFs in freshwater and seawater improves the rheological and fluid loss properties and fluid thermal stability. When incorporating CNCs at lower concentrations into ATT/SEP-WDFs in freshwater and seawater, results showed improved carrying capacity of the cuttings, wellbore stability, fast penetration rate, high yield stress during the aging period, low viscosity at a high shear rate, and excellent shear-thinning behaviors.

DEDICATION

To God Almighty for strengthening his powerful hand upon me; my marvelous father (Lotanga Nkoy) and mother (Wanzo Apota) and to my entire family and my wife Ntumba Kazadi for their material and spiritual support and encouragement that make difference in my life.

ACKNOWLEDGEMENTS

I would like to thank my supervisors, Professor Diakanua Nkazi and Professor Geoffrey Simate, for their support. A special thanks to my main supervisor Professor Nkazi for his particular support and inspiration. You have always been there aligning my thought towards the success of this project, encouraging me that made me to believe in myself and in my work.

I would like to express my sincere gratitude to CHIETA for providing funding towards my studies. The financial assistance of the National Research Foundation (NRF) towards this research is hereby acknowledged.

I would also like to thank all the staff members who help me to achieve my goal, Civil Engineering soil lab (Sam, Steven) for the use of their Filter press equipment, Chemical Engineering workshop (Rodney, Phatu, Hopewell) for the use of the drilling press equipment, Janet and Mutlanti, Professor Sigalas for the use of their rheometer, Dr Mukayi for assistance, Mr. Bruce for taking me to U.J.

TABLE OF CONTENTS

ABSTRACT 3

DEDICATION 4

ACKNOWLEDGEMENTS 5

TABLE OF CONTENTS 6

LIST OF FIGURES 11

LIST OF TABLES 15

LIST OF EQUATION 16

NOMENCLATURE 18

SYMBOLS 19

CHAPTER 1. BACKGROUND AND MOTIVATION 20

1.1. INTRODUCTION 20

1.2. RESEARCH QUESTIONS 23

1.3. RESEARCH AIM AND OBJECTIVES 23

1.4. THESIS CONTENTS 24

CHAPTER 2. DRILLING FLUID TECHNOLOGY AND DESIGN 25

2.1. MATERIALS USED AS DRILLING FLUIDS 25

2.1.1. BENTONITE 25

2.1.2. ATTAPULGITE 28

2.1.3. SEPIOLITE 30

2.1.4. DISCUSSION 31

2.2. ASSESSMENT OF DRILLING FLUID ADDITIVE ON THE DRILLING OF THE ROCK SAMPLES 32

2.2.1. RATE OF PENETRATION 32

2.2.2. DRILLING FLUID PROPERTIES 34

2.2.3. FORMATION CHARACTERISTICS 35

2.2.4. BIT TYPE 35

2.2.5. WOB AND ROTATY SPEED 36

2.2.6. BIT TOOTH WEAR 37

2.2.7. BIT HYDRAULICS 37

2.2.8. BOURGOYNE AND YOUNGS' RATE OF PENETRATION 37
2.3. PAMETERS FOR DRILLING FLUID PROPERTIES 39
2.3.1. DRILLING TEMPERATURE AND PRESSURE 39
2.3.2. RHEOLOGICAL PROPERTIES 42
2.3.3. FILTRATION 46
2.4. CELLULOSE NANOCRYSTALS AND ITS RHEOLOGICAL PROPERTIES 47
2.4.1. SYNTHESIS OF CELLULOSE NANOCRYSTALS 47
2.4.2. RHEOLOGICAL PROPERTIES OF CNCs SUSPENSIONS 49
CHAPTER 3. EXPERIMENTAL AND ANALYTICAL TECHNIQUES 51
3.1. METHODOLOGY 51
3.1.1. MATERIALS 51
3.1.2. EXPERIMENTAL PROCEDURE 51
3.1.2.1. PREPARATION OF CELLULOSE NANOCRYSTALS 51
3.1.2.2. MUD PRAPARATION 52
3.1.2.2.1. FORMULATION OF DIFFERENT MUD SYSTEMS (CNC/BT, ATT, SEP-WDFs) 52
3.1.2.2.2. ULTRASONICATION PROCESS 54
3.1.3. CNCs CHARACTERIZATION 55
3.1.4. ANALYSIS OF RHEOLOGICAL AND FLUID LOSS PROPERTIES 57
3.1.4.1. RHEOLOGICAL ANALYSIS 57
3.1.4.2. RHEOLOGICAL PROPERTIES MEASUREMENT 57
3.1.4.3. FLUID LOSS ANALYSIS 60
3.1.4.4. FILTRATION PROPERTIES MEASUREMENT 61
CHAPTER 4. CELLULOSE NANOCRYSTALS BENTONITE WATER-BASE DRILLING FLUIDS 63
4.1. ANALYSIS OF RHEOLOGICAL PROPERTIES OF CNC/BT-WDFs (FW) 63
4.1.1. RHEOLOGICAL CURVES AT DIFFERENT CNC CONCENTRATION FOR VARIOUS TEMPERATURES 63
4.1.2. RHEOLOGICAL CURVES AT DIFFERENT TEMPERATURES FOR VARIOUS CNC CONCENTRATIONS 66
4.1.3. THE EFFECT OF CNC CONCENTRATION ON THE VISCOSITY OF CNC/BT-WDFs (FW) AS DRILLING FLUID 69
4.1.4. THE EFFECT OF TEMPERATURE ON THE VISCOSITY OF CNC/BT-WDFs (FW) AS DRILLING FLUID 72

4.2. ANALYSIS OF THE RHEOLOGICAL PROPERTIES OF CNC/BT-WDFs (SW) 76

4.2.1. RHEOLOGICAL CURVES AT DIFFERENT CNC CONCENTRATIONS FOR VARIOUS TEMPERATURES. 76

4.2.2. RHEOLOGICAL CURVES AT DIFFERENT TEMPERATURES FOR VARIOUS CNC CONCENTRATIONS. 80

4.2.3. TEMPERATURE EFFECTS ON THE VISCOSITY OF CNC/BT-WDFs (SW) AS DRILLING FLUID 82

4.2.4. THE EFFECTS ON CONCENTRATION ON THE VISCOSITY OF CNC/BT-WDFs (SW) AS DRILLING FLUID 84

4.3. FILTRATION PROPERTIES 87

4.3.1. ANALYSIS OF FILTRATION PROPERTIES OF CNC/BT-WDFs (FW) 87

4.3.2. ANALYSIS OF FILTRATION PROPERTIES OF CNC/BT-WDFs (SW) 89

4.4. AGING AND TEMPERATURE EFFECTS ON DIFFERENT PREPARED DRILLING FLUIDS. 90

4.5. RATE OF PENETRATION 93

4.6. CONCLUSIONS 94

CHAPTER 5. CELLULOSE NANOCRYSTALS ATTAPULGITE WATER-BASED DRILLING FLUID 95

5.1. ANALYSIS OF RHEOLOGICAL BEHAVIOUR OF CNC/ATT-WDFs IN FRESHWATER 95

5.1.1. RHEOLOGICAL CURVES AT DIFFERENT CNC CONCENTRATIONS FOR VARIOUS TEMPERATURES 95

5.1.2. RHEOLOGICAL CURVES AT DIFFERENT TEMPERATURES FOR VARIOUS CNC CONCENTRATIONS. 99

5.1.3. CNC CONCENTRATION EFFECT ON THE VISCOSITY OF CNC/ATT-WDFs (FW) AS DRILLING FLUID. 101

5.1.4. TEMPERATURE EFFECT ON THE VISCOSITY OF CNC/ATT-WDFs (FW) AS DRILLING FLUID. 103

5.2. ANALYSIS OF THE RHEOLOGICAL PROPERTIES OF CNC/ATT-WDFs IN SEAWATER. 105

5.2.1. RHEOLOGICAL CURVES AT DIFFERENT CNC CONCENTRATIONS FOR VARIOUS TEMPERATURES. 105

5.2.2. RHEOLOGICAL CURVES OF CNC/ATT-WDFs (SW) AT DIFFERENT TEMPERATURES FOR VARIOUS CNC CONCENTRATIONS 109

5.2.3. THE EFFECT OF CNC CONCENTRATION ON THE VISCOSITY OF CNC/ATT-WDFs (SW) AS DRILLING FLUID. 111

5.3. FILTRATION PROPERTIES 117
5.3.1. ANALYSIS OF FILTRATION PROPERTIES OF CNC/ATT-WDFs (FW) 117
5.3.2. ANALYSIS OF FILTRATION PROPERTIES OF CNC/ATT-WDFs (SW) 118
5.4. AGING TIME 119
5.5. RATE OF PENETRATION. 122
5.6. CONCLUSIONS 123
CHAPTER 6. CELLULOSE NANOCRYSTALS SEPIOLITE WATER-BASED DRILLING FLUIDS. 125
6.1. ANALYSIS OF RHEOLOGICAL BEHAVIOUR OF CNC/SEP-WDFs (FW). 125
6.1.1. RHEOLOGICAL CURVES OF CNC/SEP-WDFs (FW) AT DIFFERENT CNC CONCENTRATIONS FOR VARIOUS TEMPERATURES. 125
6.1.2. RHEOLOGICAL CURVES AT DIFFERENT TEMPERATURES FOR VARIOUS CNC CONCENTRATIONS. 128
6.1.3. CNC CONCENTRATION EFFECT ON THE VISCOSITY OF CNC/SEP-WDFs (FW) AS DRILLING FLUID 130
6.1.4. TEMPERATURE EFFECT ON THE VISCOSITY OF CNC/BT-WDFs (FW) AS DRILLING FLUID. 132
6.2. ANALYSIS OF THE RHEOLOGICAL PROPERTIES OF CNC/SEP-WDFs IN SEAWATER 137
6.2.1. RHEOLOGICAL CURVES AT DIFFERENT CNC CONCENTRATIONS FOR VARIOUS TEMPERATURES. 137
6.2.2. RHEOLOGICAL CURVES OF CNC/SEP-WDFs (SW) AT DIFFERENT TEMPERATURES FOR VARIOUS CNC CONCENTRATIONS 140
6.2.3. THE EFFECT OF CNC CONCENTRATION ON THE VISCOSITY OF CNC/SEP-WDFs (SW) AS DRILLING FLUID. 142
6.3. FILTRATION PROPERTIES 148
6.3.1. ANALYSIS OF FILTRATION PROPERTIES OF CNC/SEP-WDFs (FW) 148
6.3.2. ANALYSIS OF FILTRATION PROPERTIES OF CNC/SEP-WDFs (SW) 148
6.4. AGING TIME 150
6.5. RATE OF PENETRATION. 152
6.6 . CONCLUSIONS 153
CHAPTER 7. COMPARISON OF DIFFERENT DRILLING FLUIDS 154
7.1. FILTRATION PROPERTIES 154
7.1.1. FILTRATION IN PROPERTIES IN FRESHWATER 154

7.1.2. FILTRATION IN PROPERTIES IN SEAWATER 154
7.2. AGING AND TEMPERATURE EFFECTS ON DIFFERENT PREPARED DRILLING FLUIDS. 155
7.3. RATE OF PENETRATION 161
7.4. CONCLUSIONS 170
CHAPTER 8. CONCLUSIONS AND RECOMMENDATIONS. 173
8.1. CONCLUSIONS 173
8.2. RECOMMENDATIONS 175
REFERENCES 176
INDEX A: RHEOLOGICAL DATA 192
RHEOLOGICAL DATA OF CNC/BT-WDFs (FW) 192
RHEOLOGICAL DATA OF CNC/ATT-WDFs (FW) 209
RHEOLOGICAL DATA OF CNC/SEP-WDFs (FW) 237
RHEOLOGICAL DATA OF CNC/BT-WDFs (SW) 258
RHEOLOGICAL DATA OF CNC/ATT-WDFs (SW) 286
RHEOLOGICAL DATA OF CNC/SEP-WDFs (SW) 314
INDEX B: FLUID LOSS DATA 329
INDEX C: AGING TIME DATA 332
INDEX D: RATE OF PENETRATION DATA 348

LIST OF FIGURES

Figure 1. Crystalline structure of sodium montmorillonite with interlamellar water layer. 25
Figure 2. Molecular structure of attapulgite. 29
Figure 3. Basic Structure of SEP Clay. 30
Figure 4. Various types of drill bits. 36
Figure 5. Typical response of penetration rate to increasing bit weight. 36
Figure 6. Typical response of penetration rate to increasing rotary speed. 37
Figure 7.Percentage of thermal conductivity increase against temperature for MIX-1 (a) and MIX-2 (b). 40
Figure 8. The variation of shear stress against shear rate at different temperature (25, 55 and 80°C) and different nanoFe_2O_3 (a) 0 wt.%, (b) 0.2 wt.%, (c) 0.6 wt.% and (d) 1 wt.%. 41
Figure 9. The variation of yield stress against temperature at different nanoFe_2O_3 (0 wt. %, 0.2 wt. %, 0.6 wt. % and 1 wt. %). 41
Figure 10. Graphs showing properties of Newtonian fluid. 42
Figure 11.Graphs showing properties of non-Newtonian fluids (Retrieved March 28, 2015. 43
Figure 12. Viscosity curve for bentonite. 44
Figure 13. A schematic representation of mud losses while drilling in the case of (a) typical LCM; and (b) NP. 46
Figure 14. Cellulose nanocrystals (CNCs) structure and transmission electron microscopy (TEM) image extracted from cotton. 48
Figure 15. Viscosity vs shear rate for the suspensions of whiskers at different concentrations of cellulose (wt. %). 50
Figure 16. Steady-state viscosity versus shear rate for (a) unsonicated CNC suspensions, and (b) CNC suspensions sonicated with concentrations varying from 1 to 7 wt. %. 50
Figure 17. Synthesis of Cellulose Nanocrystals (CNCs) / Oil and Gas Laboratory (Chemical Engineering / Wits University 2019). 52
Figure 18. Schematic diagram of the experimental process. 54
Figure 19. The ultrasonic processor UP200S (200 watts, 24 kHz). 55
Figure 20. TEM micrographs of the CNCs. 56
Figure 21. TEM micrographs of the CNC/BT-WDFs. 56
Figure 22. TEM micrographs of the CNC/ATT-WDFs (A) and CNC/SEP-WDFs (B). 57
Figure 23. Rotational Rheometer (Rheolab QC SN897839 / FW1.31, Chemical Engineering / Wits University, 2018). 60
Figure 24. Filter press HPHT 1L 5 bars (Soil Lab, Civil Engineering/Wits University, 2018). .. 61
Figure 25. The plots A, B, C, D, E, F and G of the variation of shear stress against shear rate for CNC/BT-WDFs (FW) at various CNC concentrations at different temperatures. 64
Figure 26.The plots A, B, C, D, E, F, G and H of shear stress as a function of shear rate for CNC/BT-WDFs (FW) at various temperatures for different CNC concentrations. 67
Figure 27. The plot of the variation of shear stress against temperature for CNC/BT-WDFs (FW) at various CNC concentrations taken at high shear rate 1200 s^{-1}. 68
Figure 28. The plots of viscosity as a function of shear rate for CNC/BT-WDFs (FW) at various CNC concentrations for different temperatures. 70
Figure 29. Variation of viscosity of CNC/BT-WDFs (FW) with CNC concentration at different temperature (0.999 s^{-1}) using Herschel-Bulkley (HB) models. 71

Figure 30. Viscosity of CNC/BT-WDFs (FW) at various CNC concentrations for different temperature. 72
Figure 31. The plot of viscosity as a function of shear rate for CNC/BT-WDFs (FW) at various temperatures for different CNC concentrations. 73
Figure 32. The plot of the viscosity of CNC/BT-WDFs (FW) as a function temperature at various CNC concentrations at low and high shear rate (0.999 s^{-1} and 1200 s^{-1}). 75
Figure 33.The plots A, B, C, D, E, F and G of shear stress of CNC/BT-WDFs (SW) as a function of shear rate at various CNC concentrations for different temperatures. 77
Figure 34. The plots A, B, C, D, E, F and G of shear stress of CNC/BT-WDFs (SW) as a function of shear rate at different temperatures for various CNC concentrations. 80
Figure 35. Plot of shear stress as a function temperature for CNC/BT-WDFs (SW) at various CNC concentrations taken at high shear rate 1200 s^{-1}. 81
Figure 36. The plot of viscosity as a function CNC concentrations for CNC/BT-WDFs in sea-water at various temperatures at low shear rate 0.999 s^{-1}. 82
Figure 37. The plot of viscosity as a function temperatures for CNC/BT-WDFs (SW) at various CNC concentrations at low and high shear rate (0.999 s^{-1} and 1200 s^{-1} respectively). 83
Figure 38. The plot of viscosity as a function of shear rate for CNC/BT-WDFs (SW) at various CNC concentrations for different temperatures. 84
Figure 39. The plot of viscosity as a function of shear rate for CNC/BT-WDFs (SW) at various temperatures for different CNC concentrations. 86
Figure 40. The plot of fluid loss volume (at 30 min) of CNC/BT-WDFs (FW) as a function of pressure at different CNC concentrations and 22°C. 87
Figure 41. The plot of fluid loss volume (at 30 min) of CNC/BT-WDFs (FW) as a function of temperatures at 450KPa for 1.0 wt. % CNC concentrations. 87
Figure 42. The plot of fluid loss volume as a function of time for CNC/BT-WDFs (FW) at 450KPa and 80°C for different CNC concentrations. 88
Figure 43. The plot of fluid loss volume as a function of time for CNC/BT-WDFs (FW) at 450 KPa for different temperatures. 89
Figure 44. The plot of fluid loss volume as a function of time for CNC/BT-WDFs (SW) at 450 KPa for different temperatures. 90
Figure 45. The plot of shear stress as a function of shear rate at different aging time at 25℃ and 80℃ for CNC/BT-WDFs in fresh-water and sea-water. 91
Figure 46. Plots of the rate of penetration as a function of pressure (stress) or weight on bit of different rock samples in CNC/BT-WDFs (FW) and CNC/BT-WDFs (SW). 93
Figure 47. The plots of shear stress as a function of shear rate for CNC/ATT-WDFs in fresh-water at various CNCs concentrations for different temperatures. 96
Figure 48. The plots A, B, C, D, E, F and G of shear stress as a function of shear rate for CNC/ATT-WDFs (FW) at various temperatures for different CNC concentrations. 99
Figure 49. The plot of the shear stress of CNC/ATT-WDFs (FW) as a function of temperature at various CNC concentration at low and high shear rate (0.999s^{-1} and 1200 s^{-1}). 100
Figure 50. The plot of the viscosity of CNC/BT-WDFs (FW) as a function of shear rate at various CNC concentrations for different temperatures. 102
Figure 51. Viscosity of CNC/ATT-WDFs (FW) as a function of temperature at various CNC concentrations taken at low and high shear rate (1 s^{-1} (a) and 1200 s^{-1}(b)). 103
Figure 52. The plot of viscosity of CNC/ATT-WDFs (FW) as a function of shear rate at various temperatures for different CNC concentrations. 104

Figure 53. The plots of shear stress as a function of shear rate for CNC/ATT-WDFs in seawater at various CNC concentrations for different temperatures. 106
Figure 54. The plot of shear stress as a function temperature for CNC/ATT-WDFs in seawater at various CNC concentrations taken at high shear rate 1200 s^{-1}. 109
Figure 55. Plots of shear stress of CNC/ATT-WDFs (SW) as a function of shear rate at different temperature for various CNC concentrations. 110
Figure 56. The plot of the viscosity of CNC/ATT-WDFs (SW) as a function of shear rate at various CNC concentrations for different temperatures. 111
Figure 57. Variation of viscosity of CNC/ATT-WDFs (SW), determined from low shear rates (0.999 1/s), with CNC concentrations at different temperatures. 113
Figure 58. The plot of viscosity as a function temperature for CNC/ATT-WDFs in fresh-water at various CNC temperature taken at low and high shear rate (1 s^{-1} and 1200 s^{-1})..... 113
Figure 59. The plot of the flow consistency coefficient (K) as a function temperature of CNC/ATT-WDFs (SW) at various CNCs temperatures. 114
Figure 60. The plot of the viscosity of CNC/ATT-WDFs (SW) as a function of shear rate at various temperatures for different CNC concentrations. 115
Figure 61. The plot of fluid loss volume as a function of time for CNC/ATT-WDFs (FW) at 450KPa and 80°C for different CNC concentrations..... 117
Figure 62. The plot of fluid loss volume as a function of time for CNC/ATT-WDFs (SW) 1.2 wt. % CNC concentration at 450 KPa for different temperatures. 118
Figure 63. The plot of shear stress as a function of shear rate at different aging time at 25℃ and 80℃ for CNC/ATT-WDFs in fresh water and seawater. 119
Figure 64. The plot of the rate of penetration as a function of pressure (stress) or weight on bit of different rock samples in CNC/ATT-WDFs (FW) and CNC/ATT-WDFs (SW). 122
Figure 65. The plot of shear stress as a function of shear rate of CNC/SEP-WDFs (FW) at various CNCs concentrations for different temperatures..... 126
Figure 66.The plot of shear stress as a function temperature for CNC/SEP-WDFs in freshwater at various CNC concentration and high shear rate (1200 s^{-1}). 128
Figure 67. The plots of shear stress as a function of shear rate of CNC/SEP-WDFs in freshwater at various temperatures for different CNC concentrations. 129
Figure 68. Variation of viscosity of CNC/SEP-WDFs (FW) with CNC concentrations at different temperatures and low shear rates (0.999 s^{-1}). 130
Figure 69. The plot of viscosity as a function of shear rate for CNC/SEP-WDFs (FW) at various CNC concentrations for different temperatures. 131
Figure 70. The plot of viscosity as a function of shear rate for CNC/SEP-WDFs (FW) at various temperatures for different CNC concentrations. 133
Figure 71. Plot of viscosity as a function temperature for CNC/SEP-WDFs in freshwater at various CNC concentration at low (0.999 s^{-1}) and high shear rate (1200 s^{-1})..... 135
Figure 72. The plot of shear stress as a function of shear rate of CNC/SEP-WDFs (SW) at various CNC concentrations for different temperatures. 138
Figure 73. The plot of shear stress as a function temperature for CNC/SEP-WDFs (SW) at various CNC concentrations taken at high shear rate 1200 s^{-1}. 140
Figure 74. The plot of shear stress as a function of shear rate of CNC/SEP-WDFs in seawater at different temperature and various CNC concentrations..... 141
Figure 75. The plot of viscosity as a function of shear rate for CNC/SEP-WDFs (SW) at various CNC concentrations for different temperatures. 143

Figure 76. Variation of viscosity of CNC/SEP-WDFs (SW) with CNC concentrations at shear rates 0.999 s^{-1} and different temperatures. 144
Figure 77. The plot of viscosity as a function temperature for CNC/SEP-WDFs in sea-water at various CNC temperature taken at low and high shear rate (1 s^{-1} and 1200 s^{-1})..... 145
Figure 78. The plot of the flow consistency coefficient (K) as a function temperature of CNC/SEP-WDFs (SW) at various CNC concentrations..... 145
Figure 79.The plot of viscosity as a function of shear rate for CNC/SEP-WDFs (SW) at various temperatures for different CNC concentrations..... 146
Figure 80. The plot of fluid loss volume as a function of time for CNC/SEP-WDFs (FW) 1.2 wt. % CNC concentration at 450 KPa for different temperatures. 148
Figure 81. The plot of fluid loss volume as a function of time for CNC/SEP-WDFs (SW) 1.2 wt. % CNC concentration at 450 KPa for different temperatures. 149
Figure 82. The plot of shear stress as a function of shear rate at different aging time at 25℃ and 80℃ for CNC/ SEP-WDFs in fresh water and seawater. 150
Figure 83.The plot of the rate of penetration as a function of pressure (stress) or weight on bit of different rock samples in CNC/SEP-WDFs (FW) / (SW). 152
Figure 84. The plot of fluid loss volume of CNC/BT, ATT, SEP-WDFs (FW) as a function of time at 80°C, 450KPa and 1.2 wt. % CNC concentration. 154
Figure 85. The plot of fluid loss volume of CNC/BT, ATT, SEP-WDFs (SW) as a function of time at 80°C, 450KPa and 1.2 wt. % CNC concentration. 155
Figure 86. Consistency index and yield point as a function of aging time at different temperatures for CNC/BT, ATT, SEP-WDFs (FW). 156
Figure 87. Consistency index (a) and yield point (b) as a function of aging time at different temperatures for CNC/BT, ATT, SEP-WDFs (SW)..... 156
Figure 88. Effective viscosity as a function of aging time at different temperatures for CNC/BT, ATT, SEP-WDFs (SW). 156
Figure 89. The plot of shear stress as a function of shear rate at different aging time at 25℃ and 80℃ for CNC/BT, ATT, SEP-WDFs in fresh water and seawater. 160
Figure 90. Drill press (RPM 885/ Bit diameter 6 mm, Workshop of Chemical Engineering/Wits University, 2019). 163
Figure 91. The plots of the rate of penetration as a function of pressure (stress) or weight on bit of different rock samples in CNC/BT, ATT, SEP-WDFs (FW)..... 164
Figure 92. The plots of the rate of penetration as a function of pressure (stress) of different rock samples in CNC/BT, ATT, SEP-WDFs (SW). 164

LIST OF TABLES

Table 1. Formulation of CNC/BT-WDFs, CNC/ATT-WDFs and CNC/SEP-WDFs in freshwater and seawater. 53
Table 2. . Calculated parameters CNC/BT-WDFs (FW) at various CNC Concentrations for different temperature using Herschel-Bulkley (HB) Models..... 65
Table 3. Variation of shear stress of CNC/BT-WDFs (FW) with temperature at different CNC concentrations determined at high shear rate (1200 s^{-1}). 68
Table 4. Variation of viscosity of CNC/BT-WDFs (FW) with temperature at different CNC concentration, determined at low shear rates (0.999 s^{-1}). 74
Table 5. Variation of viscosity of CNC/BT-WDFs (FW) with temperature at different CNC concentration, determined from high shear rates (1200 s^{-1}). 74
Table 6. Calculated parameters CNC/BT-WDFs (SW) at various CNC concentrations for different temperature using Herschel-Bulkley (HB) Models..... 78
Table 7. Variation of shear stress of CNC/BT-WDFs (SW) versus temperature at different CNC concentration, determined at high shear rates (1200 s^{-1}). 79
Table 8. Variation of viscosity of CNC/BT-WDFs (SW) versus temperature at different CNC concentration, determined at low shear rates (0.999 s^{-1}). 83
Table 9. Calculated parameters of CNC/BT-WDFs (FW)/(SW) at different aging time for different temperature using Herschel-Bulkley (HB) Models..... 91
Table 10. Calculated parameters of CNC/ATT-WDFs (FW) at various CNC Concentrations for different temperatures using Herschel-Bulkley (HB) models. 98
Table 11. Calculated parameters of CNC/ATT-WDFs (SW) at various CNC concentrations for different temperatures using Herschel−Bulkley model. 108
Table 12. Viscosity of CNC/ATT-WDFs (SW) at various CNC concentrations for different temperatures. 112
Table 13. Calculated parameters of CNC/ATT-WDFs (FW) at different aging time for different temperature using Herschel-Bulkley (HB) Models. 119
Table 14. Calculated parameters of CNC/ATT-WDFs (FW) at different aging time for different temperature using Herschel-Bulkley (HB) Models. 120
Table 15. Calculated parameters CNC/SEP-WDFs (FW) at various CNC Concentrations for different temperature using Herschel-Bulkley (HB) Models..... 127
Table 16. Variation of viscosity of CNC/SEP-WDFs (FW) with temperature at low shear rates (0.999 s-1) and different CNC concentrations. 134
Table 17. Variation of viscosity of CNC/SEP-WDFs (FW) with temperature at high shear rates (1200 s^{-1}) and different CNC concentrations. 134
Table 18. Calculated parameters of CNC/SEP-WDFs (SW) at various CNC concentrations for different temperatures using Herschel-Bulkley model. 139
Table 19. Viscosity of CNC/SEP-WDFs (SW) at various CNC concentrations for different temperatures. 144
Table 20. Calculated parameters of CNC/SEP-WDFs (FW) at different aging time for different temperature using Herschel-Bulkley (HB) Models. 151
Table 21. Calculated parameters of CNC/SEP-WDFs (SW) at different aging time for different temperature using Herschel-Bulkley (HB) Models. 151
Table 22. Yield point, consistency index and effective viscosity as a function of aging time for different temperatures. 158

Table 23. Variation of the rate of penetration of CNC/BT-WDFs (SW) versus of pressure (stress) of different rock samples in CNC/BT, ATT, SEP-WDFs (FW). 161
Table 24. Variation of the rate of penetration of CNC/BT-WDFs (SW) versus of pressure (stress) of different rock samples in CNC/BT, ATT, SEP-WDFs (SW). 162

LIST OF EQUATION

Equation 1. $dDdt = Exp(a1 + j - 28ajxi)$ 37
Equation 2. $x1 = 1$ 38
Equation 3. $x2 = 10{,}000 - TVD$ 38
Equation 4. $x3 = TVD0.69(gp - 9.0)$ 38
Equation 5. $x4 = TVD(gp - \rho c)$ 38
Equation 6. $x5 = ln[WOBdb - [WOBdb]t4.0 - [WOBdb]t]$ 38
Equation 7. $x6 = ln[N100]$ 38
Equation 8. $x7 = -h$ 38
Equation 9. $x8 = \rho g350\mu dn$ 38
Equation 10. $\tau_{gel} = (\rho_p - \rho_f)*gD/6$ 45
Equation 11. $\tau = \tau_o + \mu_p \times \dot{\gamma}$ 57
Equation 12. $\tau = K \times (\dot{\gamma})^n$ 58
Equation 13. $\tau = \tau_0 + K\times (\dot{\gamma})^n$ 58
Equation 14. $\tau = K\times (\dot{\gamma}_0 + \dot{\gamma})^n$ 59
Equation 15. $\tau = \mu_\infty\times\dot{\gamma} + K\times (\dot{\gamma})^n$ 59
Equation 16. $\tau^{0.5} = \tau_o + K \times (\dot{\gamma})^n$ 59
Equation 17. $\tau^n = \dot{\gamma}_o^n + K\times (\dot{\gamma})^n$ 60
Equation 18 ROP = (1.13949 ± 1.23859) σ + (8.45004 ± 3.06883) R^2 = 0.22005 R = 0.47 165
Equation 19 ROP = (0.35416 ± 1.29968) σ + (11.64189 ± 3.22019) R^2= 0.02415 R = 0.16 165
Equation 20 ROP = (5.1664 ± 2.46105) σ + (-2.13312 ± 6.0977) R^2= 0.59497 R = 0.77 165
Equation 21 ROP = (1.32275 ± 0.47962) σ + (-1.52044 ± 1.18834) R^2= 0.71715 R = 0.85 165
Equation 22 ROP = (3.34042 ± 1.37127) σ + (-4.59654 ± 3.39758) R^2= 0.66421 R = 0.82 165
Equation 23 ROP = (0.45236 ± 0.13544) σ + (0.02939 ± 0.33558) R^2= 0.78806 R = 0.89 166
Equation 24 ROP = (0.19653 ± 0.09509) σ + (0.14351 ± 0.2356) R^2= 0.58744 R = 0.77 166
Equation 25 ROP = (0.32277 ± 0.06188) σ + (-0.25188 ± 0.15331) R^2= 0.9007 R = 0.95 166
Equation 26 ROP = (0.93373 ± 0.15936) σ + (-1.41766 ± 0.39485) R^2= 0.91964 R = 0.96 166
Equation 27 ROP = (1.1324 ± 0.35808) σ + (-1.24414 ± 0.88721) R^2= 0.76925 R = 0.88 166

Equation 28 ROP = (0.22478 ± 0.01776) σ + (-0.0129 ± 0.044) R^2= 0.98162 R = 0.991 166
Equation 29 ROP = (0.52732 ± 0.12063) σ + (-0.15065 ± 0.29888) R^2= 0.86431 R = 0.93 167
Equation 30 ROP = (2.03075 ± 0.95363) σ + (2.9108 ± 2.36279) R^2= 0.60184 R = 0.76 167
Equation 31 ROP = (-2.36344 ± 0.96388) σ + (12.49517 ± 2.3882) R^2= 0.66712 R = 0.82 167
Equation 32 ROP = (2.70363 ± 1.25613) σ + (2.43931 ± 3.1123) R^2= 0.60695 R = 0.78 167
Equation 33 ROP = (0.19501 ± 0.05884) σ + (-0.13626 ± 0.14578) R^2= 0.78548 R = 0.89 167
Equation 34 ROP = (0.08735 ± 0.09699) σ + (0.14987 ± 0.24031) R^2= 0.21281 R = 0.46 168
Equation 35 ROP = (0.5985 ± 0.10377) σ + (-0.83219 ± 0.25711) R^2= 0.91728 R = 0.96 168
Equation 36 ROP = (-0.00102 ± 0.10155) σ + (0.31714 ± 0.25162) R^2= 0.33329 R = 0.57 168
Equation 37 ROP = (0.13836 ± 0.05496) σ + (0.00465 ± 0.13618) R^2= 0.6787 R = 0.82 168
Equation 38 ROP = (0.13831 ± 0.05472) σ + (-0.05324 ± 0.13558) R^2= 0.68048 R = 0.82 168
Equation 39 ROP = (0.02689 ± 0.11613) σ + (0.38604 ± 0.28774) R^2= 0.30993 R = 0.56 168
Equation 40 ROP = (0.1652 ± 0.03749) σ + (0.26145 ± 0.0929) R^2= 0.86616 R = 0.93 169
Equation 41 ROP = (0.51868 ± 0.1232) σ + (-0.69901 ± 0.30524) R^2= 0.85526 R = 0.93 169

NOMENCLATURE

Abbreviations

AARD	Average Absolute Relative Deviation
API	American Petroleum Institute
ATT	Attapulgite
BT	Bentonite
CNC	Cellulose Nanocrystals
H_3PO_4	Phosphoric Acid
HCL	Hydrochloric Acid
HTHP	High Temperature High Pressure
LTLP	Low Temperature Low Pressure
MFC	Microfibrillated Cellulose
Mt	Montmorillonite
NaBr	Sodium Bromide
NaCIO	Sodium Hypochlorite
NaOH	Sodium Hydroxide
NP	Nanoparticles
PR	Penetration Rate
R^2	Squared Correlation Coefficient
RMSD	Root-Mean-Square Deviation
RMSE	Root Mean Square of Error
ROP	Rate Of Penetration
RPM	Revolutions Per Minute
SEM	Scanning Electron Microscope
SEP	Sepiolite
TEM	Transmission Electron Microscope
TEMPO	2,2,6,6-Tetramethylpiperidin-1-Oxyl
WDF	Water-Based Drilling Fluid

SYMBOLS

°C	Temperature unit: Degree Celsius
AV	Apparent viscosity
D	Diameter
K	Flow consistency index
n	Flow behavior index
ppg	pound per gallon
SG	Specific gravity
y_o	Yield Stress
$\dot{\gamma}$	Shear rate
ϑ	Shear rate
τ_{gel} (lb/100ft^2)	Gel strength in pounds per square feet
ρ_f	Fluid density
ρ_p	SG for particle
τ_0	Yield Stress
τ	Shear Stress

CHAPTER 1. BACKGROUND AND MOTIVATION

1.1. INTRODUCTION

Actually, the world is experiencing a great demand of crude oils that hastens the growth of industrial sector to satisfy human being needs. Global energy supply exhibited an increase of 107% from 1973 to 2010 with 12,717 Metric tons of oil equivalent (Mtoe) by end-2010 (IEA 2014). As well the global total primary energy consumption (TPEC) was estimated at 8677 Mtoe in end-2010 and rose to 86% from 1973 to 2010. Crude oil and natural gas (NG) contributed 55% to the world energy need by 2035 (BP 2016). The oil and gas industry decides to access the unattainable hydrocarbons resources by drilling into deeper formations. As the well goes deeper, the deeper formations are being disclosed and the drilling fluid system undergoes harsh conditions not only of high pressure and high temperature (HTHP) and shear degradation but also of being contaminated with high level of soluble salts (salinity). Thus the drilling mud rheology is drastically affected as the payzone depth increases. HPHT well conditions are related to oil and gas wells where temperature and pressure are successively greater than 300°F (150°C) and 10,000 psi (69 MPa) (Amani 2015). These are new challenges encountered when the drilling operation is carrying out at the present conditions. The overall cost of drilling process represents 25 to 40 % of the total well (Khodja et al 2010; Elkatatny et al 2020). A new drilling fluid system is necessarily required to accommodate these extreme conditions (Larsen 2007; Khodja 2010).

Drilling into a deep wells characterized by harsh conditions of pressure and temperature (HPHT) requires a drilling fluid with stable rheological properties and very less filtration loss capable to stabilize the wellbore system. Many problems are encountered during drilling operation that affect the performance of drilling fluids which constitute challenges for the oil and gas industry. These challenges include: pressure losses, fluid gelation, poor hole cleaning, loss circulation zones, reservoir fluid invasions, hard rock, and all together causing severe wellbore instability (Bland et al 2005; Rocha et al 2003; Rogers et al 2004; Kelessidis 2009; Amani 2015; Larsen 2007; Khodja 2010). Thus, oil and gas industry has to develop efficient drilling fluids susceptible of good performance and overwhelm challenges **(**Kelessidis 2009).

Most works have been done to improve the rheological properties of drilling fluid mud at HPHT condition. The choice of the appropriate drilling fluid additive remains a challenge. One of the keys to address this issue is frequently the addition of several additives either individually or concurrently. It has been seen at high temperature the conventional additives (water and oil mud) appear generally unstable whereas several natural and synthetic polymers are stable in terms of bacterial, thermal and mechanical degradation (Larsen 2007).

A double effect has been noticed when the drilling fluid reacts with salt at HPHT conditions, the molecular structure of the polymer is affected leading to deflocculating of the drilling fluid. This deflocculating of the drilling fluid leads to the reduction of the viscosity. On the other hand, as the temperature increases, the mobility of the particles also increases in the drilling fluid solution. Especially bentonite (BT) structures which have more ionic components at their surface react rapidly as a consequence the behavior of bentonite is affected and the changes in the properties such as viscosity and density of the mud fluid are occurring. The effect of salinity on the correlation between the structure and reactivity of the bentonite clay is broadly increased at such conditions (Amani 2015).

The success of drilling operation in a deep well depends on the selection of good drilling fluid that performs well to minimize the amount of lost time during drilling well. Therefore this drilling fluid should be simple, economical, and flexible for future requirements and contains few additives for successful maintenance and control of its rheological properties (Max & Martin 1974). Drilling fluid or mud or drilling mud are fluids used during drilling operation of subterranean containing a continuous phase such as water, oil, and synthetic materials respectively named water-based drilling fluids(WDFs), oil-based drilling fluids(ODFs), and Synthetic-based drilling fluids (SDFs) in which clay and additives are added to improve its viscosity and density. Water-based drilling fluids (WDFs) are the most used in the oil and gas industry due to their lower cost and being environmentally friendly as compared to oil-based drilling fluids (ODFs) and synthetic-based drilling fluids (SDFs). Despite the ability of ODFs and SDFs to maintain the wellbore stability and to lubricate the drilling tools, WDFs remain the best choice (Zakaria et al 2012; Kelessidis et al 2013). Besides, WDFs improve fast penetration rate and beneficial cooling and cutting removal capacity (Fink 2015).

Bentonite suspensions are widely used in industrial processes and particularly in the petroleum industry because of their outstanding rheological properties (Ali & Barrufet 2001; Kok 2004, 2011; Wan et al 2011, Yao et al 2011; Jung 2011; Richard et al 2017; Yildiz et al 1999) and its unique swelling capacity (Jung et al 2011; Li et al 2015; Temraz & Hassanien 2016). Despite the principal role, a drilling fluid is designed to fulfill any purpose. A drilling fluid is designed for transporting the cuttings from the bottom of the wellbore to the surface; for cooling and lubricating the drill bits and pipes; for preventing cuttings from swelling and sedimentation; for alleviating friction between drilling equipment and formation; and for stabilizing wellbore walls and controlling formation pressure (Hamed & Belhadri 2009; Bailey et al 1994; Jones & Hughes 1996; Kelessidis et al 2011; Kosynkin et al 2011). Bentonite water-based drilling fluid should present high tolerance for temperature and salt. Also, it has to be cheaper, less reactive, environmentally friendly, and non-corrosive (Wan et al 2011; Khalil & Mohamed 2012; Yan et al 2013; Okon et al 2014; Ouaer & Gareche 2019).

Some problems are encountered when the drilling operation is being done such as variation of mineral compositions in the shale and the change in the formation conditions in terms of temperature and pressure. To address these problems affecting the drilling fluids, a good understanding of the shale basins' local conditions can generate best practices and lowering the drilling cost. WDFs could remove most of the supplementary cost but must defeat the challenge of wellbore stability and comparative drilling performance. The WDFs consist of water, clay, rheological modifier, and fluid loss controller. Bentonite (BT) is the most important clay used in WDFs among all due to its ability to give an outstanding swelling capacity and great rheological property (Jung et al 2011).

The role of BT is to improve the viscosity and prevent fluid loss into the formation. For this to be possible, a more quantity of BT is needed to reach desired rheological and filtration properties. Contrarily to this situation, when excess BT is used a negative effect occurs producing much thicker filter cake which could lead to formation damage and allow the pipe to get stuck during drilling operation as result the drilling productivity will be reduced (William et al 2014; Fan et al 2015; Anyanwu & Mustapha 2016; Song et al 2016). These challenges could be overwhelmed by introducing different additives in bentonite dispersions to control the rheological behavior of the dispersions such as electrolytes (Luckham & Rossi 1999), surfactants and polymers (Mahto &

Sharma 2004), amphoteric cellulose (Warren et al 2003), carboxymethyl cellulose (Iscan & Kok 2007), xanthan gum (Navarrete et al 2000), rice husk, starch (Dias et al 2015), polyacrylamide and polyacrylates (Nunes et al 2014; Li et al 2015b; Li et al 2015**)**. However, many works have been done using sodium chloride (NaCl) into bentonite dispersions to evaluate its effect on the rheological behavior of bentonite at different concentrations (Adachi et al 1998; Abend & Lagaly 2000; Ramos et al 2001; M'bodj et al 2004; Tombacz & Szekeres 2004, Tombacz & Szekeres 2004; Basim 2011). Therefore, the rheological and filtration properties of WDFs are two important aspects to ensure the safety and success of oil well drilling. Considering economic, sustainable, and environmental effects, utilization of natural polymers as modifiers for rheology and fluid loss in WDFs is highly preferred.

Drilling operations process in harsh conditions of high temperature and high pressure including high electrolyte influx (salt contamination) constitutes a great obstacle for the use of bentonite clay-based water mud. The intervention of attapulgite (ATT) or sepiolite (SEP) clays minerals to replace BT with the possibility of the incorporation of CNC particles could be the key to solve problems in the deep well. As these minerals have a fibrous structure with low surface energy, their low reactivity in the presence of salt contaminants and their high stability in high temperature can result in good rheological and fluid loss properties to sort out BT clay limitation in the drilling operation. The attapulgite (ATT) or sepiolite (SEP) suspension viscosity is owing to the effect of the shear forces leading to the formation of gel structure and the attractive forces established between particles that had been created by broken-bond charges on the edges of broken fibers through shearing force effects (Rahman 1988; Al-marhoun 2015). In this work, ATT clay will be used due to its ability to withstand the effect of salt. SEP clay as well will be used for its ability to resist both high saline concentration and HPHT conditions.

Nanotechnology represents the core of all aspects of science and technology. It is characterized by using nanoparticles (NPs) of 1-100nm in size having an extra-large surface area to volume ratio which increases their reactivity. As result, much less amount of nanoparticles is required for a particular for preparing a drilling fluid with improved rheological and filtration properties. This can contribute to the reduction of the cost of the drilling operation. The application of NPs in the oil and gas industry provides a new generation of drilling fluids named smart drilling fluids where NPs have been mixed as an additive in WDFs to improve their rheological and filtration properties including maintaining borehole stability, improving cutting removal ability, eliminating differential pipe sticking, reducing fluid loss and enhancing oil recovery (Song 2016). Most of the works have been done to optimize the utilization of NPs over the years (Kosynkin et al 2011; Jung et al 2011; Cai et al 2012; William et al 2014; Fazelabdolabadi et al 2014; and Li et al 2015). They showed that the optimum concentration of NPs used is usually <1.0 wt. %. Besides, it has been depicted that NPs offer great ability to plug pore throats in shale rather than microparticles and establish a thin filter cake to protect the wellbore from a fluid invasion that could affect formation stability and drilling productivity by providing good lubrication and lowering the torque and drag problems. The following work depicts that 98% of water penetration was reduced compared to seawater into Atoka shale and a factor of 5 to 50 was kept for the reduction of the permeability of the Atoka shale due to the use of NPs (Sensoy et al 2009).

Nevertheless, most of the NPs are inorganic materials that mean nonsoluble, nonbiodegradable, and express negative effects on human health. In this situation, the need for clean, renewable, recyclable, cheap, biodegradable, and environmentally friendly NPs as additives in WDFs is essential to denigrate the environmental hazard, health risk as well as lower the cost.

Cellulose nanocrystals (CNCs) called also nanocellulose as nanostructured have been found convenient to cover all needed characteristics by the fact of being versatile, low toxic, and carbon neutral. CNCs are the future materials that found many applications in diverse fields (Kangas 2013). It is the most abundant in the world (about 90 billion tons of production per year), a safe and more sustainable alternative to plastic in the coming generation (2041) (Malmsheimer et al 2008). Moreover, the tensile strengths of nanocellulose are below 10 MPa whereas the tensile modulus is about 220 GPa. His lightweight gives it a strong promise to be used as reinforcements in polymer matrix composites including a high surface area to volume ratio and engineered surface chemistries (Moon et al. 2011, 2013; Hamad 2006; and Lee & Deng 2011).

In this project, we will investigate the behavior of CNCs in BT-WDFs compared with that of CNCs in ATT-WDFs and CNCs in SEP-WDFs under the effect of CNCs concentration, temperature changes, and salt content. This study will investigate the behavior of CNCs incorporated into three different based-clays BT, ATT and SEP-WDFs in the perspective of improving their rheological and filtration properties. While CNCs are used as a rheological modifier and fluid loss reducer. Therefore, the assessment of the rate of penetration performed by using CNC/BT, ATT and SEP/WDFs to drill different rock samples at different CNC concentrations is carrying on.

1.2. RESEARCH QUESTIONS

- How does the addition of CNCs in water-bentonite, water-attapulgite and water-sepiolite suspensions improve the fluid loss properties and viscosity of the drilling mud?
- Which of these three CNC/BT-WDF, CNC/ATT-WDFs and CNC/SEP-WDFs show more stability under HPHT conditions?
- How do the CNCs affect the lowering of the fluid loss?
- What is the contribution of CNCs as an additive in terms of thermal stability of CNC/BT-WDF, CNC/ATT-WDFs and CNC/SEP-WDFs?
- What is the impact of the addition of CNCs into water-bentonite, water-attapulgite and water sepiolite suspensions on the penetration rate during the drilling operation?

1.3. RESEARCH AIM AND OBJECTIVES

This project aims to investigate the effect of nanocellulose on the drilling fluid behavior and compare its effect on bentonite, attapulgite and sepiolite. Of course, to meet the aims of this project, the below objectives will be investigated:

- Investigate the effect of concentration of CNC on the rheological and filtration properties of CNC/BT-WDFs, CNC/ATT-WDFs, and CNC/SEP-WDFs;
- Investigate the effect of temperature and pressure on the fluid loss behavior of CNC/BT-WDFs compared to CNC/ATT-WDFs and CNC/SEP-WDFs at different CNC concentrations;
- Investigate the penetration rate of some rock samples drilled with CNC/BT-WDFs, CNC/ATT-WDFs and CNC/SEP-WDFs in rotary drilling;
- Investigate the fluid stability of CNC/BT-WDFs compared to CNC/ATT-WDFs, and CNC/SEP-WDFs through aging at different temperatures.

1.4. THESIS CONTENTS

This research focuses on the effect of the nanocellulose concentrations and temperature effect on Bentonite, Attapulgite and Sepiolite water-based drilling fluids in fresh-water and sea-water on their rheological and filtration properties. The effect of temperature and pressure on the fluid loss behavior of CNC/BT-WDFs, CNC/ATT-WDFs, and CNC/SEP-WDFs has been investigated. Besides, the fluid stabilities of the CNC/BT-WDFs, CNC/ATT-WDFs and CNC/SEP-WDFs were also studied and compared.

The research report is set out in eight chapters. Chapter 1 sets out the introduction and the scope of the research. Chapter 2 summarize the drilling fluid technology and design. Chapters 3 introductions of the experimental and analytical techniques by describing the sample preparation and experiment procedure for laboratory testing. Chapter 4-6 investigate the effect of CNC concentrations, temperatures, and pressure on the rheological and filtration properties of CNC/BT-WDFs, CNC/ATT-WDFs, and CNC/SEP-WDFs. Chapter 7 compares different drilling fluids based on their fluid loss, aging time and rate of penetration. Chapter 8 outlines the main findings by concluding the research results and recommendations for future studies.

CHAPTER 2. DRILLING FLUID TECHNOLOGY AND DESIGN

2.1. MATERIALS USED AS DRILLING FLUIDS

2.1.1. BENTONITE

Bentonite (BT) is used in the drilling operation of wells. As Clay, BT participates in the formulation of oil and water well drilling due to its rheological and thixotropic properties. Its main function is to seal the borehole walls, lubricate the drilling bit and string, and remove drilling cuttings, cooling and cleaning the drill and stabilizing the borehole. The structure of BT is depicted in the following figure 1 (Anderson et al 2010):

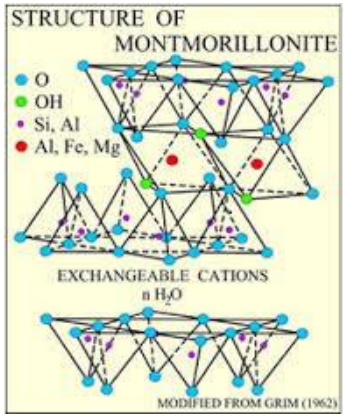

Figure 1. Crystalline structure of sodium montmorillonite with interlamellar water layer.

BT is a natural material made up predominantly of the clay mineral montmorillonite that belongs to the class of phyllosilicates named smectites. BT has a high water adsorption capacity resulting in its swell and expansion. The type of exchangeable ions contained in BT impacts its level of hydration and swelling. For sodium BT, the swelling is due to sodium cation that allows water adsorption at platelets surface level whereas calcium BT does not allow water adsorption to penetrate through the platelets. In this case, the platelets flake off instead of swelling. The dispersion of BT in water establishes a highly stable colloidal suspension which is formed with high viscosity and thixotropy. When BT adsorbs water suspensions are formed which means the hydrogen bridge bonds formed between hydrogen atoms coming from water molecules penetrating at platelet surface level and repel them apart. On the other hand, these platelets become free when mechanical stress is applied. In this condition, the viscosity of BT is lower than at rest which conducts to the process of thixotropy. These properties of BT colloidal suspension are very important and used in drilling slurries.

Once BT is hydrated, it does have the ability to expand to ten times its volume. It becomes very viscous then acts as a lubricant. So its viscosity could be controlled either by adding water or more BT to make it thin or thicker. This renders the BT very useful as a material in the process of mud rotary borehole drilling. The dispersion of sodium BT in water results in an increased viscosity and yield point of the drilling fluid. This increase of viscosity allows the drilling fluid to carry drill cuttings and raise them to the surface where they are easily removed (Alexander et al 1984).

Most drilling muds use BT for viscosity and fluid loss control. The solids build up in the drilling mud is the main problem that makes the viscosity difficult to be controlled therefore the use of BT becomes difficult. Furthermore, variable proportions of polymers contained in many so-called "BT clays" make the viscosity unpredictable.

The addition of BT to freshwater: i) increases the hole cleaning properties, ii) builds a thin filter cake of low permeability, iii) reduces fluid loss into porous formation, iv) promotes the stability of hole in poorly cemented formations, v) increases mud viscosity and lastly overtakes loss circulation. The use of high clay content, on the one hand, abridged the penetration rate and on the other hand, allows the sticking due to differential pressure leading to excessive torque and drag. BT-based drilling fluids have the limitation of flocculation and instability at high temperature and pressure conditions. Because of high water absorption capability and swelling characteristics, the dispersion behavior of BT is non-uniform and has a huge problem of flocculation, which results in insufficient and inconsistent rheology of drilling fluids (Emilio & Singer 2011).

2.1.1.1 BEHAVIOR OF BENTONITE USED AT HPHT CONDITIONS

Hiller (1963) studied the rheological behavior of 4% mass dispersions of Wyoming bentonite. These dispersions of Wyoming bentonite converted to sodium bentonite in the presence of electrolytes. He established that at low electrolytes, the increase of the temperature (up to 176°C) decreased both plastic viscosity and yield stress. Meanwhile, with pressure (up to 550 bar), both plastic viscosity and yield stress increased slightly. However, at high electrolyte concentration, Hiller observed an increase in yield stress and a decrease in plastic viscosity with increasing temperature.

Annis (1967) studied the dispersions of sodium bentonite prepared in water which became more shear-thinning as temperature increased to 150°C, giving higher yield values but lower plastic viscosities. He observed that the decrease in plastic viscosity was similar to the decrease of water viscosity with temperature, thus concluded that higher temperatures essentially affected only the yield stress values.

Alderman et al (1988) studied the rheological properties of sodium-bentonite, with 85% montmorillonite and with a Na^{+}/Ca^{++} ratio of 1.71, in neat form and with additives. They found a continuous decrease of high-shear viscosity with increasing temperature, in a similar way to the decrease of water viscosity with temperature. The yield stress increased exponentially with the temperature only after a characteristic temperature. However, they showed that the effect of pressure on the rheology of water-based drilling fluids is minimal.

Gray & Darley (1988) found that the rheological properties of water-bentonite dispersions could be influenced by the temperature in several ways: (i) physically, the viscosity of the liquid phase decreases with increasing temperature, (ii) chemically, at temperatures above 90 °C, all hydroxides react with clay minerals; at low alkalinity, no significant effect on the rheological properties, but at high alkalinity, the effect may be severe and (iii) electrochemically, the increase of the temperature increases both the ionic activity of any electrolyte and the solubility of any partially present soluble salts in the dispersion. The resulting changes in ionic and base-exchange equilibria modify the balance between interparticle attractive and repulsive forces thus greatly affecting the degree of aggregation (flocculation) or dispersion of the bentonite particles in the water medium.

Briscoe et al (1994) found that for 7 to 10% mass water- sodium-based bentonite dispersions, the rise of temperature increased significantly the yield stress whereas the plastic viscosity decreased significantly at temperatures up to 140°C but no significant change with pressure (up to 1400 bar).

Rossi et al (1999) studied the temperature and pressure effect on the rheological property of sodium montmorillonite dispersions containing different electrolytes. They stated that the temperature rise increased the yield stress owing to thermal-induced swelling.

Santoyo et al (2001) described the rheological property of four different types of bentonites water-based drilling fluids utilized in geothermal drilling. They noted a slight decrease of apparent viscosity up to temperatures between 80°C to 120°C and a sweeping increase from 125°C to 175°C.

Jung et al (2011) studied the rheological and filtration properties of iron oxide nanoparticles as additives into bentonite water-based. The experiment took place at ambient and harsh conditions (high temperature and high pressure ranging from 25°C to 200°C under 100 bar atmosphere). The outcomes of their experiments showed that an increase of iron oxide particle content into bentonite suspension resulted in increasing viscosity, yield stress, and strength of particle interaction obtained through probed flow stress. However, concerning the concentration of iron oxide particle in suspension, the addition of smaller size nanoparticles (5 wt. % bentonite with 5 wt. % 3 nm-size iron oxide particle) was found enough to improve the viscosity of the fluid system. Therefore, the viscosity increase due to the variation of the temperature was observed in all sample fluids of different sizes but was more pronounced as the iron oxide particles size decreased.

Lin et al (2016) studied the rheological property of commercial kaolinite and bentonite water dispersions, at 3°C (close to seabed temperature) and 25°C and found that the yield stress of these dispersions increased with increasing temperature.

Vryzas et al (2017) studied the effect of temperature on the rheological properties of 7% mass bentonite dispersions. They found that at low shear rates, the shear stress increased significantly with the increasing temperature between 25 and 80°Cat atmospheric pressure, with almost doubling of the shear stress values at the lowest shear rate measured. However, at high shear rates, it showed a reduction of the temperature effect that leading almost to similar shear stresses values. A linear increase in the yield stress with temperature as well was observed. They depicted an exponential decrease of the flow consistency index by a factor of almost five. However, about 20% of the increase of the flow behavior index tended towards the Newtonian value.

Mohammed (2017) studied the effect of temperature on the rheology and weight loss of 6 % mass bentonite dispersion modified with iron oxide nanoparticle (nanoFe_2O_3). The nanoFe_2O_3 content varied between 0 and 1wt % as the temperature changed from 25°C to 85°C. The results showed that 1wt % of nanoFe_2O_3 increased the rheological properties of the drilling mud. This modification increased the yield stress and plastic viscosity by 45–200% and 20–105% respectively based on the bentonite content and temperature of the drilling mud. The hyperbolic model quantified the shear-thinning behavior of the bentonite drilling fluids with and without nanoFe_2O_3 and compared it with three parameters Herschel-Bulkley model. Thus the hyperbolic model fitted very well the shear-thinning relationship between the shear stress and shear rate of the nanoFe_2O_3 modified bentonite drilling fluids.

Elochukwu & Sia (2019) investigated the filtration properties of polystyrene nanoparticle additives to water-based drilling fluid. The polystyrene nanoparticle additives a new nanoparticle that is nonconductive and less expensive. Polystyrene nanoparticle added to water-based drilling fluid design and tested for filtration loss at Low-Pressure Low Temperature (LPLT) condition (25°C and 100 psi) and High-Pressure High Temperature (HPHT) condition (150°C and differential pressure of 500 psi). The result showed that only the water-based drilling fluid constituted of active

additives such as anionic cellulose (PAC), Nano polystyrene, methyl ester sulphonate (MES) including bentonite water-based drilling fluid showed the best reduction in filtrate volume reduction, non-erodible filter cake and very low permeability. It can be concluded, that this synergy of Nano polystyrene and methyl ester sulphonate surfactant improved filtrate loss control of water-based drilling fluid.

2.1.2. ATTAPULGITE

Naturally, Attapulgite (ATT) clay is presented as a fibrillary mineral and it is a hydrated magnesium aluminum silicate. Generally, it contains three different kinds of water at room temperature: adsorption water on the mineral surface by physical effect; zeolitic water weakly bound in the micro-channel; and crystalline water tightly bound water molecules completing the coordination of the (Mg, Al) cations at the borders of each octahedral layer (structural water). Many structural hydroxyl groups are found on it such as Al-OH and Mg-OH. Moreover, some isomorphic substitutions in the tetrahedral layer, such as Al^{3+} for Si^{4+}, develop negatively charged adsorption sites to electro-statically adsorb cation ions.

Because of the special structure of attapulgite that contains much micro-channel and permanent negative charge surface that can be modified by organic matter to enhance the contaminant retention, to adsorb and to retard contaminant migration on its surface or in its micro-channel (Fan et al 2007).

The general physical properties of the ATT clay are distinctly different from those of BT or SEP clays. ATT is more sensitive to flocculation and is much more easily dispersed following coagulation. It does not form gels at such low concentrations as montmorillonite clay although at higher concentrations it will form a relatively stable gel in both distilled and saltwater (Kerr 1937).

The utilization of ATT by the industry as a distinct clay mineral has been for a long time because of its chemical composition and some properties depicted similar to montmorillonite. It has been found that its unusual properties derive qualitatively from its particular structure respectively its needle-like particle sharp and size (Preisinger 1963).

ATT consists of a long double chain of silica that is parallel to the fiber axis joined by magnesium and aluminum in octahedral coordination to yield strips like three-layer minerals which are linked to Si-O-Si bonds at the corners and around 3.7 by 6.0 Å free channel in cross-section running the length of the needle. ATT is composed of magnesium (Mg), aluminum (Al), silicate (Si) forming elongated crystals (needle-shaped) with an open-channel structure for the sake of some substitution happening between magnesium and aluminum by iron (Fe), and other elements. Its particular molecular formula is $(Mg, Al, Fe)_5Si_8O_{20}(OH_2)_4 \bullet 4H_2O$ and its molecular structure is given in figure 2 below. Besides, Murray (1999) showed that the elongate particles, when mixed with any liquid, are subjected to cause higher viscosity.

From the structure of ATT, two unusual characteristics have been denoted: no montmorillonite-type swelling can occur due to its three-dimensional structure and from the cleavage of Si-O-Si bonds holding together the three-layer strips derive the needle-like rather than plate-like particle shape. Its length is about 1 µm and width of about 0.01 µm. For more than 40 years Pal had been used by industry before it was recognized as a distinct clay mineral. It derives its nonswelling needle-like morphology from its three-dimensional crystal structure as seen in figure 2 below (Asghari & Esmaeilzadeh 2014). The shape and size of the needles result in unique colloidal properties, especially resistance to high concentrations of electrolytes, give high surface area and

high porosity particles when thermally activated. Pal is currently used in drilling fluids as a viscosifier to improve drilling fluid's ability to remove cuttings from the wellbore and to keep the cuttings and weighing materials dispersed during periods of no circulation (Abdo & Haneef 2013).

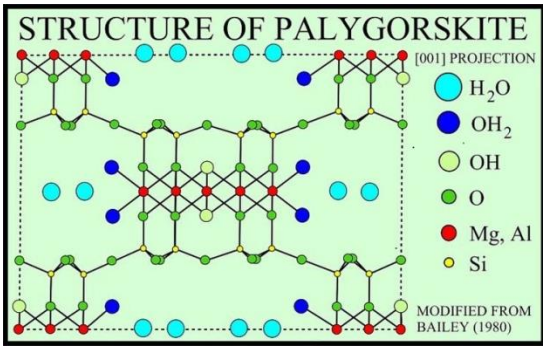

Figure 2. Molecular structure of attapulgite.

ATT is obtained naturally from mined clay. As SEP, ATT provides low-shear-rate viscosity when used in saltwater mud to lift cuttings to the surface. ATT clay cannot control the filtration properties of the drilling mud. ATT clay does not improve the filter cake once used as an oil-mud additive. However, it can only provide gel structure. Therefore, ATT clay can offer good colloidal properties such as high absorbing and decoloring capabilities, salt and alkali resistance, including a specific feature in dispersion, high-temperature endurance. Hence, it is suitable for many commercial applications (Abdo & Haneef 2013). Furthermore, ATT shows plastic and an adhesive property once wet and has a strong ability to absorb water molecular and hence it is suitable for use in drilling fluids (Bergaya & Lagaly 2006).

Recently, it has been found that ATT was used in drilling fluid as a viscosifier. To improve the ability of the mud system to remove cuttings from the wellbore. During the period of no circulation, to keep the cuttings and weighing materials dispersed in the fluid.

The colloidal properties of ATT become effective when the particles are separated into individual needles by mechanical action and the attractive forces linking the needles in a particle remain much appreciable. No swelling action is taken among the three-dimensional structure of ATT however BT shows swelling caused by penetration of water between the unit layers (Haden 1963). The dispersion becomes effective under shear when free movement is observed among individual needles or at least small bundles. In water, such a dispersion provides thixotropy and apparent viscosity under low shear. However, at high shear, nearly water-thin is obtained. Once high shear is removed, the high viscosity recovery is directly observed in pure water and a definite yield point at rest as well (Abdo & Haneef 2013).

Abdo (2014) showed that ATT can be used in drilling fluid to replace regular additives. ATT was purified, dispersed, and broken down to nano-size. During the sonication process, ATT is dispersed in ethanol as a chemical shield to protect it against flocculation. The yielded nano-attapulgites (NATT) remain dispersed without flocculation and settling to the bottom and with particle size diameter as small as 10 nm. NATT used as a drilling fluid additive in drilling fluids provides stable rheology. This confirms the test made for NATT-modified drilling fluids in HPHT environment showing great rheological stability at high temperature and pressure. The special nanorod structure

and large specific surface area can provide Pal with many unique physical and chemical properties. Therefore, Pal shows great interest to be used as an efficient and stable rheology modifier for drilling fluids (Abdo & Haneef 2013). However, because of its stability at high temperature and pressure conditions (HTHP), ATT is used as a thixotropic gelling viscosity builder and suspending agent in drilling fluids along with brines and electrolytes (Abdo & Haneef 2013).

Attapulgite suspending agent was designed for saltwater applications. In saltwater, the attapulgite suspending agent swells to approximately 10 times its original volume. It is used for increasing slurry volume and decreasing slurry weight. It is effective at temperatures up to 500°F (260°C). Typical attapulgite suspending agent concentrations are 2 to 10%. Attapulgite suspending agent has a shelf-life of up to 24 months and is not classified as hazardous waste by the Environmental Protection Agency (EPA) (www.halliburton.com H02085 08/07 © 2007 Halliburton).

2.1.3. SEPIOLITE

Sepiolite (SEP) as a natural magnesium silicate clay forms needle-like particles. The suspension of Sepiolite in water leads to the formation of a random network responsible for the viscosifying effect due to the nonswelling needle aggregation and association. This viscosifying effect is favored at low pH value or alkaline pH through the addition of electrolytes which lead to the reduction of the negative charge of the silanol surface groups allowing the individual particles to aggregate along their surfaces, thereby increasing the viscosity of the suspension (Echt & Plank 2019).

SEP is a hydrated magnesium silicate with a fibrous texture having an ideal formula of $Si_{12}Mg_8O_{30}(OH)_4(OH_2)_4.8H_2O$. SEP is non-swelling, porous, lightweight clay with a large range specific surface area of about 300 m^2/g. It has been revealed that SEP clays manifest a temperature resistance up to 260°C with low filtration properties (Carney & Meyer 1976; Carney et al 1980; Serpen et al 1992; Serpen 1999). However, Bourgogne et al (1991) reported that SEP remained stable at temperature up to 425°C (800 F). The SEP structure is depicted in the following figure 3 (Altun et al 2010):

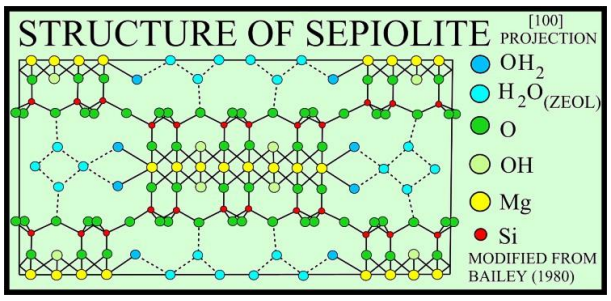

Figure 3. Basic Structure of SEP Clay.

Many of its properties make it a valuable material for a very large range of applications. Besides its high surface area, SEP has high porosity; an unusual particle shape says needle-like morphology, an outstanding sorption capacity and colloidal properties with an average length of 1

μm to 2 μm, a width of 0.01 μm containing various open channels and tunnels. SEP provides thixotropy, pseudo-plasticity, stability and rheological behavior.

SEP has found many industrial applications because it is not easily flocculated due to its elongate shape which makes it useful as a viscosifier and suspending agent (Clarke 1989; Bish & Guthrie 1993; and Heivilin & Murray 1994). The important use of SEP in drilling fluids is based on its viscosity and gel strength that is not affected by salinity variations and high temperature met at deep and geothermal wells. The clay mineral SEP remains stable at HPHT conditions and in the presence of salt (Murray 1986; Clarke 1989).

Regardless the high temperature and/or high salinity, SEP suspensions are still providing better rheological behaviors and remain insensitive. One of its important disadvantages is about having a very high API water loss. Hence, it is necessary that its rheological and filtration properties be controlled during drilling operations. The expectation of having zero water loss in harsh conditions should be achieved by means of additives (Altun et al 2014).

The studies of Altun et al (2010, 2014, 2015) proved that different additives used at high temperature and high pressure are capable to control the amount of water loss and rates in SEP-based drilling fluids below 20 ml at 200°C. Carney's work (Carney & Meyer 1976) denoted the capability of a drilling fluid to withstand temperatures in the ultra-high range. This was demonstrated through a study on the rheology of SEP slurries subjected to temperature up to 800°C including other additives resulting by improving rheological and fluid loss properties over wide temperature ranges.

In general, SEP clay depicts a great resistance to high temperature and saline environment. In these studies, SEP based muds having good rheological properties have been used for hostile drilling environments since late 1970.

2.1.4. DISCUSSION

As the payzone depth increases, the drilling mud rheology changes drastically due to high pressure, temperature, contamination and shear degradation. The WBM has inorganic bentonite clay dissolved in it or acquired while drilling through clay formation. This inorganic particle causes thermal instability resulting in clay complex decomposition (Shah et al 2010).

Both mineral dissolution and ion exchange reaction can favor the chemical modification of bentonite then lead to the alteration of chemical and physical properties of the clay barrier or host rock permeability (Berkowitz 2002; Savage et al 2002).

During the drilling operation, once the drilling stops, the drilling mud may stay static for a long time while it is exposed to a high temperature then a strong gel may develop which causes excessive pressure drop when flowing and does not form good filter cakes. Therefore, water-bentonite suspensions should be treated with various materials, to enable them to resist these high temperatures (Clark 1994).

The improvement of bentonite suspensions stability at high temperatures may be done either by modifying the bentonite surface charge or by introducing a steric barrier against agglomeration using various additives which may be either modified or non-modified, natural products like lignosulfonate complexes with various metals, tannins, humic acid, lignite and modified lignite, synthetic polymer products, mono- or poly-acrylic acid (Rabaioli et al 1993; Giovanni et al 1995).

Water bentonite suspensions showed exceptional rheological and filtration properties at low temperatures which deteriorate at temperatures higher than 120°C. The addition of additives can restore these properties. However, the thermal instability affects many of them at the temperatures encountered, for example in oil-well and geothermal drilling. The flocculation of water-bentonite suspension at high temperatures showed a great challenge for the use of BT clay. The flocculation phenomenon increases the drilling cost and affects the drilling process very unfavorably. Therefore, the use of 3 wt. % of Greek lignite into water-bentonite suspension improved significantly the filtration properties at temperatures up to 177°C with a drastic reduction in the permeability of filter cakes derived after thermal aging of the suspension (kelessidis et al 2007).

Cho et al 2000; Jacinto et al 2007; Zihms et al 2015 found that at temperatures below 100°C, the sealing performance of BT clays is not significantly affected. However, above this temperature, illitisation and mechanical degradation of BT clay could lead to a performance reduction (Zheng et al 2015).

The brine intrusion encountered during drilling operation constitutes another worse case situation related to the flocculation phenomenon. The harsh conditions of high temperature combined with salt contamination conduct consequently disrupt the achievement of getting acceptable rheological and filtration properties for the use of fresh-water BT mud.

Drilling operations process in harsh conditions of high temperature and high pressure including high electrolyte influx (salt contamination) constitute a great obstacle for the use of bentonite clay-based water mud. However, the hydration ability of commercial BT is greatly affected by the salinity of the water, the mud system should necessarily be renewed. As these minerals have a fibrous structure with low surface energy, their low reactivity in the presence of salt contaminants and their high stability in high temperature can result in good rheological and fluid loss properties to sort out bentonite clay limitation in the drilling operation. The ATT or SEP suspension viscosity is owing to the effect of the shear forces leading to the formation of gel structure and the attractive forces established between particles that had been created by broken-bond charges on the edges of broken fibers through shearing force effects. Most results based on the filtration control properties of ATT or SEP present inferior values due to the fibrous structure (Al-marhoun, 2015).

Therefore, ATT clay mineral may be used at the place of commercial BT. Nevertheless, the intervention of the ATT has been found inadequate in terms of performance as based drilling muds at the high-temperature environment and remains the subject of research for a new substitute. Consequently, SEP clay has been found capable of taking the ATT position because it has great resistance to both high temperature and high saline concentration conditions. Thus, the intervention of ATT or SEP clays minerals including CNC particles as additives to replace bentonite could be the key to solving problems in the deep well.

2.2. ASSESSMENT OF DRILLING FLUID ADDITIVE ON THE DRILLING OF THE ROCK SAMPLES

2.2.1. RATE OF PENETRATION

Bourgoyne et al. (1984) observed that once the ROP or the drilling efficiency is influenced, the hydraulic factors affect the drilling rate. However, several laboratory studies confirm the effect of the drilling fluid upon the drilling rate.

Rabia (1985) reported that the drilling capability of the state-of-the-art drilling equipment alone could not ensure the drilling success at a fast rate and getting a rapid rate of penetration. This rapid ROP depends on other things on the type and weight of drilling fluid used.

In 1996, two researchers named Reddish and Yasar performed rotary drilling tests in the laboratory using a modified industrial rotary hammer drill with a 10 mm masonry bit sharpened to 118 degrees. The larger blocks of material used drill stand and a hand-held model. The same basic operating mode and drill bit geometry were applied for all tests. They obtained an index called 'stall penetration rate' from the graphs of penetration rate versus specific energy. They found out that the stall penetration rates were strongly correlated with the modulus ratio values (Kahraman 2003).

Therefore, Bilgesu et al (1997) showed that during drilling activity a fast ROP remained the target. Once it is achieved, it can mitigate the cost of the drilling well. Hence, modern drilling practices necessitate identifying operations that can make drilling cost reduction possible.

Robinson & Morgan (2010) including Becker et al 1991 reveal that the rate of penetration (ROP) was strongly impacted by the capacity of the drilling mud to remove drilling cuttings from the borehole. More energy consumption occurred once the settled cuttings have to be ground at the bottom. However, they could be removed more effectively from the borehole only once supportive yield stress was reached. The more energy is conserved by no grinding the settled cuttings at the bottom of the well, the higher the ROP is improved. The drilling mud should manifest a shear thinning behavior to improve a proper cleaning of the borehole meaning it should have considerable viscosity at the low shear rate and yield point to suspend the drilling cuttings once the circulation is cut off. However, many drilling muds demonstrate strong thermal thinning that means they could not keep their suspending properties under downhole conditions while temperature kept on increasing resulting in the reduction of the ROP due to the low shear rate viscosity and failed to remove properly the drill solids from the bottom borehole of the well.

Akpabio et al (2015) found out that the most deciding factor that enhanced the ROP was the low mud density which is done by keeping other parameters of the fluid constant. They observed that the ROP remained relatively constant by maintaining uniform mud density as drilling progressed.

The weight on the bit and rotary speed as mechanical factors are then linearly related to the drilling rate providing the hydraulic factors are in proper balance to ensure proper cleaning of the hole. It has been found that the hydrostatic pressure (HP) was controlled by the mud weight in a wellbore. This mud weight was able to prevent the influx of fluid into the well, the casing to collapse and the open hole. On the other hand, the excessive mud weight will cause the weight of the drilling mud to go higher above the pressure gradient of the formation, which in turn, impacts the ROP. However, it has been observed that the effect of the rheological properties of the drilling fluids as for the viscosity, yield point, and gel strength upon the ROP was less than that of the mud density. It is convenient for the drilling fluid to have low solids content so that it could move with great velocity. This leads to fast removal of cuttings within a short time resulting in a fast ROP (Juhari & Isham 1998).

Drilling operation consists of establishing a complete production conduit to form a hole between the reservoir and the surface. As drilling remains an important part of the oil industry, the rate of penetration (ROP) must be increased to ascertain rapid completion of the drilling operation. It is very important to identify and understand the factors that affect the ROP such as weight on bit, formation characteristics, circulating system hydraulics, drill bit type, drilling fluid type, and

properties (Simmons 1986). During drilling activities, drilling fluid plays an important role such as minimizing fluid loss, extend bits life, and control well pressure, etc. Drilling mud must keep hydrostatic pressure higher than formation pressure to avoid back pressure which may lead to a blowout (Black et al. 1985 and Ismail 1999). Mud density has been identified for a long time as one of the factors that affect the ROP. Mud density of drilling fluid can control hydrostatic pressure into the well, prevent both the influx of formation fluid into the well and also the open hole and the collapse of the casing. The challenge occurs when an excessive mud density is applied at the bottom of the wellbore. The PR is affected as the density of the drilling mud goes higher above the pressure gradient of the formation. The increase in the density of drilling mud affects the rate of penetration. The target in every drilling operation is to get a higher penetration rate (PR), once if achieved the choice of good mud density remains a challenge during drilling operations (Akgun 2002a, 2002b).

It has been found that when the plastic viscosity, solid content, and mud density increase, the penetration rate decreases (Paiaman et al 2009). However, the penetration rate is significantly increased by the appropriate choice of mud density which must be as low as possible and more constant while other parameters of the fluid system are kept constant e.g. water-based mud density of 8.9 ppg and oil-based mud weight of 8.6 ppg (Scholar 2015). Kahraman (2003) investigated the performance analysis of drilling machines using the rock modulus ratio. He concluded that the penetration rates of rotary and diamond drills exhibited a strong correlation with modulus ratio through the uniaxial compressive strength as rock property whereas only significant correlations were exhibited between the penetration rates of percussive drills with the modulus ratio.

Drilling a well as part of oil and gas activities is complex to carry out. Many encountered parameters have to be satisfied through a good selected drilling fluid that offers a fast penetration rate to ensure speedy completion of the drilling operation. The drilling rate analysis is rigorously complicated by the difficulty of completely isolating the variable under study as long as factors affecting the rate of penetration (ROP) are exceedingly numerous to be counted: a) drilling fluid properties e.g. viscosity, solid content, mud weight, and filtrate loss; b) mechanical factors e.g. bit type, rotary speed and weight on the bit; c) rig efficiency; d) hydraulic factors e.g. bottom-hole-cleaning, jet velocity; e) personal efficiency; and f) formation characteristics e.g. state of underground formations stress, strength, elasticity, hardness and/or abrasiveness, fluid content and interstitial pressure, stickiness or balling tendency, porosity and permeability.

In the oil and gas industry, the rate of penetration (ROP), also known as penetration rate (PR) corresponds to the speed at which a drill bit breaks the rock under it to excavate the borehole. This speed is usually reported in units of feet per hour or meters per hour. The ROP is mostly affected by the following important variables: drilling fluid properties, formation characteristic, bit type, bit operating conditions means bit weight and rotary speed, bit tooth wear, and bit hydraulics (Bourgoyne et al 1986).

2.2.2. DRILLING FLUID PROPERTIES

It has been reported that the drilling fluid properties that affected the ROP include rheological and filtration properties, solid content and size distribution, density, and chemical composition. It is observed that once the viscosity, solids content, and fluid density of the drilling fluids increase, the penetration rate tends to decrease. However, the increase in the filtration rate leads to an increase in the penetration rate. Therefore, the pressure differential across the zone of crushed rock beneath the bit can be controlled by the density, solids content, and filtration characteristics of the

drilling fluid. The parasitic frictional losses in the drill string and, thus, the hydraulic energy available at the bit jets for cleaning is controlled by the fluid viscosity controls. The mud properties with significant impact on hole cleaning are the mud density and viscosity. The mud properties contribute significantly to the prevention of formation-fluid intrusion into the wellbore. On the other hand, the mud density functions as mechanical stabilization of the wellbore. Increasing the mud density beyond the required value is detrimental to ROP, and may generate induced losses by fracturing the formation under the in-situ stress condition. This may lead to an increase in bottom hole pressure beneath the bit causing a chip hold-down effect. Thus, increasing the mud density will cause a decrease in ROP. The increase of the viscosity in drilling fluids tends to decrease ROP. During drilling operation, the higher viscosity mud leads to settling down cuttings on the bottom of the hole that causes their re-drilling and poor performance of the bit. This affects the hydraulic energy available at the bit nozzles for cleaning due to parasitic frictional losses in the drill string.

It has been approved experimentally that the increase of the drilling fluid leads to the reduction of the penetration rate whatsoever the cleanness of the bit. Thus, the penetration rate, hydration rate, and bit balling tendency of some clays are affected by the chemical composition of the drilling fluid. The penetration rate for the rolling cutter bit decrease with increasing fluid density. This increase in mud density contributes to the increase of the bottom hole pressure beneath the bit and, thus increasing the pressure differential between the borehole pressure and the formation fluid pressure (Bourgoyne et al 1986).

2.2.3. FORMATION CHARACTERISTICS

The most important formation properties affecting the penetration rate are the elastic limit and ultimate strength of the formation. It is mentioned that the crater volume produced beneath a single tooth is inversely proportional to both the compressive strength of the rock and the shear strength of the rock. The penetration rate is significantly affected by the formation permeability. The penetration rate is also affected by the mineral composition of the rock.

2.2.4. BIT TYPE

The selection of drill bit is based generally on past bit performance records. However, the key factors in selecting the right bit for the right hole interval to be drilled are based on their experience and learning. The selection also depends on the type of formation to be drilled with a significant effect on ROP. Drill bits selected have a significant effect on penetration rate. They are classified into two categories named roller cone and drag as showed in figure 11 below. However, the roller cones bits are grouped into two types include milled-tooth and insert. They are used to drill rocks of various types and strengths. The former is used when tooth wear is not a critical issue, the latter with tungsten carbide inserts are used when tooth wear comes to be the limiting factor in the life of the bit. The roller cone bits make use of a shoveling (gouging) action in soft formations and of a crushing (chiseling) action in hard formations to accomplish the rock-cutting mechanisms. The polycrystalline diamond cutters (PDCs) and diamond matrix bodies constitute the drag bits. The rock-cutting mechanisms and a lack of bearings constitute the main differences from the roller cone bits. The rock shearing and the rock grinding are respectively cutting mechanisms for the PDC bit and diamond matrix. During the drilling process in extremely hard abrasive formations, mostly the diamond matrix bits are used while in all nonabrasive regardless of strength, PDC bits are used (Azar 2004). For Hossain and Al-Majed, the matrix is desirable as a bit material, because its hardness is resistant to abrasion and erosion. It can withstand relatively high compressive loads.

However, compared with steel, has low resistance to impact loading. PDC bits are generally used for drilling soft but firm, and medium-hard, nonabrasive formations that are not sticky. The choice of bit, therefore, has a significant impact on ROP (Hossain & Al-Majed 2015; Adeniran et al 2018).

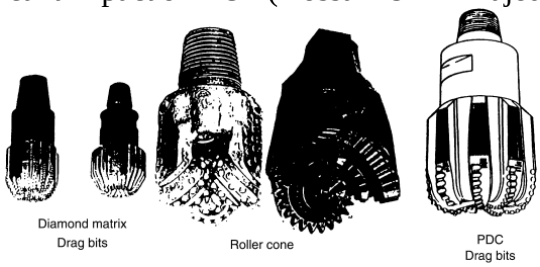

Figure 4. Various types of drill bits.

2.2.5. WOB AND ROTATY SPEED

In order to successfully break the rock, an amount of force should be added to the drill bit. Weight on the Bit, or WOB, is the amount of downward force exerted on the drill bit provided by thick-walled tubular pieces in the drilling assembly that are known as drill collars. The downward force of gravity on these steel tubes provide force for the drill bit in order to effectively break the rock. Figure 5 depicts the experimental plot of the variation of penetration rate with bit weight as all other drilling variables are held constant. In this figure 5, point (a) shows that no significant penetration rate is observed until the threshold bit weight is applied. At segment (a-b), the penetration rate increased with increasing bit weight values. At segment (b-c), it is showed that a higher increase in ROP is observed with increasing weight on bit. However, at segment (c-d), subsequent increase in the weight of bit lead to just a slight improvements in the ROP. Segment (d-e) showed a decrease in the ROP at extremely high values of bit weight. Such behavior is called bit floundering. This poor response of the ROP at high bit weight values usually is attributed to less efficient bottom hole cleaning at higher rates of cuttings generation or to a complete penetration of the cutting elements of the bit into the well bore bottom. At such bit weight values, wear on the bit is extremely high.

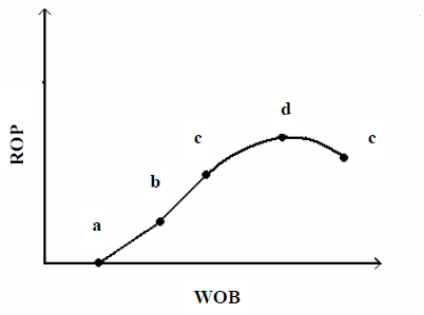

Figure 5. Typical response of penetration rate to increasing bit weight.

Figure 5 depicts the experimental plot of the variation of penetration rate with bit weight as all other drilling variables are held constant. A linear increased of the penetration rate versus rotary speed with all other variables maintained constant is depicted in figure 6 through segment (a-b), it is shown that the penetration rate increased linearly with increasing rotary speed. After a certain rotary speed values, it observed a deceleration in the increase of the ROP as the rotation speed

continued to increase in segment (b-c). Behind point (c), the ROP is slightly influenced by rotary speed as shown in the figure. This reduced impact of rotary speed at high values on the penetration rate rotation is attributed to less wellbore stability and his enlargement (Ahmed et al 2018).

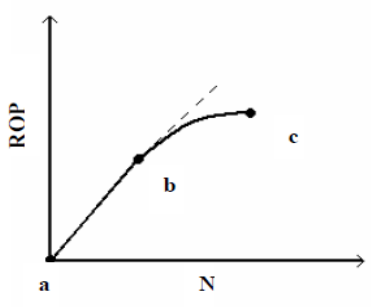

Figure 6. Typical response of penetration rate to increasing rotary speed.

2.2.6. BIT TOOTH WEAR

The common cause that leads most bits to drill slower as the drilling time elapses is tooth wear. It showed that the tooth length reduction of milled tooth rolling cutter bits is due to continuous abrasion. The tungsten carbide insert-type rolling cutter bits and PDC bits teeth fail by breaking rather than abrasion. Therefore, the breakage occurrence leads to the loss of the entire tooth. Mostly, the bit wears cause a reduction in the penetration rate. This bit wear usually is not as severe for insert bits as for milled tooth bits unless a large number of teeth break during the bit run.

2.2.7. BIT HYDRAULICS

The effect of bit hydraulics on ROP is described by commonly used objective functions, including Reynolds number, a bit of hydraulic horsepower, jet impact force, etc. A proper jetting action at the bit allows considerable improvements in penetration rate and promotes better cleaning of the bit face along with the hole bottom. Therefore, the best appropriate hydraulic's objective function selection to be used emerges certain doubt in characterizing the effect of hydraulics on penetration rate.

2.2.8. BOURGOYNE AND YOUNGS' RATE OF PENETRATION

Bourgoyne and Young's ROP model is the most popular to be used for calculating the ROP. The mathematical model presented in their model used a complex drilling model to capture the change effects in the various drilling parameters. In their correlation, eight variables included depth, formation compression, pressure difference at the bottom of well, bit diameter, WOB, bit rotation speed, bit wear, and bit hydraulic have been considered (Bourgoyne & Young 1974; Irawan et al 2012; and Ahmed et al 2018). Bourgoyne and Young have proposed the following equation to model the drilling process when using roller cone bits (Bourgoyne & Young 1974; Osgouei & Özbayoğlu 2007). The equation form is:

Equation 1. $$\frac{dD}{dt} = Exp(a_1 + \sum_{j-2}^{8} a_j x_i)$$

Where x_i stand for the set of dimensionless drilling parameters calculated from the actual collected drilling data, and a_j stand for the set of constants that relates with each of the drilling parameters considered. Dimensionless drilling parameters in this equation is described as following:

Formation Resistance:

Equation 2. $x_1 = 1$

Consolidation Effect:

Equation 3. $x_2 = 10{,}000 - TVD$

Overpressure Effects:

Equation 4. $x_3 = TVD^{0.69}(g_p - 9.0)$

Differential pressure:

Equation 5. $x_4 = TVD(g_p - \rho_c)$

Bit Diameter and WOB:

Equation 6. $x_5 = ln[\frac{{}^{WOB}/_{d_b} - [{}^{WOB}/_{d_b}]_t}{4.0 - [{}^{WOB}/_{d_b}]_t}]$

Rotary Speed:

Equation 7. $x_6 = ln[\frac{N}{100}]$

Tooth Wear:

Equation 8. $x_7 = -h$

Bit Hydraulic:

Equation 9. $x_8 = \frac{\rho g}{350\mu d_n}$

Seyed et al (2019) also develop a new model. The new model estimated the ROP in one of the Iranian oil fields by implementation genetic programming. The new model is related to 11 effective parameters reported in the drilling master log, sonic log, and constituted of weight on bit, bit rotational speed, mud weight, mud yield point, fluid loss, total nozzle area size, and sonic time. The statistical parameters include root-mean-square deviation (RMSD), squared correlation coefficient (R^2), and average absolute relative deviation (AARD), have been calculated to evaluate the proposed model. The developed model was declared accurate for estimating ROP and can provide beneficial information during drilling operations through real data verification. The values of squared correlation coefficient and root-mean-square deviation depicted the consistency of the model.

2.3. PAMETERS FOR DRILLING FLUID PROPERTIES

2.3.1. DRILLING TEMPERATURE AND PRESSURE

The establishment of wellbore temperature during drilling operation depends on many factors such as geothermal gradients, flow rate, wellbore depth, formation properties, and drilling fluid properties. The estimation of the drilling fluid temperature depends on the heat transfer assessment of the circulating fluid with the formation at the downhole. During the drilling operation, the downhole temperature impacts on the drilling mud viscosity and later on the drilling fluid density, the friction pressure losses, and the performance of drilling bits in hot wells.

The density of drilling mud under downhole conditions is a very important parameter to be known as long as it is not the same as that is measured at the surface. A significant difference has been found between those two densities in deep and hot wells. Its determination allows the computation of the actual hydrostatic pressure into the drilling well. The effect of pressure and temperature on the density of the formation fluid is crucial to be estimated because it will induce more accurate anticipation of differential pressure at the bottom-hole and abridge the fluid losses resulting from misestimating pressure differentials.

The control of the fluid density and viscosity by estimating the fluid temperature in both flow conduits (drill pipe or tubing and annulus) was conducted by Kabir et al (1996). On the other hand, the computation of the pressure drop for a number of operations was done by assuming a steady-state heat transfer in the wellbore. The result showed a limited sensitive study.

The major challenge is to design stable drilling fluid systems with optimal cooling and high thermal conductivity properties for drilling in deep wells under extreme downhole conditions or HPHT conditions. Furthermore, as drilling operations generate exuberant heat owing to friction between the drilling bit and the rock surface, the need for designing new drilling fluids with optimal heat transfer properties is of significant importance.

Excessive heating of equipment will lead to stern drilling problems which have a direct impact on the cost and efficiency of drilling operations. Consequently, the elaboration of new drilling fluids with excellent heat transfer potentiality is highly required.

Most efforts have been made by several researchers over the past years based on the investigation of the thermal properties of the drilling fluid systems containing different NPs. Generally speaking, they conclude that the achievement of enhanced thermal conductivity properties was made possible by the addition of NPs. The increase of thermal conductivity demonstrates the ability of the drilling fluid to a quick release of heat as moving up to the surface. Most of the nanoparticles were inorganic (Li et al 2010; Sedaghatzadeh & Khodadadi 2012; William et al 2014; Ho et al 2014; Fezelabdolabadi & Khodadadi 2015; Sabbaghi et al 2015; Halali et al 2016).

Fazelabdolabadi & Khodadadi (2015) analyzed the effect of carbon nanotubes (CNTs) presence on the performance of water/oil-based drilling fluids. Due to their hydrophobicity, CNTs cannot easily be dispersed in water. By acid treatment (Nitric acid 69 %), the hydrophilic functional groups were introduced onto the surface CNT surfaces. The new CNTs are termed functionalized CNTs. This acid treatment allowed more effective dispersion of CNTs in water-based drilling fluids. Therefore, CNTs become able to conduct heat more efficiently by passing through bentonite layers. Also, the milling process was applied to CNTs to investigate the effect of ball-milling on the thermal properties of CNTs-formulated mud.

They found out that CNTs form more uniform dispersion in non-polar environments (such as oil-based systems) rather than in polar environments (such as water-based systems).

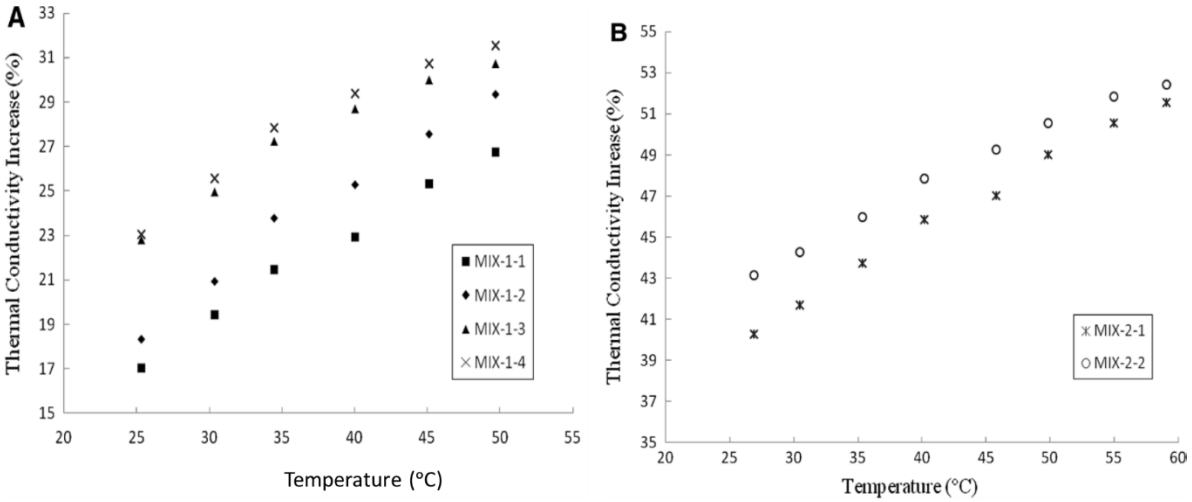

Figure 7.Percentage of thermal conductivity increase against temperature for MIX-1 (a) and MIX-2 (b).

Four different kinds of CNT-formulated mud samples were prepared by adding various amounts of unfunctionalized (MIX-1-1), ball-milled (MIX-1-2), functionalized (MIX-1-3), and functionalized and ball-milled (MIX-1-4) CNTs for CNTs water-based mud (MIX-1); and two for sample preparation in MIX-2 for both unfunctionalized (MIX-2-1) and functionalized cases (MIX-2-2).

They found, in figure 7, that the percentage of thermal conductivity increase with increasing temperature in both nanofluid mixtures comprised of CNTs water-based mud (MIX-1) and CNTs oil-based mud (MIX-2). They denoted that the increase rate was decreased after a threshold temperature of 35°C (MIX-1) and 40°C (MIX-2). This behavior describes the destruction of a functional group at a high temperature which likely declines the CNT dispersion quality and provokes instability in functionalized cases. In figure 7(a), they recorded 31.8 % of the increase in thermal conductivity for CNT-formulated mud samples (functionalized and ball-milled CNT (MIX-1.4)) at 50°C. They found out that, at elevated temperature, the effect of ball-milling on the thermal condition was magnified. In figure 7(b), they found out at higher temperatures (55°C) that the increasing temperature rate of thermal conditions was leveled off for Mix-2. Therefore, they found out that 51.8 % and 52.9 % of the increase in percentage values were respectively established through measurement at 60°C for sample preparation in MIX-2 for both unfunctionalized (MIX-2-1) and functionalized cases (MIX-2-2).

The researches of Ahmed (2016) on the effect of temperature on the rheological properties with shear stress limit of iron oxide nanoparticle modified bentonite drilling muds showed in figure 8 that the variation of shear stress against the shear rate at different temperature and different nanoFe_2O_3 concentration. The rheological properties of the mud were well fitted with the Herschel-Bulkley model. It is recorded that the coefficient of determination R^2 varied from 0.98 to 0.99; the root means square of error (RMSE) or RMSD varied from 0.50 Pa to 2.25 Pa. However, the yield stress (y_o) for 6.0 wt. % BT-WDFs without nanoFe_2O_3 at 25°C was 26.5 Pa. Once the temperature increases to 85° C, the yield stress (y0) decreased to 8.3 Pa, a reduction of 69% was

observed. It is observed that by adding 1.0 wt. % of nanoFe_2O_3 to the 6.0 wt. % BT-WDFs at 25°C, the yield stress increases by 43 %. Briefly, the more nanoFe_2O_3 concentration increases, the more the yield stress (y_o) increases.

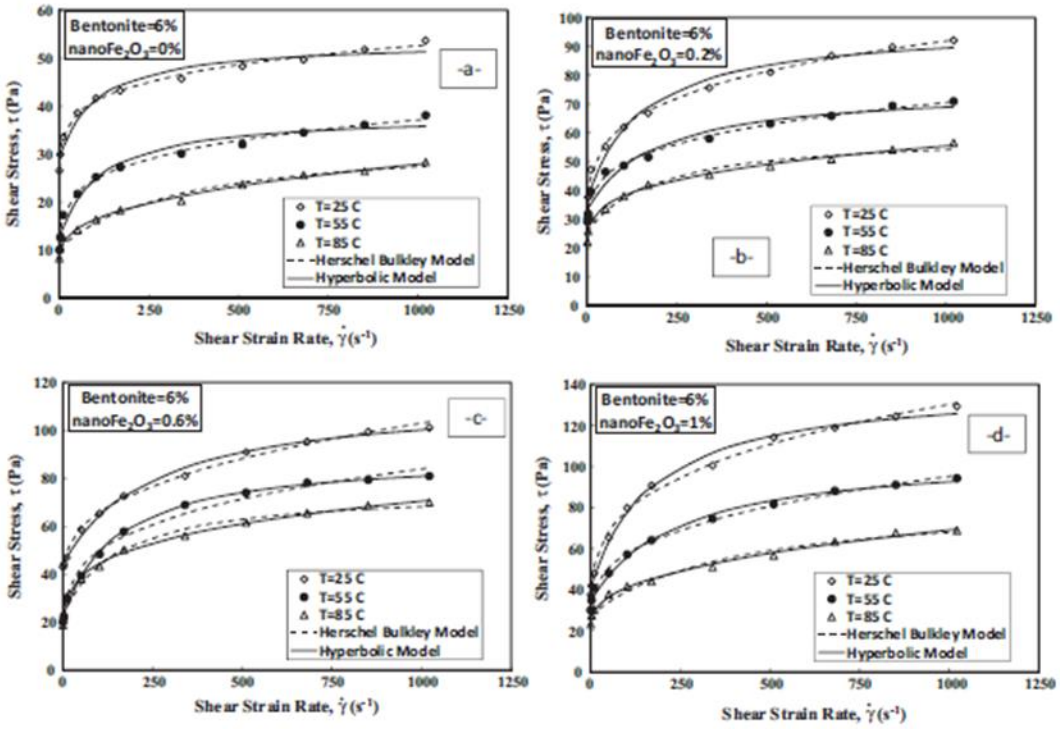

Figure 8. The variation of shear stress against shear rate at different temperature (25, 55 and 80°C) and different nanoFe_2O_3 (a) 0 wt.%, (b) 0.2 wt.%, (c) 0.6 wt.% and (d) 1 wt.%.

In figure 9 below, contrary, the increase of temperature decreases the yield stress at different nanoFe_2O_3 concentrations (Ahmed 2016).

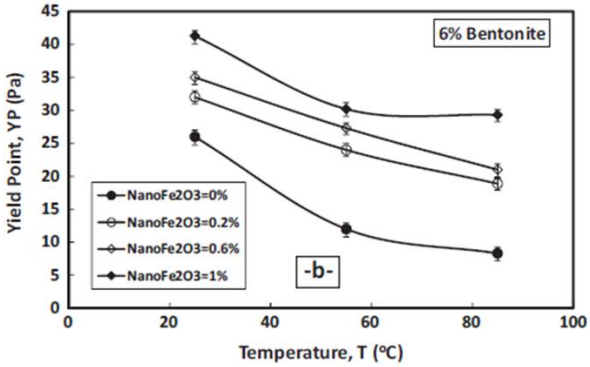

Figure 9. The variation of yield stress against temperature at different nanoFe_2O_3 (0 wt. %, 0.2 wt. %, 0.6 wt. % and 1 wt. %).

2.3.2. RHEOLOGICAL PROPERTIES

Successful drilling of oil and gas wells depends on how the rheological properties of drilling fluids are monitored and controlled. However, accurate knowledge of the rheology of drilling fluids helps to accurately predict friction losses. As drilling fluids flow through the wellbore, their rheological profile is subject to alterations due to the combination of the effect of temperature, pressure, time and shear force which makes the characterization and prediction of drilling fluids a complex task (Vryzas et al 2016). It is very important to have a deep understanding of the drilling fluid properties, particularly the impact of the related microstructure mechanisms of the flow properties to carry out a correct determination of rheological characteristics of smart fluids (Vryzas et al 2015).
Since the flow characteristics of a drilling fluid under different flow conditions are described by their properties named flow properties, the flow behavior of the drilling fluid recognized at various points of interest in the mud circulating system is sufficient enough to predict the effects of this flow. When the fluid is subjected to an applied force (shear stress) many categories of drilling fluid are determined.

The frictional drag applied by a circulating fluid on the surface of a pipe is defined as a shear stress in which the magnitude depends on the frictional drag within adjacent layers of fluid moving at different speed and the difference in velocities of adjacent layers next to the wall of the pipe. The shear rate constitutes the difference in the velocities within adjacent layers across a flow conduit and at the maximum shear stress and shear rate the effect of the flow at the wall is called area of concern.

According to the behavior of the fluid, two categories of fluids are defined “Newtonian and non-Newtonian fluids” depends on the viscosity of the fluid as shown in figure 10-11 (from http://people.sju.edu/~phabdas/physics/rheo.html and http://www.foodelphi.com/non-newtonian-fluids/). In the case of Newtonian fluids, the viscosity is represented by the ratio of shear stress and shear rate. Water and oil are good examples of Newtonian fluids. When a shear force is applied on them, the Newtonian behavior does not delay to occur instantly. The variation of shear rate leads to a high effective viscosity at low shear rate and a low effective viscosity at the high shear rate which let appear a phenomenon known as “shear thinning”.

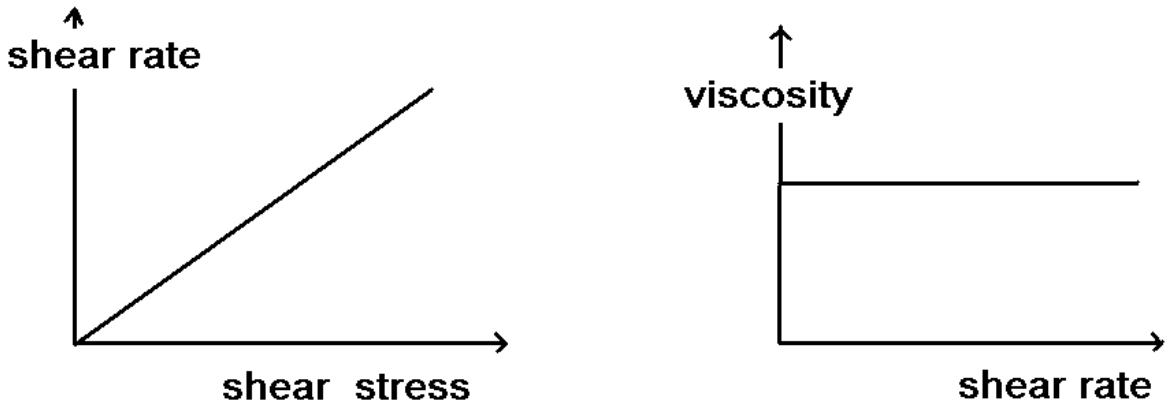

Figure 10. Graphs showing properties of Newtonian fluid.

In the case of non-Newtonian fluids, shear stress and shear rate present a non-linear relationship. These fluids necessitate an amount of shear force to start flow, and thereafter, as the shear rate keeps increasing an additional stress is needed. They are used as drilling fluids and their solid content connected together to form a structure which causes the flow to stop when shear stress is abridged to a certain level or point which is less than the shear strength of the structure. This point is named "yield stress" where the shear stress is required to start the flow. Once the non-Newtonian fluids stand static for a time interval, there will be a semi-rigid structure built on them causing the increase of shear stress required to start the flow. At this point, the shear stress is named the gel strength. The more the gel strength increases, the more rigid the structure becomes with time. Shear rate are of predominant interest in these four important areas: 1) the pit, where the shear rates values are almost zero, 2) the bits, having a super high shear rates 3) the annulus, with low shear rates, and 4) the drill string and collars, through which hydraulic power is supplied to the bit from a pump.

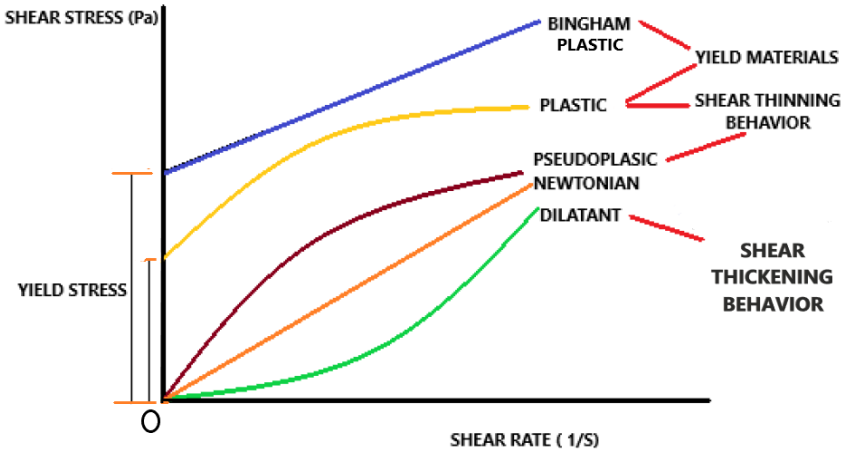

Figure 11.Graphs showing properties of non-Newtonian fluids (Retrieved March 28, 2015.

2.3.2.1. PLASTIC VISCOSITY

The plastic viscosity relates to the measurement of the internal resistance to flow owing to the type, size, and amount of solids in the drilling fluids. The plastic viscosity depends on the viscosity of the liquid phase and the volume of solids contained in the drilling fluid. Once, these solids collide one another and with the liquid phase of the drilling fluid, they create a mechanical friction that tries to prevent movement. The plastic viscosity has to be decreased in order to minimize the shear rate. By doing so, the viscosity at the bit will be reduced too in order to promote a rise to higher ROP. The increase in plastic viscosity will lead to increased pressure drop which compromises the rate of flow and tends to offset any increase in the lifting ability. In fact, the addition of any type of solid to the drilling fluid increases the plastic viscosity, but the use of solids like clay absorbing water and swelling increases the plastic viscosity due to hydration. The best is

to minimize the plastic viscosity by keeping the amount of drilled solids in the mud at a very minimal level. This is addressed by lowering the concentration of the solids or make use of the flocculants to increase the size of the particles which leads to the reduction of the available surface area. This is illustrated by the figure 12 that displays the effect of the bentonite suspension at different shear rate ranges (Annis & Smith 1996).

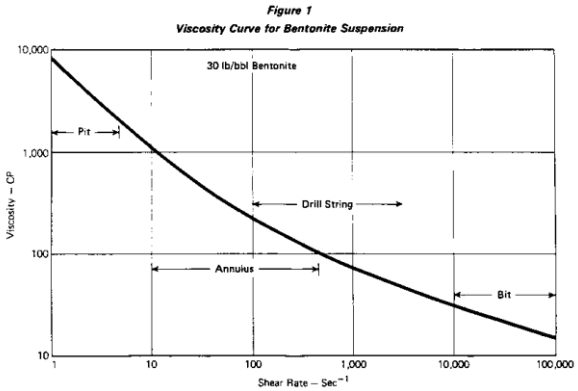

Figure 12. Viscosity curve for bentonite.

2.3.2.2. YIELD POINT

Yield point measures the attraction forces between particles in the drilling fluid. These attraction forces coming from opposite charges found on the surfaces of the particles that cause initial resistance to flow. The yield point does not depend on the type of solids present, their concentration, respective surface charges, and concentration and type of other ions or salt present in drilling fluid. The yield point can be increased in the following ways: 1) when the solids concentration is increased for instance the increase of BT which brings more surface charges mostly when the solids are in active mode whereas if they are inactive, there is a reduction of the space between the particles; 2) less chemical treatment; 3) introduction of contaminants that cause the flocculation of the drilling fluid particles e.g. salt, cement; and 4) action of the bit by grinding of the particles which expose active surface charges.

The collision between either long molecules or colloidal solids into a drilling fluid produces large resistance to the flow. The particles that are quite long compared to their thickness will have large inter-particles interference causing them to link together when they are randomly oriented in the flow stream. The yield point of the drilling fluid will then be determined by the combination of the two following effects: the broken linked bonds and the increase of fluidity due to the reduced effect of particles interaction at a high shear rate as the particles are arranged in the line in the flow stream.

In fact, the flocculation of clay solids or high concentrations of colloidal solids causes a high yield point to occur. However, this flocculation may be produced by lack of deflocculant or addition of contaminant or high temperature. Thus the achievement of a higher yield point is done by adding flocculating agents or clay extenders e.g. soda, ash, polyacrylates, and several calcium compounds. The yield point is related to two drilling fluid functions: hole cleaning capacity and pressure control capability of drilling fluid. Talking about hole cleaning, a higher yield point increases the circulating annular pressure drop and the carrying capacity of a drilling fluid. The lost circulation

problems and swabbing have been made detrimental due to an increased yield point but the latter is good for the hole cleaning, so a compromise must be reached. As the increased mud weight improves hole cleaning, high weight mud does not usually need a higher yield point to ensure good cuttings carrying capacity. Furthermore, in terms of pressure control, high weight mud requirement is often critical. As a consequence, the need of getting the yield point to a minimum usually outweighs any advantages of maintaining a high yield point in high-density mud (Annis & Smith 1996).

2.3.2.3.. GEL STRENGTH

Gel strength relates to mud's ability to suspend cuttings when circulation stops. Gel strength is a very important mud property that measures the necessary shear stress able to start the flow of drilling fluid that has been inert for a period of time (10 seconds and 10 minutes in the standard API procedure, even though measurement after 30 minutes or 16 hours may also be made) e.g. a thixotropic character measurement.

The development of gelled structures has been noticed when drilling fluids were stagnant and liquefying when sheared. These drilling fluids are termed thixotropic.

Drilling fluid needs to have gel strength in order to keep particles under static conditions. Especially, in the absence of a gel structure, barite cannot be kept in suspension over a long period without circulation, even if the viscosity is very high. The gravitational force must be required in order to balance the flow resistance force of non-moving particles so that the minimum gel strength can be estimated. For single barite, the particle must be kept in suspension. This requires a minimum gel strength that can be given by the following equation (Ehrhorn & Saasen 1996):

Equation 10. $\tau_{gel} = (\rho_p - \rho_f) * gD/6$

For example, a particle with 100μ diameter (D), respectively 4.2 and 1.0 SG for particle (ρ_p) and fluid density (ρ_f), necessitates gel strength of 0.5 Pa to keep the barite particles suspended.

Drilling fluids rheology is characterized by using widely the API yield point and plastic viscosity and their ratio. However, this should not be the case in order to prevent barite sag, since their values are normally acceptable only when the shear rate is above a few hundred reciprocal seconds.

In the case of water-based drilling fluid, the gel formation is controlled by the type and content of the clay. The gel properties can be controlled only by the clay particles coming from the drilled formation or those added to the drilling fluid. Thus, the tendency to gelate or give a gel formation results from the interaction between electrical charged edges and faces of the particles.

The high viscosity of drilling fluid does not mean high gel strength as both of them are two different phenomena and should not be mixed up. During the drilling operation, the introduction into the mud system of solids coming from drilled cuttings, barite, and so on leads to an increase in both viscosity and gel strength. However, the addition of more fluids or the surface removal of mud solids will be able to reduce the increase of viscosity and gel strength. The beginning of the flocculation could be easily perceived through an increase in gel strength while the latter is reduced by the action of deflocculants. The drilling fluid system does not desire excessive gel strength as they cause the following problems: 1) prevent solids from settling down; 2) large surge pressure while running the pipe that causes a possible breakdown of formation; 3) swabbing causing the hole to cave in below the bit.

2.3.3. FILTRATION

Filtration is considered a fundamental unit operation based on the separation of suspended solid particles from a process fluid stream. It is a process whereby suspended solid particles in a liquid are removed by the use of a porous substance referred to as a filter medium that allows the fluid to pass through the voids of the filter medium but retains the solid particles on the surface and in the pores of the medium. The fluid that passes through is called filtrate (Cheremisinoff 1998).

During drilling operations, the driller should minimize the fluid loss to promote safer and loss costly drilling activities. The most common causes of formation damage that leads to expensive stimulation treatments and even loss of production are the invasion of foreign fluids named drilling mud filtrate. This invasion of foreign fluids is a process that takes place when a well is being drilled with higher wellbore pressure (excessive mud weights) than formation pressure. As the mud filtrate invades the porous and permeable formation, solids contained in the mud, for instance, BT, are being deposited and impeding sufficient pores to form a filter mud cake on the formation face. Those problems of excessive formation damage can be palliated only if the deposition of thin permeable filter cake and acceptable fluid loss value is established (Mahmoud et al 2016).

Studies conducted by Borisov et al 2015 on nanoparticles-based invert emulsion drilling fluids (oil-based drilling fluids) were carried out in the field to evaluate nanofluids in real conditions. They found that a significant decrease in fluid loss and formation of a thinner filter cake was obtained when lost circulation materials (LCM) were combined with NPs drilling fluid compared to fluids containing LCM alone. This difference is illustrated in figure 13 below. They showed that NPs were able to fill the gaps between the micron-sized particles of the formation. As result, lower permeability and a decreased fluid loss were obtained. They conclude that the use of 0.5 wt. % calcium NP reduced the total mud losses by 22-34 % giving a good correlation with what was obtained in the lab. A schematic representation of mud losses while drilling in the case of (a) typical LCM; and (b) NP. A representation of mud losses is shown in figure 13 below (Borisov et al 2015; Vryzas & Kelessidis 2017)

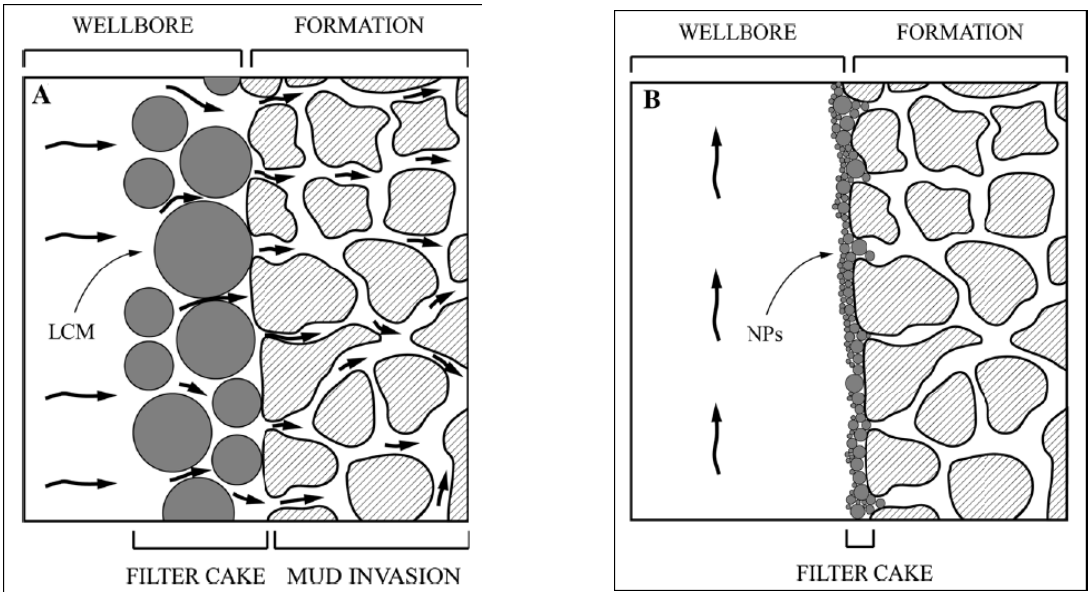

Figure 13. A schematic representation of mud losses while drilling in the case of (a) typical LCM; and (b) NP.

Three types of filtration could occur:

Beneath-the-bit filtration

As the drilling operation goes on, the drill bit is penetrating the formation, and filtration from mud which is being discharged through the nozzles on the drilling bit continues to invade the formation. Filtration is acquiring a very large driving force from the hydraulic forces. Therefore since the drilling work is carrying on, the trend of generating a filter cake would be competed by its removal and the resultant fluid loss could be significant.

Dynamic filtration

This filtration process referred to the tendency of the filter cake to be eroded by the mudflow as it is deposited. The filter cake compiles until an equilibrium thickness is established where the rate of deposition is equal to the rate of erosion. At this point the rate of filtration and cake thickness becomes constant.

There is an achievement of the equilibrium quasi-steady-state fluid loss rate. Thus this showed that both physical conditions in the circulating borehole and properties of the components in the fluid system are dependent on the dynamic fluid loss. Dynamic filtration should be controlled to check the invasion of filtrate.

Static filtration

The filter cake thickness grows continually with time increasing and results in a continuous reduction in filtration rate. Better control of the static filtration allows better control of the filter cake thickness (Peden 1982).

2.4. CELLULOSE NANOCRYSTALS AND ITS RHEOLOGICAL PROPERTIES

2.4.1. SYNTHESIS OF CELLULOSE NANOCRYSTALS

Cellulose nanocrystals (CNCs), a biopolymer and green nano-size materials, are derived from cellulose, one of the most abundant and unlimited natural polymer. They are hydrophilic, non–toxic, carbon-neutral, odorless, tasteless, insoluble in water and most organic solvents, biodegradable, and renewable. CNCs serve as sustainable and environmentally friendly materials.

Microfibrils, cell biology, are composed of cellulose chains. Once microfibrils are broken down they form cellulose nanofibrils (CNF) and CNCs that can be extracted from biomass and used to create renewable-based materials capable of competing in performance and price with petroleum-derived plastics and metal in various applications. CNCs are made of rod-shaped particles (50-500 nm in length, 3-4 nm wide) and highly crystalline whereas CNFs with the longer structures (500 to several microns in length, 5-50 nm wide) contain both amorphous and crystalline regions. CNCs extracted by acid hydrolysis are characterized by high tensile strength (~7.5 GPa), high axial stiffness (~150 GPa), low coefficient of thermal expansion (~1 ppm/K), low density (~1.6 g/cm^3), relatively low cost, chemical tunability, high aspect ratio (10-100), thermal stability up to ~300˚C, lyotropic liquid crystalline behavior, and shear-thinning rheology in aqueous suspensions (Azizi et al 2005; Van den Berg et al 2007; Wu et al 2007; Capadona et al 2007; Habibi et al 2010, Leung et al 2011, Peng et al 2011, Moon et al 2013).

Qin et al (2011) process the oxidation of cotton nanocrystals in the TEMPO-NaBr-NAClO system with ultrasonic treatment and conclude that the CNCs found out have high carboxylate content. The results depict that the carboxylate group was obtained from the conversion of the C6 primary

hydroxyl group of cellulose fiber. It is noticed that an amount up to 1.66 mmol/g of nanocrystals was achieved with width and length of 5 to 10 nm and 200 to 400 nm respectively. The CNCs produced demonstrate high stability and are very well dispersed in the aqueous suspension (Qin et al 2011).

CNCs are used as a nanomaterial for nanotechnology due to their well-known advantages. They can easily replace synthetic fibers with carbon nanotube because of their high cost and non-biodegradability (Moon et al 2011). The structure of CNCs is depicted in the following figure 14 below (Ryan et al 2010; Zhou & Wu 2012):

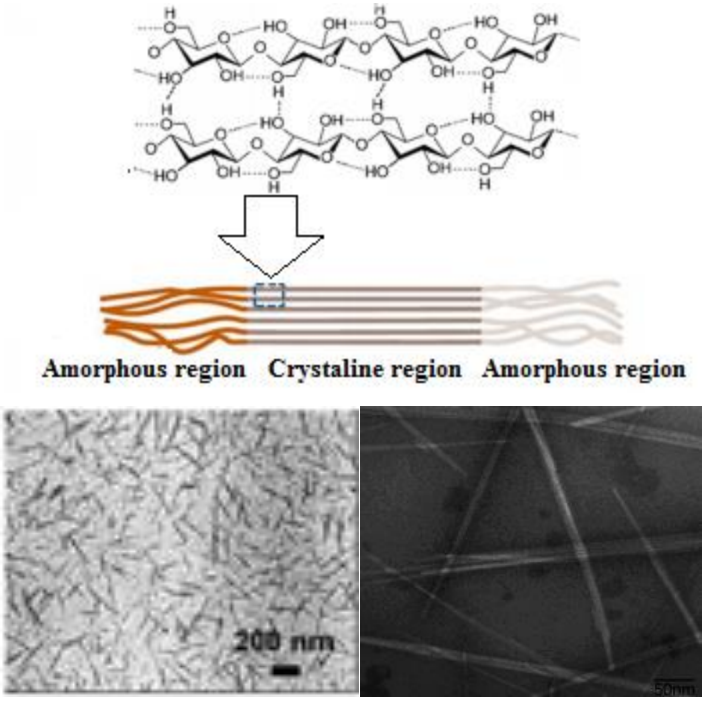

Figure 14. Cellulose nanocrystals (CNCs) structure and transmission electron microscopy (TEM) image extracted from cotton.

CNCs become the centre of much significant interest owing to their chemical, optical, mechanical, and rheological properties. The development of high-performance nanocomposites implying the use of hydrophobic matrices is one of the various challenging requirements that the CNCs have been allowed to meet due to their great surface-functionalized (George & Sabapathi 2015).

CNCs possess excellent properties which make them ideal materials for processing polymer nanocomposites (Dufresne 2006, 2013). CNCs found many applications in polymer nanocomposites such as good reinforcement fillers wide range of polymeric matrices. According to his properties, CNCs are used as rheology modifier in paints, cosmetics, polymers, and pharmaceutical products, and actually as a powerful rheological modifier in drilling fluids and cement (Turbak et al 1983; Šturcová et al 2005; Ching & Ng 2014; Li et al 2015a, 2015b; Cao et al 2015).

Several methods are involved in the synthesis of CNCs from natural cellulosic source materials for example the Tempo-mediated Oxidation and acid hydrolysis as the chemical method,

enzymatic hydrolysis, and mechanical treatment. In terms of yield and quality of CNCs, a combination of those methods is very important.

Research shows that ultra-sonication treatment is a highly efficient method for synthesizing CNCs nanoparticles. CNCs produced by the ultra-sonication treatment exhibit relatively high thermal stability that is much appreciable to be used as drilling fluid additives in HPHT wells during drilling operations (Lu et al 2014).

2.4.2. RHEOLOGICAL PROPERTIES OF CNCs SUSPENSIONS

The Physico-chemical properties of the particles influence substantially the rheological behavior of CNC suspensions. The incidence of phase transitions in the suspension is ascertained by the dimension and surface properties of rode-like CNCs and the ionic strength of the system (Dong & Gray 1997; Beck-Candenedo et al 2005; Shafiei-sabet et al 2013). The study of the rheological behavior of the rode-like particles by using cellulose whiskers suspension has been done through the work of Bercea & Navard 2000 and Azizi et al 2005. It has been found that a similarity between the flow properties of cellulose whiskers above a critical concentration and those of liquid crystal polymer solutions and the whisker can be simply oriented. They observed three distinct regions for the aqueous suspension of a cotton linter. The first region is at a low shear rate ($<1s^{-1}$). They observed high viscosity that decreases with shear rate and the alignment of whiskers underflow has been shown by the shear-thinning observed in the aqueous medium (Ortz et al 1995; Ebeling et al 1999). The second region is at an intermediate shear rate (1-10 s^{-1}) with a slighter decrease in viscosity. Whiskers present a high level of order due to the interparticle interactions that result in a high viscosity to flow. The last region is at a higher shear rate (>10 s^{-1}). It has been observed, a break of the ordered structure, conducted to the individualized whiskers. This is the typical rheological behavior of liquid crystalline polymers.

The structure-morphology-rheology relationships for cellulose nanoparticles (CNPs), including CNCs, were directly studied by Li et al 2015a. They found a proportional increase of the viscosity of CNCs suspension related to their concentration due to the augmentation in the collision possibility of CNCs. Nevertheless, over the entire investigated shear rate, it is observed that the viscosity is monotonically declined as the shear rate increased, showing a typical shear shinning behavior. A strong dependence of the viscosity of CNCs on the shear rate, CNC concentration, and CNC aspect ratio has been depicted. They observed two transition zones in the rheological behavior: a transition from isotropic to the liquid crystal and from the liquid crystal to gel with increasing CNC concentrations of the suspension in water. Figure 15 below shows the viscosity vs shear rate curves for the range of 0-0.85 wt. %. At low shear rates, a Newtonian plateau shows an isotropic sample with a shear-thinning at intermediate shear rates as the shear direction aligns parallel the nanocrystals. Another plateau in the viscosity at high shear rates demonstrates that all the particles are aligned (Bercea & Navard 2000; Shafiei-sabet et al 2012, 2013, 2014). The viscosity profile shows three regions of the formation of the liquid crystal phase suspension above the first critical concentration, typical of the liquid crystal of polymer solutions (Onogi & Asada 1980). This viscosity profile describes three different regions: 1) at low shear rates with a shear-thinning region due to the alignment of chiral nematic liquid crystal domains; 2) at the intermediate shear rates as the entire domains have been deformed and aligned along the shear direction; 3) at high shear rates with a second shear-thinning where there is the destruction of the liquid crystal domains and freed due to the high shear stress. Thus, there is an alignment of particles along the shear flow direction.

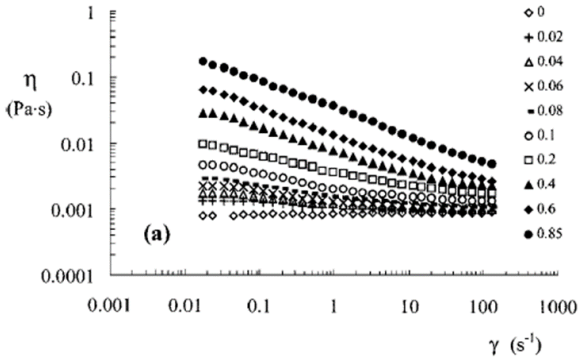

Figure 15. Viscosity vs shear rate for the suspensions of whiskers at different concentrations of cellulose (wt. %).

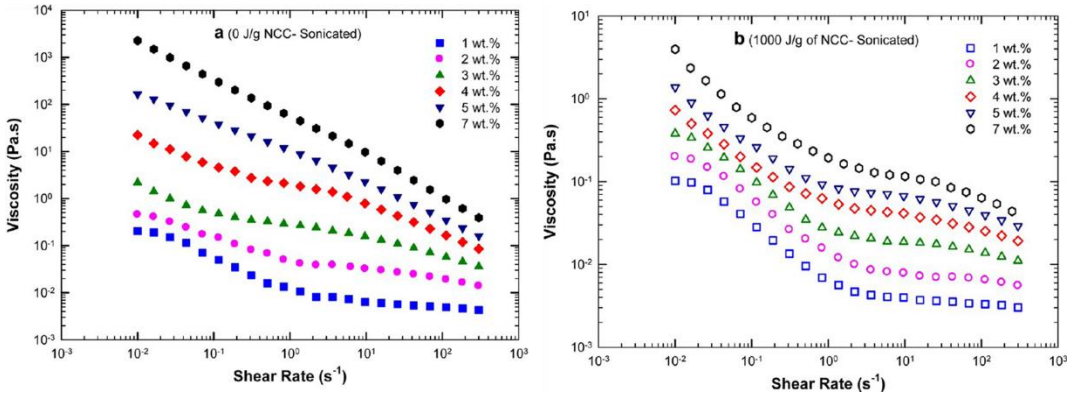

Figure 16. Steady-state viscosity versus shear rate for (a) unsonicated CNC suspensions, and (b) CNC suspensions sonicated with concentrations varying from 1 to 7 wt. %.

Figure 16(a-b) shows the plot of the viscosity vs shear rate of unsonicated CNC suspensions and CNC suspensions sonicated respectively, at various concentrations ranging from 1 to 7 wt. %. As seen for figure 16(a), a Newtonian plateau is shown for 1 wt. % sample at low shear rates followed by a shear-thinning region at intermediate shear rates and another plateau at high shear rates, typical of an isotropic sample. However from 2 to 4 wt. % CNC, the three-region viscosity profile, typically associated with lyotropic polymer liquid crystals, was observed. For 5 and 7 wt. % NCC, a single shear-thinning behavior was observed over the entire range of shear rate. That is the characteristic of a gel formation preventing the formation of chiral nematic ordered phases. Figure 16(b) depicts the shear viscosity plot of the sonicated suspensions. This shows a drastic decrease of the viscosity at all concentrations where 3-7 wt. % NCC samples show a shear viscosity plot similar to those seen in liquid crystalline systems.

`

CHAPTER 3. EXPERIMENTAL AND ANALYTICAL TECHNIQUES

3.1. METHODOLOGY

3.1.1. MATERIALS

Micro-fibrillated cellulose (MFC) in solid form was provided by South Africa Pulp and Paper Industries (SAPPI). Na-Bentonite (montmorillonite) powder was provided by Sigma-Aldrich, U.S.A. Milled Attapulgite (ATT) powder was provided by SAPPI. Sepiolite (SEP) powder was provided by Sigma-Aldrich, Spain (Concentration 13%; ≤ 10% loss on drying). TEMPO (2,2,6,6 tetramethylpiperidine-1-oxyl), 13% sodium hypochlorite (NaClO) provided by Rochelle Chemicals & Lab Equipment C.C., S.A. ; Sodium bromide (NaBr) and 0.5M sodium hydroxide (NaOH) pellets, and deionized water were used to prepare CNCs. Seawater from Durban South Africa and freshwater from deionized water were used to prepared different mud systems. BT, ATT, and SEP clay were used as the principal mud material to increase the efficiency of the drilling operation. CNCs were used at different concentrations as an additive to be mixed into Bentonite, Attapulgite and Sepiolite water-based drilling fluids (BT-WDFs, ATT-WDFs and SEP-WDFs).

3.1.2. EXPERIMENTAL PROCEDURE

3.1.2.1. PREPARATION OF CELLULOSE NANOCRYSTALS

CNCs were synthesized from MFC through TEMPO-mediated oxidation process as followed: 750ml of 3.2% MFC (24g solids) slurry diluted into deionized water (3877.5 ml) previously mixed with 0.369g TEMPO and 3.69g NaBr. Deionized water and Slurry were prestored at 9°C. The oxidation reaction took 6 hours by adding 172.5ml of 13-15% NaClO solution under mechanical agitation and controlled temperature at 10°C using an ice bath varying between 9°C and 11°C and keeping the pH of 10 by continuously adding droplets of 0.5M NaOH solution. The reaction stopped after 6 hours, filtered, washed, and suspended in 1000 ml of deionized water before proceeding with the ultrasonication. Ultrasonicator (USM20 output power of at least 300W) was used for 45 min in an ice bath. Care was taken during the filtration process to avoid any contamination that could occur by sealing the Buckner funnel with parafilm and transferred the CNCs into a clean container for storage. As the filtration process was unable to be conducted due to the presence of CNCs, the centrifugation process led to the separation of CNCs formed and excess of deionized water. The CNC from the centrifuge was transferred into a clean container and dried into an oven at 30°C for 24 hours or exposed to a room temperature for 48 hours. Thus, the dried CNCs were stored in a firmly sealed container. Figure 16 showed the preparation of CNCs into the Oil and Gas Laboratory at the school of Chemical and Metallurgical Engineering.

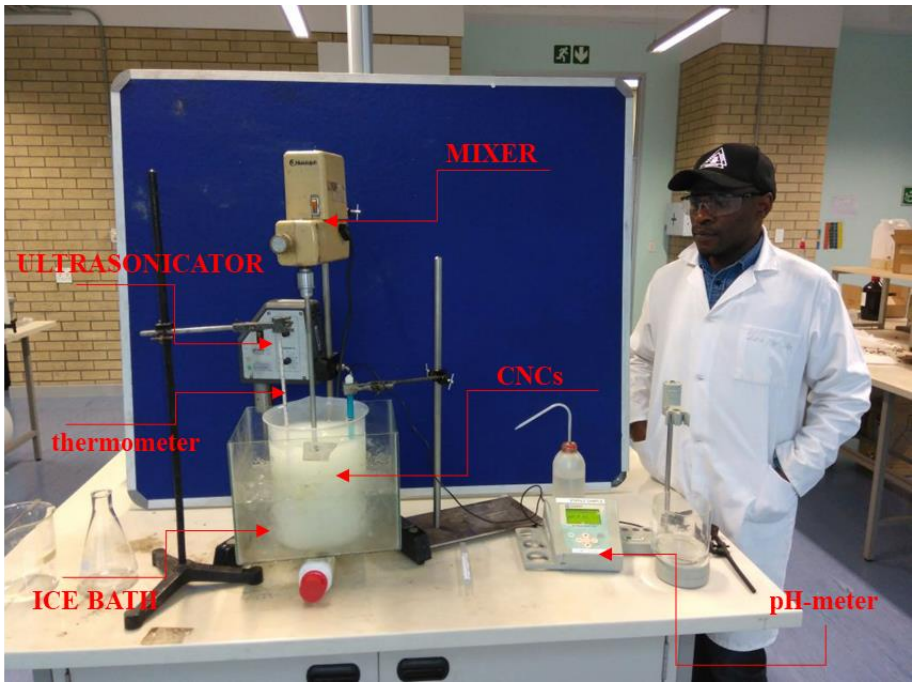

Figure 17. Synthesis of Cellulose Nanocrystals (CNCs) / Oil and Gas Laboratory (Chemical Engineering / Wits University 2019).

3.1.2.2. MUD PRAPARATION

3.1.2.2.1. FORMULATION OF DIFFERENT MUD SYSTEMS (CNC/BT, ATT, SEP-WDFs).

The investigation of the effect of concentration of CNCs on the rheological and filtration properties of CNC/BT, ATT, and SEP-WDFs was made effective through a simple preparation method describes as follow: two kinds of WDFs based on fresh water and seawater were used as the medium to drive the investigation. In the first group, there is CNC/BT, ATT, and SEP-WDFs in freshwater (FW) and the second group constitutes CNC/BT, ATT, and SEP-WDFs in seawater (SW). It has proceeded in such a way that different CNC concentrations of 0.0 (control), 0.4, 0.8, 1.2, 1.6, 2.0, and 2.4 wt. % were mixed with 6 wt. % of BT, ATT and SEP to show only the behavior of CNC/BT, ATT, and SEP-WDFs in FW and SW. Those CNC concentrations were dispersed in an aqueous solution, of deionized water or seawater. The dispersion was done with strong mechanical stirring using a mixer for 45 min. This dispersion was mixed with droplets of NaOH (sodium hydroxide) to adjust the pH to approximately a pH of 9 before adding any solid particles, and then bentonite or attapulgite or sepiolite of fixed concentration 6 wt. % was added slowly in the two groups followed by strongly mechanical stirring using a mixer for 45 min to form water-based fluids (Balhoff et al 2011). Before each run on the rheometer, the formulated drilling fluids (CNC/BT, ATT, SEP-WDFs in FW/SW) were vigorously agitated using a mixer for 20 min, and then about 20 mL of drilling fluid was carefully injected into the stainless steel cup using a syringe. The rheological curves were obtained by measuring the viscosity or shear stress as a function of shear rate ranging from 0.1 to 1200 s-1 at 20, 30, 40, 50, 60, 70, and 80°C. Table 1 summarizes the formulation of CNC/BT, ATT, and SEP-WDFs at various concentrations of CNCs. The experimental procedure of the preparation of CNCs and mud is illustrated in figure 18 below.

This range of concentration of CNC was chosen as the whole range of accessible concentration based on the researches of the following researchers: Bercea & Navard (2000) through their studies of the shear dynamics of aqueous suspensions of cellulose whiskers used CNC at different concentration as follow: 0.0, 0.02, 0.04, 0.06, 0.08, 0.1, 0.2, 0.4, 0.6, 0.85, 1.0, 1.25, 1.5, 1.75, 2.0, 2.25, 2.5, 3 and 3.5 wt. %; Wu & Li (2019), as well on their studies on the effect of modified cellulose nanocrystals on the salt resistance of bentonite drilling fluids where the concentration of modified cellulose nanocrystals in bentonite/modified cellulose nanocrystal-water based drilling fluids were varied from 0.5 to 2 wt. %; and Songa et al (2016) on their studies of prepared water-based drilling fluids of BT and CNPs (CNCs and CNFs) varied from 10 g to 20 g and from 0.35 g to 3.50 g respectively.

The choice of pH of 9 was based on the following researches: (a) Li et al (2018) found that at a low shear rate of 0.1 s-1, BT and ChNC/BT-WDFs at pH of 9.0 had viscosity values of 3.18 × 10-3 and 1.04 × 10-1 Pa.s, respectively. The incorporation of only 0.1 wt. % ChNCs resulted in a roughly 33 times improvement in the viscosity value. Therefore, it is speculated that once the negatively charged ChNCs were added into the negatively charged BT suspension at pH of 9.0, ChNCs acted depletants, which pushed the MMT platelets to link together via the entropic depletion forces. This also led to the improvement of the rheological properties of BT suspension; (b) Luckham & Rossi (1999) studied the colloidal and rheological properties of bentonite suspensions found that electrolyte concentration and pH impacts on the association of montmorillonite particles. At a sufficiently high clay concentration and low electrolyte content, the platelets may flex according to their relative positions and the relative magnitude of their surface and edge potentials. Once the edges are positive, the platelets flex towards a negative face. Once the edges are negative, the platelets are forced to assume a more parallel type orientation. Therefore, the pH of the medium is an important parameter related to the gel structure of the suspension; (c) Keren et al (1988) found a high gel volume for dilute (0.1% w/w) Na+-montmorillonite suspensions at pH~9.8 that indicated the existence of an open three-dimensional structure, where FF type association is predominant and the ability to trap more water between the layers than for lower pH values, where EE and EF type association prevails; and (d) Caenn et al (2011) found that the optimum pH control for the mud made with bentonite and fresh water varied between pH of 8 to 9.

Table 1. Formulation of CNC/BT-WDFs, CNC/ATT-WDFs and CNC/SEP-WDFs in freshwater and seawater.

SAMPLES	**(wt. %)**	**(wt. %)**	**(wt. %)**	**(wt. %)**	**(wt. %)**	**(wt. %)**	**(wt. %)**
BT	6	6	6	6	6	6	6
CNCs	0	0.4	0.8	1.2	1.6	2.0	2.4
ATT	6	6	6	6	6	6	6
CNCs	0	0.4	0.8	1.2	1.6	2.0	2.4
SEP	6	6	6	6	6	6	6
CNCs	0	0.4	0.8	1.2	1.6	2.0	2.4

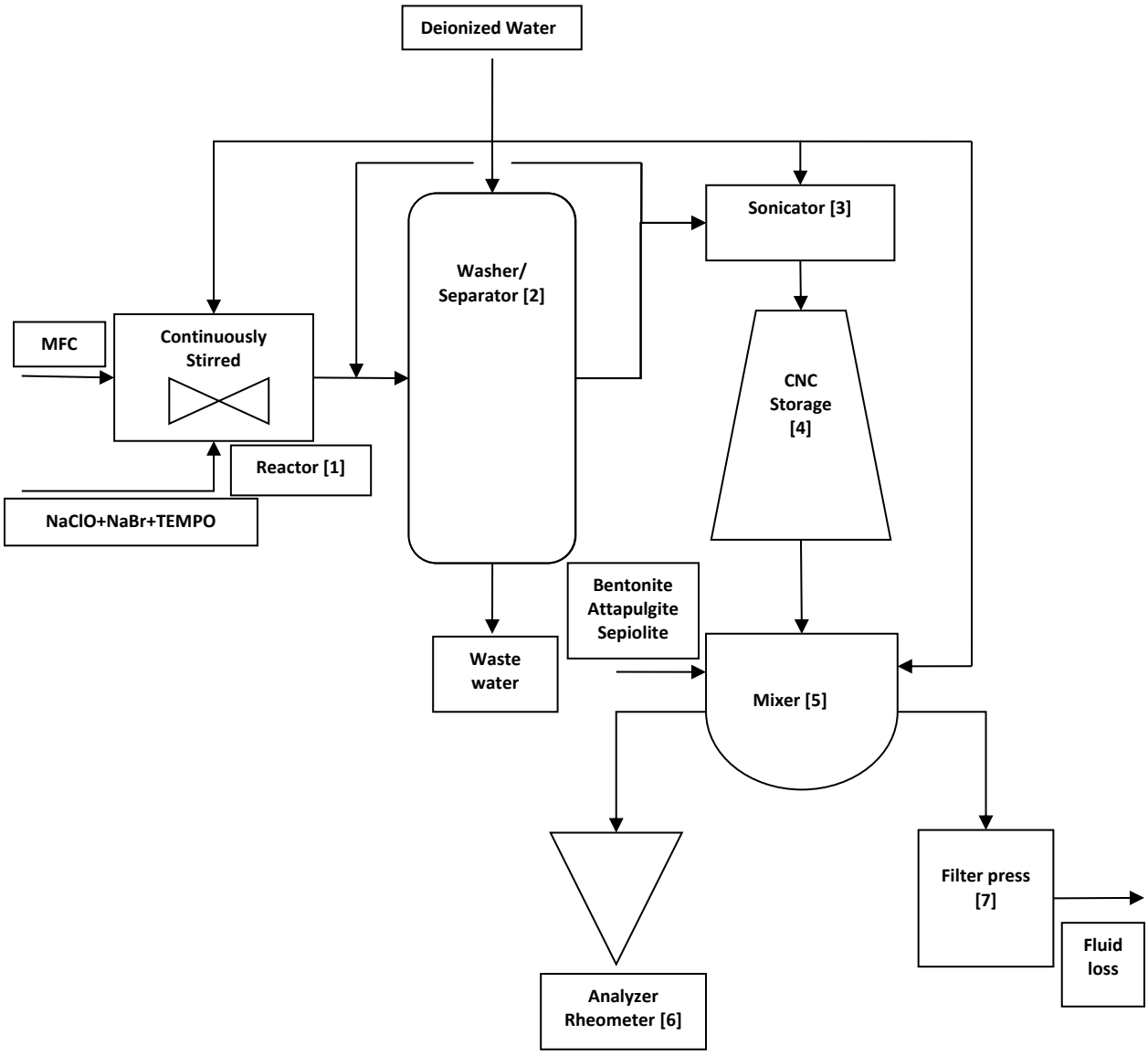

Figure 18. Schematic diagram of the experimental process.

3.1.2.2.2. ULTRASONICATION PROCESS

During this experimental procedure of the preparation of CNCs, ultrasonication process has been used to convert MFC to CNCs. Ultrasonication is the process of using sound waves to agitate particles in a given solution for the purpose of cleaning or separating different substances including the production of nanoparticles, liposomes, extraction of anthocyanins and antioxidants. Ultrasonication sends ultrasonic frequencies into a solution or a sample. In addition, it converts an electrical signal into physical vibration that can break substances apart. Usually, Ultrasonication treatment has been in the range of 10 to 1000 W/cm2 and frequencies of 20 to 100 kHz. It has a prominent effect on physical and chemical properties of liquids (Cucheval & Chow 2008; Asaad et al 2016).

Ultrasonicator is a powerful piece of lab equipment with an ultrasonic electric generator which creates a signal to power a transducer. This transducer converts the electric signal using piezoelectric crystals i.e. the crystals that respond directly to electricity by creating a mechanical vibration. Figure 18 shows the ultrasonic processor similar to the one used in the course of this project.



Figure 19. The ultrasonic processor UP200S (200 watts, 24 kHz).

The device is suitable for sample volumes from 0.1 to 1000ml. It can be used in medical or biological laboratories for the sonication of very small samples up to bigger samples in the chemical or environmental range (Cucheval & Chow 2008; Al-Hilphy et al 2016).

3.1.3. CNCs CHARACTERIZATION

The transmission electron microscopy (TEM, JEM 1400, JEOL) was used to take the morphology at an accelerating voltage of 120 kV. CNCs suspension were diluted at 0.1 wt. % by adding deionized water. A droplet of 5 µl of 0.1 wt. % CNCs suspension has been deposited onto 300 mesh Lacey Carbon film grid (LC300-CU-100) then a drop of 2 wt. % of uranyl acetate solution has been placed on the CNCs coated grid to stain the CNCs for about 2 min. Randomly selection has been done for 50 CNC particles to calculate the average dimension of CNCs from the TEM micrograms. The same, a droplet of 5 µl of 1.2 wt. % of CNC/BT-WDFs (FW), CNC/ATT-WDFs (FW) and CNC/SEP-WDFs (FW) suspension has been deposited onto 300 mesh Lacey Carbon film grid (LC300-CU-100) and observed by TEM to get the microstructure of the different mud systems.

The TEM morphology of each of them is shown in figures 20-22. It can be seen that figure 20 keeps spherical morphologies of CNCs with apparent diameters in the order of 20 nm (Soledad et al 2018). It can be seen that in figure 21 (CNC/BT-WDFs (FW)), the electrostatic repulsive forces

between CNCs and bentonite promoted their individual aggregations and consequent phase separations, resulting in the CNCs and bentonite dominated regions formed distinctly. BT was composed of a large number of plate-like layers with a permanent negative charge on the flat surface.

In figure 22(A), CNC/ATT-WDFs (FW) keeps spherical morphologies of CNCs with apparent diameters in the order of 20 nm (Soledad et al 2018) and a fibrous shape mostly with 1 μm in length and 50 nm in width similar to the TEM micrographs of attapulgite powders as found by Feng et al (2014). In figure 22(B), CNC/SEP-WDFs (FW) keeps spherical morphologies of CNCs with apparent diameters in the order of 20 nm (Soledad et al 2018) with needle like particles with a length of around 1 μm and a diameter of approximately 20 nm of the sepiolite similar to the TEM micrographs of the sepiolite found by Echt & Plank (2019).

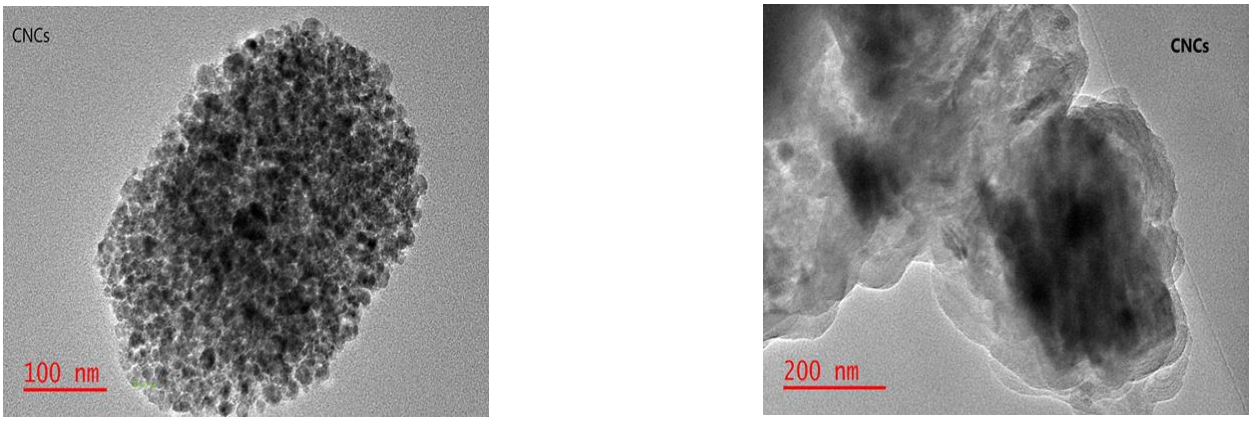

Figure 20. TEM micrographs of the CNCs.

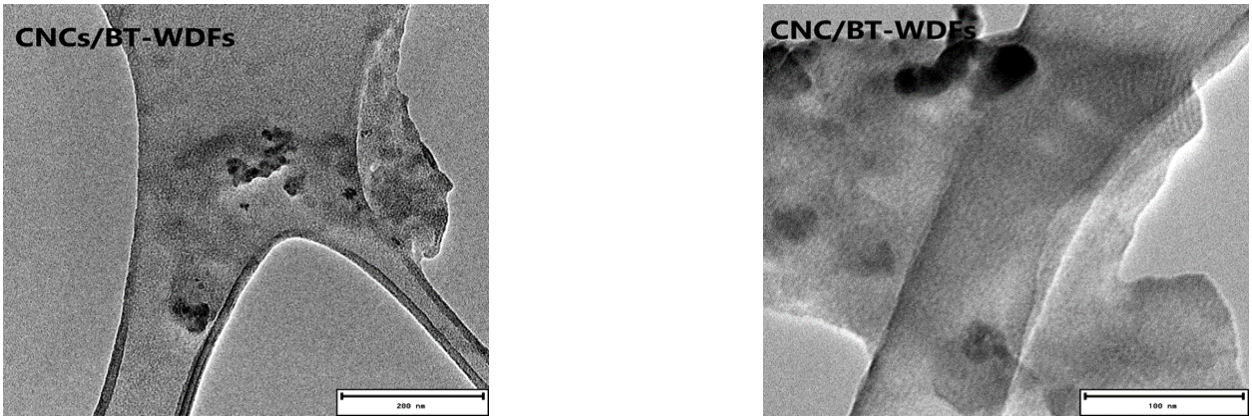

Figure 21. TEM micrographs of the CNC/BT-WDFs.

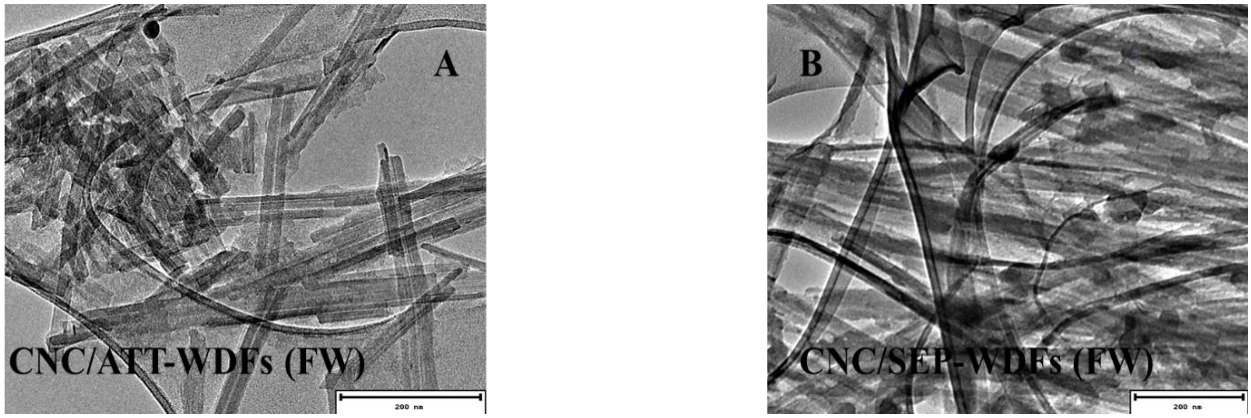

Figure 22. TEM micrographs of the CNC/ATT-WDFs (A) and CNC/SEP-WDFs (B).

3.1.4. ANALYSIS OF RHEOLOGICAL AND FLUID LOSS PROPERTIES

3.1.4.1. RHEOLOGICAL ANALYSIS

The rheological tests was conducted using the rotational rheometer "RheolabQC" (Figure 23). The rheological test was conducted as followed: 25 ml of the prepared mud sample was poured into the measuring cup, placed it on the rheometer, the appropriate flow curve was chosen and the required parameters were fixed before analysis. The rheometer was started to run the experiment. The rheoplus software installed into the rheometer executed all the set-up for the flow curves chosen. The rheological data obtained as data collection from the rheoplus software were used for further analysis as data analysis.

3.1.4.2. RHEOLOGICAL PROPERTIES MEASUREMENT

All the rheological properties of CNC/BT, ATT, and SEP-WDFs in fresh and sea water were measured with a Rheolab QC viscometer from Anton Paar, Germany. RheolabQC is equipped with DIN concentric cylinders geometry constitutes of a rotator of 28.03 mm diameter and a stainless steel cup of 30.38 mm diameter where 20 ml of the WDFs will be poured after a vigorous agitation through a mixer for 20 min. The rheological flow curves were obtained by measuring the shear stress or viscosity against the shear rate from a range of 0.999 to 1200 s^{-1} at different temperature varying from 20°C up to 80°C with an interval of 10°C. As WDFs are non-Newtonian fluids, many mathematical model could be used to fit the relationship between shear stress and shear.

The analysis of rheological data of CNC/BT-W CNC/BT, ATT, and SEP-WDFs was effective by applying Herschel-Bulkley model which is the combination of Bingham plastic and power-law models using the commercial software, OriginPro 2018. Herschel-Bulkley model was used due to the fact of not having other three parameter models available inside of OriginPro 2018 software.

Bingham plastic model is described as follow:

Equation 11. $\tau = \tau_o + \mu_p \times \dot{\gamma}$

Where τ stands for the shear stress, τ_o stands for the yield stress or yield point as the origin, μp stands for the plastic viscosity as the slope, and $\dot{\gamma}$ stands for the shear rate. The equation has two parameter easily found after fitting. However, WDFs as non-Newtonian fluids demonstrates a complex behavior to be considered as a simple linear model. With the Bingham plastic model, the

yield point and plastic viscosity can be easily obtained. However, the Bingham plastic model cannot be used to suite a complex fluid as long as the relationship between the shear stress and shear rate is no longer linear. Hence, given the fact that the analysis of complex fluid systems through the Bingham-plastic model generates a high value of yield stress thus it has been declared inadequate to be applied for complex fluid systems (Jung et al 2011).

Then, the power-law model was developed to overwhelm this challenge and it is given as follow in the bellow equation (12):

Equation 12. $\tau = K \times (\gamma)^{\wedge} n$

Where K stands for the flow coefficient or consistency index (Pa.sn), n for the flow behavior index, τ and $\dot{\gamma}$ stand for shear stress and shear rate respectively. As we can see the two parameters k and n are easy to obtain but comparatively with the Bingham plastic behavior the yield stress is missed that makes this model to be inaccurate to fit the rheological curves at low shear rates. The power law model gives a better information in the low shear rate condition but has drawbacks in high shear rate conditions (Becker et al 2003).

Hence, the Herschel-Bulkey model provides a combination of the two previous model and defines a fluid with three parameters. It can be represented mathematically as follows:

Equation 13. $\tau = \tau_o + K \times (\gamma)^{\wedge} n$

where τ stands for the shear stress, τ_o stands for the yield stress or yield point that is the magnitude of the shear stress needed to initiate flow, K stands for the flow consistency coefficient or consistency index or correction parameter that is the viscosity of the a material at 1 reciprocal second, n stands for the flow behavior index that is the degree with which a material exhibits non-Newtonian flow behavior; and τ and $\dot{\gamma}$ stand for shear stress and shear rate respectively.

As Newtonian materials exhibit linear behavior in shear stress as a function of shear rate, the flow index indicates how non-linear a material is. Li et al 2016 showed that the flow consistency coefficient value consistently increased as the CNC concentration increased, whereas the n value constantly decreased suggesting that PAC/CNC/BT-WDFs at higher CNC concentrations had a stronger dependence of shear stress on the shear rate.

Therefore, when $\tau > \tau_o$ the material is about to flow as a Power law fluid. For $\tau < \tau_o$ the material remains rigid. The model assumes that below the yield stress (τ_o), the slurry behaves as a rigid solid, similar to the Bingham plastic model. When $n < 1$, it means that the apparent viscosity of the material decreases as the shear rate increases due to shear thinning or pseudoplastic behavior, in this case the slurries are considered as shear thinning. The shear thinning gets larger as n approaches 0. However, when $n > 1$, the apparent viscosity increases as the shear rate increases due to shear-thickening or dilatant behavior. The fluids are considered as shear thickening (Caenn et al 2011; Mohammed 2017).

The interaction between the charges on the platelets also increases the effective viscosity at low rates of shear, thereby influencing the values of n and K, and is responsible for the formation of a gel when agitation ceases. Therefore, if K is very small, the accuracy of the results obtained by using Herschel-Bulkey model is not affected as long as the accuracy of the result depends on squared correlation coefficient (R^2). However, when $R^2 > 0.99$, the three-parameter model is accurate; when $R^2 < 0.99$, the model of three-parameter used is not accurate. In this project, the rheological results showed that the more K decreases (tend to the very small value), the more n increases (n>1 tend to shear thickening behavior).

Ouaer & Gareche (2019) studied the rheological properties of the hydroxyethyl cellulose (HEC) as a rheology modifier for water-based drilling fluids formulated with Algerian bentonite and found that by adding 0.05 wt. % of HEC to the basic bentonite suspension, a significant increase in the consistency index (K) from 0.008 to 0.042 Pa was observed. This increase in the consistency index (K) showed that the resistance of the system bentonite-HEC to the applied force (shear stress) was increasing with increasing HEC concentration.

The model should be used for non-Newtonian and time-dependent materials with a yield stress. Once a certain amount of shear stress is applied, the materials with yield stresses will start to flow. Yield stress, which is the amount of shear stress needed to initiate flow, represent the magnitude of the strength of attraction between the particles in the suspension that is related to the volume fraction of solids, particle size and the composition of a particle network. Just once the volume fraction, particle size and structure of the network are held constant then the relative magnitude of the strength of attraction between the particles could be studied. This situation is encountered in suspensions, the structure of the particle network with identical powder and volume fraction can be maintained constant by pre-heating the suspension prior to the yield stress measurement (Franks 2002). Therefore, the rheological parameters are determined by applying a nonlinear regression for the Herschel-Bulkley model.

Herschel-Bulkey model gave great design of the rheological behaviors of most drilling fluids (Kelessidis et al 2007; Baba & Belhadri 2009; Khalil & Jan 2011; Khalil & Jan 2012a; Khalil & Jan 2012b; Karen et al 2014; Li et al 2015; Ziaee et al 2015; Ouaer & Gareche 2019). It has been found that an equivalent fit of the rheological data can be obtained from numerous sets of parameter values (e.g., no unique fit for a given data set). This constitutes the main disadvantage of Herschel-Bulkey model. Subsequently, several improved three-parameter models, namely, the Robertson-Stiff, Sisko, Mizhari-Berk, and Heinz-Casson, were established for more complex fluids.

The Robertson−Stiff model is described as follow:

Equation 14. $\tau = K\times (\dot{\gamma_o} + \gamma)\text{^}n$

Where γ_o is the shear rate correction factor, K is the flow consistency coefficient, and n is the flow behavior index. This model was proposed for relating shear stress to shear rate in drilling fluids and cement slurries in 1976 (Robertson & Stiff 1976).

The Sisko model is described as follow:

Equation 15. $\tau = \mu_\infty\times\dot{\gamma} + K\times (\gamma)\text{^}n$

Where μ_∞ is the viscosity at infinite shear rate, K is the flow consistency coefficient (Pa.sn), and n is the flow behavior index. This model was primarily proposed to describe the rheological properties of lubricating greases in 1958 (Sisko 1958).

The Mizhari-Berk model is described as follow:

Equation 16. $\tau^{0.5} = \tau_o + K\times (\gamma)\text{^}n$

Where τ_o is the yield stress, K is the flow consistency coefficient (Pa.sn) and n is the flow behavior index. This model was formerly developed to characterize the flow behavior of orange juice in 1972 (Mizrahi & Berk 1972).

The Heinz-Casson model is described as follow:

Equation 17. $\tau^n = \dot{\gamma_o}^n + K \times (\gamma)^n$

Where $\dot{\gamma_o}$ is the shear rate correction factor, K is the flow consistency coefficient (Pa.sn) and n is the flow behavior index. This Heinz-Casson model was a modification of the Casson model and was primary proposed in 1959 (Heinz W. 1959).



Figure 23. Rotational Rheometer (Rheolab QC SN897839 / FW1.31, Chemical Engineering / Wits University, 2018).

3.1.4.3. FLUID LOSS ANALYSIS

The invasion of the drilling fluid into the formations (e.g., uncontrolled lost circulation of the drilling fluid) can results can result in a dangerous well control problem and some cases also in the loss of the well. This can as well lead to other effects such as increasing nonproductive time, resulting in a stuck pipe because of the poor hole cleaning conditions (Elkatatny et al 2003). It can also result in significant cases of swelling leading to the wellbore collapse, filter cake deposited on the wellbore wall due to the clay flocculation under certain conditions (salt contaminants or HPHT) encounter in the wellbore leading to sticking pipe issues, well damage, and causing

differential pressure sticking (Kosynkin et al 2011; Zakaria et al 2012; Blkoor & Fattah 2013). Thus, the use of suitable drilling fluid with desire filtration properties having low fluid loss volume with thin and dense filter cake that includes nanoparticles to maintain the stability of the wellbore during the drilling operation process is required.

The expectation of what is going on in the real well during the drilling operation will be carried out using filtration tests making it possible to simulate downhole conditions. Measuring filtration behavior and wall cake building characteristics are essential to drilling fluid control and treatment. The filtrate characteristics are very important as they depend on the types and amount of solids in the mud and their physical and chemical interactions. The latter ones are affected by the temperature and pressure. Therefore, it is necessary to determine the filtration properties of drilling mud by running the tests at both low-temperature/low-pressure (LTLP) and high-temperature/high-pressure (HTHP) using filter press as seen in Figure 23.

Fluid loss test will be conducted by using different mud samples subject to a certain range of pressure (100, 200, 300, and 400 KPa) and at room temperature, and the filtrate will be recorded after 30 minutes.

The mud system with viscosity and filtration loss ranging in the acceptable limit will be used for penetration rate tests with different selected rock samples in the Soil Lab, Civil Engineering/Wits University 2018.



Figure 24. Filter press HPHT 1L 5 bars (Soil Lab, Civil Engineering/Wits University, 2018).

3.1.4.4. FILTRATION PROPERTIES MEASUREMENT

Filtration measurements were achieved by using an HTHP standard filter press equipment see figure 23 (built-in soil Lab civil engineering at Wits University with pressure and temperature limit of 5 bars and 150°C respectively) with ceramic disc filter according to API guidelines. The ceramic disk has been soaked in the based fluid being tested for at least 30 minutes before usage (HTHP

Filter Press for Ceramic Disks with 1L, Double-Capped Test Cell, and air Pressuring Assemblies by Sam 2019). The air is used as a pressure source into a cylinder at 450 KPa. A timer and a graduated cylinder were also used. Before starting every measurement 100 ml of the sample were vigorously stirred within 10 minutes then poured into the filter cell. The sample was run at two different temperatures 20°C and 80°C. Sample temperatures were measured using a thermometer. The thermometer was placed into submerged samples in a cold or heated water bath to measure both temperatures. An ice bath reached 20°C while a heated bath to 80 ° C. During the experiment, the outer wall of the cylinder was covered with a sponge capable of absorbing cold (20°C) or heated (80°C) water from the water bath to maintain the temperature constant. The top cap of the filter cell was sealed and firmly tightened with a T-screw. Set the regulator so that it could be ready to release the pressure of 450 KPa into the filter cell then set the timer and the graduated cylinder ready to collect the filtrate volumes at the different slots of 1.0, 7.5, 15, 20, 25, and 30 min. At the end of each measurement, the remaining fluids were removed and the filter cake formed was now taken for Field Emission-Scanning Electron Microscopy (FE-SEM, an FEI QuantaTM 3D FEG dual beam SEM/FIB system, Hillsboro, OR) at a 20 kV accelerating voltage). The filter cake has been dried overnight at 30°C in the oven and spin-coated with gold before observations, then brought to FE-SEM to observe the small structure (as small as 1 nm) on their surfaces and cross-sectional microstructure. The surface morphology of each filter cake was performed using field emission scanning electron microscopy (FE-SEM, an FEI Quanta TM 3D FEG dual beam SEM/FIB system, Hillsboro, OR) at a 20 kV accelerating voltage.

CHAPTER 4. CELLULOSE NANOCRYSTALS BENTONITE WATER-BASE DRILLING FLUIDS

4.1. ANALYSIS OF RHEOLOGICAL PROPERTIES OF CNC/BT-WDFs (FW)

4.1.1. RHEOLOGICAL CURVES AT DIFFERENT CNC CONCENTRATION FOR VARIOUS TEMPERATURES

The rheological properties of the types of water-based drilling fluids (fresh water and seawater) were measure using the rheometer named "RheolabQC SN897839/FW1.31" with RHEOPLUS/32 V3.62 21002331-33025 as the application from Anton Paar, Germany. The plots of the variation of shear stress as a function of shear rate for CNC/BT-WDFs in fresh water at different CNC concentrations are depicted in figure 25. All the plots in figure 25 showed a strong dependence of the shear stress on the shear rate and the concentration of CNCs. The higher the shear rate, the higher the shear stress. The increase of CNC concentration from 0.2 to 2.4 wt. % eventually affected the shear stress that increased as well.

Generally speaking, figure 25 showed the variation of shear stress as a function of shear rate for CNC/BT-WDFs in fresh water at different CNCs concentrations. It is observed for all graphs at the highest shear rate 1200 s^{-1} that the shear stress increased with increasing CNC concentrations. As it is observed in Figure 25(A), the shear stress increased from 21.7 Pa at 0 wt. % to 19.1, 22.3, 20.4, 21.7, 28.4 and 36.2 Pa at 0.4, 0.8, 1.2, 1.6, 2.0 and 2.4 wt. % respectively at 20˚C; Figure 25(B), the shear stress increased from 21.4 Pa at 0.0 wt. % to 20.4, 20.7, 21.4, 25.3, 30.3 and 39.7 Pa at 0.4, 0.8, 1.2, 1.6, 2.0 and 2.4wt % respectively at 30˚C; Figure 25(C), the shear stress increased from 19.6 Pa at 0.0 wt. % to 19.6, 20.6, 20.8, 24.4, 29.7 and 36.1 Pa at 0.4, 0.8, 1.2, 1.6, 2.0 and 2.4 wt. % respectively at 40˚C; Figure 25(D), the shear stress increased from 20.9 Pa to 19.1, 18.7, 20.8, 21.9, 31 and 33.6 Pa at 0.4, 0.8, 1.2, 1.6, 2.0 and 2.4wt % respectively at 50˚C; Figure 25(E), the shear stress increased from 18.9 Pa at 0.0 wt. % to 18.8, 20.1, 20.9, 23.5, 30 and 35.4 Pa at 0.4, 0.8, 1.2, 1.6, 2.0 and 2.4wt % respectively at 60˚C; Figure 25(F), the shear stress increased from 19.3 Pa at 0.0 wt. % to 18.5, 19.7, 20, 21.8, 29.3 and 35.3 Pa at 0.4, 0.8, 1.2, 1.6, 2.0 and 2.4wt % respectively at 70˚C; and Figure 25(G), the shear stress increased from 18.6 Pa at 0.0 wt. % to 17.9, 18.5, 19.2, 21, 26.1 and 33 Pa at 0.4, 0.8, 1.2, 1.6, 2.0 and 2.4wt % respectively at 80˚C. From figure 25, it is clear that the shear stress is enhanced with the increase in CNC concentration demonstrating the requirement of the high force to start the flow of the fluids.

Rheological parameters obtained after fitting the rheological data of CNC/BT-WDFs (FW) describe the strongest dependence of y_o and K on the CNC concentrations. In figure 25(A), it is shown that the yield stress values (y_o) increase from the control BT-WDFs (FW) up until the CNC concentration was gradually added. However, from figure 25(B) to 25(G), it is shown that y_o values of the control were higher than that of the first CNC concentration added and started to increase as CNC concentration was added in the mud system. The Herschel-Bulkley as a complex rheological model with three parameters describes accurately the rheological behavior of the present mud system. It fitted very well all the experimental data shown in figure 25. It was appropriated to describe the rheological behavior for CNC/BT-WDFs in freshwater based on the results in table 2. These results demonstrate that there is a high correlation between shear stress and shear rate as R^2 values are closer to 1 (R^2>0.99). Thus, table 2 indicates that the correlation coefficient of the regression model (R^2) was greater than 0.99.

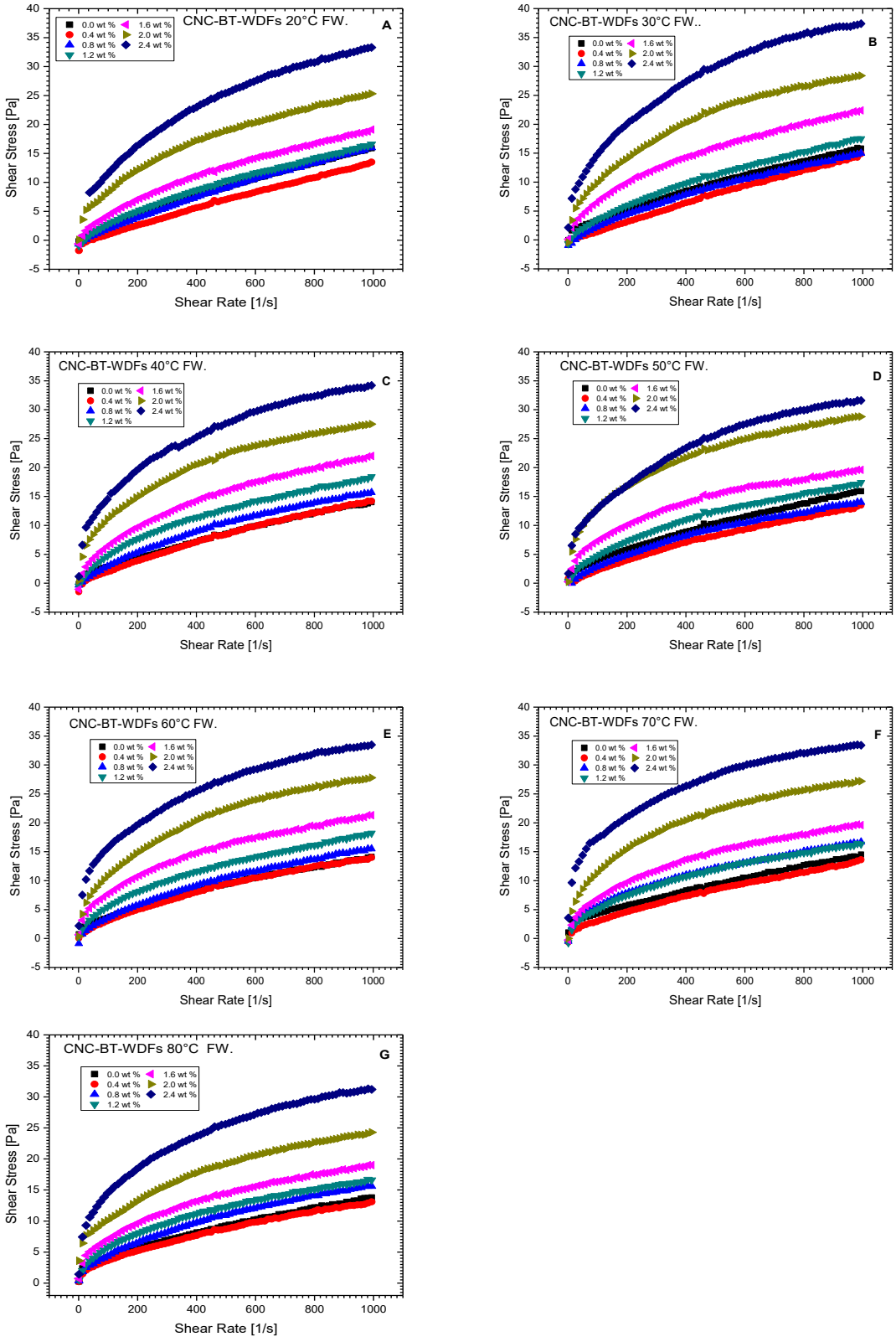

Figure 25. The plots A, B, C, D, E, F and G of the variation of shear stress against shear rate for CNC/BT-WDFs (FW) at various CNC concentrations at different temperatures.

Table 2. . Calculated parameters CNC/BT-WDFs (FW) at various CNC Concentrations for different temperature using Herschel-Bulkley (HB) Models.

T(°C)	CNC Conc (wt. %)	y_o (Pa)	K(Pa.S)	n	R^2	RMSD	SSR
20°C	0.0	0,00608	0,05739	0,8153	0,99979	0,06542	0,34242
	0.4	0,13734	0,01638	0,97421	0,9937	0,31698	8,03799
	0.8	0,22112	0,05565	0,82495	0,99134	0,43532	15,1601
	1.2	0,12248	0,10121	0,7393	0,99781	0,21618	3,73878
	1.6	0,13175	0,27021	0,61765	0,99854	0,19295	2,97832
	2.0	0,25704	1,06391	0,46054	0,99797	0,27136	5,8909
	2.4	0,42066	1,63167	0,43967	0,99714	0,4204	14,13915
30°C	0.0	0,61389	0,09419	0,8153	0,99904	0,12999	1,35173
	0.4	0,20926	0,03372	0,88408	0,98963	0,44062	15,53136
	0.8	0,18182	0,10542	0,71862	0,99464	0,31178	7,77652
	1.2	0,12127	0,17148	0,67206	0,99836	0,19409	3,01363
	1.6	0,16714	0,6508	0,51362	0,99871	0,20001	3,20034
	2.0	0,57849	1,38636	0,44286	0,99287	0,58314	27,20375
	2.4	0,66015	2,40737	0,40282	0,99528	0,59337	28,16686
40°C	0.0	0,5 421	0,06194	0,78194	0,99843	0,15129	1,83105
	0.4	0,16471	0,06618	0,78262	0,99438	0,30781	7,57955
	0.8	0,17325	0,1498	0,67776	0,99597	0,27973	7,57955
	1.2	0,2058	0,39535	0,55737	0,99676	0,26972	5,82008
	1.6	0,28355	0,66852	0,5095	0,99631	0,33625	9,04514
	2.0	0,56269	1,9382	0,38849	0,99401	0,48353	18,70414
	2.4	0,55496	2,85019	0,36373	0,99654	0,43873	15,39849
50°C	0.0	0,72835	0,14079	0,67804	0,99933	0,10528	0,88669
	0.4	0,21232	0,1022	0,70971	0,99076	0,35947	10,33742
	0.8	0,1877	0,17724	0,63566	0,99461	0,2834	6,42533
	1.2	0,18919	0,42736	0,53806	0,99708	0,23849	4,55038
	1.6	0,34961	1,11332	0,41817	0,99479	0,32895	8,65648
	2.0	0,54259	2,61528	0,35066	0,99564	0,40913	13,39107
	2.4	0,60989	2,22306	0,38957	0,99459	0,52591	22,12623
60°C	0.0	0,88677	0,13052	0,66975	0,99811	0,15453	1,91032
	0.4	0,11753	0,16817	0,64302	0,99776	0,17962	2,58114
	0.8	0,12177	0,21977	0,61912	0,99813	0,17879	2,55732
	1.2	0,10862	0,54525	0,50812	0,99917	0,12841	1,3192
	1.6	0,21066	1,12836	0,42692	0,99829	0,20325	3,30468
	2.0	0,54381	1,76326	0,40424	0,99421	0,49092	19,27981
	2.4	0,48696	3,38336	0,33543	0,99752	0,34639	9,59915
70°C	0.0	2,17026	0,05895	0,77313	0,99715	0,18233	2,65952
	0.4	0,47115	0,10221	0,70042	0,99926	0,09454	0,71507
	0.8	0,09435	0,66244	0,4666	0,99933	0,10114	0,81833
	1.2	0,1434	0,54709	0,4945	0,99833	0,16438	2,16156
	1.6	0,25621	0,91537	0,44704	0,99691	0,26117	5,4569
	2.0	0,61807	2,20427	0,36818	0,99332	0,4963	19,70476
	2.4	0,60464	4,55945	0,29192	0,99694	0,35598	10,13779
80°C	0.0	1,20019	0,15046	0,64053	0,9974	0,16858	2,27363
	0.4	0,45003	0,19421	0,60474	0,99895	0,10619	0,90203
	0.8	0,05631	0,36765	0,54473	0,99913	0,11624	1,08086
	1.2	0,1089	0,70662	0,45904	0,99916	0,11453	1,04939
	1.6	0,15296	1,05649	0,41981	0,99888	0,14461	1,67302
	2.0	2,25638	1,17446	0,42706	0,99645	0,30259	7,32485
	2.4	0,44725	3,11696	0,33738	0,99759	0,3206	8,22291

The corresponding rheological and statistical parameters are summarized in to table 2 below. It showed that the increase in CNC concentration from 0.0 wt. % to 2.4 wt. % was slightly decreasing R^2 at the same temperature and SSR/RMSD values were gradually increased from R^2 = 0,99979 at 0.0 wt. % to R^2 = 0,99714 at 2.4 wt. % and SSR = 0,34242 / RMSD = 0,06542 at 0.0 wt. % to SSR = 14,13915 / RMSD = 0,4204 at 2.4 wt. % for 20˚C; R^2 = 0,99904 at 0.0 wt. % to

R^2 = 0,99528 at 2.4 wt. % and SSR = 1,35173 / RMSD = 0,12999 at 0.0 wt. % to SSR = 28,16686 / RMSD = 0,59337 at 2.4 wt. % for 30˚C; R^2 = 0,99843 at 0.0 wt. % to R^2 = 0,99654 at 2.4 wt. % and SSR = 1,83105 / RMSD = 0,15129 at 0.0 wt. % to SSR = 15,39849 / RMSD = 0,43873 at 2.4 wt. % for 40˚C; R^2 = 0,99933 at 0.0 wt. % to R^2 = 0,99459 at 2.4 wt. % and SSR = 0,88669 / RMSD = 0,10528 at 0.0 wt. % to SSR = 22,12623 / RMSD = 0,52591 at 2.4 wt. % for 50˚C; R^2 = 0,99811 at 0.0 wt. % to R^2 = 0,99752 at 2.4 wt. % and SSR = 1,91032 / RMSD = 0,15453 at 0.0 wt. % to SSR = 9,59915 / RMSD = 0,34639 at 2.4 wt. % for 60˚C; R^2 = 0.99715 at 0.0 wt. % to R^2 = 0,99694 at 2.4 wt. % and SSR = 2,65952 / RMSD = 0,18233 at 0.0 wt. % to SSR = 10,13779 / RMSD = 0,35598 at 2.4 wt. % for 70˚C; and R^2 = 0.9974 at 0.0 wt. % to R^2 = 0,99759 at 2.4 wt. % and SSR = 2,27363 / RMSD = 0,16858 at 0.0 wt. % to SSR = 8,22291 / RMSD = 0,3206 at 2.4 wt. % for 80˚C; this illustrated that the relationship between shear stress and shear rate was nonlinear.

Generally speaking, the higher the concentration, the higher the yield stress at each set of temperatures. Besides, table 2 shows the impact of the temperature on the yield stress. At the same concentration, the control mud system shows an increase of the yield stress with increasing temperature. The same applied CNC concentration is added into the control BT-WDFs (FW) to get CNC/BT-WDFs (FW). This improvement of the yield stress facilitates the transportation of the cuttings into the mud system. As the yield stress represents the minimum stress needed to move the mud system, it will be disadvantageous to handle mud systems with a great value of the yield stress, as much energy will be needed for pumping the fluid down through the wellbore (Lummus & Azar 1986; Nwosu et al 2014; Li et al 2015).

Due to the impact of the effect of the energy on the transportation of the drilling cuts, 1.2 wt. % was selected from table 2 as the optimum concentration of CNCs to be used in CNC/BT-WDFs (FW) during drilling operation in the offshore well.

4.1.2. RHEOLOGICAL CURVES AT DIFFERENT TEMPERATURES FOR VARIOUS CNC CONCENTRATIONS

From figure 26 below, plots A, B, C, D, E, F, and G showed the variation of shear stress with the shear rate for CNC/BT-WDFs in fresh water at different temperatures for various CNC concentrations. It can be seen that at the high shear rate, there is no significant trend as the temperature increased at different CNC concentrations from the control BT-WDFs to 1.6 wt. % CNCs added followed by a slight variation of shear stress as the temperature was increasing. This is evidence of thermal stability of CNC/BT-WDFS (FW) as the shear stress did not vary much with increased temperature.

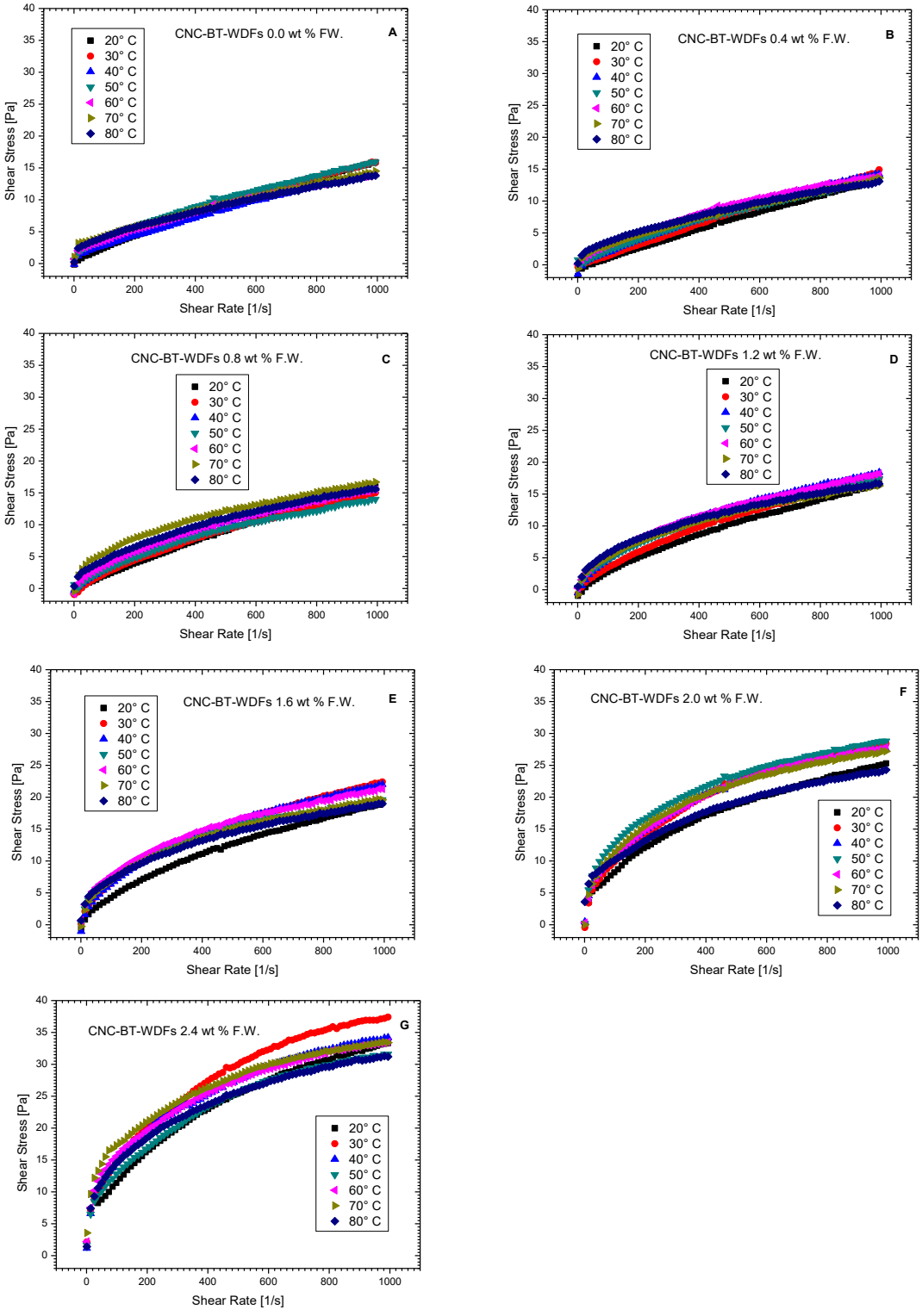

Figure 26.The plots A, B, C, D, E, F, G and H of shear stress as a function of shear rate for CNC/BT-WDFs (FW) at various temperatures for different CNC concentrations.

The rheological data based on the variation of the shear stress with the temperature at the high shear rate and various CNC concentrations for CNC/BT-WDFs (FW) was recorded in table 3 below. The graphical representation of table 3 is drawn in figure 27 below.

Table 3. Variation of shear stress of CNC/BT-WDFs (FW) with temperature at different CNC concentrations determined at high shear rate (1200 s^{-1}).

Temperature	Shear Rate	Shear Stress	Shear Stress	Shear Stress	Shear Stress	Shear Stress	Shear Stress	Shear Stress
[°C]	[1/s]	[Pa]	[Pa]	[Pa]	[Pa]	[Pa]	[Pa]	[Pa]
		BT-CNC-WDFs(FW) (0.0 wt % CNC)	BT-CNC-WDFs(FW) (0.4 wt % CNC)	BT-CNC-WDFs(FW) (0.8 wt % CNC)	BT-CNC-WDFs(FW) (1.2 wt % CNC)	BT-CNC-WDFs(FW) (1.6 wt % CNC)	BT-CNC-WDFs(FW) (2.0 wt % CNC)	BT-CNC-WDFs(FW) (2.4 wt % CNC)
20	1 200	21,7	19,1	22,3	20,4	21,7	28,4	36,2
30	1 200	21,4	20,4	20,7	21,4	25,3	30,3	39,7
40	1 200	19,6	19,6	20,6	20,8	24,4	29,7	36,1
50	1 200	20,9	19,1	18,7	20,8	21,9	31	33,6
60	1 200	18,9	18,8	20,1	20,9	23,5	30	35,4
70	1 200	19,3	18,5	19,7	20	21,8	29,3	35,3
80	1 200	18,6	17,9	18,5	19,2	21	26,1	33

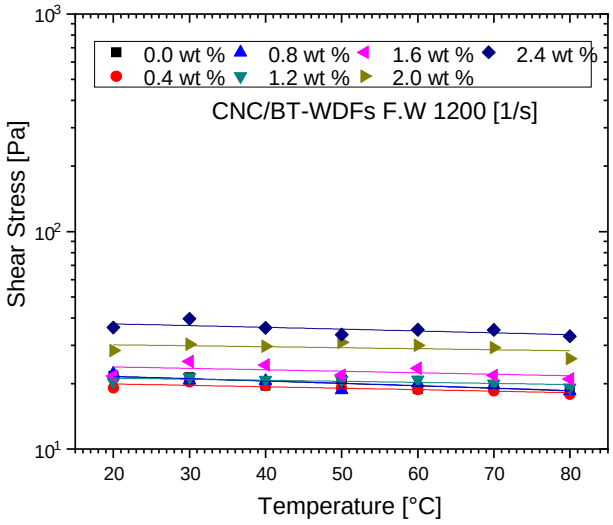

Figure 27. The plot of the variation of shear stress against temperature for CNC/BT-WDFs (FW) at various CNC concentrations taken at high shear rate 1200 s^{-1}.

Figure 27 shows at the higher shear rate (1200 s^{-1}) and particular CNC concentration, a decrease of the shear stress as the temperature was increasing that led to the decrease of the viscosity of CNC/BT-WDFs (FW) as well in figure 32. This decrease in the viscosity confirms the shear-thinning behavior of CNC/BT-WDFs (FW). This decrease of the shear stress with increasing temperature is attributed to the thermal dispersion and thermal dehydration of the bentonite clay particles in the suspension. This means dispersion and dehydration due to the effect of temperature. However, the plastic viscosity, related to the measurement of the internal resistance to flow owing to the type, size, and amount of solids in the drilling fluids, increased with the degree of dispersion of solid particles whereas its structural viscosity decreased with increasing shear rate. Despite this increase in plastic viscosity, the decrease in structural viscosity remained higher that led to the fast reduction of the shear stress with increasing temperature at a high shear rate (Wang et al 2012).

Renken & Meechan (1995) established the energy equation that accounts for the thermal dispersion effect which highlights the influence that the flow variation has on temperature. Popp & Kern (1993) observed that progressive thermal dehydration reactions induce an opening of pore space accompanied by lowered saturation conditions whereby the rate of fluid release depends mainly on temperature and also on the drainage conditions of the system. The dehydration behavior of the various hydrous rock types was found to be different because the changes in the rock physical properties are closely linked to the internally created pore fluid, the changes in the porosity and pore geometry, and the resulting pore pressure.

Furthermore, it is observed at a high shear rate that the increase of the temperature leads to a very slight decrease of shear stress. This result confirms the higher stability of CNC/BT-WDFs (FW) with increasing temperatures from 20 to 80°C. The temperature effect has almost not affected the stability of CNC/BT-WDFs (FW).

4.1.3. THE EFFECT OF CNC CONCENTRATION ON THE VISCOSITY OF CNC/BT-WDFs (FW) AS DRILLING FLUID

Figure 28 shows plots of viscosity of CNC/BT-WDFs (FW) as a function of shear rate at various CNC concentrations for different temperatures. In figure 28(A), the variation of viscosity against the shear rate at different CNC concentrations at 20°C depicts different trends. Without CNC, the BT-WDFs displayed a very low viscosity value at a low shear rate and yielded a poor shear thinning behavior with a slight decrease of viscosity as the shear rate increases. A poor surface interaction was exhibited with BT-WDFs in the absence of CNCs molecules. For this reason, the viscosity remained lower at a low shear rate. Gradually addition of CNCs on BT-WDFs (FW) modified the pattern of the rheograms. However, comparing with the control, the addition of CNC concentration from 1.2 to 0.4 wt. % was decreasing the viscosity of CNC/BT-WDFs (FW) at the lower shear rate (0.999 s^{-1}) then followed by a slight increase in viscosity as the shear rate was increasing, and reached a plateau at the high shear rate (100 s^{-1}) then a slight decreased was observed for 1.2 wt. % of CNCs. From 1.6 wt. % of CNCs, it was observed a low viscosity at the low shear rate (0.999 s^{-1}). This viscosity increased with increasing shear rate (13 s^{-1}) and displayed a viscosity above the control. This viscosity was decreasing gradually as the shear rate was increasing tending to the higher values. At 2.0 and 2.4 wt. % of CNC concentrations, CNC/BT-WDFs (FW) exhibited low viscosity at high shear rates whereas at low shear rates a high viscosity was observed which are commonly known as shear-thinning fluids. The CNC/BT-WDFs (FW) yielded nearly linear shear-thinning curves that improved the shear-thinning behavior revealed by the potential use of CNC additive as an effective rheological modifier for drilling fluids. As observed at higher CNC concentrations nearly linear shear-thinning curves were observed indicating the transformation of CNC dispersions from anisotropic to isotropic as the surface interaction was enhanced. This increase of the viscosity with CNCs at the appropriate 6 wt. % of BT concentration leads to the enhancement of the shear-thinning behavior of CNC/BT-WDFs (FW) which was advantageous for drilling fluid application (Li et al 2016). From figure 28(B) to 28(D), the flow curves of 0.4, 0.8, and 1.2 wt. % of CNCs continued to exhibit a plateau followed by a slight decrease of the viscosity at the high shear rate. Contrary, at high CNC concentration (1.6 to 2.4 wt. %) nearly linear shear-thinning curves were observed approving the shear-thinning behavior of CNC/BT-WDFs (FW). From figure 28(E) to 28(G), good performance has been seen as nearly all the flow curves exhibited nearly linear shear-thinning behavior. The viscosity decreased over the broad range of the shear rates.

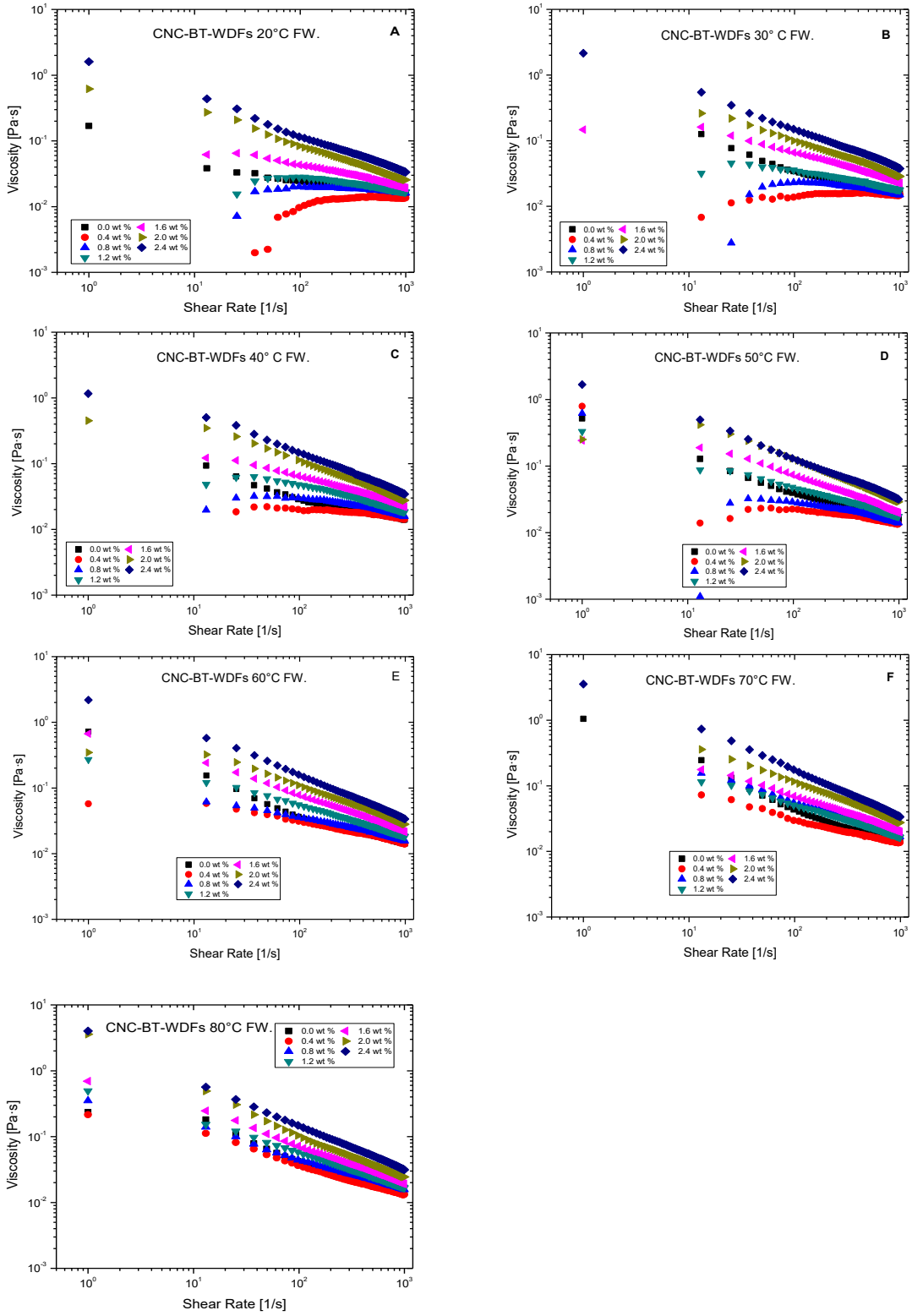

Figure 28. The plots of viscosity as a function of shear rate for CNC/BT-WDFs (FW) at various CNC concentrations for different temperatures.

Therefore, it is denoted that at 0.4 to 0.8 wt. % of CNC concentrations, CNC/BT-WDFs (FW) exhibited low viscosity than BT-WDFs (FW) along with all the range of the shear rate. Nevertheless, from 1.2 to 2.4 wt. % of CNC concentrations, CNC/BT-WDFs (FW) displayed high viscosity value along with all the range of the shear rate that was above the control viscosity value. This gives the profound shear-thinning behavior as the viscosity was decreasing with increasing shear rates. The shear-thinning behavior is commonly attributed to the non-Newtonian fluids having high viscosity at low shear rates to improve the carrying capacity or suspension of the drilled cuttings from the wellbore followed by the low viscosity at high shear rates to allow the fast pumping of the fluid into the bottom of wellbores as well as to facilitate the release of the drilled cuttings.

Generally speaking, it is denoted that the viscosity of CNC/BT-WDFs (FW) increased exponentially with the increase in the CNC concentrations as seen in figure 29. However, at the lowest shear rate (0.999 s^{-1}), the first flow curve (at 20°C) showed that the viscosity of the CNC/BT-WDFs (FW) increased from 0.169 Pa.s at 0.0 wt. % of CNC to 1.79, 0.649, 0.973, 0.617, 0.434 and 1.6 Pa.s at 0.4, 0.8, 1.2, 1.6, 2.0, and 2.4 wt. % of CNCs respectively; the second flow curve (at 30°C) showed that the viscosity increased from 0.009 Pa.s at 0.0 wt. % of CNC to 0.323, 0.649, 0.644, 0.147, 0.434 and 2.15 Pa.s at 0.4, 0.8, 1.2, 1.6, 2.0 and 2.4 wt. % of CNCs respectively; the fourth flow curve (at 40°C) showed that the viscosity increased from 0.113 Pa.s at 0.0 wt. % of CNC to 1.46, 0.301, 0.49, 1.04, 0.45 and 1.16 Pa.s at 0.4, 0.8, 1.2, 1.6, 2.0 and 2.4 wt. % of CNCs respectively; the fifth flow curve (at 50°C) showed that the viscosity increased from 0.52 Pa.s at 0.0 wt. % of CNC to 0.792, 0.622, 0.33, 0.242, 0.251 and 1.68 Pa.s at 0.4, 0.8, 1.2, 1.6, 2.0 and 2.4 wt. % of CNCs respectively; the sixth flow curve (at 60°C) showed that the viscosity increased from 0.718 Pa.s at 0.0 wt. % of CNC to 0.0572, 0.866, 0.27, 0.668, 0.346 and 2.19 Pa.s at 0.4, 0.8, 1.2, 1.6, 2.0 and 2.4 wt. % of CNCs respectively; the seventh flow curve (at 70°C) showed that the viscosity increased from 1.05 Pa.s at 0.0 wt. % of CNC to 0.619, 0.46, 0.742, 0.262, 4.32E-4 and 3.55 Pa.s at 0.4, 0.8, 1.2, 1.6, 2.0 and 2.4 wt. % of CNCs respectively; and the eighth flow curve (at 80°C) showed that the viscosity increased from 0.236 Pa.s at 0.0 wt. % of CNC to 0.215, 0.352, 0.494, 0.693, 0.359 and 1.42 Pa.s at 0.4, 0.8, 1.2, 1.6, 2.0 and 2.4 wt. % of CNCs respectively.

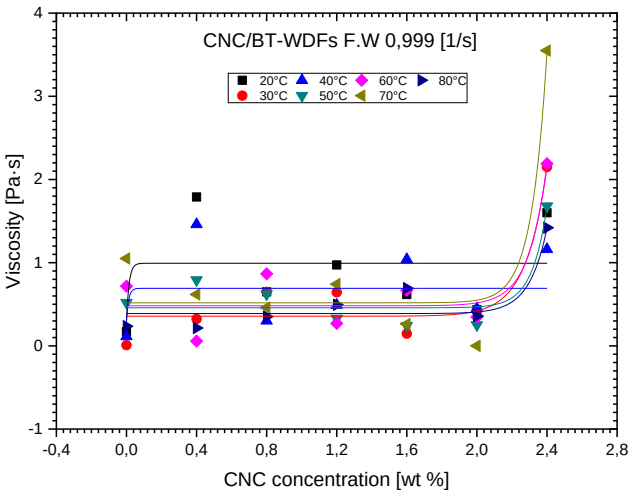

Figure 29. Variation of viscosity of CNC/BT-WDFs (FW) with CNC concentration at different temperature (0.999 s^{-1}) using Herschel-Bulkley (HB) models.

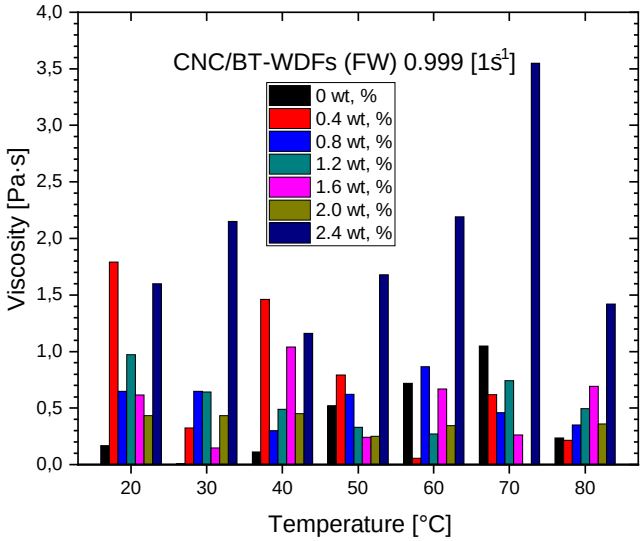

Figure 30. Viscosity of CNC/BT-WDFs (FW) at various CNC concentrations for different temperature.

The rheological data collected and represented in figure 30 describes the variation of viscosity as a function of temperatures at different CNC concentrations. This confirms the rise of the viscosity with increasing CNC concentrations at a low shear rate.

4.1.4. THE EFFECT OF TEMPERATURE ON THE VISCOSITY OF CNC/BT-WDFs (FW) AS DRILLING FLUID

The following figure 31 depicts the variation of viscosity as a function of the shear rate of CNC/BT-WDFs in freshwater for different CNC concentrations at various temperatures. The plot (A) has shown the variation of the viscosity of BT-WDFs (FW) without CNCs as a function of shear rate at various temperatures. The viscosity decreased with an increase of the shear rate that revealed the shear-thinning behavior of BT-WDFs. The drilling fluid exhibited low viscosity at a high shear rate but high viscosity at a low shear rate, which is commonly known as shear-thinning fluid. This shear-thinning phenomenon becomes more significant as the concentration of CNCs and temperature increase in the mud system from 0.4 to 2.4 wt. % and from 20°C to 80°C respectively. At a low shear rate (0.999 s^{-1}), the plots showed an increase in the viscosity at various temperatures. In figure 31, CNC/BT-WDFs (FW) exhibited nearly linear shear-thinning behavior as followed: for the plot (B) and (C) at CNC concentration of 0.4 and 0.8 wt. % from 60°C to 80°C; for the plot (D) and (E) at CNC concentrations of 1.2 and 1.6 wt. % from 50°C to 80°C; and for the plot (F) and (H) at CNC concentrations of 2.0 and 2.4 wt. %, it is shown through all over the temperature range a notable increase in the viscosity above the control BT-WDFs. However, all the temperature variation on the drilling fluid (CNC/BT-WDFs in freshwater) below 60°C dealing with 0.4, 0.8, 1.2 and 1.6 wt. % for the one below 50°C, were not appreciable as their viscosities were increasing with the increase in shear rate leading to a shear thickening behavior. Thus, these rheological curves exhibited a shear thickening behavior that limited their application in the drilling fluid field as they could not be pumped under the borehole.

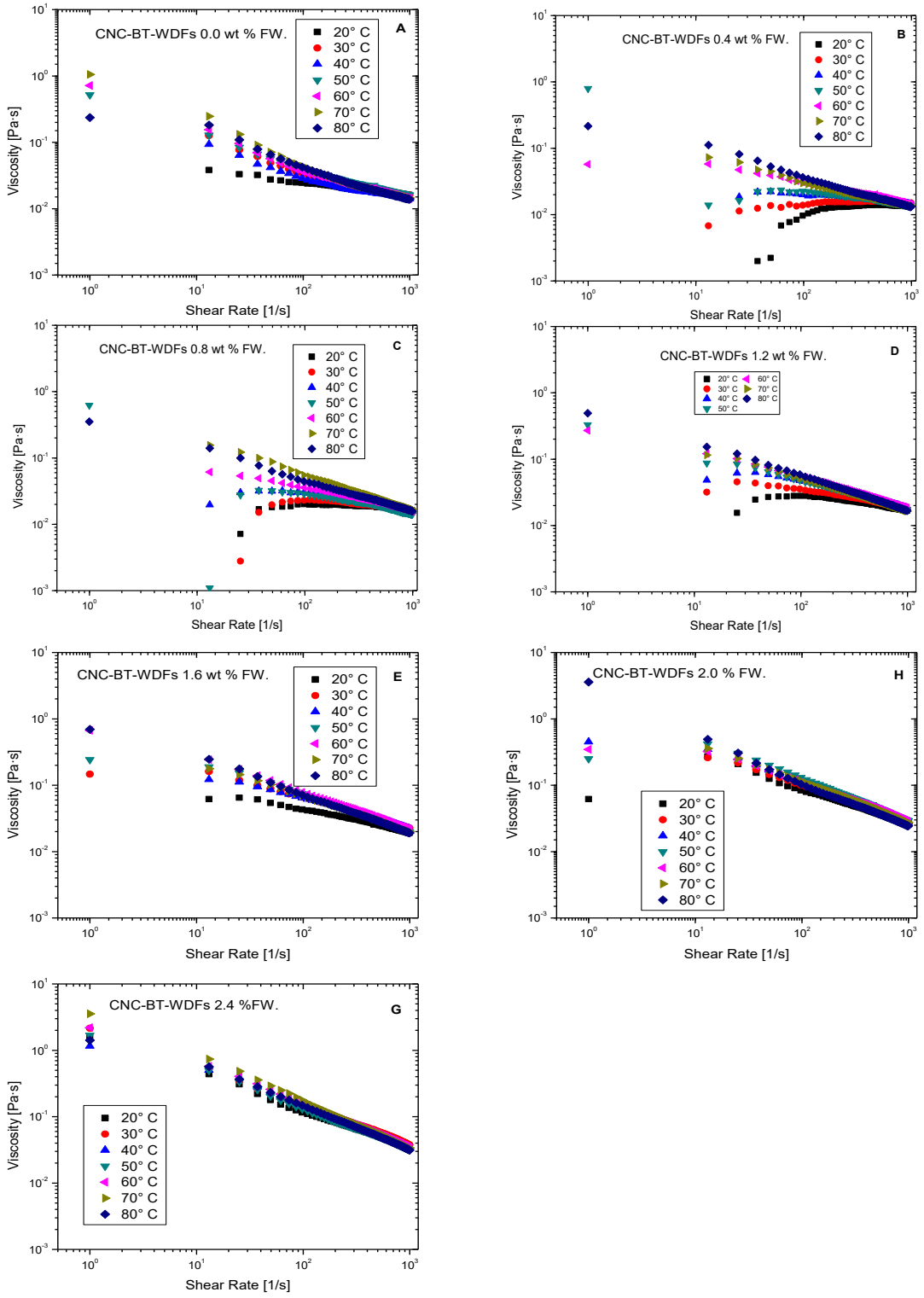

Figure 31. The plot of viscosity as a function of shear rate for CNC/BT-WDFs (FW) at various temperatures for different CNC concentrations.

Therefore, the temperature can modify the viscosity and play a role in the drilling fluid selection used in the wellbore. The only problem that remained is an excess of temperature from the wellbore that could damage the drilling fluids and lost their intrinsic properties then become useless. Thus, they should be managed with care. The shear-thinning behavior performs well at the highest temperature of 80°C without any observed damage or deformation of the flow curve. Therefore, the 80°C is well-suitable for good drilling fluid application.

Table 4. Variation of viscosity of CNC/BT-WDFs (FW) with temperature at different CNC concentration, determined at low shear rates (0.999 s^{-1}).

Temperature	Shear Rate	Viscosity	Viscosity	Viscosity	Viscosity	Viscosity	Viscosity	Viscosity	Viscosity
[°C]	[1/s]	[Pa·s]	[Pa·s]	[Pa·s]	[Pa·s]	[Pa·s]	[Pa·s]	[Pa·s]	[Pa·s]
		BT-CNC-WDFs(FW) (0.0 wt % CNC)	BT-CNC-WDFs(FW) (0.4 wt % CNC)	BT-CNC-WDFs(FW) (0.8 wt % CNC)	BT-CNC-WDFs(FW) (1.2 wt % CNC)	BT-CNC-WDFs(FW) (1.6 wt % CNC)	BT-CNC-WDFs(FW) (2.0 wt % CNC)	BT-CNC-WDFs(FW) (2.4 wt % CNC)	BT-CNC-WDFs(FW) (4.0 wt % CNC)
20	0,999	0,169	1,79	0,649	0,973	0,617	0,0617	1,6	7,55
30	0,999	0,009	0,323	0,954	0,644	0,147	0,434	2,15	6,12
40	0,999	0,113	1,46	0,301	0,49	1,04	0,45	1,16	8,02
50	0,999	0,52	0,793	0,622	0,33	0,242	0,251	1,68	9,61
60	0,999	0,718	0,0575	0,866	0,27	0,668	0,346	2,19	9,69
70	0,999	1,05	0,619	0,46	0,742	0,262	4,32E-4	3,55	11,8
80	0,999	0,236	0,215	0,352	0,494	0,693	3,59	1,42	8

Table 5. Variation of viscosity of CNC/BT-WDFs (FW) with temperature at different CNC concentration, determined from high shear rates (1200 s^{-1}).

Temperature	Shear Rate	Viscosity	Viscosity	Viscosity	Viscosity	Viscosity	Viscosity	Viscosity	Viscosity
[°C]	[1/s]	[Pa·s]	[Pa·s]	[Pa·s]	[Pa·s]	[Pa·s]	[Pa·s]	[Pa·s]	[Pa·s]
		BT-CNC-WDFs(FW) (0.0 wt % CNC)	BT-CNC-WDFs(FW) (0.4 wt % CNC)	BT-CNC-WDFs(FW) (0.8 wt % CNC)	BT-CNC-WDFs(FW) (1.2 wt % CNC)	BT-CNC-WDFs(FW) (1.6 wt % CNC)	BT-CNC-WDFs(FW) (2.0 wt % CNC)	BT-CNC-WDFs(FW) (2.4 wt % CNC)	BT-CNC-WDFs(FW) (4.0 wt % CNC)
20	1 200	0,0181	0,0159	0,0186	0,017	0,0181	0,0237	0,0302	0,0688
30	1 200	0,0178	0,017	0,0173	0,0179	0,0211	0,0253	0,0331	0,0703
40	1 200	0,0163	0,0164	0,0171	0,0174	0,0203	0,0247	0,0301	0,0658
50	1 200	0,0174	0,0159	0,0156	0,0174	0,0183	0,0258	0,028	0,0641
60	1 200	0,0157	0,0157	0,0168	0,0174	0,0196	0,025	0,0295	0,0639
70	1 200	0,0161	0,0154	0,0164	0,0167	0,0181	0,0244	0,0294	0,0632
80	1 200	0,0155	0,0149	0,0154	0,016	0,0175	0,0217	0,0275	0,0599

The rheological data from the HB model resumed, in tables 4-5, give the value of the viscosity of CNC/BT-WDFs (FW) as a function of temperature at different CNC concentrations, low and high shear rates. Those two figures included in figure 32 derived from tables 4-5 can describe in a specific way the temperature effect on the viscosity of CNC/BT-WDFs (FW) at different CNC concentrations, low and high shear rate. The statistical data analysis by performing a linear fitting results with different slope values as CNC concentration was varied at low shear rate (0.999 s^{-1}) as seen in figure 32(A): 0.01031 ± 0.0063, -0.01977 ± 0.01021, -0.00469 ± 0.00469, -0.00522 ± 0.00448, 3.07143E-4 ± 0.00662, -2.82986E-4 ± 0.00368 and 0.01175 ± 0.01551 for 0.0, 0.4, 0.8, 1.2, 1.6, 2.0 and 2.4 wt. % respectively. The negative slope value stands for a decrease in the viscosity, while the positive slope value stands for an increase. It seems like without the addition of CNC, the viscosity of the control BT-WDFs was quite unstable as a change in the temperature at a low shear rate offers a positive slope value. However, a great negative slope value also exhibited poor thermal stability. Therefore, samples of 0.4, 0.8, 1.2, and 2.0 wt. % CNC concentrations with low negative slope exhibited good thermal stability at the low shear rate as viscosity was almost constant with increasing temperature.

The drilling operations necessary require a drilling fluid with shear-thinning behavior that means drilling fluid reducing their viscosity with increasing temperature should be used during drilling operations. Thus, all drilling fluids with a positive slope or increasing viscosity with the increase of temperature are useless in the drilling operation.

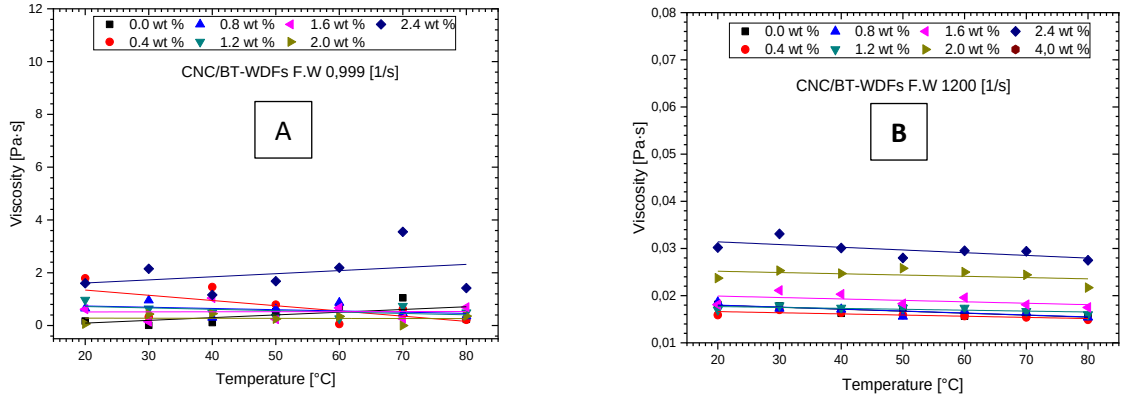

Figure 32. The plot of the viscosity of CNC/BT-WDFs (FW) as a function temperature at various CNC concentrations at low and high shear rate (0.999 s^{-1} and 1200 s^{-1}).

The result shows only CNC/BT-WDFs (FW) at CNC concentrations 0.4, 0.8, 1.2, and 2.0 wt. % with negative slope values develop consistence resistance in temperature change at low shear allowing the carrying capacity of the cuttings. On the other hand, the statistical data analysis by performing a linear fitting offered different slope values as CNC concentration at high shear rate (1200 s^{-1}) as seen in figure 32(B): -4.21429E-5 ± 1.08468E-5, -2.46429E-5 ± 8.65289E-6, -4.17857E-5 ± 1.26158E-5, 1.92857E-5 ± 9.43831E-6, -3.03571E-5 ± 2.426E-5, -2.67857E-5 ± 2.5334E-5 and -5.75E-5 ± 2.74787E-5 for 0.0, 0.4, 0.8, 1.2, 1.6, 2.0 and 2.4 wt. % respectively. It shows that at the high shear rate, all slopes present low negative values. Their viscosities are well maintained over a wide temperature range due to the rigid network formed between the CNC, BT layers, and immobilized water molecules. These water molecules were merely entrapped within the core-shell structure and immobilized at the vicinity of CNCs. It results in great resistance to temperature changes. In fact, during the drilling operation of the deeper well, the excessive friction between the drill bit and the formation released much heat resulting in a significant increase in the wellbore temperature. From the perspective of the performance of the drilling fluids in the cutting transportation, it is worthy to prepare a mud system with minimum temperature effect. A low-temperature effect on the viscosity demonstrates the resistance of the drilling fluid. This resistance of the drilling fluid is due to the strong surface interaction of CNC/BT-WDFs (FW). By studying the effect of temperature change on viscosity, there is usually a decrease in viscosity as the temperature increases due to the increased mobility of water molecules. This confirms the CNC/BT-WDFs (FW) at CNC concentration of 1.2 wt % as the optimum concentration to be used in the drilling operation for the lowest effect of the temperature on the viscosity (low slope value: -1.92857E-5 ± 9.43831E-6) showing the greatest resistance of the drilling fluid against the rise of the temperature.

4.2. ANALYSIS OF THE RHEOLOGICAL PROPERTIES OF CNC/BT-WDFs (SW)

4.2.1. RHEOLOGICAL CURVES AT DIFFERENT CNC CONCENTRATIONS FOR VARIOUS TEMPERATURES.

The rheological properties analysis of CNC/BT-WDFs in seawater was conducted in the same condition as for CNC/BT-WDFs in freshwater. The plots of the variation of shear stress against shear rate for CNC/BT-WDFs in seawater at different CNC concentrations are illustrated in figure 33. From shear stress versus shear rate flow curves in figure 33, an enhancement of the shear stress with increasing CNC concentration is observed, indicating the requirement of higher force to start the flow of the fluids. Particularly for this case, the enhancement is observed from dilatant flow curves to shear-thinning flow curves by increasing CNC concentrations. This improvement in the shear stress is due to the highly entangled CNC able to retain the bentonite particles, which leads to the formation of a flexible three-dimensional network throughout the mud system. It is observed that the presence of seawater, salt as a contaminant significantly affects the rheological properties and filtration of CNC/BT-WDFs. At a range of CNC concentration from 0.0 wt. % to 1.6 w % dilatant curves with n>1 as are shown from all plots in figure 33.

Besides, all the shear thinning behavior demonstrates by CNC/BT-WDFs in freshwater turned into shear thickening behavior in the presence of seawater at this range of CNC concentration 0.4 up to 1.6 wt. % despite any change in the temperature. Some yield stress values of the flow curves in the control BT-WDFs or CNC/BT-WDFs (SW) show negative yield stress values were regarded as behavior such as a sol and determine to be meaningless (Choo & Bai 2015). This simply means the BT-WDFs or CNC/BT-WDFs (SW) could not give any resistance in the presence of salt contained in seawater. By the way, the incorporation of CNCs from 2.0 wt. % and 2.4 wt. % from all plots in figure 33 gradually changed the pattern of the rheological curves and were capable to stand against the effect of salt in the suspension formed by CNC/BT-WDFs (SW). This salt resistance is attributed to the strong surface interactions between CNCs, bentonite, and water immobilized as a stiff network was built based on the attraction between the negatively-charged cellulose nanocrystals (carboxylated cellulose nanocrystals) to the positively-charged edge surfaces of bentonite found in the alkaline water-based drilling fluid (pH=10), resulting to improve the rheological properties of CNC/BT-WDFs (SW). This strong interaction, between the carboxylated CNCs or modified CNCs produced by Tempo-mediated oxidation of MFC followed by ultra-sonication and the exfoliated bentonite clay suspension, rests via van der Waals forces and electrostatic attraction on the sides and surfaces of the clays platelets.

Therefore, the strong interaction imparts rigidity to the CNC-bentonite networks that increase the salt resistance of CNC/BT-WDFs (SW) by impeding invasion by salt ions, enhance water barrier capacity, and decrease fluid loss. However, as the negatively charged face surfaces of bentonite platelets continue to be exposed, it has been observed at the high shear rate some created flocculation or aggregated microstructures in the seawater-based drilling fluid.

.

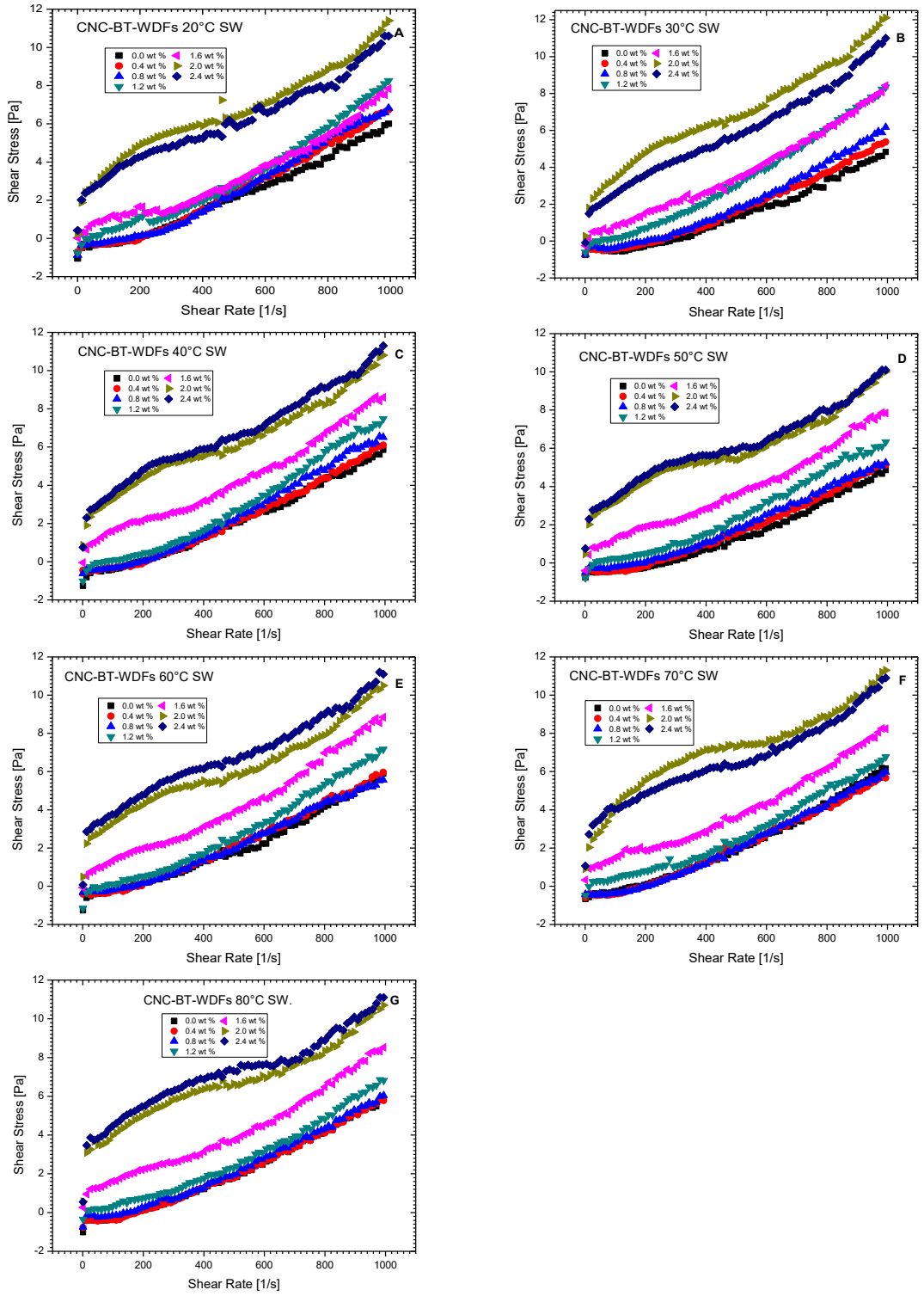

Figure 33.The plots A, B, C, D, E, F and G of shear stress of CNC/BT-WDFs (SW) as a function of shear rate at various CNC concentrations for different temperatures.

A better fitting of the rheological data is given through Herschel-Bulkley model in table 6 below where an increase in the yield stress (y_0) as function of CNC concentration is observed at different temperature as followed: from 0.65351 Pa at 0.0 wt. % CNC to -0.63085,-0.58812, 0.09306, 0.74961, 1.96446 and 2.2737 Pa at 0.4, 0.8, 1.2, 1.6, 2.0 and 2.4 wt. % respectively for 20˚C; from -0.65021 Pa at 0.0 wt. % CNC to -0.63227, -0.50136, -0.2141, 0.45462, 2.04659 and 1.66471 Pa at 0.4, 0.8, 1.2, 1.6, 2.0 and 2.4 wt. % respectively for 30˚C; from -0.7602 Pa at 0.0 wt. % CNC to - 0.60146, -06671, -035884, 1.15631, 2.34567 and 2.46343 Pa at 0.4, 0.8, 1.2, 1.6, 2.0 and 2.4 wt. % respectively for 40˚C; from -56529 Pa at 0.0 wt. % CNC to -0.5953, -46743, -0.19222, 0.85782, 2.36548 and 2.40184 Pa at 0.4, 0.8, 1.2, 1.6, 2.0 and 2.4 wt. % % respectively for 50˚C; from -0.49843 Pa at 0.0 wt. % CNC to -0.56081, 0.49562, -0.29343, 0.93931, 2.61247 and 2.39559 Pa at 0.4, 0.8, 1.2, 1.6, 2.0 and 2.4 wt. % respectively for 60˚C ; from -0.48552 Pa at 0.0 wt. % CNC to -0.67799, -0.6357, 0.13887, 1.17982, 0.85688 and 3.18524 Pa at 0.4, 0.8, 1.2, 1.6, 2.0 and 2.4 wt. % respectively for 70˚C; and from -0.55961 Pa at 0.0 wt. % CNC to -0.58262, 0.38726, 0.1512, 1,34084, 2.60478 and 2.42332 Pa at 0.4, 0.8, 1.2, 1.6, 2.0 and 2.4 wt. % respectively for 80˚C. The results in table 6 show that all suspension of CNC/BT-WDFS (SW) have a yield stress (y_0). The maximum yield stress is reached at 2.4 wt. % CNC concentration for 20˚C; 2.0 wt. % for 30˚C; 2.4 wt.% for 40˚C; 2.4 wt. % for 50˚C; 2.0 wt.% for 60˚C; 1.6 wt.% for 70˚C then decrease and increase at 2.4 wt. %; 2.0 wt.% for 80˚C. This increase in the yield stress should be attributed to the entanglements of the polymer macromolecules (CNCs) absorbed onto Bentonite particle surfaces.

Table 6. Calculated parameters CNC/BT-WDFs (SW) at various CNC concentrations for different temperature using Herschel-Bulkley (HB) Models.

T(°C)	Conc (wt %)	y_0 (Pa)	K(Pa.S)	n	R^2	RMSD	SSR
20°C	0.0	-0,65351	8,99265E-4	1,2889	0,99689	0,11107	0,98698
	0.4	-0,63085	5,70247E-4	1,37277	0,9968	0,12794	1,30953
	0.8	-0,58812	3,67839E-4	1,44128	0,99532	0,16068	2,06546
	1.2	0,09306	1,33016E-4	1,59717	0,99569	0,16386	2,14813
	1.6	0,74961	5,42725E-5	1,70283	0,99265	0,18132	2,63003
	2.0	1,96446	0,03911	0,7758	0,9623	0,45626	16,6537
	2.4	2,2737	0,00934	0,96936	0,96969	0,38779	12,03047
30°C	0.0	-0,65021	1,05533E-4	1,57238	0,99537	0,11351	1,03082
	0.4	-0,63227	1,97791E-4	1,49651	0,99828	0,07672	0,47089
	0.8	-0,50136	9,41983E-5	1,61847	0,99847	0,07995	0,51131
	1.2	-0,2141	5,18905E-4	1,40704	0,99901	0,08214	0,53978
	1.6	0,45462	6,05073E-4	1,36904	0,99574	0,15277	1,86704
	2.0	2,04659	0,02231	0,87152	0,97541	0,41518	13,79028
	2.4	1,66471	0,00623	1,048	0,9836	0,32921	8,67052
40°C	0.0	-0,7602	8,31205E-4	1,29951	0,99709	0,10678	0,91223
	0.4	-0,60146	3,63508E-4	1,42454	0,99854	0,07875	0,49612
	0.8	-0,6671	4,88694E-4	1,39614	0,99746	0,1149	1,05607
	1.2	-0,35881	3,08023E-4	1,47452	0,99602	0,15612	1,94996
	1.6	1,15631	3,98141E-4	1,42611	0,99077	0,22028	3,88196
	2.0	2,34567	0,00976	0,96606	0,97406	0,36575	10,70201
	2.4	2,46343	0,01475	0,91379	0,97788	0,35146	9,88182
50°C	0.0	-0,56529	5,77558E-5	1,66029	0,99793	0,07622	0,46482
	0.4	-0,5953	2,09475E-4	1,48287	0,99817	0,07614	0,46381
	0.8	-0,46743	2,93572E-4	1,43562	0,99686	0,10082	0,81323
	1.2	-0,19222	3,67908E-4	1,42229	0,99404	0,15909	2,02474
	1.6	0,85782	4,98761E-4	1,383	0,9898	0,21527	3,70739
	2.0	2,36548	0,00975	0,94791	0,94955	0,45358	16,45859
	2.4	2,40184	0,02019	0,84499	0,95983	0,40034	16,45859

60°C	0.0	-0,49843	2,29281E-4	1,48039	0,99466	0,14027	1,57403
	0.4	-0,56081	5,87596E-4	1,34965	0,99787	0,09152	0,67003
	0.8	-0,49562	6,31936E-4	1,33316	0,99616	0,11802	1,11434
	1.2	-0,29343	4,02625E-4	1,42536	0,99656	0,13499	1,45769
	1.6	0,93931	3,73864E-4	1,44312	0,99365	0,19277	2,97293
	2.0	2,61247	0,0041	1,08189	0,95905	0,43975	15,47013
	2.4	2,39559	0,02956	0,80932	0,96688	0,41058	13,48634
70°C	0.0	-0,48552	1,97473E-4	1,5111	0,99884	0,06947	0,38611
	0.4	-0,67799	7,44173E-4	1,31387	0,99789	0,08992	0,64683
	0.8	-0,6357	4,36045E-4	1,39637	0,99803	0,0904	0,6538
	1.2	0,13887	1,56669E-4	1,54504	0,99523	0,14171	1,60644
	1.6	1,17982	1,62056E-4	1,54787	0,99446	0,16112	2,07667
	2.0	0,85688	0,38058	0,46101	0,96385	0,41536	13,80199
	2.4	3,18524	0,00605	1,01874	0,96051	0,40838	13,34204
80°C	0.0	-0,55961	4,04113E-4	1,40195	0,99804	0,08677	0,60236
	0.4	-0,58262	4,30761E-4	1,39309	0,99875	0,06936	0,38482
	0.8	-0,38726	3,43779E-4	1,42632	0,99757	0,09742	0,75919
	1.2	0,1512	1,16209E-4	1,58905	0,99783	0,09603	0,73777
	1.6	1,34084	2,01718E-4	1,51764	0,99257	0,18855	2,84402
	2.0	2,60478	0,04097	0,74668	0,94965	0,4502	16,21405
	2.4	2,42332	0,11859	0,60345	0,94999	0,45358	16,45886

The amount of salinity in seawater is roughly estimated to 35000 ppm equivalent to 35 g of salt per one litter or Kg of water of the concentration of salts (e.g., Na^+ and Ca^{2+} salts). The cations are electrostatically attracted to the negatively charged surface of bentonite platelets creating a charge imbalance in the double layer resulting in flocculation and aggregation. Consequently, the filtrate volume increases, giving place to a thicker filter cake, leading in turn to the pipe sticking problems, wellbore swelling, and formation collapse.

Table 7. Variation of shear stress of CNC/BT-WDFs (SW) versus temperature at different CNC concentration, determined at high shear rates (1200 s^{-1}).

Temperature	Shear Rate	Shear Stress	Shear Stress	Shear Stress	Shear Stress	Shear Stress	Shear Stress	Shear Stress
[°C]	[1/s]	[Pa]	[Pa]	[Pa]	[Pa]	[Pa]	[Pa]	[Pa]
		BT-CNC-WDFs(SW) (0.0 wt % CNC)	BT-CNC-WDFs(SW) (0.4 wt % CNC)	BT-CNC-WDFs(SW) (0.8 wt %CNC)	BT-CNC-WDFs(SW) (1.2 wt % CNC)	BT-CNC WDFs(SW) (1.6 wt %CNC)	BT-CNC-WDFs(SW) (2.0 wt % CNC)	BT-CNC-WDFs(SW) (2.4 wt %CNC)
20	1 200	8,62	9	9,29	10,9	10,5	14,9	13,9
30	1 200	7,08	7,5	7,88	11,2	11,2	15,5	14,3
40	1 200	8,55	8,37	8,66	10,1	11,5	14,3	14,7
50	1 200	6,98	7,05	7,17	8,38	10,4	13,2	13,3
60	1 200	7,94	8,01	7,95	9,43	11,8	13,5	14,6
70	1 200	8,73	8,15	8,5	9,37	11,1	14,6	14,3
80	1 200	8,4	8,09	8,34	9,24	11,3	13,9	14,1

The flow curves of the CNC/BT-WDFs (SW) at the highest shear rate of 1200 s^{-1} generally speaking depict that the shear stress increased with an increase in the CNC concentration at different temperatures as resume in table 7.

4.2.2. RHEOLOGICAL CURVES AT DIFFERENT TEMPERATURES FOR VARIOUS CNC CONCENTRATIONS.

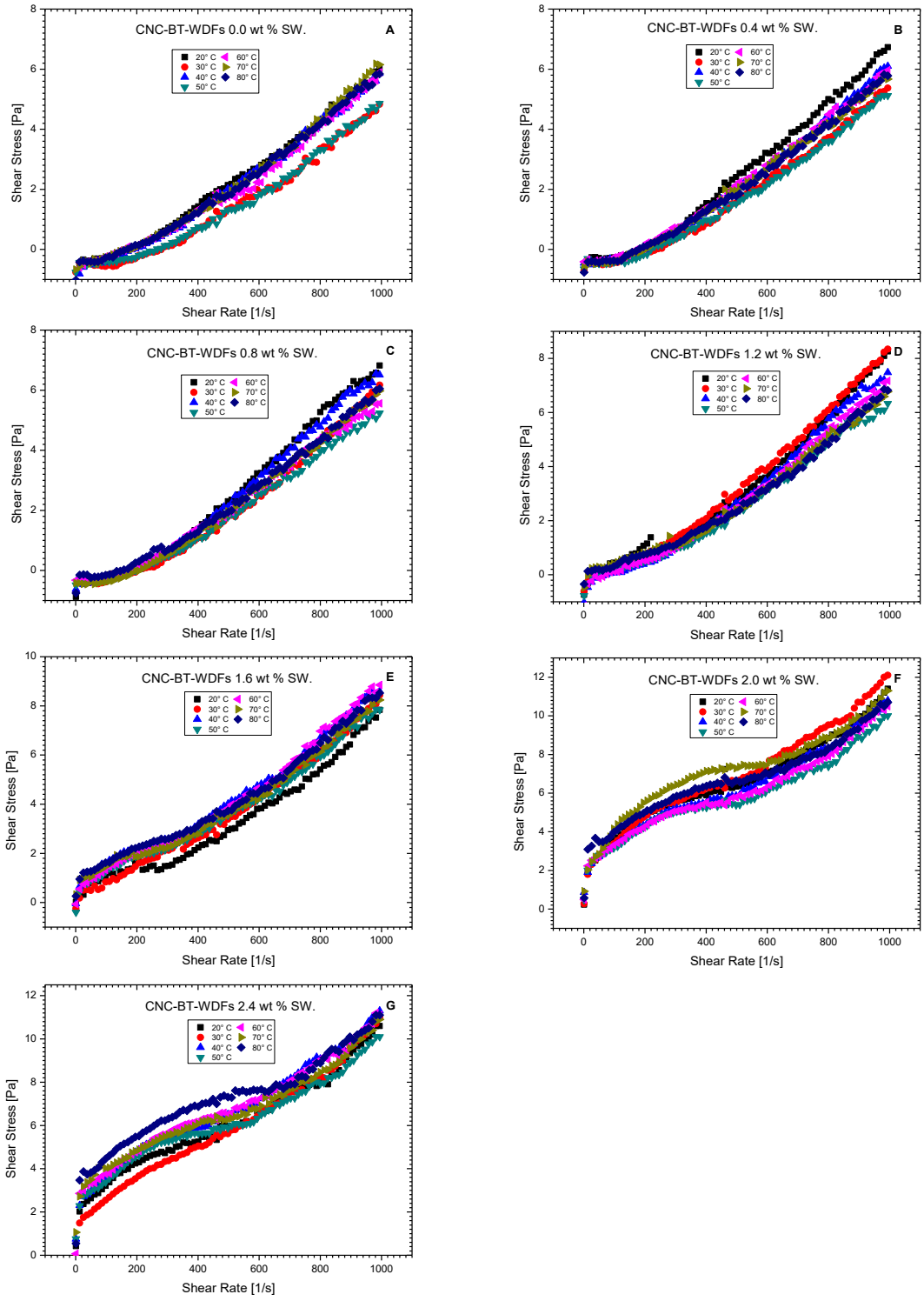

Figure 34. The plots A, B, C, D, E, F and G of shear stress of CNC/BT-WDFs (SW) as a function of shear rate at different temperatures for various CNC concentrations.

The rheological properties of CNC/BT-WDFs (SW) were measured with the Rotational Rheometer (RheolabQC SN897839/FW1.31) at atmospheric pressure. The variation of the shear stress of CNC/BT-WDFs (SW) as a function of shear rate at different temperatures for various CNC concentrations is shown in figure 34. The experimental results indicate that the CNC/BT-WDFs in seawater behaved as shear thickening fluids from the control BT-WDFs (SW) to CNC/BT-WDFs (SW) at 1.6 wt. % of CNCs for all ranges of temperature including 2.0 wt. % of CNCs at 60°C with n>1 then as a shear-thinning fluid at 2.0 wt. % of CNCs for all range of temperature except at 60°C and for all temperatures except 30°C, 60°C and 70°C for 2.4 wt. % of CNCs.

From figure 34, plots A, B, C, D, E, F, and G show the variation of shear stress with the shear rate for CNC/BT-WDFs in seawater at different temperatures for various CNC concentrations. It can be seen that at a low shear rate, there is no significant change in the variation of shear stress as the temperature increased. However, at a high shear rate, few variations are observed.

However, the shear-thinning behavior of CNC/BT-WDFs (SW) is the most interesting as it is applied in the drilling operation. For the shear-thinning behavior of CNC/BT-WDFs (SW) at 2.0 wt. % and 2.4 wt. % of CNCs, the shear stress showed a very slight decrease as temperature increased at the high shear rate (1200 s^{-1}) in figure 35 below which means no significant change over a broad range of temperature from 20 to 80 °C.

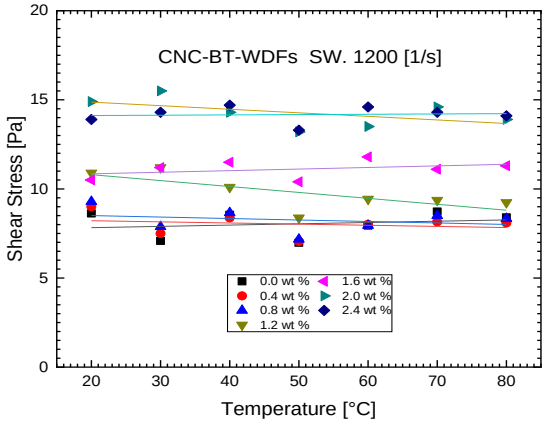

Figure 35. Plot of shear stress as a function temperature for CNC/BT-WDFs (SW) at various CNC concentrations taken at high shear rate 1200 s^{-1}.

4.2.3. TEMPERATURE EFFECTS ON THE VISCOSITY OF CNC/BT-WDFs (SW) AS DRILLING FLUID

From figure 36, it is depicted that the addition of 0.4 to 2.4 wt. % of CNC concentrations to BT-WDFS suspension increases exponentially, the viscosity of CNC/BT-WDFs (SW). This increase favored the transport of cuttings not over the broad range of CNC concentration but only from 2.0 to 2.4 wt. % as described in this project. This can be projected as well for the higher CNC concentration based on the trend given in figure 36 below. So far, this increase in the viscosity of CNC/BT-WDFs (SW) can be attributed to the hydrogen bond formed between the hydrogen and the hydroxyl of BT clay, and those from the group carboxylate of CNC molecules. Besides, it may be attributed to the number of entanglements caused by long polymer chains.

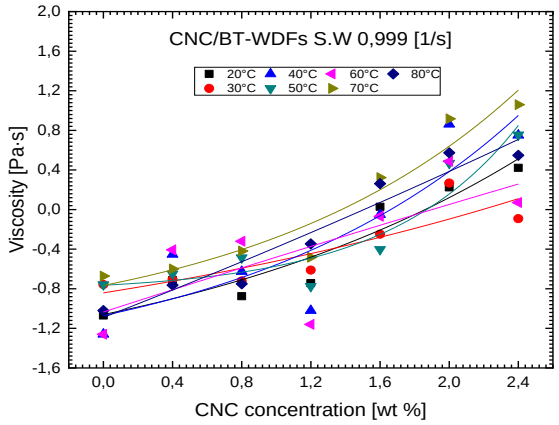

Figure 36. The plot of viscosity as a function CNC concentrations for CNC/BT-WDFs in sea-water at various temperatures at low shear rate 0.999 s^{-1}.

The following table 8 showed the variation of viscosity of CNC/BT-WDFs (SW) with the temperature at different CNC concentrations. As reported above that the strong resistance to salt effect was attributed to the rigid CNCs-bentonite network built with 2.0 and 2.4 wt. % CNCs into BT-WDFs (SW) especially the strong surface interaction of CNC/BT-WDFs (SW). This can be demonstrated through the investigation of the dependence of viscosity upon the temperature variation. Generally speaking, when the temperature increased, the viscosity of the drilling fluid decreased, this result from the mobility of water molecules. Though in the presence of a strong surface interaction it could be led to the reduction of sensitivity upon the temperature change (Yan et al 2013).

Table 8. Variation of viscosity of CNC/BT-WDFs (SW) versus temperature at different CNC concentration, determined at low shear rates (0.999 s^{-1}).

Temperature	Shear Rate	Viscosity	Viscosity	Viscosity	Viscosity	Viscosity	Viscosity	Viscosity
[°C]	[1/s]	[Pa.s]	[Pa.s]	[Pa.s]	[Pa.s]	[Pa.s]	[Pa.s]	[Pa.s]
		CNC- BT-WDFs(SW) (0.0 wt % CNC)	CNC- BT-WDFs(SW) (0.4 wt % CNC)	CNC- BT-WDFs(SW) (0.8 wt % CNC)	CNC- BT-WDFs(SW) (1.2 wt % CNC)	CNC- BT-WDFs(SW) (1.6 wt % CNC)	CNC- BT-WDFs(SW) (2.0 wt % CNC)	CNC- BT-WDFs(SW) (2.4 wt % CNC)
20	0,999	-1,07	-0,711	-0,876	-0,743	0,0285	0,224	0,422
30	0,999	-0,757	-0,704	-0,722	-0,612	-0,249	0,268	-0,0922
40	0,999	-1,26	-0,453	-0,626	-1,02	-0,0512	0,862	0,751
50	0,999	-0,758	-0,649	-0,486	-0,776	-0,403	0,469	0,755
60	0,999	-1,26	-0,407	-0,32	-1,16	-0,0684	0,487	0,0715
70	0,999	-0,672	-0,599	-0,419	-0,482	0,323	0,917	1,06
80	0,999	-1,02	-0,763	-0,75	-0,347	0,262	0,573	0,548

The temperature effect on the viscosity of CNC/BT-WDFs (SW) at low and high shear rate is shown in figure 37 below. It can be seen that for the control BT-WDFs (SW) and CNC/BT-WDFs (SW) with CNC concentration less than 2.0 wt. % of CNC concentration, the viscosity value is negative and no impact on the thermal stability as well as it produced also a shear-thickening behavior. However, most interestingly are from CNC concentrations 2.0 and 2.4 wt. % of CNC/BT-WDFs (SW) in which the viscosity is well maintained over the broad range of temperature from 20 to 80 °C. This stability is due to the formation of the strong network between CNCs, BT layers, and immobilized water molecules caught in the core-shell structure and immobilized at the proximity of CNCs resulting in high resistance over the change of temperature (Yan et al 2013).

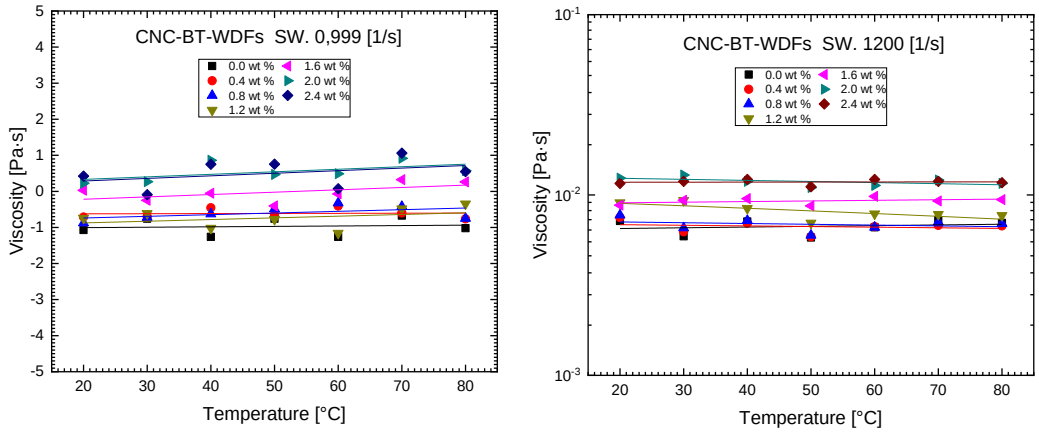

Figure 37. The plot of viscosity as a function temperatures for CNC/BT-WDFs (SW) at various CNC concentrations at low and high shear rate (0.999 s^{-1} and 1200 s^{-1} respectively).

4.2.4. THE EFFECTS ON CONCENTRATION ON THE VISCOSITY OF CNC/BT-WDFs (SW) AS DRILLING FLUID

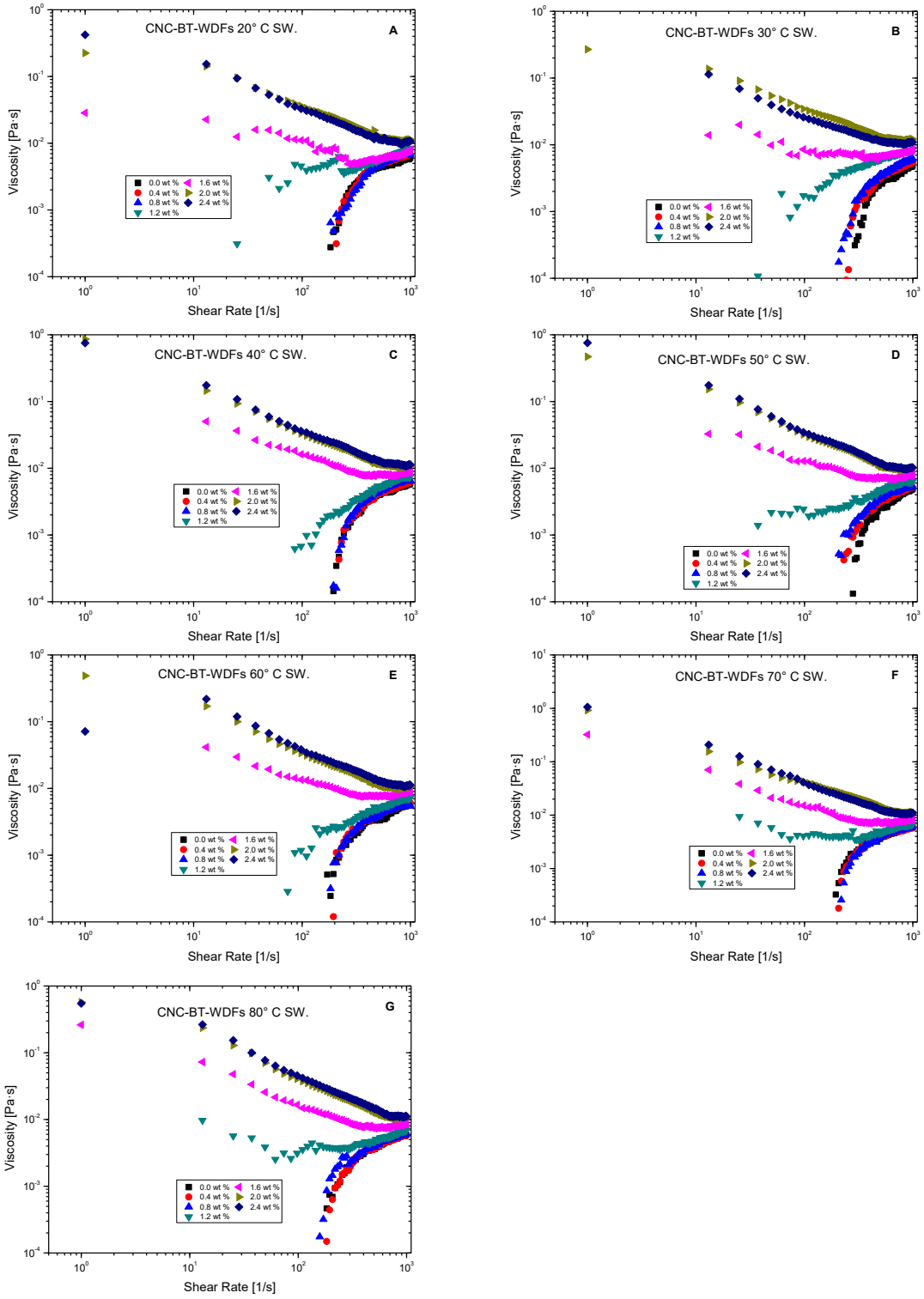

Figure 38. The plot of viscosity as a function of shear rate for CNC/BT-WDFs (SW) at various CNC concentrations for different temperatures.

The analysis of the rheological curves based on the variation of the viscosity with the shear rate at various CNC concentrations shown in figure 38 demonstrates a reduction in viscosity over a broad range of shear rate from 0.999 s^{-1} to 900 s^{-1} than followed by a slight increase in viscosity as the shear rate is going to reach 1200 s^{-1} from 2.0 wt. % to 2.4 wt. % CNC concentrations for all the ranges of temperature. These rheograms represent the shear-thinning behavior of CNC/BT-WDFs (SW) due to the strong interaction between charged bentonite clay and the carboxylated CNCs with immobilized water. This reduction has been seen as well at 1.6 wt. % CNC concentration but was interrupted with an increase in viscosity from 600 s^{-1} due to a weak interaction between carboxylated CNCs and BT-WDFs that let appear a shear thickening behavior at high shear over a broad range of temperature from 20°C to 80°C. However, the viscosity continues to increase over a broad range of shear rate for the control BT-WFDs (SW) to 1.2 wt. % CNC concentration of CNC/BT-WDFs (SW) that confirms a shear thickening behavior over the broad range of temperature from 20°C to 80°C.

The effect of temperature on the viscosity of CNC/BT-WDFs (SW) over the broad range of shear rate for different CNC concentrations is shown in figure 39. In figure 39(A-D), it depicted an increase in viscosity with an increasing shear rate over the broad range of the temperature. In figure 39(E), a slight decrease in viscosity is shown from 0.999 s^{-1} to 350 s^{-1} than followed by a very slight increase in viscosity till 1200 s^{-1} for 60°C and 80°C. This was applicable as well as for 40°C to 50°C but with very low viscosity. From 20°C to 30°C, the CNC/BT-WDFs (SW) viscosity was almost in a linear relationship with the progress shear rate over a broad range of temperature. In figure 37(F-G), it can be seen that the viscosity of the mud decreases with increasing shear rate from 0.999 s^{-1} to 900 s^{-1} and plateaued till 1200 s^{-1} over a broad range of temperature from 20°C to 80°C. Therefore, this reduction of viscosity with an increase in shear rate results in a shear thinning behavior. As it could be seen, in figure 39(F-G), the effect of temperature upon viscosity remained almost constant at a high shear rate confirming the thermal stability of CNC/BT-WDFs (SW). Thus, it can be said that CNC/BT-WDFs (SW) at 2.0 wt. % and 2.4 wt. % CNC concentrations develop high resistance in salinity or in the presence of salt content in seawater. This salt content favored the improvement in yield stress, viscosity, and gel strength of CNC/BT-WDFs (SW) at 2.0 wt. % and 2.4 wt. % CNC concentrations as seen in figure 39(F-G).

This behavior of the different rheological properties of the mud system under high temperature could be the result of the thermal degradation of the solid content, polymers, and other components of the mud system and the expansion of the molecules which will lower the resistance of the fluid to flow, hence, its viscosity, yield stress and gel strength **(**Amani & Al-Jubouri 2012). By contrast, the present case of CNC/BT-WDFs (SW) shows an improvement of the rheological properties with the incorporation of the CNC polymers in the presence of seawater and high temperature into ATT-WDFs (SW) including the improvement of the yield stress, viscosity, and gel strength of the mud system. A transformation from the shear thickening curves to shear-thinning curves has been observed through the incorporation of CNCs as nanoparticles in WDFs (SW) confirming the rheological modifier and fluid loss reducer of CNCs. Thus 2.0 wt. % of CNCs can be considered as the optimum concentration to be used for improving the rheological properties of CNC/ATT-WDFs in seawater.

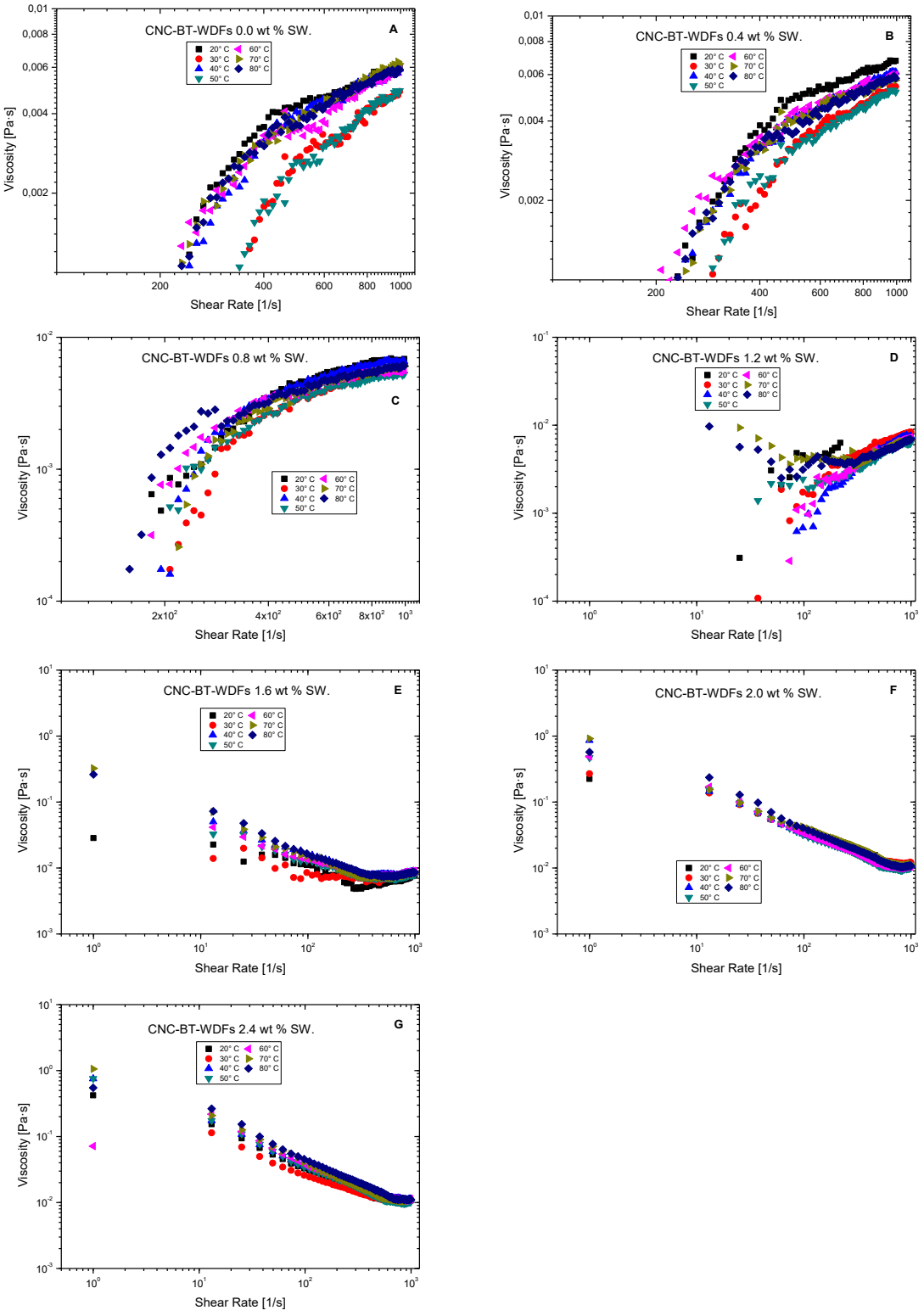

Figure 39. The plot of viscosity as a function of shear rate for CNC/BT-WDFs (SW) at various temperatures for different CNC concentrations.

4.3. FILTRATION PROPERTIES

4.3.1. ANALYSIS OF FILTRATION PROPERTIES OF CNC/BT-WDFs (FW)

The filtration properties of CNC/BT-WDFs (FW) were analyzed by using API filter press as shown in figure 23. The API fluid loss tests, the filtrate volume in ml per 30 min, were run in figure 40. Figure 40 shows the fluid loss as a function of pressure (150, 250, 350, and 450 KPa) for three different CNC concentrations (0.8, 1.0, and 1.2 wt. % CNCs) at room temperature (22°C). The filtration process has been run to determine the best pressure that gives less filtrate lost to accommodate the requirement of HPHT fluid. It is noted that the pressure limit on the API equipment being used to run the filtration process is 5 bars.

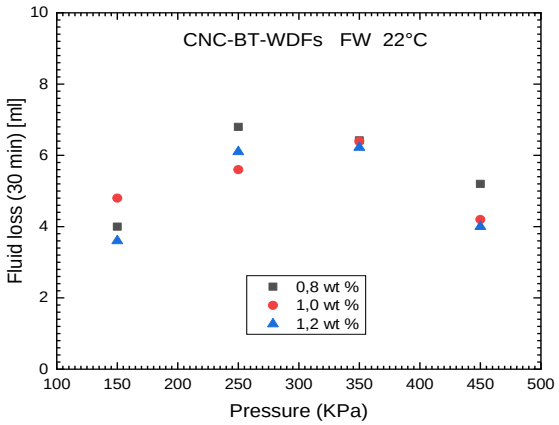

Figure 40. The plot of fluid loss volume (at 30 min) of CNC/BT-WDFs (FW) as a function of pressure at different CNC concentrations and 22°C.

From figure 40, it is shown that the lowest fluid loss volume is given at low pressure (150 KPa) and high pressure (450 KPa). Because the prepared fluid is to be used for the HPHT environment, the high pressure of 450 KPa convenes to be considered. However, it is shown that a 450 KPa, the best CNC concentration among the three giving less fluid loss is 1.2 wt. %. Therefore, the working pressure taken is 450 KPa and it should be applied along all the filtration process.

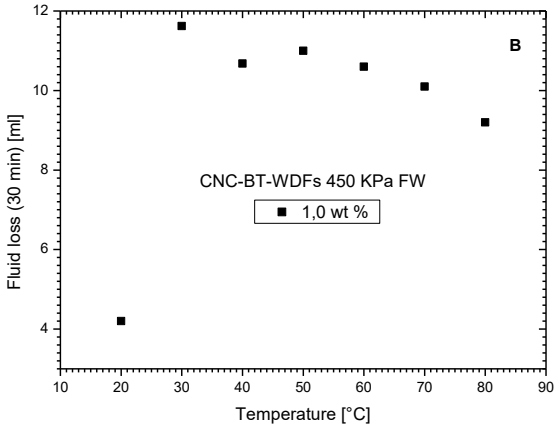

Figure 41. The plot of fluid loss volume (at 30 min) of CNC/BT-WDFs (FW) as a function of temperatures at 450KPa for 1.0 wt. % CNC concentrations.

Figure 41 depicted the dependence of the filtrate loss upon the temperature for CNC/BT-WDFs (FW) at 1.0 wt. % and 450 KPa. At 20°C and 5 bars, this present condition is that of low temperature and high pressure (LTHP), it could be said that the dispersed state that could increase the thermal resistance and facilitates the colloidal packing to form filter cakes of low permeability for improving filtration properties was not yet established. The low filtration observed was due to the action of CNC molecules to stabilize the water dispersion and close the pores of the API filter press. This reduction in the filtration was due to the action of the non-reacted CNC particles to block the API filter pores.

However, the cause for the fluid loss jump from 20 to 30°C is due to the increase in temperature. Knowing that with an increase in temperature, the particles move fast as they gain kinetic energy, resulting in increased collision rates and an increased rate of diffusion. As temperature increases, the Bentonite platelet started to collide with CNC molecules. Therefore, the carboxylated CNCs with his effect on the reduction of edge-to-face bonding between bentonite platelet results to enhance disaggregation during hydration. This means that carboxylated CNCs (as polymers) enhance the performance of sodium bentonite primarily by promoting the disaggregation of bentonite platelets.

The addition of water into the bentonite/CNCs system results in the absorption of the anionic functional groups of the CNCs (as a polymer) onto and the neutralization of the positively charged bentonite platelet edges This reaction assists platelet separation as the polymer overcomes the bond forces of the macrostructure (www.cetco.com). Meanwhile, the filtrate volume increases as the water dispersions were not yet completely absorb into the bentonite/CNCs system before the CNCs establish a protective encapsulation around hydrated bentonite platelets that increases a bentonite's contaminant resistance.

A decrease of fluid loss with increasing temperature is observed from 30°C up to 80°C. This simply means that at high temperatures, the interaction between BT layers, carboxylated CNCs and immobilized water is more reinforced resulting in a rigid and stable structure. This rigid and stable structure of CNC/BT-WDFs (FW) does not allow invasion of water. It is worth avoiding the collapse of the wellbore due to the invasion of fluids into the formation. This could only be done by designing a suitable drilling fluid that is following API standards (the API recommended value for WDFs is 15.0 ml) (American Petroleum Institute 1993).

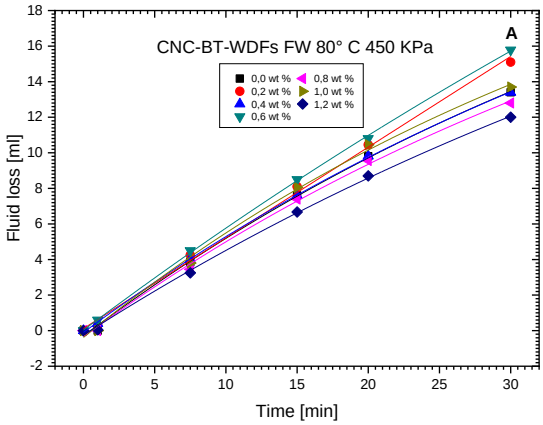

Figure 42. The plot of fluid loss volume as a function of time for CNC/BT-WDFs (FW) at 450KPa and 80°C for different CNC concentrations.

Figure 42 shows the effect of CNC concentration on the filtration property of CNC/BT-WDFs (FW). The incorporation of CNCs impacts the API fluid loss. The CNC/BT-WDFs (FW) with 0.0, 0.2, 0.4, 0.6, 0.8, 1.0 and 1.2 wt. % of CNCs had the API fluid loss values of 13.4, 15.1, 13.4, 15.78, 12.8, 13.7, and 12 mL/30 min respectively, showing an increase of 11.3 %, 0.0 %, 15.1 %, a decrease of 4.5 %, an increase of 2.2 % and a decrease of 10.5 % when compared to the original BT-WDFs (FW). It could be seen that CNCs yielded a significant reduction of the fluid loss volume, especially at 1.2 wt. % CNC concentration. This significant reduction of the fluid loss volume is due to (a) the considerable viscosity of CNC/BT-WDFs (FW); the great interaction between CNC particles and BT layers; (b) the addition of CNCs might modify the microstructure of the filter cakes, leading to the change in the permeability (Warren et al 2003).

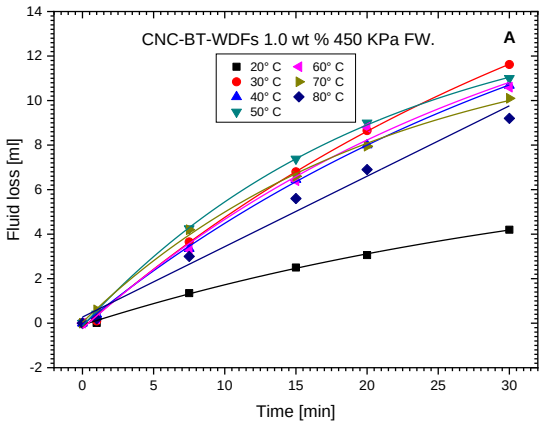

Figure 43. The plot of fluid loss volume as a function of time for CNC/BT-WDFs (FW) at 450 KPa for different temperatures.

Figure 43 shows the effect of temperature on the filtration property of CNC/BT-WDFs (FW) at 1.0 wt. % CNC concentration. It could be seen that the fluid loss decreased as temperature increased showing the great water retention exhibited by the addition of CNCs into BT-WDFs (FW). This result is significantly different from any expectation of the effect of temperature on the fluid loss that can cause the reduction in the viscosity and free water molecules. Especially in the case of colloids, continuous random movement is observed by a bombardment of the water molecules in the dispersion medium. The increase of temperature induces the Brownian motion to become more energetic. Therefore, this reduction in fluid loss volume is due to the higher stability of the CNCs into BT-WDFs (FW) at high temperatures. The lower fluid loss volume observed at 20°C is not taken into account because the focus of this research is based on the HPHT wells.

4.3.2. ANALYSIS OF FILTRATION PROPERTIES OF CNC/BT-WDFs (SW)

Bunphot (2017) studied the physical and chemical properties of Gellan Gum (GLG) in freshwater and seawater-based drilling mud on 0.1, 0.3, and 1.0 % by weight of GLG concentrations and tested at 30, 45, 60, and 80°C. He found out that the drilling mud with 1.0 % of GLG concentration improved significantly the rheological properties of freshwater and seawater-based drilling mud. The temperature has positive effects on the filtration properties of freshwater-based drilling mud by increasing the effectiveness of polymer but decreasing the effectiveness of bentonite suspension. However, the temperature effects and salinity affected negatively the filtration properties of seawater-based drilling mud by decreasing the effectiveness of both polymer and bentonite suspension.

The filtration properties of CNC/BT-WDFs (SW) were analyzed by using API filter press as showed in figure 23. The API fluid loss was recorded by measuring the volume of the filtrate after 30 min recorded as followed at 0.0, 7.5, 15, 20, and 30 min respectively. The tests run are shown in figure 44. Moreover, the variation of the fluid loss of CNC/BT-WDFs (SW) as a function of times at different temperatures showed the effect of temperature on the fluid loss. The more the temperature increases, the more the fluid is getting lost from the drilling fluid. This loss of drilling fluid is due to the weak interaction between bentonite clay and carboxylated CNCs in the presence of a salt contaminant in seawater that prevents the swelling of bentonite and result in fast aggregation and flocculation of bentonite clays.

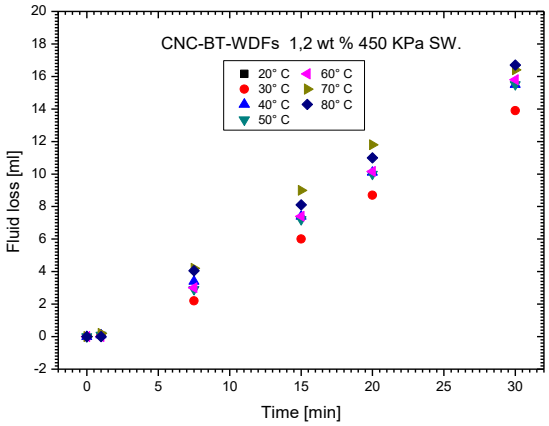

Figure 44. The plot of fluid loss volume as a function of time for CNC/BT-WDFs (SW) at 450 KPa for different temperatures.

It could be said that CNC particles have little impact on the prevention of fluid loss from CNC/BT-WDFs (SW). As it is well-known that the fluid loss volume affects negatively the formation leading to serious wellbore collapse and significant swelling resulting in the deposition by flocculation of their filter cake on the wellbore wall causing differential pressure sticking, stuck pipe problems, and well damage (Zakaria et al 2012). Nevertheless, when 1.2 wt. % of CNCs was incorporated, the minimum API fluid loss of 12 ml/30 min was obtained for CNC/BT-WDFs (FW), which was much less than the API recommended value (15.0 ml) for WDFs (American Petroleum Institute 1993). By contrast, the CNC/BT-WDFs (SW) at the same condition of CNC concentration, temperature, and pressures produced an API fluid loss of 16.7 ml/30 min about 28 % of API fluid loss more than that of CNC/BT-WDFs (FW) and above the API recommended value.

4.4. AGING AND TEMPERATURE EFFECTS ON DIFFERENT PREPARED DRILLING FLUIDS.

Figure 45 and table 9 displayed the plot of shear stress as a function of shear rate at the different aging times and the calculated parameters of CNC/BT-WDFs (FW) at a different aging time for different temperatures using Herschel-Bulkley (HB) Models.

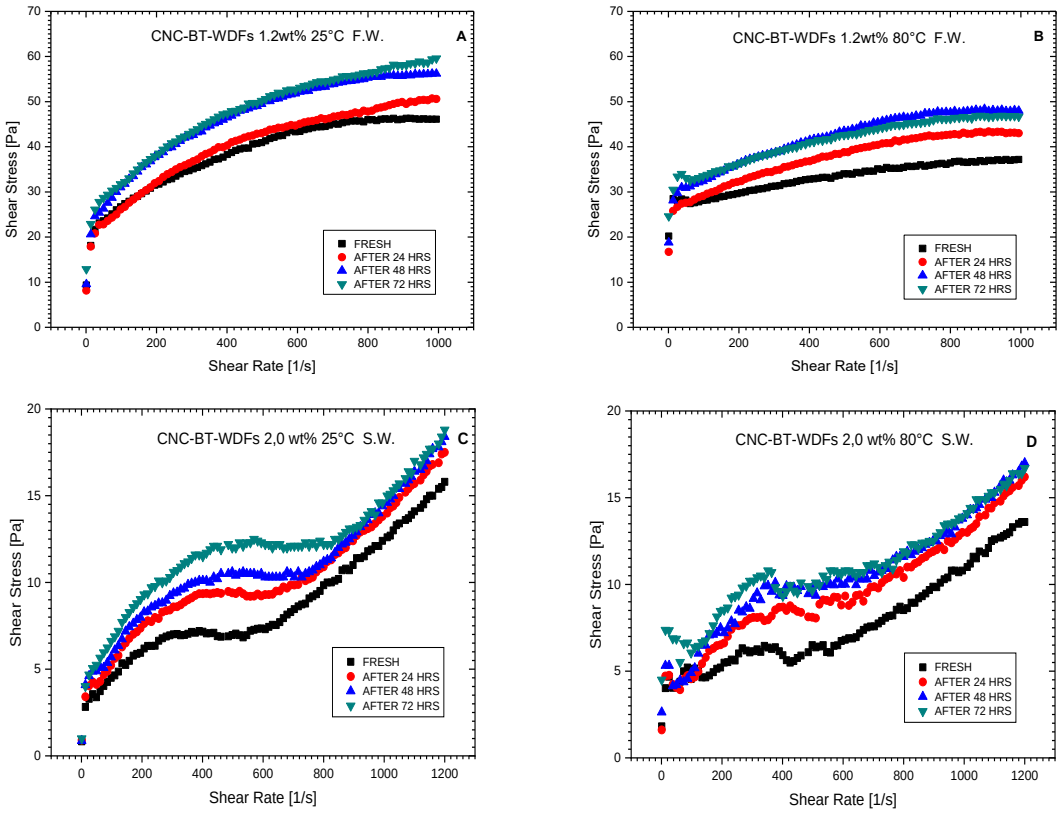

Figure 45. The plot of shear stress as a function of shear rate at different aging time at 25℃ and 80℃ for CNC/BT-WDFs in fresh-water and sea-water.

Table 9. Calculated parameters of CNC/BT-WDFs (FW)/(SW) at different aging time for different temperature using Herschel-Bulkley (HB) Models.

CNC-BT-WDFs 1.2wt% 25°C F.W.				
Model	Herschel			
Equation	y = y0 + K*x^n;			
Plot	Shear Stress	Shear Stress	Shear Stress	Shear Stress
y0	3,26239 ± 1,63173	2,616 ± 1,15433	0 ± 1,74854	8,53336 ± 1,0625
K	6,82763 ± 0,95583	6,23382 ± 0,61915	9,83688 ± 1,07788	5,38162 ± 0,51118
n	0,27281 ± 0,01548	0,29807 ± 0,01131	0,25755 ± 0,01187	0,32776 ± 0,01114
Reduced Chi-Sqr	0,76165	0,48938	0,74021	0,53701
R-Square (COD)	0,98876	0,99443	0,99306	0,99508
Adj. R-Square	0,98847	0,99429	0,99289	0,99496
CNC-BT-WDFs 1.2wt% 80°C F.W.				
Model	Herschel			
Equation	y = y0 + K*x^n;			
Plot	Shear Stress	Shear Stress	Shear Stress	Shear Stress
y0	23,12145 ± 0,6991	16,10176 ± 1,02402	17,34374 ± 1,2318	25,69103 ± 0,76294
K	0,67404 ± 0,21023	3,01758 ± 0,50011	3,73847 ± 0,62938	1,2006 ± 0,25107
n	0,44399 ± 0,0395	0,32375 ± 0,01937	0,31151 ± 0,01945	0,42282 ± 0,0262
Reduced Chi-Sqr	0,49958	0,48262	0,62918	0,52925
R-Square (COD)	0,95779	0,9851	0,9844	0,97984
Adj. R-Square	0,95673	0,98473	0,98401	0,97934

CNC-BT-WDFs 1.2wt% 25°C S.W.				
Model	Herschel			
Equation	y = y0 + K*x^n;			
Plot	Shear Stress	Shear Stress	Shear Stress	Shear Stress
y0	4,72034 ± 0,19263	4,72272 ± 0,3693	4,71759 ± 0,4985	0,96705 ± 1,1662
K	5,40077E-5 ± 4,09869E-5	0,00646 ± 0,00435	0,0247 ± 0,01671	1,08011 ± 0,45252
n	1,7192 ± 0,10712	1,05206 ± 0,09294	0,86566 ± 0,09212	0,3706 ± 0,04964
Reduced Chi-Sqr	0,60625	0,99506	1,25023	1,02508
R-Square (COD)	0,94671	0,91901	0,8975	0,90904
Adj. R-Square	0,9456	0,91732	0,89537	0,90715
CNC-BT-WDFs 1.2wt% 80°C S.W.				
Model	Herschel			
Equation	y = y0 + K*x^n;			
Plot	Shear Stress	Shear Stress	Shear Stress	Shear Stress
y0	4,8302 ± 0,10749	4,43881 ± 0,2667	4,27235 ± 0,37734	6,73258 ± 0,27777
K	4,35669E-6 ± 2,84298E-6	0,00662 ± 0,00335	0,03714 ± 0,01759	0,00339 ± 0,00232
n	2,05026 ± 0,09243	1,04048 ± 0,07	0,80506 ± 0,06406	1,11185 ± 0,09468
Reduced Chi-Sqr	0,23961	0,50847	0,6199	0,62245
R-Square (COD)	0,96924	0,95166	0,94241	0,92211
Adj. R-Square	0,9686	0,95065	0,94121	0,92049

It is observed that shear stress increased with an increase in aging time. This means the shear stress decreases with the aging time in freshwater. The same effect is observed in seawater but the action of the salt upon the drilling fluids was detrimental as CNC/BT-WDFs (SW) at low and high temperature could not display proper shear thinning behavior. It can be also seen that CNC/BT-WDFs (FW) at 80℃ offered great yield stress value demonstrating the high carrying capacity of the mud at high temperature. It has been observed that the drilling fluid properties are affected by the variation of the temperature and aging time. As seen in this project, the impact of temperature and aging time upon the yield stress, viscosity, and shear stress so far on the gel strength. Therefore, by the fact of maintaining at the optimum values these rheological properties, many drilling issues could be avoided. Thus, the drilling fluid rheology remained very important as the viscosity of the drilling fluid is practically affecting the rate of penetration during the drilling operation. Keeping proper gel strength is advantageous for holding cuttings in suspension, and for a high penetration rate relatively low gel strength is needed that will cause less pressure drop in the borehole. The cutting slip velocity gives a better correlation with yield stress than any other rheological parameters. Furthermore, the incorporation of the cellulose nanocrystals in the clay-based fluids maintained a better viscosity of the mud system that means CNCs reduced the viscosity at the optimum value leading to the reduction of the amount of energy needed for rotating drill stem and drill bit.

4.5. RATE OF PENETRATION

The experimental data are given in tables 23-24 show the variation of the rate of penetration as a function of pressure (stress) or weight on the bit of different rock samples with CNC/BT, ATT, SEP-WDFs in fresh-water and sea-water. Only the one for CNC/BT-WDFs in fresh-water and sea-water has to be considered in this case. Generally, it is observed in figure 46 that CNC/BT-WDFs (FW), at 1.2 wt. % CNC concentration, exhibit a more significant rate of penetration values than CNC/BT-WDFs (SW) at 1.2 wt % CNC concentration into plot B over all the drilled rock samples sample. Besides, the fast ROP is attributed to 1.2 wt % CNC concentration of CNC/BT-WDFs (FW) as drilling is done into Shale, Dolomite, and Sandstone rock samples except for Breccia rock sample. A more significant correlation between the ROP and the stress (pressure) or weight on bit is given to 1.2 wt. % CNC concentration of CNC/BT-WDFs (FW) when drilled in Dolomite and Sandstone rock samples.

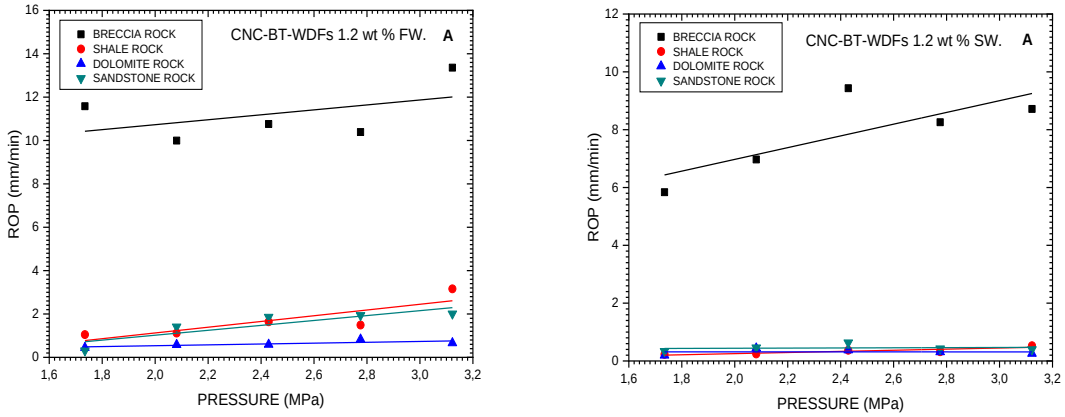

Figure 46. Plots of the rate of penetration as a function of pressure (stress) or weight on bit of different rock samples in CNC/BT-WDFs (FW) and CNC/BT-WDFs (SW).

4.6. CONCLUSIONS

The effect of CNC concentrations, temperature and pressure on the rheological and filtration properties of CNC/BT-WDFs was investigated in fresh-water and sea-water. Herschel-Bulkley model as statistical modelling technology was used for better understanding of the rheological behaviors. The penetration rate onto different rock samples with CNC/BT-WDFs was investigated in fresh-water and sea-water. The aging and temperature effect of CNC/BT-WDFs was investigated in fresh-water and sea-water. Some significant results observed during the study of this project are:

- CNCs had considerable effect on the rheological and filtration properties of CNC/BT-WDFs in fresh-water whereas less effect in sea-water.
- Effect of salinity had considerably affected the rheological and filtration properties of CNC/BT-WDFs.
- Effect of temperature on the rheological and filtration properties affected more the CNC/BT-WDFs (FW) than CNC/BT-WDFs (SW).
- Fast penetration rate was reached by using CNC/BT-WDFs (FW) than CNC/BT-WDFs (SW) through rotary drilling on different rock samples.
- Salinity have negative effects on the aging time of CNC/BT-WDFs in sea-water. Meaning that the salinity affected the carrying capacity of cuttings (yield stress) of CNC/BT-WDFs (SW) whereas the increase in temperature tried to improve the yield stress of the affected mud during aging period.
- Effect of aging time of CNC/BT-WDFs in fresh-water was improved by increasing temperature as it has great impact on the increase of the yield stress.

CHAPTER 5. CELLULOSE NANOCRYSTALS ATTAPULGITE WATER-BASED DRILLING FLUID

5.1. ANALYSIS OF RHEOLOGICAL BEHAVIOUR OF CNC/ATT-WDFs IN FRESHWATER

5.1.1. RHEOLOGICAL CURVES AT DIFFERENT CNC CONCENTRATIONS FOR VARIOUS TEMPERATURES

The rheological properties of the types of water-based drilling fluids (fresh and sea water) were measure using the rheometer named RheolabQC SN897839/FW1.31with RHEOPLUS/32 V3.62 21002331-33025 as application from Anton Paar, Germany. The plots of shear stress as a function of shear rate for CNC/ATT-WDFs in fresh water at different CNC concentrations are depicted in figure 45.

Drilling operations process in harsh condition of high temperature and high pressure including high electrolyte influx (salt contamination) constitute a great obstacle for the use of bentonite clay-base water mud. The intervention of attapulgite or sepiolite clays minerals to replace bentonite with addition of CNC particles could be the key solving problems in deep well. As these minerals have fibrous structure with low surface energy, their low reactivity in the presence of salt contaminants and their high stability in high temperature can result with a good rheological and fluid loss properties to sort out bentonite clay limitation in drilling operation. The attapulgite or sepiolite suspension viscosity is owing to the effect of the shear force leading to the formation of gel structure and the attractive forces established between particles that had been created by broken-bond charges on the edges of broken fibers through shearing force effects. Most results based on the filtration control properties of attapulgite or sepiolite present inferior values due to the fibrous structure (Al-marhoun, 2015). As drilling fluid is subjected to a continuous shear rate in the dynamic flow loop, the combine application of shear rate and temperature favors the attapulgite for enhancing rheological properties in the presence of CNC particles. The drilling fluids kept being dilatant despite certain amount of CNC particles added as shown in figure 45. However, the fibrous structure of attapulgite clay does not contribute to the formation of a thin filter cake of low permeability. Hence, the values of fluid loss for both API and dynamic filtration are observed to be higher. In this research project, the cellulose nanocrystals (CNCs) are used as additives to improve the rheological properties of attapulgite.

All the plots in figure 47 showed a dependence of the shear stress on the shear rate and the concentration of CNCs. The increase of CNC concentration from 0 to 2.4 wt. % affected the shear stress that was eventually increased. The flow curves of the CNC/ATT-WDFs (FW) at the highest shear rate of 1200 s^{-1} depicted an increase in the shear stress with CNC concentration as followed: in figure 47(A) the shear stress increased from 10,1 Pa at 0 wt. % to 10, 9.85, 10.1, 11.4, 11.4 and 12.9 Pa at 0.4, 0.8, 1.2, 1.6, 2.0 and 2.4 wt. % respectively; in figure 47(B) the shear stress increased from 9.96 Pa at 0.0 wt. % to 9.09, 9.01, 9.58, 10.2, 10.4 and 11.6 Pa at 0.4, 0.8, 1.2, 1.6, 2.0 and 2.4 wt. % respectively; in figure 47(C) the shear stress increased from 8.78 Pa at 0.0 wt. % to 8.54, 8.62, 9.12, 8.97, 10.2 and 11.3 Pa at 0.4, 0.8, 1.2, 1.6, 2.0 and 2.4 wt. % respectively; in figure 47(D) the shear stress increased from 10.3 Pa to 9.73, 9.77, 11.5, 13.2, 15.7 and 17 Pa at 0.4, 0.8, 1.2, 1.6, 2.0 and 2.4 wt. % respectively; in figure 47(E) the shear stress increased from 18.9 Pa at 0.0 wt. % to 9.65, 9.51, 10.6, 12.6, 14, 15.2 and 17.6 Pa at 0.4, 0.8, 1.2, 1.6, 2.0 and 2.4 wt. % respectively at 60˚C; in figure 47(F) the shear stress increased from 8.65 Pa at 0.0 wt. % to 8.38,

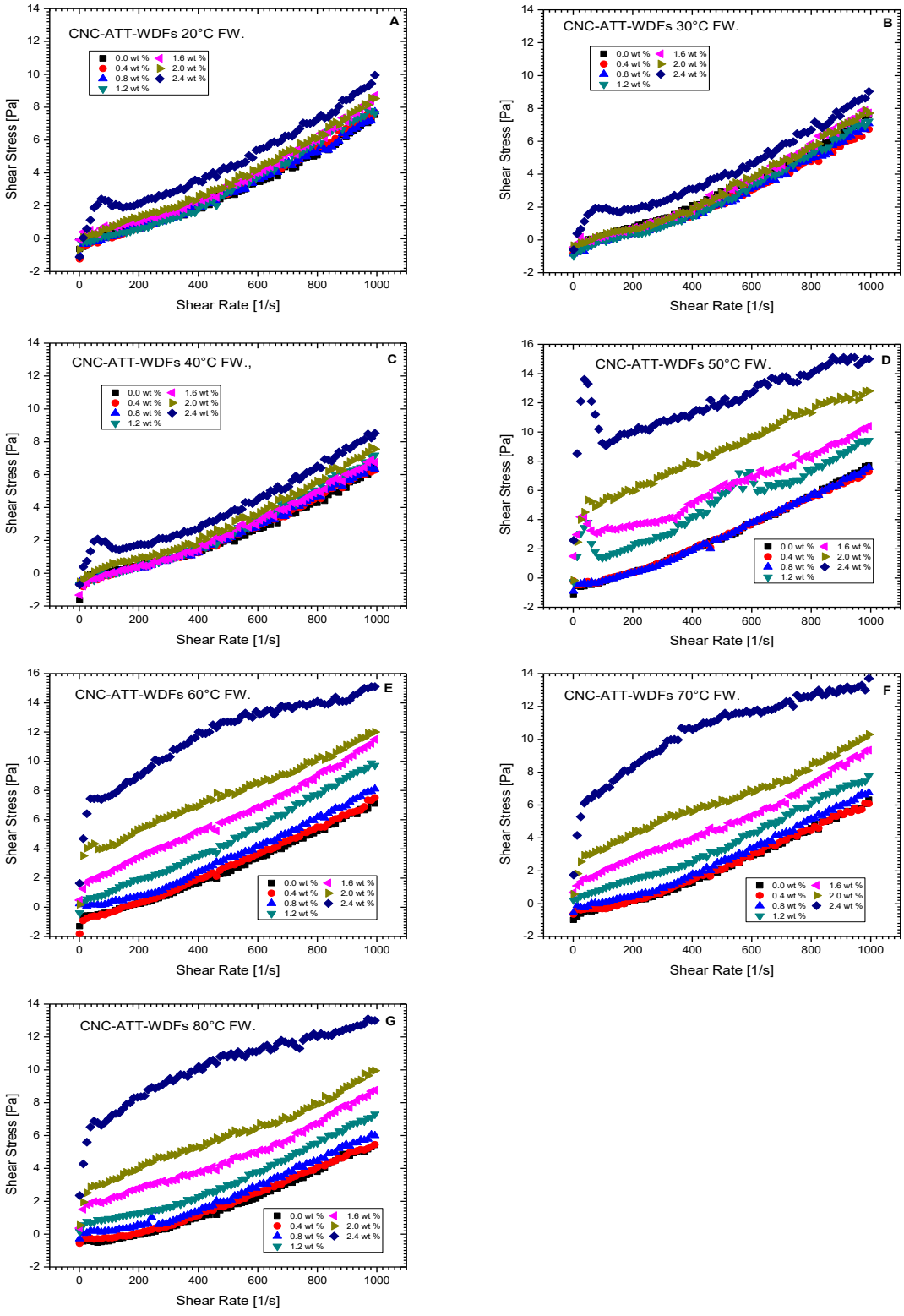

Figure 47. The plots of shear stress as a function of shear rate for CNC/ATT-WDFs in fresh-water at various CNCs concentrations for different temperatures.

8.67, 10.1, 11.9, 13.1 and 15.8 Pa at 0.4, 0.8, 1.2, 1.6, 2.0 and 2.4 wt. % respectively; and in figure 47(G) the shear stress increased from 7.7 Pa at 0.0 wt. % to 7.56, 8.18, 9.84, 11, 12.3 and 15.3 Pa at 0.4, 0.8, 1.2, 1.6, 2.0, and 2.4 wt. % respectively. From the figure 47, it is clear that the shear stress is slightly enhanced with the increasing in CNC concentrations that shows the need of the high force to start the flow of the fluids.

Herschel-Bulkley model describes the rheological behavior of CNC/ATT-WDFs (FW). All the rheological and statistical parameters are given in table 11. As it is observed for the statistical parameters, the increase of CNC concentration from 0.0 wt. % to 2.4 wt. % decreases R^2 whereas SSR/RMSD was increasing as followed (the variation of the value of R^2 at 0.0 wt. % / 2.4 wt. % and the variation of the value of SSR at 0.0 wt. % / RMSD at 0.0 wt. % to SSR at 2.4 wt. % /RMSD at 2.4 wt. % respectively) : 0,99571/0,97679 and 1,70271/0,14589 to 12,02864/0,38776 respectively at 20˚C; 0,99756/0,98466 and 1,02247/0,11305 to 6,87414/0,29313 respectively at 30˚C; 0,98892/0,98294 and 3,54067/0,21038 to 7,28523/0,30177 respectively at 40˚C; 0,99894/0,71857 and 0,54375/0,08244 to 9,56658/1,11783 respectively at 50˚C; 0,99843/0,97998 and 0,71834/0,09476 to 12,14912/0,3897 respectively at 60˚C; 0,99787/0,99054 and 0,75912/0,09741 to 4,50956/0,23742 respectively at 70˚C; and 0,99816/0,9894 and 0,51841/0,0805 to 4,00082/0,22363 respectively at 80˚C. This illustrated that the relationship between shear stress and shear rate was nonlinear.

Generally speaking, the CNC concentrations had a significant impact on the rheological parameters (i.e., y_o, K, and n). As shown in table 10, with the increase in the CNC concentration, both the y_o (Pa) and K (Pa.S) values gradually increased while the n value constantly decreased.

Rheological parameters obtain after fitting the rheological data of CNC/ATT-WDFs (FW) in table 10 showed a poor dependence of y_o, K and n on the CNC concentration due to shear thickening behavior of CNC/ATT-WDFs (FW) under certain conditions. It is shown from 20°C to 40°C, the yield stress values (y_o) poorly increased over a broad range of CNC concentration. However, from 50°C to 80°C, an increase in yield stress values (y_o) was observed from 2.0 wt. % to 2.4 wt. % CNC concentrations. A maximum yield stress values (y_o) was reached at 2.0 wt. % of 2.44968, 2.80068, 2.11002 and 2.14734 Pa respectively as the temperature was increased from 50°C to 80°C. This confirms a strong surface interaction between CNCs and attapulgite which improve significantly the cuttings transport performance and wellbore cleaning efficiency of CNC/ATT-WDFs (FW). Furthermore, these two CNC concentrations offer a shear thinning behavior with the flow behavior index n<1 as shown in table 10. As it is seen the addition of CNCs into ATT-WDFs improves the rheological property of CNC/ATT-WDFs (FW). This results in the modification of the flow curve from shear thickening to shear thinning behavior. Furthermore, the improvement of the yield stress facilitates the transportation of the cuttings into the mud system. As the yield stress represent the minimum stress needed to move the mud system.

All the finds in figure 47 and table 10 are in a good agreement. The result in table 10 showed a great correlation between shear stress and shear rate as R^2 is closed to 1 for CNC/BT-WDFs (FW). However, the flow index (n) of the most flow curves showed a shear thickening behavior as n>1 even at high temperature. This can be seen for CNC concentration from 0.4 to 1.6 wt % through all the range of temperature (20 to 80°C). Also, this includes CNC/ATT-WDFs (FW) at 2.0 and 2.4 wt. % till 40°C and 50°C respectively. But, from 50°C and 60°C up to 80°C respectively for 2.0 and 2.4 wt. %, the flow index (n) is showed a decrease in value lower than 1 (n<1). This decrease in the flow index n = 0.65118 for 2.0 wt. % of CNC in ATT-WDFs (FW) at

50°C and n = 0.29779 at 60°C for 2.4 wt. % of CNC in ATT-WDFs (FW) confirmed the shear thinning behavior of the mud system.

Table 10. Calculated parameters of CNC/ATT-WDFs (FW) at various CNC Concentrations for different temperatures using Herschel-Bulkley (HB) models.

T(°C)	CNC Conc (wt %)	y_0 (Pa)	K(Pa.S)	n	R^2	RMSD	SSR
20°C	0.0	0,04482	3,19781E-4	1,45385	0,99571	0,14589	1,70271
	0.4	0,04861	9,25576E-4	1,31398	0,99642	0,14592	1,70335
	0.8	0,04865	8,31115E-4	1,32268	0,99602	0,14682	1,72445
	1.2	0,04364	3,17216E-4	1,47367	0,99679	0,14356	1,64865
	1.6	0,39545	1,33556E-4	1,59561	0,9978	0,11625	1,0811
	2.0	0,23063	5,49334E-4	1,39281	0,99564	0,16537	2,18789
	2.4	1,21264	5,34518E-4	1,3977	0,97679	0,38776	12,02864
30°C	0.0	0,03686	6,80548E-4	1,34913	0,99756	0,11305	1,02247
	0.4	0,04222	4,79952E-4	1,39086	0,99622	0,13269	1,40857
	0.8	0,04229	3,46328E-4	1,44458	0,99633	0,13698	1,50111
	1.2	0,0423	3,33514E-4	1,45839	0,99668	0,13804	1,52448
	1.6	0,0368	2,38368E-4	1,51195	0,99752	0,12347	1,21962
	2.0	0,0394	3,37722E-4	1,46075	0,99727	0,12873	1,32572
	2.4	1,15856	2,06539E-4	1,52502	0,98466	0,29313	6,87414
40°C	0.0	0,06155	1,47974E-4	1,54908	0,98892	0,21038	3,54067
	0.4	0,04005	3,78157E-4	1,42095	0,99627	0,12804	1,31145
	0.8	0,0325	2,12447E-4	1,5056	0,99736	0,10869	0,94505
	1.2	0,03846	3,48679E-4	1,44664	0,99708	0,1247	1,24394
	1.6	0,04882	5,88668E-4	1,36773	0,9955	0,15139	1,83354
	2.0	0,01305	3,5058E-4	1,44715	0,9957	0,1528	1,86771
	2.4	1,12495	1,20753E-4	1,59906	0,98294	0,30177	7,28523
50°C	0.0	0,02805	0,00121	1,2812	0,99894	0,08244	0,54375
	0.4	0,03627	0,00141	1,25274	0,99813	0,10462	0,87557
	0.8	0,03511	0,00113	1,28941	0,99828	0,10375	0,86106
	1.2	1,32546	0,00307	1,14106	0,93222	0,65022	33,8227
	1.6	2,88935	6,73902E-4	1,34968	0,97737	0,34581	9,56658
	2.0	2,44968	0,11466	0,65118	0,97139	0,46733	17,47194
	2.4	9,5856	7,19715E-4	1,30623	0,71857	1,11783	99,9629
60°C	0.0	0,03192	0,00103	1,29642	0,99843	0,09476	0,71834
	0.4	0,04728	0,00296	1,15062	0,99742	0,1268	1,2862
	0.8	0,03915	7,37024E-4	1,35076	0,9977	0,12019	1,15556
	1.2	0,40706	0,00203	1,22488	0,99761	0,14054	1,58019
	1.6	1,57725	0,00504	1,0923	0,99402	0,21844	3,81713
	2.0	2,80068	0,03268	0,81048	0,9768	0,38116	11,62251
	2.4	0,59582	1,84549	0,29779	0,97998	0,3897	12,14912
70°C	0.0	0,0321	7,09606E-4	1,33149	0,99787	0,09741	0,75912
	0.4	0,03679	7,66021E-4	1,31809	0,99716	0,11071	0,98057
	0.8	0,0324	5,48582E-4	1,3746	0,9979	0,10087	0,81405
	1.2	0,47728	7,50372E-4	1,33276	0,99655	0,13241	1,40253
	1.6	1,5217	0,00116	1,27361	0,99139	0,21513	3,70235
	2.0	2,11002	0,02234	0,84457	0,98042	0,30509	7,44651
	2.4	0,0554	1,97033	0,27737	0,99054	0,23742	4,50956
80°C	0.0	0,02395	1,76334E-4	1,51517	0,99816	0,0805	0,51841
	0.4	0,02767	3,47577E-4	1,41601	0,99775	0,08824	0,62284
	0.8	0,04332	1,50011E-4	1,54147	0,99408	0,14752	1,74087
	1.2	0,63068	1,79544E-4	1,52723	0,99721	0,10972	0,96302
	1.6	1,81578	4,72298E-4	1,38643	0,98743	0,23196	4,30431
	2.0	2,14734	0,01417	0,9034	0,97631	0,32466	8,43222
	2.4	1,32164	1,49724	0,29511	0,9894	0,22363	4,00082

5.1.2. RHEOLOGICAL CURVES AT DIFFERENT TEMPERATURES FOR VARIOUS CNC CONCENTRATIONS.

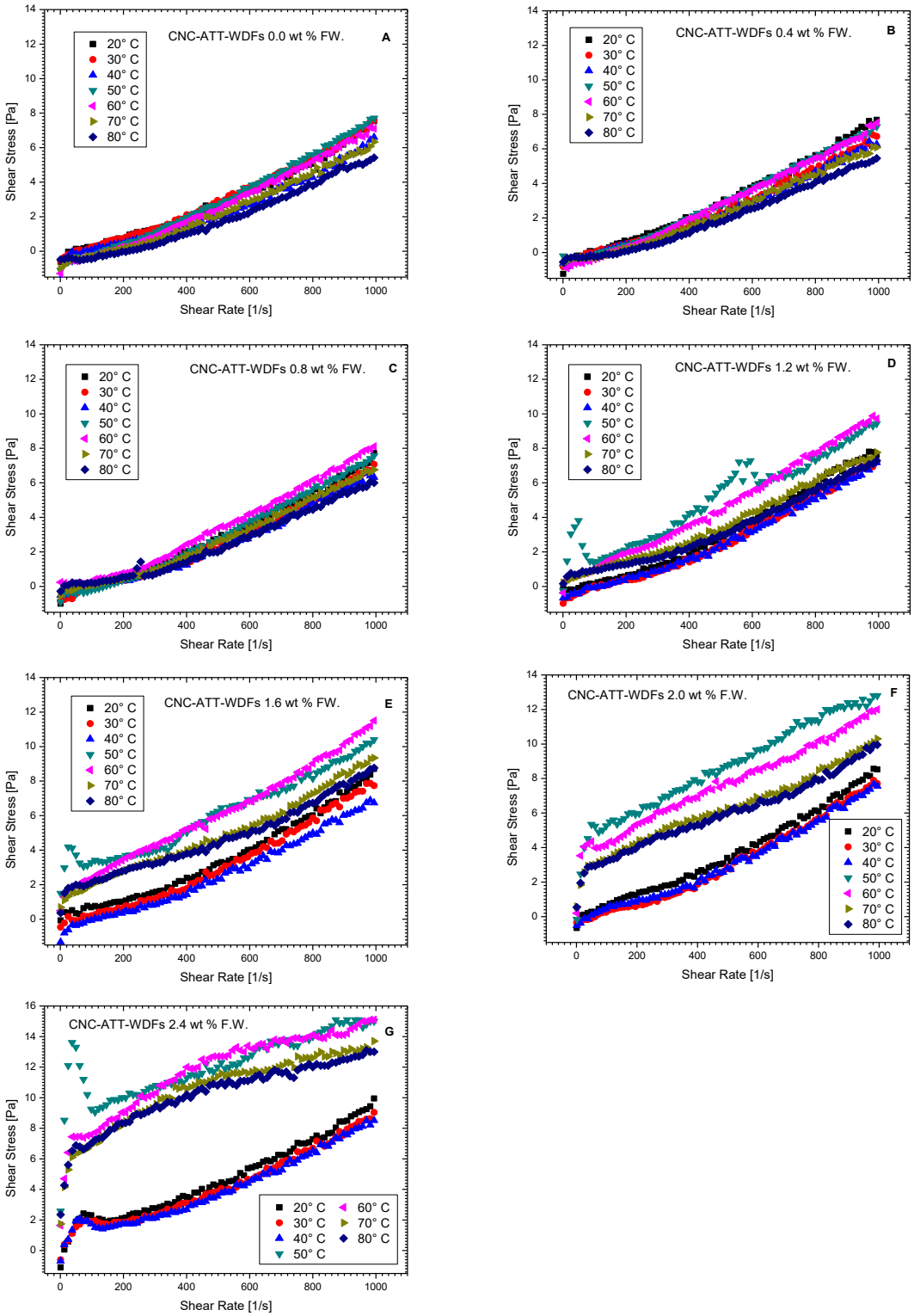

Figure 48. The plots A, B, C, D, E, F and G of shear stress as a function of shear rate for CNC/ATT-WDFs (FW) at various temperatures for different CNC concentrations.

This effect of temperature upon the shear stress as shown in table 10 was the result of figure 48 demonstrating the improvement of the rheological property of CNC/ATT-WDFs (FW) at elevated CNC concentration. Less variation of shear stress has been seen with increase in temperature, this results to the high thermal stability of CNC/ATT-WDFs (FW).

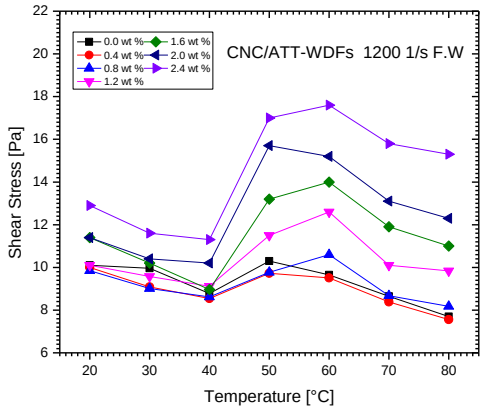

Figure 49. The plot of the shear stress of CNC/ATT-WDFs (FW) as a function of temperature at various CNC concentration at low and high shear rate (0.999s^{-1} and 1200 s^{-1}).

In figure 49, it is observed that the shear stress decrease as the temperature was increasing from 20˚C to 40˚C then a sudden increase is showed at 50˚C intensively for 1.2 wt. % to 2.4 wt. % follow by a decrease in shear stress as temperature kept on increasing from 50˚C to 80 ˚C at high shear rate (1200 s^{-1}) that led to the decrease of the viscosity of CNC/ATT-WDFs (FW). This decrease in viscosity confirm the shear thinning behavior of CNC/ATT-WDFs (FW) at 2.0 and 2.4 wt. % CNC concentrations from 50˚C to 80˚C. Firstly, the increase in shear stress is due to the increased temperature condition that ameliorated the interaction between CNC molecules and ATT water-based drilling fluids. Secondly, this decrease in shear stress is due to the instability of both materials above 60 ˚C. Therefore, additive of thermal stability agent could be needed to keep the shear stress at the expected behavior. It could be seen that under shear force, the structure of a drilling fluid is destroyed and the viscosity decreased. The recovery of the structure of a drilling fluid brings an increase in viscosity when shear is removed. Yin & Chen (2009) noticed an obvious shear thinning behavior of attapulgite nanoparticles in fluids at high shear rate, indicating that all curves were located in the non-Newtonian region. What's more, the low content of rod-like clay minerals was easy to diffuse in the solution and the rods oriented in the flow direction under shear force. In this experiment, the mixture of attapulgite with cellulose nanocrystals (CNCs) offered a shear thinning behavior only at high temperature and elevated CNC concentration. This is due to the interaction between CNCs and attapulgite rod-like clay minerals that improve the rheological and filtration properties of CNC/ATT-WDFs (FW).

5.1.3. CNC CONCENTRATION EFFECT ON THE VISCOSITY OF CNC/ATT-WDFs (FW) AS DRILLING FLUID.

The viscosity of CNC/ATT-WDFs (FW) as a function of shear rate at different CNC concentrations at figure 50(A-C) depict different trends offering an increase in viscosity with increasing temperature except for 2.4 wt. % CNC concentration where almost two plateau including a fast decrease in viscosity were observed. This result in shear thickening behavior observed for CNC/ATT-WDFs (FW). However, from figure 50(D-G), some flow curves offer a decrease in viscosity with increase in shear rate. From figure 50(D), CNC/ATT-WDFs (FW) with 0.0 to 0.8 wt. % of CNC concentration showed an increase in viscosity with shear rate resulting in a shear thickening behavior; with 1.2 wt. % of CNC concentration two plateau were observed with a fast decrease in viscosity around 100 s^{-1} that end up with a continuous viscosity that give place to a Newtonian fluid; with 1.6 wt. % of CNC concentration, the viscosity decreased till shear rate 350 s^{-1} than end up with a plateau showing that the mud fluid change to a Newtonian fluid; with 2.0 wt. % of CNC concentration, a continuous decrease in viscosity was observed that showing a thinning behavior of the mud system; and with 2.4 wt. % of CNC concentration a fluctuation in the decease of the viscosity has been observed with a great decrease around 70 s^{-1} showing a poor shear thinning behavior of CNC/ATT-WDFs (FW). From figure 50(E-F), CNC/ATT-WDFs (FW) with 0.0 to 0.8 wt. % of CNC concentration showed an increase in viscosity with shear rate resulting in a shear thickening behavior; with 1.2 wt. % of CNC concentration, a slight decrease followed by a plateau leading to a Newtonian fluid; with 1.6 wt. % of CNC concentration, the viscosity decrease and end up with a plateau at high shear rate leading to a Newtonian fluid; and with 2.0 wt. % and 2.4 wt. % of CNC concentration, a nonlinear decrease in viscosity was observed leading to a nonlinear shear thinning behavior of CNC/ATT-WDFs (FW). From figure 50(G), CNC/ATT-WDFs (FW) with 0.0 to 0.8 wt. % of CNC concentration continue to show an increase in viscosity with shear rate resulting in a shear thickening behavior; with 1.2 wt. % of CNC concentration, the decrease in viscosity is followed by an increase from 200 s^{-1} leading to a shear thickening fluid; with 1.6 wt. % and 2.0 wt. % of CNC concentrations, a nonlinear decrease of viscosity end up with a plateau at high shear rate leading to a Newtonian fluid; and with 2.4 wt. % CNC concentration, a linear decrease in viscosity was observed leading to a linear shear thinning behavior of CNC/ATT-WDFs (FW). The CNC/ATT-WDFs (FW) yields nearly linear shear-thinning curves at high CNC concentration that improve the shear-thinning behavior revealed by the potential use of CNCs additive as effective rheological modifier for drilling fluids. As observed at higher CNC concentrations nearly linear shear-thinning curves was observed indicating the transformation of CNC dispersion from anisotropic to isotropic with enhancement of the surface interaction. This increase of the viscosity with CNCs into ATT-WDFs lead to the enhancement of the shear- thinning behavior of CNC/ATT-WDFs (FW) which was advantageous for drilling fluid application. In general the viscosity value remained low whatever the increase of CNC concentration. The shear-thinning behavior is commonly attributed to the non-Newtonian fluids

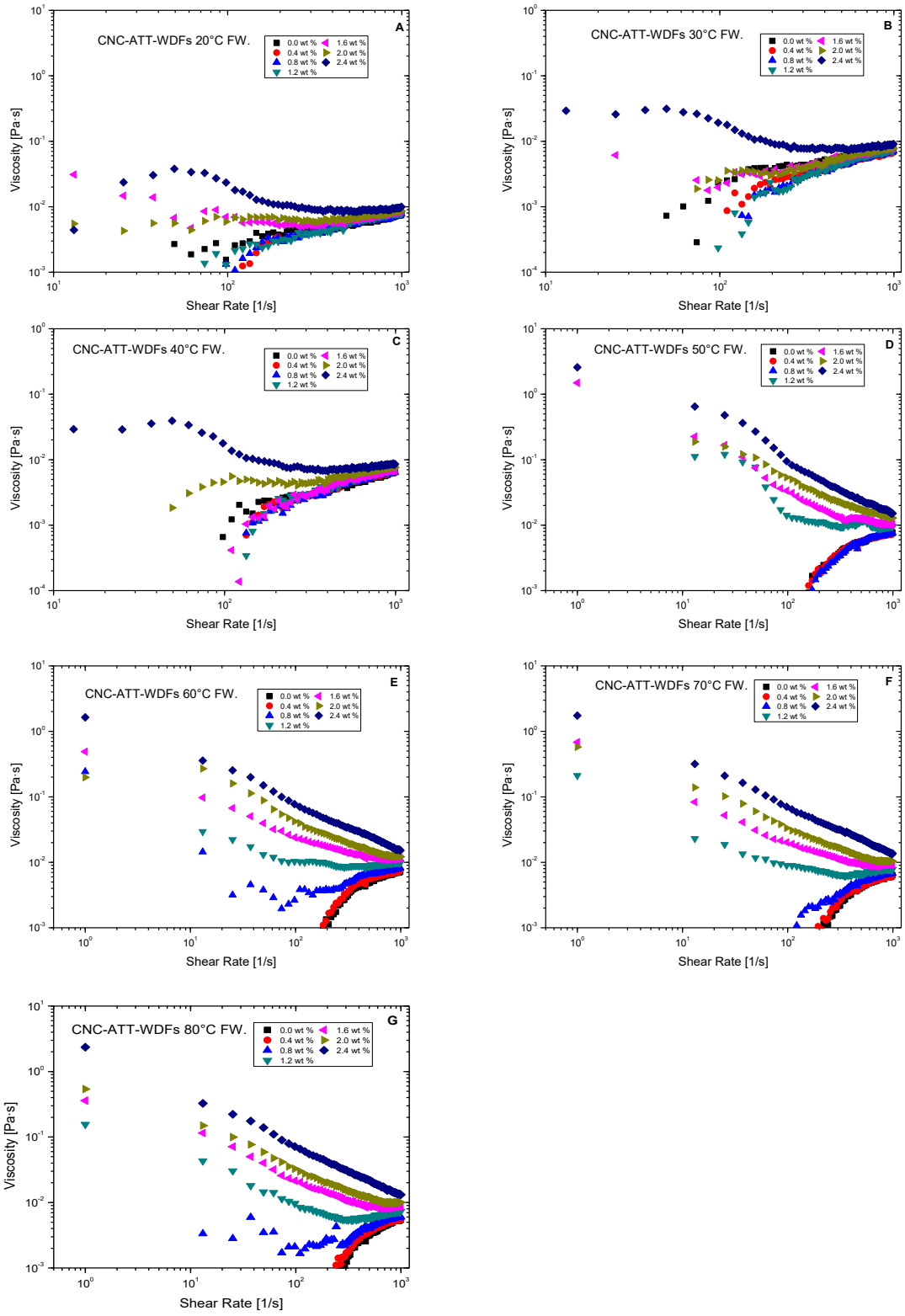

Figure 50. The plot of the viscosity of CNC/BT-WDFs (FW) as a function of shear rate at various CNC concentrations for different temperatures.

having high viscosity at low shear rates to improve the carrying capacity or suspension of the drilled cuttings from the wellbore followed by the low viscosity at high shear rates to allow the fast pumping of the fluid into the bottom of wellbores as well as to facilitate the release of the drilled cuttings. Therefore, 2.0 wt. % and 2.4 wt. % of CNC concentrations were convenient to offer a shear thinning behavior to CNC/ATT-WDFs (FW) and confirm CNCs as rheological modifier additive into ATT-WDFs in freshwater.

5.1.4. TEMPERATURE EFFECT ON THE VISCOSITY OF CNC/ATT-WDFs (FW) AS DRILLING FLUID.

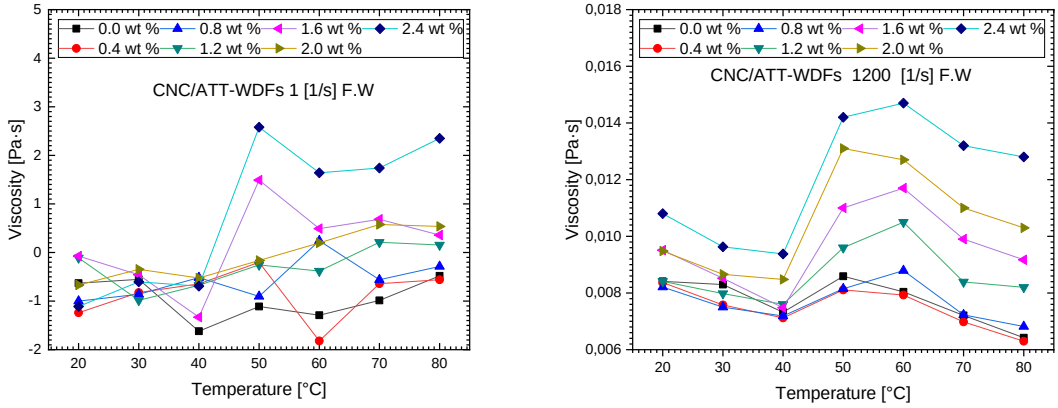

Figure 51. Viscosity of CNC/ATT-WDFs (FW) as a function of temperature at various CNC concentrations taken at low and high shear rate (1 s^{-1} (a) and 1200 s^{-1}(b)).

As shown in this figure 51(a), temperature effect on the viscosity of CNC/ATT-WDFs (FW) at low shear rate (1 s^{-1}). It is observed that for the plot of viscosity as a function of temperatures at different CNC concentration, the increase of temperature till 40°C continued to offer negative values for the viscosity at low shear rate (1 s^{-1}) over a broad range of CNC concentrations. This low viscosity value at low shear stress already weaken the carrying capacity of cuttings as well as their suspension into CNC/ATT-WDFs (FW). However, it is observed from 50°C only 1.6 wt % and 2.4 wt % of CNC in ATT-WDFs showed an increase of the viscosity and above 50°C two others CNC concentrations (1.2 wt % and 2.0 wt %) emerged with noticed viscosity (positive values) showing a good carrying capacity of cuttings and sustanable suspension in the mud system. At 80°C the plot depicts a significant increase of the initial viscosity that allowed the drilling cuttings suspension with increase in CNC concentrations and temperature as well. Contrary, in figure 51(b) for high shear stress (1200 s^{-1}), the trend of decreasing viscosity with increased temperature was interrupted between 40°C and 50°C showing a slight increase in the viscosity value at the higher temperature. Despite this sudden slight variation of viscosity at 50°C, this trend remains constant. These low viscosity values confirm a fast pumping of the fluid into the bottom of wellbores. Therefore, it facilitates the release of the drilled cuttings.

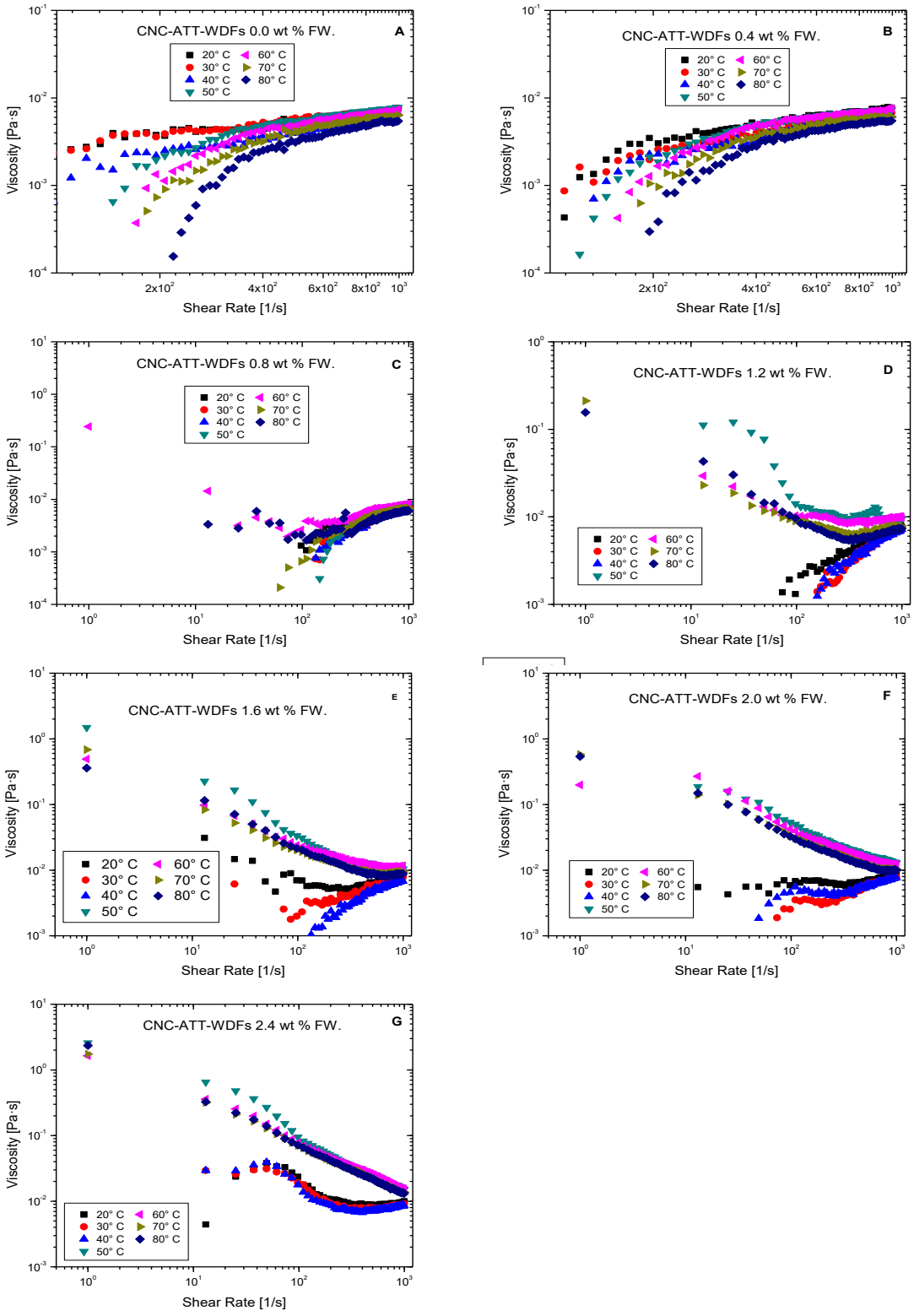

Figure 52. The plot of viscosity of CNC/ATT-WDFs (FW) as a function of shear rate at various temperatures for different CNC concentrations.

Figure 52 shows the variation of the viscosity against shear rate at different temperature for various CNC concentration. In figure 52(A-B), the viscosity increases with increasing shear rate for all the set of temperature resulting in a shear thickening behavior for BT-WDFs and CNC/BT-WDFs at 0.4 wt. % CNC concentration respectively. However, the temperature effect upon the viscosity shows a decrease of viscosity as temperature is increasing from 20˚C to 80˚C leading to more shear thickening behavior for BT-WDFs and CNC/BT-WDFs at 0.4 wt. % CNC concentration respectively. In figure 52(C), the shear thickening behavior is maintained except at 60˚C and 80˚C where CNC/BT-WDFs at 0.8 wt. % CNC concentration shows a decrease in viscosity as the shear rate increases till 100 s^{-1} then increases again till 1200 s^{-1}. The same applied in figure 52(D) from 50˚C to 80˚C for CNC/BT-WDFs at 0.8 wt. % CNC concentration. In figure 52(E-G), the shear thickening behavior is maintained from 20˚C to 40˚C as the viscosity increases with increasing shear rate whereas from 50˚C to 80˚C a shear thinning behavior is observed as the viscosity decreases with increasing shear rate. This decrease of the viscosity of CNC/ATT-WDFs (FW) over the broad range of shear rate results in a shear thinning behaviour that confirms the thixotropy property of CNC/ATT-WDFs (FW).

By investigating the effect of the change in the temperature on the viscosity, generally a decrease in viscosity as the temperature increases is observed due to the increase in the mobility of water molecules. This confirms the CNC/ATT-WDFs (FW) at 2.0 wt. % and 2.4 wt. % of CNC concentrations as the optimum concentration to be used in the drilling operation for the lowest effect of the temperature on the viscosity. In fresh water, long chain, negatively charged polymers as in the case of the carboxylated CNCs are subject to forces, which induce elongation as a result of the mutual repulsion of like charges. This affects the wrap up of the carboxylated CNCs onto attapulgite particles. In that way, the platelets approach one another so closely so that the attractive forces predominated and gives rise to a state of dispersion with edge-to-face contact of the platelets. For this reason further increase in temperature causes the platelets to aggregate and finally leads to a state of flocculation in the case where CNC concentrations are less than 2.0 wt. %.

5.2. ANALYSIS OF THE RHEOLOGICAL PROPERTIES OF CNC/ATT-WDFs IN SEAWATER.

5.2.1. RHEOLOGICAL CURVES AT DIFFERENT CNC CONCENTRATIONS FOR VARIOUS TEMPERATURES.

During the salt contamination of the drilling formation, the attapulgite, unlike bentonite, was able to form a gel structure in saltwater and be used in brine drilling fluids. Attapulgite particles can be considered as charged particles with zones of positive and negative charge. The formation of gel suspensions in salt and fresh water was made possible by the bonding of these alternating charges. The establishment of hydrogen bonds was capable to form special structures of network gel of aqueous suspensions of attapulgite able to suspend large lattice cuttings and require during the circulation of drilling fluid low power for mud pump (Luckham & Rossi 1999; Kelessidis et al 2007; Zhang et al 2017). As known a rise in temperature increases the activity of any electrolyte and increases the solubility of any salt that may be present. For this, the presence of electrolytes as in the case of seawater, the repulsive forces between negative charged polymers (carboxylated CNCs) are suppressed, thus allowing the like charges to approach one another more closely and giving rise to a coiled structure. This results in a rise of shear thinning behavior that improves the rheological property of CNC/ATT-WDFs in seawater.

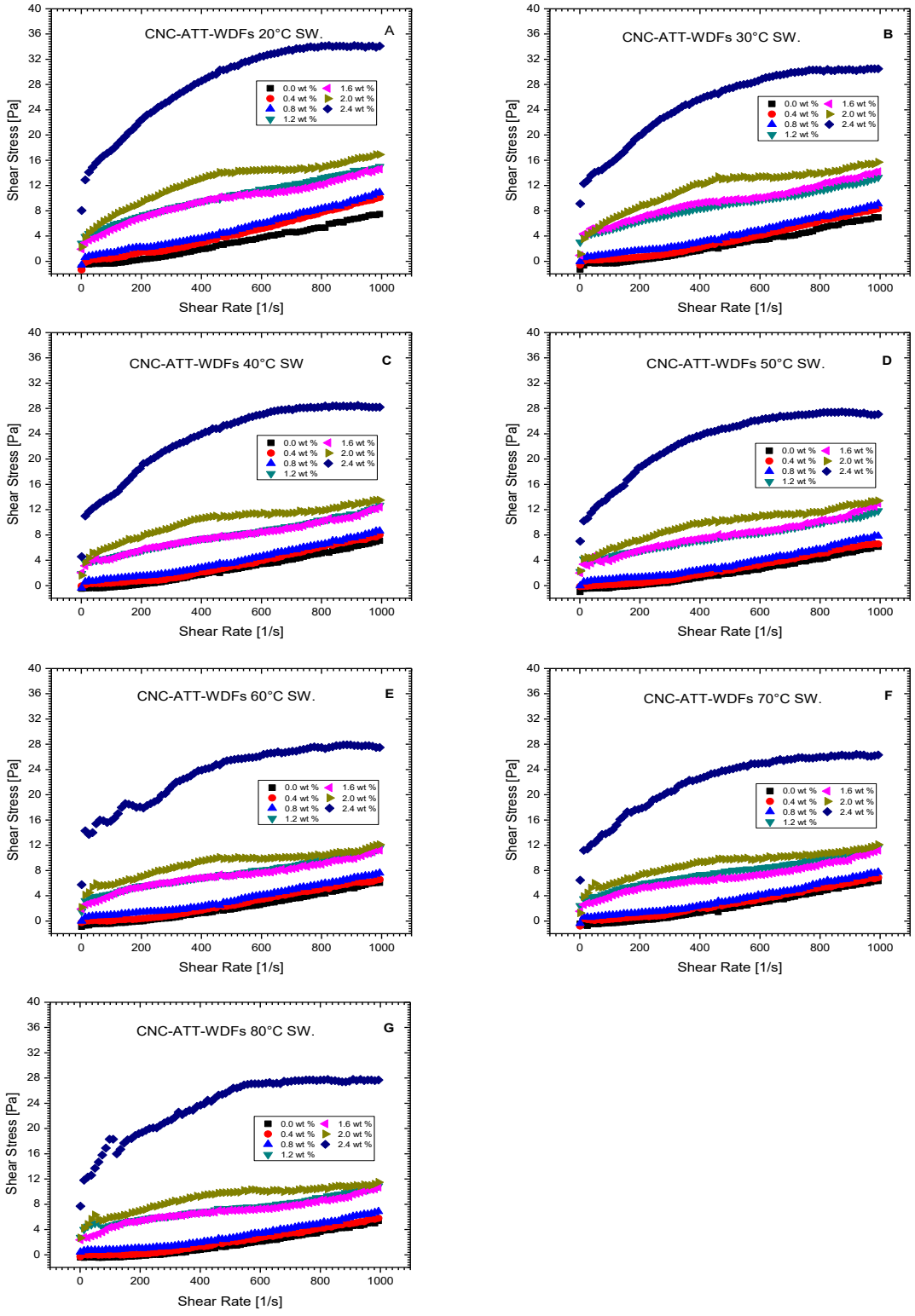

Figure 53. The plots of shear stress as a function of shear rate for CNC/ATT-WDFs in seawater at various CNC concentrations for different temperatures.

The rheological properties analysis of CNC/ATT-WDFs (SW) has been conducted in the same condition as for CNC/ATT-WDFs in freshwater. The plots of the shear stress of CNC/ATT-WDFs in seawater as a function of shear rate at different CNC concentrations are illustrated in figure 53. From shear stress versus shear rate flow curves, an enhancement of the shear stress with the increase in CNC concentration is observed, indicating the requirement of a higher force to start the flow of the fluids. However, generally speaking, it is observed that the control (0.0 wt. % of CNC concentration) ATT-WDFs (SW), 0.4 wt. % and 0.8 wt. % CNC/ATT-WDFs (SW) keep offering dilatant curves that relate to a shear thickening behavior ($n>1$). Furthermore, the release of his shear-thinning behavior is manifested from 1.2 wt. % CNC concentration and above as the flow index became lesser than 1 ($n<1$). This enhancement is observed from dilatant flow curves to shear-thinning flow curves by increasing CNC concentration. The enhancement in shear stress is due to the high surface interaction between CNCs, attapulgite, and immobilized water that can offer strong resistance to flow under a shear force that built a card-house structure.

It is observed that in the presence of seawater, the salt as a contaminant could not affect the attapulgite water-based drilling fluids. However, high tolerance is shown by CNC/ATT-WDFs in the presence of high salinity. This confirms the research of Al-marhoun (2015) reported on the fibrous structure of attapulgite minerals that were less reactive toward salt and temperature as they possess low surface energy.

The experiment results in figure 53 displayed more shear-thinning curves than the shear thickening curves and 1.2 wt. % of CNC concentration was shown as the minimum concentration capable to offer a good shear-thinning behavior of CNC/ATT-WDFs in seawater. By the way, the incorporation of CNCs into ATT-WDFs (SW) gradually changed the pattern of the rheological curves and were capable to stand against the salt effect in the suspension formed by CNC/ATT-WDFs (SW), especially from 1.2 wt. % to 2.4 wt. % of CNC concentrations. This salt resistance is attributed to the strong surface interactions between CNCs, attapulgite, and water immobilized as a stiff network was built based on the attraction between carboxylated CNCs to the positively charged edge surfaces of the attapulgite. This improves the rheological properties of CNC/ATT-WDFs (SW). Therefore, the strong interaction imparts rigidity to the CNC-attapulgite networks that increase the salt resistance of CNC/ATT-WDFs (SW) by preventing invasion by salt ions, enhancing water barrier capacity, and decreasing fluid loss.

The results in figure 53 show that all suspensions of CNC/ATT-WDFS (SW) have yield stress (y_o). The maximum yield stress is reached at 1.2 wt. % of CNC concentration for the entire range of temperatures. This increase in the yield stress should be attributed to the absorption of the polymer macromolecules (CNCs) onto attapulgite particle surfaces.

From figure 53(A), the yield stress (y_o) varied from 0.04606 Pa at 0.0 wt. % CNC to 0.06081, 0.71899, 3.1348, 1.50173, 0.83326 and 2.81456 Pa at 0.4, 0.8, 1.2, 1.6, 2.0 and 2.4 wt. % respectively; From figure 53(B), the yield stress (y_o) varied from 0.04974 Pa at 0.0 wt. % CNC to 0.04335, 0.62812, 3.35335, 2.80046, 0.85481and 4.52407 Pa at 0.4, 0.8, 1.2, 1.6, 2.0 and 2.4 wt. % respectively; From figure 53(C), the yield stress (y_o) varied from 0.02931 Pa at 0.0 wt. % CNC to 0.03725, 0.58704, 3.19322, 3.07088, 0.574 and 1.75228 Pa at 0.4, 0.8, 1.2, 1.6, 2.0 and 2.4 wt. % respectively; From figure 53(D), the yield stress (y_o) varied from 0.02484 Pa at 0.0 wt. % CNC to 0.03401, 0.68785, 3.52026, 2.95168, 1.61822 and 0.2548 Pa at 0.4, 0.8, 1.2, 1.6, 2.0 and 2.4 wt. % respectively; From figure 53(E), the yield stress (y_o) varied from 0.02106 Pa at 0.0 wt. % CNC to 0.0504, 0.62693, 2.96847, 2.20012, 0.8403 and 3.66412 Pa at 0.4, 0.8, 1.2, 1.6, 2.0 and 2.4 wt. % respectively; From figure 53(F), the yield stress (y_o) varied from 0.02759 Pa at 0.0 wt. % CNC

to 0.04744, 0.53658, 3.04866, 2.49568, 0.54512 and 1.34556 Pa at 0.4, 0.8, 1.2, 1.6, 2.0 and 2.4 wt. % respectively; and from figure 53(G), the yield stress (y_o) varied from 0.02337 Pa at 0.0 wt. % CNC to 0.03732, 0.59417, 0.59417, 4.15802, 2.41918, 1.53609 and 2.39824 Pa at 0.4, 0.8, 1.2, 1.6, 2.0 and 2.4 wt. % respectively.

Table 11. Calculated parameters of CNC/ATT-WDFs (SW) at various CNC concentrations for different temperatures using Herschel−Bulkley model.

T(°C)	CNC Conc (wt %)	y_0 (Pa)	K(Pa.S)	n	R^2	RMSD	SSR
20°C	0.0	0,04606	0,00146	1,25255	0,99721	0,13284	1,41173
	0.4	0,06081	0,00125	1,30638	0,99661	0,18165	2,63978
	0.8	0,71899	0,00138	1,28795	0,99564	0,20125	3,24007
	1.2	3,1348	0,11811	0,66446	0,99824	0,13003	1,35261
	1.6	1,50173	0,3277	0,52623	0,9879	0,3381	9,14505
	2.0	0,83326	2,01714	0,31473	0,97575	0,54412	23,68511
	2.4	2,81456	3,85085	0,31286	0,97737	0,98669	0,97355
30°C	0.0	0,04974	0,001	1,29785	0,9961	0,14779	1,74732
	0.4	0,04335	4,28849E-4	1,436	0,99719	0,13977	1,56282
	0.8	0,62812	7,83962E-4	1,34498	0,99703	0,13968	1,56076
	1.2	3,35335	0,06379	0,72361	0,99525	0,17796	2,53346
	1.6	2,80046	0,17237	0,59716	0,97525	0,43691	15,27116
	2.0	0,85481	2,29121	0,29397	0,97647	0,50815	20,65764
	2.4	4,52407	2,60701	0,3428	0,97124	0,97426	75,93397
40°C	0.0	0,02931	7,63728E-4	1,33503	0,99853	0,08913	0,63558
	0.4	0,03725	2,67761E-4	1,49589	0,99612	0,15541	1,93224
	0.8	0,58704	5,4041E-4	1,39211	0,9964	0,1472	1,73351
	1.2	3,19322	0,02684	0,83745	0,98914	0,25838	5,34095
	1.6	3,07088	0,03558	0,79263	0,98381	0,3038	7,38355
	2.0	0,574	1,73399	0,29748	0,9819	0,3469	9,62727
	2.4	1,75228	4,88	0,26785	0,97341	0,91279	66,65488
150°C	0.0	0,02484	3,17786E-4	1,44379	0,99848	0,08041	0,51723
	0.4	0,03401	4,00118E-4	1,41872	0,99752	0,1086	0,94355
	0.8	0,68785	1,25408E-4	1,58905	0,99668	0,12811	1,3129
	1.2	3,52026	0,02002	0,86406	0,99026	0,22072	3,89747
	1.6	2,95168	0,03296	0,81159	0,9783	0,3745	11,22023
	2.0	1,61822	0,61254	0,42437	0,98773	0,28841	6,65432
	2.4	0,2548	4,48324	0,26934	0,96671	0,95423	72,84461
60°C	0.0	0,02106	3,90348E-4	1,41582	0,99896	0,06713	0,36056
	0.4	0,0504	5,71481E-4	1,36661	0,99484	0,15621	1,95207
	0.8	0,62693	2,5538E-4	1,4823	0,9956	0,14365	1,65083
	1.2	2,96847	0,03742	0,77585	0,98498	0,27248	5,93961
	1.6	2,20012	0,09933	0,63777	0,97638	0,33238	8,83813
	2.0	0,8403	1,3552	0,29802	0,96516	0,38111	11,6197
	2.4	3,66412	3,54603	0,28479	0,96337	0,91084	66,3708
70°C	0.0	0,02759	4,58E-4	1,39949	0,99841	0,08714	0,60753
	0.4	0,04744	5,5842E-4	1,36929	0,99537	0,14725	1,7345
	0.8	0,53658	3,1789E-4	1,45431	0,9955	0,14725	1,77719
	1.2	3,04866	0,05397	0,72524	0,99097	0,21058	3,54736
	1.6	2,49568	0,03666	0,77594	0,97174	0,36883	10,88256
	2.0	0,54512	1,81913	0,2692	0,98151	0,28603	6,54484
	2.4	1,34556	4,15063	0,26733	0,97635	0,72763	42,35589
80°C	0.0	0,02337	9,23725E-5	1,60277	1,60277	0,08196	0,53733
	0.4	0,03732	1,96012E-4	1,49938	1,49938	0,12443	1,2386
	0.8	0,59417	8,19359E-5	1,6294	1,6294	0,09155	0,67058
	1.2	4,15802	0,0065	0,99375	0,99375	0,2751	6,05461
	1.6	2,41918	0,09942	0,62042	0,62042	0,37596	11,30749
	2.0	1,53609	1,07829	0,32016	0,32016	0,35938	10,33258
	2.4	2,39824	4,27403	0,26642	0,26642	0,92032	67,75873

The Herschel-Bulkley model offered better fitting of the rheological data as shown in table 11 where an increase in the yield stress (y_o) as a function of CNC concentration is observed at different temperatures. However, the CNC concentrations had a significant impact on the rheological parameters (i.e., y_o, K, and n). As shown in table 12, with the increase in the CNC concentration, both y_o (Pa) and K (Pa.S) values gradually increased while the n value constantly decreased.

5.2.2. RHEOLOGICAL CURVES OF CNC/ATT-WDFs (SW) AT DIFFERENT TEMPERATURES FOR VARIOUS CNC CONCENTRATIONS

The rheological properties of CNC/ATT-WDFs (SW) were measured with the Rotational Rheometer (RheolabQC SN897839/FW1.31) at atmospheric pressure and various temperatures.

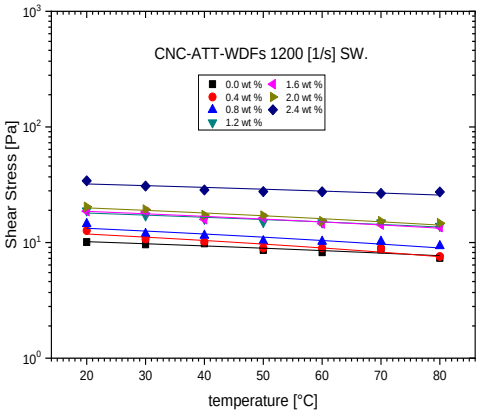

Figure 54. The plot of shear stress as a function temperature for CNC/ATT-WDFs in seawater at various CNC concentrations taken at high shear rate 1200 s^{-1}.

On the other hand figure 54 shows that at the higher shear rate (1200 s^{-1}) and constant CNC concentration, a decrease of the shear stress was observed as the temperature was increasing that led to the decrease of the viscosity of CNC/ATT-WDFs (SW) as well in figure 56. The decrease in viscosity confirms the shear-thinning behavior of CNC/ATT-WDFs (SW). This decrease of the shear stress with an increase in temperature is attributed to the thermal dispersion and thermal dehydration of the attapulgite clay particles in the suspension. The shear stress versus shear rate curves is shown in figure 55. The experimental results indicate that the CNC/ATT-WDFS in seawater behaved as shear thickening fluids from figure 55(A-C) over a broad range of temperature with a consistency index greater than 1 (n>1). By increasing the amount of CNCs added into ATT-WDFs (SW), shear-thinning fluids appear from figure 55(D-G) over a broad range of temperatures. However, the shear-thinning behavior of CNC/ATT-WDFs (SW) is the most interesting as it is needed during the drilling operation. For the shear-thinning behavior of CNC/ATT-WDFs (SW) from figure 54(D-G), the shear stress showed a slight decrease as temperature increased at the high shear rate (1200 s^{-1}) in figure 54 that means less change was observed over a broad range of temperature from 20 to 80 °C. Generally speaking, the combined application of shear rate and temperature favored the attapulgite for enhancing rheological properties.

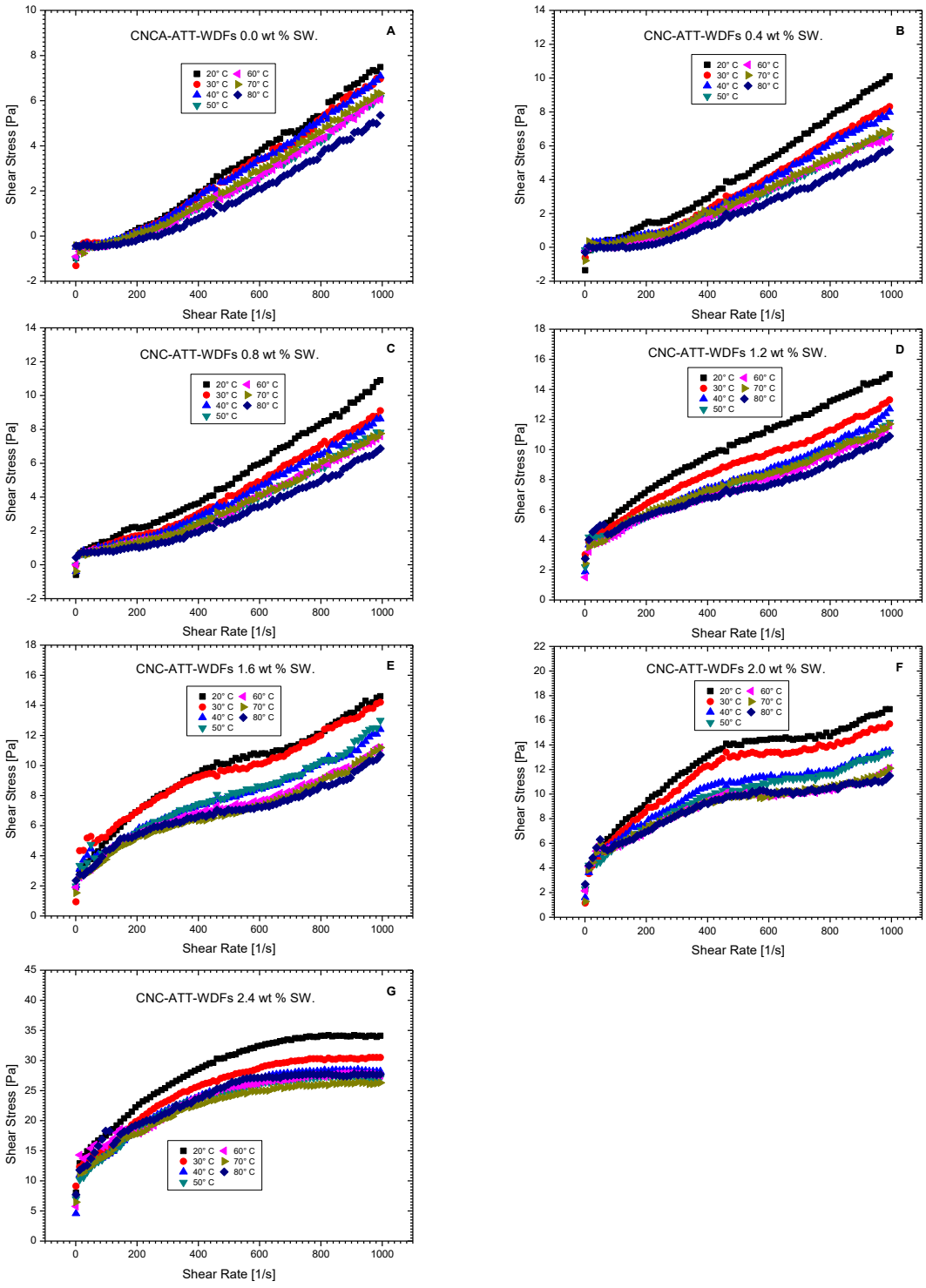

Figure 55. Plots of shear stress of CNC/ATT-WDFs (SW) as a function of shear rate at different temperature for various CNC concentrations.

5.2.3. THE EFFECT OF CNC CONCENTRATION ON THE VISCOSITY OF CNC/ATT-WDFs (SW) AS DRILLING FLUID.

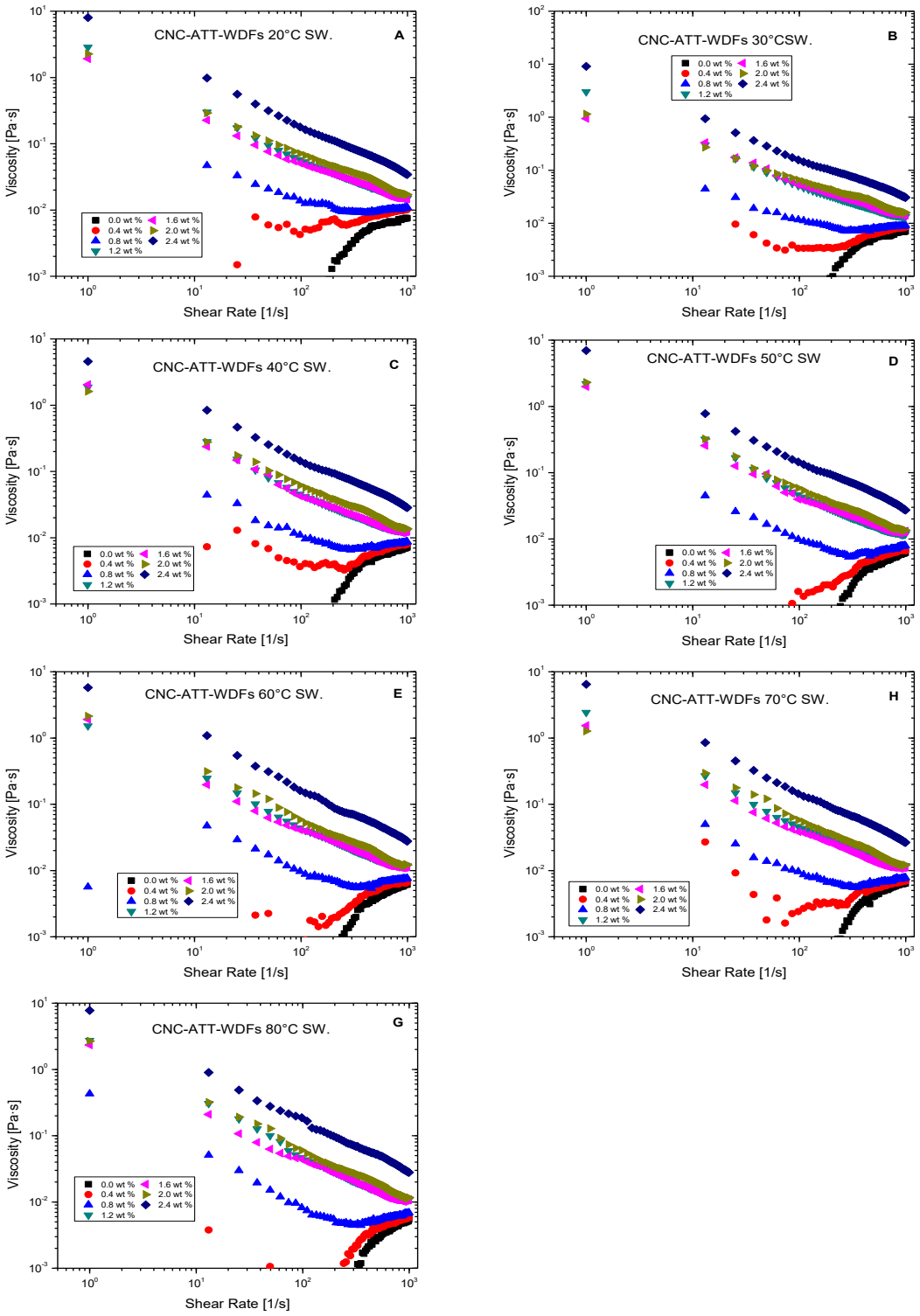

Figure 56. The plot of the viscosity of CNC/ATT-WDFs (SW) as a function of shear rate at various CNC concentrations for different temperatures.

The analysis of the rheological curves based on the variation of the viscosity with the shear rate at various CNC concentrations shown in figure 56 demonstrates a reduction in viscosity over a broad range of shear rate from 0.999 s^{-1} to 1200 s^{-1} from 1.2 to 2.4 wt. % CNC concentrations from plot A to G. These rheograms represent the shear-thinning behavior of CNC/ATT-WDFs (SW) due to the strong interaction between charged attapulgite and carboxylated CNCs with immobilized water. This reduction has been seen as well at 0.8 wt. % CNC concentration but was interrupted with an increase in viscosity. This interruption is due to a weak interaction between carboxylated CNCs and ATT-WDFs. This interruption is showed from 200 s^{-1} to 1200 s^{-1} that let appear a shear thickening behavior over a broad range of temperature from plot A to G. However, the viscosity continues to increase over a broad range of shear rate for 0.0 and 0.4 wt. % CNC concentration that confirms a shear thickening behavior of these mud systems over a broad range of temperatures from plot A to G.

The rheological data given in table 12 below provides the description of the variation of viscosity as a function of CNC concentration at different temperatures.

Table 12. Viscosity of CNC/ATT-WDFs (SW) at various CNC concentrations for different temperatures.

CNC concentration	Shear Rate	Viscosity	Viscosity	Viscosity	Viscosity	Viscosity	Viscosity	Viscosity
[wt %]	[1/s]	[Pa·s]	[Pa·s]	[Pa·s]	[Pa·s]	[Pa·s]	[Pa·s]	[Pa·s]
		CNC-ATT-WDFs S.W. [20°C]	CNC-ATT-WDFs S.W. [30°C]	CNC-ATT-WDFs S.W. [40°C]	CNC-ATT-WDFs S.W. [50°C]	CNC-ATT-WDFs S.W. [60°C]	CNC-ATT-WDFs S.W. [70°C]	CNC-ATT-WDFs S.W. [80°C]
0.0	0,999	-0,985	-1,31	-0,491	-1,01	-0,91	-0,421	-0,428
0,4	0,999	-1,35	-0,607	-0,0727	-0,15	-0,249	-0,783	-0,304
0,8	0,999	-0,599	-0,0273	-0,397	-0,0259	0,00565	-0,384	0,43
1,2	0,999	2,86	3,02	1,88	2,19	1,52	2,43	2,74
1,6	0,999	1,92	0,941	2,04	1,99	1,91	1,54	2,34
2.0	0,999	2,26	1,15	1,61	2,3	2,14	1,27	2,68
2,4	0,999	8,03	9,14	4,57	6,97	5,76	6,46	7,74

Generally speaking, it denotes that the viscosity of CNC/ATT-WDFs (SW) increases exponentially with the increase in the CNC concentrations as shown in figure 57. Figure 57 plots from values in table 12 shows that the viscosity of the CNC/ATT -WDFs (SW) increases from -0.985 Pa.s at 0.0 wt. % of CNC to -1.35, -0.599, 2.86, 1.92, 2.26 and 8.03 Pa.s at 0.4, 0.8, 1.2, 1.6, 2.0 and 2.4 wt. % of CNCs respectively for 20°C; from -1.31 Pa.s at 0 wt. % of CNC to -0.607, -0.0273, 3.02, 0.941, 1.15 and 9.14 Pa.s at 0.4, 0.8, 1.2, 1.6, 2.0 and 2.4 wt. % of CNCs respectively for 30°C; from -0.491 Pa.s at 0 wt. % of CNC to -0.0727, -0.397, 1.88, 2.04, 1.61 and 4.57 Pa.s at 0.4, 0.8, 1.2, 1.6, 2.0 and 2.4 wt. % of CNCs respectively for 40°C; from -1.01 Pa.s at 0 wt. % of CNC to -0.15, -0.0259, 2.19, 1.99, 2.3 and 6.97 Pa.s at 0.4, 0.8, 1.2, 1.6, 2.0 and 2.4 wt. % of CNCs respectively for 50°C; from -0.91 Pa.s at 0 wt. % of CNC to -0.249, 0.00565, 1.52, 1.91, 2.14 and 5.76 Pa.s at 0.4, 0.8, 1.2, 1.6, 2.0 and 2.4 wt. % of CNCs respectively for 60°C; from -0.421 Pa.s at 0 wt. % of CNC to -0.783, -0.384, 2.43, 1.54, 1.27 and 6.46 Pa.s at 0.4, 0.8, 1.2, 1.6, 2.0 and 2.4 wt. % of CNCs respectively for 70°C; and from -0.428 Pa.s at 0 wt. % of CNC -0.304, 0.43, 2.74, 2.34, 2.68 and 7.74 Pa.s at 0.4, 0.8, 1.2, 1.6, 2.0 and 2.4 wt. % of CNCs respectively for 80°C.

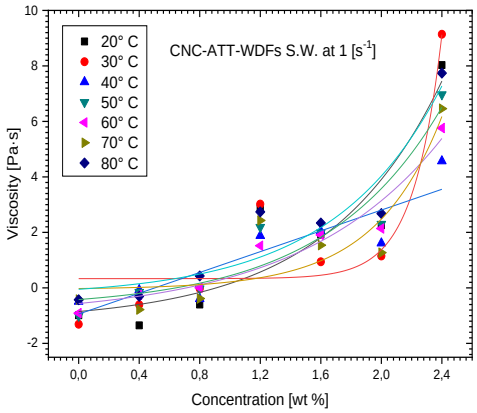

Figure 57. Variation of viscosity of CNC/ATT-WDFs (SW), determined from low shear rates (0.999 1/s), with CNC concentrations at different temperatures.

As a negative value of the viscosity stands for lost viscosity, 1.2 wt. % CNC concentration into ATT-WDFs (SW) has taken as the starting concentration that offers a significant viscosity value that induces a shear-thinning behavior of the drilling fluids in seawater and allows the carrying of cuttings at the low shear rate (0.999 s^{-1}). It can be seen in table 13 that the incorporation of CNCs from 1.2 to 2.4 wt. % to the attapulgite suspension increases the viscosity of CNC/ATT-WDFs (SW) significantly, which increases the carrying cuttings performance. The hydrogen bonding built between hydrogen and hydroxyl of attapulgite clay and the carboxylated CNCs can be the reason for this increase in viscosity of CNC/ATT-WDFs (SW).

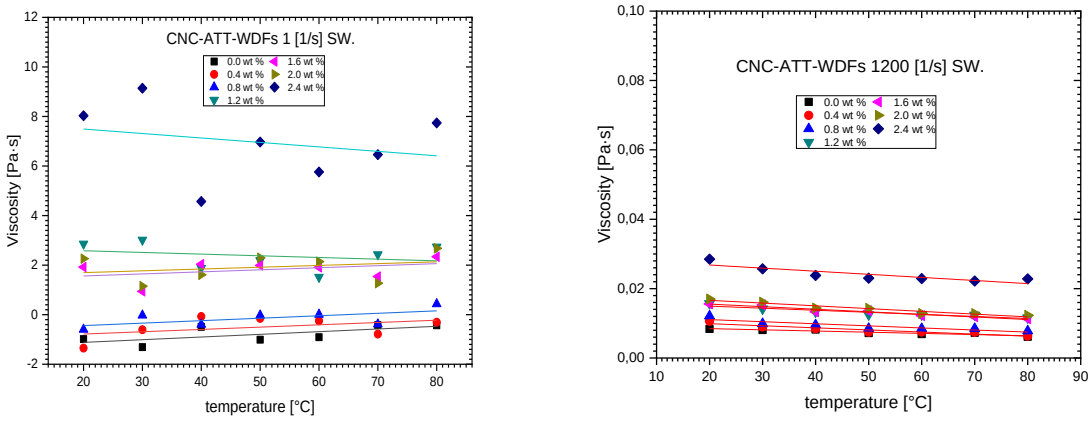

Figure 58. The plot of viscosity as a function temperature for CNC/ATT-WDFs in fresh-water at various CNC temperature taken at low and high shear rate (1 s^{-1} and 1200 s^{-1}).

Generally, the increase in temperature induces a reduction of the viscosity but in the presence of some strong surface interaction, there will be less sensitivity to the change of temperature. In this way, it can be conducted any investigation for the evidence of an existing strong surface interaction upon CNC/ATT-WDFs (SW). Figure 58 depicts the effect of temperature on the viscosity of CNC/ATT-WDFs (SW) at a low shear rate. It has been observed that from 0.0 to 0.8 wt. % CNC

concentrations into ATT-WDFs (SW) as the viscosity remained below zero, the temperature could not impact them. Their viscosities were unstable with change in the temperature and exhibited poor thermal stability as certainly they were increasing with increased shear rate leading to a shear thickening behavior. However, from 1.2 to 2.4 wt. % CNC concentrations into ATT-WDFs (SW), it can be seen that their viscosity was not affected by the change in temperature due to the firm network among ATT rods, CNCs, and immobilized water molecules in which the core-shell structure caught water molecules and fastened at the proximity of CNCs, offering less effect of temperature change upon the viscosity. This behavior has been shown at the high shear rate in which CNC/ATT-WDFs (SW) displayed more resistance to the temperature change (Yan et al 2013).

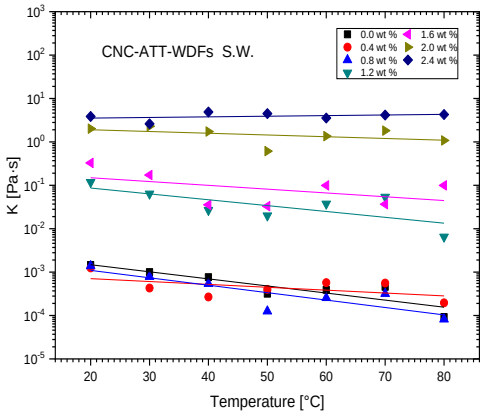

Figure 59. The plot of the flow consistency coefficient (K) as a function temperature of CNC/ATT-WDFs (SW) at various CNCs temperatures.

Figure 59 describes the variation of the flow consistency coefficient of CNC/ATT-WDFs (SW) against temperature at different CNC concentrations. By performing a linear fitting, the statistical data analysis results with different slope values as CNC concentration was varied: -0.01631 ± 0.00362, -0.00663 ± 0.00445, -0.0171 ± 0.0047, -0.0135 ± 0.00585, -0.00876 ± 0.00695, -0.00401 ± 0.00367 and 0.00143 ± 0.00173 for 0.0, 0.4, 0.8, 1.2, 1.6, 2.0 and 2.4 wt. % respectively. As it is seen negative slope value stands for a decrease of the flow consistency coefficient whereas a positive slope value stands for an increase of CNC/ATT-WDFs (SW) as a function of temperature at different CNC concentrations. As seen in this figure 59, the flow consistency coefficient (K) which is a measure of the shear viscosity (the resistance to flow at $1s^{-1}$) is slightly maintained constant over the broad range of temperature from 20°C to 80°C at 0.4, 1.2, 1.6 and 2.0 wt. % CNC concentrations that mean after the yield stress is exceeded, the flow is maintained constant along with the change of temperature. These lowest values of the slope are related to the lowest effect of the temperature on the flow consistency coefficient. Therefore, the CNC/ATT-WDFs (SW) with a low resistance to flow develop great thermal stability.

It depicted that the viscosity increased with increasing shear rate over the broad ranges of the temperature, as seen in figure 60(A-B). However, in figure 60(B), a discrepancy trend is observed due to the poor stability between CNC molecules and ATT clay particles and the temperature effect. However, this discrepancy trend occurred due to the less impact of fewer CNC concentrations added to the ATT-WDFs (SW). This less impact of CNC leads to establish a weak interaction between CNCs, Attapulgite, and immobilized water. This amount of CNC concentration (0.4 wt. %) was not enough for a significant shift into the drilling fluid from the shear-thickening behavior to the shear-thinning behavior. Therefore, the rheogram was able to

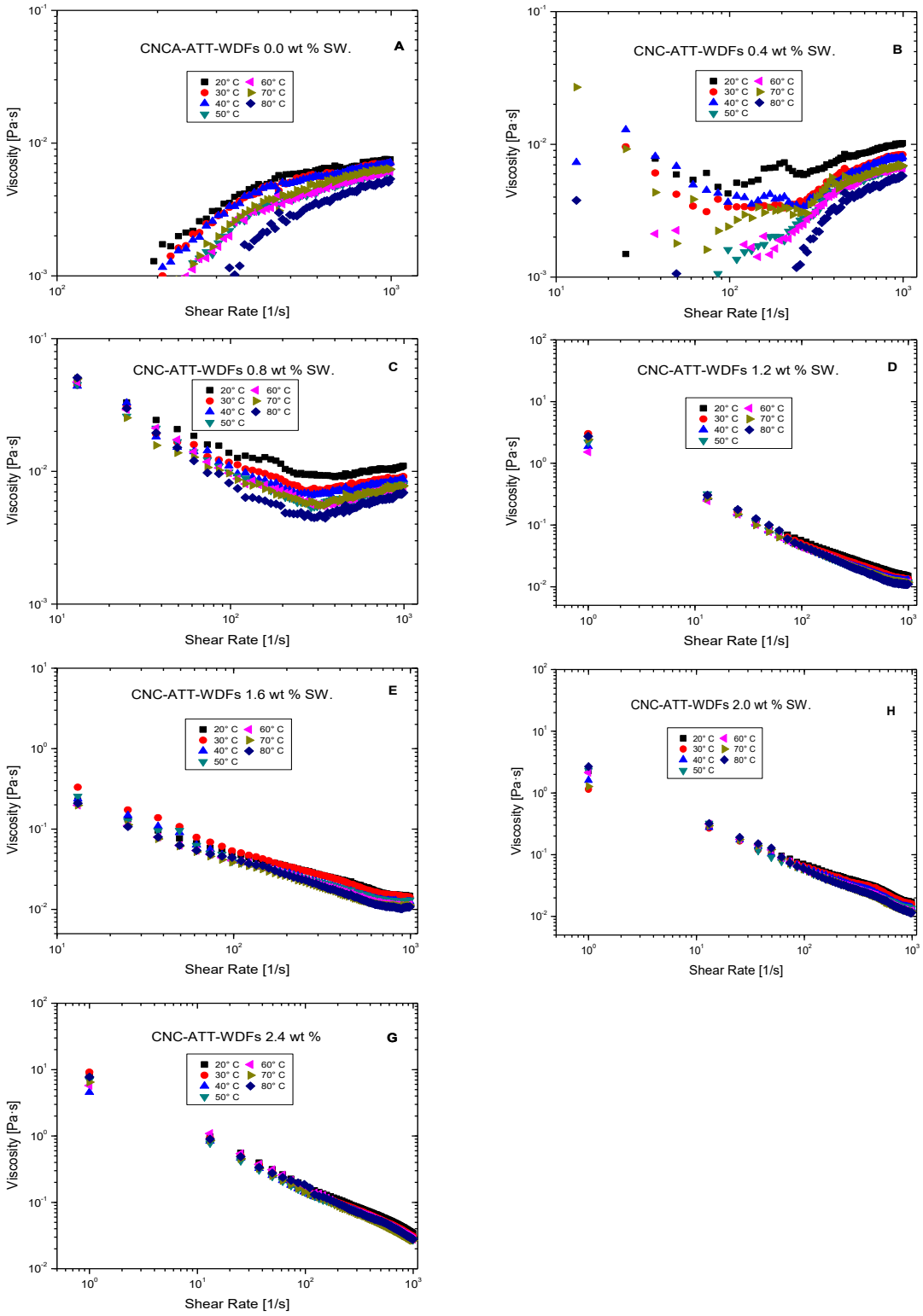

Figure 60. The plot of the viscosity of CNC/ATT-WDFs (SW) as a function of shear rate at various temperatures for different CNC concentrations.

show up this trend of shear-thinning behavior. By the way, the temperature change affected this weak interaction by displaying this discrepancy trend. Thus, the temperature effect on the viscosity of 0.4 wt. % CNC/ATT-WDFs (SW) impacted as well on the shear-thinning at the low shear rate (10-350 s-1); in figure 60(C), it can be seen that the viscosity decreased (0.999 s^{-1} to 300 s^{-1}) than increased (till 1200 s^{-1}); and from figure 60(D-G), it can be seen that the viscosity of the mud decreased with increasing shear rate at all the range of temperature. Therefore, this reduction of viscosity with increasing shear rate resulted in a shear thinning behavior. As it could be seen that the temperature effect on the viscosity remained mostly constant at high temperatures confirming the thermal stability of CNC/ATT-WDFs (SW). Thus, it can be seen that attapulgite develops a high resistance in salinity or the presence of salt content in seawater. This salt content favors the improvement in yield stress, viscosity, and gel strength of CNC/ATT-WDFs.

This behavior of the different rheological properties of the mud system under high temperature could be the result of the thermal degradation of the solid content, polymers, and other components of the mud system and the expansion of the molecules which will lower the resistance of the fluid to flow, hence, its viscosity, yield stress and gel strength **(**Amani & Al-Jubouri 2012). By contrast, the present case of CNC/ATT-WDFs (SW) shows an improvement of the rheological properties with the incorporation of the CNC polymers in the presence of seawater and high temperature into ATT-WDFs (SW) including the improvement of the yield stress, viscosity, and gel strength of the mud system. It has been seen as well the transformation from the shear thickening curves to shear-thinning curves through the incorporation of CNCs as nanoparticles in WDFs (SW) confirming the rheological modifier and fluid loss reducer of CNCs. Thus, 1.2 wt. % of CNCs can be considered as the optimum concentration to be used to improve the rheological properties of CNC/ATT-WDFs in seawater.

5.3. FILTRATION PROPERTIES

5.3.1. ANALYSIS OF FILTRATION PROPERTIES OF CNC/ATT-WDFs (FW)

The drilling fluid based on attapulgite clay has been investigated by incorporating different CNC concentrations as followed 0.0, 0.8, 1.0, and 1.2 wt. % respectively at 20°C and 80°C to design a suitable drilling fluid that is following API standards (15ml/30 min) as shown in figure 61

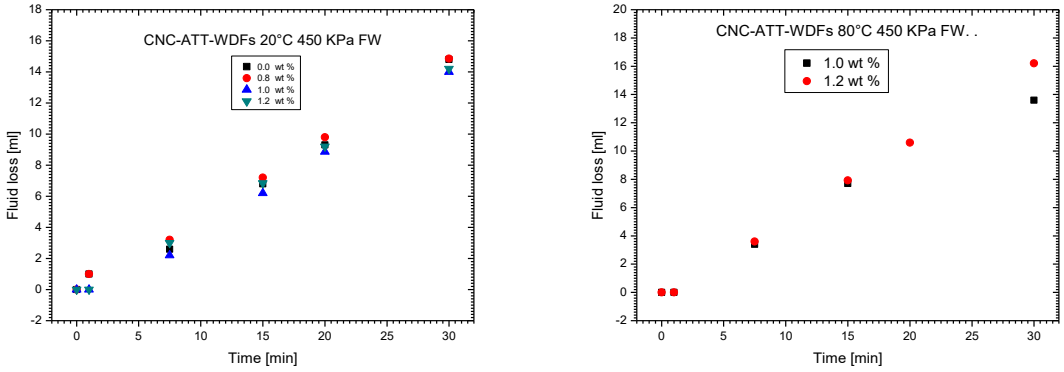

Figure 61. The plot of fluid loss volume as a function of time for CNC/ATT-WDFs (FW) at 450KPa and 80°C for different CNC concentrations.

The CNC/ATT-WDFs (FW) with 0.0, 0.8, 1.0 and 1.2 wt. % of CNCs had the API fluid loss values of 14.8, 14.85, 14, and 14.2 ml/30 min, respectively at 20°C. For 80°C, these API fluid loss values were recorded 13.6 and 16.2 ml/30 min at 1.0 and 1.2 wt. % respectively. It is seen that at low temperature (20°C), the fluid loss volume decreases whereas, at high temperature (80°C), the fluid loss volume of CNC/ATT-WDFs (FW) increases.

5.3.2. ANALYSIS OF FILTRATION PROPERTIES OF CNC/ATT-WDFs (SW)

The fluid loss properties of CNC/ATT-WDFs (FW) at 1.2 wt. % CNC concentration was investigated by varying the temperature from 20°C to 80°C to design a suitable drilling fluid that is following API standards (15ml/30 min) as shown in figure 62.

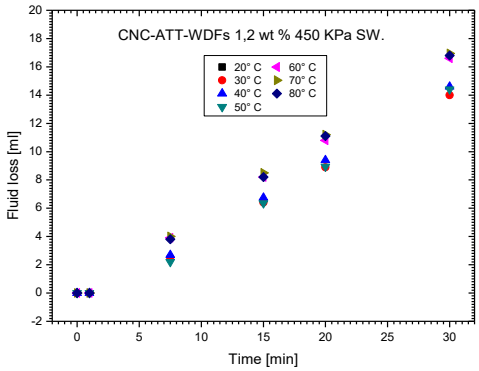

Figure 62. The plot of fluid loss volume as a function of time for CNC/ATT-WDFs (SW) 1.2 wt. % CNC concentration at 450 KPa for different temperatures.

The effect of temperature on the fluid loss is observed in figure 62 for 1.2 wt. % CNC concentration of CNC/ATT-WDFs (SW). The CNC/ATT-WDFs (SW) with 1.2 wt. % offers 14, 14.6, 14.4, 16.6, 16.95 and 16.8 ml/30 min API fluid loss volume at 30°C, 40°C, 50°C, 60°C, 70°C, and 80°C respectively. It could be seen that the fluid loss increased as temperature increased demonstrating less retention of the filtrate at high temperature that could lead to serious wellbore collapse and deposition by flocculation of their filter cake on the wellbore wall causing differential pressure sticking, stuck pipe problems, and well damage (Zakaria et al 2012). These API fluid volumes of CNC/ATT-WDFs (SW) are above the API standard given from 60°C to 80°C.

Nevertheless, when 1.2 wt. % of CNCs was incorporated, the minimum API fluid loss of 16.2 ml/30 min was obtained at 80°C for CNC/ATT-WDFs (FW) whereas the CNC/BT-WDFs (SW) at the same condition of CNC concentration, temperature, and pressures produced an API fluid loss of 16.8 mL/30 min about 3.6 % of API fluid loss more than that of CNC/ATT-WDFs (FW).

5.4. AGING TIME

Figure 63 shows the plot of shear stress as a function of shear rate at the different aging times and the calculated parameters of CNC/ATT-WDFs (FW) at different aging times for different temperatures using Herschel-Bulkley (HB) Models. Tables 13-14 displayed the calculated parameters of CNC/ATT-WDFs (FW) / (SW) at different aging times for different temperatures using Herschel−Bulkley (HB) Models.

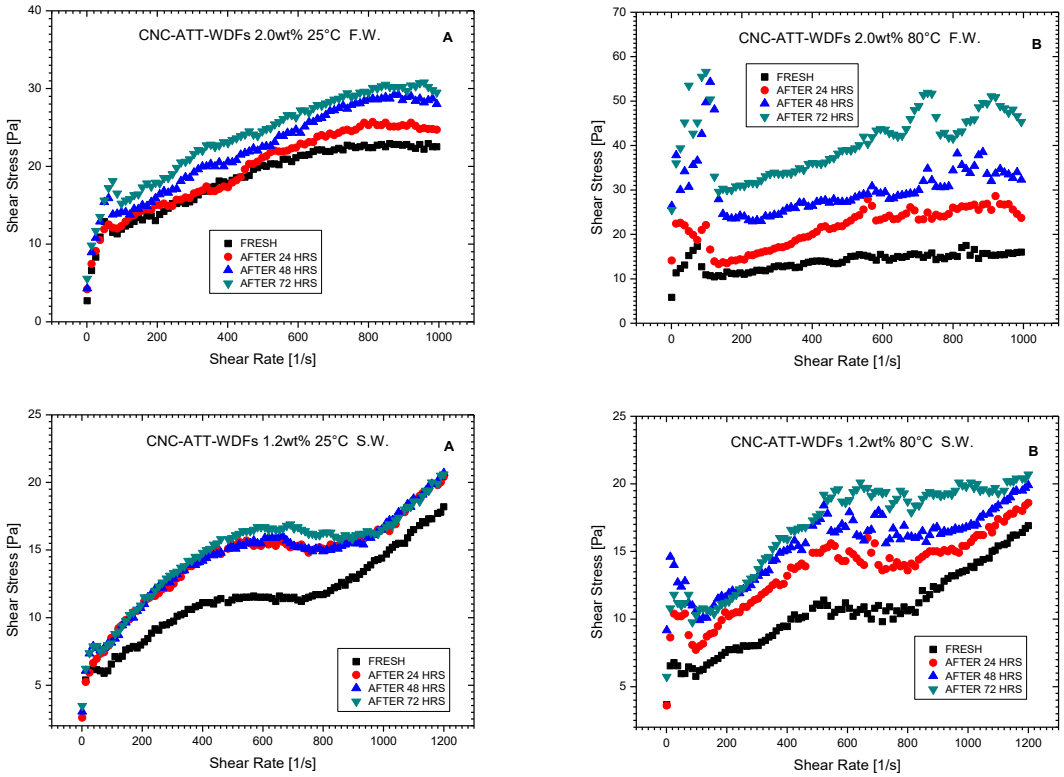

Figure 63. The plot of shear stress as a function of shear rate at different aging time at 25℃ and 80℃ for CNC/ATT-WDFs in fresh water and seawater.

Table 13. Calculated parameters of CNC/ATT-WDFs (FW) at different aging time for different temperature using Herschel-Bulkley (HB) Models.

CNC-ATT-WDFs 2.0wt% 25°C F.W.				
Model	Herschel			
Equation	y = y0 + K*x^n;			
Plot	Shear Stress	Shear Stress	Shear Stress	Shear Stress
y0	1,02542 ± 1,22432	4,96536 ± 0,83546	7,02608 ± 0,81878	6,06176 ± 0,95155
K	2,59874 ± 0,61837	0,81131 ± 0,21886	0,56396 ± 0,16197	1,42212 ± 0,32091
N	0,31467 ± 0,02757	0,47565 ± 0,03465	0,5378 ± 0,03774	0,41698 ± 0,02818
Reduced Chi-Sqr	0,63883	0,8386	1,06408	0,79594
R-Square (COD)	0,96943	0,96982	0,96947	0,97637
Adj. R-Square	0,96867	0,96906	0,96871	0,97578

CNC-ATT-WDFs 2.0wt% 80°C F.W.				
Model	Herschel			
Equation	y = y0 + K*x^n;			
Plot	Shear Stress	Shear Stress	Shear Stress	Shear Stress
y0	11,09718 ± 0,66457	16,60854 ± 0,83656	30,36864 ± 4,1862E7	36,29723 ± 1,28766
K	0,01442 ± 0,02745	0,00137 ± 0,00272	0,01719 ± 4,1862E7	2,5271E-6 ± 1,3574E-5
n	0,85171 ± 0,26553	1,30827 ± 0,28493	8,55929E-34 ± 34,2377	2,25616 ± 0,7826
Reduced Chi-Sqr	1,82182	6,25983	35,33436	32,25181
R-Square (COD)	0,54787	0,66327	-2,93458E-5	0,38148
Adj. R-Square	0,53657	0,65485	-0,02503	0,36601

Table 14. Calculated parameters of CNC/ATT-WDFs (FW) at different aging time for different temperature using Herschel-Bulkley (HB) Models.

CNC-ATT-WDFs 2.0wt% 25°C S.W.				
Model	Herschel			
Equation	y = y0 + K*x^n;			
Plot	Shear Stress	Shear Stress	Shear Stress	Shear Stress
y0	4,66121 ± 0,55285	0 ± 1,44521	0,98115 ± 1,47474	0 ± 1,69732
K	0,09033 ± 0,0494	2,45501 ± 0,78833	2,10802 ± 0,76432	2,81128 ± 0,97936
n	0,68182 ± 0,07259	0,28333 ± 0,03518	0,29723 ± 0,04034	0,26764 ± 0,03744
Reduced Chi-Sqr	0,94443	0,76521	0,91094	0,89739
R-Square (COD)	0,91016	0,93832	0,92316	0,92706
Adj. R-Square	0,90828	0,93703	0,92156	0,92554
CNC-ATT-WDFs 2.0wt% 80°C S.W.				
Model	Herschel			
Equation	y = y0 + K*x^n;			
Plot	Shear Stress	Shear Stress	Shear Stress	Shear Stress
y0	6,10435 ± 0,27673	5,54324 ± 0,97811	10,32767 ± 0,72585	5,51418 ± 1,32348
K	0,00294 ± 0,00196	0,50039 ± 0,27829	0,07522 ± 0,07013	0,95377 ± 0,46405
n	1,14014 ± 0,09245	0,44263 ± 0,06869	0,66663 ± 0,12339	0,39473 ± 0,05856
Reduced Chi-Sqr	0,64619	1,11961	1,55211	1,54836
R-Square (COD)	0,92794	0,86542	0,77272	0,8853
Adj. R-Square	0,92643	0,86262	0,76798	0,88291

It is observed in figure 63(A) that shear stress increased with an increase in aging time. This means the shear stress decreases with the aging time in freshwater. The same effect is observed in seawater but the action of the salt upon the drilling fluids was shown up as CNC/ATT-WDFs (SW) at low and high temperature could not display proper shear thinning behavior. It can be also seen that CNC/ATT-WDFs (FW) at 80℃ shown up critical yield point. It has been observed that the drilling fluid properties are affected by the variation of the temperature and aging time. As seen in this project, the impact of temperature and aging time upon the yield stress, viscosity, and shear stress so far on the gel strength.

It is observed in figure 63(B) for CNC/ATT-WDFs (FW) 2.0 wt. % that the effect of temperature on the shear stress displays a critical point in the flow curve at 80°C. However, the critical point intensity increases as much as the aging time increases which indicate the appropriate shear stress to break the connected aggregates and fiber at 80°C. The shear stresses corresponding to the critical points are 18 Pa for CNC/ATT-WDFs (FW) fresh, 23.2 Pa for CNC/ATT-WDFs (FW) after 24 hours, 55.5 Pa for CNC/ATT-WDFs (FW) after 48 hours, and 57 Pa for CNC/ATT-WDFs (FW) after 74 hours aged at 80°C. Thus, CNC/ATT-WDFs (FW) after 74 hours show the best gel strength.

In figure 63(B) for CNC/ATT-WDFs (SW) 1.2 wt. %, it is observed that the effect of temperature on the shear stress displays as well a critical point of less intensity in the flow curve at 80°C. This

reduction of the critical point intensity could be justified by the presence of salt content in the mud system. As the high salt content favored a strong interaction between CNC particles and ATT-WDFs (SW). The shear stresses corresponding to the critical points are 7.02 Pa for CNC/ATT-WDFs (SW) fresh, 10.7 Pa for CNC/ATT-WDFs (SW) after 24 hours, 11.4 Pa for CNC/ATT-WDFs (SW) after 48 hours, and 14.9 Pa for CNC/ATT-WDFs (SW) after 74 hours aged at 80°C. Therefore, CNC/ATT-WDFs (SW) after 74 hours show the best gel strength (Zhuang & Zhang 2018).

Therefore, by the fact of maintaining at the optimum values these rheological properties, many drilling issues could be avoided. Thus, the drilling fluid rheology remained very important as the viscosity of the drilling fluid is practically affecting the rate of penetration during the drilling operation. Keeping proper gel strength is advantageous for holding cuttings in suspension, and for a high penetration rate relatively low gel strength is needed that will cause less pressure drop in the borehole. The cutting slip velocity gives a better correlation with yield stress than any other rheological parameters. Furthermore, the incorporation of the cellulose nanocrystals in the clay-based fluids maintained a better viscosity of the mud system that means CNCs reduced the viscosity at the optimum value leading to the reduction of the amount of energy needed for rotating drill stem and drill bit.

5.5. RATE OF PENETRATION.

The experimental data are given in tables 24 and 25 shown the variation of the rate of penetration as a function of pressure (stress) or weight on the bit of different rock samples with CNC/BT, ATT, SEP-WDFs in fresh-water and sea-water. Only the one for CNC/ATT-WDFs in freshwater and seawater has to be considered in this case. Generally, it is observed in figure 64 plot (A) that CNC/ATT-WDFs (FW) at 2.0 wt. % CNC concentration exhibits a more significant rate of penetration values than CNC/ATT-WDFs (SW) at 1.2 wt. % CNC concentration into plot B except when drilling is done with Sandstone rock sample. Besides, the fast ROP is attributed to CNC/ATT-WDFs (FW) at 2.0 wt. % CNC concentration as drilling is done into Breccia, Shale, Dolomite, and Sandstone rock samples with a more significant correlation between the ROP and the stress (pressure) or weight on bit.

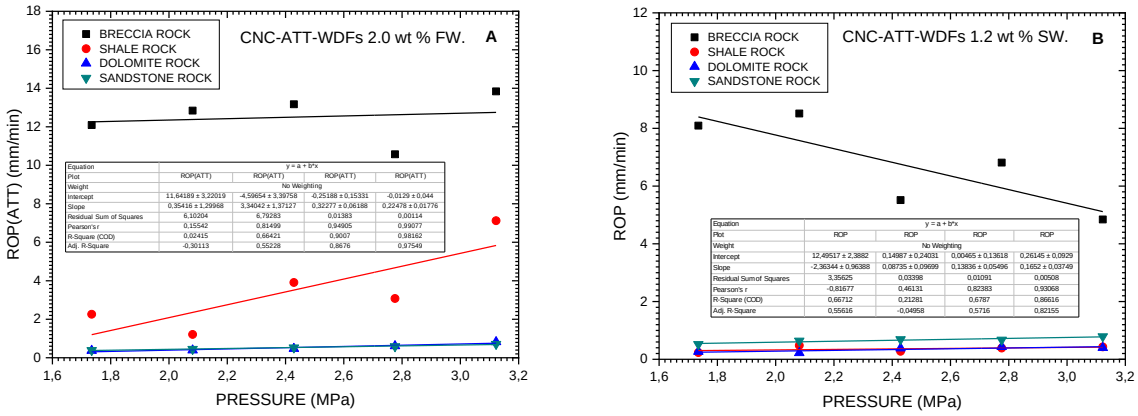

Figure 64. The plot of the rate of penetration as a function of pressure (stress) or weight on bit of different rock samples in CNC/ATT-WDFs (FW) and CNC/ATT-WDFs (SW).

5.6. CONCLUSIONS

The effect of CNC concentrations, temperature, and pressure on the rheological and filtration properties of CNC/ATT-WDFs was investigated in fresh water and seawater. Herschel-Bulkley's model as a statistical modeling approach was used for a better understanding of the rheological behaviors. The penetration rate onto different rock samples with CNC/ATT-WDFs was investigated in fresh water and seawater. The aging and temperature effect of CNC/ATT-WDFs was investigated in fresh water and seawater some significant results observed during the study of this project are:

- CNC concentration had a significant effect on the improvement of the rheological properties of CNC/ATT-WDFs (SW) whereas less effect was seen on the rheological properties of CNC/ATT-WDFs (FW). This CNC concentration effect is shown, firstly during the variation of shear stress against the shear rate at 80°C for various CNC concentrations of CNC/ATT-WDFs (SW): the shear stress increased from 7.37 Pa at 0.0 wt.% of CNC to 7.57, 9.35, 13.9, 13.6, 14.7 and 27.4 Pa at 0.4, 0.8, 1.2, 1.6, 2.0 and 2.4 wt.% of CNCs respectively; in comparison with CNC/ATT-WDFs FW): the shear stress increased from 7.7 Pa at 0.0 wt.% of CNC to 7.56, 8.18, 9.84, 11, 12.3, and 15.3 at 0.4, 0.8, 1.2, 1.6, 2.0 and 2.4 wt.% of CNCs respectively. Secondly, during the variation of the yield stress against CNC concentration at 80°C for CNC/ATT-WDFs (SW): the yield stress increased from 0.02337 Pa at 0.0 wt. % of CNC to 0.03732, 0.59417, 4.15802, 2.41918, 1.53609 and 2.39824 Pa at 0.4, 0.8, 1.2, 1.6, 2.0 and 2.4 wt.% of CNCs respectively; in comparison with CNC/ATT-WDFs (FW): the yield stress increased from 0.02395 Pa at 0.0 wt. % of CNC to 0.02767, 0.04332, 0.63068, 1.81578, 2.14734 and 1.32164 Pa at 0.4, 0.8, 1.2, 1.6, 2.0 and 2.4 wt.% of CNCs respectively.

- CNC concentration had a significant effect on the improvement of the viscosity of CNC/ATT-WDFs (SW) whereas less effect was seen on the viscosity of CNC/ATT-WDFs (FW). The variation of the viscosity against shear rate for CNC/BT-WDFs (SW) at various CNC concentrations for different temperatures exhibited more shear-thinning properties than for CNC/BT-WDFs (FW). As observed at the low shear rate (0.999 s-1) and 80°C: the viscosities of the CNC/BT-WDFs (SW) increased from -0.428 Pa·s at 0.0 wt. % of CNC to -0.305, 0.43, 2.75, 2.35, 2.68 and 7.7 Pa·s at 0.4, 0.8, 1.2, 1.6, 2.0 and 2.4 wt.% of CNCs, respectively; in comparison with the CNC/BT-WDFs (FW), the viscosities increased from -0.481 Pa·s at 0.0 wt. % of CNC to -0.56, -0.286, 0.156, 0.36, 0.538 and 2.35 Pa·s at 0.4, 0.8, 1.2, 1.6, 2.0 and 2.4 wt.% of CNCs, respectively.

- CNC concentration had a significant effect on the improvement of the filtration properties of CNC/ATT-WDFs (FW) whereas less effect was seen on the filtration properties of CNC/ATT-WDFs (SW). As it is observed, the API fluid loss values of CNC/BT-WDFs (FW) indicated better fluid loss control properties at 1.0 wt.% of CNCs at low temperature (20°C) and high temperature (80°C) of 14 ml/30 min and 13.6 ml/30 min, respectively lower than the API standards (15 ml/30 min). Besides, at 1.2 wt. % of CNC/ATT-WDFs (FW), API fluid loss values of 14.2 ml/30 min and 16.2 ml/30 min, respectively were observed. Meanwhile, the API fluid loss values of 1.2 wt. % CNCs in CNC/BT-WDFs (SW) at 20°C and 80°C were about 13.8 ml/30 min (20°C) and 16,8 ml/30 min (80°C), respectively.

- Effect of salinity had considerably improved the rheological properties of CNC/ATT-WDFs in seawater. This effect of salinity was detrimental for the filtration properties as the fluid loss was slightly above the API standard value at high temperature whereas at low temperature his filtration property was acceptable.
- The effect of temperature on the rheological and filtration properties affected more the CNC/ATT-WDFs (SW) than CNC/ATT-WDFs (FW).
- The fast penetration rate was reached by using CNC/ATT-WDFs (FW) than CNC/ATT-WDFs (SW) through rotary drilling on different rock samples (Breccia, Shale, Dolomite, and Sandstone) except when drilling in Sandstone rock sample.
- Salinity has negative effects on the aging time of CNC/ATT-WDFs in seawater. Meaning that the salinity affected the carrying capacity of cuttings (yield stress) of CNC/ATT-WDFs (SW) whereas the increase in temperature tried to improve the yield stress of the affected mud during the aging period. In freshwater, this yield stress was increased due to the increase in temperature for CNC/ATT-WDFs (FW) during the aging time.
- The effect of the aging time of CNC/ATT-WDFs in freshwater was improved by increasing temperature as it has a great impact on the increase of the yield stress.

CHAPTER 6. CELLULOSE NANOCRYSTALS SEPIOLITE WATER-BASED DRILLING FLUIDS.

6.1. ANALYSIS OF RHEOLOGICAL BEHAVIOUR OF CNC/SEP-WDFs (FW).

6.1.1. RHEOLOGICAL CURVES OF CNC/SEP-WDFs (FW) AT DIFFERENT CNC CONCENTRATIONS FOR VARIOUS TEMPERATURES.

The rheological properties of the types of water-based drilling fluids (freshwater and seawater) were measure using the rheometer named RheolabQC SN897839/FW1.31with RHEOPLUS/32 V3.62 21002331-33025 as an application from Anton Paar, Germany. The plots of shear stress as a function of shear rate for CNC/SEP-WDFs in fresh water at different CNCs concentrations are depicted in figure 65.

All the plots in figure 65 showed a dependence of the shear stress on the shear rate and the concentration of CNCs. The increase of CNC concentration from 0.0 to 2.4 wt. % affected the shear stress that was eventually increased. The flow curves of the CNC/SEP-WDFs (FW) are depicted an increase in the shear stress at the highest shear rate of 1200 s^{-1} as followed: in figure 65(A) from 62.2 Pa at 0 wt. % to 16.1, 15.3, 16.5, 18.3, 22.4 and 33 Pa at 0.4, 0.8, 1.2, 1.6, 2.0 and 2.4 wt. % respectively; in figure 65(B), the shear stress increased from 82.1 Pa at 0.0 wt. % to 17.8, 16.2, 16.5, 18.4, 21.7 and 29.4 Pa at 0.4, 0.8, 1.2, 1.6, 2.0 and 2.4 wt. % respectively; in figure 65(C), the shear stress increased from 89.8 Pa at 0.0 wt. % to 16.1, 14.1, 15, 17.3, 19.9 and 27.2 Pa at 0.4, 0.8, 1.2, 1.6, 2.0 and 2.4 wt. % respectively; in figure 65(D), the shear stress increased from 91.9 Pa to 17.3, 14.6, 15.2, 17.1, 19.3 and 25.7 Pa at 0.4, 0.8, 1.2, 1.6, 2.0 and 2.4 wt. % respectively; in figure 65(E), the shear stress increased from 90.4 Pa at 0.0 wt. % to 15.3, 13.1, 13.8, 15.5, 18.2 and 23.4 Pa at 0.4, 0.8, 1.2, 1.6, 2.0 and 2.4 wt. % respectively; in figure 65(F), the shear stress increased from 87.4 Pa at 0.0 wt. % to 15.2, 12.9, 12.7, 14.7, 17.2 and 21.8 Pa at 0.4, 0.8, 1.2, 1.6, 2.0 and 2.4 wt. % respectively; and in figure 65(G), the shear stress increased from 101 Pa at 0.0 wt. % to 19.3, 13.2, 13.3, 15, 17.3 and 21.7 Pa at 0.4, 0.8, 1.2, 1.6, 2.0, and 2.4 wt. % respectively. From figure 65, it is clear that the shear stress is enhanced with increasing CNC concentrations that require a high force to start the flow of the fluids.

All the rheological curves were well fitted with H-B model and results are displayed in table 15 below which summarized all the values of the rheological and statistical parameters. It is revealed that the increase in CNC concentrations from 0.4 to 2.4 wt. % enable a slight decrease of R^2 at the same temperature and SSR/RMSD values were gradually increased from R^2 = 0,98932 at 0.0 wt. % to R^2 = 0,96168 at 2.4 wt. % and SSR = 9,15158 / RMSD = 0,33822 at 0.0 wt. % to SSR = 119,7748 / RMSD = 1,2236 at 2.4 wt. % for 20˚C; 0,991 to 0,96471 and 6,88549 / 0,29337 to 78,46413 / 0,99035 for 30˚C; 0,99142 to 0,96646 and 4,96102 / 0,24902 to 62,3962 / 0,88315 for 40˚C; 0,9909 to 0,95221 and 4,96102 / 0,24902 and 62,3962 / 0,88315 for 50˚C; 0,98803 to 0,96333 and 3,56093 / 0,21098 to 80,77764 / 1,00485 for 60˚C; 0,97742 to 0,94438 and 4,20565 / 0,22928 to 58,87383 / 0,85786 for 70˚C; and from 0,99298 to 0,95935 and 2,09303 / 0,16175 to 28,18971 / 0,59361 for 80˚C. This proves that the relationship between shear stress and shear rate was nonlinear.

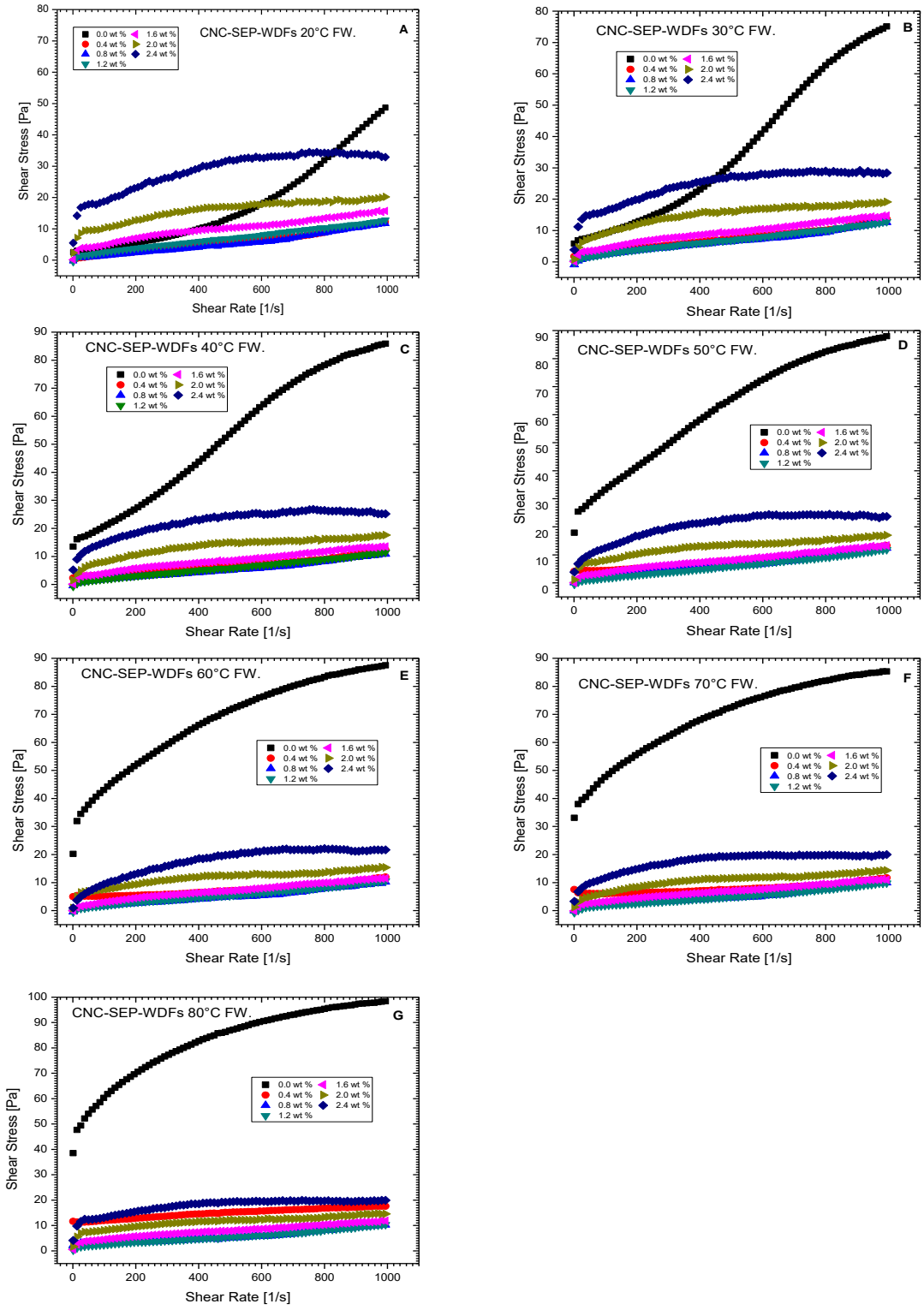

Figure 65. The plot of shear stress as a function of shear rate of CNC/SEP-WDFs (FW) at various CNCs concentrations for different temperatures.

It has been seen in table 15 that the Herschel-Bulkley model as a complex rheological model with three parameters was able to describe accurately the rheological behavior of CNC/SEP-WDFs (FW) as R^2 is closer to 1.

Table 15. Calculated parameters CNC/SEP-WDFs (FW) at various CNC Concentrations for different temperature using Herschel-Bulkley (HB) Models.

T(°C)	CNC Conc (wt %)	y_0 (Pa)	K(Pa.S)	n	R^2	RMSD	SSR
20°C	0.0	3,83595	7,69036E-6	2,259	0,99902	0,42827	14,67335
	0.4	0,94726	0,00238	1,21981	0,98932	0,33822	9,15158
	0.8	1,03747	5,71035E-4	1,42295	0,9923	0,28211	6,36681
	1.2	0,80447	0,02679	0,87875	0,99564	0,21883	3,83086
	1.6	1,59889	0,21924	0,59625	0,98594	0,41379	13,69745
	2.0	1,0431	3,81642	0,24736	0,98206	0,4836	18,70962
	2.4	2,87408	7,4404	0,23369	0,96168	1,2236	119,7748
30°C	0.0	5,66747	0,0027	1,48227	0,99321	1,8874	284,98109
	0.4	2,6152	0,00351	1,15643	0,991	0,29337	6,88549
	0.8	0,76806	0,01679	0,94065	0,98389	0,41196	13,57685
	1.2	0,75991	0,02795	0,87301	0,99548	0,22321	3,98573
	1.6	1,38839	0,14938	0,64721	0,99218	0,30604	7,49307
	2.0	1,06197	5,74297	0,2108	0,98972	0,38593	11,9156
	2.4	3,64107	11,26221	0,17596	0,96471	0,99035	78,46413
40°C	0.0	11,40958	0,11629	0,94668	0,99058	2,26964	412,10055
	0.4	2,98938	5,39847E-4	1,40523	0,99142	0,24902	4,96102
	0.8	0,93662	0,00262	1,18805	0,98894	0,30304	7,34668
	1.2	0,4931	0,01593	0,94107	0,99472	0,22314	3,98318
	1.6	1,59118	0,08878	0,70808	0,98997	0,32226	8,30806
	2.0	0,90167	3,8084	0,24428	0,9862	0,41032	13,46885
	2.4	2,85686	8,84738	0,19041	0,96646	0,88315	62,3962
50°C	0.0	17,35503	0,79423	0,65727	0,99346	2,26964	412,10055
	0.4	4,27724	4,66331E-4	1,41901	0,9909	0,24902	4,96102
	0.8	1,84225	9,22769E-4	1,35125	0,98843	0,30304	7,34668
	1.2	0,46206	0,00967	1,01955	0,99624	0,22314	3,98318
	1.6	1,47143	0,07118	0,73744	0,99168	0,32226	8,30806
	2.0	-0,92019	2,71724	0,26794	0,9869	0,41032	13,46885
	2.4	-7,53012	8,83967	0,19247	0,95221	0,88315	62,3962
60°C	0.0	18,57987	3,19185	0,4494	0,99611	1,02648	84,29223
	0.4	5,22082	5,81144E-6	2,0137	0,98803	0,21098	3,56093
	0.8	0,9593	0,00261	1,17579	0,98691	0,30197	7,29489
	1.2	0,57211	0,01317	0,95432	0,99222	0,24636	4,85563
	1.6	0,62801	0,1018	0,67472	0,99457	0,21258	3,61537
	2.0	0,96578	3,25456	0,23408	0,97708	0,4122	13,59262
	2.4	2,25271	5,8305	0,24104	0,96333	1,00485	80,77764
70°C	0.0	27,93245	2,53893	0,45743	0,99501	0,98613	77,79649
	0.4	6,31555	7,40359E-7	2,27894	0,97742	0,22928	4,20565
	0.8	1,66202	2,34374E-4	1,51738	0,9853	0,30871	7,62435
	1.2	0,78955	0,00469	1,0899	0,98808	0,28342	6,42634
	1.6	1,16341	0,07569	0,70406	0,99105	0,25184	5,07383
	2.0	0,68435	2,5756	0,26383	0,98487	0,34826	9,70275
	2.4	7,44547	17,81568	0,10727	0,94438	0,85786	58,87383
80°C	0.0	28,91653	7,07222	0,33537	0,99468	1,05531	89,0949
	0.4	10,75586	0,0471	0,72516	0,99298	0,16175	2,09303
	0.8	2,94804	2,25441E-5	1,84032	0,99476	0,16382	2,14686
	1.2	1,66595	0,00361	1,12132	0,98759	0,27732	6,15269
	1.6	2,00363	0,1334	0,61789	0,98687	0,28569	6,5293
	2.0	0,80635	2,96787	0,22884	0,98017	0,33199	8,81725
	2.4	12,61191	28,76719	0,06614	0,95935	0,59361	28,18971

The rheological parameter results are given in table 15 that displayed the strongest dependence of y_0 and K on the CNC concentration changes. It is shown through all range of temperature, the SEP-WDFs (FW) offers the highest yield stress values (y_0). By contrast, the addition of CNCs at 0.4 wt. % into SEP-WDFs (FW) first decreases the yield stress and further additions of the higher concentration till 2.4 wt. % are characterized by a fluctuated increase in the yield stress over the broad range of temperature from 20°C to 80°C. Besides, table 15 shows the effect of the temperature on the yield stress. At the same concentration, the control mud system and 0.4 wt. % CNC concentration showed an increase of the yield stress as temperature increased. Further addition of CNC into SEP-WDFs (FW) showed a decrease follows by an increase of the yield stress generally observed as the temperature was increasing. This improvement of the yield stress facilitates the transportation of the cuttings into the mud system. As the yield stress represents the minimum stress needed to move the drilling fluid. It will be disadvantageous to handle drilling that has a great yield stress value where much energy is needed for pumping the fluid down through the wellbore (Lummus & Azar 1986; Nwosu & Ewulonu 2014; Li et al 2015; Zhuang et al 2018; Echt & Plank 2019). Due to the impact of the effect of the energy on the transportation of the drilling cuts, 1.2 wt. % and 1.6 wt. % could be selected from table 15 as the optimum concentration of CNCs to be used for CNC/SEP-WDFs (FW) during drilling operation in the offshore well.

6.1.2. RHEOLOGICAL CURVES AT DIFFERENT TEMPERATURES FOR VARIOUS CNC CONCENTRATIONS.

Figure 66 showed a very slight decrease of the shear stress as temperature increased at the high shear rate (1200 s^{-1}). This means the variation of shear stress over the broad range of temperature from 20 to 80 °C showed no significant change while adding CNC concentration into SEP-WDFs (FW). This decrease of the shear stress with an increase in temperature is attributed to the thermal dispersion and thermal dehydration of the sepiolite clay particles in the suspension.

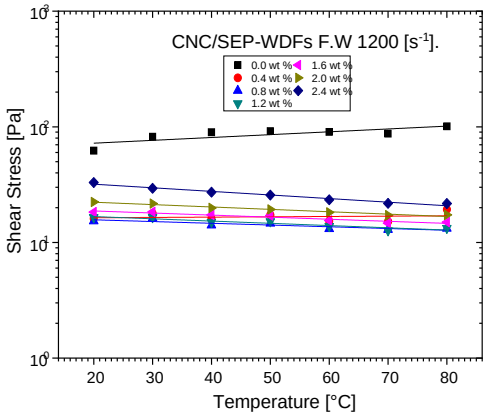

Figure 66.The plot of shear stress as a function temperature for CNC/SEP-WDFs in freshwater at various CNC concentration and high shear rate (1200 s^{-1}).

From figure 67 below, plots A, B, C, D, E, F, G, and H showed the variation of shear stress with the shear rate for CNC/SEP-WDFs (FW) at different temperatures for various CNCs concentrations. It can be seen that at the high shear rate, there is a significant trend as the temperature increased at different CNC concentrations. This is depicted from 1.2 wt. % to 2.4 wt. % of the CNC concentration added. This is the evidence of the effect of CNC concentration upon

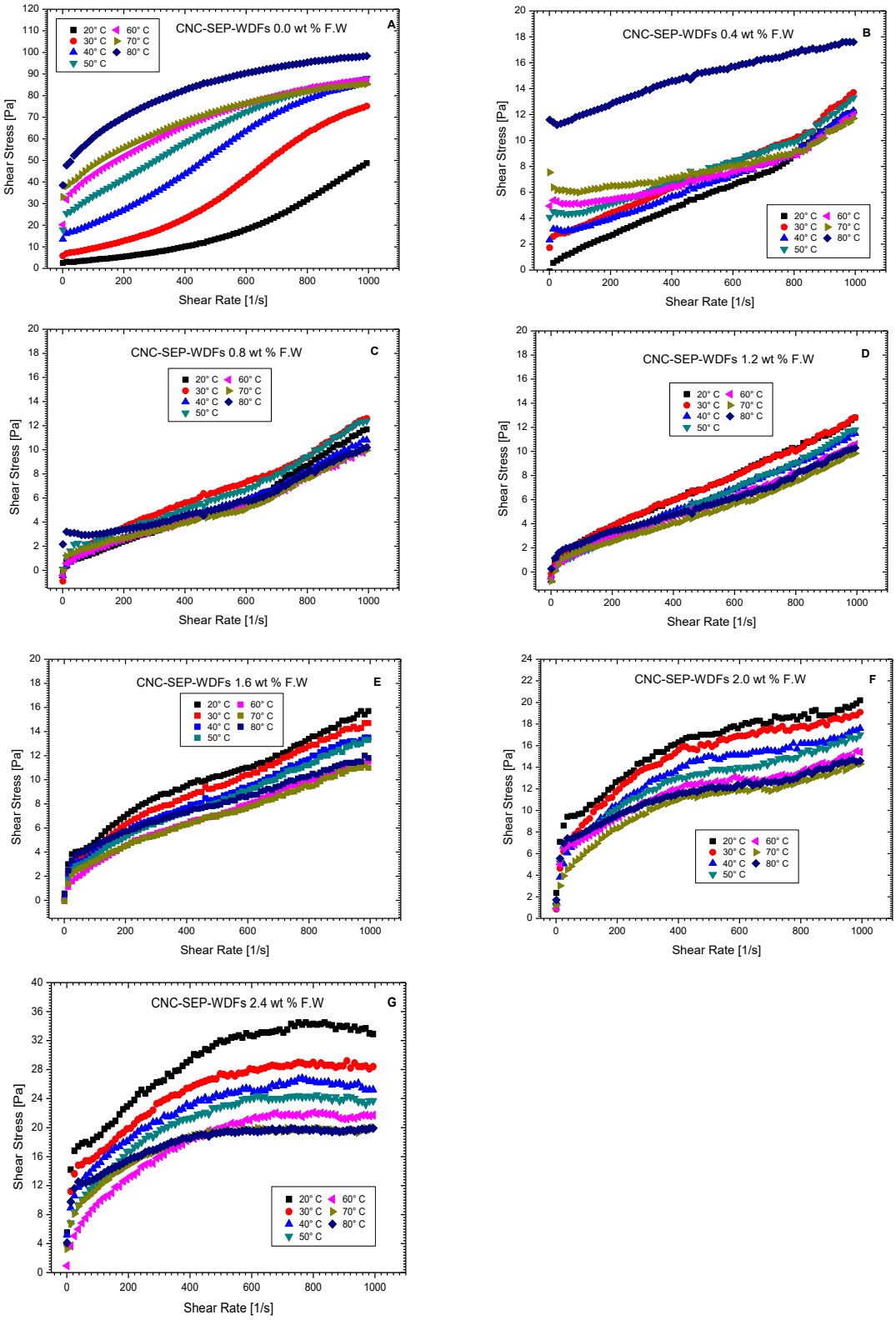

Figure 67. The plots of shear stress as a function of shear rate of CNC/SEP-WDFs in freshwater at various temperatures for different CNC concentrations.

SEP-WDFs (FW) in the improvement of rheological properties of CNC/SEP-WDFs (FW). The more the CNC concentration increased, the more the shear stress increased. Furthermore, it observed at a high shear rate that the rise of the temperature leads to the decrease of shear stress. This is the result of the thermal dispersion and thermal dehydration of SEP clay particles in the suspension (Wang et al 2011).

6.1.3. CNC CONCENTRATION EFFECT ON THE VISCOSITY OF CNC/SEP-WDFs (FW) AS DRILLING FLUID

The rheological data expressed in figure 68 below describes the variation of viscosity as a function of CNC concentration at different temperatures and a low shear rate of 0.999 s-1. Generally, it denotes that the viscosity of CNC/SEP-WDFs (FW) decreases exponentially till 1.2 wt. % then increases again exponentially with the increase in the CNC concentrations.

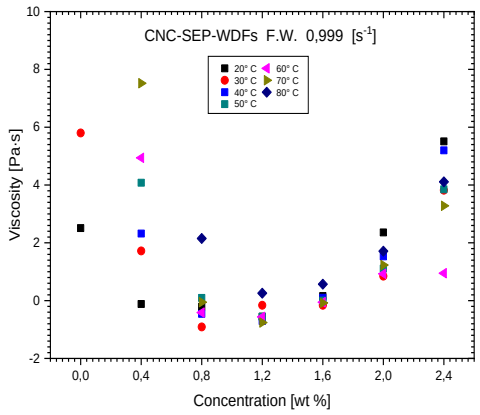

Figure 68. Variation of viscosity of CNC/SEP-WDFs (FW) with CNC concentrations at different temperatures and low shear rates (0.999 s^{-1}).

Figure 69 shows the effect of the CNC concentration on the viscosity of CNC/SEP-WDFs (FW). It is observed in figure 69(A) that the incorporation of CNCs into SEP-WDFs (FW) from 0.4 to 2.4 wt. % increases significantly the viscosity. A poor shear thinning behavior is observed as the viscosity decreases over the broad range of shear rate from 0.999 s-1 to 1200 s-1 and gets lower for 0.4, 0.8, and 1.2 wt. % CNC concentrations. This offered a poor surface interaction between CNCs and SEP-WDFs (FW). This viscosity started to increase with nearly linear shear thinning behavior from 1.6 to 2.4 wt. % showing a good surface interaction between CNCs and SEP-WDFs (FW). However, the control SEP-WDFs (FW) shows a progressed decrease as the shear rate is increasing till 300 s-1 then started to increase up to the higher shear rate. In figure 69(B), it notices an increase in viscosity for the control SEP-WDFs (FW) and 0.4 wt. % CNCs and particularly a slight decrease of the viscosity for all the remaining CNC concentrations incorporated into WDFs (FW). In figure 69(C), a slight decrease in viscosity is observed except for the control SEP-WDFs (FW) and 0.4 wt. % CNCs added in which a slight increase in the viscosity is noticed. In figure 69(D), same as in the previous case, much increases in the viscosity of SEP-WDFs (FW) and 0.4 wt. % CNC concentration was observed. In figure 69(E), the same applied as the previous case with much increase in the viscosity of SEP-WDFs (FW) and 0.4 wt. % CNC concentration was observed a well, followed by a decrease in the following additions of CNC concentration in SEP-WDFs (FW).

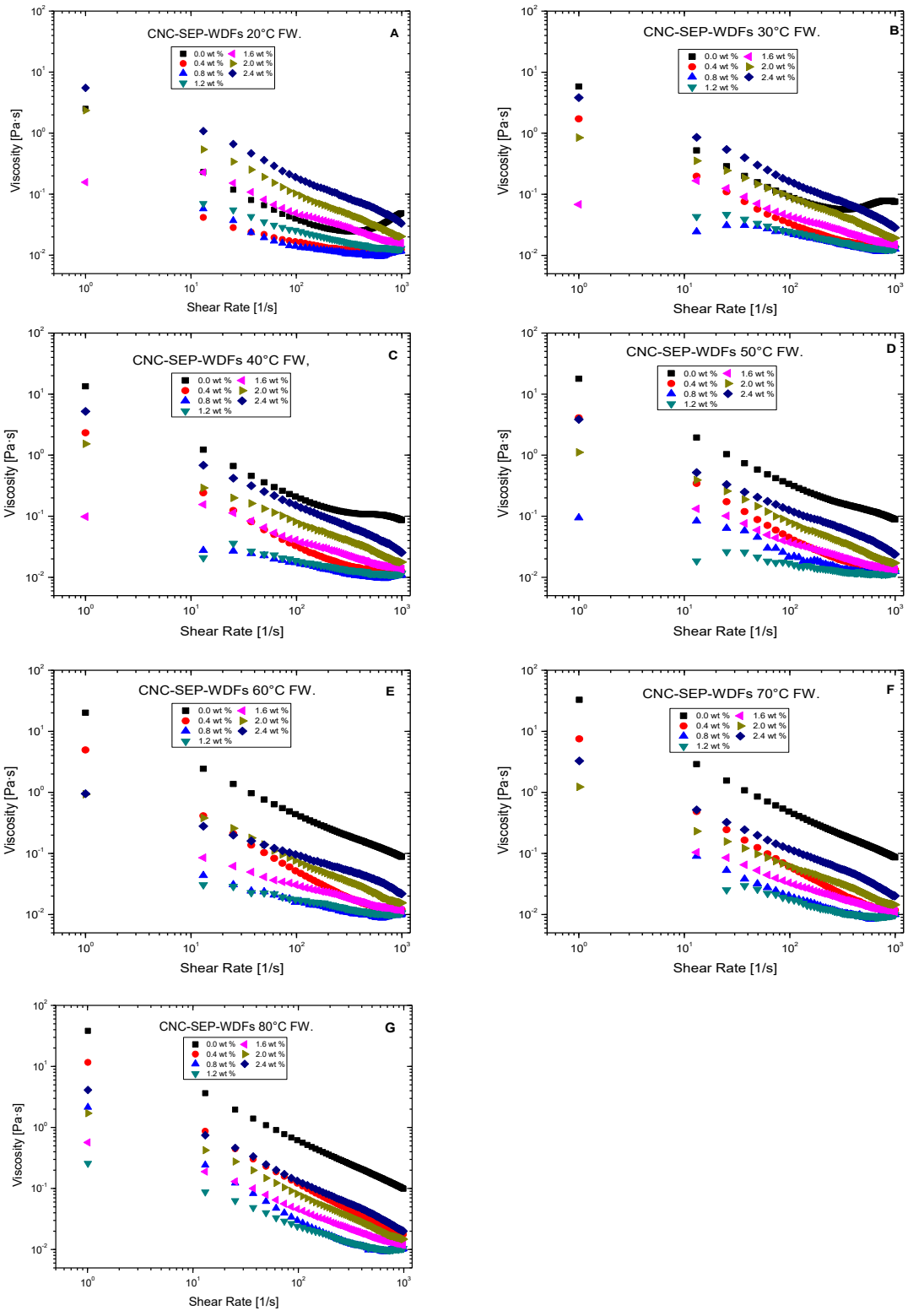

Figure 69. The plot of viscosity as a function of shear rate for CNC/SEP-WDFs (FW) at various CNC concentrations for different temperatures.

In figure 69(F), an increase in the viscosity with nearly linear shear-thinning curves was observed for SEP-WDFs (FW) and 0.4, 0.8, 1.2, 1.6, 2.0, and 2.4 wt. % CNC concentrations. In figure 69(G), finally, it is noticed that linear shear-thinning curve improving the shear-thinning behavior revealed the potential use of CNC additive as an effective rheological modifier for drilling fluids. This is noticed as their viscosity was decreasing linearly with increasing shear rate.

Hence, the effect of the concentration upon the viscosity of CNC/SEP-WDFs (FW) kept decreased from the higher viscosity of SEP-WDFs (FW) to 1.2 and 1.6 wt. % CNCs as minimum viscosity value then increased again from 1.6 to 2.4 wt. % with continuous increase in shear rate. It has been seen that the variation of the viscosity with the shear rate at different CNC concentrations for different temperatures demonstrates great surface interaction between CNCs and SEP-WDFS (FW). The shear-thinning behavior is commonly attributed to the non-Newtonian fluids having high viscosity at low shear rates, to improve the carrying capacity or suspension of the drilled cuttings from the wellbore. It is followed by the low viscosity at high shear rates allowing the fast pumping of the fluid into the bottom of wellbores and facilitate the release of the drilled cuttings.

6.1.4. TEMPERATURE EFFECT ON THE VISCOSITY OF CNC/BT-WDFs (FW) AS DRILLING FLUID.

Figure 70 displayed the plot of the variation of viscosity with a shear rate of CNC/SEP-WDFs (FW) at various temperatures for different CNC concentrations. Plot A shows the variation of the viscosity of the control SEP-WDFs (FW) as a function of shear rate at various temperatures. It is observed that the viscosity decreased with increasing shear rate that revealed the shear-thinning behavior of SEP-WDFs (FW). It has been seen that the mud system displays high viscosity at a low shear rate and low viscosity at a high shear rate, which is commonly known as shear-thinning fluids. These shear-thinning phenomena become more significant as CNC concentration and temperature increase in the mud system. However, it is observed at a low shear rate (0,999 s^{-1}), plots showed that viscosity increases with temperature changes. Plot A illustrates the viscosity variation of the control SEP-WDFs (FW) over the broad range of shear rate (from 0.999 s^{-1} to 1200 s^{-1}) at different temperatures (from 20°C to 80°C). It depicts a linear decrease of the viscosity with increasing shear rate resulting in a shear-thinning behavior of the control SEP-WDFs (FW) from 60°C to 80°C. At 50°C, a nearly linear decrease of the viscosity is observed. From 20°C to 40°C, a very poor shear thinning is observed as the decrease in viscosity was inverted at 400 s^{-1} and started to increase up to 1200 s^{-1} allowing the shear thickening behavior of the control SEP-WDFs (FW) to take place.

Therefore, the temperature change improves the shear-thinning behavior of the control SEP-WDFs (FW) and leads to greater viscosity values at high temperatures. From plot B, it is noticed that the incorporation of CNCs into SEP-WDFs (FW) at 0.4 wt % concentration increases the viscosity at a low shear rate as a function of temperature change. However, the decrease of the viscosity with increasing shear rate leads to a poor shear-thinning behavior as the rheological curves started to increase at the high shear. This is seen from 20°C to 70°C then at 80°C, the rheological curve exhibited a linear shear thinning behavior with high viscosity value good enough for cuttings transportation at a low shear rate and pumping at a high shear rate as the viscosity goes lower. From plot C, the rheological curves were not good enough to express the behavior of the drilling fluid at 0.8 wt. % CNC concentration of CNC/SEP-WDFs (FW).

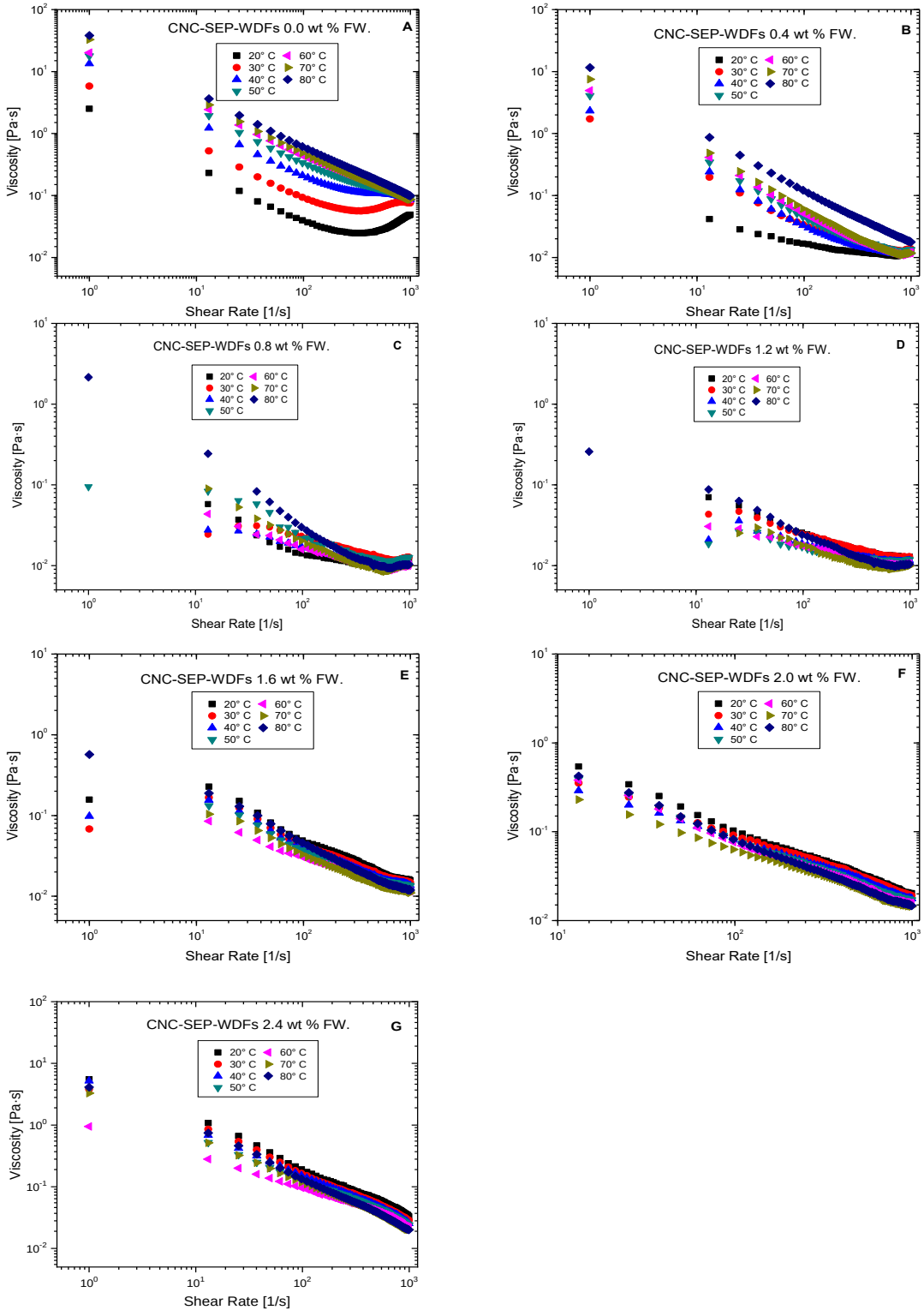

Figure 70. The plot of viscosity as a function of shear rate for CNC/SEP-WDFs (FW) at various temperatures for different CNC concentrations.

It displays low viscosity values with the possibility of getting a shear thickening behavior. From plot D, the rheological curves were not good enough to express as well the behavior of the drilling fluid at 1.2 wt. % CNC concentration of CNC/SEP-WDFs (FW). It displays low viscosity values with the possibility of getting a shear thickening behavior. This viscosity increases, decrease and end up with a plateau or increases again at a high shear rate. From plot E, the rheological curves exhibit a nearly linear shear thinning behavior for the drilling fluid at 1.6 wt. % CNC concentration of CNC/SEP-WDFs (FW). It is noticed that the viscosity decreases with increasing temperature up to 80°C at a high shear rate of 1200 s^{-1}. Thus, from plot F and G for the two last (2.0 wt. % and 2.4 wt. % respectively) CNC concentrations for CNC/SEP-WDFs (FW), the viscosity decreases with increasing shear rate over the broad range as well as with increasing temperature from 20°C to 80°C at a high shear rate of 1200 s^{-1}.

The analysis of the rheological data of CNC/SEP-WDFs (FW) shows in table 16 and 17 how the viscosity of CNC/SEP-WDFs (FW) varies with temperatures at different CNC concentrations at low and high shear rate.

Table 16. Variation of viscosity of CNC/SEP-WDFs (FW) with temperature at low shear rates (0.999 s-1) and different CNC concentrations.

Temperature	Shear Rate	Viscosity	Viscosity	Viscosity	Viscosity	Viscosity	Viscosity	Viscosity
[°C]	[s^{-1}]	[Pa·s]	[Pa·s]	[Pa·s]	[Pa·s]	[Pa·s]	[Pa·s]	[Pa·s]
		CNC/SEP-WDFs (FW) (0.0 wt % CNC)	CNC/SEP-WDFs (FW) (0.4 wt % CNC)	CNC/SEP-WDFs (FW) (0.8 wt % CNC)	CNC/SEP-WDFs (FW) (1.2 wt % CNC)	CNC/SEP-WDFs (FW) (1.6 wt % CNC)	CNC/SEP-WDFs (FW) (2.0 wt % CNC)	CNC/SEP-WDFs (FW) (2.4 wt % CNC)
20	1	2,51	-0,116	-0,217	-0,553	0,157	2,36	5,51
30	1	5,8	1,72	-0,91	-0,161	0,068	0,847	3,82
40	1	13,4	2,32	-0,457	-0,707	0,0981	1,53	5,2
50	1	17,8	4,08	0,0946	-0,56	1,91E-4	1,11	3,85
60	1	20,1	4,94	-0,413	-0,564	-0,0567	0,927	0,948
70	1	32,9	7,52	-0,0541	-0,759	-0,0797	1,23	3,28
80	1	38,2	11,6	2,15	0,258	0,569	1,71	4,11

Table 17. Variation of viscosity of CNC/SEP-WDFs (FW) with temperature at high shear rates (1200 s^{-1}) and different CNC concentrations.

Temperature	Shear Rate	Viscosity	Viscosity	Viscosity	Viscosity	Viscosity	Viscosity	Viscosity
[°C]	[s^{-1}]	[Pa·s]	[Pa·s]	[Pa·s]	[Pa·s]	[Pa·s]	[Pa·s]	[Pa·s]
		CNC/SEP-WDFs (FW) (0.0 wt % CNC)	CNC/SEP-WDFs (FW) (0.4 wt % CNC)	CNC/SEP-WDFs (FW) (0.8 wt % CNC)	CNC/SEP-WDFs (FW) (1.2 wt % CNC)	CNC/SEP-WDFs (FW) (1.6 wt % CNC)	CNC/SEP-WDFs (FW) (2.0 wt % CNC)	CNC/SEP-WDFs (FW) (2.4 wt % CNC)
20	1 200	0,0518	0,0134	0,0128	0,0137	0,0152	0,0186	0,0275
30	1 200	0,0684	0,0149	0,0135	0,0138	0,0154	0,0181	0,0245
40	1 200	0,0748	0,0134	0,0117	0,0125	0,0144	0,0166	0,0227
50	1 200	0,0766	0,0144	0,0122	0,0127	0,0143	0,0161	0,0214
60	1 200	0,0753	0,0128	0,0109	0,0115	0,0129	0,0151	0,0195
70	1 200	0,0729	0,0126	0,0108	0,0106	0,0122	0,0143	0,0181
80	1 200	0,084	0,0161	0,011	0,0111	0,0125	0,0144	0,0181

The temperature effects on the viscosity of CNC/SEP-WDFs (FW) at different CNC concentrations, low and high shear rates are given from the rheological data in table 16-17 was expressed graphically through figure 71. It is known the drilling operations necessary require a drilling fluid with shear thinning behavior. On the

other hand, the drilling fluid that depicts a reduction of the viscosity as the temperature increases is convenient for being used during drilling operations. Thus, all drilling fluid with a positive slope or increasing viscosity while the temperature is increasing is useless in the drilling operation.

Figure 71 below describes the effect of temperature on the viscosity of CNC/SEP-WDFs (FW) at different CNC concentrations at low and high shear rates. From figure 71, it can be seen that at a low shear rate, the viscosity of control SEP-WDFs (FW) and CNC/SEP-WDFs (FW) at 0.4 wt. % increases as the temperature was increasing with great positive slope 0.01868 and 0.01646 respectively. For 0.8 wt. % to 1.6 wt. % CNC concentrations, the variation of their viscosity against temperature was quite unstable to give a straight line reason why their linearization could not offer a proper fitting. However, for 2.0 wt. % and 2.4 wt. % CNC concentrations, it is observed that their fittings offered a low negative slope value of 0.00112 and 0.00448 respectively. This complied with the requirement of the drilling operation that claimed a drilling fluid with a shear-thinning behavior to be used for the drilling of a well as it can reduce their viscosity with increasing temperature. Hence, these drilling fluids with great positive slope values are excluded from being used during drilling operations as viscosity increased with increasing temperature.

From figure 71, it can be seen that at a high shear rate, only the viscosity of control SEP-WDFs (FW) increases as the temperature was increasing leading to a great positive slope of 0.00246 and a very low positive slope of 2,62989E-4 was obtained from CNC/BT-WDFs (FW) at CNC concentrations 0.4 wt. %. As CNC concentration increases 0.8, 1.2, 1.6, 2.0 and 2.4 wt. %, the statistical data analysis by performing linear fitting results with different negative slope values of CNC/BT-WDFs (FW): -0.00151, -0.00193, -0.0018, 0.00207, and -0.00312 respectively. It can be seen that the viscosity was well maintained over a broad range of temperature due to the stiff network formed among CNCs, SEP layers, and immobilized water molecules where these water molecules were simply entrapped within the core-shell structure and immobilized at the vicinity of CNCs resulting to great resistance to the temperature changes. In fact, during the drilling operation of the deeper well, the excessive friction between the drill bit and the formation released much heat resulting in a significant increase in temperature into the wellbore. In the perspective of the performance of the drilling fluids in the cutting transportation, it is worthy to develop the mud system with less effect of temperature. This very low effect of temperature in the viscosity is due to the resistance of the drilling fluid.

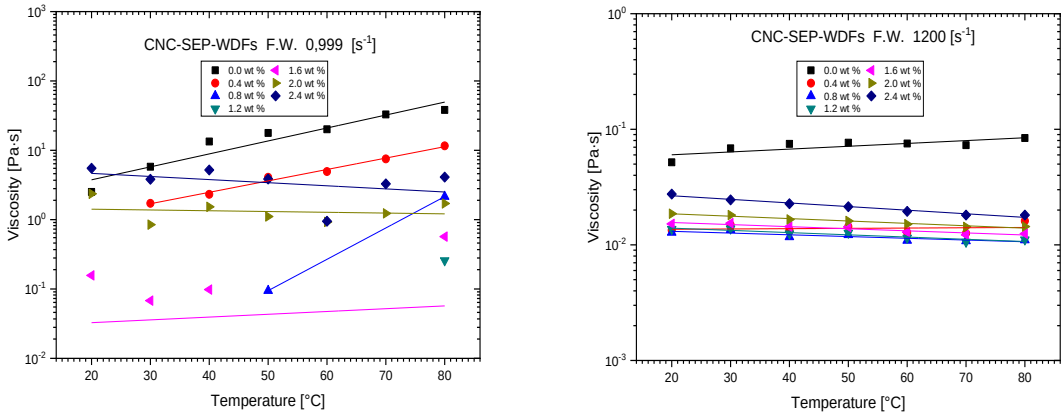

Figure 71. Plot of viscosity as a function temperature for CNC/SEP-WDFs in freshwater at various CNC concentration at low (0.999 s^{-1}) and high shear rate (1200 s^{-1}).

This resistance of CNC/SEP-WDFs (FW) is due to the strong surface interaction of CNCs and SEP-WDFs (FW). By investigating the effect of temperature on the viscosity, generally a decrease

in viscosity as the temperature increases are observed due to the increase in the mobility of water molecules. It is known that the more the raising temperature, the more the kinetic energy of the molecules increases leading to the weakening of intermolecular hydrogen bonds. As the mixture of CNCs and SEP in aqueous solution results in the attachment of the CNCs to the edge of SEP layers via hydrogen bond formed between their hydroxyl group and the possible ionic bond between the carboxylated CNCs with negatively charged carboxylate groups and the positively charged edge site of SEP, therefore, it could suggest that the increase of temperature affects the hydrogen bonds in CNC/SEP-WDFs (FW) that could lead to the reduction of viscosity with increasing temperature at high shear rate. So far, it could be seen the increase of viscosity of SEP-WDFs owing to the absorption of water into the sepiolite channels that cause more swelling. This confirms the CNC/SEP-WDFs (FW) at CNC concentrations of 1.2 wt. % at low temperature and 1.6 wt. % as the optimum concentration to be used in the drilling operation for the lowest effect of the temperature on the viscosity. Therefore, the CNC/SEP-WDFs (FW) at CNC concentration of 0.8 wt. % cannot be used as drilling fluid during drilling operation as long as it produced a shear thickening behavior and the same for the CNC/SEP-WDFs (FW) at CNC concentration of 1.2 wt. % at high temperature and high shear rate.

6.2. ANALYSIS OF THE RHEOLOGICAL PROPERTIES OF CNC/SEP-WDFs IN SEAWATER

6.2.1. RHEOLOGICAL CURVES AT DIFFERENT CNC CONCENTRATIONS FOR VARIOUS TEMPERATURES.

Sepiolite as a natural magnesium silicate clay forms needle-like particles. The suspension of Sepiolite in water leads to the formation of a random network responsible for the viscosifying effect due to the nonswelling needle aggregation and association. This viscosifying effect is favored at low pH value or alkaline pH through the incorporation of electrolytes which lead to the reduction of the negative charge of the silanol surface groups allowing the individual particles to aggregate along their surfaces, thereby increasing the viscosity of the suspension (Echt & Plank 2019).

As known, a rise in temperature increases the activity of any electrolyte and increases the solubility of any salt that may be present. This presence of electrolytes as in the case of seawater leads to the suppression of the repulsive forces between negatively charged polymers (carboxylated CNCs) and allow the like charges to approach one another more closely and giving rise to a coiled structure. As a result, a rise of shear-thinning behavior was observed that leads to the improvement of the rheological property of CNC/SEP-WDFs in seawater.

The rheological properties analysis of CNC/SEP-WDFs (SW) conducted in the same condition as all the previous drilling muds. Figure 72 illustrates the plots of shear stress as a function of shear rate for CNC/SEP-WDFs (SW) at different CNC concentrations. The figure shows better enhancement of the shear stress as CNC concentration was increasing. This indicates the requirement of a very high force to start the flow of the fluids. However, a general trend was observed as CNCs were added into SEP-WDFs (SW) at different concentrations offering a shear-thinning behavior for all drilling muds over the broad range of the shear rate from 0.999 s^{-1} to 1200 s^{-1}. This enhancement of the shear stress is due to the very higher surface interaction between CNCs, sepiolite, and immobilized water which was able to offer strong resistance to flow under shear force for the establishment of a card-house structure. Figure 72 shows an increase in the yield stress (y_o) as a function of CNC concentration. This is observed at different temperatures as followed: in figure 72(A), from 4.89972 Pa at 0.0 wt. % CNC to 3.32239, 19.10717, 4.97544, 5.50913, 12.49176 and 10,28925 Pa at 0.4, 0.8, 1.2, 1.6, 2.0 and 2.4 wt. % respectively; in figure 72(B), from 2.39298 Pa at 0.0 wt. % CNC to 4.55342, 32.66222, 4.73254, 66.1749, 13.29487 and 108.7711 Pa at 0.4, 0.8, 1.2, 1.6, 2.0 and 2.4 wt. % respectively; in figure 72(C), from 6.33751 Pa at 0.0 wt. % CNC to 5.41761, 6.05853, 8.86258, 11.92096, 44.81562 and 123.4327 Pa at 0.4, 0.8, 1.2, 1.6, 2.0 and 2.4 wt. % respectively; in figure 72(D), from 14.65309 Pa at 0.0 wt. % CNC to 4.86935, 5.31999, 14.8701, 23.44082, 30.37459 and 17.48043 Pa at 0.4, 0.8, 1.2, 1.6, 2.0 and 2.4 wt. respectively; in figure 72(E), from 6.672 Pa at 0.0 wt. % CNC to 6.46678, 19.09796, 23.2716, 10.31326, 22.62047 and 16.94121 Pa at 0.4, 0.8, 1.2, 1.6, 2.0 and 2.4 wt. % respectively; in figure 70(F), from 3.58001 Pa at 0.0 wt. % CNC to 26.79503, 51.9444, 43.42833, 6.24559, 12.08523 and 51.20858 Pa at 0.4, 0.8, 1.2, 1.6, 2.0 and 2.4 wt. % respectively; and in figure 72(G), from 23.41879 Pa at 0.0 wt. % CNC to 40.62112, 28.58876, 2.82284, 28.46116, 16.31808 and 19.11969 Pa at 0.4, 0.8, 1.2, 1.6, 2.0 and 2.4 wt. % respectively.

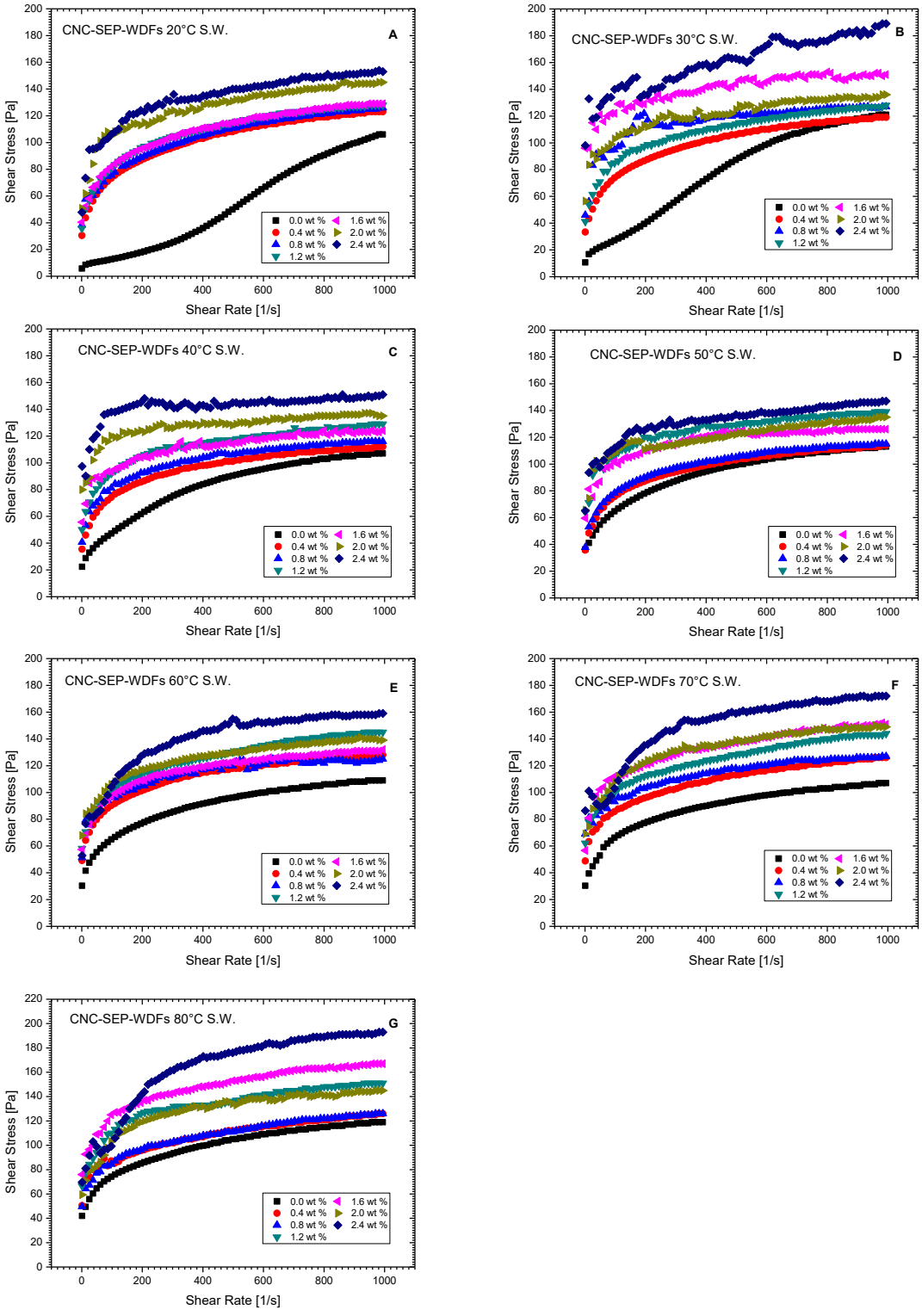

Figure 72. The plot of shear stress as a function of shear rate of CNC/SEP-WDFs (SW) at various CNC concentrations for different temperatures.

This increase in the yield stress should be attributed to the high enhancement of the surface interaction between CNCs and SE-WDFs (SW). It is observed that high yield stress values were observed in the presence of seawater, the salt as a contaminant favored significantly the rheological properties of CNC/SEP-WDFs (SW).

This increase in the yield stress should be attributed to the high enhancement of the surface interaction between CNCs and SE-WDFs (SW). It is observed that high yield stress values were observed in the presence of seawater, the salt as a contaminant favored significantly the rheological properties of CNC/SEP-WDFs (SW).

Therefore, the control SEP-WDFs (SW) gradually changed the pattern of their rheological curves with temperature change and was able to stand against the effect of salt in the suspension This salt resistance shown with all CNC/ SEP-WDFs (SW) was attributed to the strong surface interactions between CNCs, sepiolite and immobilized water as a stiff network built base on the attraction between carboxylated CNCs to the positively-charged edge surfaces of sepiolite. This improves the rheological properties of CNC/SEP-WDFs (SW). Therefore, the strong interaction imparts rigidity to the CNC-sepiolite networks that increase the salt resistance of CNC/SEP-WDFs (SW) by preventing invasion by salt ions, enhance water barrier capacity, and decrease fluid loss.

A better fitting of the rheological data is given through the Herschel-Bulkley model in table 19 below. From table 18, it is observed that the Herschel-Bulkley model gives a good correlation between shear stress and shear rate as R^2 is close to 1. However, the flow behavior index n < 1 leads to a shear-thinning behavior of the CNC/SEP-WDFs (SW). The high value of the yield stress proves the great carrying capacity of cuttings by CNC/SEP-WDFs (SW).

Table 18. Calculated parameters of CNC/SEP-WDFs (SW) at various CNC concentrations for different temperatures using the Herschel-Bulkley model.

Table 18. Calculated parameters of CNC/SEP-WDFs (SW) at various CNC concentrations for different temperatures using Herschel-Bulkley model.

T(°C)	CNC Conc (wt %)	y_0 (Pa)	K(Pa.S)	n	R^2	RMSD	SSR
20	0.0	4,89972	1,25748	1,25748	0,99012	3,28884	865,31767
	0.4	3,32239	2,25508	0,22716	0,99561	1,35479	146,83725
	0.8	19,10717	1,69057	0,26895	0,99415	1,49276	178,26625
	1.2	4,97544	3,6261	0,20293	0,99267	1,70255	231,89379
	1.6	5,50913	2,6729	0,21199	0,995	1,37958	152,25857
	2.0	12,49176	10,33325	0,15376	0,97843	2,71141	588,14008
	2.4	10,28925	8,54573	0,152	0,98718	2,19024	383,77076
30	0.0	2,39298	1,28151	0,66637	0,98383	4,36435	1523,80684
	0.4	4,55342	28,70936	0,20887	0,99259	1,63059	212,70468
	0.8	32,66222	57,27615	0,11879	0,90078	4,52813	1640,31911
	1.2	4,73254	37,0504	0,1808	0,99443	1,34519	144,7637
	1.6	66,1749	25,13988	0,18025	0,95856	2,51616	506,48374
	2.0	13,29487	59,06395	0,12078	0,98232	1,89825	288,26741
	2.4	108,77114	2,47137	0,49974	0,94583	4,49875	1619,10295
40	0.0	6,33751	8,15806	0,37037	0,98845	2,40785	463,82076
	0.4	5,41761	32,45994	0,18217	0,99063	1,55898	194,43455
	0.8	6,05853	39,22816	0,15985	0,99151	1,40425	157,7538
	1.2	8,86258	47,65734	0,14561	0,98755	1,75314	245,87903
	1.6	11,92096	55,79431	0,11704	0,98424	1,60955	207,25231
	2.0	44,81562	80,04544	0,07867	0,92422	2,92896	686,30641
	2.4	123,43272	100,08398	0,05973	0,77474	4,80069	1843,73353

50	0.0	14,65309	13,93077	0,28757	0,99112	1,78101	253,75897
	0.4	4,86935	33,0127	0,18186	0,99265	1,39729	156,19374
	0.8	5,31999	36,26017	0,17023	0,99249	1,36951	150,0452
	1.2	14,8701	62,40522	0,1175	0,98051	2,02186	327,03245
	1.6	23,44082	61,18855	0,10875	0,95322	2,77488	327,03245
	2.0	30,37459	67,22445	0,09835	0,93862	2,99733	718,7203
	2.4	17,48043	69,24456	0,10888	0,97896	2,07398	344,1113
60	0.0	6,672	19,42996	0,24394	0,99607	1,10783	98,1832
	0.4	6,46678	45,31184	0,1522	0,99262	1,37961	152,26668
	0.8	19,09796	56,07502	0,11952	0,96113	2,67644	573,06619
	1.2	23,2716	30,46836	0,20293	0,99546	1,25429	125,85997
	1.6	10,31326	52,75836	0,13443	0,98629	1,77718	252,66935
	2.0	22,62047	41,28609	0,15332	0,99096	1,40848	158,70542
	2.4	16,94121	48,32241	0,17802	0,95965	4,69472	1763,2332
70	0.0	3,58001	24,76926	0,21402	0,99381	1,33166	141,86547
	0.4	26,79503	20,75537	0,22819	0,99886	0,54732	23,96476
	0.8	51,9444	13,47544	0,25246	0,98749	1,49123	177,9018
	1.2	43,42833	17,99624	0,25048	0,99803	0,77139	47,603
	1.6	6,24559	58,87413	0,13708	0,99589	1,11345	99,18141
	2.0	12,08523	47,67609	0,15584	0,97921	2,55324	521,52334
	2.4	51,20858	18,28941	0,28075	0,927	6,5182	3398,95202
80	0.0	23,41879	14,16126	0,27955	0,99682	1,0063	81,01048
	0.4	40,62112	13,86374	0,26304	0,99301	1,26063	127,13587
	0.8	28,58876	19,53833	0,23373	0,99737	0,82803	54,85035
	1.2	2,82284	56,1324	0,14171	0,97836	2,59874	540,27471
	1.6	28,46116	42,17673	0,174	0,99152	1,75585	246,63972
	2.0	16,31808	51,82194	0,1521	0,96523	3,47733	967,34813
	2.4	19,11969	32,04178	0,25151	0,94661	7,41126	4394,13985

6.2.2. RHEOLOGICAL CURVES OF CNC/SEP-WDFs (SW) AT DIFFERENT TEMPERATURES FOR VARIOUS CNC CONCENTRATIONS

The rheological properties of CNC/SEP-WDFs (SW) were measured with the Rotational Rheometer (RheolabQC SN897839/FW1.31) at atmospheric pressure and various temperatures.

Figure 73 shows the variation of the shear stress against temperature at the higher shear rate (1200 s^{-1}) and different CNC concentrations. It depicts almost a plateau as the shear stress was varied against temperature. This thermal stability is attributed to the thermal dispersion and thermal dehydration of the sepiolite clay particles in the suspension.

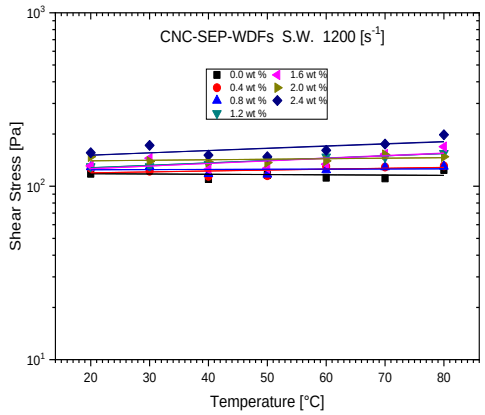

Figure 73. The plot of shear stress as a function temperature for CNC/SEP-WDFs (SW) at various CNC concentrations taken at high shear rate 1200 s^{-1}.

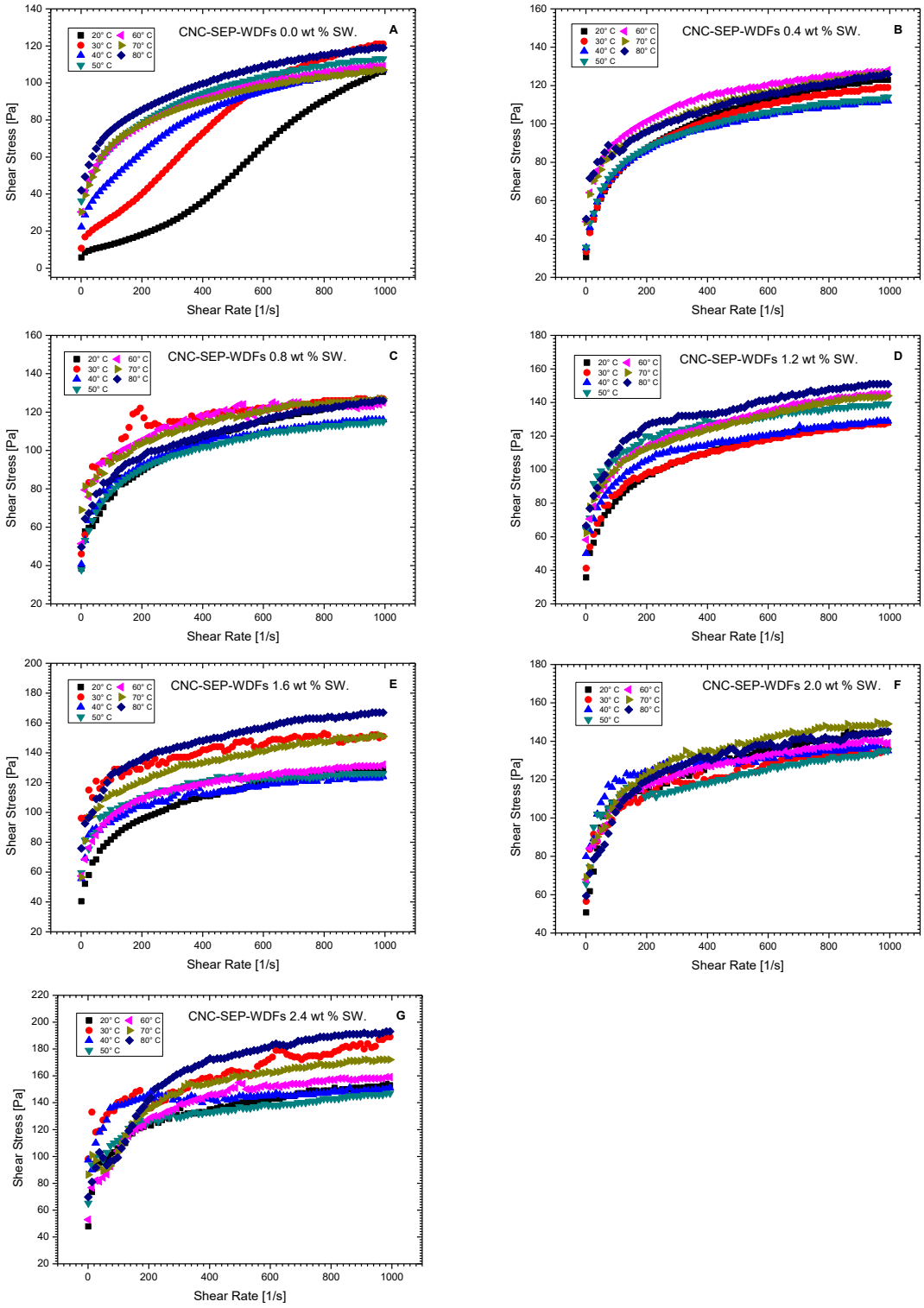

Figure 74. The plot of shear stress as a function of shear rate of CNC/SEP-WDFs in seawater at different temperature and various CNC concentrations.

The shear stress versus shear rate curves of CNC/SEP-WDFs (SW) at different temperatures and various CNC concentrations are shown in Figure 74.

The experimental results indicate that the CNC/SEP-WDFS (SW) behaved as shear-thinning fluids from 0.0 wt. % to 2.4 wt. % CNC concentrations over a broad range of temperature with the consistency index less than 1 ($n<1$) except only for the control SEP-WDFs (SW) at 20°C. However, the shear-thinning behavior of CNC/SEP-WDFs (SW) is the most interesting as it is needed during the drilling operation. Generally speaking, the combined application of shear rate and temperature favored the CNC/SEP-WDFs (SW) for enhancing rheological properties.

6.2.3. THE EFFECT OF CNC CONCENTRATION ON THE VISCOSITY OF CNC/SEP-WDFs (SW) AS DRILLING FLUID.

The analysis of the rheological curves based on the variation of the viscosity with the shear rate at various CNC concentrations shown in figure 75 demonstrates a linear reduction in the viscosity over a broad range of shear rate from 0.999 s^{-1} to 1200 s^{-1} for almost all the CNC concentrations for all range of temperature except for the control SEP-WDFs (SW) at 20°C where the viscosity decreases and increases at 400 s^{-1} to 800 s^{-1} than decreases again. As well as at 30°C where the viscosity decreases and reaches a plateau at 800 s^{-1} then decreases again till 1200 s^{-1}. These rheograms of represent the shear-thinning behavior of CNC/SEP -WDFs (SW) due to the strong interaction between charged sepiolite and carboxylated CNCs with immobilized water.

Most of the CNC/SEP-WDFs (SW) except the control SEP-WDFs (SW) at 20°C and 30°C offer significant viscosity values that induce a shear-thinning behavior of the drilling fluids in seawater and allows the carrying of cuttings at the low shear rate (0.999 s^{-1}). It can be seen in figure 75 that the incorporation of CNCs from 0.4 wt. % to 2.4 wt. % to the sepiolite suspension increases the viscosity of CNC/SEP-WDFs (SW) significantly, which increases the carrying cuttings performance. The hydrogen bonding built between hydrogen and hydroxyl of sepiolite clay and the carboxylated CNCs can be the reason for this increase in viscosity of CNC/SEP-WDFs (SW).

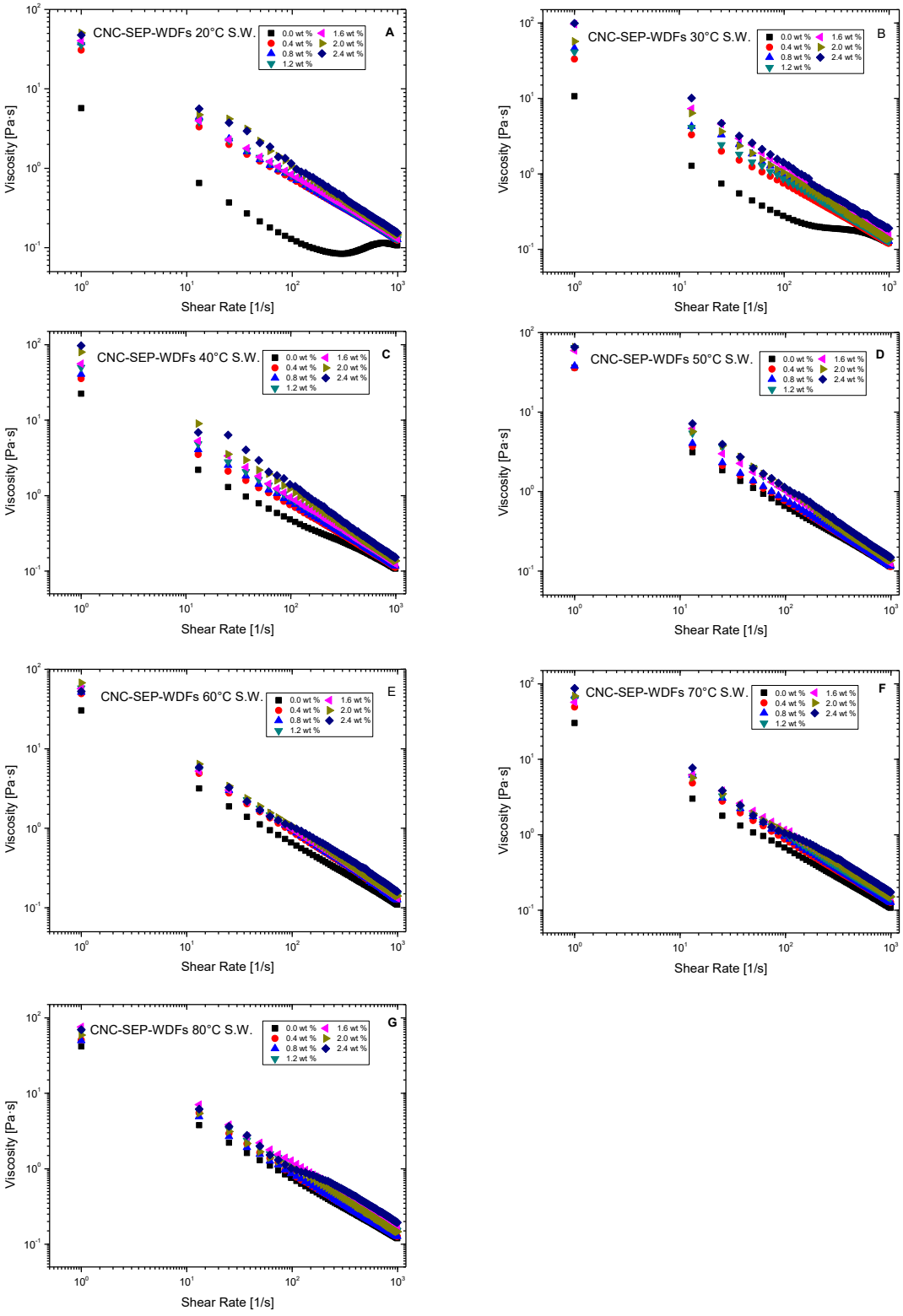

Figure 75. The plot of viscosity as a function of shear rate for CNC/SEP-WDFs (SW) at various CNC concentrations for different temperatures.

The rheological data given in table 19 below provides the description of the variation of viscosity as a function of CNC concentration at different temperatures.

Table 19. Viscosity of CNC/SEP-WDFs (SW) at various CNC concentrations for different temperatures.

CNC concentration	Shear Rate	Viscosity	Viscosity	Viscosity	Viscosity	Viscosity	Viscosity	Viscosity
[wt %]	[1/s]	[Pa·s]	[Pa·s]	[Pa·s]	[Pa·s]	[Pa·s]	[Pa·s]	[Pa·s]
		CNC-SEP-WDFs S.W. [20°C]	CNC- SEP -WDFs S.W. [30°C]	CNC- SEP -WDFs S.W. [40°C]	CNC- SEP-WDFs S.W. [50°C]	CNC- SEP-WDFs S.W. [60°C]	CNC- SEP-WDFs S.W. [70°C]	CNC- SEP-WDFs S.W. [80°C]
0.0	0,999	5,73	10,7	22,4	36,2	30,4	30,2	41,8
0,4	0,999	30,8	33,2	35,5	35,9	49,4	49,1	50,8
0,8	0,999	38,2	46,2	40,5	38,1	51,5	68,8	49,9
1,2	0,999	35,7	41,1	50	64,6	58	62,6	66,2
1,6	0,999	40,3	96	55,9	59,5	57,2	56,8	75,8
2.0	0,999	50,6	56,9	79,7	65,5	67,5	68,9	59,1
2,4	0,999	47,6	98,9	97,1	65,6	52,6	87	69,6

Generally speaking, it is denoted that the viscosity of CNC/SEP-WDFs (SW) increased with the increase in the CNC concentrations as seen in figure 76.

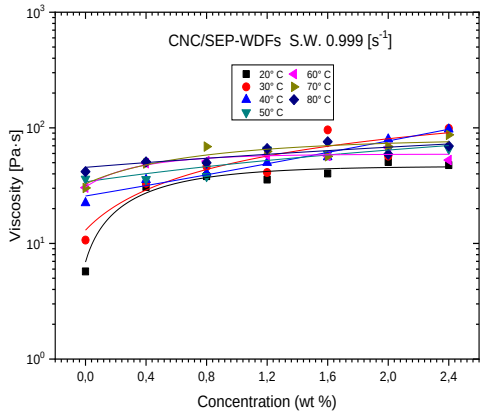

Figure 76. Variation of viscosity of CNC/SEP-WDFs (SW) with CNC concentrations at shear rates 0.999 s^{-1} and different temperatures.

Generally, the increase in temperature induces a reduction of the viscosity but in the presence of some strong surface interaction, there will be less sensitivity to the change of temperature. In this way, it can be conducted any investigation for the evidence of an existing strong surface interaction upon CNC/SEP-WDFs (SW). Figure 77 depicts the effect of temperature on the viscosity of CNC/SEP-WDFs (SW) at a low shear rate, much increase of the viscosity with temperature was observed from 0.0 to 1.2 wt. % CNC concentrations into SEP-WDFs (SW). However, from 1.6 to 2.4 wt. % CNC concentrations into SEP-WDFs (SW), it can be seen that their viscosity was not affected much by the change in temperature but kept on slightly increasing. This was due to the firm network among SEP rods, CNCs, and immobilized water molecules in which the core-shell structure caught water molecules and fastened at the proximity of CNCs, offering less effect of temperature change upon the viscosity. Therefore, it favored the carrying capacity of cuttings into the drilling fluids at a low shear rate. However, despite the very low increase in viscosity as a function of temperature that is observed CNC/SEP-WDFs (SW) demonstrated thermal stability at

a high shear rate as well due to the strong interaction between SEP rods, carboxylated CNCs, and immobilized water.

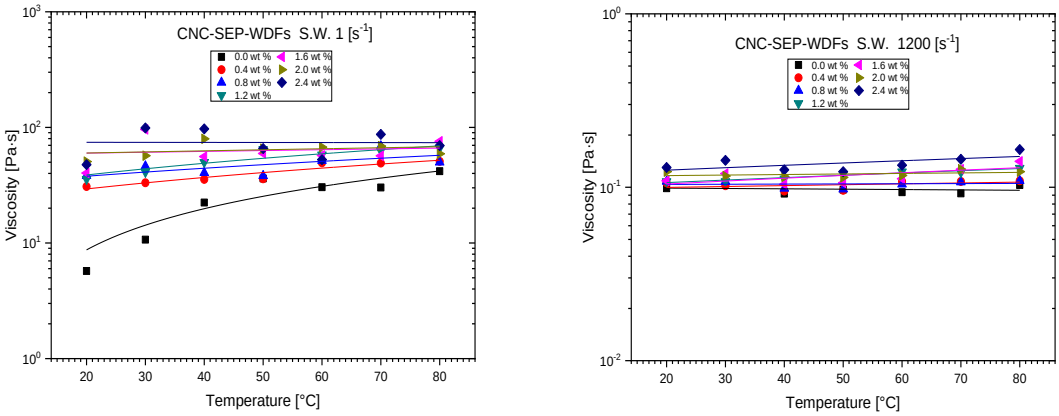

Figure 77. The plot of viscosity as a function temperature for CNC/SEP-WDFs in sea-water at various CNC temperature taken at low and high shear rate (1 s $^{-1}$ and 1200 s $^{-1}$).

This behavior of CNC/SEP-WDFs (SW) at a high shear rate offers more resistance toward the temperature change (Yan et al 2013).

The plot in this figure 78 shows the effect of the temperature upon the flow consistency coefficient which is a measure of the shear viscosity or the resistance to flow at 0.999 s $^{-1}$. It is observed that K is kept increasing for the control SEP-WDFs (SW) as the temperature was increasing. On the other hand, it could be seen that the addition of CNCs particles into SEP-WDFs (SW) first increased the consistency coefficient of all the CNC/SEP-WDFs (SW) from 20°C to 40°C then from there it started to decrease slightly as the temperature increased from 40°C to 80°C. This means after the yield stress is exceeded, the flow is almost maintained constant along with the higher temperature change.

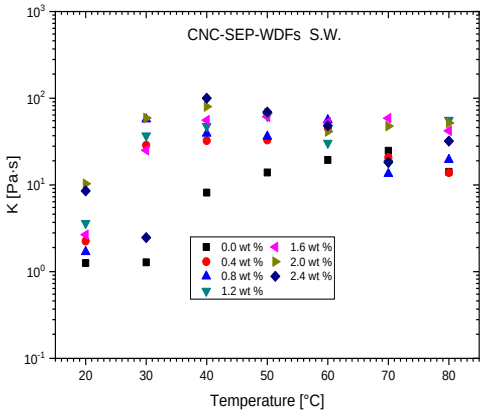

Figure 78. The plot of the flow consistency coefficient (K) as a function temperature of CNC/SEP-WDFs (SW) at various CNC concentrations.

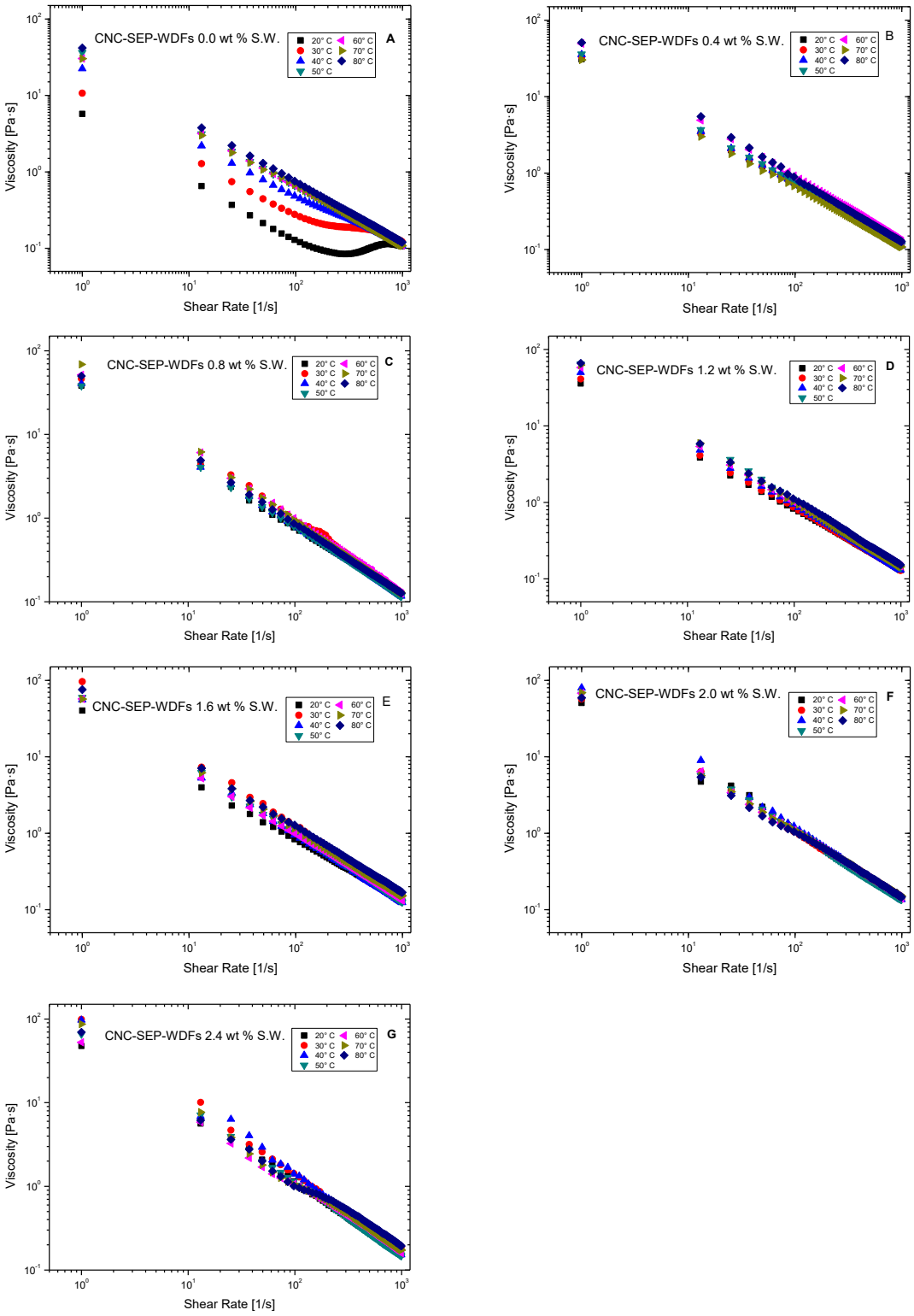

Figure 79.The plot of viscosity as a function of shear rate for CNC/SEP-WDFs (SW) at various temperatures for different CNC concentrations.

As it can be seen, in figure 79 above, the effect of temperature on the viscosity of CNC/SEP-WDFs (SW) over a broad range of shear rate is exactly manifested at 0.0 wt. % of CNC concentration from 20°C to 40°C. Plot A of figure 79 shows how the increase in temperature affected the viscosity that was increasing as well. At 20°C, the viscosity of the control SEP-WDFs (SW) depicted a nonlinear decrease over the broad range of shear rate from 0.999 s^{-1} to 1200 s^{-1}. It decreased then increases and decreased again; at 30°C, it decreased then reached a plateau then decreased again; and at 40°C, it decreased with slight shift then continued to decrease. However, from 50°C to 80°C, a linear decrease of the viscosity was observed over the broad range of the shear rate from 0.999 s^{-1} to 1200 s^{-1}. From plot B to plot G, it is observed that this effect of the temperature upon the viscosity was much less manifested. The temperature effect was almost non-significant upon the viscosity of CNC/SEP-WDFs (SW). Therefore, the reduction of viscosity with an increase in shear rate results in a shear-thinning behavior of the CNC/SEP-WDFs (SW) at CNC concentrations from 0.4 wt. % to 2.4 wt. %. As it could be seen, the effect of temperature upon viscosity remained mostly constant over the broad range of temperature from 20°C to 80°C for 0.4, 0.8, 1.2, 1.6, 2.0, and 2.4 wt. % CNC concentrations respectively. This confirms the thermal stability of CNC/SEP-WDFs (SW). Thus, it can be attributed to the high resistance in salinity content in sea-water of the CNC/SEP-WDFs. Thus, the salt content favors the improvement in yield stress, viscosity, and gel strength of CNC/SEP-WDFs as drilling fluids.

This behavior of the different rheological properties of the mud system under high temperature could be the result of the thermal degradation of the solid content, polymers, and other components of the mud system and the expansion of the molecules which will lower the resistance of the fluid to flow, hence, its viscosity, yield stress and gel strength (Amani & Al-Jubouri 2012). By contrast, the present case of CNC/SEP-WDFs (SW) shows an improvement of the rheological properties with the incorporation of the CNC polymers in the presence of seawater and temperature change into SEP-WDFs including the enhancement of the yield stress, viscosity, and gel strength of the mud system. This incorporation of CNCs as nanoparticles in SEP-WDFs (SW) leads to the shear-thinning behavior of the drilling muds confirms the rheological modifier and fluid loss reducer property of CNCs.

6.3. FILTRATION PROPERTIES

6.3.1. ANALYSIS OF FILTRATION PROPERTIES OF CNC/SEP-WDFs (FW)

The fluid loss properties of CNC/SEP-WDFs (FW) at 1.2 wt. % CNC concentration was investigated by varying the temperature from 20°C to 80°C to design a suitable drilling fluid that is following API standards (15mL/30 min) as shown in figure 80. The effect of temperature on the fluid loss of CNC/SEP-WDFs (FW) was observed at 30°C, 40°C, 50°C, 60°C, 70°C, and 80°C and offers 13.4, 13.8, 14.8, 15.8, 16 and 17.2 ml/30 min API fluid loss volume respectively.

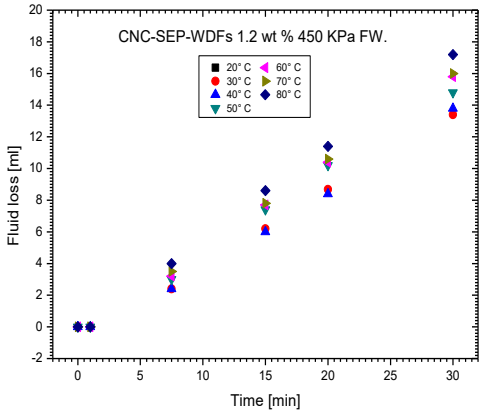

Figure 80. The plot of fluid loss volume as a function of time for CNC/SEP-WDFs (FW) 1.2 wt. % CNC concentration at 450 KPa for different temperatures.

It could be seen that the fluid loss increased as temperature increased demonstrating less retention of the filtrate at high temperature that could lead to serious wellbore collapse and deposition by flocculation of their filter cake on the wellbore wall causing differential pressure sticking, stuck pipe problems, and well damage (Zakaria et al 2012). These API fluid volumes of CNC/SEP-WDFs (SW) are above the API standard given from 60°C to 80°C.

6.3.2. ANALYSIS OF FILTRATION PROPERTIES OF CNC/SEP-WDFs (SW)

The fluid loss properties of CNC/SEP-WDFs (FW) at 1.2 wt. % CNC concentration was also investigated by varying the temperature from 20°C to 80°C to design a suitable drilling fluid that is following API standards (15ml/30 min) as shown in figure 81.

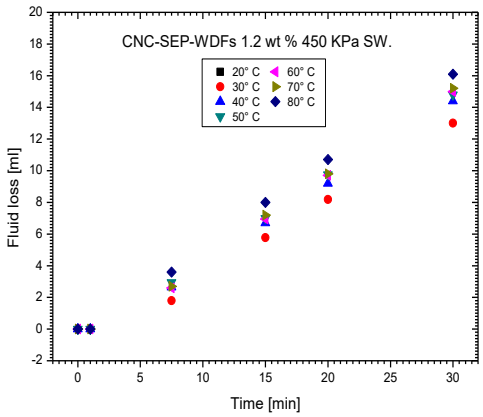

Figure 81. The plot of fluid loss volume as a function of time for CNC/SEP-WDFs (SW) 1.2 wt. % CNC concentration at 450 KPa for different temperatures.

The effect of temperature on the fluid loss is observed through figure 81 for 1.2 wt. % CNC concentration of CNC/SEP-WDFs (SW). The CNC/SEP-WDFs (SW) with 1.2 wt. % offers 13, 14.4, 14.8, 15.0, 15.2 and 16.1 mL/30 min API fluid loss volume at 30°C, 40°C, 50°C, 60°C, 70°C, and 80°C respectively. It could be seen that the fluid loss increased as temperature increased demonstrating less retention of the filtrate that could lead to serious wellbore collapse and deposition by flocculation of their filter cake on the wellbore wall causing differential pressure sticking, stuck pipe problems, and well damage (Zakaria et al 2012). These API fluid volumes of CNC/SEP-WDFs (SW) are above the API standard given from 60°C to 80°C.

Nevertheless, when 1.2 wt. % of CNCs was incorporated, the minimum API fluid loss of 17.2 ml/30 min was obtained at 80°C for CNC/SEP-WDFs (FW) whereas the CNC/SEP-WDFs (SW) at the same condition of CNC concentration, temperature, and pressures produced an API fluid loss of 16.1 mL/30 min about 6.4 % of API fluid loss less than that of CNC/SEP-WDFs (FW).

6.4. AGING TIME

It can be observed that figure 82 and table 21-22 displayed the plot of shear stress as a function of shear rate at different aging times and the calculated parameters of CNC/SEP-WDFs (FW) at different aging times for different temperature using Herschel-Bulkley (HB) Models. It is observed in figure 80(A-B) for CNC/SEP-WDFs (FW) that shear stress increased with an increase in aging time. This means the shear stress decreases with the aging time in freshwater. The same effect is observed in seawater except for CNC/SEP-WDFs (SW) in figure 80(A) where the shear stress decreases with increasing aging time. However, in figure 80(B) for CNC/SEP-WDFs (SW), the shear stress increases with increasing aging time. It has been observed that the drilling fluid properties are affected by the variation of the temperature and aging time.

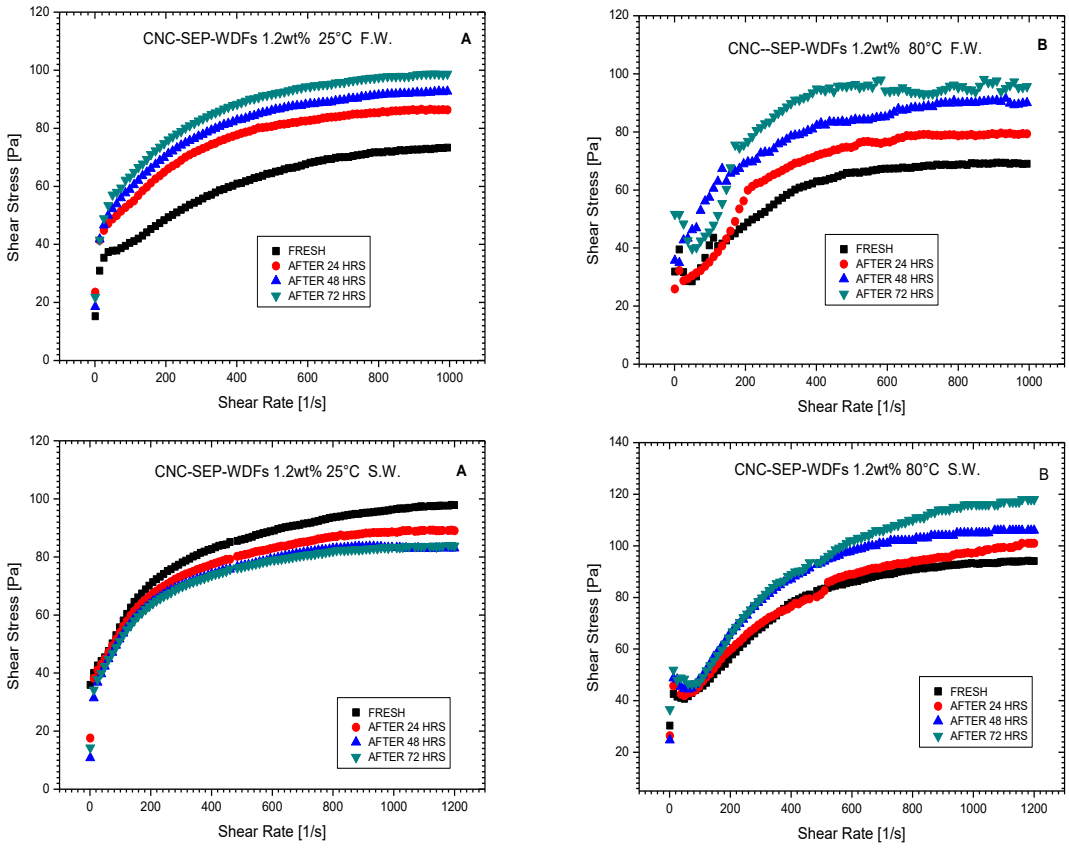

Figure 82. The plot of shear stress as a function of shear rate at different aging time at 25℃ and 80℃ for CNC/ SEP-WDFs in fresh water and seawater.

Table 20. Calculated parameters of CNC/SEP-WDFs (FW) at different aging time for different temperature using Herschel-Bulkley (HB) Models.

1.2 wt. % CNC-SEP-WDFs (FW) at 25°C				
Model	Herschel			
Equation	y = y0 + K*x^n;			
Plot	Shear Stress	Shear Stress	Shear Stress	Shear Stress
y0	8,20216 ± 2,54924	0 ± 5,9003	0 ± 5,69734	0 ± 6,00949
K	8,89858 ± 1,3894	23,65335 ± 4,41602	25,09186 ± 4,25044	26,91946 ± 4,4921
n	0,29357 ± 0,0177	0,19336 ± 0,018	0,19454 ± 0,01638	0,19382 ± 0,01611
Reduced Chi-Sqr	2,2879	3,49536	3,32279	3,65361
R-Square (COD)	0,98629	0,98062	0,98432	0,98475
Adj. R-Square	0,98595	0,98014	0,98393	0,98436
1.2 wt. % CNC-SEP-WDFs (FW) at 80°C				
Model	Herschel			
Equation	y = y0 + K*x^n;			
Plot	Shear Stress	Shear Stress	Shear Stress	Shear Stress
y0	16,65198 ± 5,06382	0 ± 9,8615	4,05579 ± 7,53799	14,71954 ± 16,37162
K	5,54584 ± 2,3411	13,63431 ± 5,91622	21,45007 ± 5,41153	14,98593 ± 10,09279
n	0,3383 ± 0,04996	0,26573 ± 0,04755	0,20822 ± 0,02513	0,25753 ± 0,07298
Reduced Chi-Sqr	13,26756	25,78965	7,21494	64,87904
R-Square (COD)	0,91225	0,90468	0,96429	0,79018
Adj. R-Square	0,91006	0,9023	0,9634	0,78494

Table 21. Calculated parameters of CNC/SEP-WDFs (SW) at different aging time for different temperature using Herschel-Bulkley (HB) Models.

1.2 wt. % CNC-SEP-WDFs (SW) at 25°C				
Model	Herschel			
Equation	y = y0 + K*x^n;			
Plot	Shear Stress	Shear Stress	Shear Stress	Shear Stress
y0	5,2315 ± 5,995	0 ± 6,26725	0 ± 8,63964	0 ± 7,07267
K	19,93701 ± 4,03551	23,28708 ± 4,56302	22,37736 ± 6,32647	22,20542 ± 5,17016
n	0,22157 ± 0,02027	0,19572 ± 0,01862	0,19374 ± 0,02675	0,19433 ± 0,02206
Reduced Chi-Sqr	6,38883	4,74349	8,72848	5,90654
R-Square (COD)	0,97364	0,97653	0,95385	0,96766
Adj. R-Square	0,97309	0,97604	0,95289	0,96699
1.2 wt. % CNC-SEP-WDFs (SW) at 80°C				
Model	Herschel			
Equation	y = y0 + K*x^n;			
Plot	Shear Stress	Shear Stress	Shear Stress	Shear Stress
y0	13,70017 ± 5,2256	17,53423 ± 3,61692	3,92708 ± 7,61875	23,78337 ± 3,96713
K	8,30555 ± 2,39058	6,25098 ± 1,39746	14,87588 ± 4,20118	4,43236 ± 1,13953
n	0,32982 ± 0,03304	0,37164 ± 0,02651	0,28034 ± 0,03083	0,44049 ± 0,03172
Reduced Chi-Sqr	15,17846	9,93085	20,63827	18,20486
R-Square (COD)	0,95211	0,97235	0,95112	0,96772
Adj. R-Square	0,95112	0,97177	0,9501	0,96704

As seen in this project, the impact of temperature and aging time upon the yield stress viscosity and shear stress so far on the gel strength. Therefore, by the fact of maintaining at the optimum values these rheological properties, many drilling issues could be avoided. Thus, the drilling fluid rheology remained very important as the viscosity of the drilling fluid is practically affecting the rate of penetration during the drilling operation. Keeping proper gel strength is advantageous for holding cuttings in suspension, and for a high penetration rate relatively low gel strength is needed that will cause less pressure drop in the borehole. The cutting slip velocity gives a better correlation with yield stress than any other rheological parameters. Furthermore, the incorporation of the cellulose nanocrystals in the clay-based fluids maintained a better viscosity of the mud system that means CNCs reduced the viscosity at the optimum value leading to the reduction of the amount of energy needed for rotating drill stem and drill bit.

6.5. RATE OF PENETRATION.

The experimental data are given in tables 23 and 24 show the variation of the rate of penetration as a function of pressure (stress) or weight on the bit of different rock samples with CNC/BT, ATT, SEP-WDFs in freshwater and sea-water. Only the one for CNC/SEP-WDFs in freshwater and seawater has to be considered in this case. Generally, it is observed in figure 81 that CNC/SEP-WDFs (FW) at 1.2 wt. % CNC concentration exhibits a more significant rate of penetration values than CNC/SEP-WDFs (SW) at 1.2 wt. % CNC concentration into plot B. In addition, the fast ROP is attributed to CNC/SEP-WDFs (FW) at 1.2 wt. % CNC concentration as drilling is done into Breccia, Dolomite, and Sandstone rock samples except into Shale rock sample where CNC/SEP-WDFs (SW) at 1.2 wt. % CNC concentration shows fast ROP.

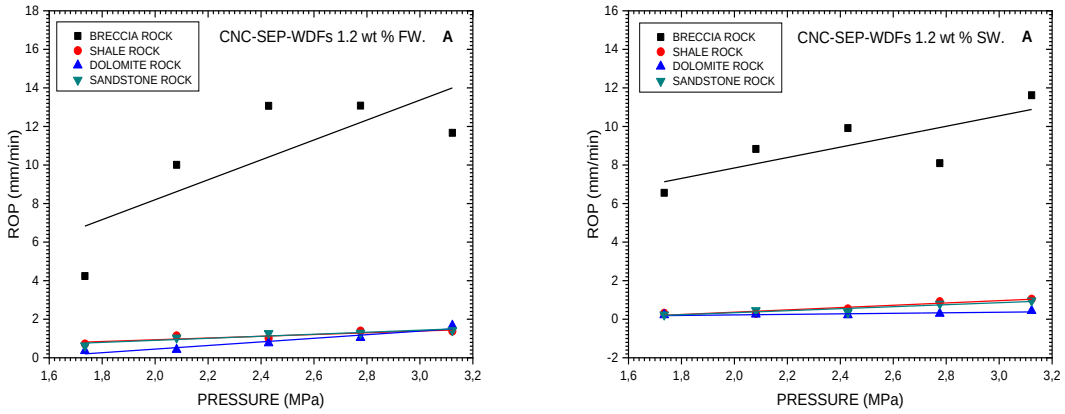

Figure 83.The plot of the rate of penetration as a function of pressure (stress) or weight on bit of different rock samples in CNC/SEP-WDFs (FW) / (SW).

6.6 . CONCLUSIONS

The effect of CNC concentrations, temperature, and pressure on the rheological and filtration properties of CNC/SEP-WDFs was investigated in fresh-water and sea-water. Herschel-Bulkley's model as a statistical modeling technique was used for a better understanding of the rheological behaviors. The penetration rate onto different rock samples with CNC/SEP-WDFs was investigated in freshwater and seawater. The aging and temperature effect of CNC/SEP-WDFs was investigated in fresh-water and sea-water some significant results observed during the study of this project are:

- CNC concentrations had a great effect on the rheological properties of CNC/SEP-WDFs in seawater as little increase in the CNC concentration produced considerable augmentation of the drilling viscosity whereas less effect has been observed for CNC/SEP-WDFs in freshwater. The fluid loss property of CNC/SEP-WDFs (SW) was less affected than that of CNC/SEP-WDFs (FW) even though both offered a high fluid loss value (16.1 and 17.2 ml/30 min, respectively) than the API standard value (15 ml/30 min) at high temperature (80°C). At low temperature (30°C), their fluid loss values (13 and 13.4 ml/30 min, respectively) were acceptable as they are less than the API standard value (15 ml/30 min).
- Effect of salinity had considerably improved the rheological properties of CNC/SEP-WDFs in seawater. It improved as well the filtration properties as the fluid loss was slightly above the API standard value at high temperature whereas at low temperature his filtration property was acceptable.
- The temperature effects on the rheological properties were much improved in CNC/ SEP-WDFs (SW) than CNC/SEP-WDFs (FW) as it increased the carrying capacity and the viscosity of the drilling mud in sea-water more than in fresh-water for CNC/SEP-WDFs.
- The fast penetration rate was reached by using CNC/SEP -WDFs (FW) than CNC/SEP-WDFs (SW) through rotary drilling on different rock samples (Breccia, Shale, Dolomite, and Sandstone) except when drilling in Shale rock sample.
- Salinity has positive effects on the aging time of CNC/SEP-WDFs in seawater. Meaning that the salinity increases the carrying capacity of cuttings (yield stress) of CNC/SEP-WDFs (SW) at high temperature during the aging period. In freshwater, this yield stress was improved due to the increase in temperature for CNC/SEP-WDFs (FW) during the aging time.
- The effect of the aging time of CNC/SEP-WDFs in freshwater was improved by increasing temperature as it has a great impact on the increase of the yield stress for both CNC/SEP-WDFs in freshwater and seawater.

CHAPTER 7. COMPARISON OF DIFFERENT DRILLING FLUIDS

7.1. FILTRATION PROPERTIES

7.1.1. FILTRATION IN PROPERTIES IN FRESHWATER

The filtration properties of CNC/BT-WDFs (FW), CNC/ATT-WDFs (FW), and CNC/SEP-WDFs (FW) were analyzed by using API filter press as shown in figure 84. The API fluid loss was recorded by measuring the volume of the filtrate after 30 min recorded as followed at 0.0, 7.5, 15, 20, and 30 min respectively.

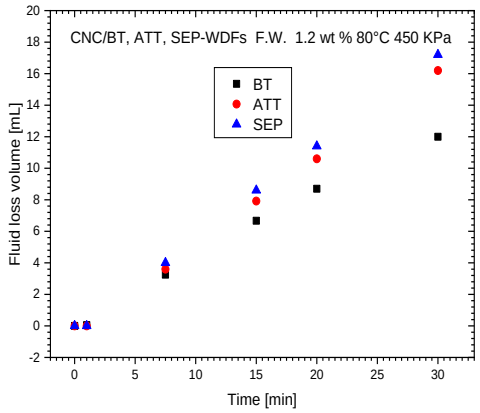

Figure 84. The plot of fluid loss volume of CNC/BT, ATT, SEP-WDFs (FW) as a function of time at 80°C, 450KPa and 1.2 wt. % CNC concentration.

By comparing the three drilling fluids CNC/BT, ATT, SEP-WDFs (FW) based on their filtration at 80°C, 450KPa, and 1.2 wt. % CNC concentration, it is observed that the amounts of fluid loss produced in terms of ml/30 min are 12, 16.2, and 17.2 ml/30 min for CNC/BT-WDFs (FW), CNC/ATT-WDFs (FW), and CNC/SEP-WDFs (FW) respectively. This result shows less filtrate loss and more water retention for CNC/BT-WDFs (FW) due to the high bentonite swelling

7.1.2. FILTRATION IN PROPERTIES IN SEAWATER

The filtration properties of CNC/BT-WDFs (SW), CNC/ATT-WDFs (SW), and CNC/SEP-WDFs (SW) were analyzed by using API filter press as showed in figure 85. The API fluid loss was recorded by measuring the volume of the filtrate after 30 min recorded as followed at 0.0, 7.5, 15, 20, and 30 min respectively.

By comparing the three drilling fluids CNC/BT, ATT, SEP-WDFs (SW) on base on their filtration at 80°C, 450KPa, and 1.2 wt. % CNC concentration, it is observed that the amounts of fluid loss produced in terms of mL/30 min are 16.7, 16.8, and 16.1 ml/30 min for CNC/BT-WDFs (SW), CNC/ATT-WDFs (SW), and CNC/SEP-WDFs (SW) respectively. This result shows less filtrate loss and more water retention for CNC/SEP-WDFs (SW) due to the great surface interaction observed between sepiolite clay and the carboxylated CNC with immobilized water.

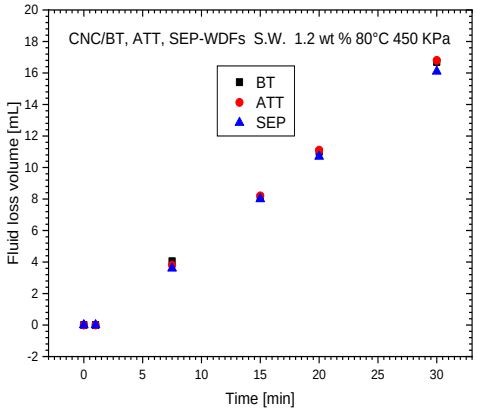

Figure 85. The plot of fluid loss volume of CNC/BT, ATT, SEP-WDFs (SW) as a function of time at 80°C, 450KPa and 1.2 wt. % CNC concentration.

7.2. AGING AND TEMPERATURE EFFECTS ON DIFFERENT PREPARED DRILLING FLUIDS.

The studies of properties of a drilling fluid under downhole conditions are attributed to the concept of aging for simulating the properties of drilling mud since the properties on the surface do not reflect the faithful picture of the bottom-hole conditions (Awele 2014). The process in which drilling fluids were previously subjected to a shear period and allowed to more freely develop their rheological and filtration properties is summarized by what is called aging (Makinde 2011). It is through any variation from static to dynamic conditions or even from ambient temperature to very high temperature that aging takes place.

The properties of drilling mud change due to high temperature, pressure, and aging, which causes problems in drilling a successful well, especially deep wells. This causes the properties of the mud to decrease, leading to severe affectation in drilling operations known as non-productive time (NPT), thereby increasing the cost of operation and possibly causing a kick or blowout. Fluid loss and differential sticking are some examples of poor monitoring of the down-hole condition of a drilling system. As a result, due to the poor conditioning of drilling muds, the industry faced many problems (Echt & Plank 2019).

From the results shown in figure 86-88, it can be seen that the rheological properties of the drilling fluids CNC/BT, ATT, SEP-WDFs in fresh water and seawater are affected by aging and temperature. In the following step, the variation and reason based on the changes of properties with time and temperature will be given (Amani & Al-Jubouri 2012).

It is observed in figure 86(a) and table 22, the consistency index that is the viscosity of the material at one reciprocal second of CNC/BT, ATT, SEP-WDFs (FW) are different as aging time and temperature change even though an equal amount of clay materials has been added and mixed in the same condition. It is observed that the increase of temperature from 25°C to 80°C decreases the consistency index of CNC/BT, ATT, SEP-WDFs (FW). For the same range of aging time, a temperature rise causes the consistency index to reduce through all the freshwater mud systems. For the same temperature (25°C or 80°C), the increase of the aging time causes fluctuation of the consistency index values of the mud system. Except for 1.2 wt. % of CNC/SEP-WDFs at 25°C,

the increase of the aging time increases the consistency index. On contrary, the one for 2.0 wt. % CNC/ATT-WDFs at 80°C, the consistency index remained constant along with the range of the

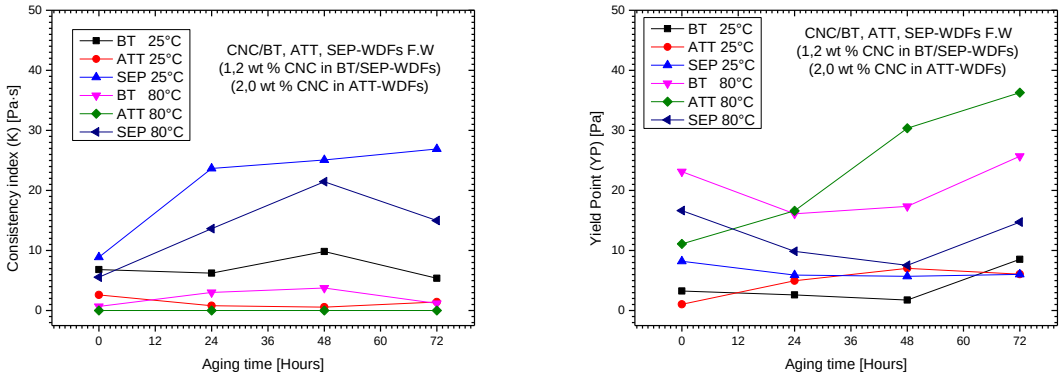

Figure 86. Consistency index and yield point as a function of aging time at different temperatures for CNC/BT, ATT, SEP-WDFs (FW).

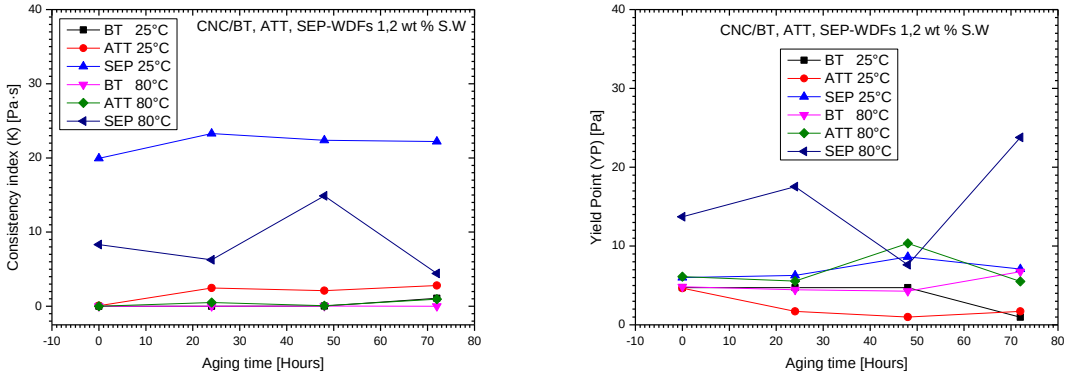

Figure 87. Consistency index (a) and yield point (b) as a function of aging time at different temperatures for CNC/BT, ATT, SEP-WDFs (SW).

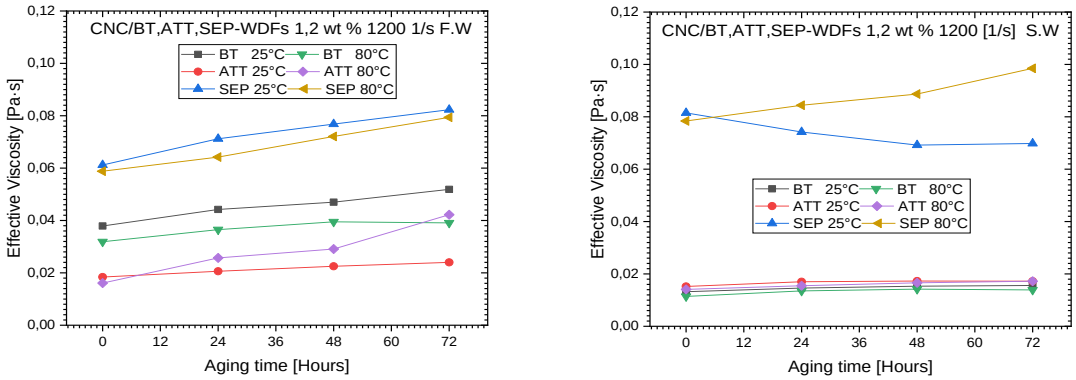

Figure 88. Effective viscosity as a function of aging time at different temperatures for CNC/BT, ATT, SEP-WDFs (SW).

aging time. However, the yield stress in figure 86(b) increased with an increase in temperature for all the freshwater mud systems. For the same range of aging time, an increase in temperature cause

the yield stress to increase through all the freshwater mud system. At the same temperature, as aging time increases, the yield stress is generally speaking increased for CNC/BT- ATT-WDFs (FW) and slightly decreased for CNC/SEP-WDFs (FW).

In contrast, in figure 87 and table 22, the consistency index for CNC/BT-WDFs (SW) is slightly increased with an increase in temperature for each particular 24 hours including zero-hours but except at 72 hours in which a decrease is shown. For CNC/ATT-WDFs (SW), the consistency index is started with the same value for both of the temperatures (25°C and 80°C) at zero hours then decreased with an increase in temperature for each particular 24 hours. For CNC/SEP-WDFs (SW), the consistency index extremely decreases with an increase in temperature. For the same range of aging time, a temperature rise causes the consistency index to reduce through all the seawater mud systems. At the same temperature, as aging time increases, the consistency index is slightly increased at both temperature (25°C and 80°C) for CNC/BT-WDFs (SW), slightly increased at both temperature (25°C and 80°C) for CNC/ATT-WDFs (SW) and increased at 25°C and increased then decreased at 80°C for CNC/SEP-WDFs (SW).

Figure 88 showed the variation of the effective viscosity with aging time at different temperatures for CNC/BT, ATT, SEP-WDFs (FW,) and CNC/BT, ATT, SEP-WDFs (SW). It is observed in figure 88(a) that the effective viscosity slightly increased with an increase in aging time at any temperature for CNC/BT, ATT, and SEP-WDFs (FW) at the high shear rate (1200 s-1) at a point it could be taken as maintained stable. However, a temperature rise showed a decrease in the effective viscosity only for CNC/BT, SEP-WDFs (FW) and it increases for CNC/ATT-WDFs (FW). This demonstrates the continuous flow of the drilling fluids at a high shear rate with good maintenance of its effective viscosity.

Figure 88(b) shows the plot of the effective viscosity as a function of aging time at different temperatures for CNC/BT, ATT, and SEP-WDFs (SW). It is observed that the effective viscosity of CNC/BT-WDFs (SW) decreased significantly in seawater but was slightly maintained at a lower level due to the action of carboxylated CNCs that improves its resistance to flow. The effective viscosity was drastically affected in seawater leading to flocculation and aggregation of BT clay particles. However, the effective viscosity of CNC/ATT, SEP-WDFs (SW) was maintained in a plateau over a broad range of aging time, and for CNC/SEP-WDFs (SW), it is decreased at low temperature and increased at high temperature over a broad range of aging time

It is also observed through table 22 that CNC/BT-WDFs (FW) were mostly affected in the presence of seawater than in freshwater as the consistency index is widely reduced to very low values in both temperatures. This means the mud system is widely affected in the presence of salt contaminant confirming the reduction of the rheological and filtration properties. The effect of salt upon CNC/BT-WDFs is widely affecting its resistance to flow leading to BT clay flocculation and aggregation. For CNC/ATT-WDFs as shown in table 22, an improvement in rheological property was observed in seawater even under high temperature as the yield stress and consistency index values increased demonstrating a high capacity to carry the drilling cuttings, good pumping of the drilling fluid as consistency index and effective viscosity are maintained with appreciable values. In the case of CNC/SEP-WDFs, it is observed that yield stress, consistency index and effective viscosity were well maintained. A temperature rise improves the carrying capacity of cuttings and a well-pumping capacity of the drilling fluid in seawater.

The behavior of the different rheological properties of the mud system under high temperature resulting in thermal degradation of the solid, polymers, and other components of the mud system

including molecules expansion which lowered the resistance of the fluid to flow (yield point) and, hence, its viscosity (consistency index), effective viscosity, and gel strength was not effective due to the action of carboxylated-CNCs as nanoparticles impacting upon different water-based drilling fluids involved in this project (CNC/BT, ATT, SEP-WDFs).

Table 22. Yield point, consistency index and effective viscosity as a function of aging time for different temperatures.

Temperature	Aging time	Yield Point (YP)	Consistency index (K)	Yield Point (YP)	Consistency index (K)	Yield Point (YP)	Consistency index (K)
	[Hours]	[Pa]	[Pa·s]	[Pa]	[Pa·s]	[Pa]	[Pa·s]
		CNC-BT-WDFs 1.2wt% F.W.	CNC-BT-WDFs 1.2wt% F.W.	CNC-ATT-WDFs 2.0wt% F.W.	CNC-ATT-WDFs 2.0wt% F.W.	CNC-SEP-WDFs 1.2wt% F.W.	CNC-SEP-WDFs 1.2wt% F.W.
25°C	0	3,26239	6,82763	1,02542	2,59874	8,20216	8,89858
	24	2,616	6,23382	4,96536	0,81131	5,9003	23,65335
	48	1,74854	9,83688	7,02608	0,56396	5,69734	25,09186
	72	8,53336	5,38162	6,06176	1,42212	6,00949	26,91946
80°C	0	23,12145	0,67404	11,09718	0,01442	16,65198	5,54584
	24	16,10176	3,01758	16,60854	0,00137	9,8615	13,63431
	48	17,34374	3,73847	30,36864	0,01719	7,53799	21,45007
	72	25,69103	1,2006	36,29723	2,52705E-6	14,71954	14,98593
		CNC-BT-WDFs 1.2wt% S.W.	CNC-BT-WDFs 1.2wt% S.W.	CNC-ATT-WDFs 1.2wt% S.W.	CNC-ATT-WDFs 1.2wt% S.W.	CNC-SEP-WDFs 1.2wt% S.W.	CNC-SEP-WDFs 1.2wt% S.W.
25°C	0	4,72034	5,40077E-5	4,66121	0,09033	5,995	19,93701
	24	4,72272	0,00646	1,69732	2,45501	6,26725	23,28708
	48	4,71759	0,0247	0,98115	2,10802	8,63964	22,37736
	72	0,96705	1,08011	1,69732	2,81128	7,07267	22,20542
80°C	0	4,8302	4,35669E-6	6,10435	0,00294	13,70017	8,30555
	24	4,43881	0,00662	5,54324	0,50039	17,53423	6,25098
	48	4,27235	0,03714	10,32767	0,07522	7,61875	14,87588
	72	6,73258	0,00339	5,51418	0,95377	23,78337	4,43236
		Effective viscosity [Pa·s] at 1200 1/s					
		CNC-BT-WDFs 1.2wt% F.W.	CNC-ATT-WDFs 2.0wt% F.W.	CNC-SEP-WDFs 1.2wt% F.W.	CNC-BT-WDFs 1.2wt% S.W.	CNC-ATT-WDFs 1.2wt% S.W.	CNC-SEP-WDFs 1.2wt% S.W.
25°C	0	0,0379	0,0184	0,0612	0,0132	0,0152	0,0815
	24	0,0442	0,0206	0,0712	0,0146	0,017	0,0742
	48	0,047	0,0225	0,0768	0,0153	0,0173	0,0692
	72	0,0519	0,024	0,0823	0,0156	0,0172	0,0698
		CNC-BT-WDFs 1.2wt% F.W.	CNC-ATT-WDFs 2.0wt% F.W.	CNC-SEP-WDFs 1.2wt% F.W.	CNC-BT-WDFs 1.2wt% S.W.	CNC-ATT-WDFs 1.2wt% S.W.	CNC-SEP-WDFs 1.2wt% S.W.
80°C	0	0,0319	0,0161	0,0588	0,0114	0,0141	0,0784
	24	0,0365	0,0257	0,0642	0,0135	0,0155	0,0844
	48	0,0395	0,0291	0,0721	0,0142	0,0166	0,0887
	72	0,0391	0,0422	0,0794	0,0139	0,0172	0,0985

As it can be seen on figures 86-88 and in table 22, the consistency index and effective viscosity of CNC/BT, ATT, SEP-WDFs (FW or SW) are different even though equal amount of clay materials and CNCs particles were added in equal amount of water and mixed for the same period of time. The consistency index and effective viscosity of fresh (zero hour) CNC/BT-WDFs compared to fresh CNC/ATT, SEP-WDFs in freshwater at 25°C were found to be 6.82763/0.0379, 2.59874/0.0184 and 8.89858/0.0612 Pa.s respectively and the one in seawater at 25°C were found to be 5.40077E-5/0.0132, 0.09033/0.0152 and 19.93701/0.0815 Pa.s respectively. By comparing the effect of consistency index and effective viscosity at 25°C even though at 80°C, this is clearly shown that in fresh water mud a lesser amount of CNCs particles in SEP-WDFs will be needed to obtain a particular viscosity as compared to CNCs particles in BT-WDFs than followed by the one in ATT-WDFs; in seawater by contrast, a lesser amount of CNCs in SEP-WDFs will be needed to produce the same effect as compare to the one in ATT-WDFs followed by the one in BT-WDFs at both of the temperatures. Those comparisons are applied over the broad range of aging time. The yield stress of CNC/BT-WDFs (FW) was found to be 2.616/4.43881 Pa after 24 hours at 25°C and 80°C respectively while that of CNC/ATT-WDFs (FW) was 4.96536/5.54324 Pa and of

CNC/SEP-WDFs (FW) was 5.9003/17.53423 Pa. This means that CNC/SEP-WDFs (FW) offers a better hole cleaning capacity than CNC/ATT-WDFs (FW) followed by CNC/BT-WDFs (FW). By the way, the yield stress of CNC/BT-WDFs (SW) was found to be 0,0442/0,0365 Pa after 24 hours at 25°C and 80°C respectively while that of CNC/ATT-WDFs (SW) was 0,0712/0,0642 Pa

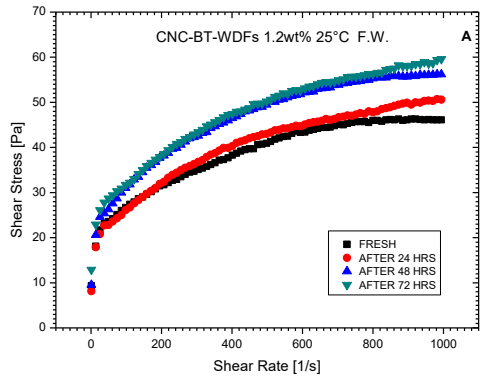

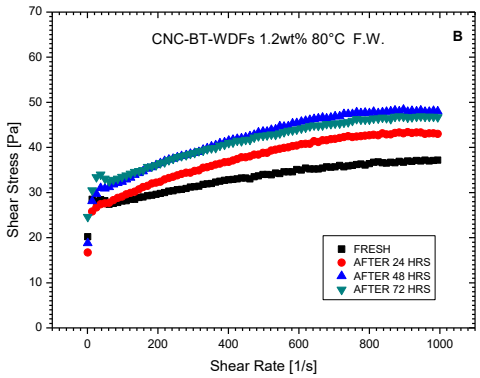

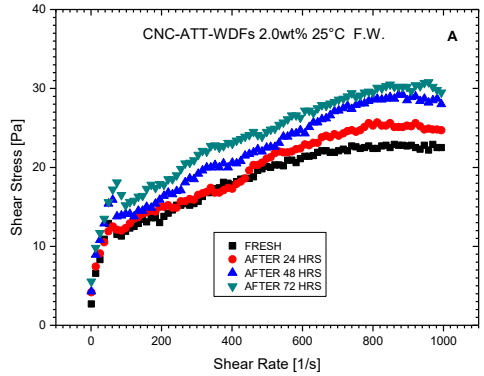

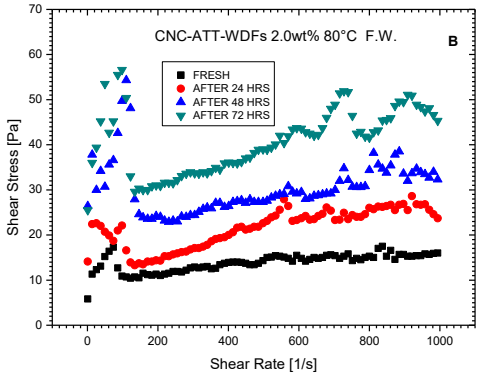

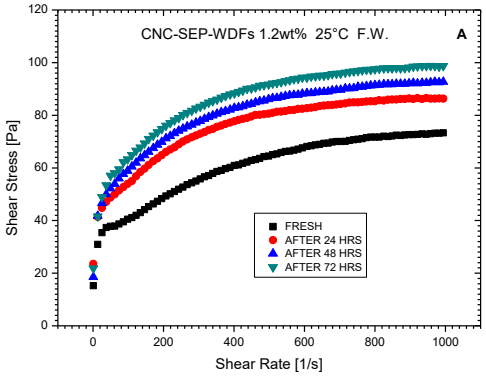

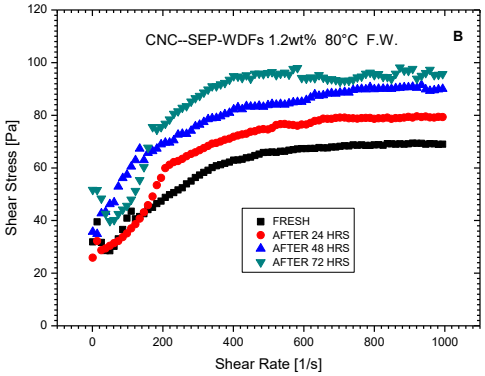

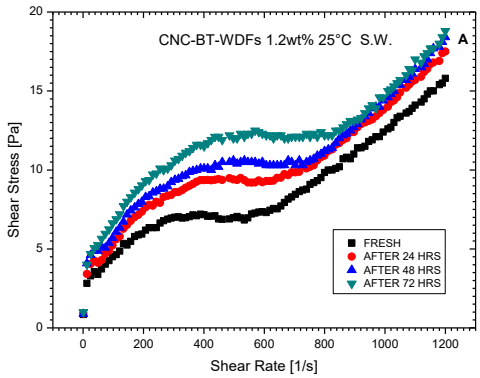

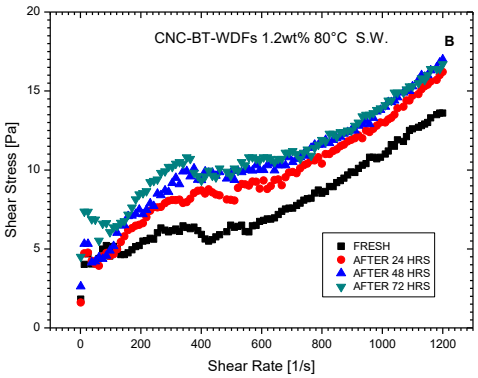

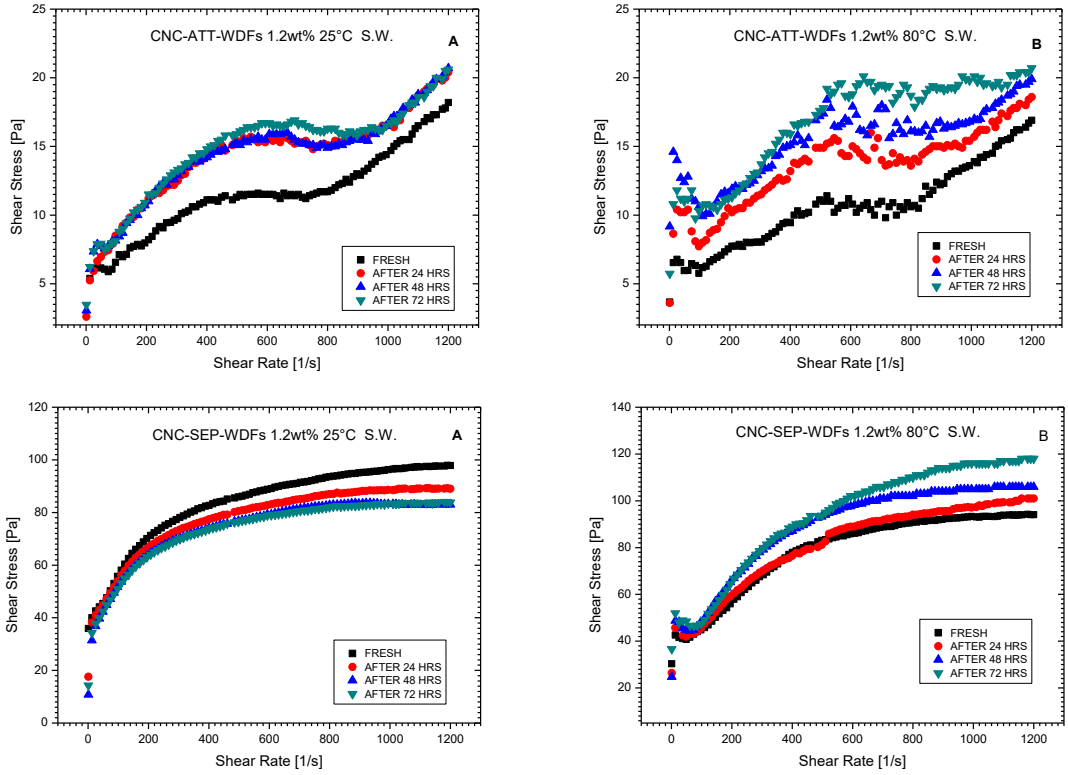

Figure 89. The plot of shear stress as a function of shear rate at different aging time at 25°C and 80°C for CNC/BT, ATT, SEP-WDFs in fresh water and seawater.

and of CNC/SEP-WDFs (SW) was 0,017/0,0155 Pa. This means that CNC/ATT-WDFs (SW) offers a better hole cleaning capacity than CNC/BT-WDFs (SW) followed by CNC/SEP-WDFs (SW). Therefore, this shows that the yield stress of the all drilling fluids was affected by salt, temperature and aging time.

Furthermore, figure 89 displayed the plot of shear stress as a function of shear rate at different aging times. It is observed that shear stress increased with an increase in aging time. This means the shear stress decreases with the aging time in freshwater. The same effect is observed in seawater but the action of the salt upon the drilling fluids was shown up as CNC/BT-WDFs (SW) at low and high temperature could not display proper shear thinning behavior as shown for CNC/BT, ATT, SEP-WDFs in freshwater. It has been observed that the drilling fluid properties are affected by the variation of the temperature and aging time. As seen in this project, the impact of temperature and aging time upon the yield stress, viscosity, and shear stress so far on the gel strength. Therefore, by the fact of maintaining at the optimum values these rheological properties many drilling issues could be avoided. Thus, the drilling fluid rheology remained very important as the viscosity of the drilling fluid is practically affecting the rate of penetration during the drilling operation. Keeping proper gel strength is advantageous for holding cuttings in suspension, and for a high penetration rate relatively low gel strength is needed that will cause less pressure drop in the borehole. The cutting slip velocity gives a better correlation with yield stress than any other rheological parameters. Furthermore, the incorporation of the cellulose nanocrystals in different clay-based fluids maintained a better viscosity of the mud system that means CNCs reduced the

viscosity at the optimum value leading to the reduction of the amount of energy needed for rotating drill stem and drill bit.

7.3. RATE OF PENETRATION

It is important to know that in drilling activities, the most indispensable drilling fluid feature remains the removal and transport of drilling cuttings to the surface whatever its ability for accommodating weighting materials is of paramount importance as this contributes to the stabilization of the wellbore (Adam 1998). The more the mud weight is light with low solids content, the more ROP will be fast during the drilling operation as all other variables are kept constant (Gribble & Hall 2000).

The focus in this project is based on the preparation of the lighter drilling mud weight through the incorporation of the CNC nanoparticles into clay-based water drilling fluids to enhance the fast penetration rate during the rotary drilling through different rock samples selected based on their properties and their appearance in the petroleum wells (e.g., breccia, shale, dolomite and sandstone rocks). Three samples of drilling fluids were selected in the course of this project (e.g., CNC/BT-WDFs (FW/SW) at 1.2 wt. % CNC concentrations respectively; CNC/ATT-WDFs (FW/SW) at 2.0 wt. % and 1.2 wt. % CNC concentrations respectively; and CNC/SEP-WDFs FW/SW at 1.2 wt. % CNC concentration respectively based on their rheological and filtration properties.

Table 23. Variation of the rate of penetration of CNC/BT-WDFs (SW) versus of pressure (stress) of different rock samples in CNC/BT, ATT, SEP-WDFs (FW).

STRESS	**ROP(BT)**				**ROP(ATT)**				**ROP(SEP)**			
MPa	mm/min											
	BRECCIA ROCK/ CNC-BT-WDFs (FW)1,2 wt % CNCs				**BRECCIA ROCK/ CNC-ATT-WDFs (FW) 2,0 wt % CNCs**				**BRECCIA ROCK/ CNC-SEP-WDFs (FW) 1,2 wt % CNCs**			
	RUN1	**RUN2**	**RUN3**	**MEAN**	**RUN1**	**RUN2**	**RUN3**	**MEAN**	**RUN1**	**RUN2**	**RUN3**	**MEAN**
1,7348	11,85	11,11	11,78	11,58	11,91	12,44	11,91	12,09	5,38	3,62	3,72	4,24
2,0812	9,21	9,14	11,64	9,997	14,03	14,02	10,48	12,84	13,89	11,85	4,29	10,01
2,4287	10,37	11,14	3,52	10,76	12,47	12,84	14,21	13,17	15,8	14,59	8,82	13,07
2,7757	10,32	10,47	10,38	10,39	8,97	10,67	12,07	10,57	14,61	10,82	13,82	13,08
3,1226	13,43	14,56	12,09	13,36	13,65	11,55	16,33	13,84	8,12	9,3	17,6	11,67
	SHALE ROCK/ CNC-BT-WDFs (FW) 1,2 wt % CNCs				**SHALE ROCK/ CNC-ATT-WDFs (FW) 2,0 wt % CNCs**				**SHALE ROCK/ CNC-SEP-WDFs (FW) 1,2 wt % CNCs**			
	RUN1	**RUN2**	**RUN3**	**MEAN**	**RUN1**	**RUN2**	**RUN3**	**MEAN**	**RUN1**	**RUN2**	**RUN3**	**MEAN**
1,7348	0,86	1,27	1,02	1,05	3,88	1,27	1,64	2,26	0,7	0,73	0,74	0,72
2,0812	1,05	1,19	0,13	1,12	1,15	1,17	1,3	1,21	1,75	0,91	0,75	1,14
2,4287	1,51	1,42	1,99	1,64	1,59	4,59	5,54	3,91	1	0,97	1,07	1,01
2,7757	1,52	1,17	1,77	1,49	2	6,13	1,11	3,08	1,22	1,17	1,77	1,39
3,1226	1,87	3,64	3,98	3,16	4,53	9,28	7,56	7,12	1,2	1,73	1,22	1,38
	DOLOMITE ROCK/ CNC-BT-WDFs (FW) 1,2 wt % CNCs				**DOLOMITE ROCK/ CNC-ATT-WDFs (FW) 2,0 wt % CNCs**				**DOLOMITE ROCK/ CNC-SEP-WDFs (FW) 1,2 wt % C NCs**			
	RUN1	**RUN2**	**RUN3**	**MEAN**	**RUN1**	**RUN2**	**RUN3**	**MEAN**	**RUN1**	**RUN2**	**RUN3**	**MEAN**
1,7348	0,34	0,39	0,59	0,444	0,47	0,39	0,15	0,37	0,35	0,43	0,29	0,36
2,0812	0,44	0,7	0,59	0,58	0,58	0,22	0,38	0,39	0,37	0,55	0,34	0,42
2,4287	0,48	0,87	0,43	0,59	0,15	0,47	0,14	0,47	0,5	0,65	1,13	0,76
2,7757	0,86	1,08	0,56	0,83	0,55	0,61	0,67	0,61	1,12	0,91	1,1	1,04
3,1226	0,68	0,7	0,61	0,66	1,03	0,61	0,38	0,82	2,04	1,43	1,54	1,67
	SANDSTONE ROCK/ CNC-BT-WDFs (FW) 1,2 wt % CNCs				**SANDSTONE ROCK/ CNC-ATT-WDFs (FW) 2,0 wt % CNCs**				**SANDSTONE ROCK/ CNC-SEP-WDFs (FW) 1,2 wt % CNCs**			
	RUN1	**RUN2**	**RUN3**	**MEAN**	**RUN1**	**RUN2**	**RUN3**	**MEAN**	**RUN1**	**RUN2**	**RUN3**	**MEAN**
1,7348	0,25	0,16	0,51	0,31	0,45	0,33	0,11	0,39	0,58	0,58	0,72	0,63
2,0812	1,58	1,19	1,45	1,41	0,46	0,46	0,42	0,45	1,02	1,05	1,06	1,04
2,4287	1,82	1,97	1,8	1,86	0,52	0,53	0,32	0,525	1,3	1,31	1,21	1,27
2,7757	1,79	1,8	2,24	1,94	0,65	0,53	0,53	0,59	1,25	1,33	1,2	1,29
3,1226	2,02	2,1	1,92	2,01	0,93	0,49	0,25	0,71	1,42	0,93	1,01	1,42

The experimental data are given in tables 23-24 that showed the variation of the rate of penetration as a function of pressure (stress) or weight on the bit of different rock samples with CNC/BT, ATT, SEP-WDFs in fresh-water and seawater.

In this experiment, the rotary drilling tests were performed in the workshop of our School of Chemical and Metallurgical Engineering using a drill press loaded with different weights from 5, 6, 7, 8, and 9 kg respectively with a concrete drill bit of 6 mm of diameter and a cylinder of 30 ml mounted on top of the rock sample for retaining 25 ml of the drilling fluid samples to ensure that the mud weight controls hydrostatic pressure (HP) at the bottom hole and prevents unwanted loss of the fluid by using a plastic cylinder to simulate the bottom hole behavior for the test as shown in figure 90. The rate of penetration was measured in mm per 1 min at RPM 885 for 5 different stress values (pressure or weight on the bit). All the experimental data were recorded in table 23-24 and the evaluation was done by using perform linear fitting analysis. Generally speaking, tables 23-24 showed that the lesser the ROP, the harder the rock sample and the lower the rock porosity property.

Table 24. Variation of the rate of penetration of CNC/BT-WDFs (SW) versus of pressure (stress) of different rock samples in CNC/BT, ATT, SEP-WDFs (SW).

STRESS	**ROP(BT)**				**ROP(ATT)**				**ROP(SEP)**			
MPa	mm/min											
	BRECCIA ROCK/ CNC-BT-WDFs (SW) 1,2 wt % CNCs				**BRECCIA ROCK/ CNC-ATT-WDFs (SW) 1,2 wt % CNCs**				**BRECCIA ROCK/ CNC-SEP-WDFs (SW) 1,2 wt % CNCs**			
	RUN1	**RUN2**	**RUN3**	**MEAN**	**RUN1**	**RUN2**	**RUN3**	**MEAN**	**RUN1**	**RUN2**	**RUN3**	**MEAN**
1,7348	9,31	7,66	0,54	5,83667	10,43	6,79	7,06	8,09333	8,09	9,07	2,52	6,56
2,0812	7,89	9,11	3,91	6,97	9,11	8,63	7,8	8,51333	8,96	8,48	9,06	8,83333
2,4287	10,39	8,46	9,45	9,43333	10,29	2,45	3,8	5,51333	10,35	10,35	9,05	9,91667
2,7757	3,58	9,81	11,38	8,25667	8,85	10,33	1,26	6,81333	10,9	2,88	10,51	8,09667
3,1226	11,12	9,31	5,72	8,71667	7,06	3,01	4,46	4,84333	11,71	11,01	12,14	11,62
	SHALE ROCK/ CNC-BT-WDFs (SW) 1,2 wt % CNCs				**SHALE ROCK/ CNC-ATT-WDFs (SW) 1,2 wt % CNCs**				**SHALE ROCK/ CNC-SEP-WDFs (SW) 1,2 wt % CNCs**			
	RUN1	**RUN2**	**RUN3**	**MEAN**	**RUN1**	**RUN2**	**RUN3**	**MEAN**	**RUN1**	**RUN2**	**RUN3**	**MEAN**
1,7348	0,28	0,19	0,21	0,22667	0,21	0,15	0,34	0,23333	0,32	0,31	0,31	0,31333
2,0812	0,24	0,22	0,27	0,24333	0,45	0,63	0,36	0,48	0,24	0,36	0,29	0,29667
2,4287	0,31	0,31	0,49	0,37	0,44	0,19	0,2	0,27667	0,69	0,6	0,33	0,54
2,7757	0,29	0,31	0,36	0,32	0,51	0,38	0,28	0,39	0,97	0,35	1,42	0,91333
3,1226	0,46	0,59	0,53	0,52667	0,37	0,34	0,58	0,43	1,02	1,05	1,06	1,04333
	DOLOMITE ROCK/ CNC-BT-WDFs (SW) 1,2 wt % CNCs				**DOLOMITE ROCK/ CNC-ATT-WDFs (SW) 1,2 wt % CNCs**				**DOLOMITE ROCK/ CNC-SEP-WDFs (SW) 1,2 wt % CNCs**			
	RUN1	**RUN2**	**RUN3**	**MEAN**	**RUN1**	**RUN2**	**RUN3**	**MEAN**	**RUN1**	**RUN2**	**RUN3**	**MEAN**
1,7348	0,14	0,17	0,27	0,19333	0,32	0,24	0,24	0,26667	0,35	0,14	0,16	0,21667
2,0812	0,48	0,42	0,42	0,44	0,19	0,25	0,22	0,22	0,2	0,42	0,14	0,25333
2,4287	0,34	0,51	0,27	0,37333	0,28	0,65	0,22	0,38333	0,15	0,14	0,35	0,21333
2,7757	0,21	0,36	0,36	0,31	0,32	0,53	0,45	0,43333	0,22	0,32	0,34	0,29333
3,1226	0,23	0,28	0,26	0,25667	0,45	0,28	0,47	0,4	0,52	0,4	0,39	0,43667
	SANDSTONE ROCK/ CNC-BT-WDFs (SW) 1,2 wt % CNCs				**SANDSTONE ROCK/ CNC-ATT-WDFs (SW) 1,2 wt % CNCs**				**SANDSTONE ROCK/ CNC-SEP-WDFs (SW) 1,2 wt % CNCs**			
	RUN1	**RUN2**	**RUN3**	**MEAN**	**RUN1**	**RUN2**	**RUN3**	**MEAN**	**RUN1**	**RUN2**	**RUN3**	**MEAN**
1,7348	0,35	0,33	0,33	0,33667	0,48	0,38	0,7	0,52	0,21	0,23	0,26	0,23333
2,0812	0,44	0,46	0,48	0,46	0,49	0,7	0,73	0,64	0,46	0,48	0,43	0,45667
2,4287	0,65	0,66	0,59	0,63333	0,76	0,71	0,6	0,69	0,43	0,37	0,26	0,35333
2,7757	0,48	0,47	0,33	0,42667	0,8	0,57	0,65	0,67333	0,6	0,75	1,04	0,79667
3,1226	0,32	0,49	0,39	0,4	0,91	0,85	0,61	0,79	0,73	1,12	1,04	0,96333

The results are shown in figures 91-92 demonstrating a linear relationship between the rate of penetration (ROP) and the stress or pressure.

Generally, these two figures 91-92 showed the dependence of the rate of penetration upon different weights on bit or stress changes. In the meantime, the effect of the mud weight of different drilling fluids is to be considered. Even though these mud weights or densities are constant for each particular drilling fluid but remain different as all packages of drilling fluids are to be considered in a such way that they are different from each other in terms of mud properties. Mud weight is defined as the density of drilling fluid (mass divided by volume), which is expressed in pounds per gallon (ppg or Ib/gal), pounds per cubic feet (lb/ft3), or kilograms per cubic meter (kg/m3) and it has been identified as one of the factors that impact the ROP (Akpabio et al 2015). The variation of the ROP into different rock samples depends on rock properties or formation characteristics and also on the drilling fluid's rheological and filtration properties. Different trends are given as the drilling operation was run under drill press operation carried on with different drilling fluid samples.

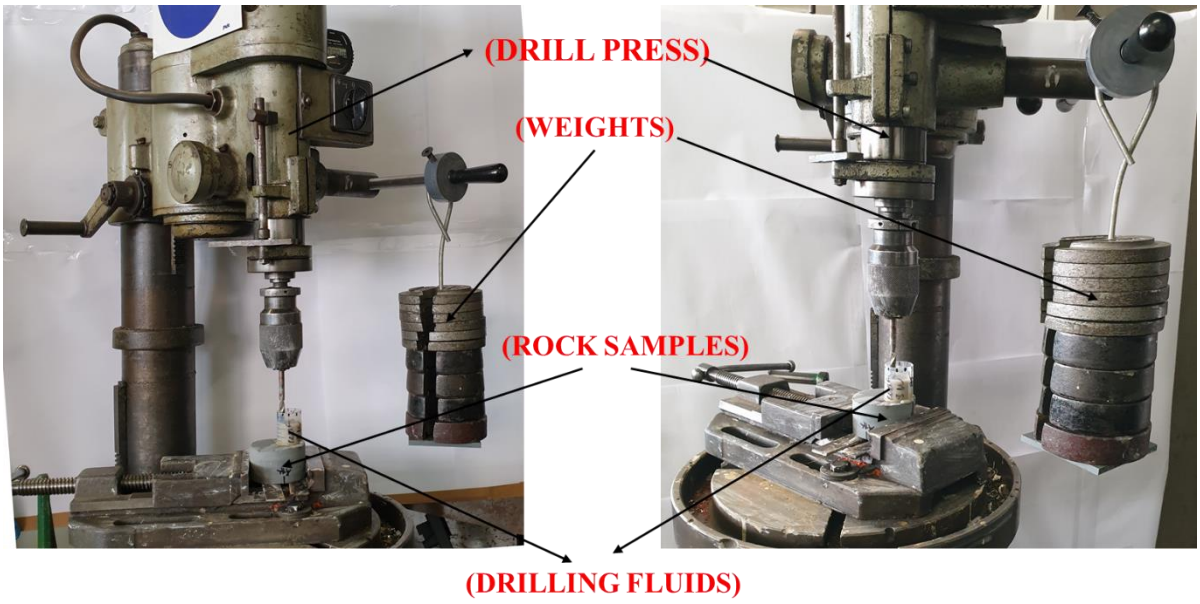

Figure 90. Drill press (RPM 885/ Bit diameter 6 mm, Workshop of Chemical Engineering/Wits University, 2019).

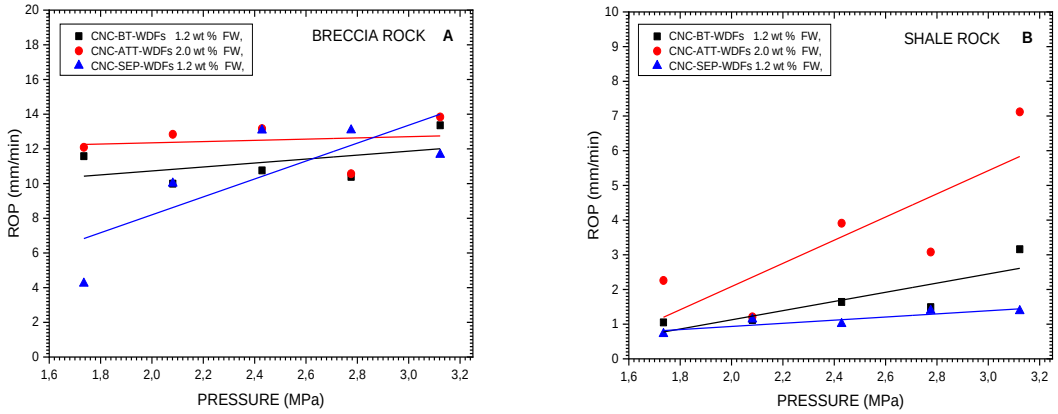

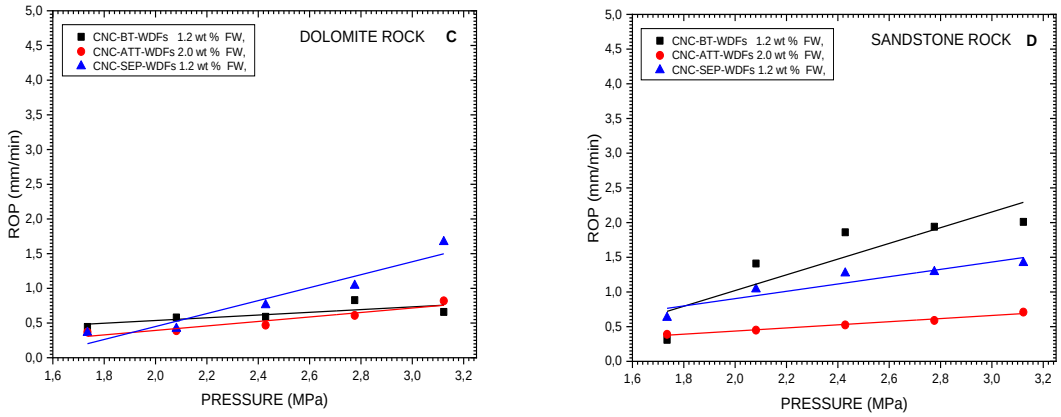

Figure 91. The plots of the rate of penetration as a function of pressure (stress) or weight on bit of different rock samples in CNC/BT, ATT, SEP-WDFs (FW).

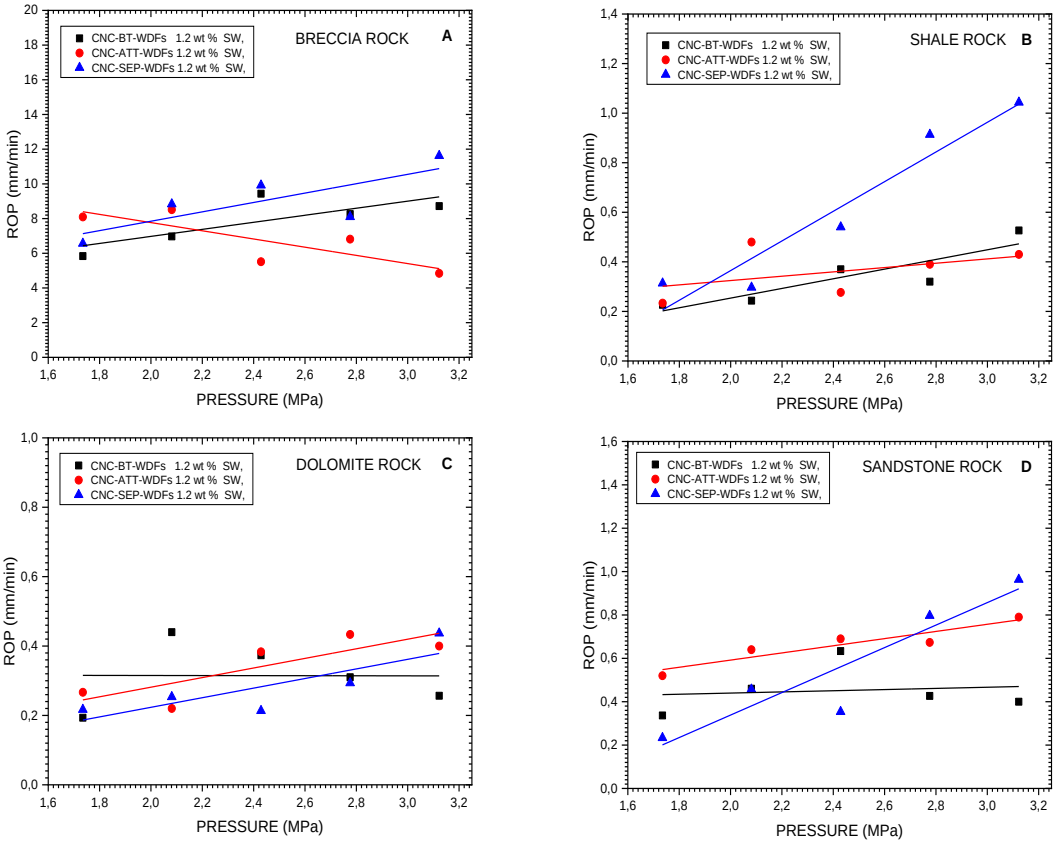

Figure 92. The plots of the rate of penetration as a function of pressure (stress) of different rock samples in CNC/BT, ATT, SEP-WDFs (SW).

For the drilling operation of Breccia rock sample in figure 91 plot A with

- CNC/BT-WDFs in freshwater showed a linear relationship between the ROP and the stress or the weight on the bit. There is no significant correlation between the ROP and the stress (pressure). For the rotary drilling, the ROP increases with increasing stress or pressure (σ). The equation of the line is:

Equation 18 $ROP = (1.13949 \pm 1.23859)\,\sigma + (8.45004 \pm 3.06883)$ $R^2 = 0.22005$ $R = 0.47$

- CNC/ATT-WDFs in freshwater showed a linear relationship between the ROP and the stress. There is no significant correlation between the ROP and the stress (pressure). For the rotary drilling, the ROP increases with increasing stress or pressure (σ). The equation of the line is:

Equation 19 $ROP = (0.35416 \pm 1.29968)\,\sigma + (11.64189 \pm 3.22019)$ $R^2 = 0.02415$ $R = 0.16$

- CNC/SEP-WDFs in freshwater showed a linear relationship between the ROP and the stress. There is no significant correlation between the ROP and the stress (pressure). For the rotary drilling, the ROP increases with increasing stress or pressure (σ). The equation of the line is:

Equation 20 $ROP = (5.1664 \pm 2.46105)\,\sigma + (-2.13312 \pm 6.0977)$ $R^2 = 0.59497$ $R = 0.77$

For the drilling operation of Shale rock sample in figure 91 plot B with

- CNC/BT-WDFs in freshwater showed a linear relationship between the ROP and the stress. There is a significant correlation between the ROP and the stress (pressure). For the rotary drilling, the ROP increases with increasing stress or pressure (σ). The equation of the line is:

Equation 21 $ROP = (1.32275 \pm 0.47962)\,\sigma + (-1.52044 \pm 1.18834)$ $R^2 = 0.71715$ $R = 0.85$

- CNC/ATT-WDFs in freshwater showed a linear relationship between the ROP and the stress. There is a significant correlation between the ROP and the stress (pressure). For the rotary drilling, the ROP increases with increasing stress (pressure). The equation of the line is:

Equation 22 $ROP = (3.34042 \pm 1.37127)\,\sigma + (-4.59654 \pm 3.39758)$ $R^2 = 0.66421$ $R = 0.82$

- CNC/SEP-WDFs in freshwater showed a linear relationship between the ROP and the stress. There is a significant correlation between the ROP and the stress (pressure). For the rotary drilling, the ROP increases with increasing stress or pressure (σ). The equation of the line is:

Equation 23 $ROP = (0.45236 \pm 0.13544)\,\sigma + (0.02939 \pm 0.33558)$ $R^2 = 0.78806$ $R = 0.89$

For the drilling operation of Dolomite rock sample in figure 91 plot C with

- CNC/BT-WDFs in freshwater showed a linear relationship between the ROP and the stress. No significant correlation between the ROP and the stress or pressure (σ) was found. For the rotary drilling, the ROP increases with increasing stress or pressure (σ). The equation of the line is:

Equation 24 $ROP = (0.19653 \pm 0.09509)\,\sigma + (0.14351 \pm 0.2356)$ $R^2 = 0.58744$ $R = 0.77$

- CNC/ATT-WDFs in freshwater showed a linear relationship between the ROP and the stress. A very strong correlation between the ROP and the stress (presure) was found. For the rotary drilling, the ROP increases with increasing stress or pressure (σ). The equation of the line is:

Equation 25 $ROP = (0.32277 \pm 0.06188)\,\sigma + (-0.25188 \pm 0.15331)$ $R^2 = 0.9007$ $R = 0.95$

- CNC/SEP-WDFs in freshwater showed a linear relationship between the ROP and the stress. A strong correlation between the ROP and the stress (presure) was found. For the rotary drilling, the ROP increases with increasing stress or pressure (σ). The equation of the line is:

Equation 26 $ROP = (0.93373 \pm 0.15936)\,\sigma + (-1.41766 \pm 0.39485)$ $R^2 = 0.91964$ $R = 0.96$

For the drilling operation of Sandstone rock sample in figure 91 plot D with

- CNC/BT-WDFs in freshwater showed a linear relationship between the ROP and the stress. There is a significant correlation between the ROP and the stress (presure). For the rotary drilling, the ROP increases with increasing stress or pressure (σ). The equation of the line is:

Equation 27 $ROP = (1.1324 \pm 0.35808)\,\sigma + (-1.24414 \pm 0.88721)$ $R^2 = 0.76925$ $R = 0.88$

- CNC/ATT-WDFs in freshwater showed a linear relationship between the ROP and the stress. A very strong correlation between the ROP and the stress (presure) was found. For the rotary drilling, the ROP increases with increasing stress or pressure (σ). The equation of the line is:

Equation 28 $ROP = (0.22478 \pm 0.01776)\,\sigma + (-0.0129 \pm 0.044)$ $R^2 = 0.98162$ $R = 0.991$

- CNC/SEP-WDFs in freshwater showed a linear relationship between the ROP and the stress. There is a strong correlation between the ROP and the stress (presure).For the rotary drilling, the ROP increases with increasing stress or pressure (σ). The equation of the line is:

Equation 29 $ROP = (0.52732 \pm 0.12063)\ \sigma + (-0.15065 \pm 0.29888)$ $R^2 = 0.86431$ $R = 0.93$

With ROP standing for the rate of penetration and σ standing for stress related to σ = F/A where F is the thrust or weight on the bit and A is the area of the bit diameter.

Therefore, it has been observed through figure 91 that: a) from plot A, the rotary drilling operated through Breccia rock sample with different mud systems attributes a fast ROP and great correlation between the ROP and the stress or weight on the bit to the CNC/SEP-WDFs (FW) at 1.2 wt. % of CNC concentration; b) from plot B with Shale rock sample, the fast ROP is attributed to CNC/ATT-WDFs (FW) at 2.0 wt. % CNC concentration and great correlation to CNC/SEP-WDFs (FW)) at 1.2 wt. % of CNC concentration; c) from plot C with Dolomite rock sample, the fast ROP and great correlation between the ROP and the stress or weight on the bit are attributed to the CNC/SEP-WDFs (FW) at 1.2 wt. % of CNC concentration; and from plot D with Sandstone rock sample, the fast ROP is attributed to CNC/BT-WDFs (FW) at 1.2 wt. % CNC concentration and great correlation to CNC/ATT-WDFs (FW)) at 2.0 wt. % of CNC concentration.

For the drilling operation of Breccia rock sample in figure 92 plot A with

- CNC/BT-WDFs in seawater showed a linear relationship between the ROP and the stress or weight on the bit. There is no significant correlation between the ROP and the stress (presure). For the rotary drilling, the ROP increases with increasing stress (pressure). The equation of the line is:

Equation 30 $ROP = (2.03075 \pm 0.95363)\ \sigma + (2.9108 \pm 2.36279)$ $R^2 = 0.60184$ $R = 0.76$

- CNC/ATT-WDFs in seawater showed a linear relationship between the ROP and the stress. There is no significant correlation between the ROP and the stress (presure). For the rotary drilling, the ROP decreases with increasing stress (pressure). The equation of the line is:

Equation 31 $ROP = (-2.36344 \pm 0.96388)\ \sigma + (12.49517 \pm 2.3882)$ $R^2 = 0.66712$ $R = 0.82$

- CNC/SEP-WDFs in seawater showed a linear relationship between the ROP and the stress. There is no significant correlation between the ROP and the stress (presure). For the rotary drilling, the ROP increases with increasing stress (pressure). The equation of the line is:

Equation 32 $ROP = (2.70363 \pm 1.25613)\ \sigma + (2.43931 \pm 3.1123)$ $R^2 = 0.60695$ $R = 0.78$

For the drilling operation of Shale rock sample in figure 92 plot B with

- CNC/BT-WDFs in seawater showed a linear relationship between the ROP and the stress. There is a significant correlation between the ROP and the stress (presure).v For the rotary drilling, the ROP increases with increasing stress (pressure). The equation of the line is:

Equation 33 $ROP = (0.19501 \pm 0.05884)\ \sigma + (-0.13626 \pm 0.14578)$ $R^2 = 0.78548$ $R = 0.89$

- CNC/ATT-WDFs in seawater showed a linear relationship between the ROP and the stress. There is no significant correlation between the ROP and the stress (presure). For the rotary drilling, the ROP increases with increasing stress (pressure). The equation of the line is:

Equation 34 $ROP = (0.08735 \pm 0.09699)\ \sigma + (0.14987 \pm 0.24031)$ $R^2 = 0.21281$ $R = 0.46$

- CNC/SEP-WDFs in seawater showed a linear relationship between the ROP and the stress. There is a strong correlation between the ROP and the stress (presure).For the rotary drilling, the ROP increases with increasing stress (pressure). The equation of the line is:

Equation 35 $ROP = (0.5985 \pm 0.10377)\ \sigma + (-0.83219 \pm 0.25711)$ $R^2 = 0.91728$ $R = 0.96$

For the drilling operation of Dolomite rock sample in figure 92 plot C with

- CNC/BT-WDFs in seawater showed a linear relationship between the ROP and the stress. No significant correlation between the ROP and the stress (presure) was found. For the rotary drilling, the ROP decreases with increasing stress (pressure). The equation of the line is:

Equation 36 $ROP = (-0.00102 \pm 0.10155)\ \sigma + (0.31714 \pm 0.25162)$ $R^2 = 0.33329$ $R = 0.57$

- CNC/ATT-WDFs in seawater showed a linear relationship between the ROP and the stress. No significant correlation between the ROP and the stress (presure) was found. For the rotary drilling, the ROP increases with increasing stress (pressure). The equation of the line is:

Equation 37 $ROP = (0.13836 \pm 0.05496)\ \sigma + (0.00465 \pm 0.13618)$ $R^2 = 0.6787$ $R = 0.82$

- CNC/SEP-WDFs in seawater showed a linear relationship between the ROP and the stress. . No significant correlation between the ROP and the stress (presure) was found. For the rotary drilling, the ROP increases with increasing stress (pressure). The equation of the line is:

Equation 38 $ROP = (0.13831 \pm 0.05472)\ \sigma + (-0.05324 \pm 0.13558)$ $R^2 = 0.68048$ $R = 0.82$

For the drilling operation of Sandstone rock sample in figure 92 plot D with

- CNC/BT-WDFs in seawater showed a linear relationship between the ROP and the stress. There is no significant correlation between the ROP and the stress (presure). For the rotary drilling, the ROP increases with increasing stress (pressure). The equation of the line is:

Equation 39 $ROP = (0.02689 \pm 0.11613)\ \sigma + (0.38604 \pm 0.28774)$ $R^2 = 0.30993$ $R = 0.56$

- CNC/ATT-WDFs in seawater showed a linear relationship between the ROP and the stress. A strong correlation between the ROP and the stress (presure) was found. For the rotary drilling, the ROP increases with increasing stress (pressure). The equation of the line is:

Equation 40 $ROP = (0.1652 \pm 0.03749)\,\sigma + (0.26145 \pm 0.0929)$ $R^2 = 0.86616$ $R = 0.93$

- CNC/SEP-WDFs in seawater showed a linear relationship between the ROP and the stress. There is a strong correlation between the ROP and the stress (presure).For the rotary drilling, the ROP increases with increasing stress (pressure). The equation of the line is:

Equation 41 $ROP = (0.51868 \pm 0.1232)\,\sigma + (-0.69901 \pm 0.30524)$ $R^2 = 0.85526$ $R = 0.93$

Therefore, it has been observed through figure 92 that: a) from plot A, the rotary drilling operated through Breccia rock sample with different mud systems attributes a fast ROP and great correlation between the ROP and the stress or weight on the bit to the CNC/SEP-WDFs (FW) at 1.2 wt. % of CNC concentration; b) from plot B with Shale rock sample, the rotary drilling operated with different mud systems attributes a fast ROP and great correlation between the ROP and the stress or weight on the bit to the CNC/SEP-WDFs (SW) at 1.2 wt. % of CNC concentration; c) from plot C with Dolomite rock sample, the fast ROP is attributed to CNC/ATT-WDFs (SW) at 2.0 wt. % CNC concentration and great correlation to CNC/SEP-WDFs (FW)) at 1.2 wt. % of CNC concentration; and from plot D with Sandstone rock sample, the fast ROP is attributed to CNC/SEP-WDFs (SW) at 1.2 wt. % CNC concentration and great correlation to CNC/ATT-WDFs (SW)) at 2.0 wt. % of CNC concentration.

On the other hand, it is observed that at the higher stress or weight on the bit, mostly there are CNC/SEP-WDFs that come with the higher ROP as shown in plots A and C for freshwater figure 91 and plots A, B, and D for seawater in figure 92.

Besides, it is observed from figure 91 that the lowest rate of penetration (ROP) values are given by the rotary drilling of the Dolomite rock sample with 1.2, 2.0, and 1.2 wt. % of CNCs in BT, ATT, SEP-WDFs (FW) followed by Sandstone rock, Shale rock, and Breccia rock samples. The same observation is made by the rotary drilling of those rock samples with 1.2 wt. % of CNCs in BT, ATT, SEP-WDFs (SW) in figure 92. The resistance in drilling operation could be attributed to the hardness of the rock samples thereby considered as part of the formation. Therefore, the lower the rate of penetration (ROP), the harder the formation. Hence, it could be concluded that the order in the hardness of the formation is observed in this project as follow: The hardness order by drilling with 1.2, 2.0, and 1.2 wt. % of CNCs in BT, ATT, SEP-WDFs (FW), and 1.2 wt. % of CNCs in BT, ATT, SEP-WDFs (SW) is given in this way Dolomite rock followed by Sandstone rock, Shale rock, and Breccia rock samples respectively

7.4. CONCLUSIONS

The effect of CNC concentrations, temperature, and pressure on the rheological and filtration properties of CNC/BT, ATT, SEP-WDFs was investigated in freshwater and seawater. Herschel-Bulkley's model as a statistical modeling approach was used for a better understanding of the rheological behaviors. The penetration rate onto different rock samples using CNC/BT, ATT, SEP-WDFs was also investigated in freshwater and seawater. The aging and temperature effects of CNC/BT, ATT, SEP-WDFs were investigated in freshwater and seawater as well. Some significant results observed during the study of this project are:

- CNC concentration had a significant effect on the improvement of the filtration properties as the API fluid loss of CNC/BT-WDFs (FW) at 80°C decreased until 12 ml/30 min compared with the API standard (15 mL/30 min) as the concentration of CNCs increased. A positive effect was observed with CNC/ATT-WDFs (FW) at 80°C as the decrease in CNC concentration decreased the API fluid loss from 16.2 mL/30 min at 1.2 wt. % of CNCs to 13.6 ml/30 min at 1.0 wt. % of CNCs.
- CNC concentration had a significant effect on the improvement of the filtration properties as well at low temperatures. As it was observed, an API fluid loss of 11.63 mL/30 min for CNC/BT-WDFs (FW) at 30°C; an API fluid loss of 14.4 ml/30 min for CNC/ATT-WDFs (FW) at 20°C; and an API fluid loss of 13.4 ml/30 min for CNC/SEP-WDFs (FW) at 30°C.
- The salinity effect had significantly improved the filtration properties of CNC/BT, ATT, SEP-WDFs (SW) at low temperature (30°C). As it was observed during the experiment: the API fluid loss of 13.9, 14, and 13 ml/30 min for CNC/BT-WDFs (SW), CNC/ATT-WDFs (SW), and CNC/SEP-WDFs (SW) respectively lower than the API standard (15 ml/30 min). This effect of salinity was detrimental for the filtration properties as the fluid loss was slightly above the API standard value (15 ml/30 min) at high temperatures (80°C). As it was observed during the experiment: the API fluid loss of 16.7, 16.8, and 16.1 ml/30 min for CNC/BT-WDFs (SW), CNC/ATT-WDFs (SW), and CNC/SEP-WDFs (SW) respectively higher than the API standard (15 ml/30 min). As a result, this will directly affect the cost of the well. Therefore, this could be mitigated by the incorporation of the filtration control agent like polyanionic cellulose (PAC) to reduce the fluid loss during the filtration process.
- Temperature effect on filtration properties affected drastically both the CNC/ATT, SEP-WDFs (FW) and CNC/BT, ATT, SEP-WDFs (SW), except CNC/BT-WDFs (FW). Especially, at 80°C, with the API fluid loss of 16.2 and 17.2 ml/30 min for CNC/ATT-WDFs (FW) and CNC/SEP-WDFs (FW) respectively; and 16.7, 16.8 and 16.1 mL/30 min for CNC/BT-WDFs (SW) CNC/ATT-WDFs (SW) and CNC/SEP-WDFs (SW) respectively higher than the API standard (15 ml/30 min), except 12 ml/30 min for CNC/BT-WDFs (FW) at 80°C.
- The variation of the consistency index (K), yield stress (y_o), and effective viscosity at different temperatures under aging conditions were investigated in this project. It is observed that:
    a) The flow consistency index (K) of CNC/BT, ATT, SEP-WDFs (FW) under aging conditions decreased with increasing temperature from 20 to 80°C. As their flow curves keep exhibiting a shear thinning, the flow consistency index leads to a good pumping capacity.

b) The yield stress (y_o) of CNC/BT, ATT, SEP-WDFs (FW), and CNC/ATT, SEP-WDFs (SW) under aging conditions increased with increasing temperature from 20 to 80°C. This results in a great carrying capacity of the cuttings, except for CNC/BT-WDFs (SW).
c) The flow consistency index (K) of CNC/BT-WDFs (SW) under aging conditions present a very poor K value that slightly increased with increasing temperature from 20 to 80°C. It does not show a shear-thinning behavior due to the flocculation and aggregation of the BT platelets in the presence of the salt contents.
d) The flow consistency index (K) of CNC/ATT-WDFs (SW) under aging conditions depicted a significant value that decreased with increasing temperature from 20 to 80°C. It exhibited nearly linear shear-thinning curves due to the enhanced surface interaction between CNCs, ATT, and water molecules.
e) The flow consistency index (K) of CNC/SEP-WDFs (SW) under aging conditions decreased with increasing temperature from 20 to 80°C. This leads to the shear thinning behavior and good pumping capacity of the drilling fluid as K was maintained with appreciable values.
f) The effective viscosity of CNC/BT, ATT, SEP-WDFs (FW) slightly increased with increasing aging time at any temperature (20 or 80°C) at a high shear rate. This allowed a good pumping capacity of the drilling fluid and the carrying capacity of cuttings at a low shear rate.
g) The effective viscosity under the aging condition of the CNC/BT-WDFs (SW) decreased significantly but was slightly maintained at a lower value. This decrease of the effective viscosity was due to the flocculation and aggregation of BT platelets and was detrimental to the pumping capacity of the CNC/BT-WDFs (SW).
h) The effective viscosity under the aging condition of the CNC/ATT-WDFs (SW) was maintained in a plateau with a significant value as the temperature was increased from 20 to 80°C leading to a good pumping capacity of the drilling fluid.
i) The effective viscosity under the aging condition of the CNC/SEP-WDFs (SW) was decreased at low temperature (20°C) then increased at high temperature (80°C) resulting in a good pumping capacity of the drilling fluid.

- The ROP onto different rock samples using CNC/BT, AT, SEP-WDFs was investigated in freshwater and seawater.

  It was observed that the drilling operation conducted with freshwater on:
  a) Breccia rock sample showed that 1.2 wt. % of CNCs into CNC/SEP-WDFs gave a fast ROP with a slope value of 5.1664 ± 2.46105.
  b) Shale rock sample showed that 2.0 wt. % of CNCs into CNC/ATT-WDFs gave a fast ROP with a slope value of 3.34042 ± 1.37127.
  c) Dolomite rock sample showed that 1.2 wt. % of CNCs into CNC/SEP-WDFs gave a fast ROP with a slope value of 0.93373 ± 0.15936.
  d) Sandstone rock sample showed that 1.2 wt. % of CNCs into CNC/BT-WDFs gave a fast ROP with a slope value of 1.1324 ± 0.35808.

  It was observed that the drilling operation conducted with seawater on:
  a) Breccia rock sample showed that 1.2 wt. % of CNCs into CNC/SEP-WDFs gave a fast ROP with a slope value of 2.7036 ± 1.25613.

b) Shale rock sample showed that 1.2 wt. % of CNCs into CNC/SEP-WDFs gave a fast ROP with a slope value of 0.5985 ± 0.10377.
c) Dolomite rock sample showed that 1.2 wt. % of CNCs into CNC/ATT-WDFs gave a fast ROP with a slope value of 0.13836 ± 0.05496.
d) Sandstone rock sample showed that 1.2 wt. % of CNCs into CNC/SEP-WDFs gave a fast ROP with a slope value of 0.51868 ± 0.1232.

CHAPTER 8. CONCLUSIONS AND RECOMMENDATIONS.

8.1. CONCLUSIONS

The mud systems synthesized on the base of attapulgite and sepiolite clays using cellulose nanocrystals as an additive for water-based drilling fluids demonstrate a considerable improvement of the rheological and filtration properties and a great capacity to replace bentonite during drilling operation in HTHP conditions.

CNCs as additive showed a great contribution to yield stress, consistency index, and flow behavior index of attapulgite or sepiolite-based drilling fluid due to the electrostatic attractive interactions between carboxylated CNCs and attapulgite or sepiolite rods with immobilized water. These interactions favored the improvement of the yield stress of the attapulgite and/or sepiolite-based drilling mud as they were able to regulate the electrolyte level of the dispersions, impact on the surface charge of the clay mineral particles, broken up the aggregated configuration of attapulgite, and/or sepiolite gel. This improvement of the yield stress contributed to an increase in the viscosity then will allow the transport of the cutting at the surface of the wellbore at low velocity.

The CNC concentration, temperature, and pressure effects on rheological properties and CNC / BT-WDF filtration were investigated in freshwater and seawater. Herschel-Bulkley's model as a statistical modeling technique was used for a better understanding of the rheological behaviors. The penetration rate on different rock samples using CNC/BT-WDFs was investigated in freshwater and seawater. The aging times and temperature effect of CNC/BT-WDFs were investigated in freshwater and seawater. Significant results observed during the study of this project are:

- CNC concentrations have a considerable effect on the rheological and filtration properties of CNC/BT, ATT-WDFs (FW), and CNC/SEP-WDFs (SW) as a few increase in the CNC concentration produced considerable augmentation of the viscosity. While less effect was observed in CNC/SEP-WDFs (FW) and CNC/BT, ATT-WDFs (SW).
- Effect of salinity has considerably improved the rheological properties of CNC/ATT, SEP-WDFs (SW) more than CNC/BT-WDFs (SW) that was considerably affected. This effect of salinity has significantly affected the filtration properties of CNC/BT-WDFs (SW) 1.2 wt. % CNC concentration (16.7 mL/30 min). It has a considerable effect on the filtration properties of CNC/ATT-WDFs (SW) 1.2 wt. % CNC concentration as the fluid loss was slightly above the API standard value (15 ml/30 min) at high temperature (with 16.8 ml/30 min at 80°C) whereas, at low temperature, his filtration property was acceptable (with 14 ml/30 min at 80°C). Thus, it affected as well the filtration property of CNC/SEP-WDFs (SW) with 16.1 ml/30 min at 80°C that is above the API standard value (15 ml/30 min) whereas, at low temperature (30°C), his filtration property was acceptable (13 ml/30 min).
- The effect of temperature on the rheological and filtration properties affected more the CNC/BT-WDFs (FW) and CNC/ATT-WDFs (SW) than CNC/BT-WDFs (SW) and CNC/ATT-WDFs (FW). This temperature effect improved the rheological properties of CNC/ SEP-WDFs (SW) more than CNC/SEP-WDFs (FW) as it increased the cuttings carrying capacity.
- The hardness order during rotary drilling of different rock samples with 1.2, 2.0, and 1.2 wt. % of CNCs in BT, ATT, SEP-WDFs (FW) respectively, and 1.2 wt. % of CNCs in BT,

ATT, SEP-WDFs (SW) respectively, was given in this way: Dolomite rock harder than Sandstone rock followed by Shale rock and Breccia rock samples. This hardness order was due to the resistance of the rock samples during rotary drilling using different drilling fluids resulting in the degree of penetration depth of the drill bit into different rock samples.

8.2. RECOMMENDATIONS

For future rheological studies, the following is recommended:

- The use of a rheometer made of equipment incorporated with a device for controlling the temperature and pressure during the measurement to simulate the deep well downhole condition.
- Effects of pH of the drilling fluid on the drilling performance.
- Effects of CNC on the abrasion of the drilling equipment.

For future fluid loss studies, the following is recommended:

- The use of an appropriate API filter press incorporated with a proper jacket for controlling the temperature variation with a great range of pressure variation to simulate the downhole condition of the normal deep well.
- The incorporation of the filtration control agent like polyanionic cellulose (PAC) to reduce the fluid loss during filtration process into CNC/SEP-WDFs (FW) and CNC/BT, ATT, SEP- WDFs (SW) at high temperature.

For future rheological analysis, the following is recommended:

- The use of the performed Origin software is needed. This software should incorporate more three-parameter models (e.g., the Sisko model, Robertson-Stiff model, Mizhari-Berk model, and Heinz-Casson model) to compare rheological data.

REFERENCES

Abdo, J. and Haneef, M.D., 2013. Clay nanoparticles modified drilling fluids for drilling of deep hydrocarbon wells. *Applied Clay Science*, *86*, pp.76-82.Dias, F. T. G.; Souza, R. R.; Lucas, E. F., 2015, Influence of modified starches composition on their performance as fluid loss additives in invert-emulsion drilling fluids. Fuel, 140, 711−716.

Abdo, J., 2014. Nano-attapulgite for improved tribological properties of drilling fluids. *Surface and Interface Analysis*, *46*(10-11), pp.882-887.

Abend, S. and Lagaly, G., 2000. Sol–gel transitions of sodium montmorillonite dispersions. *Applied clay science*, *16*(3-4), pp.201-227.

Abu-Jdayil, B., 2011. Rheology of sodium and calcium bentonite–water dispersions: Effect of electrolytes and aging time. *International journal of mineral processing*, *98*(3-4), pp.208-213.

Adams, N.J., Drilling Engineering, A Complete Well Planning Approach, 1985. *Tulsa, Oklahoma.: Penn Well Books-Penn Well Publishing Company*.

Ahmed, O., Adeniran, A. and Samsuri, A., 2018. Rate of penetration prediction utilizing hydromechanical specific energy. In *Drilling* (pp. 105-131). IntechOpen.

Akgun, F., 2002a, January. How to Etimate the Maximum Achievable Drilling Rate Without Jeopardizing Safety. In *Abu Dhabi International Petroleum Exhibition and Conference*. Society of Petroleum Engineers.

Akgun, F., 2002b, January. How to Etimate the Maximum Achievable Drilling Rate Without Jeopardizing Safety. In *Abu Dhabi International Petroleum Exhibition and Conference*. Society of Petroleum Engineers.

Alderman, N.J., Gavignet, A., Guillot, D. and Maitland, G.C., 1988, January. High-temperature, high-pressure rheology of water-based muds. In *SPE Annual Technical Conference and Exhibition*. Society of Petroleum Engineers.

Alexander, W. and Odom, I.E., American Colloid Company, 1984. *Extrusion of bentonite clay for fluid loss reduction in drilling fluids*. U.S. Patent 4,462,470.

Al-hilphy, A.R.S., Verma, D.K., Niamah, A.K., Billoria, S.U.D.H.A.N.S.H.I. and Srivastar, P., 2016. Principles of ultrasonic technology for treatment of milk and milk products. *Food process engineering: Emerging trends in research and their applications*, pp.178-202.

Ali, L. and Barrufet, M.A., 2001. Using centrifuge data to investigate the effects of polymer treatment on relative permeability. *Journal of Petroleum Science and Engineering*, *29*(1), pp.1-16.

Al-Marhoun, M.A. and Rahman, S.S., 1988. Optimizing the properties of water-based polymer drilling fluids for penetrating formations with electrolyte influx. *Erdol Erdgas*, pp.318-323.

Al-Marhoun, M.A. and Rahman, S.S., 1988. Optimizing the properties of water-based polymer drilling fluids for penetrating formations with electrolyte influx. *Erdol Erdgas*, pp.318-323.

Altun, G. and Osgouei, A.E., 2014. Investigation and remediation of active-clay contaminated sepiolite drilling muds. *Applied Clay Science*, *102*, pp.238-245.

Altun, G., Osgouei, A.E. and Serpen, U., 2010, April. Controlling rheological and fluid loss properties of sepiolite based muds under elevated temperatures. In *Proceedings World Geothermal Congress, Bali, Indonesia, April* (pp. 25-29).

Altun, G., Osgouei, A.E., Ozyurtkan, M.H. and Serpen, U., 2015. Sepiolite based muds as an alternate drilling fluid for hot environments. In *Proceedings of the 2015 World Geothermal Congress. Melbourne: International Geothermal Association*.

Amani, M. and Al-Jubouri, M., 2012. The effect of high pressures and high temperatures on the properties of water based drilling fluids. *Energy Science and Technology*, *4*(1), pp.27-33.

Amani, M., Khorasani, M.H.M. and Ghamary, M.H., 2016, March. Effect of salinity on the viscosity of water based drilling fluids at elevated pressures and temperatures. In *Qatar Foundation Annual Research Conference Proceedings Volume 2016 Issue 1* (Vol. 2016, No. 1, p. EEPP2318). Hamad bin Khalifa University Press (HBKU Press).

Anderson, R.L., Ratcliffe, I., Greenwell, H.C., Williams, P.A., Cliffe, S. and Coveney, P.V., 2010. Clay swelling—a challenge in the oilfield. *Earth-Science Reviews*, *98*(3), pp.201-216

Annis, M.R. and Smith, M.V., 1996. Drilling fluids technology. *Revised Edition Exxon Company*.

Annis, M.R., 1967. High-temperature flow properties of water-base drilling fluids. *Journal of Petroleum Technology*, *19*(08), pp.1-074.

Anyanwu C, Mustapha Unubi M , 2016, Experimental evaluation of particle sizing in drilling fluid to minimize filtrate losses and formation damage. SPE-184303-MS, presented at SPE Nigiria international conference and exhibition held in Lagos;

Asghari, I. and Esmaeilzadeh, F., 2014. Manipulation of key parameters in RESS process for attapulgite particles utilizing in drilling mud and investigation on its rheological characteristics. *Journal of Petroleum Science and Engineering*, *122*, pp.789-799.

Azar, J.J., 2004. Oil and Natural Gas Drilling.

Azizi Samir, M.A.S., Alloin, F. and Dufresne, A., 2005. Review of recent research into cellulosic whiskers, their properties and their application in nanocomposite field. *Biomacromolecules*, *6*(2), pp.612-626.

Bailey L, Keall M, Audibert A, Lecourtier J., 1994, Effect of clay/polymer interactions on shale stabilization during drilling. Langmuir 10:1544–1549.

Balhoff, M.T., Lake, L.W., Bommer, P.M., Lewis, R.E., Weber, M.J. and Calderin, J.M., 2011. Rheological and yield stress measurements of non-Newtonian fluids using a Marsh Funnel. *Journal of petroleum Science and Engineering*, *77*(3), pp.393-402.

Balhoff, M.T., Lake, L.W., Bommer, P.M., Lewis, R.E., Weber, M.J. and Calderin, J.M., 2011. Rheological and yield stress measurements of non-Newtonian fluids using a Marsh Funnel.

Beck-Candanedo, S., Roman, M. and Gray, D.G., 2005. Effect of reaction conditions on the properties and behavior of wood cellulose nanocrystal suspensions. *Biomacromolecules*, *6*(2), pp.1048-1054.

Becker, T.E., Azar, J.J., Okrajni, S.S., 1991. Correlations of mud rheological properties with cuttings-transport performance in directional drilling. SPE Drill. Eng. 6.

Becker, T.E., Morgan, R.G., Chin, W.C. and Griffith, J.E., 2003, January. Improved rheology model and hydraulics analysis for tomorrow's wellbore fluid applications. In *SPE production and operations symposium*. Society of Petroleum Engineers.

Bercea, M. and Navard, P., 2000. Shear dynamics of aqueous suspensions of cellulose whiskers. *Macromolecules*, *33*(16), pp.6011-6016.

Bercea, M. and Navard, P., 2000. Shear dynamics of aqueous suspensions of cellulose whiskers. *Macromolecules*, *33*(16), pp.6011-6016.

Bergaya, F. and Lagaly, G., 2006. General introduction: clays, clay minerals, and clay science. *Developments in clay science*, *1*, pp.1-18.

Berkowitz, B., 2002. Characterizing flow and transport in fractured geological media: A review. Advances in water resources, 25(8-12), pp.861-884.

Bilgesu, H. I., Tetrick, L. T.,Altmis, U., Mohaghegh, S. and Ameri, S. (1997). A New Approach for the Prediction of Rate of Penetration Values Paper SPE 39231 presented at the SPE Eastern Regional meeting, Lexington, October 22-24 1997.

Bish, D.L. and Guthrie Jr, G.D., 1993. *Mineralogy of clay and zeolite dusts (exclusive of 1: 1 layer silicates)* (No. CONF-9310406--Vol. 28). Mineralogical Society of America, Washington, DC (United States).

Black, A.D., Dearing, H.L. and DiBona, B.G., 1985. Effects of pore pressure and mud filtration on drilling rates in a permeable sandstone. *Journal of petroleum technology*, *37*(09), pp.1-671.

Bland, R., Mullen, G., Gonzalez, Y., Harvey, F. And Pless, M., 2005. Drilling fluid meets deep gas drilling challenges. Drilling contractor, 61(3), pp.50-54.

Blkoor, S. O. and Fattah K.A, 2013. The Influence of XC-Polymer on Drilling Fluid Filter Cake Properties and Formation Damage. J. Pet. Environ. Biotechnol, 4(5).

Borisov, A.S., Husein, M. and Hareland, G., 2015. A field application of nanoparticle-based invert emulsion drilling fluids. *Journal of Nanoparticle Research*, *17*(8), p.340.

Bourgoyne, A.T., Millheim, K.K., Chenevert, M.E. and Young, F.S., 1986. *Applied drilling engineering* (Vol. 2, p. 514). Richardson, TX: Society of Petroleum Engineers.

Bourgoyne Jr, A.T. and Young Jr, F.S., 1974. A multiple regression approach to optimal drilling and abnormal pressure detection. Society of Petroleum Engineers Journal, 14(04), pp.371-384.

Bourgoyne Jr, A.T., Millheim, K.K., Chenevert, M.E. and Young Jr, F.S., 1986. Applied drilling engineering. Volume 2.

Bourgoyne Jr, A.T., Millheim, K.K., Chenevert, M.E. and Young Jr, F.S., 1991. Applied Drilling Engineering, SPE Textbook Series Vol. 2, Second Printing, 152-155. *Society of Petroleum Engineers*.

BP. BP Energy Outlook 2016 edition. BP; 2016.

Briscoe, B.J., Luckham, P.F., Ren, S.R., 1994. The properties of drilling muds at high-pressures and high-temperatures. Phil. Trans. R. Soc. London Ser. A 348 (1687), 179–207

Bunphot, T., 2017. *Performange of freshwater and seawater drilling mud with gellan gum* (Doctoral dissertation, School of Geotechnology Institute of Engineering Suranaree University of Technology).

Caenn R, Darley HC, Gray GR. Composition and properties of drilling and completion fluids. Gulf professional publishing; 2011 Sep 29).

Caenn, R., Darley, H.C. and Gray, G.R., 2011. *Composition and properties of drilling and completion fluids*. Gulf professional publishing.

Cai, J., Chenevert, M.E., Sharma, M.M. and Friedheim, J.E., 2012. Decreasing water invasion into Atoka shale using nonmodified silica nanoparticles. *SPE Drilling & Completion, 27*(01), pp.103-112.

Cao, Y., Zavaterri, P., Youngblood, J., Moon, R. and Weiss, J., 2015. The influence of cellulose nanocrystal additions on the performance of cement paste. *Cement and Concrete Composites*, *56*, pp.73-83.

Capadona, J.R., Van Den Berg, O., Capadona, L.A., Schroeter, M., Rowan, S.J., Tyler, D.J. and Weder, C., 2007. A versatile approach for the processing of polymer nanocomposites with self-assembled nanofibre templates. *Nature Nanotechnology*, *2*(12), pp.765-769.

Carney, L.L. and Guven, N., 1980. Investigation of changes in the structure of clays during hydrothermal study of drilling fluids. *Society of Petroleum Engineers Journal*, *20*(05), pp.385-390.

Carney, L.L. and Meyer, R.L., 1976. A New Approach to High Temperature Drilling Fluids. SPE 6025. In *51st SPE Annual Fall Meeting of Society of Petroleum Engineers, New Orleans, LA, USA, October* (pp. 3-6).

Cheremisinoff, N.P., 1998. *Liquid filtration*. Butterworth-Heinemann

Ching, Y.C. and Ng, T.S., 2014. Effect of preparation conditions on cellulose from oil palm empty fruit bunch fiber. *BioResources*, *9*(4), pp.6373-6385.

Cho, W.J., Lee, J.O. and Kang, C.H., 2000. Influence of temperature elevation on the sealing performance of a potential buffer material for a high-level radioactive waste repository. Annals of Nuclear Energy, 27(14), pp.1271-1284.

Choo, K.Y. and Bai, K., 2015. Effects of bentonite concentration and solution pH on the rheological properties and long-term stabilities of bentonite suspensions. *Applied Clay Science*, *108*, pp.182-190.

Clark, R.K., 1994. Impact of environmental regulations on drilling-fluid technology. Journal of Petroleum Technology, 46(09), pp.804-809.

Clarke, G.M., 1989. Sepiolite: the Spanish mineral. *Ind. Clays*, *85*.

Cucheval, A. and Chow, R.C.Y., 2008. A study on the emulsification of oil by power ultrasound. *Ultrasonics sonochemistry*, *15*(5), pp.916-920.

Dias, F.T.G., Souza, R.R. and Lucas, E.F., 2015. Influence of modified starches composition on their performance as fluid loss additives in invert-emulsion drilling fluids. *Fuel*, *140*, pp.711-716.

Dong, X.M. and Gray, D.G., 1997. Effect of counterions on ordered phase formation in suspensions of charged rodlike cellulose crystallites. *Langmuir, 13*(8), pp.2404-2409.

Dufresne, A., 2006. Comparing the mechanical properties of high performances polymer nanocomposites from biological sources. *Journal of Nanoscience and Nanotechnology*, *6*(2), pp.322-330.

Dufresne, A., 2013. Nanocellulose: a new ageless bionanomaterial. *Materials Today*, *16*(6), pp.220-227.

Ebeling, T., Paillet, M., Borsali, R., Diat, O., Dufresne, A., Cavaille, J.Y. and Chanzy, H., 1999. Shear-induced orientation phenomena in suspensions of cellulose microcrystals, revealed by small angle X-ray scattering. *Langmuir*, *15*(19), pp.6123-6126.

Echt, T. and Plank, J., 2019. An improved test protocol for high temperature carrying capacity of drilling fluids exemplified on a sepiolite mud. Journal of Natural Gas Science and Engineering, 70, p.102964.

Ehrhorn, C. and Saasen, A., 1996. Barite sag in drilling fluids. *Ann. Trans. Nordic Rheology Soc*, *4*, p.66

Elkatatny, S., Gamal, H., Ahmed, A., Sarmah, P., Sangaru, S. and Alohaly, M., 2020. A Novel Solution for Severe Loss Prevention While Drilling Deep Wells. *Sustainability*, *12*(4), p.1339.

Elochukwu, H. and Sia, L.K.S.L., 2019, April. Improved Filtration Properties of Polystyrene Nanoparticle additives to Water Based Drilling Fluid. In IOP Conference Series: Materials Science and Engineering (Vol. 495, No. 1, p. 012072). IOP Publishing.

Fan J, Zhu H, Li R, Chen N, 2015, Montmorillonite modified by cationic and nonionic surfactants as high-performance fluid-losscontrol additive in oil-based drilling fluids. J Dispers Sci Technol 36:569–576.

Fan, J., Zhu, H., Li, R. and Chen, N., 2015. Montmorillonite modified by cationic and non-ionic surfactants as high-performance fluid-loss-control additive in oil-based drilling fluids. Journal of Dispersion Science and Technology, 36(4), pp.569-576.

Fan, J., Zhu, H., Li, R. and Chen, N., 2015. Montmorillonite modified by cationic and nonionic surfactants as high-performance fluid-loss-control additive in oil-based drilling fluids. *Journal of Dispersion Science and Technology*, *36*(4), pp.569-576..

Fazelabdolabadi, B., Khodadadi, A.A. and Sedaghatzadeh, M., 2015. Thermal and rheological properties improvement of drilling fluids using functionalized carbon nanotubes. *Applied Nanoscience*, *5*(6), pp.651-659.

Fink, J., 2015. Water-based chemicals and technology for drilling, completion, and workover fluids.

Friedheim, J. E.; Tour, J. M. 2011. Graphene Oxide as a High-Performance Fluid-Loss-Control Additive in Waterbased Drilling Fluids. ACS Appl. Mater. Interfaces, 4, pp 222−227.

George, J. and Sabapathi, S.N., 2015. Cellulose nanocrystals: synthesis, functional properties, and applications. *Nanotechnology, science and applications*, *8*, p.45.

Giovanni, B., Fausto, M., Stefano, C. and Lockhart, T.P., 1995, January. New Chemistry for Chromium-Free Bentonite Drilling Fluids Stable at High Temperatures. In SPE International Symposium on Oilfield Chemistry. Society of Petroleum Engineers.

Gray, H.C.H., Darley, G.R., 1988. Composition and Properties of Oil–Well Drilling Fluids.Gulf Pub, Co.

Gribble, C. D. and Hall, A. J., 2000. A Practical Introduction to Optical Mineralogy, London. George Allen and Unwin Publishers.

Zhuang, G., Zhang, Z. and Chen, H., 2018. Influence of the interaction between surfactants and sepiolite on the rheological properties and thermal stability of organo-sepiolite in oil-based drilling fluids. *Microporous and Mesoporous Materials*, *272*, pp.143-154.

Rabia, H., 1985. *Oilwell drilling engineering: principles and practice* (pp. 96-98). London: Graham & Trotman.

Habibi, Y., Lucia, L.A. and Rojas, O.J., 2010. Cellulose nanocrystals: chemistry, self-assembly, and applications. *Chemical reviews*, *110*(6), pp.3479-3500.

Haden Jr, W.L., 1963. Attapulgite: properties and uses. *Clays Clay Miner*, *10*, pp.284-290.

Halali, M.A., Ghotbi, C., Tahmasbi, K. and Ghazanfari, M.H., 2016. The role of carbon nanotubes in improving thermal stability of polymeric fluids: Experimental and modeling. *Industrial & Engineering Chemistry Research*, *55*(27), pp.7514-7534.

Hamad, W., 2006. On the development and applications of cellulosic nanofibrillar and nanocrystalline materials. *The Canadian Journal of Chemical Engineering*, *84*(5), pp.513-519.

Hamed, S.B. and Belhadri, M., 2009. Rheological properties of biopolymers drilling fluids. *Journal of Petroleum Science and Engineering*, *67*(3-4), pp.84-90.

Heinz, W., 1959. The Casson flow equation: Its validity for suspension of paints. Material Prüfung, 1, p.311.

Heivilin, F.G. and Murray, H.H., 1994. Hormites: palygorskite (attapulgite) and sepiolite. *Industrial Minerals and Rocks (ed. Carr, DD) Littleton, Colarado, Society of Mining, Metallurgy, and Exploration, Inc*, pp.249-154.

Hiller, K.H., 1963. Rheological measurements of clay suspensions at high temperatures and pressures. J. Pet. Technol. 17, 779–789.

Ho, C.Y., Yusup, S. and Soon, C.V., 2014. Study on the effect of nanoparticle loadings in base fluids for improvement of drilling fluid properties. *J. Adv. Chem. Eng*, *4*, p.115.

Ho, C.Y., Yusup, S. and Soon, C.V., 2014. Study on the effect of nanoparticle loadings in base fluids for improvement of drilling fluid properties. *J. Adv. Chem. Eng*, *4*, p.115.

Hossain, M.E. and Al-Majed, A.A., 2015. Fundamentals of sustainable drilling engineering. John Wiley & Sons.

HPHT Filter Press Instruction Manual, 2017. Manual no. 209486, revision N instrument No. Models 175ct and 500ct. Fann Instrument Company.

IEA. Key world Energy Statistics. Paris: International Energy Agency; 2014, ⟨https://www.iea.org/publications/freepublications/publication/key-worldenergy statistics.html⟩, [accessed 3.12.16].

Irawan, S., Rahman, A. and Tunio, S., 2012. Optimization of weigth on bit during drilling operation based on rate of penetration model. Research Journal of Applied Sciences, Engineering and Technology, 4(12), pp.1690-1695.

Iscan, A. G.; Kok, M. V., 2007, Effects of Polymers and CMC Concentration on Rheological and Fluid Loss Parameters of Water-Based Drilling Fluids. Energy Sources, Part A, 29, 939–949.

Ismail, A.R., Aftab, A., Ibupoto, Z.H. and Zolkifile, N., 2016. The novel approach for the enhancement of rheological properties of water-based drilling fluids by using multi-walled carbon nanotube, nanosilica and glass beads. *Journal of Petroleum Science and Engineering, 139*, pp.264-275.

Ismail, I., Ismail, A.R. and Yang, J., 1999. Managing drilling mud weight using ilmenite.

Jacinto, A., Gomez-Espina, R., Villar, M.V. and Ledesma, A., 2007, September. Effect of temperature on the retention capacity of compacted bentonite: An experimental and numerical investigation. In Proceedings of the International Meeting on Clays in Natural & Engineered Barriers for Radioactive Waste Confinement, Lille, France (pp. 17-20).

Jones TGJ, Hughes TL, 1996, drilling fluid suspensions. In: Suspensions: fundamentals and applications in the petroleum industry. Advances in chemistry series, vol 251, American Chemical Society, Washington, DC, pp 10–463.

Juhari, Y. and Isham, I., 1998. Managing Drilling Mud Weight Using Ilmenite. In *Faculty of Chemical and Natural resources Engineering Conference, Universiti Teknologi Malaysia (UTM), Johor, Bahru*.

Jung, Y., Barry, M., Lee, J.K., Tran, P., Soong, Y., Martello, D. and Chyu, M., 2011, April. Effect of nanoparticle-additives on the rheological properties of clay-based fluids at high temperature and high pressure. In AADE national technical conference and exhibition (pp. 1-4). Houston, TX: American Association of Drilling Engineers.

Jung, Y., Barry, M., Lee, J.K., Tran, P., Soong, Y., Martello, D. and Chyu, M., 2011, April. Effect of nanoparticle-additives on the rheological properties of clay-based fluids at high temperature and high pressure. In *AADE National Technical Conference and Exhibition, Texas, USA*.

Jung, Y., Son, Y.H., Lee, J.K., Phuoc, T.X., Soong, Y. and Chyu, M.K., 2011. Rheological behavior of clay–nanoparticle hybrid-added bentonite suspensions: specific role of hybrid additives on the gelation of clay-based fluids. *ACS applied materials & interfaces, 3*(9), pp.3515-3522.

Kabir, C.S., Hasan, A.R., Kouba, G.E. and Ameen, M., 1996. Determining circulating fluid temperature in drilling, workover, and well control operations. *SPE Drilling & Completion, 11*(02), pp.74-79.

Kahraman, S., 2003. Performance analysis of drilling machines using rock modulus ratio. *Journal of The Southern African Institute of Mining and Metallurgy*, *103*(8), pp.515-522.

Kangas, H., 2013. Cellulose nanofibrils—a class of materials with unique properties and many potential applications. *Production and Applications of Cellulose Nanomaterials*.

Kelessidis, V.C., Poulakakis, E. and Chatzistamou, V., 2011. Use of Carbopol 980 and carboxymethyl cellulose polymers as rheology modifiers of sodium-bentonite water dispersions. *Applied clay science*, *54*(1), pp.63-69.

Kelessidis, V.C., 2009. Drilling fluid challenges for oil-well deep drilling. International Multidisciplinary Scientific GeoConference: SGEM: Surveying Geology & mining Ecology Management, 1, p.595.

Kelessidis, V.C., Poulakakis, E. and Chatzistamou, V., 2011. Use of Carbopol 980 and carboxymethyl cellulose polymers as rheology modifiers of sodium-bentonite water dispersions. *Applied clay science*, *54*(1), pp.63-69.

Kelessidis, V.C., Tsamantaki, C. and Dalamarinis, P., 2007. Effect of pH and electrolyte on the rheology of aqueous Wyoming bentonite dispersions. *Applied Clay Science*, *38*(1-2), pp.86-96.
Kelessidis, V.C., Tsamantaki, C. and Dalamarinis, P., 2007. Effect of pH and electrolyte on the rheology of aqueous Wyoming bentonite dispersions. Applied Clay Science, 38(1-2), pp.86-96.

Kelessidis, V.C., Tsamantaki, C., Pasadakis, N., Repouskou, E. and Hamilaki, E., 2007. Permeability, porosity and surface characteristics of filter cakes from water–bentonite suspensions. WIT Transactions on Engineering Sciences, 56, pp.173-182.).

Kelessidis, V.C., Zografou, M. and Chatzistamou, V., 2013, March. Optimization of drilling fluid rheological and fluid loss properties utilizing PHPA polymer. In SPE Middle East Oil and Gas Show and Conference. Society of Petroleum Engineers.

Kerr, P.F., 1937. Attapulgus clay. *Am. Mineral*, *22*, pp.534-540.

Khalil M, Mohamed Jan B, 2012, Viscoplastic modeling of anovel lightweight biopolymer drilling fluid for underbalanced drilling. Ind Eng Chem Res 51:4056–4068.

Khalil, M. and Mohamed Jan, B., 2012. Herschel-Bulkley rheological parameters of a novel environmentally friendly lightweight biopolymer drilling fluid from xanthan gum and starch. *Journal of Applied Polymer Science*, *124*(1), pp.595-606.

Khalil, M. and Mohamed Jan, B., 2012. Viscoplastic modeling of a novel lightweight biopolymer drilling fluid for underbalanced drilling. *Industrial & engineering chemistry research*, *51*(10), pp.4056-4068.

Khalil, M., Jan, B.M. and Raman, A.A.A., 2011. Rheological and statistical evaluation of nontraditional lightweight completion fluid and its dependence on temperature. *Journal of Petroleum Science and Engineering*, *77*(1), pp.27-33.

Khodja, M., Khodja-Saber, M., Canselier, J.P., Cohaut, N. and Bergaya, F., 2010. Drilling fluid technology: performances and environmental considerations. In Products and services; from R&D to final solutions (pp. 227-256). Sciyo Publications.

Khodja, M., Khodja-Saber, M., Canselier, J.P., Cohaut, N. and Bergaya, F., 2010. Drilling fluid technology: performances and environmental considerations. In *Products and services; from R&D to final solutions*. InTech.

Kok, M.V., 2010. A rheological characterization and parametric analysis of a bentonite sample. *Energy Sources, Part A: Recovery, Utilization, and Environmental Effects*, *33*(4), pp.344-348.

Kosynkin, D.V., Ceriotti, G., Wilson, K.C., Lomeda, J.R., Scorsone, J.T., Patel, A.D., Friedheim, J.E. and Tour, J.M., 2011. Graphene oxide as a high-performance fluid-loss-control additive in water-based drilling fluids. *ACS applied materials & interfaces*, *4*(1), pp.222-227.

Larsen, H., 2007. Behaviour of polymer muds under high pressure–high temperature conditions (Master's thesis, Institutt for petroleumsteknologi og anvendt geofysikk.

Lee, J. and Deng, Y., 2011. The morphology and mechanical properties of layer structured cellulose microfibril foams from ice-templating methods. *Soft Matter*, *7*(13), pp.6034-6040.

Leung, A.C., Hrapovic, S., Lam, E., Liu, Y., Male, K.B., Mahmoud, K.A. and Luong, J.H., 2011. Characteristics and properties of carboxylated cellulose nanocrystals prepared from a novel one-step procedure. *Small*, *7*(3), pp.302-305.

Li M, Wu Q, Song K, Qing Y, Wu Y,2015, Cellulose nanoparticles as modifiers for rheology and fluid loss in bentonite water-based fluids. ACS Appl Mater Interfaces 7:5006–5016.
Li, D., Hong, B., Fang, W., Guo, Y. and Lin, R., 2010. Preparation of well-dispersed silver nanoparticles for oil-based nanofluids. *Industrial & Engineering Chemistry Research*, *49*(4), pp.1697-1702.

Li, M.C, Wu Q, Song, K, De Hoop, C.F., Lee, S. Qing, Y. and Wu Y., 2016. Cellulose Nanocrystals and Polyanionic Cellulose as Additives in Bentonite Water-Based Drilling Fluids: Rheological Modeling and Filtration Mechanisms. Industrial & Engineering Chemistry Research, 55(1). Pp 133-143.

Li, M.C., Wu, Q., Song, K., French, A.D., Mei, C. and Lei, T., 2018. pH-responsive water-based drilling fluids containing bentonite and chitin nanocrystals. *ACS Sustainable Chemistry & Engineering*, *6*(3), pp.3783-3795.

Li, M.C., Wu, Q., Song, K., Lee, S., Qing, Y. and Wu, Y., 2015a. Cellulose nanoparticles: structure–morphology–rheology relationships. *ACS Sustainable Chemistry & Engineering*, *3*(5), pp.821-832.

Li, M.C., Wu, Q., Song, K., Qing, Y. and Wu, Y., 2015. Cellulose nanoparticles as modifiers for rheology and fluid loss in bentonite water-based fluids. *ACS applied materials & interfaces*, *7*(8), pp.5006-5016.

Li, M.C., Wu, Q., Song, K., Qing, Y. and Wu, Y., 2015b. Cellulose nanoparticles as modifiers for rheology and fluid loss in bentonite water-based fluids. *ACS applied materials & interfaces*, *7*(8), pp.5006-5016.

Lin, Y., Cheah, L.K.-J., Phan-Thiena, N., Khoo, B.C., 2016. Effect of temperature on rheological behavior of kaolinite and bentonite suspensions. Colloids Surf. A Physicochem. Eng. Asp. 506, 1–5

Lu, Q., Tang, L., Lin, F., Wang, S., Chen, Y., Chen, X. and Huang, B., 2014. Preparation and characterization of cellulose nanocrystals via ultrasonication-assisted FeCl3-catalyzed hydrolysis. *Cellulose*, *21*(5), pp.3497-3506.

Keren, R., Shainberg, I. and Klein, E., 1988. Settling and flocculation value of sodium-montmorillonite particles in aqueous media. *Soil Science Society of America Journal*, *52*(1), pp.76-80.

Luckham, P.F. and Rossi, S., 1999. The colloidal and rheological properties of bentonite suspensions. *Advances in colloid and interface science*, *82*(1-3), pp.43-92.

Lummus, J.L. and Azar, J.J., 1986. Drilling fluids optimization: a practical field approach.

Mahmood Amani and Mohammed Al-Jubouri, 2012 the effect of high pressures and high temperatures on the properties of water based drilling fluids.

Mahmoud, O., Nasr-El-Din, H.A., Vryzas, Z. and Kelessidis, V.C., 2016, February. Nanoparticle-based drilling fluids for minimizing formation damage in HP/HT applications. In *SPE International Conference and Exhibition on Formation Damage Control*. Society of Petroleum Engineers.

Mahto, V. and Sharma, V.P., 2004. Rheological study of a water based oil well drilling fluid. *Journal of Petroleum Science and Engineering*, *45*(1), pp.123-128.

Mahto, V.; Sharma, V. P., 2004, Rheological Study of a Water Based Oil Well Drilling Fluid. J. Pet. Sci. Eng., 45, 123−128.

Malmsheimer, R.W., Heffernan, P., Brink, S., Crandall, D., Deneke, F., Galik, C., Gee, E., Helms, J.A., McClure, N., Mortimer, M. and Ruddell, S., 2008. Forest management solutions for mitigating climate change in the United States. *Journal of Forestry*, *106*(3), p.115.

Max R. A and Martin V. S (1974) Drilling Fluids Technology

M'bodj, O., Kbir Ariguib, N., Trabelsi Ayadi, M., Magnin, A., 2004. Plastic and elastic properties of the systems interstratified clay–water–electrolyte–xanthan. Journal of Colloid and Interface Science 273, 675–684.

Menezes, R.R., Marques, L.N., Campos, L.A., Ferreira, H.S., Santana, L.N.L. and Neves, G.A., 2010. Use of statistical design to study the influence of CMC on the rheological properties of bentonite dispersions for water-based drilling fluids. *Applied Clay Science*, *49*(1-2), pp.13-20.

Miyahara, K., Adachi, Y. and Nakaishi, K., 1998. The viscosity of a dilute suspension of sodium montmorillonite in an alkaline state. *Colloids and Surfaces A: Physicochemical and Engineering Aspects*, *131*(1-3), pp.69-75.

Mizrahi, S. and Berk, Z., 1972. Flow behaviour of concentrated orange juice: mathematical treatment. Journal of Texture Studies, 3(1), pp.69-79.

Mohammed, A.S., 2017. Effect of temperature on the rheological properties with shear stress limit of iron oxide nanoparticle modified bentonite drilling muds. Egyptian journal of petroleum, 26(3), pp.791-802.

Moon, R., Beck, S. and Rudie, A., 2013. Cellulose nanocrystals-a material with unique properties and many potential applications. *Review Process: Non-Refereed (Other)*.

Moon, R.J., Martini, A., Nairn, J., Simonsen, J. and Youngblood, J., 2011. Cellulose nanomaterials review: structure, properties and nanocomposites. *Chemical Society Reviews*, *40*(7), pp.3941-3994.

Murray, H.H., 1999. Applied clay mineralogy today and tomorrow. *Clay minerals*, *34*(1), pp.39-39.

Nan, F., Xu, Y., Xu, B., Gao, F., Wu, Y. and Tang, X., 2014. Effect of natural attapulgite powders as lubrication additive on the friction and wear performance of a steel tribo-pair. *Applied surface science*, *307*, pp.86-91.

Navarrete, R. C.; Himes, R. E.; Seheult, J. M., 2000, Applications of Xanthan Gum in Fluid-Loss Control and Related Formation Damage. SPE Permian Basin Oil and Gas Recovery Conference, Midland, TX, March 23−26; Society of Petroleum Engineers: Richardson, TX, 2000; SPE Paper No. 59535.

Navarrete, R.C., Himes, R.E. and Seheult, J.M., 2000, January. Applications of xanthan gum in fluid-loss control and related formation damage. In *SPE Permian Basin Oil and Gas Recovery Conference*. Society of Petroleum Engineers.

Nunes, R. de C. P.; Pires, R. V.; Lucas, E. F.; Vianna, A.; Lomba, R., 2014, New filtrate loss controller based on poly(methyl methacrylate-covinyl acetate). J. Appl. Polym. Sci., 131, DOI: 10.1002/app.40646.

Nunes, R.D.C.P., Pires, R.V., Lucas, E.F., Vianna, A. and Lomba, R., 2014. New filtrate loss controller based on poly (methyl methacrylate-co-vinyl acetate). *Journal of Applied Polymer Science*, *131*(16).

Nwosu, O.U. and Ewulonu, C.M., 2014. Rheological behaviour of eco-friendly drilling fluids from biopolymers. *J. Polym. Biopolym. Phys. Chem*, *2*(3), pp.50-54.

Okon, A.N., Udoh, F.D. and Bassey, P.G., 2014, August. Evaluation of rice husk as fluid loss control additive in water-based drilling mud. In *SPE Nigeria Annual International Conference and Exhibition*. Society of Petroleum Engineers.

Onogi, S. and Asada, T., 1980. Rheology and rheo-optics of polymer liquid crystals. In *Rheology* (pp. 127-147). Springer US.

Orts, W.J., Godbout, L., Marchessault, R.H. and Revol, J.F., 1995. Shear-Induced Alignment of Liquid-Cystalline Suspensions of Cellulose Microfibrils.

Osgouei, R.E. and Özbayoğlu, M., 2007, September. Rate of penetration estimation model for directional and horizontal wells. In 16th international petroleum and natural gas congress and exhibition of Turkey.

Ouaer, H. and Gareche, M., 2019. Hydroxyethyl cellulose as a rheology modifier for water-based drilling fluids formulated with Algerian bentonite. Journal of the Brazilian Society of Mechanical Sciences and Engineering, 41(3), p.123.

Paiaman, A.M., Al-Askari, M.K., Salmani, B., Alanazi, B.D. and Masihi, M., 2009. Effect of drilling fluid properties on rate of Penetration. *Nafta*, *60*(3), pp.129-134.

Pech-Cohuo, S.C., Canche-Escamilla, G., Valadez-González, A., Fernández-Escamilla, V.V.A. and Uribe-Calderon, J., 2018. Production and modification of cellulose nanocrystals from Agave tequilana weber waste and its effect on the melt rheology of PLA. *International Journal of Polymer Science*, *2018*.

Peden, J.M., Avalos, M.R. and Arthur, K.G., 1982, January. The analysis of the dynamic filtration and permeability impairment characteristics of inhibited water based muds. In *SPE Formation Damage Control Symposium*. Society of Petroleum Engineers.

Peng, B.L., Dhar, N., Liu, H.L. and Tam, K.C., 2011. Chemistry and applications of nanocrystalline cellulose and its derivatives: a nanotechnology perspective. *The Canadian Journal of Chemical Engineering*, *89*(5), pp.1191-1206.

Popp, T. and Kern, H., 1993. Thermal dehydration reactions characterised by combined measurements of electrical conductivity and elastic wave velocities. *Earth and planetary science letters*, *120*(1-2), pp.43-57.

Powell, J.W., Stagg, T., Reiley, R.H. and Dobson, J., 1991, January. Thixotropic, Crosslinking Polymer/Borate/Salt Plug: Development and Application. In *International Arctic Technology Conference*. Society of Petroleum Engineers.

Preisinger, A., 1963. Clays and clay minerals. *Earth Sci. Series*, *12*, p.365.

Qin, Z.Y., Tong, G., Chin, Y.F. and Zhou, J.C., 2011. Preparation of ultrasonic-assisted high carboxylate content cellulose nanocrystals by TEMPO oxidation. BioResources, 6(2), pp.1136-1146).

Rabaioli, M.R., Miano, F., Lockhart, T.P. and Burrafato, G., 1993, January. Physical/chemical studies on the surface interactions of bentonite with polymeric dispersing agents. In SPE International Symposium on Oilfield Chemistry. Society of Petroleum Engineers.

Ramos-Tejada, M.M., Arrovo, F.J., Peren, R., Duran, J.D.G., 2001. Scaling behavior of the rheological parameters of montmorillonite suspensions: correlation between interparticle interaction and degree of flocculation. Journal of Colloid and Interface Science 235, 251–259.

Renken, K.J. and Meechan, K., 1995. Impact of thermal dispersion during forced convection condensation in a thin porous/fluid composite system. *Chemical Engineering Communications*, *131*(1), pp.189-205.

Richard O. et al., 2017, Predictive modelling of the impact of silica nanoparticles on fluid loss of Water based Mud.

Robertson, R.E. and Stiff Jr, H.A., 1976. An improved mathematical model for relating shear stress to shear rate in drilling fluids and cement slurries. Society of Petroleum Engineers Journal, 16(01), pp.31-36.

Robinson, L., Morgan, M., 2010. Effect of hole cleaning on drilling rate and performance. In: AADE Fluids Conference and Exhibition. Houston, USA, AADE-04-DF-HO-42.

Rocha, L.A.S., Junqueira, P. and Roque, J.L., 2003, January. Overcoming deep and ultra-deep water drilling challenges. In Offshore Technology Conference. Offshore Technology Conference.

Rogers, J.D., Lambert, S.W., Schlumberger, D.C.S. and Steve, W., 2004. Benchmarking Deep Drilling, and Completion Technologies.

Rossi, S., Luckham, P.F., Zhu, S., Briscoe, B.J., 1999. High-pressure/High-temperature Rheology of Na+-Montmorillonite Clay Suspensions, Paper SPE 50725 Presented at the SPE Int. Symposium on Oilfield Chemistry, Houston, TX, 16–19 Febr

Ryan Wagner, Xiawa Wu, Ashlie Marini, Arvind Raman, and Robert Moon. 2010. Deformation Mechanics of Cellulose Nanocrystals. Poster-presentation, Birck Nanotechnology Center, School of Mechanical Engineering, Department of Physics, Purdue University

Sabbaghi, S.; Saboori, R. and Barahoeti, M., 2015. Enhance heat transfert of drilling fluid with titania nanofluid. *Research & Reviews: Journal of Engineering and Technology, 4*, pp.12-17.

Santoyo, E., Santoyo–Gutierrez, S., Garcia, A., Espinosa, G., Moya, S.I., 2001. Rheological property measurement of drilling fluids used in geothermal wells. Appl. Therm. Eng. 21, 283–302

Savage, D., Noy, D. and Mihara, M., 2002. Modelling the interaction of bentonite with hyperalkaline fluids. Applied Geochemistry, 17(3), pp.207-223.

Scholar, P.G., 2015. The Effect of Drilling Mud Density on Penetration Rate.

Sedaghatzadeh, M. and Khodadadi, A., 2012. An improvement in thermal and rheological properties of water-based drilling fluids using multiwall carbon nanotube (MWCNT). *Iranian Journal of Oil & Gas Science and Technology*, *1*(1), pp.55-65.

Sensoy, T., Chenevert, M.E. and Sharma, M.M., 2009, January. Minimizing water invasion in shales using nanoparticles. In *SPE Annual Technical Conference and Exhibition*. Society of Petroleum Engineers.

Serpen, U., 1999. Use of sepiolite clay and other minerals for developing geothermal drilling fluids. *Applied Mechanics and Engineering*, *4*(spec.), pp.309-313.

Serpen, U., Haciislamoglu, M. and Tuna, O., 1992, February. Use of sepiolite resources of turkey in geothermal muds. In *Proceedings, 9th International Petroleum Congress of Turkey, Ankara* (pp. 17-21).

Seyed alangi, S.A., Nabavizadeh, M.J. and Hajipour, M., 2019. Mathematical Modeling to Predict the Rate of Penetration (ROP) Using Genetic Programming. Journal of Gas Technology, JGT, p.57.

Shafeiei-Sabet, S., Hamad, W.Y. and Hatzikiriakos, S.G., 2013. Influence of degree of sulfation on the rheology of cellulose nanocrystal suspensions. *Rheologica Acta*, *52*(8-9), pp.741-751.

Shafeiei-Sabet, S., Hamad, W.Y. and Hatzikiriakos, S.G., 2013. Influence of degree of sulfation on the rheology of cellulose nanocrystal suspensions. *Rheologica Acta*, *52*(8-9), pp.741-751.

Shafiei Sabet, S., 2013. *Shear rheology of cellulose nanocrystal (CNC) aqueous suspensions* (Doctoral dissertation, University of British Columbia).

Shafiei-Sabet, S., Hamad, W.Y. and Hatzikiriakos, S.G., 2012. Rheology of nanocrystalline cellulose aqueous suspensions. *Langmuir*, *28*(49), pp.17124-17133.

Shafiei-Sabet, S., Hamad, W.Y. and Hatzikiriakos, S.G., 2014. Ionic strength effects on the microstructure and shear rheology of cellulose nanocrystal suspensions. *Cellulose*, *21*(5), pp.3347-3359.

Shah, S.N., Shanker, N.H. and Ogugbue, C.C., 2010, April. Future challenges of drilling fluids and their rheological measurements. In AADE fluids conference and exhibition, Houston, Texas. sn.

Simmons, E.L., 1986, January. A Technique for accurate bit programming and drilling performance optimization. In *SPE/IADC Drilling Conference*. Society of Petroleum Engineers.

Sisko, A.W., 1958. The flow of lubricating greases. Industrial & Engineering Chemistry, 50(12), pp.1789-1792.

Song, K., Wu, Q., Li, M., Ren, S., Dong, L., Zhang, X., Lei, T. and Kojima, Y., 2016. Water-based bentonite drilling fluids modified by novel biopolymer for minimizing fluid loss and formation damage. *Colloids and Surfaces A: Physicochemical and Engineering Aspects*, *507*, pp.58-66.

Šturcová, A., Davies, G.R. and Eichhorn, S.J., 2005. Elastic modulus and stress-transfer properties of tunicate cellulose whiskers. *Biomacromolecules*, *6*(2), pp.1055-1061.

Temraz MG, Hassanien I, 2016, Mineralogy and rheological properties of some Egyptian bentonite for drilling fluids. J Nat Gas Sci Eng 31:791–799.

Turbak, A.F., Snyder, F.W. and Sandberg, K.R., 1983, January. Microfibrillated cellulose, a new cellulose product: properties, uses, and commercial potential. In *J. Appl. Polym. Sci.: Appl. Polym. Symp.;(United States)* (Vol. 37, No. CONF-8205234-Vol. 2). ITT Rayonier Inc., Shelton, WA.

Van den Berg, O., Capadona, J.R. and Weder, C., 2007. Preparation of homogeneous dispersions of tunicate cellulose whiskers in organic solvents. *Biomacromolecules*, *8*(4), pp.1353-1357.

Vryzas, Z. and Kelessidis, V.C., 2017. Nano-Based Drilling Fluids: A Review. *Energies*, *10*(4), p.540.

Vryzas, Z., Kelessidis, V.C., Nalbantian, L., Zaspalis, V., Gerogiorgis, D.I. and Wubulikasimu, Y., 2017. Effect of temperature on the rheological properties of neat aqueous Wyoming sodium bentonite dispersions. Applied Clay Science, 136, pp.26-36.

Vryzas, Z., Mahmoud, O., Nasr-El-Din, H.A. and Kelessidis, V.C., 2015, December. Development and testing of novel drilling fluids using Fe 2 O 3 and SiO 2 nanoparticles for enhanced drilling operations. In *International Petroleum Technology Conference*. International Petroleum Technology Conference.

Vryzas, Z., Wubulikasimu, Y., Gerogiorgis, D. and Kelessidis, V.C., 2016, May. Understanding the temperature effect on the rheology of water-bentonite suspensions. In *Proceedings of the Nordic Polymer Days and Nordic Rheological Conference, Helsinki, Finland* (Vol. 30).

Wan T, Yao J, Zishun S, Li W, Juan W., 2011, Solution and drilling fluid properties of water soluble AM–AA–SSS copolymers by inverse microemulsion. J Pet Sci Eng 78:334–337.

Wang, F., Tan, X., Wang, R., Sun, M., Wang, L. and Liu, J., 2012. High temperature and high pressure rheological properties of high-density water-based drilling fluids for deep wells. Petroleum Science, 9(3), pp.354-362).

Warren, B., van der Horst, P. and Stewart, W., 2003, January. Application of amphoteric cellulose ethers in drilling fluids. In *International Symposium on Oilfield Chemistry*. Society of Petroleum Engineers.

William, J.K.M., Ponmani, S., Samuel, R., Nagarajan, R. and Sangwai, J.S., 2014. Effect of CuO and ZnO nanofluids in xanthan gum on thermal, electrical and high pressure rheology of water-based drilling fluids. *Journal of Petroleum Science and Engineering*, *117*, pp.15-27.

Wu, X., Wagner, R., Raman, A., Moon, R., Martini, A. and Center, B.N., 2010. Elastic deformation mechanics of cellulose nanocrystals. *Review Process: Non-Refereed (Other)*.

Ouaer, H. and Gareche, M., 2019. Hydroxyethyl cellulose as a rheology modifier for water-based drilling fluids formulated with Algerian bentonite. *Journal of the Brazilian Society of Mechanical Sciences and Engineering*, *41*(3), pp.1-10.

Yan, L., Wang, C., Xu, B., Sun, J., Yue, W. and Yang, Z., 2013. Preparation of a novel amphiphilic comb-like terpolymer as viscosifying additive in low-solid drilling fluid. *Materials Letters*, *105*, pp.232-235.
Yildiz et al., 1999.

Yin, H., Mo, D. and Chen, D., 2009. Orientation behavior of attapulgite nanoparticles in poly (acrylonitrile)/attapulgite solutions by rheological analysis. *Journal of Polymer Science Part B: Polymer Physics*, *47*(10), pp.945-954.

Zakaria, M., Husein, M.M. and Harland, G., 2012, January. Novel nanoparticle-based drilling fluid with improved characteristics. In *SPE International Oilfield Nanotechnology Conference and Exhibition*. Society of Petroleum Engineers.

Zhang, T., Li, T., Liu, Y., Li, Y., Guo, G., Cui, J. and Zhou, F., 2017, February. Preparation and rheological properties of attapulgite gel for aqueous suspensions. In *2016 7th International Conference on Education, Management, Computer and Medicine (EMCM 2016)* (pp. 547-559). Atlantis Press.

Zheng, L., Rutqvist, J., Birkholzer, J.T. and Liu, H.H., 2015. On the impact of temperatures up to 200 C in clay repositories with bentonite engineer barrier systems: A study with coupled thermal, hydrological, chemical, and mechanical modeling. Engineering Geology, 197, pp.278-295.

Zhou, C. and Wu, Q., 2012. Recent development in applications of cellulose nanocrystals for advanced polymer-based nanocomposites by novel fabrication strategies. In *Nanocrystals-synthesis, characterization and applications*. Intech.

Zhuang, G., Zhang, Z. and Chen, H., 2018. Influence of the interaction between surfactants and sepiolite on the rheological properties and thermal stability of organo-sepiolite in oil-based drilling fluids. *Microporous and Mesoporous Materials*, *272*, pp.143-154.

Zhuang, G., Zhang, Z., Yang, H. and Tan, J., 2018. Structures and rheological properties of organo-sepiolite in oil-based drilling fluids. *Applied Clay Science*, *154*, pp.43-51.

Ziaee, H., Arabloo, M., Ghazanfari, M.H. and Rashtchian, D., 2015. Herschel–Bulkley rheological parameters of lightweight colloidal gas aphron (CGA) based fluids. *Chemical Engineering Research and Design*, *93*, pp.21-29.

Zihms SG, Harrington JF. Thermal cycling: impact on bentonite permeability. Mineralogical Magazine. 2015 Nov; 79 (6):1543-50.

INDEX A: RHEOLOGICAL DATA

RHEOLOGICAL DATA OF CNC/BT-WDFs (FW)

Time	Shear Rate	Shear Stress	Viscosity	Shear Stress	Viscosity	Shear Stress	Viscosity	Shear Stress	Viscosity	Shear Stress	Viscosity	Shear Stress	Viscosity	Shear Stress	Viscosity
[s]	[1/s]	[Pa]	[Pa.s]	[Pa]	[Pa.s]	[Pa]	[Pa.s]	[Pa]	[Pa.s]	[Pa]	[Pa.s]	[Pa]	[Pa.s]	[Pa]	[Pa.s]
Number of Intervals:		*BT-CNC-WDFs (6 wt %) 0.0 % 20°C*	*BT-CNC-WDFs (6 wt %) 0.0 % 20°C*	*BT-CNC-WDFs (6 wt %) 0.4 % 20°C*	*BT-CNC-WDFs (6 wt %) 0.4 % 20°C*	*BT-CNC-WDFs (6 wt %) 0.8 % 20°C*	*BT-CNC-WDFs (6 wt %) 0.8 % 20° C*	*BT-CNC-WDFs (6 wt. %) 1.2 % 20° C*	*BT-CNC-WDFs (6 wt %) 1.2 % 20° C*	*BT-CNC-WDFs (6 wt %) 1.6 % 20° C*	*BT-CNC-WDFs (6 wt %) 1.6 % 20° C*	*BT-CNC-WDFs (6 wt %) 2.0 % 20° C*	*BT-CNC-WDFs (6 wt %) 2.0 % 20° C*	*BT-CNC-WDFs (6 wt %) 2.4 % 20° C*	*BT-CNC-WDFs (6 wt %) 2.4 % 20° C*
2	0,999	0,168	0,169	1,79	1,79	0,649	0,649	0,971	0,973	0,617	0,617	0,0616	0,0617	1,6	1,6
4	13,1	0,502	0,0383	0,609	0,0465	0,11	0,0084	0,336	0,0256	0,811	0,0619	3,57	0,272	5,71	0,436
6	25,2	0,833	0,033	0,278	0,011	0,18	0,00715	0,391	0,0155	1,64	0,0649	5,23	0,208	7,74	0,307
8	37,3	1,2	0,0322	0,0743	0,00199	0,631	0,0169	0,916	0,0245	2,28	0,0611	5,75	0,154	8,23	0,22
10	49,4	1,36	0,0275	0,11	0,00223	0,894	0,0181	1,33	0,0269	2,67	0,0541	6,17	0,125	8,78	0,178
12	61,6	1,64	0,0266	0,422	0,00686	1,13	0,0184	1,68	0,0274	3,1	0,0503	6,58	0,107	9,35	0,152
14	73,7	1,86	0,0253	0,567	0,0077	1,38	0,0187	2,02	0,0274	3,46	0,0469	7,14	0,097	9,99	0,136
16	85,8	2,14	0,0249	0,718	0,00837	1,71	0,0199	2,4	0,028	3,8	0,0443	7,74	0,0902	10,8	0,125
18	97,9	2,4	0,0246	0,943	0,00963	1,97	0,0201	2,73	0,0279	4,22	0,0431	8,21	0,0839	11,4	0,116
20	110	2,63	0,0239	1,15	0,0104	2,17	0,0198	3,07	0,0279	4,59	0,0418	8,71	0,0792	12,1	0,11
22	122	2,9	0,0238	1,35	0,0111	2,41	0,0197	3,34	0,0274	5,01	0,0411	9,29	0,0761	12,7	0,104
24	134	3,16	0,0235	1,55	0,0116	2,68	0,02	3,6	0,0268	5,34	0,0398	9,86	0,0735	13,4	0,0997
26	146	3,36	0,023	1,8	0,0123	2,85	0,0195	3,93	0,0269	5,67	0,0388	10,4	0,0708	14	0,0956
28	158	3,59	0,0226	1,94	0,0122	3,09	0,0195	4,22	0,0267	6,04	0,0381	10,8	0,0681	14,5	0,0915
30	171	3,8	0,0223	2,17	0,0127	3,33	0,0195	4,46	0,0262	6,26	0,0367	11,2	0,0657	15	0,088
32	183	4,03	0,0221	2,32	0,0127	3,6	0,0197	4,68	0,0256	6,56	0,0359	11,6	0,0635	15,6	0,0852
34	195	4,25	0,0218	2,51	0,0129	3,84	0,0197	4,91	0,0252	6,94	0,0356	12	0,0615	16,2	0,0832
36	207	4,4	0,0213	2,71	0,0131	4,05	0,0196	5,21	0,0252	7,22	0,0349	12,3	0,0596	16,6	0,0805
38	219	4,63	0,0211	2,85	0,013	4,26	0,0195	5,37	0,0245	7,49	0,0342	12,6	0,0577	17,1	0,0783
40	231	4,77	0,0206	3	0,013	4,45	0,0192	5,64	0,0244	7,72	0,0334	13	0,0563	17,6	0,0761
42	243	4,95	0,0203	3,18	0,0131	4,64	0,0191	5,88	0,0242	8,03	0,033	13,3	0,0548	18	0,0739
44	255	5,19	0,0203	3,34	0,0131	4,88	0,0191	6,06	0,0237	8,33	0,0326	13,7	0,0536	18,4	0,0723
46	267	5,39	0,0201	3,56	0,0133	5,11	0,0191	6,26	0,0234	8,47	0,0317	14	0,0524	18,9	0,0709
48	280	5,61	0,0201	3,71	0,0133	5,33	0,0191	6,53	0,0233	8,81	0,0315	14,4	0,0514	19,3	0,0691
50	292	5,75	0,0197	3,91	0,0134	5,49	0,0188	6,79	0,0233	9,05	0,031	14,7	0,0503	19,7	0,0677
52	304	5,98	0,0197	4,09	0,0135	5,73	0,0189	6,99	0,023	9,29	0,0306	14,9	0,049	20,2	0,0665
54	316	6,17	0,0195	4,28	0,0136	5,97	0,0189	7,22	0,0228	9,57	0,0303	15,2	0,048	20,4	0,0647
56	328	6,41	0,0195	4,43	0,0135	6,16	0,0188	7,47	0,0228	9,9	0,0302	15,6	0,0475	20,9	0,0636
58	340	6,61	0,0194	4,68	0,0138	6,45	0,019	7,6	0,0224	10	0,0295	15,8	0,0465	21,3	0,0628
60	352	6,82	0,0194	4,87	0,0138	6,68	0,019	7,81	0,0222	10,2	0,0291	16	0,0456	21,7	0,0617
62	364	7	0,0192	5	0,0137	6,83	0,0188	8,09	0,0222	10,5	0,0289	16,4	0,0451	22,1	0,0606
64	376	7,22	0,0192	5,26	0,014	7,11	0,0189	8,28	0,022	10,7	0,0285	16,6	0,0442	22,5	0,0598
66	389	7,42	0,0191	5,46	0,014	7,25	0,0187	8,5	0,0219	11	0,0282	17	0,0437	22,7	0,0584
68	401	7,59	0,0189	5,63	0,014	7,49	0,0187	8,68	0,0217	11,1	0,0277	17,2	0,0429	23	0,0574
70	413	7,84	0,019	5,73	0,0139	7,71	0,0187	8,85	0,0214	11,4	0,0276	17,4	0,0421	23,4	0,0566
72	425	8,08	0,019	5,93	0,0139	8	0,0188	9,01	0,0212	11,6	0,0274	17,5	0,0413	23,7	0,0557
74	437	8,19	0,0187	6,07	0,0139	8,09	0,0185	9,27	0,0212	11,9	0,0272	17,9	0,041	24	0,0549
76	449	8,38	0,0187	6,35	0,0141	8,34	0,0186	9,41	0,021	12	0,0267	18	0,04	24,4	0,0543

78	461	8,53	0,0185	6,87	0,0149	8,31	0,018	9,46	0,0205	11,8	0,0255	18,3	0,0396	24,5	0,0531
80	473	8,76	0,0185	6,62	0,014	8,7	0,0184	9,82	0,0208	12,3	0,0261	18,4	0,0389	24,9	0,0526
82	485	8,93	0,0184	6,87	0,0142	8,9	0,0183	9,99	0,0206	12,5	0,0257	18,6	0,0383	25,2	0,052
84	498	9,06	0,0182	6,99	0,014	8,99	0,0181	10,3	0,0206	12,7	0,0255	18,9	0,0379	25,4	0,051
86	510	9,25	0,0181	7,19	0,0141	9,18	0,018	10,4	0,0205	12,8	0,0251	19	0,0373	25,6	0,0503
88	522	9,54	0,0183	7,35	0,0141	9,51	0,0182	10,5	0,0201	13	0,0249	19,2	0,0368	25,9	0,0497
90	534	9,65	0,0181	7,5	0,014	9,62	0,018	10,7	0,02	13,2	0,0246	19,3	0,0362	26,2	0,049
92	546	9,87	0,0181	7,61	0,0139	9,81	0,018	10,9	0,0199	13,4	0,0245	19,6	0,0359	26,4	0,0484
94	558	9,98	0,0179	7,8	0,014	9,92	0,0178	11,1	0,0199	13,5	0,0242	19,7	0,0353	26,6	0,0477
96	570	10,2	0,018	7,86	0,0138	10,2	0,0178	11,2	0,0197	13,8	0,0241	20	0,035	26,9	0,0472
98	582	10,4	0,0179	8,03	0,0138	10,4	0,0178	11,3	0,0194	14	0,024	20,2	0,0347	27,2	0,0467
100	594	10,5	0,0177	8,22	0,0138	10,5	0,0176	11,6	0,0195	14,1	0,0237	20,2	0,0341	27,4	0,0461
102	607	10,8	0,0177	8,43	0,0139	10,8	0,0178	11,7	0,0192	14,3	0,0235	20,4	0,0337	27,7	0,0456
104	619	10,9	0,0176	8,58	0,0139	10,9	0,0176	11,8	0,0191	14,5	0,0234	20,5	0,0332	27,9	0,0451
106	631	11	0,0175	8,77	0,0139	11,1	0,0175	12	0,0191	14,6	0,0231	20,7	0,0328	28,2	0,0447
108	643	11,3	0,0175	8,82	0,0137	11,2	0,0175	12,1	0,0188	14,7	0,0229	20,9	0,0325	28,5	0,0443
110	655	11,5	0,0175	9,03	0,0138	11,5	0,0176	12,2	0,0186	14,8	0,0226	21	0,032	28,7	0,0438
112	667	11,6	0,0174	9,14	0,0137	11,6	0,0174	12,3	0,0185	15	0,0226	21,2	0,0318	28,8	0,0431
114	679	11,7	0,0172	9,36	0,0138	11,7	0,0172	12,6	0,0185	15,1	0,0222	21,4	0,0315	28,9	0,0426
116	691	11,9	0,0172	9,45	0,0137	11,9	0,0172	12,7	0,0184	15,3	0,0221	21,6	0,0312	29,2	0,0422
118	703	12,1	0,0172	9,64	0,0137	12,1	0,0172	12,8	0,0182	15,4	0,0219	21,7	0,0309	29,5	0,0419
120	716	12,2	0,017	9,73	0,0136	12,1	0,017	13	0,0182	15,7	0,0219	22	0,0307	29,5	0,0412
122	728	12,5	0,0172	9,88	0,0136	12,5	0,0172	13,1	0,018	15,9	0,0218	22,1	0,0304	29,9	0,0411
124	740	12,6	0,0171	10	0,0136	12,6	0,0171	13,2	0,0179	15,9	0,0215	22,3	0,0301	30	0,0406
126	752	12,7	0,0168	10,2	0,0136	12,6	0,0168	13,5	0,018	16,1	0,0214	22,4	0,0297	30,1	0,04
128	764	12,9	0,0169	10,4	0,0136	12,9	0,0169	13,6	0,0178	16,3	0,0213	22,6	0,0295	30,3	0,0397
130	776	13	0,0168	10,6	0,0136	13,1	0,0169	13,8	0,0178	16,3	0,0211	22,6	0,0292	30,5	0,0393
132	788	13,2	0,0167	10,7	0,0136	13,3	0,0169	13,9	0,0176	16,5	0,0209	22,8	0,0289	30,7	0,039
134	800	13,3	0,0166	10,8	0,0135	13,3	0,0166	14,2	0,0177	16,7	0,0209	23,1	0,0288	30,7	0,0383
136	812	13,5	0,0166	10,9	0,0134	13,5	0,0166	14,3	0,0176	16,9	0,0209	23,3	0,0286	30,9	0,0381
138	825	13,5	0,0163	11,3	0,0138	13,6	0,0165	14,5	0,0176	17	0,0206	23,5	0,0285	31,4	0,0381
140	837	13,9	0,0166	11,3	0,0135	13,9	0,0167	14,5	0,0173	17,2	0,0205	23,5	0,0281	31,3	0,0374
142	849	14	0,0165	11,5	0,0135	14,1	0,0166	14,7	0,0173	17,3	0,0204	23,6	0,0278	31,4	0,0371
144	861	14,1	0,0164	11,7	0,0135	14,2	0,0165	14,9	0,0173	17,4	0,0203	23,7	0,0276	31,6	0,0367
146	873	14,4	0,0165	11,8	0,0135	14,5	0,0166	15	0,0172	17,6	0,0202	23,9	0,0274	31,8	0,0364
148	885	14,5	0,0164	12	0,0136	14,6	0,0165	15,1	0,0171	17,6	0,0199	23,9	0,027	32	0,0362
150	897	14,7	0,0164	12,1	0,0135	14,8	0,0165	15,2	0,017	17,9	0,02	24,1	0,0268	32,2	0,0358
152	909	14,8	0,0162	12,2	0,0134	14,8	0,0163	15,6	0,0171	18,1	0,0199	24,4	0,0268	32,1	0,0353
154	921	15	0,0162	12,3	0,0134	15,1	0,0163	15,6	0,0169	18,2	0,0197	24,5	0,0265	32,4	0,0352
156	934	15,1	0,0161	12,5	0,0134	15,2	0,0163	15,8	0,0169	18,3	0,0196	24,6	0,0263	32,5	0,0349
158	946	15,3	0,0162	12,7	0,0134	15,4	0,0163	15,9	0,0168	18,5	0,0196	24,7	0,0262	32,7	0,0346
160	958	15,4	0,016	12,9	0,0135	15,4	0,0161	16,2	0,0169	18,5	0,0193	24,8	0,0259	32,9	0,0343
162	970	15,5	0,016	13,1	0,0135	15,6	0,0161	16,3	0,0168	18,7	0,0193	25	0,0258	33,1	0,0341
164	982	15,8	0,0161	13,2	0,0135	16	0,0163	16,3	0,0166	18,8	0,0192	25,1	0,0255	33,2	0,0338
166	994	15,9	0,016	13,5	0,0136	16	0,0161	16,6	0,0167	19,1	0,0192	25,3	0,0255	33,3	0,0335
168	1 010	16	0,0159	13,9	0,0138	16,2	0,0161	16,7	0,0166	19,2	0,0191	25,5	0,0253	33,5	0,0333
170	1 020	16,2	0,016	14,2	0,014	16,4	0,0161	16,9	0,0166	19,5	0,0191	25,6	0,0252	33,6	0,033
172	1 030	16,3	0,0158	14,8	0,0143	16,6	0,0161	16,9	0,0164	19,3	0,0188	25,7	0,025	33,8	0,0328
174	1 040	16,5	0,0158	15,1	0,0145	16,7	0,0161	17,1	0,0164	19,3	0,0185	26	0,0249	33,8	0,0325
176	1 050	16,8	0,016	15,8	0,015	17,1	0,0162	17,2	0,0163	19,3	0,0183	26	0,0247	34	0,0323
178	1 070	17,4	0,0163	16	0,015	17,4	0,0163	17,4	0,0163	19,6	0,0184	26,4	0,0247	34,2	0,032
180	1 080	17,9	0,0166	16,6	0,0153	17,9	0,0166	17,6	0,0163	19,7	0,0183	26,4	0,0245	34,3	0,0318
182	1 090	18,3	0,0168	17	0,0156	18,2	0,0167	17,9	0,0164	19,9	0,0182	26,6	0,0244	34,5	0,0316
184	1 100	18,9	0,0171	17,4	0,0157	18,7	0,017	18	0,0163	20,2	0,0183	26,8	0,0243	34,8	0,0316
186	1 120	19,3	0,0173	17,6	0,0158	19,1	0,0171	18,2	0,0163	20,2	0,0181	26,8	0,024	34,9	0,0313
188	1 130	19,9	0,0176	17,6	0,0156	19,6	0,0174	18	0,016	20,3	0,018	27	0,0239	35,1	0,0312

190	1 140	20,4	0,0179	17,7	0,0156	20	0,0175	18,1	0,0159	20,6	0,0181	27,3	0,024	35,2	0,0309
192	1 150	20,9	0,0181	18,1	0,0157	20,5	0,0178	18,4	0,016	20,7	0,018	27,5	0,0238	35,4	0,0308
194	1 160	21	0,018	18,3	0,0158	21	0,018	18,7	0,0161	21	0,018	27,8	0,0239	35,6	0,0306
196	1 180	21,2	0,018	18,7	0,0159	21,6	0,0183	19,6	0,0167	21,1	0,018	28	0,0238	35,8	0,0305
198	1 190	21,4	0,018	18,8	0,0159	21,9	0,0185	20	0,0169	21,4	0,0181	28,3	0,0238	36	0,0303
200	1 200	21,7	0,0181	19,1	0,0159	22,3	0,0186	20,4	0,017	21,7	0,0181	28,4	0,0237	36,2	0,0302

Time	Shear Rate	Shear Stress	Viscosity	Shear Stress	Viscosity	Shear Stress	Viscosity	Shear Stress	Viscosity	Shear Stress	Viscosity	Shear Stress	Viscosity	Shear Stress	Viscosity
[s]	[1/s]	[Pa]	[Pa·s]	[Pa]	[Pa·s]	[Pa]	[Pa·s]	[Pa]	[Pa·s]	[Pa]	[Pa·s]	[Pa]	[Pa·s]	[Pa]	[Pa·s]
Number of Intervals:		*BT-CNC-WDFs (6 wt %) 0.0 % 30°C*	*BT-CNC-WDFs (6 wt %) 0.0 % 30°C*	*BT-CNC-WDFs (6 wt %) 0.4 % 30°C*	*BT-CNC-WDFs (6 wt %) 0.4 % 30°C*	*BT-CNC-WDFs (6 wt %) 0.8 % 30°C*	*BT-CNC-WDFs (6 wt %) 0.8 % 30°C*	*BT-CNC-WDFs (6 wt %) 1.2 % 30°C*	*BT-CNC-WDFs (6 wt %) 1.2 % 30°C*	*BT-CNC-WDFs (6 wt %) 1.6 % 30°C*	*BT-CNC-WDFs (6 wt %) 1.6 % 30°C*	*BT-CNC-WDFs (6 wt %) 2.0 % 30°C*	*BT-CNC-WDFs (6 wt %) 2.0 % 30°C*	*BT-CNC-WDFs (6 wt %) 2.4 % 30°C*	*BT-CNC-WDFs (6 wt %) 2.4 % 30°C*
2	0,999	0,00899	0,009	0,323	0,323	0,953	0,954	0,643	0,644	0,147	0,147	0,434	0,434	2,15	2,15
4	13,1	1,65	0,126	0,089	0,00679	0,564	0,043	0,417	0,0318	2,11	0,161	3,41	0,26	7,17	0,547
6	25,2	1,94	0,0768	0,285	0,0113	0,0701	0,00278	1,15	0,0454	3,01	0,119	5,49	0,218	8,76	0,347
8	37,3	2,28	0,0612	0,464	0,0124	0,565	0,0151	1,63	0,0436	3,7	0,0991	6,42	0,172	9,8	0,262
10	49,4	2,43	0,0491	0,679	0,0137	0,973	0,0197	1,97	0,0398	4,36	0,0882	7,17	0,145	10,9	0,221
12	61,6	2,72	0,0442	0,787	0,0128	1,33	0,0216	2,42	0,0393	4,92	0,08	7,97	0,13	11,9	0,193
14	73,7	2,89	0,0392	1,05	0,0142	1,65	0,0224	2,71	0,0368	5,46	0,0741	8,74	0,119	12,9	0,175
16	85,8	3,1	0,0362	1,15	0,0134	1,95	0,0228	3,1	0,0361	6,04	0,0704	9,27	0,108	13,8	0,161
18	97,9	3,35	0,0342	1,35	0,0138	2,25	0,023	3,47	0,0355	6,45	0,0659	9,83	0,1	14,7	0,15
20	110	3,62	0,0329	1,56	0,0142	2,57	0,0234	3,75	0,0341	7,01	0,0637	10,4	0,0948	15,4	0,14
22	122	3,8	0,0311	1,8	0,0147	2,83	0,0232	4,02	0,0329	7,43	0,0608	11,1	0,0905	16,2	0,132
24	134	4,02	0,03	2,03	0,0151	3,07	0,0229	4,31	0,0321	7,84	0,0584	11,6	0,0867	16,8	0,125
26	146	4,31	0,0294	2,23	0,0152	3,34	0,0229	4,65	0,0318	8,23	0,0562	12,2	0,0832	17,5	0,12
28	158	4,54	0,0286	2,47	0,0156	3,62	0,0229	4,97	0,0314	8,67	0,0547	12,5	0,0791	18,2	0,115
30	171	4,81	0,0282	2,66	0,0156	3,86	0,0226	5,29	0,031	9,1	0,0533	13,1	0,0765	18,8	0,11
32	183	4,97	0,0272	2,85	0,0156	4,1	0,0224	5,58	0,0305	9,42	0,0516	13,5	0,0741	19,3	0,106
34	195	5,17	0,0266	3,02	0,0155	4,32	0,0222	5,85	0,03	9,72	0,0499	13,9	0,0716	19,8	0,102
36	207	5,36	0,0259	3,24	0,0156	4,57	0,0221	6,04	0,0292	10,1	0,049	14,3	0,0692	20,4	0,0984
38	219	5,6	0,0256	3,41	0,0156	4,75	0,0217	6,34	0,0289	10,4	0,0476	14,8	0,0676	20,8	0,0951
40	231	5,76	0,0249	3,61	0,0156	4,97	0,0215	6,59	0,0285	10,9	0,0469	15,2	0,0657	21,2	0,0919
42	243	5,95	0,0245	3,82	0,0157	5,17	0,0212	6,79	0,0279	11	0,0454	15,6	0,0642	21,7	0,0893
44	255	6,08	0,0238	3,95	0,0155	5,36	0,021	7,08	0,0277	11,3	0,0443	16	0,0628	22,2	0,0869
46	267	6,28	0,0235	4,14	0,0155	5,47	0,0205	7,36	0,0275	11,6	0,0433	16,4	0,0614	22,5	0,0842
48	280	6,48	0,0232	4,35	0,0156	5,7	0,0204	7,59	0,0272	11,8	0,0424	16,7	0,0599	23	0,0822
50	292	6,69	0,0229	4,63	0,0159	5,98	0,0205	7,75	0,0266	12,2	0,0418	17,1	0,0586	23,5	0,0804
52	304	6,85	0,0226	4,77	0,0157	6,14	0,0202	7,98	0,0263	12,4	0,0407	17,5	0,0575	23,9	0,0787
54	316	7,1	0,0225	4,97	0,0157	6,33	0,02	8,28	0,0262	12,6	0,04	17,9	0,0568	24,3	0,0771
56	328	7,24	0,0221	5,16	0,0157	6,63	0,0202	8,5	0,0259	12,9	0,0394	18,2	0,0555	24,8	0,0757
58	340	7,48	0,022	5,33	0,0157	6,72	0,0198	8,77	0,0258	13,2	0,0387	18,6	0,0548	25,2	0,0742
60	352	7,68	0,0218	5,53	0,0157	6,93	0,0197	9	0,0256	13,4	0,0381	19,1	0,0541	25,8	0,0732
62	364	7,85	0,0215	5,8	0,0159	7,26	0,0199	9,15	0,0251	13,7	0,0375	19,3	0,053	26,2	0,072
64	376	8,1	0,0215	6	0,0159	7,41	0,0197	9,43	0,0251	13,9	0,0369	19,7	0,0522	26,6	0,0707
66	389	8,26	0,0213	6,25	0,0161	7,65	0,0197	9,61	0,0247	14,1	0,0362	20	0,0516	27	0,0695
68	401	8,49	0,0212	6,45	0,0161	7,9	0,0197	9,82	0,0245	14,3	0,0358	20,3	0,0506	27,4	0,0683
70	413	8,58	0,0208	6,57	0,0159	8,02	0,0194	10	0,0243	14,5	0,035	20,5	0,0496	27,8	0,0674
72	425	8,8	0,0207	6,72	0,0158	8,13	0,0191	10,3	0,0242	14,6	0,0344	20,8	0,049	28,1	0,0661
74	437	8,95	0,0205	7	0,016	8,42	0,0193	10,4	0,0238	14,9	0,0342	21	0,0481	28,5	0,0651
76	449	9,26	0,0206	7,19	0,016	8,51	0,0189	10,6	0,0237	15,1	0,0337	21,4	0,0477	28,7	0,064
78	461	8,95	0,0194	7,77	0,0169	8,8	0,0191	11,1	0,0241	15,2	0,0329	22,1	0,0479	29,5	0,0639
80	473	9,51	0,0201	7,57	0,016	8,9	0,0188	10,9	0,023	15,6	0,033	21,9	0,0462	29,4	0,0621
82	485	9,73	0,02	7,78	0,016	9,02	0,0186	11,1	0,023	15,8	0,0325	22,3	0,0458	29,6	0,061
84	498	9,83	0,0198	8,01	0,0161	9,3	0,0187	11,2	0,0226	16	0,0322	22,4	0,0451	29,9	0,0602
86	510	10	0,0197	8,21	0,0161	9,41	0,0185	11,4	0,0224	16,2	0,0318	22,7	0,0446	30,3	0,0594
88	522	10,2	0,0195	8,25	0,0158	9,44	0,0181	11,7	0,0224	16,2	0,0311	23	0,044	30,6	0,0587
90	534	10,4	0,0194	8,5	0,0159	9,68	0,0181	11,8	0,0221	16,5	0,0309	23,2	0,0434	30,8	0,0578
92	546	10,5	0,0192	8,6	0,0158	9,85	0,018	12	0,0219	16,7	0,0306	23,4	0,0429	31,1	0,057
94	558	10,7	0,0192	8,84	0,0158	10	0,018	12,1	0,0216	16,9	0,0303	23,6	0,0423	31,4	0,0563
96	570	10,8	0,0189	8,9	0,0156	10,2	0,0178	12,3	0,0215	17,1	0,0299	23,8	0,0417	31,8	0,0558

98	582	10,9	0,0187	9,04	0,0155	10,3	0,0177	12,5	0,0214	17,2	0,0296	24	0,0411	32	0,055
100	594	11,1	0,0187	9,37	0,0158	10,5	0,0177	12,5	0,0211	17,5	0,0295	24	0,0404	32,2	0,0542
102	607	11,3	0,0186	9,42	0,0155	10,5	0,0174	12,8	0,0211	17,5	0,0288	24,2	0,04	32,4	0,0535
104	619	11,5	0,0185	9,63	0,0156	10,7	0,0174	12,9	0,0209	17,7	0,0286	24,4	0,0395	32,8	0,053
106	631	11,6	0,0184	9,83	0,0156	10,9	0,0173	13,1	0,0207	17,9	0,0284	24,6	0,039	32,8	0,0521
108	643	11,7	0,0182	9,92	0,0154	11	0,0171	13,3	0,0206	18	0,0279	24,8	0,0386	33,1	0,0516
110	655	11,9	0,0182	9,97	0,0152	11	0,0169	13,5	0,0206	18	0,0276	25	0,0382	33,4	0,051
112	667	12	0,018	10,1	0,0152	11,2	0,0168	13,5	0,0203	18,3	0,0275	25,1	0,0376	33,8	0,0506
114	679	12,2	0,018	10,4	0,0154	11,5	0,0169	13,7	0,0201	18,5	0,0273	25,2	0,0371	33,8	0,0498
116	691	12,3	0,0178	10,6	0,0153	11,6	0,0168	13,8	0,02	18,6	0,027	25,3	0,0366	34	0,0492
118	703	12,5	0,0178	10,7	0,0152	11,7	0,0166	14	0,02	18,8	0,0267	25,5	0,0362	34,2	0,0487
120	716	12,6	0,0176	10,9	0,0152	12	0,0167	14,1	0,0197	19,1	0,0266	25,5	0,0357	34,4	0,0481
122	728	12,7	0,0175	10,9	0,015	12	0,0164	14,4	0,0198	19,1	0,0263	25,9	0,0356	34,7	0,0476
124	740	12,9	0,0174	11,1	0,015	12	0,0163	14,5	0,0197	19,2	0,026	26	0,0351	34,9	0,0472
126	752	13	0,0174	11,4	0,0152	12,4	0,0165	14,6	0,0194	19,6	0,026	26	0,0346	34,9	0,0464
128	764	13,2	0,0172	11,5	0,015	12,4	0,0162	14,8	0,0194	19,6	0,0257	26,3	0,0344	35,1	0,0459
130	776	13,3	0,0172	11,7	0,0151	12,5	0,0161	15	0,0193	19,8	0,0255	26,4	0,034	35,2	0,0454
132	788	13,5	0,0172	11,8	0,015	12,6	0,016	15,2	0,0193	19,9	0,0252	26,6	0,0337	35,4	0,045
134	800	13,6	0,017	12,1	0,0151	12,9	0,0162	15,2	0,019	20,2	0,0252	26,5	0,0331	35,6	0,0445
136	812	13,7	0,0168	12,2	0,015	13	0,0161	15,3	0,0188	20,3	0,025	26,6	0,0328	35,9	0,0441
138	825	13,9	0,0169	12,3	0,0149	13,2	0,016	15,4	0,0187	20,3	0,0247	26,6	0,0323	35,6	0,0432
140	837	14	0,0167	12,4	0,0149	13,2	0,0158	15,7	0,0188	20,5	0,0245	27	0,0323	36	0,043
142	849	14,2	0,0167	12,7	0,0149	13,3	0,0157	15,9	0,0188	20,7	0,0244	27,1	0,032	36,1	0,0425
144	861	14,3	0,0167	12,9	0,0149	13,5	0,0157	16	0,0186	20,8	0,0242	27,2	0,0316	36,1	0,042
146	873	14,4	0,0165	12,9	0,0148	13,5	0,0155	16,2	0,0186	20,9	0,0239	27,3	0,0313	36,4	0,0417
148	885	14,7	0,0166	13	0,0147	13,6	0,0154	16,4	0,0185	21,1	0,0238	27,5	0,0311	36,5	0,0412
150	897	14,8	0,0165	13,2	0,0147	13,7	0,0153	16,5	0,0184	21,2	0,0236	27,6	0,0308	36,7	0,0409
152	909	14,8	0,0163	13,5	0,0149	14,1	0,0155	16,4	0,018	21,4	0,0236	27,6	0,0303	36,8	0,0405
154	921	15	0,0163	13,5	0,0147	14,1	0,0153	16,6	0,018	21,5	0,0233	27,7	0,0301	36,9	0,0401
156	934	15,1	0,0162	13,8	0,0147	14,4	0,0154	16,8	0,018	21,7	0,0232	27,8	0,0298	36,9	0,0395
158	946	15,3	0,0162	13,8	0,0146	14,3	0,0152	17,1	0,0181	21,7	0,023	28	0,0296	36,9	0,039
160	958	15,5	0,0162	14,1	0,0147	14,6	0,0153	17,2	0,018	22	0,023	28	0,0293	36,9	0,0386
162	970	15,6	0,0161	14,3	0,0147	14,7	0,0151	17,4	0,0179	22,2	0,0229	28,2	0,0291	37,1	0,0382
164	982	15,9	0,0161	14,3	0,0146	14,8	0,015	17,5	0,0179	22,2	0,0226	28,3	0,0289	37,2	0,0379
166	994	15,8	0,0159	14,9	0,015	15	0,0151	17,5	0,0176	22,4	0,0226	28,4	0,0285	37,4	0,0376
168	1 010	16	0,0159	15,2	0,0151	15,1	0,015	17,7	0,0176	22,5	0,0224	28,5	0,0283	37,6	0,0373
170	1 020	16,1	0,0158	15,5	0,0153	15,3	0,015	17,8	0,0175	22,7	0,0223	28,6	0,0281	37,7	0,037
172	1 030	16,4	0,0159	16,2	0,0157	15,4	0,0149	18,1	0,0176	22,9	0,0222	28,8	0,028	37,7	0,0366
174	1 040	16,5	0,0159	16,7	0,016	15,7	0,015	18,2	0,0174	23,2	0,0222	28,9	0,0277	38	0,0364
176	1 050	16,8	0,0159	17	0,0161	15,8	0,015	18,5	0,0175	23,2	0,022	29,1	0,0276	38	0,036
178	1 070	16,8	0,0157	17,4	0,0163	16,2	0,0152	18,5	0,0173	23,4	0,0219	29,2	0,0274	38,4	0,036
180	1 080	17	0,0158	17,9	0,0165	16,5	0,0153	18,8	0,0174	23,5	0,0218	29,3	0,0272	38,4	0,0356
182	1 090	17,2	0,0158	18,3	0,0168	16,9	0,0155	18,9	0,0173	23,8	0,0218	29,3	0,0268	38,5	0,0353
184	1 100	17,5	0,0158	18,2	0,0165	17,2	0,0156	19,1	0,0173	23,8	0,0216	29,4	0,0267	38,7	0,0351
186	1 120	18,1	0,0162	18,5	0,0166	17,5	0,0157	19,4	0,0174	24	0,0215	29,5	0,0265	38,5	0,0346
188	1 130	18,6	0,0165	18,8	0,0167	17,9	0,0159	19,6	0,0174	24,2	0,0214	29,7	0,0263	38,6	0,0342
190	1 140	19	0,0167	19	0,0167	18,4	0,0161	19,8	0,0173	24,4	0,0214	29,7	0,0261	38,8	0,034
192	1 150	19,6	0,017	19,3	0,0168	18,8	0,0164	20	0,0174	24,5	0,0213	29,9	0,0259	38,7	0,0336
194	1 160	20,1	0,0173	19,6	0,0169	19,4	0,0167	20,4	0,0175	24,8	0,0213	30	0,0258	39,1	0,0336
196	1 180	20,6	0,0175	19,9	0,017	19,9	0,0169	20,7	0,0176	25	0,0212	30	0,0255	39,2	0,0333
198	1 190	21	0,0177	20,2	0,017	20,5	0,0172	21	0,0177	25,2	0,0212	30,2	0,0254	39,5	0,0333

200	1 200	21,4	0,0178	20,4	0,017	20,7	0,0173	21,4	0,0179	25,3	0,0211	30,3	0,0253	39,7	0,0331

Time	Shear Rate	Shear Stress	Viscosity	Shear Stress	Viscosity	Shear Stress	Viscosity	Shear Stress	Viscosity	Shear Stress	Viscosity	Shear Stress	Viscosity	Shear Stress	Viscosity
[s]	[1/s]	[Pa]	[Pa·s]	[Pa]	[Pa·s]	[Pa]	[Pa·s]	[Pa]	[Pa·s]	[Pa]	[Pa·s]	[Pa]	[Pa·s]	[Pa]	[Pa·s]
Number of Intervals:		BT-CNC-WDFs (6 wt %) 0.0 % 40°C	BT-CNC-WDFs (6 wt %) 0.0 % 40°C	BT-CNC-WDFs (6 wt %) 0.4 % 40°C	BT-CNC-WDFs (6 wt %) 0.4 % 40°C	BT-CNC-WDFs (6 wt %) 0.8 % 40°C	BT-CNC-WDFs (6 wt %) 0.8 % 40°C	BT-CNC-WDFs (6 wt %) 1.2 % 40°C	BT-CNC-WDFs (6 wt %) 1.2 % 40°C	BT-CNC-WDFs (6 wt %) 1.6 % 40°C	BT-CNC-WDFs (6 wt %) 1.6 % 40°C	BT-CNC-WDFs (6 wt %) 2.0 % 40°C	BT-CNC-WDFs (6 wt %) 2.0 % 40°C	BT-CNC-WDFs (6 wt %) 2.4 % 40°C	BT-CNC-WDFs (6 wt %) 2.4 % 40°C
2	0,999	0,113	0,113	1,46	1,46	0,301	0,301	0,49	0,49	1,04	1,04	0,449	0,45	1,16	1,16
4	13,1	1,22	0,0933	0,156	0,0119	0,258	0,0197	0,634	0,0484	1,6	0,122	4,56	0,348	6,6	0,503
6	25,2	1,61	0,0639	0,467	0,0185	0,76	0,0301	1,56	0,0618	2,83	0,112	6,54	0,259	9,66	0,383
8	37,3	1,76	0,047	0,818	0,0219	1,19	0,0318	2,36	0,0632	3,56	0,0954	7,57	0,203	10,5	0,282
10	49,4	2,07	0,0418	1,09	0,0221	1,57	0,0317	2,9	0,0587	4,25	0,0859	8,43	0,17	11,4	0,23
12	61,6	2,26	0,0367	1,3	0,0211	1,96	0,0319	3,37	0,0547	4,8	0,0781	9,16	0,149	12,3	0,199
14	73,7	2,51	0,034	1,55	0,021	2,21	0,0299	3,84	0,0521	5,43	0,0737	9,78	0,133	13,2	0,179
16	85,8	2,64	0,0308	1,76	0,0205	2,61	0,0305	4,27	0,0498	5,85	0,0682	10,4	0,122	13,8	0,161
18	97,9	2,81	0,0287	1,96	0,02	2,93	0,03	4,67	0,0477	6,36	0,065	11,1	0,113	14,5	0,148
20	110	2,99	0,0272	2,11	0,0192	3,23	0,0294	5,1	0,0464	6,8	0,0618	11,6	0,105	15,5	0,14
22	122	3,16	0,0258	2,36	0,0193	3,52	0,0289	5,5	0,0451	7,26	0,0595	12,2	0,0995	15,9	0,13
24	134	3,43	0,0256	2,67	0,0199	3,79	0,0283	5,87	0,0437	7,69	0,0573	12,5	0,0934	16,5	0,123
26	146	3,57	0,0244	2,9	0,0198	4,12	0,0281	6,25	0,0427	8,09	0,0553	13	0,0891	17,1	0,117
28	158	3,81	0,024	3,13	0,0198	4,43	0,028	6,63	0,0419	8,47	0,0535	13,4	0,0846	17,7	0,112
30	171	3,98	0,0233	3,33	0,0195	4,74	0,0278	6,97	0,0408	8,87	0,052	13,9	0,0817	18,2	0,107
32	183	4,18	0,0229	3,61	0,0198	4,95	0,0271	7,26	0,0397	9,27	0,0507	14,3	0,0784	18,9	0,103
34	195	4,34	0,0223	3,8	0,0195	5,17	0,0266	7,54	0,0387	9,54	0,049	14,8	0,0758	19,4	0,0997
36	207	4,45	0,0215	3,95	0,0191	5,46	0,0264	7,79	0,0377	9,78	0,0473	15,1	0,073	19,9	0,0961
38	219	4,63	0,0211	4,18	0,0191	5,68	0,0259	8,04	0,0367	10,2	0,0465	15,5	0,0708	20,4	0,0931
40	231	4,77	0,0206	4,37	0,0189	5,92	0,0256	8,34	0,0361	10,5	0,0452	15,9	0,0687	20,9	0,0902
42	243	4,87	0,02	4,53	0,0186	6,16	0,0253	8,6	0,0353	10,8	0,0442	16,3	0,067	21,4	0,088
44	255	5,08	0,0199	4,76	0,0187	6,35	0,0249	8,82	0,0346	11,1	0,0434	16,6	0,0652	21,7	0,0852
46	267	5,22	0,0195	4,93	0,0184	6,49	0,0243	9,03	0,0338	11,3	0,0424	17	0,0637	22	0,0824
48	280	5,43	0,0194	5,16	0,0185	6,73	0,0241	9,28	0,0332	11,7	0,0417	17,4	0,0621	22,3	0,0799
50	292	5,57	0,0191	5,31	0,0182	7,06	0,0242	9,59	0,0329	11,9	0,0409	17,7	0,0607	22,7	0,0779
52	304	5,78	0,019	5,53	0,0182	7,23	0,0238	9,84	0,0324	12,2	0,0403	18	0,0594	23,2	0,0764
54	316	5,91	0,0187	5,72	0,0181	7,41	0,0235	10	0,0317	12,5	0,0396	18,4	0,0583	23,6	0,0746
56	328	6,17	0,0188	5,96	0,0182	7,68	0,0234	10,3	0,0314	12,8	0,039	18,6	0,0568	23,8	0,0725
58	340	6,27	0,0184	6,14	0,0181	7,81	0,023	10,5	0,0308	13,1	0,0384	19	0,0559	23,5	0,069
60	352	6,45	0,0183	6,36	0,0181	8,04	0,0228	10,6	0,0302	13,3	0,0378	19,3	0,0549	23,9	0,0678
62	364	6,75	0,0185	6,58	0,018	8,37	0,023	10,9	0,03	13,6	0,0373	19,6	0,0538	24,3	0,0666
64	376	6,84	0,0182	6,74	0,0179	8,53	0,0227	11,1	0,0294	13,8	0,0366	20	0,0532	24,5	0,0652
66	389	7,02	0,0181	6,96	0,0179	8,76	0,0225	11,2	0,0289	14	0,036	20,3	0,0521	24,9	0,0641
68	401	7,18	0,0179	7,12	0,0178	8,97	0,0224	11,4	0,0285	14,3	0,0356	20,5	0,0513	25,3	0,063
70	413	7,43	0,018	7,41	0,018	9,16	0,0222	11,5	0,028	14,6	0,0353	20,7	0,0501	25,6	0,0621
72	425	7,59	0,0179	7,55	0,0178	9,28	0,0218	11,7	0,0275	14,8	0,0349	20,9	0,0492	25,9	0,061
74	437	7,77	0,0178	7,69	0,0176	9,55	0,0219	12	0,0274	15,1	0,0345	21,1	0,0482	26,3	0,0601
76	449	7,81	0,0174	7,8	0,0174	9,67	0,0215	12,1	0,0269	15,2	0,0339	21,4	0,0475	26,4	0,0588
78	461	8,36	0,0181	8,29	0,018	10,2	0,0222	12,1	0,0263	15,2	0,0329	21,2	0,0461	27,1	0,0588
80	473	8,23	0,0174	8,18	0,0173	10,1	0,0213	12,4	0,0263	15,6	0,033	21,8	0,046	27,1	0,0572
82	485	8,3	0,0171	8,26	0,017	10,2	0,021	12,6	0,026	15,7	0,0324	22,1	0,0456	27,2	0,0561
84	498	8,53	0,0171	8,4	0,0169	10,5	0,021	12,8	0,0258	15,9	0,032	22,2	0,0447	27,6	0,0554
86	510	8,62	0,0169	8,53	0,0167	10,6	0,0208	13	0,0255	16,1	0,0317	22,6	0,0443	27,8	0,0546
88	522	8,91	0,0171	8,85	0,017	10,6	0,0204	13	0,0249	16,4	0,0315	22,8	0,0436	28	0,0536
90	534	8,98	0,0168	8,95	0,0168	10,9	0,0203	13,2	0,0248	16,5	0,0309	22,9	0,043	28,3	0,0529
92	546	9,2	0,0168	9,18	0,0168	11	0,0202	13,3	0,0244	16,7	0,0306	23,1	0,0422	28,6	0,0524
94	558	9,31	0,0167	9,26	0,0166	11,2	0,0201	13,5	0,0243	16,8	0,0302	23,3	0,0417	28,8	0,0516
96	570	9,58	0,0168	9,56	0,0168	11,3	0,0198	13,8	0,0241	17,2	0,0301	23,3	0,0409	29,2	0,0512
98	582	9,73	0,0167	9,74	0,0167	11,4	0,0196	13,9	0,0238	17,3	0,0298	23,5	0,0404	29,5	0,0506
100	594	9,85	0,0166	9,76	0,0164	11,7	0,0197	14,2	0,0238	17,4	0,0293	23,7	0,0398	29,6	0,0499

102	607	9,94	0,0164	9,98	0,0165	11,7	0,0193	14,2	0,0235	17,6	0,029	23,8	0,0392	29,8	0,0491
104	619	10,1	0,0163	10,1	0,0163	11,9	0,0192	14,4	0,0233	17,7	0,0286	24	0,0387	30	0,0486
106	631	10,1	0,0161	10,2	0,0161	12,1	0,0191	14,5	0,023	17,8	0,0282	24,1	0,0382	30,2	0,0478
108	643	10,4	0,0162	10,5	0,0163	12,1	0,0188	14,6	0,0228	18,1	0,0282	24,1	0,0376	30,4	0,0474
110	655	10,5	0,016	10,6	0,0162	12,2	0,0186	14,6	0,0223	18,3	0,0279	24,4	0,0373	30,5	0,0466
112	667	10,7	0,016	10,7	0,0161	12,4	0,0186	14,8	0,0222	18,4	0,0277	24,4	0,0366	30,8	0,0461
114	679	10,7	0,0157	10,7	0,0157	12,6	0,0185	15	0,0221	18,4	0,027	24,6	0,0363	30,8	0,0454
116	691	10,9	0,0158	10,9	0,0158	12,7	0,0184	15,1	0,0219	18,6	0,0269	24,7	0,0358	31	0,0449
118	703	11	0,0156	11,1	0,0157	12,8	0,0182	15,2	0,0217	18,7	0,0266	24,8	0,0353	31,2	0,0443
120	716	11,2	0,0157	11,2	0,0156	13	0,0182	15,5	0,0217	18,9	0,0264	24,9	0,0348	31,4	0,0439
122	728	11,4	0,0156	11,5	0,0157	13	0,0179	15,5	0,0213	19,1	0,0263	25,1	0,0345	31,6	0,0434
124	740	11,5	0,0156	11,6	0,0157	13,2	0,0178	15,7	0,0212	19,3	0,0261	25,2	0,034	31,7	0,0429
126	752	11,6	0,0154	11,5	0,0153	13,4	0,0179	15,9	0,0211	19,3	0,0257	25,3	0,0336	31,9	0,0424
128	764	11,8	0,0154	11,8	0,0154	13,5	0,0176	15,9	0,0208	19,5	0,0255	25,5	0,0333	32,1	0,042
130	776	11,9	0,0154	11,9	0,0153	13,6	0,0176	16,1	0,0207	19,6	0,0253	25,6	0,033	32,1	0,0414
132	788	11,9	0,0151	12,1	0,0153	13,7	0,0173	16,1	0,0205	19,7	0,025	25,8	0,0327	32,2	0,0409
134	800	12,2	0,0152	12,1	0,0151	13,9	0,0174	16,4	0,0205	19,8	0,0248	25,8	0,0323	32,3	0,0404
136	812	12,4	0,0152	12,3	0,0151	14	0,0173	16,6	0,0204	20,1	0,0247	25,9	0,0318	32,5	0,04
138	825	12,3	0,015	12,3	0,015	14,2	0,0172	16,8	0,0203	20	0,0242	26,1	0,0316	32,5	0,0395
140	837	12,6	0,0151	12,7	0,0151	14,2	0,0169	16,7	0,0199	20,4	0,0244	26,1	0,0312	32,8	0,0392
142	849	12,7	0,015	12,7	0,015	14,3	0,0169	16,8	0,0198	20,5	0,0241	26,3	0,031	33	0,0389
144	861	12,8	0,0148	12,8	0,0149	14,5	0,0168	16,9	0,0197	20,5	0,0239	26,4	0,0306	33,1	0,0384
146	873	13	0,0149	13,1	0,015	14,5	0,0166	17	0,0195	20,8	0,0238	26,4	0,0303	33,2	0,0381
148	885	13	0,0146	13	0,0147	14,6	0,0165	17,1	0,0193	20,7	0,0234	26,6	0,0301	33,2	0,0375
150	897	13,2	0,0147	13,3	0,0148	14,8	0,0165	17,2	0,0192	21	0,0234	26,7	0,0297	33,3	0,0371
152	909	13,4	0,0147	13,4	0,0148	15,1	0,0166	17,5	0,0193	21,1	0,0232	26,7	0,0294	33,6	0,0369
154	921	13,4	0,0146	13,6	0,0147	15,1	0,0164	17,5	0,019	21,2	0,023	26,9	0,0292	33,6	0,0365
156	934	13,5	0,0144	13,6	0,0146	15,2	0,0163	17,7	0,0189	21,3	0,0228	27	0,029	33,7	0,0361
158	946	13,5	0,0143	13,8	0,0146	15,2	0,0161	17,7	0,0188	21,5	0,0227	27,1	0,0286	33,8	0,0358
160	958	13,5	0,0141	13,8	0,0144	15,3	0,016	17,9	0,0187	21,5	0,0224	27,3	0,0285	33,8	0,0353
162	970	13,6	0,0141	13,9	0,0143	15,5	0,016	18,1	0,0187	21,6	0,0223	27,3	0,0282	33,8	0,0349
164	982	13,8	0,0141	14,2	0,0144	15,5	0,0157	18,1	0,0184	21,9	0,0223	27,4	0,0279	34,1	0,0347
166	994	14	0,0141	14,2	0,0143	15,7	0,0158	18,4	0,0185	22	0,0221	27,5	0,0276	34,2	0,0344
168	1 010	14,1	0,014	14,4	0,0143	15,8	0,0157	18,4	0,0183	22,1	0,022	27,6	0,0274	34,3	0,0341
170	1 020	14,4	0,0142	14,7	0,0144	16	0,0157	18,6	0,0182	22,3	0,0219	27,6	0,0271	34,4	0,0338
172	1 030	14,6	0,0142	14,9	0,0144	16	0,0155	18,7	0,0182	22,4	0,0217	27,9	0,027	34,4	0,0333
174	1 040	15,1	0,0145	15,2	0,0145	16,2	0,0155	19	0,0182	22,5	0,0216	27,9	0,0268	34,5	0,0331
176	1 050	15,7	0,0148	15,7	0,0149	16,2	0,0153	19	0,018	22,6	0,0214	28,1	0,0267	34,5	0,0328
178	1 070	16,3	0,0153	16,3	0,0152	16,4	0,0154	19,2	0,018	23	0,0215	28,1	0,0263	34,9	0,0327
180	1 080	16,7	0,0154	16,7	0,0154	16,5	0,0153	19,3	0,0179	23,1	0,0214	28,3	0,0262	34,9	0,0324
182	1 090	17	0,0156	17,1	0,0157	16,7	0,0153	19,5	0,0179	23,1	0,0212	28,5	0,0261	35	0,032
184	1 100	17,5	0,0159	17,6	0,016	17	0,0154	19,6	0,0178	23,4	0,0212	28,6	0,0259	35,1	0,0318
186	1 120	17,8	0,016	17,9	0,0161	17,3	0,0155	19,7	0,0176	23,3	0,0209	28,8	0,0258	35,1	0,0315
188	1 130	17,9	0,0159	18,4	0,0163	17,6	0,0156	19,8	0,0176	23,4	0,0208	29	0,0257	35,2	0,0312
190	1 140	18,4	0,0161	18,6	0,0164	18,1	0,0159	20,1	0,0176	23,7	0,0208	29	0,0254	35,6	0,0312
192	1 150	18,5	0,016	18,7	0,0163	18,5	0,016	20,2	0,0176	23,8	0,0207	29,2	0,0254	35,6	0,0309
194	1 160	18,8	0,0161	18,9	0,0162	19,1	0,0164	20,4	0,0176	24	0,0206	29,3	0,0252	35,8	0,0307
196	1 180	19	0,0161	19,1	0,0162	19,6	0,0167	20,6	0,0175	24	0,0204	29,5	0,0251	35,7	0,0304
198	1 190	19,3	0,0163	19,4	0,0163	20,3	0,0171	20,7	0,0174	24,3	0,0204	29,5	0,0248	36	0,0303
200	1 200	19,6	0,0163	19,6	0,0164	20,6	0,0171	20,8	0,0174	24,4	0,0203	29,7	0,0247	36,1	0,0301

Time	Shear Rate	Shear Stress	Viscosity	Shear Stress	Viscosity	Shear Stress	Viscosity	Shear Stress	Viscosity	Shear Stress	Viscosity	Shear Stress	Viscosity	Shear Stress	Viscosity
[s]	[1/s]	[Pa]	[Pa·s]	[Pa]	[Pa·s]	[Pa]	[Pa·s]	[Pa]	[Pa·s]	[Pa]	[Pa·s]	[Pa]	[Pa·s]	[Pa]	[Pa·s]
Number of Intervals:		BT-CNC-WDFs (6 wt %) 0.0 % 50°C	BT-CNC-WDFs (6 wt %) 0.0 % 50°C	BT-CNC-WDFs (6 wt %) 0.4 % 50°C	BT-CNC-WDFs (6 wt %) 0.4 % 50°C	BT-CNC-WDFs (6 wt %) 0.8 % 50°C	BT-CNC-WDFs (6 wt %) 0.8 % 50°C	BT-CNC-WDFs (6 wt %) 1.2 % 50°C	BT-CNC-WDFs (6 wt %) 1.2 % 50°C	BT-CNC-WDFs (6 wt %) 1.6 % 50°C	BT-CNC-WDFs (6 wt %) 1.6 % 50°C	BT-CNC-WDFs (6 wt %) 2.0 % 50°C	BT-CNC-WDFs (6 wt %) 2.0 % 50°C	BT-CNC-WDFs (6 wt %) 2.4 % 50°C	BT-CNC-WDFs (6 wt %) 2.4 % 50°C
2	0,999	0,52	0,52	0,792	0,793	0,623	0,622	0,33	0,33	0,242	0,242	0,25	0,251	1,67	1,68
4	13,1	1,68	0,128	0,183	0,0139	0,0144	0,0011	1,15	0,0874	2,47	0,189	5,48	0,418	6,51	0,497
6	25,2	2,13	0,0843	0,411	0,0163	0,698	0,0277	2,13	0,0846	3,85	0,153	7,64	0,303	8,51	0,337
8	37,3	2,48	0,0664	0,833	0,0223	1,21	0,0324	2,77	0,0741	4,82	0,129	8,89	0,238	9,49	0,254
10	49,4	2,79	0,0564	1,14	0,0231	1,58	0,0319	3,19	0,0645	5,43	0,11	9,9	0,2	10,1	0,204
12	61,6	3,11	0,0506	1,44	0,0234	1,88	0,0306	3,61	0,0587	6,01	0,0977	10,8	0,176	10,9	0,176
14	73,7	3,31	0,045	1,62	0,022	2,22	0,0301	3,94	0,0535	6,37	0,0864	11,5	0,157	11,6	0,157
16	85,8	3,54	0,0412	1,91	0,0222	2,56	0,0298	4,33	0,0505	6,85	0,0799	12,1	0,142	12,1	0,141
18	97,9	3,9	0,0398	2,2	0,0225	2,83	0,0289	4,7	0,048	7,26	0,0742	12,7	0,13	12,8	0,131
20	110	4,14	0,0376	2,45	0,0223	3,07	0,0279	5	0,0454	7,62	0,0693	13,3	0,121	13,4	0,122
22	122	4,42	0,0362	2,64	0,0217	3,33	0,0273	5,37	0,044	8	0,0655	13,9	0,114	13,9	0,114
24	134	4,69	0,0349	2,84	0,0211	3,6	0,0268	5,66	0,0422	8,32	0,062	14,4	0,107	14,4	0,107
26	146	4,95	0,0338	3,06	0,0209	3,83	0,0262	6	0,041	8,72	0,0596	14,9	0,102	14,9	0,102
28	158	5,12	0,0323	3,27	0,0207	4,1	0,0259	6,3	0,0398	9,01	0,0569	15,4	0,097	15,4	0,0973
30	171	5,37	0,0315	3,41	0,02	4,3	0,0252	6,58	0,0386	9,37	0,055	15,8	0,0925	15,8	0,0928
32	183	5,54	0,0303	3,67	0,0201	4,53	0,0248	6,84	0,0375	9,63	0,0527	16,2	0,0886	16,2	0,0889
34	195	5,73	0,0294	3,9	0,02	4,78	0,0245	7,09	0,0364	9,96	0,0511	16,5	0,0846	16,7	0,0858
36	207	5,94	0,0287	4,07	0,0197	4,94	0,0239	7,44	0,036	10,2	0,0491	16,8	0,0813	17,1	0,0828
38	219	6,16	0,0281	4,29	0,0196	5,17	0,0236	7,62	0,0348	10,5	0,0479	17,2	0,0787	17,6	0,0805
40	231	6,34	0,0274	4,47	0,0194	5,37	0,0232	7,88	0,0341	10,8	0,0465	17,6	0,076	18	0,078
42	243	6,52	0,0268	4,61	0,019	5,57	0,0229	8,11	0,0333	11	0,0453	17,9	0,0738	18,5	0,0759
44	255	6,69	0,0262	4,85	0,019	5,83	0,0229	8,37	0,0328	11,3	0,0444	18,3	0,0716	18,9	0,074
46	267	6,9	0,0258	5,03	0,0188	6,05	0,0226	8,56	0,032	11,6	0,0434	18,6	0,0697	19,3	0,0721
48	280	7,04	0,0252	5,26	0,0188	6,28	0,0225	8,8	0,0315	11,8	0,0423	19	0,0679	19,7	0,0706
50	292	7,24	0,0248	5,38	0,0184	6,43	0,022	9,09	0,0312	12	0,0411	19,2	0,0657	20	0,0687
52	304	7,42	0,0244	5,59	0,0184	6,68	0,022	9,31	0,0307	12,3	0,0403	19,5	0,0643	20,4	0,0673
54	316	7,62	0,0241	5,79	0,0183	6,88	0,0218	9,51	0,0301	12,6	0,0397	19,9	0,0629	20,8	0,0658
56	328	7,76	0,0237	6	0,0183	7,12	0,0217	9,73	0,0297	12,8	0,039	20,1	0,0614	21,3	0,0649
58	340	8,04	0,0236	6,2	0,0182	7,29	0,0214	9,87	0,029	13	0,0382	20,4	0,06	21,7	0,0638
60	352	8,2	0,0233	6,4	0,0182	7,51	0,0213	10,1	0,0287	13,2	0,0374	20,7	0,0588	22	0,0624
62	364	8,29	0,0228	6,56	0,018	7,67	0,0211	10,4	0,0286	13,3	0,0364	20,9	0,0574	22,3	0,0611
64	376	8,57	0,0228	6,77	0,018	7,86	0,0209	10,6	0,0281	13,5	0,0359	21,2	0,0563	22,7	0,0604
66	389	8,76	0,0225	6,96	0,0179	8,05	0,0207	10,8	0,0277	13,7	0,0351	21,5	0,0553	23,1	0,0595
68	401	8,93	0,0223	7,05	0,0176	8,17	0,0204	11	0,0274	13,9	0,0347	21,7	0,0542	23,4	0,0584
70	413	9,03	0,0219	7,28	0,0176	8,4	0,0204	11,2	0,027	14,1	0,0341	22	0,0532	23,8	0,0575
72	425	9,22	0,0217	7,52	0,0177	8,62	0,0203	11,3	0,0265	14,3	0,0336	22,2	0,0523	24	0,0564
74	437	9,35	0,0214	7,6	0,0174	8,7	0,0199	11,6	0,0265	14,4	0,033	22,4	0,0513	24,2	0,0555
76	449	9,66	0,0215	7,69	0,0171	8,85	0,0197	11,7	0,0261	14,7	0,0327	22,7	0,0506	24,5	0,0545
78	461	10,3	0,0223	7,71	0,0167	9,03	0,0196	12,4	0,0268	15,3	0,0332	23,3	0,0504	25,1	0,0544
80	473	9,92	0,021	7,96	0,0168	9,14	0,0193	12,1	0,0256	15,1	0,0318	23	0,0487	25	0,0529
82	485	10,2	0,0209	8,06	0,0166	9,27	0,0191	12,2	0,0251	15,2	0,0314	23,2	0,0478	25,3	0,0521
84	498	10,3	0,0206	8,13	0,0163	9,35	0,0188	12,5	0,0251	15,3	0,0308	23,3	0,0468	25,5	0,0512
86	510	10,4	0,0205	8,3	0,0163	9,5	0,0186	12,6	0,0246	15,5	0,0304	23,5	0,0461	25,8	0,0507
88	522	10,6	0,0203	8,52	0,0163	9,78	0,0188	12,6	0,0241	15,7	0,0301	23,8	0,0456	26,2	0,0502
90	534	10,8	0,0202	8,55	0,016	9,84	0,0184	12,8	0,0239	15,8	0,0296	23,9	0,0448	26,3	0,0493
92	546	10,9	0,0199	8,7	0,0159	9,98	0,0183	12,9	0,0236	16	0,0292	24,1	0,0441	26,6	0,0487
94	558	11	0,0198	8,8	0,0158	10	0,018	13,1	0,0234	16,1	0,0289	24,3	0,0435	26,7	0,0478
96	570	11,1	0,0195	9,05	0,0159	10,2	0,0179	13,2	0,0231	16,2	0,0284	24,5	0,043	27	0,0473

98	582	11,2	0,0193	9,2	0,0158	10,4	0,0178	13,3	0,0228	16,3	0,028	24,7	0,0424	27,3	0,0469
100	594	11,4	0,0192	9,18	0,0154	10,3	0,0174	13,5	0,0227	16,4	0,0276	24,8	0,0416	27,4	0,046
102	607	11,6	0,0192	9,42	0,0155	10,5	0,0173	13,5	0,0222	16,7	0,0275	25	0,0412	27,6	0,0455
104	619	11,7	0,019	9,47	0,0153	10,6	0,0171	13,7	0,0221	16,8	0,0271	25,1	0,0406	27,8	0,045
106	631	11,9	0,0188	9,58	0,0152	10,7	0,0169	13,8	0,0219	16,8	0,0267	25,3	0,0401	27,9	0,0442
108	643	12	0,0186	9,86	0,0153	10,9	0,0169	13,9	0,0217	16,9	0,0263	25,5	0,0396	28,2	0,0438
110	655	12,2	0,0186	9,97	0,0152	11,1	0,0169	13,9	0,0213	17	0,026	25,6	0,0391	28,3	0,0432
112	667	12,2	0,0183	10,1	0,0151	11,2	0,0168	14,1	0,0212	17	0,0255	25,7	0,0385	28,5	0,0427
114	679	12,4	0,0183	10,1	0,0148	11,2	0,0164	14,3	0,021	17,1	0,0252	25,7	0,0378	28,5	0,042
116	691	12,5	0,0181	10,3	0,0149	11,3	0,0164	14,4	0,0208	17,2	0,0248	25,8	0,0374	28,7	0,0415
118	703	12,7	0,0181	10,5	0,0149	11,5	0,0163	14,4	0,0205	17,2	0,0244	26	0,037	28,9	0,0411
120	716	12,7	0,0178	10,5	0,0146	11,5	0,016	14,7	0,0205	17,2	0,024	26,1	0,0365	29	0,0405
122	728	12,9	0,0177	10,7	0,0147	11,7	0,0161	14,7	0,0202	17,5	0,024	26,4	0,0362	29,3	0,0402
124	740	13,1	0,0177	10,8	0,0147	11,7	0,0159	14,8	0,02	17,5	0,0237	26,5	0,0359	29,4	0,0398
126	752	13,2	0,0175	10,9	0,0145	11,7	0,0156	15	0,02	17,4	0,0231	26,5	0,0353	29,4	0,0391
128	764	13,3	0,0175	11,1	0,0146	11,9	0,0156	15,1	0,0197	17,7	0,0231	26,7	0,0349	29,7	0,0388
130	776	13,5	0,0174	11,2	0,0144	12	0,0154	15,2	0,0196	17,7	0,0229	26,8	0,0345	29,7	0,0383
132	788	13,7	0,0174	11,3	0,0144	12,1	0,0154	15,3	0,0194	17,8	0,0226	27	0,0343	29,9	0,038
134	800	13,8	0,0172	11,3	0,0142	12,1	0,0151	15,6	0,0195	17,9	0,0223	27	0,0337	29,9	0,0374
136	812	13,8	0,017	11,5	0,0142	12,3	0,0151	15,7	0,0193	18	0,0221	27,1	0,0333	30	0,037
138	825	14,2	0,0172	11,5	0,014	12,4	0,0151	15,8	0,0192	18,4	0,0223	27,5	0,0334	30,2	0,0366
140	837	14,2	0,017	11,8	0,0141	12,7	0,0152	15,8	0,0189	18,3	0,0218	27,4	0,0327	30,4	0,0363
142	849	14,4	0,017	11,9	0,014	12,8	0,015	15,9	0,0187	18,4	0,0217	27,5	0,0324	30,5	0,0359
144	861	14,6	0,0169	12	0,0139	12,8	0,0149	16,1	0,0187	18,4	0,0214	27,6	0,0321	30,6	0,0355
146	873	14,6	0,0167	12,2	0,014	13,1	0,015	16,1	0,0185	18,6	0,0213	27,8	0,0318	30,8	0,0353
148	885	14,9	0,0168	12,2	0,0138	13,2	0,0149	16,2	0,0183	18,8	0,0212	28	0,0316	30,8	0,0348
150	897	14,9	0,0166	12,4	0,0138	13,4	0,0149	16,2	0,0181	18,9	0,021	28,1	0,0313	31	0,0346
152	909	14,9	0,0164	12,4	0,0137	13,3	0,0146	16,6	0,0182	18,8	0,0207	28	0,0308	31,1	0,0342
154	921	15,1	0,0164	12,6	0,0137	13,5	0,0146	16,6	0,018	19	0,0206	28,2	0,0306	31,1	0,0337
156	934	15,3	0,0164	12,7	0,0136	13,5	0,0145	16,7	0,0179	19,1	0,0204	28,3	0,0304	31,1	0,0333
158	946	15,4	0,0163	12,9	0,0136	13,7	0,0145	16,8	0,0177	19,3	0,0204	28,5	0,0302	31,4	0,0332
160	958	15,6	0,0163	12,8	0,0134	13,6	0,0142	17	0,0177	19,3	0,0202	28,6	0,0298	31,3	0,0326
162	970	15,7	0,0162	12,9	0,0133	13,7	0,0141	17,1	0,0176	19,4	0,02	28,7	0,0296	31,3	0,0323
164	982	15,9	0,0162	13,3	0,0136	14	0,0143	17,1	0,0174	19,6	0,0199	28,8	0,0294	31,6	0,0321
166	994	15,9	0,016	13,5	0,0136	14	0,0141	17,4	0,0175	19,6	0,0197	28,8	0,029	31,6	0,0317
168	1 010	16	0,0159	13,8	0,0137	14,2	0,0141	17,5	0,0174	19,7	0,0196	29	0,0288	31,7	0,0315
170	1 020	16,1	0,0158	14,3	0,014	14,3	0,014	17,6	0,0173	19,8	0,0194	29,1	0,0285	31,8	0,0312
172	1 030	16,4	0,0159	14,7	0,0143	14,5	0,014	17,7	0,0172	19,9	0,0194	29,3	0,0284	31,8	0,0309
174	1 040	16,5	0,0158	15,1	0,0145	14,7	0,0141	17,9	0,0172	19,9	0,0191	29,3	0,0281	31,9	0,0306
176	1 050	16,7	0,0158	15,5	0,0147	15	0,0142	18	0,017	20,2	0,0191	29,7	0,0281	32,1	0,0305
178	1 070	16,7	0,0156	15,9	0,0149	15,3	0,0144	18,2	0,0171	20,4	0,0191	29,7	0,0278	32,3	0,0303
180	1 080	17	0,0158	16,5	0,0153	15,5	0,0144	18,4	0,017	20,5	0,019	29,7	0,0275	32,4	0,03
182	1 090	17,4	0,016	16,8	0,0154	15,8	0,0145	18,5	0,0169	20,6	0,0189	29,8	0,0274	32,5	0,0297
184	1 100	17,9	0,0162	16,7	0,0151	16,4	0,0148	18,6	0,0168	20,8	0,0188	30	0,0272	32,6	0,0296
186	1 120	18,4	0,0165	16,9	0,0151	17	0,0152	18,7	0,0168	20,9	0,0187	30,1	0,027	32,7	0,0293
188	1 130	18,9	0,0168	17,2	0,0152	17,4	0,0155	18,8	0,0167	21	0,0186	30,4	0,0269	32,7	0,029
190	1 140	19,2	0,0168	17,6	0,0154	17,8	0,0156	19,2	0,0168	21,1	0,0185	30,4	0,0267	33	0,029
192	1 150	19,8	0,0172	17,7	0,0154	18,2	0,0158	19,4	0,0168	21,3	0,0185	30,8	0,0267	33	0,0287
194	1 160	20,2	0,0173	18	0,0155	18,5	0,0159	19,7	0,017	21,4	0,0184	30,7	0,0263	33,1	0,0285
196	1 180	20,7	0,0176	18,2	0,0155	18,2	0,0155	20	0,017	21,6	0,0184	30,7	0,0261	33,3	0,0283
198	1 190	20,7	0,0174	18,6	0,0157	18,4	0,0155	20,5	0,0173	21,8	0,0184	30,9	0,026	33,4	0,0281

200	1 200	20,9	0,0174	19,1	0,0159	18,7	0,0156	20,8	0,0174	21,9	0,0183	31	0,0258	33,6	0,028

Time	Shear Rate	Shear Stress	Viscosity	Shear Stress	Viscosity	Shear Stress	Viscosity	Shear Stress	Viscosity	Shear Stress	Viscosity	Shear Stress	Viscosity	Shear Stress	Viscosity
[s]	[1/s]	[Pa]	[Pa·s]	[Pa]	[Pa·s]	[Pa]	[Pa·s]	[Pa]	[Pa·s]	[Pa]	[Pa·s]	[Pa]	[Pa·s]	[Pa]	[Pa·s]
Number of Intervals:		BT-CNC-WDFs (6 wt %) 0.0 % 60°C	BT-CNC-WDFs (6 wt %) 0.0 % 60°C	BT-CNC-WDFs (6 wt %) 0.4 % 60°C	BT-CNC-WDFs (6 wt %) 0.4 % 60°C	BT-CNC-WDFs (6 wt %) 0.8 % 60°C	BT-CNC-WDFs (6 wt %) 0.8 % 60°C	BT-CNC-WDFs (6 wt %) 1.2 % 60°C	BT-CNC-WDFs (6 wt %) 1.2 % 60°C	BT-CNC-WDFs (6 wt %) 1.6 % 60°C	BT-CNC-WDFs (6 wt %) 1.6 % 60°C	BT-CNC-WDFs (6 wt %) 2.0 % 60°C	BT-CNC-WDFs (6 wt %) 2.0 % 60°C	BT-CNC-WDFs (6 wt %) 2.4 % 60°C	BT-CNC-WDFs (6 wt %) 2.4 % 60°C
2	0,999	0,719	0,718	0,0572	0,0575	0,865	0,866	0,27	0,27	0,668	0,668	0,346	0,346	2,2	2,19
4	13,1	2,03	0,155	0,761	0,0581	0,804	0,0613	1,59	0,121	3,17	0,242	4,23	0,323	7,53	0,575
6	25,2	2,43	0,0962	1,2	0,0474	1,35	0,0537	2,57	0,102	4,36	0,173	6,2	0,246	10,2	0,405
8	37,3	2,6	0,0695	1,57	0,0419	1,84	0,0493	3,15	0,0845	5,19	0,139	7,31	0,196	11,7	0,314
10	49,4	2,8	0,0567	1,93	0,0391	2,23	0,0451	3,77	0,0763	5,82	0,118	8,15	0,165	12,8	0,258
12	61,6	3,03	0,0491	2,29	0,0372	2,58	0,0419	4,15	0,0674	6,35	0,103	8,87	0,144	13,5	0,22
14	73,7	3,21	0,0436	2,45	0,0333	2,9	0,0394	4,7	0,0638	6,76	0,0918	9,54	0,129	14,3	0,194
16	85,8	3,37	0,0393	2,75	0,0321	3,18	0,0371	5,02	0,0586	7,17	0,0835	10,2	0,119	15	0,175
18	97,9	3,56	0,0364	3,04	0,031	3,51	0,0359	5,42	0,0554	7,65	0,0781	10,8	0,11	15,6	0,16
20	110	3,77	0,0342	3,27	0,0298	3,79	0,0345	5,78	0,0526	8,03	0,073	11,3	0,103	16,2	0,147
22	122	3,99	0,0327	3,56	0,0291	4,08	0,0334	6,13	0,0502	8,42	0,069	11,8	0,0966	16,8	0,137
24	134	4,32	0,0322	3,76	0,028	4,43	0,033	6,47	0,0482	8,83	0,0658	12,3	0,092	17,3	0,129
26	146	4,45	0,0304	4,01	0,0274	4,67	0,0319	6,81	0,0465	9,23	0,0631	12,8	0,0878	17,7	0,121
28	158	4,69	0,0296	4,23	0,0267	4,92	0,031	7,16	0,0452	9,61	0,0607	13,2	0,0836	18,2	0,115
30	171	4,89	0,0287	4,47	0,0262	5,17	0,0303	7,45	0,0437	9,97	0,0585	13,7	0,0804	18,6	0,109
32	183	5,15	0,0282	4,68	0,0256	5,43	0,0297	7,72	0,0423	10,3	0,0565	14,2	0,0777	19	0,104
34	195	5,28	0,0271	4,88	0,025	5,68	0,0292	7,99	0,041	10,6	0,0546	14,7	0,0752	19,5	0,1
36	207	5,44	0,0263	5,1	0,0246	5,85	0,0283	8,19	0,0396	10,9	0,0527	15	0,0725	19,9	0,0962
38	219	5,56	0,0254	5,2	0,0238	6,09	0,0278	8,44	0,0385	11,2	0,0512	15,4	0,0705	20,3	0,0925
40	231	5,71	0,0247	5,43	0,0235	6,28	0,0272	8,65	0,0374	11,5	0,0496	15,8	0,0683	20,6	0,0893
42	243	5,87	0,0241	5,61	0,0231	6,51	0,0268	8,88	0,0365	11,8	0,0483	16,1	0,0663	21	0,0865
44	255	6,07	0,0238	5,79	0,0227	6,78	0,0265	9,17	0,0359	12	0,0471	16,5	0,0647	21,5	0,0844
46	267	6,2	0,0232	5,94	0,0222	7	0,0262	9,46	0,0354	12,4	0,0462	16,9	0,063	21,9	0,0818
48	280	6,39	0,0229	6,15	0,022	7,22	0,0258	9,63	0,0344	12,6	0,045	17,2	0,0617	22,2	0,0796
50	292	6,51	0,0223	6,37	0,0218	7,34	0,0252	9,79	0,0336	12,8	0,0438	17,6	0,0602	22,7	0,0778
52	304	6,72	0,0221	6,55	0,0216	7,57	0,0249	9,99	0,0329	13,1	0,043	17,9	0,0589	23	0,0758
54	316	6,87	0,0217	6,68	0,0212	7,78	0,0246	10,2	0,0324	13,2	0,0418	18,2	0,0577	23,4	0,0741
56	328	7,09	0,0216	6,92	0,0211	7,98	0,0243	10,4	0,0317	13,4	0,0409	18,5	0,0564	23,7	0,0723
58	340	7,21	0,0212	7,04	0,0207	8,2	0,0241	10,7	0,0314	13,7	0,0404	18,7	0,0551	24	0,0705
60	352	7,41	0,021	7,22	0,0205	8,42	0,0239	10,9	0,0309	14	0,0397	19,1	0,0543	24,2	0,0688
62	364	7,66	0,021	7,51	0,0206	8,54	0,0234	11	0,0301	14,1	0,0388	19,5	0,0535	24,7	0,0677
64	376	7,76	0,0206	7,64	0,0203	8,77	0,0233	11,2	0,0299	14,5	0,0384	19,7	0,0523	24,9	0,0661
66	389	7,98	0,0205	7,88	0,0203	8,94	0,023	11,4	0,0294	14,6	0,0375	20,1	0,0517	25,2	0,0649
68	401	8,09	0,0202	8,03	0,02	9,12	0,0228	11,6	0,0289	14,8	0,0369	20,4	0,0509	25,5	0,0637
70	413	8,33	0,0202	8,21	0,0199	9,36	0,0227	11,7	0,0284	15	0,0363	20,7	0,0502	25,8	0,0624
72	425	8,47	0,0199	8,32	0,0196	9,61	0,0226	11,9	0,0281	15,3	0,0359	21	0,0494	26	0,0612
74	437	8,65	0,0198	8,62	0,0197	9,67	0,0221	12	0,0275	15,3	0,0351	21,3	0,0486	26,4	0,0603
76	449	8,73	0,0194	8,69	0,0194	9,91	0,0221	12,3	0,0274	15,5	0,0346	21,4	0,0476	26,5	0,059
78	461	9,31	0,0202	9,26	0,0201	9,83	0,0213	12,3	0,0266	15,4	0,0333	21,6	0,0467	27	0,0584
80	473	9,13	0,0193	9,05	0,0191	10,2	0,0216	12,6	0,0266	15,9	0,0335	22	0,0464	27	0,057
82	485	9,18	0,0189	9,17	0,0189	10,4	0,0215	12,8	0,0264	16,1	0,0332	22	0,0453	27,2	0,056
84	498	9,35	0,0188	9,42	0,0189	10,5	0,0211	12,9	0,0258	16,2	0,0325	22,3	0,0447	27,6	0,0554
86	510	9,44	0,0185	9,53	0,0187	10,6	0,0209	13	0,0255	16,4	0,0322	22,5	0,0441	27,7	0,0544
88	522	9,66	0,0185	9,56	0,0183	10,9	0,021	13,3	0,0254	16,7	0,0319	22,7	0,0436	27,9	0,0535
90	534	9,76	0,0183	9,74	0,0182	10,9	0,0205	13,4	0,0251	16,8	0,0314	22,9	0,0428	28,2	0,0528
92	546	9,95	0,0182	9,87	0,0181	11,1	0,0203	13,5	0,0247	16,9	0,031	23,1	0,0423	28,4	0,052
94	558	10	0,0179	10	0,018	11,2	0,02	13,6	0,0244	17	0,0305	23,3	0,0417	28,7	0,0514
96	570	10,3	0,018	10,1	0,0178	11,4	0,0199	13,7	0,0241	17,2	0,0301	23,5	0,0413	28,9	0,0506
98	582	10,4	0,0179	10,3	0,0176	11,5	0,0197	13,9	0,0238	17,3	0,0296	23,7	0,0407	29	0,0498
100	594	10,4	0,0176	10,5	0,0176	11,5	0,0194	14	0,0235	17,3	0,0291	23,9	0,0401	29,2	0,0492
102	607	10,6	0,0175	10,5	0,0172	11,7	0,0194	14,2	0,0235	17,6	0,0289	24	0,0396	29,3	0,0483

104	619	10,7	0,0173	10,6	0,0172	11,8	0,0191	14,3	0,0232	17,6	0,0284	24,2	0,0391	29,5	0,0476
106	631	10,7	0,017	10,8	0,0171	11,9	0,0189	14,4	0,0229	17,7	0,028	24,2	0,0384	29,7	0,0471
108	643	10,9	0,017	10,9	0,017	12,1	0,0189	14,5	0,0226	17,9	0,0278	24,6	0,0382	29,9	0,0464
110	655	11,1	0,0169	10,9	0,0166	12,3	0,0188	14,7	0,0225	18,1	0,0276	24,6	0,0376	29,9	0,0457
112	667	11,2	0,0168	11,1	0,0166	12,4	0,0186	14,8	0,0222	18,1	0,0272	24,8	0,0372	30,2	0,0452
114	679	11,2	0,0165	11,3	0,0166	12,4	0,0183	14,9	0,0219	18,2	0,0267	24,8	0,0365	30,3	0,0446
116	691	11,4	0,0165	11,4	0,0164	12,6	0,0182	15	0,0217	18,3	0,0264	25	0,0362	30,5	0,0441
118	703	11,5	0,0164	11,5	0,0163	12,7	0,0181	15,2	0,0216	18,5	0,0263	25,2	0,0358	30,6	0,0435
120	716	11,7	0,0163	11,7	0,0163	12,8	0,0178	15,2	0,0213	18,5	0,0259	25,3	0,0353	30,9	0,0432
122	728	11,8	0,0162	11,6	0,016	13	0,0179	15,4	0,0212	18,7	0,0257	25,5	0,035	31	0,0426
124	740	11,9	0,0161	11,8	0,0159	13,2	0,0178	15,6	0,0211	18,9	0,0255	25,6	0,0346	31,1	0,042
126	752	11,9	0,0158	12	0,016	13,1	0,0175	15,6	0,0207	18,8	0,025	25,6	0,034	31,4	0,0418
128	764	12	0,0157	12	0,0157	13,4	0,0175	15,8	0,0207	19	0,0249	25,8	0,0337	31,4	0,0411
130	776	12,1	0,0156	12,2	0,0157	13,5	0,0174	15,9	0,0206	19,3	0,0248	25,9	0,0333	31,6	0,0407
132	788	12,2	0,0154	12,3	0,0155	13,7	0,0174	16,1	0,0205	19,5	0,0247	26	0,033	31,7	0,0402
134	800	12,3	0,0154	12,5	0,0156	13,6	0,017	16,1	0,0202	19,4	0,0243	26,1	0,0327	32	0,0399
136	812	12,5	0,0154	12,6	0,0155	13,8	0,0169	16,2	0,02	19,5	0,024	26,4	0,0324	32,2	0,0396
138	825	12,4	0,0151	12,8	0,0155	13,8	0,0168	16,3	0,0197	19,5	0,0237	26,2	0,0318	32,3	0,0392
140	837	12,7	0,0152	12,6	0,0151	14,1	0,0169	16,7	0,0199	19,9	0,0238	26,5	0,0317	32,2	0,0385
142	849	12,8	0,0151	12,7	0,015	14,3	0,0168	16,7	0,0197	20	0,0236	26,6	0,0314	32,3	0,0381
144	861	12,8	0,0149	12,9	0,0149	14,3	0,0166	16,8	0,0196	20,1	0,0234	26,7	0,031	32,5	0,0377
146	873	13,1	0,015	12,9	0,0148	14,6	0,0167	17	0,0195	20,3	0,0232	26,9	0,0308	32,6	0,0373
148	885	13,1	0,0148	12,9	0,0146	14,7	0,0166	17,2	0,0194	20,4	0,0231	26,8	0,0303	32,6	0,0368
150	897	13,2	0,0148	13,1	0,0145	14,8	0,0165	17,3	0,0192	20,5	0,0229	27,1	0,0302	32,7	0,0364
152	909	13,3	0,0147	13,4	0,0147	14,7	0,0162	17,2	0,019	20,4	0,0225	27,2	0,0299	33	0,0363
154	921	13,5	0,0146	13,4	0,0145	14,9	0,0162	17,5	0,0189	20,6	0,0224	27,3	0,0296	33	0,0358
156	934	13,5	0,0145	13,5	0,0144	15	0,0161	17,6	0,0189	20,7	0,0222	27,3	0,0293	33	0,0354
158	946	13,7	0,0145	13,5	0,0143	15,2	0,0161	17,8	0,0188	20,9	0,0221	27,4	0,029	33,1	0,035
160	958	13,6	0,0142	13,6	0,0142	15,2	0,0159	17,8	0,0186	20,9	0,0219	27,4	0,0286	33,2	0,0346
162	970	13,7	0,0142	13,7	0,0142	15,2	0,0157	17,9	0,0185	21	0,0216	27,5	0,0283	33,3	0,0343
164	982	14	0,0143	13,7	0,014	15,5	0,0158	18,1	0,0184	21,3	0,0217	27,6	0,0282	33,3	0,0339
166	994	14,1	0,0142	14	0,014	15,5	0,0156	18,2	0,0183	21,3	0,0214	27,8	0,0279	33,5	0,0337
168	1 010	14,2	0,0141	14,1	0,014	15,7	0,0156	18,3	0,0182	21,5	0,0214	27,9	0,0277	33,6	0,0333
170	1 020	14,3	0,0141	14,2	0,0139	15,8	0,0156	18,4	0,018	21,5	0,0211	28,1	0,0276	33,8	0,0331
172	1 030	14,3	0,0139	14,2	0,0138	15,9	0,0154	18,6	0,0181	21,6	0,021	28	0,0272	33,8	0,0328
174	1 040	14,5	0,0139	14,6	0,014	15,9	0,0153	18,7	0,018	21,7	0,0208	28,2	0,0271	34	0,0326
176	1 050	14,8	0,014	14,7	0,0139	16,2	0,0154	18,9	0,018	21,9	0,0208	28,2	0,0268	34	0,0322
178	1 070	15,4	0,0144	15	0,0141	16,3	0,0153	18,9	0,0177	22	0,0206	28,6	0,0268	34,2	0,032
180	1 080	15,7	0,0146	15,4	0,0142	16,5	0,0153	19,1	0,0177	22,2	0,0205	28,6	0,0265	34,3	0,0318
182	1 090	16,1	0,0148	15,8	0,0145	16,7	0,0153	19,2	0,0176	22,3	0,0204	28,7	0,0263	34,3	0,0314
184	1 100	16,7	0,0152	16,2	0,0147	17,1	0,0155	19,4	0,0176	22,5	0,0204	28,8	0,0261	34,4	0,0312
186	1 120	17	0,0152	16,6	0,0149	17,3	0,0155	19,6	0,0176	22,7	0,0203	28,8	0,0259	34,5	0,0309
188	1 130	17,5	0,0155	17	0,0151	17,7	0,0157	19,8	0,0176	22,8	0,0202	29	0,0257	34,6	0,0307
190	1 140	18	0,0158	17,6	0,0154	18	0,0158	19,7	0,0173	22,8	0,02	29,3	0,0257	34,8	0,0305
192	1 150	18	0,0156	18	0,0156	18,4	0,016	19,9	0,0173	23,1	0,02	29,4	0,0255	34,8	0,0302
194	1 160	18,2	0,0156	18,4	0,0158	18,7	0,0161	20,1	0,0172	23	0,0198	29,5	0,0254	35	0,0301
196	1 180	18,3	0,0156	18,6	0,0158	19,2	0,0163	20,3	0,0172	23,2	0,0198	29,6	0,0252	35,1	0,0299
198	1 190	18,7	0,0157	18,8	0,0158	19,8	0,0166	20,5	0,0172	23,3	0,0196	29,9	0,0251	35,3	0,0297
200	1 200	18,9	0,0157	18,8	0,0157	20,1	0,0168	20,9	0,0174	23,5	0,0196	30	0,025	35,4	0,0295

Time	Shear Rate	Shear Stress	Viscosity	Shear Stress	Viscosity	Shear Stress	Viscosity	Shear Stress	Viscosity	Shear Stress	Viscosity	Shear Stress	Viscosity	Shear Stress	Viscosity
[s]	[1/s]	[Pa]	[Pa·s]	[Pa]	[Pa·s]	[Pa]	[Pa·s]	[Pa]	[Pa·s]	[Pa]	[Pa·s]	[Pa]	[Pa·s]	[Pa]	[Pa·s]
Number of Intervals:		BT-CNC-WDEs (6 wt %) 0.0 % 70°C	BT-CNC-WDEs (6 wt %) 0.0 % 70°C	BT-CNC-WDEs (6 wt %) 0.4 % 70°C	BT-CNC-WDEs (6 wt %) 0.4 % 70°C	BT-CNC-WDEs (6 wt %) 0.8 % 70°C	BT-CNC-WDEs (6 wt %) 0.8 % 70°C	BT-CNC-WDEs (6 wt %) 1.2 % 70°C	BT-CNC-WDEs (6 wt %) 1.2 % 70°C	BT-CNC-WDEs (6 wt %) 1.6 % 70°C	BT-CNC-WDEs (6 wt %) 1.6 % 70°C	BT-CNC-WDEs (6 wt %) 2.0 % 70°C	BT-CNC-WDEs (6 wt %) 2.0 % 70°C	BT-CNC-WDEs (6 wt %) 2.4 % 70°C	BT-CNC-WDEs (6 wt %) 2.4 % 70°C
2	0,999	1,05	1,05	0,619	0,619	0,46	0,46	0,742	0,742	-0,262	0,262	4,31E-4	4,32E-4	3,56	3,55
4	13,1	3,22	0,246	0,953	0,0727	2,04	0,156	1,5	0,115	2,33	0,177	4,7	0,358	9,65	0,736
6	25,2	3,33	0,132	1,55	0,0614	3,07	0,122	2,57	0,102	3,63	0,144	6,4	0,254	12,2	0,484
8	37,3	3,38	0,0905	1,78	0,0476	3,72	0,0997	3,12	0,0836	4,36	0,117	7,54	0,202	13,3	0,357
10	49,4	3,51	0,0711	2,22	0,0449	4,33	0,0876	3,65	0,0738	5,02	0,102	8,55	0,173	14,4	0,291
12	61,6	3,76	0,0612	2,42	0,0393	4,56	0,0741	4,01	0,0652	5,63	0,0915	9,41	0,153	15,5	0,251
14	73,7	3,85	0,0523	2,66	0,0361	4,87	0,0661	4,32	0,0586	5,96	0,0809	10,1	0,136	16,5	0,224
16	85,8	4,07	0,0474	2,72	0,0317	5,18	0,0604	4,64	0,0541	6,39	0,0745	10,7	0,125	16,8	0,196
18	97,9	4,26	0,0435	2,91	0,0297	5,39	0,0551	4,98	0,0508	6,81	0,0696	11,3	0,116	17,3	0,177
20	110	4,46	0,0406	3,16	0,0288	5,74	0,0522	5,29	0,0481	7,2	0,0655	11,9	0,108	17,7	0,161
22	122	4,59	0,0376	3,33	0,0273	6,06	0,0496	5,64	0,0462	7,55	0,0619	12,4	0,102	18	0,148
24	134	4,75	0,0354	3,52	0,0262	6,38	0,0475	5,99	0,0447	7,92	0,059	13	0,0969	18,6	0,139
26	146	5,03	0,0343	3,78	0,0258	6,7	0,0458	6,31	0,0431	8,33	0,057	13,5	0,0925	19,1	0,131
28	158	5,15	0,0325	3,95	0,0249	7,01	0,0442	6,62	0,0418	8,71	0,055	14	0,0883	19,6	0,124
30	171	5,35	0,0314	4,18	0,0245	7,31	0,0429	6,89	0,0404	9,07	0,0532	14,4	0,0843	20	0,117
32	183	5,5	0,0301	4,37	0,0239	7,58	0,0415	7,15	0,0391	9,28	0,0508	14,9	0,0814	20,4	0,112
34	195	5,65	0,029	4,55	0,0234	7,75	0,0398	7,36	0,0378	9,56	0,0491	15,3	0,0785	20,9	0,107
36	207	5,84	0,0282	4,7	0,0227	8,03	0,0388	7,57	0,0366	9,9	0,0479	15,7	0,076	21,2	0,103
38	219	5,94	0,0271	4,9	0,0224	8,15	0,0372	7,81	0,0356	10,2	0,0466	16,2	0,0738	21,6	0,0988
40	231	6,06	0,0262	5,04	0,0218	8,37	0,0362	8,03	0,0347	10,5	0,0453	16,5	0,0715	22	0,0952
42	243	6,23	0,0256	5,2	0,0214	8,56	0,0352	8,25	0,0339	10,7	0,0441	16,8	0,0689	22,4	0,092
44	255	6,33	0,0248	5,36	0,021	8,71	0,0341	8,48	0,0332	10,9	0,0428	17,1	0,067	22,7	0,089
46	267	6,45	0,0241	5,57	0,0208	8,88	0,0332	8,7	0,0325	11,2	0,0418	17,4	0,0651	23,1	0,0865
48	280	6,61	0,0236	5,69	0,0203	9,07	0,0324	8,89	0,0318	11,4	0,0406	17,8	0,0635	23,5	0,0839
50	292	6,85	0,0235	5,83	0,02	9,34	0,032	9	0,0309	11,6	0,0397	18	0,0619	23,8	0,0816
52	304	6,96	0,0229	6,01	0,0198	9,5	0,0313	9,29	0,0306	11,8	0,0388	18,4	0,0605	24,1	0,0793
54	316	7,1	0,0225	6,21	0,0196	9,68	0,0306	9,43	0,0299	12,1	0,0382	18,6	0,059	24,5	0,0776
56	328	7,29	0,0222	6,33	0,0193	9,88	0,0301	9,63	0,0294	12,3	0,0374	19	0,058	24,8	0,0756
58	340	7,37	0,0217	6,59	0,0194	10	0,0294	9,88	0,0291	12,5	0,0369	19,3	0,0567	25,1	0,0738
60	352	7,54	0,0214	6,76	0,0192	10,2	0,0289	10,1	0,0286	12,8	0,0362	19,6	0,0558	25,4	0,072
62	364	7,79	0,0214	6,83	0,0187	10,5	0,0287	10,2	0,028	12,9	0,0355	19,8	0,0542	25,5	0,07
64	376	7,92	0,021	7,07	0,0188	10,6	0,0281	10,4	0,0277	13,2	0,0351	20	0,053	25,9	0,0687
66	389	8,11	0,0209	7,25	0,0187	10,8	0,0278	10,6	0,0272	13,5	0,0347	20,2	0,052	26,1	0,0673
68	401	8,3	0,0207	7,36	0,0184	11	0,0273	10,7	0,0267	13,7	0,0341	20,4	0,0508	26,4	0,0658
70	413	8,45	0,0205	7,48	0,0181	11,1	0,0268	10,9	0,0264	13,8	0,0334	20,7	0,0503	26,5	0,0643
72	425	8,52	0,02	7,67	0,018	11,1	0,0262	11,1	0,0261	14	0,0329	20,9	0,0493	26,9	0,0632
74	437	8,82	0,0202	7,75	0,0177	11,4	0,0261	11,2	0,0256	14,1	0,0323	21,2	0,0485	27	0,0618
76	449	8,86	0,0197	7,99	0,0178	11,5	0,0255	11,4	0,0253	14,4	0,0321	21,3	0,0474	27,4	0,0611
78	461	8,68	0,0188	7,78	0,0169	11,7	0,0255	11,3	0,0246	14,3	0,0309	21,2	0,046	27,5	0,0595
80	473	9,11	0,0192	8,21	0,0173	11,8	0,0249	11,7	0,0247	14,6	0,0309	21,8	0,046	27,8	0,0587
82	485	9,2	0,019	8,4	0,0173	11,9	0,0246	11,8	0,0243	14,9	0,0306	21,9	0,045	28,1	0,0579
84	498	9,42	0,0189	8,45	0,017	12,2	0,0244	11,9	0,0239	15	0,0301	22,1	0,0444	28,2	0,0568
86	510	9,49	0,0186	8,63	0,0169	12,3	0,0241	12	0,0236	15,2	0,0299	22,3	0,0438	28,5	0,056
88	522	9,48	0,0182	8,79	0,0169	12,2	0,0235	12,3	0,0237	15,4	0,0295	22,5	0,0431	28,8	0,0552
90	534	9,69	0,0182	8,9	0,0167	12,5	0,0233	12,4	0,0232	15,5	0,0291	22,6	0,0423	29	0,0543
92	546	9,82	0,018	9,01	0,0165	12,6	0,023	12,6	0,023	15,6	0,0286	22,8	0,0418	29,2	0,0535
94	558	10	0,018	9,12	0,0163	12,7	0,0228	12,6	0,0226	15,8	0,0283	23	0,0411	29,4	0,0527
96	570	10,1	0,0177	9,22	0,0162	12,7	0,0224	12,8	0,0225	15,8	0,0278	23,2	0,0407	29,6	0,0518
98	582	10,2	0,0175	9,35	0,0161	12,9	0,0221	13	0,0223	16	0,0275	23,4	0,0401	29,7	0,051
100	594	10,5	0,0176	9,43	0,0159	13,1	0,0221	13	0,0219	16,1	0,0271	23,4	0,0394	29,8	0,0501
102	607	10,5	0,0172	9,64	0,0159	13,1	0,0216	13,2	0,0218	16,3	0,0268	23,6	0,0389	30,1	0,0497

104	619	10,6	0,0172	9,75	0,0158	13,3	0,0214	13,3	0,0215	16,4	0,0265	23,7	0,0383	30,2	0,0488
106	631	10,8	0,0172	9,83	0,0156	13,5	0,0213	13,4	0,0213	16,6	0,0263	23,8	0,0377	30,3	0,0481
108	643	10,9	0,0169	9,92	0,0154	13,4	0,0209	13,5	0,021	16,6	0,0258	24,1	0,0375	30,4	0,0472
110	655	11	0,0167	10,1	0,0154	13,5	0,0206	13,7	0,0209	16,7	0,0256	24,2	0,0369	30,6	0,0467
112	667	11,2	0,0168	10,1	0,0152	13,6	0,0205	13,8	0,0206	16,8	0,0251	24,4	0,0365	30,7	0,0459
114	679	11,5	0,0169	10,2	0,0151	13,9	0,0204	13,7	0,0202	17	0,0251	24,3	0,0358	30,9	0,0455
116	691	11,5	0,0166	10,4	0,015	13,9	0,0202	13,9	0,0201	17,1	0,0247	24,5	0,0355	31	0,0449
118	703	11,5	0,0164	10,5	0,015	14	0,0199	14	0,0199	17,2	0,0244	24,6	0,035	31,2	0,0443
120	716	11,7	0,0164	10,5	0,0147	14,2	0,0199	14	0,0196	17,2	0,024	24,8	0,0347	31,2	0,0436
122	728	11,7	0,0161	10,7	0,0148	14,2	0,0195	14,3	0,0196	17,4	0,0239	25	0,0344	31,4	0,0432
124	740	11,8	0,016	10,9	0,0147	14,3	0,0193	14,4	0,0194	17,4	0,0236	25,1	0,034	31,5	0,0426
126	752	12,2	0,0162	10,9	0,0145	14,6	0,0194	14,3	0,0191	17,6	0,0234	25,2	0,0335	31,6	0,0421
128	764	12,1	0,0159	11,1	0,0146	14,6	0,0191	14,5	0,019	17,7	0,0231	25,4	0,0332	31,7	0,0415
130	776	12,3	0,0159	11,2	0,0145	14,7	0,019	14,6	0,0188	17,8	0,023	25,4	0,0328	31,9	0,041
132	788	12,4	0,0158	11,4	0,0145	14,8	0,0188	14,8	0,0188	18	0,0228	25,5	0,0323	32,1	0,0407
134	800	12,7	0,0159	11,4	0,0142	15,1	0,0188	14,8	0,0184	17,9	0,0224	25,6	0,032	32	0,04
136	812	12,8	0,0158	11,5	0,0141	15,2	0,0187	14,9	0,0183	18	0,0222	25,8	0,0317	32,1	0,0395
138	825	12,9	0,0157	11,8	0,0144	15,3	0,0185	14,8	0,018	18,3	0,0222	25,7	0,0312	32,3	0,0391
140	837	12,9	0,0154	11,8	0,0141	15,3	0,0183	15,2	0,0182	18,3	0,0219	26	0,0311	32,3	0,0386
142	849	13	0,0154	11,9	0,0141	15,4	0,0182	15,3	0,018	18,5	0,0217	26,1	0,0307	32,5	0,0383
144	861	13,2	0,0153	12	0,014	15,6	0,0181	15,4	0,0178	18,6	0,0216	26,1	0,0304	32,6	0,0378
146	873	13,2	0,0151	12,2	0,0139	15,6	0,0178	15,6	0,0179	18,7	0,0214	26,3	0,0302	32,6	0,0374
148	885	13,3	0,015	12,4	0,014	15,7	0,0177	15,6	0,0177	18,9	0,0214	26,3	0,0297	32,8	0,0371
150	897	13,4	0,0149	12,5	0,0139	15,7	0,0175	15,8	0,0176	18,9	0,021	26,5	0,0295	32,8	0,0366
152	909	13,7	0,0151	12,4	0,0136	16	0,0176	15,7	0,0173	18,9	0,0207	26,6	0,0293	32,8	0,036
154	921	13,7	0,0149	12,6	0,0137	16	0,0174	15,9	0,0172	19,1	0,0207	26,7	0,029	33	0,0358
156	934	13,8	0,0148	12,7	0,0136	16,2	0,0173	15,9	0,0171	19,3	0,0207	26,7	0,0286	33,1	0,0354
158	946	13,9	0,0147	12,8	0,0136	16,2	0,0171	16,1	0,017	19,4	0,0205	26,9	0,0284	33,2	0,0351
160	958	14,1	0,0147	13	0,0135	16,4	0,0171	16	0,0167	19,4	0,0203	26,8	0,028	33,3	0,0348
162	970	14,2	0,0146	13,2	0,0136	16,5	0,017	16,1	0,0166	19,6	0,0202	26,9	0,0277	33,4	0,0344
164	982	14,1	0,0144	13,4	0,0137	16,4	0,0167	16,4	0,0167	19,7	0,0201	27,2	0,0277	33,5	0,0341
166	994	14,5	0,0145	13,6	0,0137	16,7	0,0168	16,3	0,0164	19,6	0,0198	27,2	0,0274	33,4	0,0336
168	1 010	14,4	0,0143	14	0,014	16,7	0,0166	16,5	0,0164	19,8	0,0197	27,3	0,0271	33,6	0,0334
170	1 020	14,6	0,0143	14,4	0,0141	16,8	0,0165	16,6	0,0163	19,9	0,0195	27,5	0,027	33,7	0,0331
172	1 030	14,7	0,0142	14,8	0,0144	17	0,0165	16,7	0,0162	20,1	0,0195	27,3	0,0265	33,9	0,0329
174	1 040	15	0,0144	15,1	0,0145	17,2	0,0165	16,8	0,0161	20,2	0,0193	27,5	0,0264	33,9	0,0325
176	1 050	15,3	0,0145	15,7	0,0148	17,2	0,0163	16,9	0,0161	20,4	0,0194	27,6	0,0262	34,1	0,0323
178	1 070	15,8	0,0148	15,9	0,0149	17,3	0,0162	17,2	0,0161	20,3	0,0191	27,9	0,0262	34	0,0319
180	1 080	16,2	0,015	16,3	0,0151	17,5	0,0162	17,3	0,016	20,6	0,0191	28	0,0259	34,2	0,0317
182	1 090	16,6	0,0152	16,3	0,015	17,7	0,0162	17,4	0,0159	20,7	0,019	28,1	0,0257	34,3	0,0314
184	1 100	17	0,0154	16,7	0,0151	17,8	0,0161	17,7	0,016	20,9	0,0189	28,2	0,0256	34,4	0,0312
186	1 120	17,5	0,0157	16,9	0,0151	17,9	0,016	17,8	0,016	21,1	0,0189	28,2	0,0253	34,6	0,0311
188	1 130	17,9	0,0159	17,2	0,0152	17,9	0,0159	18	0,016	21,2	0,0188	28,4	0,0252	34,7	0,0308
190	1 140	18,4	0,0161	17,2	0,0151	18,2	0,016	18,2	0,016	21,1	0,0185	28,7	0,0252	34,7	0,0305
192	1 150	18,3	0,0159	17,5	0,0152	18,4	0,016	18,6	0,0161	21,4	0,0186	28,6	0,0249	34,9	0,0303
194	1 160	18,6	0,016	17,7	0,0152	18,7	0,0161	18,8	0,0162	21,4	0,0184	28,8	0,0247	35	0,0301
196	1 180	18,8	0,016	17,9	0,0152	19,1	0,0162	19,2	0,0163	21,6	0,0184	28,9	0,0246	35,1	0,0299
198	1 190	19,1	0,0161	18,2	0,0153	19,4	0,0164	19,5	0,0164	21,6	0,0182	29,2	0,0246	35,1	0,0296
200	1 200	19,3	0,0161	18,5	0,0154	19,7	0,0164	20	0,0167	21,8	0,0181	29,3	0,0244	35,3	0,0294

Time	Shear Rate	Shear Stress	Viscosity	Shear Stress	Viscosity	Shear Stress	Viscosity	Shear Stress	Viscosity	Shear Stress	Viscosity	Shear Stress	Viscosity	Shear Stress	Viscosity
[s]	[1/s]	[Pa]	[Pa·s]	[Pa]	[Pa·s]	[Pa]	[Pa·s]	[Pa]	[Pa·s]	[Pa]	[Pa·s]	[Pa]	[Pa·s]	[Pa]	[Pa·s]
Number of Intervals:		BT-CNC-WDEs (6 wt %) 0.0 % 80°C	BT-CNC-WDEs (6 wt %) 0.0 % 80°C	BT-CNC-WDEs (6 wt %) 0.4 % 80°C	BT-CNC-WDEs (6 wt %) 0.4 % 80°C	BT-CNC-WDEs (6 wt %) 0.8 % 80°C	BT-CNC-WDEs (6 wt %) 0.8 % 80°C	BT-CNC-WDEs (6 wt %) 1.2 % 80°C	BT-CNC-WDEs (6 wt %) 1.2 % 80°C	BT-CNC-WDEs (6 wt %) 1.6 % 80°C	BT-CNC-WDEs (6 wt %) 1.6 % 80°C	BT-CNC-WDEs (6 wt %) 2.0 % 80°C	BT-CNC-WDEs (6 wt %) 2.0 % 80°C	BT-CNC-WDEs (6 wt %) 2.4 % 80°C	BT-CNC-WDEs (6 wt %) 2.4 % 80°C
2	0,999	0,236	0,236	0,215	0,215	0,352	0,352	0,494	0,494	0,696	0,693	0,359	0,359	1,42	1,42
4	13,1	2,38	0,182	1,47	0,112	1,84	0,14	2	0,153	3,23	0,246	6,43	0,491	7,42	0,566
6	25,2	2,75	0,109	2,06	0,0815	2,52	0,1	3,06	0,121	4,44	0,176	7,69	0,305	9,29	0,368
8	37,3	2,95	0,079	2,42	0,0649	2,88	0,0771	3,63	0,0974	5,05	0,135	8,02	0,215	10,6	0,283
10	49,4	3,23	0,0654	2,63	0,0532	3,13	0,0633	4,03	0,0816	5,45	0,11	8,52	0,172	11,4	0,231
12	61,6	3,46	0,0563	2,92	0,0474	3,49	0,0567	4,5	0,0732	5,92	0,0961	8,9	0,145	12,3	0,2
14	73,7	3,67	0,0498	3,15	0,0428	3,83	0,0521	4,97	0,0675	6,28	0,0853	9,37	0,127	13,1	0,178
16	85,8	3,9	0,0454	3,41	0,0398	4,06	0,0474	5,32	0,062	6,66	0,0777	9,82	0,115	13,8	0,161
18	97,9	4,14	0,0423	3,58	0,0365	4,33	0,0443	5,77	0,059	7,03	0,0718	10,1	0,104	14,5	0,148
20	110	4,36	0,0396	3,8	0,0345	4,67	0,0425	5,97	0,0543	7,3	0,0664	10,5	0,0956	15	0,137
22	122	4,56	0,0373	3,99	0,0327	5,01	0,041	6,35	0,052	7,69	0,063	10,8	0,0887	15,6	0,127
24	134	4,75	0,0354	4,21	0,0314	5,35	0,0399	6,7	0,0499	8,01	0,0597	11,2	0,0836	16	0,12
26	146	4,97	0,034	4,43	0,0303	5,51	0,0376	6,94	0,0474	8,41	0,0574	11,5	0,0787	16,5	0,113
28	158	5,14	0,0324	4,65	0,0293	5,72	0,0361	7,16	0,0452	8,73	0,0551	11,9	0,0754	17	0,107
30	171	5,38	0,0316	4,81	0,0282	6	0,0352	7,44	0,0436	9,02	0,0529	12,3	0,0719	17,4	0,102
32	183	5,52	0,0302	4,95	0,0271	6,17	0,0338	7,69	0,0421	9,25	0,0506	12,7	0,0696	17,8	0,0975
34	195	5,6	0,0288	5,13	0,0263	6,4	0,0329	7,91	0,0406	9,54	0,049	13,1	0,0672	18,3	0,0938
36	207	5,83	0,0282	5,28	0,0255	6,63	0,032	8,12	0,0392	9,82	0,0475	13,4	0,065	18,7	0,0904
38	219	5,97	0,0273	5,46	0,0249	6,9	0,0315	8,37	0,0382	10,1	0,0461	13,8	0,0631	19,2	0,0876
40	231	6,14	0,0266	5,6	0,0242	7,11	0,0308	8,58	0,0371	10,4	0,0448	14,1	0,0611	19,5	0,0846
42	243	6,33	0,026	5,76	0,0237	7,32	0,0301	8,77	0,0361	10,6	0,0434	14,4	0,0591	20	0,0822
44	255	6,36	0,0249	5,91	0,0232	7,44	0,0291	9	0,0352	10,8	0,0422	14,7	0,0577	20,3	0,0794
46	267	6,54	0,0244	6,02	0,0225	7,69	0,0287	9,18	0,0343	11	0,0411	15	0,056	20,6	0,0771
48	280	6,65	0,0238	6,19	0,0222	7,87	0,0281	9,38	0,0336	11,2	0,04	15,3	0,0548	21	0,075
50	292	6,88	0,0236	6,32	0,0217	8,03	0,0275	9,5	0,0326	11,3	0,0389	15,5	0,0531	21,2	0,0728
52	304	6,97	0,0229	6,48	0,0213	8,26	0,0272	9,72	0,032	11,6	0,038	15,8	0,0519	21,5	0,0707
54	316	7,11	0,0225	6,62	0,021	8,47	0,0268	9,91	0,0314	11,8	0,0374	16	0,0507	21,8	0,0689
56	328	7,22	0,022	6,82	0,0208	8,62	0,0263	10,1	0,0308	12	0,0367	16,3	0,0497	22	0,0672
58	340	7,38	0,0217	6,9	0,0203	8,89	0,0261	10,4	0,0304	12,3	0,0362	16,5	0,0486	22,4	0,066
60	352	7,51	0,0213	7,07	0,0201	9,07	0,0258	10,6	0,03	12,5	0,0355	16,8	0,0477	22,7	0,0644
62	364	7,64	0,021	7,3	0,02	9,18	0,0252	10,7	0,0293	12,6	0,0345	17,1	0,047	22,9	0,0628
64	376	7,84	0,0208	7,38	0,0196	9,43	0,0251	10,9	0,0289	12,9	0,0342	17,3	0,046	23,2	0,0617
66	389	7,98	0,0205	7,54	0,0194	9,6	0,0247	11	0,0284	13,1	0,0336	17,6	0,0452	23,4	0,0601
68	401	8,16	0,0204	7,67	0,0191	9,76	0,0244	11,2	0,0279	13,2	0,033	17,7	0,0442	23,7	0,0591
70	413	8,19	0,0198	7,9	0,0191	9,89	0,024	11,4	0,0275	13,4	0,0324	18	0,0436	23,9	0,058
72	425	8,33	0,0196	8,04	0,0189	10,1	0,0237	11,6	0,0272	13,6	0,032	18,2	0,0428	24,2	0,0569
74	437	8,49	0,0194	8,18	0,0187	10,2	0,0233	11,6	0,0266	13,6	0,0312	18,4	0,042	24,4	0,0558
76	449	8,7	0,0194	8,2	0,0183	10,5	0,0233	11,8	0,0263	13,9	0,031	18,5	0,0411	24,7	0,0551
78	461	8,59	0,0186	8,59	0,0186	10,7	0,0233	11,7	0,0253	14,2	0,0308	18,7	0,0406	25,2	0,0546
80	473	8,92	0,0188	8,54	0,018	10,7	0,0225	12,1	0,0255	14,1	0,0299	18,9	0,04	25,2	0,0531
82	485	9,13	0,0188	8,56	0,0176	10,9	0,0224	12,2	0,0251	14,4	0,0296	18,9	0,039	25,5	0,0524
84	498	9,24	0,0186	8,72	0,0175	10,9	0,022	12,2	0,0246	14,4	0,029	19,2	0,0385	25,6	0,0514
86	510	9,4	0,0184	8,8	0,0173	11,1	0,0218	12,4	0,0242	14,5	0,0285	19,3	0,0378	25,8	0,0507
88	522	9,38	0,018	8,99	0,0172	11,3	0,0217	12,6	0,0242	14,8	0,0284	19,5	0,0374	26	0,0498
90	534	9,57	0,0179	9,06	0,017	11,5	0,0215	12,7	0,0237	14,9	0,0279	19,6	0,0368	26,2	0,0491
92	546	9,7	0,0178	9,24	0,0169	11,5	0,0211	12,8	0,0234	15	0,0275	19,8	0,0363	26,4	0,0483
94	558	9,91	0,0178	9,34	0,0167	11,7	0,0209	12,9	0,0231	15,1	0,027	20	0,0358	26,6	0,0476
96	570	9,9	0,0174	9,56	0,0168	11,8	0,0207	13,2	0,0231	15,2	0,0267	20,2	0,0355	26,7	0,0468
98	582	10	0,0172	9,71	0,0167	11,9	0,0205	13,3	0,0229	15,4	0,0264	20,4	0,035	26,9	0,0462
100	594	10,2	0,0172	9,8	0,0165	12	0,0202	13,3	0,0224	15,5	0,026	20,5	0,0345	27,1	0,0456
102	607	10,3	0,017	9,84	0,0162	12,2	0,0202	13,5	0,0223	15,7	0,026	20,6	0,034	27,4	0,0451
104	619	10,5	0,0169	9,96	0,0161	12,3	0,0199	13,5	0,0219	15,8	0,0256	20,8	0,0336	27,5	0,0445
106	631	10,6	0,0168	10	0,0159	12,5	0,0198	13,6	0,0216	15,9	0,0253	20,9	0,0331	27,7	0,0439

108	643	10,6	0,0165	10,3	0,016	12,5	0,0195	13,8	0,0215	16,1	0,025	21,1	0,0329	27,8	0,0433
110	655	10,7	0,0164	10,3	0,0157	12,7	0,0195	14	0,0214	16,3	0,0249	21,1	0,0323	28,1	0,0429
112	667	10,8	0,0162	10,5	0,0157	12,8	0,0192	14,1	0,0211	16,3	0,0244	21,4	0,032	28,2	0,0422
114	679	11,1	0,0163	10,4	0,0154	12,9	0,019	14	0,0207	16,4	0,0241	21,4	0,0315	28,4	0,0418
116	691	11,1	0,0161	10,6	0,0154	13	0,0188	14,2	0,0205	16,5	0,0238	21,6	0,0312	28,5	0,0412
118	703	11,2	0,016	10,7	0,0152	13,2	0,0187	14,3	0,0204	16,6	0,0237	21,6	0,0308	28,7	0,0408
120	716	11,3	0,0158	10,9	0,0152	13,2	0,0185	14,4	0,0201	16,6	0,0233	21,9	0,0305	28,7	0,0401
122	728	11,4	0,0156	11	0,0151	13,4	0,0184	14,7	0,0202	16,8	0,0231	22	0,0302	28,9	0,0397
124	740	11,4	0,0155	11,1	0,015	13,5	0,0182	14,8	0,02	17	0,023	22,1	0,0299	28,9	0,0391
126	752	11,7	0,0156	11,2	0,0149	13,6	0,0181	14,7	0,0195	16,9	0,0225	22,2	0,0295	29,1	0,0388
128	764	11,8	0,0154	11,3	0,0147	13,8	0,018	14,9	0,0195	17,1	0,0224	22,3	0,0292	29,3	0,0383
130	776	11,9	0,0154	11,3	0,0146	13,9	0,0179	14,9	0,0192	17,2	0,0222	22,4	0,0289	29,5	0,038
132	788	12,1	0,0153	11,4	0,0144	14,1	0,0178	15,1	0,0191	17,5	0,0222	22,4	0,0285	29,6	0,0376
134	800	12,2	0,0152	11,6	0,0145	14,1	0,0176	15,1	0,0189	17,4	0,0218	22,7	0,0283	29,6	0,037
136	812	12,2	0,015	11,8	0,0145	14,1	0,0174	15,2	0,0187	17,5	0,0215	22,8	0,0281	29,7	0,0366
138	825	12,5	0,0151	11,7	0,0142	14,5	0,0176	15,4	0,0186	17,7	0,0214	22,8	0,0276	30	0,0364
140	837	12,4	0,0148	11,9	0,0142	14,4	0,0172	15,5	0,0186	17,7	0,0212	22,9	0,0274	30,1	0,036
142	849	12,5	0,0148	11,9	0,0141	14,6	0,0173	15,6	0,0183	17,8	0,021	23	0,0271	30,2	0,0356
144	861	12,7	0,0147	12	0,014	14,6	0,017	15,6	0,0181	17,9	0,0208	23,1	0,0269	30,3	0,0352
146	873	12,6	0,0145	12,2	0,014	14,7	0,0168	15,8	0,0181	18	0,0207	23,2	0,0266	30,4	0,0348
148	885	12,8	0,0145	12,1	0,0137	14,9	0,0168	15,9	0,0179	18,2	0,0206	23,3	0,0263	30,7	0,0346
150	897	12,8	0,0143	12,3	0,0137	14,9	0,0166	16	0,0178	18,3	0,0204	23,5	0,0262	30,7	0,0342
152	909	13,1	0,0144	12,4	0,0137	14,9	0,0164	15,9	0,0175	18,2	0,02	23,6	0,026	30,6	0,0336
154	921	13,1	0,0142	12,5	0,0135	15,1	0,0164	16,1	0,0175	18,4	0,02	23,7	0,0257	30,7	0,0333
156	934	13,3	0,0142	12,5	0,0134	15,2	0,0163	16,1	0,0173	18,5	0,0198	23,7	0,0254	30,8	0,033
158	946	13,3	0,014	12,6	0,0133	15,3	0,0162	16,3	0,0173	18,7	0,0198	23,9	0,0253	30,9	0,0327
160	958	13,6	0,0142	12,6	0,0132	15,4	0,0161	16,3	0,017	18,7	0,0195	23,9	0,0249	31,1	0,0324
162	970	13,7	0,0141	12,7	0,0131	15,6	0,016	16,4	0,0169	18,8	0,0194	23,9	0,0247	31,1	0,0321
164	982	13,7	0,0139	12,9	0,0131	15,6	0,0159	16,7	0,017	19	0,0193	24,1	0,0245	31,3	0,0319
166	994	13,8	0,0139	13,1	0,0132	15,6	0,0157	16,6	0,0167	19	0,0191	24,3	0,0244	31,2	0,0314
168	1 010	13,9	0,0138	13,2	0,0131	15,8	0,0157	16,8	0,0167	19,1	0,0189	24,3	0,0242	31,4	0,0312
170	1 020	14	0,0137	13,4	0,0132	15,8	0,0155	16,9	0,0166	19,2	0,0188	24,5	0,024	31,4	0,0309
172	1 030	14,2	0,0138	13,6	0,0132	16	0,0156	16,9	0,0164	19,3	0,0187	24,4	0,0237	31,7	0,0308
174	1 040	14,4	0,0138	14,1	0,0135	16,1	0,0155	16,9	0,0162	19,3	0,0185	24,6	0,0236	31,7	0,0304
176	1 050	14,6	0,0138	14,4	0,0137	16,3	0,0155	17,1	0,0162	19,6	0,0186	24,6	0,0234	31,9	0,0303
178	1 070	14,8	0,0138	15	0,0141	16,3	0,0153	17,3	0,0162	19,6	0,0184	24,9	0,0234	31,8	0,0298
180	1 080	15,3	0,0142	15,4	0,0143	16,4	0,0152	17,4	0,0161	19,8	0,0183	24,9	0,0231	32,1	0,0297
182	1 090	15,7	0,0144	15,8	0,0144	16,5	0,0151	17,5	0,016	19,8	0,0182	25	0,0229	32,2	0,0295
184	1 100	16	0,0145	16,2	0,0147	16,6	0,015	17,7	0,0161	20,1	0,0182	25,1	0,0228	32,3	0,0292
186	1 120	16,5	0,0148	16,4	0,0147	16,9	0,0151	17,7	0,0159	20,2	0,0181	25,1	0,0225	32,5	0,0291
188	1 130	16,8	0,0149	16,4	0,0146	17	0,0151	18	0,0159	20,3	0,018	25,2	0,0223	32,6	0,0289
190	1 140	17,2	0,0151	16,8	0,0148	17,1	0,015	18	0,0158	20,3	0,0178	25,5	0,0224	32,5	0,0285
192	1 150	17,7	0,0154	17	0,0147	17,4	0,0151	18,2	0,0158	20,5	0,0178	25,5	0,0222	32,7	0,0284
194	1 160	18,1	0,0156	17,2	0,0148	17,7	0,0152	18,4	0,0158	20,5	0,0177	25,6	0,022	32,8	0,0282
196	1 180	18,3	0,0156	17,3	0,0147	18	0,0153	18,5	0,0158	20,7	0,0176	25,7	0,0219	32,9	0,028
198	1 190	18,4	0,0155	17,7	0,0149	18,2	0,0153	18,9	0,0159	20,7	0,0174	26	0,0219	32,9	0,0277
200	1 200	18,6	0,0155	17,9	0,0149	18,5	0,0154	19,2	0,016	21	0,0175	26,1	0,0217	33	0,0275

RHEOLOGICAL DATA OF CNC/ATT-WDFs (FW)

Time	Shear Rate	Shear Stress	Viscosity	Shear Stress	Viscosity	Shear Stress	Viscosity	Shear Stress	Viscosity	Shear Stress	Viscosity	Shear Stress	Viscosity	Shear Stress	Viscosity	Shear Stress	Viscosity
[s]	[1/s]	[Pa]	[Pa·s]	[Pa]	[Pa·s]	[Pa]	[Pa·s]	[Pa]	[Pa·s]	[Pa]	[Pa·s]	[Pa]	[Pa·s]	[Pa]	[Pa·s]	[Pa]	[Pa·s]
Number of Intervals:		CNC-ATT-WDFs (6 wt %) 0.0 % 20°C F.W.	CNC-ATT-WDFs (6 wt %) 0.0 % 20°C F.W.	CNC-ATT-WDFs (6 wt %) 0.4 % 20°C F.W.	CNC-ATT-WDFs (6 wt %) 0.4 % 20°C F.W.	CNC-ATT-WDFs (6 wt %) 0.8 % 20°C F.W.	CNC-ATT-WDFs (6 wt %) 0.8 % 20°C F.W.	CNC-ATT-WDFs (6 wt %) 1.2 % 20°C F.W.	CNC-ATT-WDFs (6 wt %) 1.2 % 20°C F.W.	CNC-ATT-WDFs (6 wt %) 1.6 % 20°C F.W.	CNC-ATT-WDFs (6 wt %) 1.6 % 20°C F.W.	CNC-ATT-WDFs (6 wt %) 2.0 % 20°C F.W.	CNC-ATT-WDFs (6 wt %) 2.0 % 20°C F.W.	CNC-ATT-WDFs (6 wt %) 2.4 % 20°C F.W.	CNC-ATT-WDFs (6 wt %) 2.4 % 20°C F.W.
2	0,999	-0,633	-0,632	-1,24	-1,24	-1	-1	-0,11	-0,11	-0,0725	-0,073	-0,668	-0,668	-1,11	-1,11		
4	13,1	-0,503	-0,03 84	-0,481	-0,0367	-0,331	-0,0252	-0,215	-0,0164	0,407	0,031	0,07 21	0,0055	0,058	0,0044 2		
6	25,2	-0,04 22	-0,00 167	-0,431	-0,0171	-0,334	-0,0132	-0,173	-0,00684	0,37	0,0147	0,108	0,00428	0,594	0,0236		
8	37,3	-0,182	-0,00 487	-0,288	-0,00771	-0,214	-0,00573	-0,201	-0,00538	0,519	0,0139	0,209	0,00559	1,13	0,0303		
10	49,4	0,133	0,00 269	-0,19	-0,00384	-0,184	-0,00372	-0,09 92	-0,00201	0,333	0,00674	0,27 8	0,00561	1,88	0,038		
12	61,6	0,115	0,00 187	-0,266	-0,00433	-0,182	-0,00296	0,04 53	7,36E-4	0,291	0,00472	0,27 1	0,00441	2,08	0,0338		
14	73,7	0,166	0,00 225	-0,066	-8,97E-4	-0,135	-0,00184	0,101	0,00137	0,628	0,00852	0,44 6	0,00606	2,42	0,0328		
16	85,8	0,238	0,00 277	0,072	8,39E-4	0,005 64	6,58E-5	0,165	0,00192	0,768	0,00895	0,59 9	0,00699	2,33	0,0272		
18	97,9	0,151	0,00 155	0,060 6	6,2E-4	0,129	0,00132	0,128	0,00131	0,684	0,00699	0,57 7	0,00589	2,3	0,0235		
20	110	0,283	0,00 258	0,047 3	4,3E-4	0,118	0,00107	0,235	0,00214	0,764	0,00695	0,74 8	0,0068	1,97	0,0179		
22	122	0,337	0,00 276	0,151	0,00124	0,198	0,00162	0,277	0,00227	0,699	0,00572	0,78 7	0,00645	2,08	0,017		
24	134	0,397	0,00 296	0,182	0,00135	0,259	0,00193	0,365	0,00272	0,77	0,00574	0,94 4	0,00704	2,01	0,015		
26	146	0,581	0,00 397	0,288	0,00197	0,347	0,00237	0,393	0,00269	0,861	0,00588	1,01	0,00688	1,88	0,0128		
28	158	0,56	0,00 354	0,395	0,00249	0,459	0,0029	0,374	0,00236	0,921	0,00581	1,1	0,00692	1,95	0,0123		
30	171	0,661	0,00 388	0,51	0,00299	0,575	0,00337	0,429	0,00252	0,976	0,00572	1,18	0,00694	1,97	0,0115		
32	183	0,737	0,00 403	0,545	0,00298	0,572	0,00313	0,546	0,00299	1,01	0,00551	1,27	0,00695	2	0,0109		
34	195	0,732	0,00 376	0,679	0,00348	0,657	0,00337	0,57	0,00293	1,01	0,00518	1,23	0,0063	2,11	0,0108		
36	207	0,763	0,00 369	0,625	0,00302	0,611	0,00295	0,658	0,00318	1,08	0,00524	1,39	0,0067	2,15	0,0104		
38	219	0,956	0,00 437	0,716	0,00327	0,767	0,0035	0,68	0,0031	1,18	0,0054	1,43	0,00651	2,31	0,0106		
40	231	1	0,00 434	0,814	0,00352	0,835	0,00361	0,703	0,00304	1,24	0,00535	1,46	0,0063	2,41	0,0104		
42	243	1,1	0,00 452	0,827	0,0034	0,859	0,00353	0,827	0,0034	1,34	0,0055	1,56	0,0064	2,45	0,0101		
44	255	1,05	0,00 409	0,921	0,00361	0,851	0,00333	1,03	0,00405	1,27	0,00499	1,62	0,00633	2,42	0,0094 8		

46	267	1,17	0,00439	1,11	0,00417	1,07	0,00399	0,971	0,00363	1,37	0,00511	1,59	0,00596	2,63	0,00985
48	280	1,21	0,00433	1,1	0,00393	1,03	0,00367	1,09	0,00391	1,44	0,00515	1,71	0,00612	2,6	0,0093
50	292	1,28	0,00437	1,17	0,004	1,15	0,00395	1,1	0,00376	1,53	0,00526	1,8	0,00617	2,76	0,00945
52	304	1,32	0,00434	1,27	0,00418	1,19	0,00392	1,19	0,0039	1,58	0,00521	1,81	0,00596	2,75	0,00904
54	316	1,36	0,0043	1,37	0,00432	1,26	0,004	1,27	0,00402	1,63	0,00517	1,87	0,00593	2,84	0,00899
56	328	1,43	0,00436	1,45	0,00441	1,33	0,00407	1,36	0,00413	1,66	0,00507	1,89	0,00577	2,91	0,00887
58	340	1,51	0,00443	1,53	0,00449	1,47	0,00431	1,34	0,00394	1,83	0,00538	2,07	0,00609	3,06	0,00901
60	352	1,41	0,004	1,61	0,00457	1,43	0,00405	1,58	0,00448	1,81	0,00513	2,12	0,00603	2,99	0,00848
62	364	1,63	0,00446	1,58	0,00432	1,62	0,00444	1,58	0,00434	2,05	0,00563	2,37	0,00651	3,16	0,00868
64	376	1,76	0,00466	1,8	0,00478	1,86	0,00495	1,57	0,00416	2,21	0,00587	2,36	0,00626	3,41	0,00905
66	389	1,83	0,00471	2,03	0,00522	2,02	0,00519	1,59	0,00408	2,2	0,00565	2,31	0,00595	3,57	0,00919
68	401	1,92	0,0048	1,93	0,00481	2,03	0,00507	1,83	0,00456	2,4	0,00598	2,59	0,00646	3,5	0,00873
70	413	1,84	0,00445	2	0,00484	1,89	0,00457	2,11	0,00511	2,33	0,00566	2,69	0,00652	3,45	0,00836
72	425	2,05	0,00482	2,22	0,00523	2,24	0,00528	2,03	0,00478	2,45	0,00578	2,6	0,00612	3,79	0,00892
74	437	2,04	0,00468	2,21	0,00505	2,13	0,00488	2,29	0,00525	2,54	0,0058	2,83	0,00647	3,8	0,00868
76	449	2,22	0,00493	2,33	0,00518	2,33	0,00518	2,29	0,00511	2,74	0,00611	2,95	0,00658	4,03	0,00897
78	461	2,64	0,00573	2,14	0,00464	2,24	0,00486	2,01	0,00436	2,5	0,00541	2,97	0,00645	3,76	0,00814
80	473	2,4	0,00507	2,61	0,00551	2,55	0,00538	2,56	0,00541	2,89	0,00611	3,03	0,00641	4,12	0,0087
82	485	2,55	0,00526	2,76	0,00568	2,71	0,00558	2,65	0,00546	3,12	0,00643	3,07	0,00632	4,32	0,0089
84	498	2,63	0,00529	2,7	0,00543	2,75	0,00552	2,85	0,00573	3,23	0,0065	3,4	0,00684	4,23	0,0085
86	510	2,76	0,00541	3,06	0,006	2,97	0,00582	2,89	0,00567	3,3	0,00647	3,21	0,0063	4,45	0,00873
88	522	2,66	0,00509	3,03	0,0058	2,81	0,00539	3,23	0,0062	3,24	0,00621	3,52	0,00675	4,37	0,00838
90	534	2,83	0,0053	2,99	0,00561	2,93	0,00548	3,28	0,00614	3,39	0,00634	3,78	0,00708	4,52	0,00847
92	546	2,94	0,00539	3,1	0,00568	2,99	0,00547	3,43	0,00628	3,49	0,00639	3,89	0,00712	4,55	0,00833
94	558	3	0,00538	3,37	0,00603	3,02	0,00541	3,59	0,00643	3,48	0,00623	3,8	0,00682	4,67	0,00837
96	570	3,29	0,00577	3,62	0,00635	3,37	0,00592	3,39	0,00595	3,7	0,00649	3,79	0,00665	5,06	0,00887
98	582	3,31	0,00568	3,47	0,00596	3,37	0,00579	3,7	0,00635	3,87	0,00665	4,18	0,00717	4,92	0,00846
100	594	3,48	0,00586	3,75	0,00631	3,65	0,00615	3,69	0,0062	4,01	0,00675	4,13	0,00695	5,38	0,00905
102	607	3,45	0,00568	3,89	0,00641	3,62	0,00598	3,87	0,00639	4,03	0,00665	4,33	0,00715	5,44	0,00897
104	619	3,53	0,00571	3,96	0,0064	3,73	0,00603	3,99	0,00644	4,16	0,00673	4,49	0,00726	5,52	0,00892
106	631	3,64	0,00577	4,03	0,00639	3,82	0,00606	4,11	0,00652	4,34	0,00688	4,57	0,00725	5,58	0,00884
108	643	3,69	0,00573	4,15	0,00646	3,9	0,00607	4,32	0,00672	4,39	0,00682	4,66	0,00725	5,8	0,00903
110	655	3,93	0,00601	4,33	0,0066	4,32	0,00659	4,17	0,00637	4,59	0,00701	4,67	0,00713	5,9	0,00901
112	667	3,8	0,0057	4,3	0,00644	4,04	0,00605	4,63	0,00693	4,51	0,00676	4,91	0,00735	5,84	0,00875

114	679	4,16	0,00613	4,26	0,00627	4,43	0,00652	4,57	0,00673	4,91	0,00723	5,15	0,00758	5,98	0,00881
116	691	4,35	0,0063	4,43	0,00641	4,6	0,00666	4,52	0,00654	5,1	0,00738	5,24	0,00759	6,25	0,00904
118	703	4,45	0,00633	4,49	0,00638	4,67	0,00664	4,66	0,00663	5,21	0,00741	5,37	0,00764	6,25	0,00889
120	716	4,28	0,00598	4,55	0,00636	4,44	0,00621	5,06	0,00707	5,21	0,00729	5,41	0,00756	6,23	0,0087
122	728	4,34	0,00596	5,01	0,00689	4,69	0,00645	5,16	0,0071	5,13	0,00705	5,3	0,00729	6,47	0,00889
124	740	4,62	0,00624	4,81	0,00651	4,8	0,00649	5,15	0,00696	5,53	0,00747	5,81	0,00785	6,68	0,00903
126	752	4,86	0,00646	5,25	0,00699	5	0,00665	5,33	0,00709	5,59	0,00744	5,7	0,00758	7,04	0,00936
128	764	4,88	0,00638	5,26	0,00688	5	0,00655	5,48	0,00717	5,7	0,00746	5,81	0,00761	7	0,00916
130	776	5,01	0,00646	5,44	0,00701	5,22	0,00672	5,58	0,00719	5,87	0,00756	6	0,00773	7,01	0,00903
132	788	5	0,00635	5,41	0,00687	5,24	0,00665	5,8	0,00736	5,97	0,00758	6,15	0,0078	7,08	0,00898
134	800	5,07	0,00634	5,64	0,00704	5,26	0,00657	5,99	0,00748	6,01	0,00751	6,1	0,00762	7,28	0,0091
136	812	5,45	0,00671	5,61	0,0069	5,63	0,00693	5,84	0,00719	6,41	0,00789	6,37	0,00784	7,52	0,00926
138	825	5,58	0,00677	5,74	0,00696	5,4	0,00655	6,21	0,00754	6,13	0,00744	6,33	0,00768	7,34	0,0089
140	837	5,38	0,00643	5,8	0,00693	5,39	0,00644	6,53	0,0078	6,47	0,00773	6,78	0,00811	7,4	0,00885
142	849	5,64	0,00664	5,87	0,00691	5,6	0,0066	6,58	0,00775	6,74	0,00794	7	0,00825	7,66	0,00902
144	861	5,71	0,00663	6,09	0,00707	5,78	0,00672	6,78	0,00788	6,8	0,0079	7,09	0,00824	7,7	0,00895
146	873	5,9	0,00675	6,54	0,00749	5,94	0,0068	6,88	0,00788	6,84	0,00783	6,92	0,00793	8,04	0,00921
148	885	6,3	0,00712	6,41	0,00724	6,4	0,00723	6,66	0,00752	7,35	0,0083	7,2	0,00814	8,43	0,00953
150	897	6,18	0,00688	6,69	0,00745	6,19	0,0069	7,16	0,00798	7,13	0,00794	7,3	0,00813	8,43	0,0094
152	909	6,4	0,00703	6,67	0,00734	6,45	0,0071	7,12	0,00783	7,39	0,00813	7,61	0,00836	8,49	0,00934
154	921	6,57	0,00714	6,89	0,00748	6,65	0,00722	7,17	0,00779	7,6	0,00824	7,72	0,00837	8,78	0,00952
156	934	6,68	0,00716	7,06	0,00756	6,74	0,00722	7,32	0,00784	7,69	0,00824	7,83	0,00839	8,91	0,00954
158	946	6,84	0,00724	7,28	0,0077	6,97	0,00737	7,39	0,00781	7,86	0,00831	7,93	0,00839	9,05	0,00957
160	958	7,05	0,00736	7,24	0,00756	7,05	0,00736	7,47	0,00779	8,15	0,00851	8,19	0,00856	9,16	0,00957
162	970	7,03	0,00725	7,61	0,00785	7,12	0,00734	7,8	0,00805	8,06	0,00831	8,14	0,00839	9,25	0,00954
164	982	7,2	0,00733	7,42	0,00755	7,16	0,00729	7,78	0,00792	8,37	0,00853	8,56	0,00872	9,44	0,00961
166	994	7,53	0,00758	7,68	0,00773	7,73	0,00777	7,61	0,00765	8,71	0,00876	8,53	0,00858	9,95	0,01
168	1 010	7,68	0,00764	8,05	0,008	7,88	0,00783	7,65	0,0076	8,83	0,00878	8,6	0,00855	10,2	0,0101
170	1 020	7,72	0,00758	8	0,00786	7,89	0,00775	7,86	0,00772	9,04	0,00888	9,01	0,00884	10,4	0,0102
172	1 030	7,53	0,00731	7,99	0,00776	7,68	0,00745	8,34	0,0081	8,96	0,0087	9,15	0,00888	10,3	0,01
174	1 040	7,92	0,0076	8,51	0,00816	8,13	0,0078	8,25	0,00791	9,15	0,00877	9,02	0,00865	10,7	0,0102
176	1 050	7,89	0,00748	8,42	0,00798	8,09	0,00767	8,64	0,00819	9,32	0,00884	9,39	0,0089	10,5	0,00994
178	1 070	8,18	0,00767	8,6	0,00806	8,36	0,00783	8,55	0,00801	9,58	0,00898	9,46	0,00887	10,8	0,0101
180	1 080	8,34	0,00773	8,77	0,00813	8,42	0,00781	8,73	0,00809	9,69	0,00898	9,51	0,00882	10,9	0,0101

182	1 090	8,42	0,00772	8,89	0,00815	8,49	0,00779	8,97	0,00822	9,81	0,00899	9,64	0,00884	11,1	0,0101
184	1 100	8,66	0,00785	9,1	0,00825	8,8	0,00798	9,02	0,00818	9,92	0,00899	9,81	0,0089	11,4	0,0104
186	1 120	9,05	0,00811	9,07	0,00813	8,99	0,00806	9,13	0,00818	10,3	0,00925	10,2	0,00913	11,4	0,0103
188	1 130	8,9	0,00789	9,42	0,00835	8,86	0,00785	9,44	0,00837	10,1	0,00899	10,1	0,00893	11,2	0,00996
190	1 140	9,28	0,00814	9,21	0,00809	8,91	0,00782	9,64	0,00846	10,5	0,00919	10,6	0,00931	11,3	0,0099
192	1 150	9,55	0,00829	9,34	0,00811	9,37	0,00813	9,54	0,00828	10,7	0,00929	10,8	0,00936	11,7	0,0102
194	1 160	9,7	0,00834	9,48	0,00815	9,51	0,00818	9,69	0,00833	10,9	0,00938	11	0,00946	12	0,0103
196	1 180	9,73	0,00828	9,61	0,00817	9,38	0,00797	10	0,00855	10,9	0,00925	11,1	0,00941	12,1	0,0103
198	1 190	9,57	0,00805	10,1	0,00848	9,43	0,00794	10,3	0,00865	10,9	0,00918	10,8	0,0091	12,4	0,0104
200	1 200	10,1	0,00841	10	0,00837	9,85	0,00821	10,1	0,00841	11,4	0,00951	11,4	0,00948	12,9	0,0108

Time	Shear Rate	Shear Stress	Viscosity	Shear Stress	Viscosity	Shear Stress	Viscosity	Shear Stress	Viscosity	Shear Stress	Viscosity	Shear Stress	Viscosity	Shear Stress	Viscosity
[s]	[1/s]	[Pa]	[Pa·s]	[Pa]	[Pa·s]	[Pa]	[Pa·s]	[Pa]	[Pa·s]	[Pa]	[Pa·s]	[Pa]	[Pa·s]	[Pa]	[Pa·s]
Number of Intervals:		*CNC-ATT-WDFs (6 wt %) 0.0 % 30°C F.W.*	*CNC-ATT-WDFs (6 wt %) 0.0 % 30°C F.W.*	*CNC-ATT-WDFs (6 wt %) 0.4 % 30°C F.W.*	*CNC-ATT-WDFs (6 wt %) 0.4 % 30°C F.W.*	*CNC-ATT-WDFs (6 wt %) 0.8 % 30°C F.W.*	*CNC-ATT-WDFs (6 wt %) 0.8 % 30°C F.W.*	*CNC-ATT-WDFs (6 wt %) 1.2 % 30°C F.W.*	*CNC-ATT-WDFs (6 wt %) 1.2 % 30°C F.W.*	*CNC-ATT-WDFs (6 wt %) 1.6 % 30°C F.W.*	*CNC-ATT-WDFs (6 wt %) 1.6 % 30°C F.W.*	*CNC-ATT-WDFs (6 wt %) 2.0 % 30°C F.W.*	*CNC-ATT-WDFs (6 wt %) 2.0 % 30°C F.W.*	*CNC-ATT-WDFs (6 wt %) 2.4 % 30°C F.W.*	*CNC-ATT-WDFs (6 wt %) 2.4 % 30°C F.W.*
2	0,999	-0,552	-0,552	-0,823	-0,824	-0,858	-0,859	-0,983	-0,983	-0,46	-0,459	-0,346	-0,346	-0,603	-0,603
4	13,1	-0,352	-0,0269	-0,713	-0,0543	-0,763	-0,0582	-0,683	-0,0521	-0,218	-0,0166	-0,351	-0,0268	0,384	0,0293
6	25,2	-0,188	-0,00744	-0,489	-0,0194	-0,683	-0,0271	-0,662	-0,0263	0,153	0,00613	-0,184	-0,0073	0,65	0,0258
8	37,3	-0,126	-0,00337	-0,377	-0,0101	-0,714	-0,0191	-0,498	-0,0133	-0,0655	-0,00176	-0,176	-0,00471	1,12	0,03
10	49,4	0,036	7,27E-4	-0,355	-0,00717	-0,44	-0,0089	-0,408	-0,00826	-0,0924	-0,00187	-0,114	-0,0023	1,54	0,0312
12	61,6	0,0623	0,00101	-0,211	-0,00342	-0,212	-0,00345	-0,339	-0,00551	-0,0699	-0,00113	-0,0105	-1,7E-4	1,71	0,0278
14	73,7	0,0211	2,86E-4	-0,0561	-7,61E-4	-0,177	-0,0024	-0,238	-0,00323	0,188	0,00255	0,138	0,00188	1,94	0,0263
16	85,8	0,105	0,00123	-0,00958	-1,12E-4	-0,1	-0,00117	-0,0776	-9,04E-4	0,152	0,00178	0,22	0,00257	1,93	0,0225
18	97,9	0,23	0,00235	-0,0398	-4,06E-4	0,00358	3,66E-5	0,023	2,35E-4	0,194	0,00198	0,248	0,00253	1,88	0,0192
20	110	0,277	0,00252	0,0954	8,67E-4	-0,0968	-8,8E-4	-0,0883	-8,02E-4	0,254	0,00231	0,387	0,00352	1,95	0,0178
22	122	0,321	0,00263	0,197	0,00162	-0,00179	-1,47E-5	0,0983	8,05E-4	0,411	0,00337	0,412	0,00337	1,82	0,0149
24	134	0,434	0,00324	0,146	0,00109	0,0988	7,36E-4	0,0518	3,86E-4	0,422	0,00314	0,482	0,00359	1,75	0,0131
26	146	0,548	0,00374	0,21	0,00143	0,103	7,02E-4	0,0843	5,76E-4	0,486	0,00332	0,515	0,00352	1,74	0,0119
28	158	0,615	0,00388	0,305	0,00192	0,239	0,00151	0,222	0,0014	0,502	0,00317	0,543	0,00343	1,68	0,0106
30	171	0,667	0,00391	0,372	0,00218	0,272	0,0016	0,272	0,0016	0,499	0,00293	0,551	0,00323	1,85	0,0108
32	183	0,717	0,00393	0,431	0,00236	0,317	0,00174	0,298	0,00163	0,642	0,00352	0,613	0,00335	1,85	0,0101
34	195	0,7	0,00359	0,384	0,00197	0,364	0,00187	0,455	0,00234	0,607	0,00312	0,579	0,00297	1,84	0,00946
36	207	0,805	0,00389	0,533	0,00258	0,347	0,00167	0,377	0,00182	0,769	0,00372	0,693	0,00335	1,86	0,00901
38	219	0,906	0,00414	0,578	0,00264	0,425	0,00194	0,377	0,00172	0,722	0,0033	0,677	0,00309	1,93	0,0088
40	231	0,965	0,00418	0,62	0,00268	0,484	0,00209	0,404	0,00175	0,778	0,00337	0,743	0,00322	2,06	0,0089
42	243	1,07	0,00439	0,698	0,00287	0,506	0,00208	0,453	0,00186	0,845	0,00347	0,822	0,00338	2,04	0,00838

44	255	1,07	0,0041 8	0,73	0,0028 6	0,55 3	0,0021 6	0,51 6	0,0020 2	1,08	0,0042 2	0,95 7	0,0037 5	1,97	0,0077 1
46	267	1,11	0,0041 5	0,70 5	0,0026 3	0,73 7	0,0027 5	0,70 9	0,0026 5	1,04	0,0038 8	0,87 3	0,0032 6	2,26	0,0084 4
48	280	1,18	0,0042 2	0,85 7	0,0030 7	0,69	0,0024 7	0,67 7	0,0024 2	1,15	0,0041	1,1	0,0039 3	2,18	0,0078
50	292	1,27	0,0043 7	0,90 4	0,0031	0,79 7	0,0027 3	0,78 2	0,0026 8	1,15	0,0039 5	1,1	0,0037 6	2,27	0,0077 9
52	304	1,32	0,0043 3	0,94 1	0,0031	0,87 5	0,0028 8	0,87	0,0028 7	1,21	0,0039 9	1,16	0,0038 3	2,35	0,0077 3
54	316	1,37	0,0043 3	1,01	0,0032 1	0,93	0,0029 4	0,93	0,0029 5	1,33	0,0042 1	1,26	0,0039 8	2,44	0,0077 2
56	328	1,38	0,0042	1,05	0,0032	1,05	0,0032 2	1,06	0,0032 4	1,43	0,0043 7	1,34	0,0040 9	2,52	0,0076 9
58	340	1,56	0,0045 9	1,22	0,0035 8	1,1	0,0032 2	1,1	0,0032 4	1,39	0,0040 9	1,4	0,0041 3	2,72	0,0080 1
60	352	1,55	0,0043 9	1,24	0,0035 2	1,14	0,0032 4	1,16	0,0033	1,68	0,0047 8	1,56	0,0044 4	2,61	0,0074 1
62	364	1,8	0,0049 3	1,44	0,0039 7	1,17	0,0032 2	1,16	0,0031 8	1,58	0,0043 5	1,66	0,0045 5	2,78	0,0076 2
64	376	1,87	0,0049 8	1,39	0,0036 8	1,35	0,0035 8	1,32	0,0035 1	1,6	0,0042 4	1,66	0,0044 2	2,97	0,0078 8
66	389	1,85	0,0047 7	1,37	0,0035 3	1,48	0,0038 2	1,58	0,0040 5	1,69	0,0043 4	1,61	0,0041 5	3,1	0,0079 7
68	401	2,11	0,0052 7	1,61	0,0040 1	1,43	0,0035 6	1,41	0,0035 1	1,76	0,0044	1,88	0,0046 9	3,1	0,0077 5
70	413	2,08	0,0050 3	1,67	0,0040 5	1,42	0,0034 4	1,52	0,0036 9	2,04	0,0049 3	2,14	0,0052	3,09	0,0074 8
72	425	2,16	0,0050 7	1,59	0,0037 5	1,73	0,0040 8	1,81	0,0042 6	2,09	0,0049 3	2,02	0,0047 5	3,26	0,0076 8
74	437	2,29	0,0052 5	1,79	0,0040 9	1,61	0,0036 8	1,74	0,0039 7	2,24	0,0051 2	2,26	0,0051 7	3,21	0,0073 6
76	449	2,46	0,0054 8	1,91	0,0042 5	1,8	0,004	1,87	0,0041 7	2,26	0,0050 3	2,35	0,0052 4	3,4	0,0075 7
78	461	2,48	0,0053 8	2,21	0,0047 9	2,27	0,0049 2	1,9	0,0041 2	2,74	0,0059 4	2,28	0,0049 4	3,68	0,0079 8
80	473	2,6	0,0054 9	2,02	0,0042 8	2,08	0,0043 8	2,13	0,0044 9	2,51	0,0053	2,49	0,0052 7	3,73	0,0078 9
82	485	2,76	0,0056 8	2,09	0,0043 1	2,18	0,0045	2,26	0,0046 6	2,57	0,0053	2,6	0,0053 5	3,81	0,0078 5
84	498	2,94	0,0059	2,34	0,0047	2,14	0,0043 1	2,18	0,0043 9	2,68	0,0053 9	2,85	0,0057 4	3,85	0,0077 3
86	510	2,84	0,0055 6	2,19	0,0042 9	2,47	0,0048 4	2,55	0,0050 1	2,88	0,0056 4	2,75	0,0053 9	4,06	0,0079 6
88	522	2,97	0,0057	2,41	0,0046 1	2,3	0,0044 1	2,48	0,0047 5	3,09	0,0059 2	3,14	0,0060 1	3,93	0,0075 3
90	534	3,22	0,0060 3	2,7	0,0050 6	2,33	0,0043 7	2,47	0,0046 3	3,06	0,0057 4	3,36	0,0063	4,03	0,0075 5
92	546	3,34	0,0061 3	2,79	0,0051 1	2,44	0,0044 8	2,6	0,0047 6	3,19	0,0058 4	3,48	0,0063 6	3,96	0,0072 5
94	558	3,26	0,0058 4	2,72	0,0048 8	2,62	0,0046 9	2,89	0,0051 7	3,46	0,0061 9	3,45	0,0061 8	4,14	0,0074 2
96	570	3,37	0,0059 1	2,68	0,0047	2,98	0,0052 2	3,18	0,0055 8	3,4	0,0059 7	3,32	0,0058 3	4,46	0,0078 2
98	582	3,64	0,0062 5	3,06	0,0052 5	2,78	0,0047 7	2,97	0,0051 1	3,51	0,0060 2	3,74	0,0064 3	4,34	0,0074 6
100	594	3,66	0,0061 5	2,97	0,005	3,09	0,0052 1	3,35	0,0056 3	3,6	0,0060 6	3,66	0,0061 5	4,66	0,0078 4
102	607	3,71	0,0061 2	3,08	0,0050 8	3,19	0,0052 5	3,43	0,0056 5	3,81	0,0062 8	3,78	0,0062 3	4,63	0,0076 3
104	619	3,83	0,0061 9	3,21	0,0051 9	3,26	0,0052 7	3,48	0,0056 3	3,87	0,0062 5	3,93	0,0063 6	4,83	0,0078 1
106	631	3,93	0,0062 3	3,36	0,0053 2	3,36	0,0053 2	3,58	0,0056 8	3,93	0,0062 3	4,11	0,0065 1	4,93	0,0078 2
108	643	3,86	0,006	3,41	0,0053	3,5	0,0054 5	3,74	0,0058 1	4,2	0,0065 3	4,27	0,0066 4	5,03	0,0078 3
110	655	4,03	0,0061 5	3,5	0,0053 4	3,73	0,0056 9	4	0,0061 1	4,14	0,0063 1	4,15	0,0063 3	5,39	0,0082 2

112	667	4,04	0,00605	3,6	0,0054	3,63	0,00545	3,94	0,0059	4,52	0,00677	4,52	0,00677	5,15	0,00772
114	679	4,38	0,00645	3,96	0,00584	3,65	0,00537	3,91	0,00576	4,38	0,00645	4,65	0,00684	5,4	0,00795
116	691	4,53	0,00655	4,02	0,00582	3,89	0,00562	4,1	0,00593	4,4	0,00636	4,62	0,00668	5,59	0,00808
118	703	4,63	0,00658	4,19	0,00596	3,95	0,00562	4,2	0,00597	4,54	0,00646	4,78	0,00679	5,81	0,00826
120	716	4,67	0,00653	4,29	0,006	3,97	0,00555	4,31	0,00603	4,92	0,00687	4,94	0,00691	5,89	0,00824
122	728	4,49	0,00617	4,05	0,00556	4,46	0,00613	4,76	0,00654	5,1	0,00701	4,81	0,00661	5,89	0,0081
124	740	4,9	0,00662	4,47	0,00604	4,3	0,00581	4,56	0,00617	5,05	0,00683	5,08	0,00686	5,97	0,00807
126	752	4,86	0,00646	4,39	0,00584	4,64	0,00617	4,86	0,00646	5,22	0,00694	5,03	0,00669	6,46	0,00859
128	764	5,05	0,00661	4,55	0,00596	4,73	0,00619	4,95	0,00648	5,38	0,00704	5,24	0,00686	6,39	0,00836
130	776	5,24	0,00675	4,7	0,00606	4,74	0,00611	4,97	0,0064	5,44	0,00701	5,39	0,00695	6,55	0,00844
132	788	5,38	0,00683	4,87	0,00618	4,82	0,00611	5,07	0,00643	5,59	0,00709	5,58	0,00708	6,52	0,00828
134	800	5,27	0,00659	4,77	0,00596	4,99	0,00623	5,26	0,00658	5,86	0,00732	5,71	0,00714	6,69	0,00836
136	812	5,6	0,00689	5,03	0,00619	5,03	0,00619	5,37	0,00661	5,7	0,00702	5,73	0,00705	7,17	0,00883
138	825	5,51	0,00668	4,77	0,00579	5,34	0,00648	5,71	0,00693	6,32	0,00766	5,86	0,0071	7	0,00849
140	837	5,79	0,00692	5,17	0,00618	5,1	0,0061	5,49	0,00656	6,32	0,00755	6,3	0,00753	6,82	0,00815
142	849	5,95	0,007	5,39	0,00635	5,17	0,00609	5,53	0,00652	6,38	0,00751	6,43	0,00758	6,97	0,00822
144	861	5,97	0,00693	5,54	0,00643	5,33	0,00619	5,67	0,00659	6,63	0,0077	6,59	0,00765	7,14	0,00829
146	873	5,89	0,00675	5,3	0,00608	5,76	0,0066	6,13	0,00702	6,72	0,0077	6,48	0,00742	7,42	0,00849
148	885	6,38	0,00721	5,68	0,00642	5,85	0,00661	6,18	0,00698	6,5	0,00735	6,55	0,0074	7,79	0,0088
150	897	6,27	0,00699	5,66	0,0063	5,95	0,00663	6,3	0,00703	6,99	0,00779	6,86	0,00764	7,54	0,0084
152	909	6,56	0,00722	5,94	0,00654	5,98	0,00657	6,33	0,00696	7,01	0,0077	7,03	0,00774	7,94	0,00873
154	921	6,66	0,00723	6,01	0,00653	6,22	0,00675	6,56	0,00712	7,12	0,00773	7,11	0,00771	8,1	0,00879
156	934	6,78	0,00726	6,07	0,0065	6,34	0,00679	6,75	0,00723	7,34	0,00787	7,17	0,00768	8,19	0,00878
158	946	6,91	0,00731	6,13	0,00648	6,55	0,00692	6,93	0,00733	7,41	0,00783	7,22	0,00763	8,44	0,00892
160	958	7,14	0,00746	6,45	0,00673	6,53	0,00682	6,92	0,00722	7,41	0,00774	7,46	0,00779	8,45	0,00882
162	970	7,04	0,00725	6,28	0,00647	6,75	0,00696	7,16	0,00739	7,86	0,0081	7,59	0,00782	8,6	0,00887
164	982	7,5	0,00763	6,81	0,00693	6,71	0,00683	6,93	0,00706	7,87	0,00801	7,89	0,00804	8,62	0,00877
166	994	7,59	0,00763	6,72	0,00676	7,07	0,00712	7,22	0,00727	7,73	0,00777	7,71	0,00776	9,03	0,00909
168	1 010	7,69	0,00764	6,82	0,00678	7,24	0,0072	7,71	0,00766	7,87	0,00783	7,84	0,00779	9,35	0,0093
170	1 020	7,88	0,00774	7,09	0,00696	7,19	0,00706	7,58	0,00745	8	0,00785	8,12	0,00797	9,44	0,00927
172	1 030	7,86	0,00763	7,15	0,00694	7,19	0,00698	7,53	0,00731	8,5	0,00824	8,49	0,00824	9,35	0,00908
174	1 040	7,92	0,0076	7,04	0,00675	7,64	0,00733	8,05	0,00772	8,55	0,0082	8,26	0,00792	9,67	0,00927
176	1 050	8,15	0,00773	7,54	0,00715	7,44	0,00706	7,68	0,00729	8,9	0,00844	8,72	0,00827	9,7	0,0092
178	1 070	8,32	0,0078	7,67	0,00719	7,64	0,00716	7,97	0,00747	8,79	0,00824	8,77	0,00822	9,96	0,00933

180	1 080	8,52	0,0079	7,82	0,00725	7,82	0,00725	8,18	0,00758	8,99	0,00833	8,94	0,00828	10,1	0,00937
182	1 090	8,64	0,00792	7,88	0,00722	7,85	0,0072	8,29	0,0076	9,18	0,00841	9,07	0,00831	10,1	0,00921
184	1 100	8,77	0,00795	7,97	0,00722	8,1	0,00734	8,54	0,00774	9,25	0,00839	9,13	0,00827	10,2	0,00925
186	1 120	9,05	0,00811	8,3	0,00744	7,98	0,00716	8,54	0,00765	9,28	0,00832	9,39	0,00842	10,3	0,00919
188	1 130	8,87	0,00787	8,08	0,00717	8,33	0,00739	8,69	0,00771	9,66	0,00857	9,44	0,00837	10,3	0,00915
190	1 140	9,14	0,00802	8,56	0,00751	8,25	0,00724	8,62	0,00756	9,73	0,00854	9,87	0,00866	10,2	0,00899
192	1 150	9,43	0,00819	8,64	0,0075	8,35	0,00725	8,91	0,00774	9,64	0,00837	9,97	0,00865	10,8	0,00934
194	1 160	9,62	0,00827	8,87	0,00762	8,52	0,00732	8,98	0,00772	9,77	0,0084	10,1	0,00866	10,8	0,00932
196	1 180	9,7	0,00825	8,96	0,00762	8,56	0,00728	9,01	0,00766	10,1	0,00862	10,3	0,00879	10,8	0,00916
198	1 190	9,55	0,00804	8,93	0,00752	9,01	0,00759	9,43	0,00794	10,5	0,0088	10,2	0,00857	11	0,00924
200	1 200	9,96	0,0083	9,09	0,00758	9,01	0,0075	9,58	0,00798	10,2	0,00852	10,4	0,00866	11,6	0,00963

Time	Shear Rate	Shear Stress	Viscosity	Shear Stress	Viscosity	Shear Stress	Viscosity	Shear Stress	Viscosity	Shear Stress	Viscosity	Shear Stress	Viscosity	Shear Stress	Viscosity
[s]	[1/s]	[Pa]	[Pa·s]	[Pa]	[Pa·s]	[Pa]	[Pa·s]	[Pa]	[Pa·s]	[Pa]	[Pa·s]	[Pa]	[Pa·s]	[Pa]	[Pa·s]
Number of Intervals:		*CNC-ATT-WDFs (6 wt %) 0.0 % 40°C F.W.*	*CNC-ATT-WDFs (6 wt %) 0.0 % 40°C F.W.*	*CNC-ATT-WDFs (6 wt %) 0.4 % 40°C F.W.*	*CNC-ATT-WDFs (6 wt %) 0.4 % 40°C F.W.*	*CNC-ATT-WDFs (6 wt %) 0.8 % 40°C F.W.*	*CNC-ATT-WDFs (6 wt %) 0.8 % 40°C F.W.*	*CNC-ATT-WDFs (6 wt %) 1.2 % 40°C F.W.*	*CNC-ATT-WDFs (6 wt %) 1.2 % 40°C F.W.*	*CNC-ATT-WDFs (6 wt %) 1.6 % 40°C F.W.*	*CNC-ATT-WDFs (6 wt %) 1.6 % 40°C F.W.*	*CNC-ATT-WDFs (6 wt %) 2.0 % 40°C F.W.*	*CNC-ATT-WDFs (6 wt %) 2.0 % 40°C F.W.*	*CNC-ATT-WDFs (6 wt %) 2.4 % 40°C F.W.*	*CNC-ATT-WDFs (6 wt %) 2.4 % 40°C F.W.*
2	0,999	-1,63	-1,62	-0,645	-0,645	-0,515	-0,517	-0,675	-0,675	-1,33	-1,33	-0,524	-0,525	-0,693	-0,692
4	13,1	-0,572	-0,0436	-0,822	-0,0627	-0,482	-0,0368	-0,632	-0,0482	-0,792	-0,0604	-0,378	-0,0288	0,385	0,0293
6	25,2	-0,278	-0,011	-0,571	-0,0226	-0,275	-0,0109	-0,469	-0,0186	-0,612	-0,0243	-0,128	-0,00507	0,732	0,029
8	37,3	-0,0342	-9,16E-4	-0,445	-0,0119	-0,378	-0,0101	-0,367	-0,00983	-0,337	-0,00903	-0,133	-0,00355	1,33	0,0356
10	49,4	-0,144	-0,00291	-0,416	-0,00841	-0,259	-0,00524	-0,441	-0,00892	-0,361	-0,0073	0,0907	0,00184	1,94	0,0393
12	61,6	-0,194	-0,00315	-0,404	-0,00657	-0,225	-0,00366	-0,285	-0,00462	-0,289	-0,0047	0,189	0,00307	2,08	0,0338
14	73,7	2,28E-4	3,09E-6	-0,252	-0,00342	-0,0774	-0,00105	-0,087	-0,00118	-0,231	-0,00314	0,283	0,00383	1,9	0,0258
16	85,8	0,00177	2,07E-5	-0,157	-0,00183	-0,00669	-7,8E-5	-0,0608	-7,08E-4	-0,091	-0,00106	0,382	0,00446	1,94	0,0227
18	97,9	0,0644	6,58E-4	-0,163	-0,00166	-0,087	-8,89E-4	-0,0856	-8,74E-4	-0,0622	-6,36E-4	0,446	0,00456	1,74	0,0178
20	110	0,134	0,00122	-0,0932	-8,48E-4	-0,0339	-3,08E-4	-0,0194	-1,76E-4	0,0456	4,14E-4	0,612	0,00556	1,51	0,0137
22	122	0,249	0,00204	0,00699	5,72E-5	3,97E-4	3,25E-6	-0,00306	-2,51E-5	0,0167	1,37E-4	0,577	0,00472	1,48	0,0121
24	134	0,216	0,00161	0,0942	7,01E-4	0,101	7,56E-4	0,0459	3,42E-4	0,139	0,00104	0,671	0,005	1,42	0,0106
26	146	0,22	0,0015	0,162	0,00111	0,158	0,00108	0,118	8,05E-4	0,195	0,00133	0,704	0,00481	1,5	0,0103
28	158	0,359	0,00226	0,226	0,00143	0,18	0,00114	0,197	0,00124	0,207	0,00131	0,709	0,00447	1,54	0,00974
30	171	0,404	0,00237	0,325	0,00191	0,217	0,00127	0,256	0,0015	0,234	0,00137	0,729	0,00427	1,6	0,0094
32	183	0,431	0,00236	0,377	0,00207	0,296	0,00162	0,357	0,00196	0,362	0,00198	0,857	0,00469	1,66	0,00909
34	195	0,425	0,00218	0,443	0,00227	0,328	0,00168	0,337	0,00173	0,346	0,00178	0,837	0,0043	1,73	0,00886
36	207	0,518	0,0025	0,473	0,00229	0,401	0,00194	0,529	0,00256	0,49	0,00237	0,973	0,0047	1,76	0,00852
38	219	0,576	0,00263	0,389	0,00178	0,333	0,00152	0,532	0,00243	0,436	0,00199	0,974	0,00445	1,73	0,00791
40	231	0,625	0,0027	0,426	0,00184	0,414	0,00179	0,526	0,00228	0,44	0,0019	0,949	0,0041	1,75	0,00755
42	243	0,693	0,00285	0,535	0,0022	0,489	0,00201	0,683	0,00281	0,54	0,00222	1,05	0,00433	1,8	0,00741

44	255	0,655	0,00257	0,707	0,00277	0,663	0,0026	0,687	0,00269	0,752	0,00294	1,17	0,00459	1,98	0,00775
46	267	0,734	0,00275	0,686	0,00257	0,627	0,00234	0,646	0,00242	0,661	0,00247	1,07	0,00401	2,11	0,00791
48	280	0,755	0,0027	0,798	0,00286	0,725	0,00259	0,832	0,00297	0,818	0,00293	1,26	0,00452	2,13	0,00762
50	292	0,844	0,00289	0,774	0,00265	0,716	0,00245	0,865	0,00297	0,803	0,00275	1,27	0,00434	2,1	0,00719
52	304	0,883	0,00291	0,855	0,00281	0,818	0,00269	0,876	0,00288	0,85	0,0028	1,31	0,0043	2,15	0,00709
54	316	0,898	0,00284	0,915	0,0029	0,887	0,00281	0,962	0,00305	0,952	0,00301	1,4	0,00443	2,29	0,00724
56	328	0,96	0,00293	1,01	0,00309	0,986	0,00301	0,994	0,00303	1,03	0,00315	1,47	0,00447	2,36	0,00719
58	340	1,13	0,00331	0,952	0,0028	0,939	0,00276	1,16	0,00342	1,06	0,00312	1,52	0,00446	2,33	0,00686
60	352	1,02	0,0029	1,22	0,00346	1,17	0,00333	1,16	0,00329	1,24	0,00352	1,71	0,00485	2,54	0,00722
62	364	1,22	0,00334	1,08	0,00297	1,1	0,00301	1,41	0,00388	1,29	0,00355	1,78	0,0049	2,49	0,00684
64	376	1,34	0,00357	1,09	0,00288	1,06	0,00282	1,36	0,00362	1,23	0,00327	1,75	0,00465	2,56	0,00679
66	389	1,31	0,00338	1,24	0,00319	1,22	0,00313	1,51	0,00389	1,35	0,00348	1,66	0,00428	2,64	0,00679
68	401	1,49	0,00371	1,24	0,0031	1,24	0,00308	1,62	0,00404	1,43	0,00358	1,98	0,00495	2,69	0,00671
70	413	1,37	0,00332	1,55	0,00375	1,53	0,00372	1,7	0,00412	1,74	0,00422	2,23	0,00541	2,94	0,00713
72	425	1,49	0,00352	1,53	0,00359	1,53	0,0036	1,56	0,00367	1,68	0,00395	2,06	0,00486	3	0,00707
74	437	1,52	0,00348	1,73	0,00396	1,71	0,00392	1,82	0,00416	1,89	0,00432	2,38	0,00544	3,15	0,0072
76	449	1,69	0,00376	1,71	0,00381	1,71	0,0038	1,94	0,00431	1,93	0,0043	2,41	0,00537	3,14	0,00698
78	461	2,1	0,00455	1,65	0,00357	2,04	0,00443	1,75	0,00379	2,25	0,00487	2,68	0,0058	3,23	0,00701
80	473	1,8	0,0038	1,95	0,00411	1,94	0,0041	2,06	0,00436	2,1	0,00444	2,51	0,00531	3,45	0,00729
82	485	1,91	0,00394	1,97	0,00406	1,96	0,00403	2,16	0,00445	2,14	0,0044	2,56	0,00527	3,44	0,00708
84	498	1,99	0,004	2,09	0,0042	2,04	0,0041	2,44	0,00489	2,33	0,00469	2,81	0,00566	3,56	0,00715
86	510	2,02	0,00396	2,17	0,00425	2,17	0,00427	2,27	0,00445	2,32	0,00455	2,74	0,00537	3,77	0,0074
88	522	1,92	0,00368	2,44	0,00467	2,4	0,00459	2,51	0,00482	2,67	0,00511	3,16	0,00606	3,86	0,00739
90	534	2,17	0,00406	2,37	0,00444	2,36	0,00441	2,78	0,0052	2,77	0,0052	3,28	0,00614	3,8	0,00712
92	546	2,28	0,00418	2,5	0,00458	2,47	0,00452	2,89	0,00529	2,96	0,00542	3,42	0,00626	3,9	0,00714
94	558	2,27	0,00406	2,72	0,00487	2,74	0,0049	2,76	0,00495	2,91	0,00522	3,38	0,00606	4,31	0,00772
96	570	2,49	0,00436	2,68	0,0047	2,66	0,00466	2,74	0,0048	2,79	0,00489	3,19	0,0056	4,29	0,00752
98	582	2,56	0,0044	2,71	0,00466	2,73	0,00469	3,2	0,0055	3,08	0,0053	3,51	0,00604	4,24	0,00728
100	594	2,7	0,00453	2,76	0,00464	2,76	0,00464	3,11	0,00524	2,93	0,00493	3,49	0,00586	4,41	0,00742
102	607	2,67	0,0044	2,96	0,00488	2,97	0,00489	3,22	0,0053	3,21	0,00529	3,7	0,0061	4,61	0,0076
104	619	2,77	0,00448	3,04	0,00491	3,05	0,00493	3,38	0,00546	3,34	0,0054	3,79	0,00612	4,74	0,00766
106	631	2,92	0,00463	3,16	0,00501	3,15	0,005	3,51	0,00557	3,51	0,00556	3,96	0,00627	4,71	0,00747
108	643	2,93	0,00455	3,37	0,00524	3,31	0,00515	3,61	0,00562	3,67	0,00572	4,15	0,00645	5,02	0,00781
110	655	3,24	0,00494	3,26	0,00497	3,24	0,00494	3,69	0,00563	3,46	0,00528	4,07	0,00621	4,98	0,00761

112	667	3,04	0,00456	3,65	0,00546	3,62	0,00542	3,8	0,00569	3,92	0,00588	4,46	0,00668	5,28	0,00791
114	679	3,43	0,00505	3,42	0,00504	3,5	0,00515	4,19	0,00616	3,86	0,00568	4,58	0,00675	5,08	0,00747
116	691	3,67	0,00531	3,43	0,00496	3,46	0,00501	4,28	0,00619	3,84	0,00555	4,46	0,00646	5,13	0,00742
118	703	3,76	0,00534	3,57	0,00508	3,61	0,00513	4,38	0,00623	4,01	0,0057	4,57	0,00649	5,27	0,00749
120	716	3,61	0,00505	3,88	0,00542	4	0,00559	4,49	0,00627	4,27	0,00597	4,88	0,00682	5,63	0,00786
122	728	3,64	0,005	4,04	0,00555	4,14	0,00569	4,2	0,00577	4,25	0,00584	4,73	0,0065	5,92	0,00814
124	740	3,93	0,00531	3,98	0,00538	4,08	0,00551	4,65	0,00628	4,35	0,00589	5	0,00675	5,69	0,00769
126	752	3,99	0,00531	4,09	0,00544	4,21	0,0056	4,56	0,00606	4,39	0,00584	4,93	0,00656	5,92	0,00787
128	764	4,01	0,00525	4,28	0,00561	4,39	0,00574	4,69	0,00614	4,59	0,00601	5,17	0,00677	6,12	0,00802
130	776	4,17	0,00537	4,34	0,0056	4,5	0,00579	4,86	0,00627	4,72	0,00608	5,29	0,00681	6,19	0,00798
132	788	4,27	0,00541	4,48	0,00568	4,63	0,00587	5,06	0,00642	4,87	0,00618	5,45	0,00692	6,31	0,00801
134	800	4,27	0,00533	4,71	0,00589	4,83	0,00604	5,02	0,00627	4,99	0,00624	5,62	0,00702	6,52	0,00815
136	812	4,69	0,00578	4,54	0,00558	4,67	0,00575	5,33	0,00656	4,92	0,00606	5,58	0,00687	6,4	0,00788
138	825	4,4	0,00534	4,89	0,00593	5,07	0,00615	5,19	0,00629	5,13	0,00622	5,77	0,007	6,93	0,0084
140	837	4,75	0,00567	5,12	0,00612	5,17	0,00618	5,54	0,00662	5,52	0,0066	6,2	0,00742	6,89	0,00823
142	849	4,95	0,00583	5,15	0,00607	5,17	0,00609	5,81	0,00684	5,59	0,00658	6,36	0,00749	6,82	0,00804
144	861	4,97	0,00577	5,37	0,00623	5,39	0,00626	5,99	0,00695	5,77	0,0067	6,43	0,00747	7,1	0,00825
146	873	4,89	0,0056	5,38	0,00617	5,59	0,00641	5,71	0,00654	5,73	0,00656	6,28	0,0072	7,38	0,00846
148	885	5,38	0,00607	5,19	0,00587	5,28	0,00596	6	0,00678	5,59	0,00632	6,26	0,00708	7,31	0,00825
150	897	5,19	0,00579	5,66	0,00631	5,71	0,00637	5,99	0,00667	6,02	0,00671	6,6	0,00735	7,65	0,00852
152	909	5,52	0,00607	5,59	0,00614	5,66	0,00622	6,22	0,00684	6,07	0,00667	6,78	0,00745	7,57	0,00833
154	921	5,61	0,00608	5,75	0,00624	5,78	0,00627	6,26	0,00679	6,15	0,00667	6,86	0,00745	7,76	0,00842
156	934	5,7	0,0061	5,93	0,00635	5,95	0,00637	6,37	0,00683	6,29	0,00674	7	0,0075	7,96	0,00853
158	946	5,78	0,00611	6,02	0,00636	6,06	0,00641	6,45	0,00682	6,33	0,0067	7,02	0,00742	8,03	0,00849
160	958	6,12	0,00639	5,98	0,00624	6,05	0,00631	6,78	0,00707	6,44	0,00672	7,24	0,00756	8,13	0,00849
162	970	6,01	0,0062	6,44	0,00664	6,54	0,00674	6,74	0,00695	6,75	0,00696	7,38	0,00761	8,48	0,00875
164	982	6,45	0,00657	6,16	0,00627	6,4	0,00652	7,12	0,00725	6,89	0,00701	7,67	0,00781	8,22	0,00837
166	994	6,6	0,00664	6,26	0,0063	6,32	0,00636	7,18	0,00722	6,74	0,00678	7,56	0,0076	8,51	0,00856
168	1 010	6,71	0,00667	6,47	0,00643	6,45	0,00641	7,07	0,00702	6,81	0,00677	7,64	0,00759	8,71	0,00865
170	1 020	6,82	0,0067	6,58	0,00646	6,56	0,00644	7,36	0,00723	7,08	0,00695	7,96	0,00781	8,72	0,00856
172	1 030	6,8	0,0066	7,07	0,00686	6,95	0,00674	7,59	0,00736	7,57	0,00735	8,31	0,00807	8,95	0,00868
174	1 040	6,85	0,00657	7,11	0,00682	7,16	0,00686	7,31	0,00701	7,34	0,00704	8,11	0,00778	9,36	0,00897
176	1 050	7,07	0,0067	7,13	0,00676	7,29	0,00691	7,75	0,00735	7,72	0,00732	8,59	0,00815	9,27	0,00879
178	1 070	7,39	0,00693	7,2	0,00675	7,22	0,00677	7,77	0,00728	7,64	0,00716	8,53	0,008	9,46	0,00887

180	1 080	7,33	0,0068	7,33	0,0067 9	7,46	0,0069 1	7,87	0,0072 9	7,74	0,0071 8	8,7	0,0080 6	9,69	0,0089 8
182	1 090	7,52	0,0068 9	7,58	0,0069 5	7,67	0,0070 3	8,02	0,0073 5	7,98	0,0073 2	8,88	0,0081 4	9,87	0,0090 5
184	1 100	7,54	0,0068 4	7,73	0,0070 1	7,71	0,0069 9	8,05	0,0073	8,03	0,0072 8	8,92	0,0080 8	10,1	0,0091 4
186	1 120	7,97	0,0071 5	7,66	0,0068 7	7,66	0,0068 7	8,29	0,0074 3	8,17	0,0073 3	9,14	0,0081 9	10	0,0089 6
188	1 130	7,6	0,0067 4	8,17	0,0072 5	8,13	0,0072 1	8,36	0,0074 2	8,31	0,0073 7	9,22	0,0081 8	10,4	0,0092 4
190	1 140	8,08	0,0070 9	8,02	0,0070 4	8,02	0,0070 4	8,82	0,0077 4	8,7	0,0076 3	9,64	0,0084 6	10,2	0,0089 7
192	1 150	8,4	0,0073	8,04	0,0069 8	8	0,0069 5	8,78	0,0076 2	8,64	0,0075	9,68	0,0084	10,4	0,0090 2
194	1 160	8,48	0,0072 9	8,06	0,0069 2	8,13	0,0069 9	8,92	0,0076 7	8,56	0,0073 6	9,76	0,0083 9	10,5	0,0090 3
196	1 180	8,52	0,0072 5	8,32	0,0070 7	8,46	0,0071 9	9,07	0,0077 2	8,95	0,0076 1	10	0,0085 3	10,7	0,0090 8
198	1 190	8,24	0,0069 4	8,77	0,0073 8	8,87	0,0074 6	9,04	0,0076 1	9,08	0,0076 5	10,1	0,0084 8	11,3	0,0094 8
200	1 200	8,78	0,0073 2	8,54	0,0071 2	8,62	0,0071 9	9,12	0,0076	8,97	0,0074 8	10,2	0,0084 8	11,3	0,0093 8

Time	Shear Rate	Shear Stress	Viscosity	Shear Stress	Viscosity	Shear Stress	Viscosity	Shear Stress	Viscosity	Shear Stress	Viscosity	Shear Stress	Viscosity	Shear Stress	Viscosity
[s]	[1/s]	[Pa]	[Pa·s]	[Pa]	[Pa·s]	[Pa]	[Pa·s]	[Pa]	[Pa·s]	[Pa]	[Pa·s]	[Pa]	[Pa·s]	[Pa]	[Pa·s]
Number of Intervals:		*CNC-ATT-WDFs (6 wt %) 0.0 % 50°C F.W.*	*CNC-ATT-WDFs (6 wt %) 0.0 % 50°C F.W.*	*CNC-ATT-WDFs (6 wt %) 0.4 % 50°C F.W.*	*CNC-ATT-WDFs (6 wt %) 0.4 % 50°C F.W.*	*CNC-ATT-WDFs (6 wt %) 0.8 % 50°C F.W.*	*CNC-ATT-WDFs (6 wt %) 0.8 % 50°C F.W.*	*CNC-ATT-WDFs (6 wt %) 1.2 % 50°C F.W.*	*CNC-ATT-WDFs (6 wt %) 1.2 % 50°C F.W.*	*CNC-ATT-WDFs (6 wt %) 1.6 % 50°C F.W.*	*CNC-ATT-WDFs (6 wt %) 1.6 % 50°C F.W.*	*CNC-ATT-WDFs (6 wt %) 2.0 % 50°C F.W.*	*CNC-ATT-WDFs (6 wt %) 2.0 % 50°C F.W.*	*CNC-ATT-WDFs (6 wt %) 2.4 % 50°C F.W.*	*CNC-ATT-WDFs (6 wt %) 2.4 % 50°C F.W.*
2	0,999	-1,11	-1,11	-0,202	-0,202	-0,902	-0,902	-0,254	-0,255	1,49	1,49	-0,164	-0,164	2,58	2,58
4	13,1	-0,543	-0,0414	-0,469	-0,0358	-0,437	-0,0333	1,47	0,112	2,97	0,226	2,46	0,187	8,52	0,65
6	25,2	-0,611	-0,0242	-0,455	-0,0181	-0,392	-0,0155	3,04	0,121	4,18	0,166	3,99	0,158	12,1	0,479
8	37,3	-0,569	-0,0153	-0,439	-0,0118	-0,313	-0,00839	3,45	0,0925	4,11	0,11	4,51	0,121	13,6	0,364
10	49,4	-0,321	-0,0065	-0,243	-0,00492	-0,44	-0,00891	3,81	0,0771	3,71	0,075	5,34	0,108	13,3	0,269
12	61,6	-0,468	-0,0076	-0,369	-0,006	-0,279	-0,00453	2,36	0,0383	3,25	0,0528	5,24	0,0851	12,1	0,197
14	73,7	-0,401	-0,00544	-0,359	-0,00488	-0,362	-0,00491	1,8	0,0245	3,06	0,0415	4,9	0,0665	11,2	0,152
16	85,8	-0,362	-0,00422	-0,322	-0,00376	-0,311	-0,00362	1,47	0,0172	3,11	0,0363	5,01	0,0584	10,2	0,119
18	97,9	-0,279	-0,00285	-0,21	-0,00215	-0,217	-0,00222	1,38	0,0141	3,28	0,0335	5,25	0,0536	9,25	0,0945
20	110	-0,188	-0,00171	-0,0562	-5,11E-4	-0,162	-0,00147	1,44	0,0131	3,41	0,031	5,49	0,0499	9,05	0,0823
22	122	-0,105	-8,63E-4	0,0199	1,63E-4	-0,114	-9,35E-4	1,57	0,0128	3,36	0,0275	5,59	0,0458	9,29	0,0761
24	134	0,00134	9,97E-6	0,0568	4,23E-4	-0,0379	-2,83E-4	1,69	0,0126	3,32	0,0247	5,35	0,0399	9,38	0,0699
26	146	0,0955	6,53E-4	0,109	7,47E-4	0,0451	3,08E-4	1,71	0,0117	3,32	0,0227	5,55	0,0379	9,53	0,0651
28	158	0,147	9,3E-4	0,189	0,00119	0,114	7,2E-4	1,82	0,0115	3,47	0,0219	5,68	0,0358	9,83	0,062
30	171	0,287	0,00168	0,242	0,00142	0,176	0,00103	1,94	0,0114	3,48	0,0204	5,95	0,0349	9,88	0,0579
32	183	0,304	0,00166	0,327	0,00179	0,269	0,00147	2,02	0,0111	3,57	0,0196	6,03	0,033	9,85	0,054
34	195	0,383	0,00196	0,414	0,00212	0,341	0,00175	2,1	0,0108	3,5	0,018	5,92	0,0304	10	0,0514
36	207	0,453	0,00219	0,386	0,00186	0,416	0,00201	2,35	0,0113	3,69	0,0178	5,98	0,0289	10	0,0485
38	219	0,54	0,00246	0,491	0,00224	0,429	0,00196	2,42	0,0111	3,71	0,0169	6,37	0,0291	10,3	0,0469
40	231	0,55	0,00238	0,577	0,0025	0,508	0,0022	2,48	0,0107	3,73	0,0162	6,39	0,0277	10,2	0,044

42	243	0,591	0,00243	0,631	0,00259	0,573	0,00236	2,5	0,0103	3,79	0,0156	6,41	0,0264	10,2	0,0419
44	255	0,689	0,0027	0,759	0,00297	0,681	0,00267	2,55	0,00999	3,78	0,0148	6,48	0,0254	10,1	0,0397
46	267	0,807	0,00302	0,838	0,00313	0,717	0,00268	2,63	0,00985	3,82	0,0143	6,45	0,0241	10,4	0,0388
48	280	0,938	0,00335	0,964	0,00345	0,806	0,00288	2,83	0,0101	3,81	0,0136	6,83	0,0244	10,6	0,0381
50	292	0,978	0,00335	0,998	0,00342	0,921	0,00316	2,8	0,00961	3,95	0,0135	6,98	0,0239	10,7	0,0368
52	304	1,12	0,00369	1,1	0,00363	1,02	0,00336	2,92	0,00961	3,97	0,0131	6,97	0,0229	10,8	0,0356
54	316	1,23	0,0039	1,2	0,0038	1,08	0,00342	2,94	0,00929	4,1	0,013	7,16	0,0227	10,7	0,0339
56	328	1,37	0,00417	1,34	0,00409	1,23	0,00374	3,06	0,00932	4,14	0,0126	7,31	0,0223	10,8	0,033
58	340	1,5	0,0044	1,44	0,00424	1,28	0,00375	3,2	0,00941	4	0,0118	7,35	0,0216	11	0,0322
60	352	1,57	0,00446	1,56	0,00442	1,41	0,004	3,66	0,0104	4,27	0,0121	7,39	0,021	10,9	0,0309
62	364	1,59	0,00436	1,65	0,00452	1,6	0,0044	3,7	0,0102	4,47	0,0123	7,51	0,0206	11,1	0,0305
64	376	1,73	0,0046	1,77	0,00471	1,67	0,00443	3,67	0,00974	4,71	0,0125	7,73	0,0205	11,1	0,0294
66	389	1,84	0,00474	1,9	0,0049	1,81	0,00466	4,01	0,0103	5,06	0,013	7,93	0,0204	11	0,0284
68	401	1,95	0,00486	1,96	0,00488	1,91	0,00476	4,22	0,0105	5,02	0,0125	7,81	0,0195	11,3	0,0282
70	413	2,08	0,00505	2,12	0,00513	2,06	0,00498	4,27	0,0103	5,28	0,0128	7,79	0,0189	11,5	0,0279
72	425	2,19	0,00515	2,27	0,00534	2,12	0,00499	4,56	0,0107	5,44	0,0128	8,36	0,0197	11,5	0,027
74	437	2,24	0,00513	2,29	0,00524	2,3	0,00525	4,34	0,00993	5,53	0,0127	8,26	0,0189	11,4	0,026
76	449	2,4	0,00534	2,38	0,0053	2,33	0,00518	4,51	0,0101	5,65	0,0126	8,43	0,0188	11,6	0,0258
78	461	2,53	0,00548	2,08	0,00451	2,01	0,00437	5,12	0,0111	5,64	0,0122	8,22	0,0178	12,2	0,0264
80	473	2,59	0,00547	2,62	0,00553	2,57	0,00542	5,13	0,0108	6,02	0,0127	8,47	0,0179	11,8	0,025
82	485	2,65	0,00546	2,67	0,0055	2,59	0,00534	5,4	0,0111	6,13	0,0126	8,66	0,0178	11,7	0,0241
84	498	2,65	0,00532	2,75	0,00552	2,75	0,00553	5,75	0,0115	6,25	0,0126	8,76	0,0176	12	0,024
86	510	2,78	0,00545	2,85	0,00558	2,77	0,00543	5,84	0,0115	6,45	0,0127	8,83	0,0173	12,3	0,0241
88	522	2,93	0,00561	3,06	0,00587	2,92	0,0056	6,02	0,0115	6,2	0,0119	9,01	0,0173	11,9	0,0229
90	534	2,92	0,00547	3,09	0,00579	3,05	0,00572	6,25	0,0117	6,48	0,0121	8,92	0,0167	12	0,0224
92	546	3,05	0,00558	3,22	0,0059	3,18	0,00583	6,56	0,012	6,57	0,012	9,09	0,0166	12,2	0,0223
94	558	3,18	0,00569	3,24	0,0058	3,3	0,00592	7,2	0,0129	6,59	0,0118	9,1	0,0163	12,1	0,0216
96	570	3,42	0,006	3,46	0,00606	3,48	0,00609	6,12	0,0107	6,65	0,0117	9,37	0,0164	12,3	0,0216
98	582	3,64	0,00625	3,6	0,00618	3,62	0,00622	7,11	0,0122	6,62	0,0114	9,36	0,0161	12,6	0,0217
100	594	3,62	0,00609	3,61	0,00608	3,76	0,00633	7,28	0,0123	6,93	0,0117	9,65	0,0162	12,6	0,0213
102	607	3,83	0,00631	3,82	0,0063	3,83	0,00631	6,49	0,0107	6,87	0,0113	9,68	0,016	12,8	0,0211
104	619	3,87	0,00625	3,9	0,00631	3,96	0,00641	5,95	0,00962	7,03	0,0114	9,73	0,0157	13,2	0,0213
106	631	3,96	0,00628	3,94	0,00625	4,04	0,0064	6,08	0,00964	7,38	0,0117	9,8	0,0155	13,3	0,0211
108	643	4,11	0,0064	4,2	0,00653	4,18	0,0065	5,98	0,00929	7,15	0,0111	10,1	0,0157	13,4	0,0208

110	655	4,24	0,0064 8	4,26	0,0065	4,19	0,0064	6,41	0,0097 9	7,2	0,011	10,1	0,0154	13,2	0,0201
112	667	4,34	0,0065	4,4	0,0066	4,36	0,0065 3	6,29	0,0094 4	7,22	0,0108	10,3	0,0155	13,7	0,0205
114	679	4,32	0,0063 6	4,37	0,0064 3	4,43	0,0065 2	6,31	0,0092 9	7,42	0,0109	10,3	0,0151	13,6	0,02
116	691	4,5	0,0065 1	4,53	0,0065 5	4,59	0,0066 4	6,54	0,0094 6	7,29	0,0105	10,6	0,0154	13,5	0,0195
118	703	4,65	0,0066 1	4,66	0,0066 3	4,67	0,0066 4	6,36	0,0090 4	7,59	0,0108	10,7	0,0151	13,8	0,0196
120	716	4,69	0,0065 6	4,74	0,0066 2	4,88	0,0068 2	6,56	0,0091 7	7,5	0,0105	10,9	0,0152	13,8	0,0192
122	728	4,99	0,0068 6	4,97	0,0068 3	4,9	0,0067 3	6,43	0,0088 4	7,65	0,0105	11,3	0,0155	13,5	0,0186
124	740	5,13	0,0069 3	5,09	0,0068 7	5,04	0,0068 1	6,64	0,0089 8	7,71	0,0104	11,1	0,015	13,4	0,0181
126	752	5,09	0,0067 7	5,06	0,0067 4	5,2	0,0069 2	6,73	0,0089 5	8,43	0,0112	11,1	0,0148	13,4	0,0179
128	764	5,28	0,0069 2	5,27	0,0069	5,3	0,0069 3	6,71	0,0087 8	8,08	0,0106	11,4	0,0149	13,9	0,0181
130	776	5,4	0,0069 6	5,32	0,0068 6	5,37	0,0069 2	6,98	0,0089 9	8,32	0,0107	11,3	0,0145	13,9	0,0179
132	788	5,58	0,0070 8	5,45	0,0069 2	5,45	0,0069 1	7,43	0,0094 3	8,4	0,0107	11,4	0,0145	13,8	0,0176
134	800	5,58	0,0069 7	5,51	0,0068 8	5,67	0,0070 8	7,3	0,0091 2	8,15	0,0102	11,3	0,0141	14	0,0175
136	812	5,76	0,0070 9	5,68	0,0069 9	5,84	0,0071 9	7,49	0,0092 2	8,48	0,0104	11,7	0,0144	14,2	0,0175
138	825	5,72	0,0069 4	5,66	0,0068 6	5,67	0,0068 8	7,67	0,0093	8,59	0,0104	12	0,0145	14,3	0,0173
140	837	6,1	0,0072 9	5,96	0,0071 3	5,95	0,0071 1	7,62	0,0091 1	8,74	0,0105	11,9	0,0142	14,5	0,0174
142	849	6,16	0,0072 6	6	0,0070 7	6,05	0,0071 3	7,96	0,0093 8	8,83	0,0104	12	0,0141	14,5	0,0171
144	861	6,23	0,0072 4	6,02	0,007	6,2	0,0072	7,97	0,0092 6	9,11	0,0106	12,1	0,014	14,7	0,0171
146	873	6,42	0,0073 6	6,27	0,0071 8	6,28	0,0071 9	8,1	0,0092 7	9,17	0,0105	12,2	0,0139	15,1	0,0173
148	885	6,57	0,0074 2	6,26	0,0070 7	6,33	0,0071 5	8,21	0,0092 8	9,19	0,0104	12,1	0,0137	14,9	0,0168
150	897	6,7	0,0074 7	6,48	0,0072 2	6,48	0,0072 2	8,54	0,0095 2	9,32	0,0104	12,4	0,0138	14,9	0,0166
152	909	6,75	0,0074 2	6,45	0,0070 9	6,75	0,0074 2	8,48	0,0093 3	9,36	0,0103	12,2	0,0134	15,1	0,0166
154	921	6,87	0,0074 5	6,6	0,0071 6	6,82	0,0074	8,68	0,0094 2	9,46	0,0103	12,4	0,0134	14,8	0,0161
156	934	7	0,0074 9	6,71	0,0071 9	6,9	0,0073 9	8,85	0,0094 8	9,73	0,0104	12,2	0,0131	15,1	0,0162
158	946	7,2	0,0076 1	6,87	0,0072 6	7,06	0,0074 6	9	0,0095 2	9,82	0,0104	12,6	0,0133	15,1	0,0159
160	958	7,21	0,0075 3	6,82	0,0071 3	7,05	0,0073 6	9,26	0,0096 7	10	0,0105	12,2	0,0127	14,6	0,0152
162	970	7,39	0,0076 2	6,96	0,0071 8	7,23	0,0074 6	9,4	0,0096 9	10,2	0,0105	12,5	0,0129	14,8	0,0153
164	982	7,65	0,0077 9	7,25	0,0073 8	7,4	0,0075 3	9,3	0,0094 8	10,2	0,0103	12,8	0,0131	15	0,0153
166	994	7,71	0,0077 6	7,29	0,0073 3	7,58	0,0076 2	9,43	0,0094 9	10,4	0,0104	12,8	0,0128	15	0,0151
168	1 010	7,79	0,0077 4	7,47	0,0074 3	7,65	0,0076 1	9,42	0,0093 6	10,5	0,0104	12,9	0,0128	15,3	0,0152
170	1 020	8,04	0,0079	7,59	0,0074 5	7,8	0,0076 6	9,64	0,0094 6	10,6	0,0104	13	0,0128	15,3	0,015
172	1 030	8,13	0,0078 9	7,59	0,0073 7	7,87	0,0076 4	9,77	0,0094 8	10,9	0,0106	13	0,0126	15	0,0146
174	1 040	8,19	0,0078 5	7,75	0,0074 3	8,01	0,0076 8	10,1	0,0096 8	11,1	0,0107	13,2	0,0126	15,2	0,0146
176	1 050	8,44	0,0080 1	7,84	0,0074 3	8,13	0,0077 1	10,1	0,0096 2	11,2	0,0106	13,2	0,0125	15,2	0,0145

178	1 070	8,6	0,00806	8,11	0,0076	8,35	0,00782	10,4	0,00971	11,2	0,0105	13,6	0,0127	15,8	0,0148
180	1 080	8,8	0,00816	8,19	0,00759	8,37	0,00776	10,6	0,0098	11,5	0,0107	13,5	0,0125	15,9	0,0148
182	1 090	8,76	0,00803	8,38	0,00768	8,56	0,00785	10,8	0,00987	11,8	0,0108	13,7	0,0125	16	0,0147
184	1 100	9,09	0,00824	8,56	0,00776	8,7	0,00788	10,8	0,0098	11,9	0,0108	14	0,0127	16,2	0,0147
186	1 120	9,07	0,00814	8,51	0,00763	8,65	0,00776	11	0,00989	12,4	0,0111	14,1	0,0126	16,1	0,0144
188	1 130	9,2	0,00816	8,76	0,00777	8,85	0,00785	11,1	0,00984	12,4	0,011	14,4	0,0127	16,2	0,0144
190	1 140	9,43	0,00828	8,93	0,00784	9,16	0,00804	11,2	0,00986	12,3	0,0108	14,8	0,013	16,6	0,0145
192	1 150	9,61	0,00835	8,98	0,00779	9,14	0,00793	11,3	0,00979	12,7	0,011	14,8	0,0129	16,9	0,0147
194	1 160	9,63	0,00827	9,12	0,00783	9,36	0,00804	11,5	0,00986	12,9	0,0111	15,3	0,0132	16,4	0,0141
196	1 180	9,73	0,00827	9,24	0,00786	9,48	0,00807	11,5	0,00978	13,3	0,0113	15,4	0,0131	16,6	0,0141
198	1 190	9,96	0,00839	9,62	0,0081	9,62	0,0081	11,5	0,00968	13,2	0,0111	15,2	0,0128	16,9	0,0142
200	1 200	10,3	0,00859	9,73	0,00811	9,77	0,00815	11,5	0,0096	13,2	0,011	15,7	0,0131	17	0,0142

Time	Shear Rate	Shear Stress	Viscosity	Shear Stress	Viscosity	Shear Stress	Viscosity	Shear Stress	Viscosity	Shear Stress	Viscosity	Shear Stress	Viscosity	Shear Stress	Viscosity
[s]	[1/s]	[Pa]	[Pa·s]	[Pa]	[Pa·s]	[Pa]	[Pa·s]	[Pa]	[Pa·s]	[Pa]	[Pa·s]	[Pa]	[Pa·s]	[Pa]	[Pa·s]
Number of Intervals:		*CNC-ATT-WDFs (6 wt %) 0.0 % 60°C F.W.*	*CNC-ATT-WDFs (6 wt %) 0.0 % 60°C F.W.*	*CNC-ATT-WDFs (6 wt %) 0.4 % 60°C F.W.*	*CNC-ATT-WDFs (6 wt %) 0.4 % 60°C F.W.*	*CNC-ATT-WDFs (6 wt %) 0.8 % 60°C F.W.*	*CNC-ATT-WDFs (6 wt %) 0.8 % 60°C F.W.*	*CNC-ATT-WDFs (6 wt %) 1.2 % 60°C F.W.*	*CNC-ATT-WDFs (6 wt %) 1.2 % 60°C F.W.*	*CNC-ATT-WDFs (6 wt %) 1.6 % 60°C F.W.*	*CNC-ATT-WDFs (6 wt %) 1.6 % 60°C F.W.*	*CNC-ATT-WDFs (6 wt %) 2.0 % 60°C F.W.*	*CNC-ATT-WDFs (6 wt %) 2.0 % 60°C F.W.*	*CNC-ATT-WDFs (6 wt %) 2.4 % 60°C F.W.*	*CNC-ATT-WDFs (6 wt %) 2.4 % 60°C F.W.*
2	0,999	-1,29	-1,29	-1,82	-1,82	0,243	0,243	-0,381	-0,381	0,491	0,491	0,199	0,198	1,64	1,64
4	13,1	-0,6	-0,0458	-0,914	-0,0697	0,189	0,0144	0,386	0,0294	1,27	0,0972	3,53	0,269	4,7	0,358
6	25,2	-0,556	-0,022	-0,761	-0,0302	0,0801	0,00317	0,561	0,0222	1,7	0,0675	4,04	0,16	6,41	0,254
8	37,3	-0,539	-0,0144	-0,647	-0,0173	0,169	0,00454	0,646	0,0173	1,88	0,0504	4,22	0,113	7,44	0,199
10	49,4	-0,577	-0,0117	-0,596	-0,012	0,186	0,00377	0,648	0,0131	1,95	0,0395	4,35	0,088	7,43	0,15
12	61,6	-0,484	-0,00786	-0,621	-0,0101	0,177	0,00288	0,735	0,0119	1,97	0,032	3,98	0,0647	7,46	0,121
14	73,7	-0,45	-0,00611	-0,491	-0,00667	0,143	0,00195	0,772	0,0105	2,21	0,03	3,99	0,0542	7,38	0,1
16	85,8	-0,373	-0,00435	-0,51	-0,00595	0,197	0,0023	0,867	0,0101	2,25	0,0263	4,08	0,0476	7,52	0,0877
18	97,9	-0,312	-0,00318	-0,397	-0,00405	0,258	0,00263	1,01	0,0103	2,34	0,0239	4,12	0,0421	7,58	0,0775
20	110	-0,305	-0,00277	-0,321	-0,00292	0,423	0,00384	1,12	0,0102	2,5	0,0227	4,35	0,0395	7,72	0,0702
22	122	-0,189	-0,00155	-0,241	-0,00198	0,469	0,00384	1,22	0,01	2,65	0,0217	4,26	0,0349	7,83	0,0641
24	134	-0,0739	-5,51E-4	-0,134	-9,98E-4	0,463	0,00345	1,4	0,0104	2,75	0,0205	4,45	0,0332	8,09	0,0603
26	146	-0,0475	-3,24E-4	0,0116	7,91E-5	0,462	0,00315	1,52	0,0104	2,86	0,0196	4,62	0,0316	8,3	0,0567
28	158	0,0116	7,34E-5	0,0673	4,24E-4	0,58	0,00366	1,61	0,0101	3,05	0,0193	4,74	0,0299	8,57	0,0541
30	171	0,0636	3,73E-4	0,143	8,38E-4	0,636	0,00373	1,69	0,00993	3,16	0,0185	4,91	0,0288	8,59	0,0504
32	183	0,17	9,32E-4	0,201	0,0011	0,668	0,00366	1,85	0,0101	3,29	0,018	5,11	0,028	8,71	0,0477
34	195	0,261	0,00134	0,247	0,00127	0,751	0,00385	1,88	0,00967	3,41	0,0175	5,31	0,0273	9,04	0,0464
36	207	0,234	0,00113	0,346	0,00167	0,773	0,00374	1,98	0,00958	3,54	0,0171	5,39	0,0261	9,02	0,0436
38	219	0,317	0,00145	0,377	0,00172	0,811	0,0037	2,02	0,00925	3,64	0,0166	5,49	0,0251	9,29	0,0424
40	231	0,37	0,0016	0,475	0,00206	0,901	0,0039	2,08	0,009	3,72	0,0161	5,59	0,0242	9,41	0,0407

42	243	0,423	0,00174	0,578	0,00238	0,941	0,00387	2,11	0,00869	3,87	0,0159	5,63	0,0232	9,68	0,0398
44	255	0,556	0,00218	0,608	0,00238	1	0,00392	2,24	0,00879	3,95	0,0155	5,83	0,0228	10,1	0,0394
46	267	0,616	0,0023	0,723	0,0027	1,08	0,00405	2,3	0,00858	4,06	0,0152	6,07	0,0227	9,99	0,0374
48	280	0,734	0,00263	0,777	0,00278	1,2	0,00428	2,4	0,00859	4,08	0,0146	6,07	0,0217	10,1	0,0362
50	292	0,77	0,00264	0,953	0,00327	1,35	0,00464	2,44	0,00835	4,26	0,0146	6,14	0,0211	10,2	0,0351
52	304	0,89	0,00293	1	0,0033	1,46	0,00479	2,61	0,0086	4,23	0,0139	6,25	0,0206	10,3	0,0341
54	316	0,977	0,00309	1,12	0,00353	1,51	0,0048	2,71	0,00859	4,42	0,014	6,38	0,0202	10,8	0,0342
56	328	1,12	0,00342	1,22	0,00371	1,66	0,00506	2,85	0,00869	4,55	0,0139	6,31	0,0192	10,8	0,033
58	340	1,21	0,00356	1,38	0,00405	1,71	0,00502	2,92	0,00859	4,58	0,0135	6,47	0,019	11	0,0324
60	352	1,34	0,00381	1,48	0,0042	1,83	0,0052	3,12	0,00886	4,64	0,0132	6,61	0,0188	11,1	0,0316
62	364	1,43	0,00393	1,61	0,00441	2,02	0,00554	3,21	0,00882	4,84	0,0133	6,82	0,0187	11,2	0,0307
64	376	1,52	0,00404	1,74	0,00461	2,14	0,00569	3,33	0,00886	4,91	0,0131	6,78	0,018	11,5	0,0305
66	389	1,62	0,00418	1,82	0,00468	2,31	0,00596	3,47	0,00893	5,14	0,0132	6,86	0,0177	11,6	0,0299
68	401	1,66	0,00415	1,98	0,00493	2,45	0,00611	3,51	0,00876	5,22	0,013	6,89	0,0172	12	0,0299
70	413	1,85	0,00449	1,99	0,00483	2,52	0,00611	3,68	0,00892	5,31	0,0129	7,15	0,0173	11,9	0,0289
72	425	1,95	0,0046	2,08	0,00489	2,62	0,00616	3,74	0,00881	5,32	0,0125	7,24	0,017	11,9	0,028
74	437	2	0,00457	2,22	0,00508	2,77	0,00635	3,84	0,0088	5,54	0,0127	7,41	0,0169	12	0,0274
76	449	2,03	0,00451	2,37	0,00528	2,85	0,00635	3,89	0,00867	5,4	0,012	7,35	0,0164	12,5	0,0278
78	461	1,97	0,00426	2,13	0,00461	3,11	0,00675	3,73	0,0081	5,23	0,0113	7,82	0,0169	12,3	0,0267
80	473	2,26	0,00477	2,53	0,00535	3,09	0,00653	4,24	0,00896	5,8	0,0123	7,48	0,0158	12,6	0,0265
82	485	2,29	0,00471	2,73	0,00561	3,22	0,00663	4,23	0,00871	5,84	0,012	7,62	0,0157	12,7	0,0261
84	498	2,38	0,00478	2,82	0,00567	3,37	0,00676	4,3	0,00865	5,96	0,012	7,85	0,0158	12,7	0,0254
86	510	2,48	0,00486	2,9	0,0057	3,48	0,00682	4,43	0,0087	6,09	0,012	7,82	0,0153	12,7	0,025
88	522	2,68	0,00514	2,91	0,00559	3,44	0,0066	4,78	0,00915	6,17	0,0118	7,72	0,0148	12,7	0,0244
90	534	2,72	0,0051	3,08	0,00576	3,56	0,00668	4,8	0,009	6,29	0,0118	7,9	0,0148	12,8	0,024
92	546	2,87	0,00526	3,15	0,00577	3,67	0,00673	4,94	0,00904	6,38	0,0117	7,97	0,0146	13,1	0,0239
94	558	2,88	0,00515	3,32	0,00595	3,82	0,00685	5,04	0,00904	6,44	0,0115	8,18	0,0147	13,3	0,0238
96	570	3,16	0,00554	3,32	0,00582	3,85	0,00675	5,28	0,00926	6,52	0,0114	8,38	0,0147	13,1	0,0229
98	582	3,28	0,00564	3,45	0,00593	3,93	0,00675	5,37	0,00923	6,69	0,0115	8,37	0,0144	13	0,0223
100	594	3,32	0,00558	3,59	0,00604	4,17	0,00702	5,39	0,00907	6,84	0,0115	8,53	0,0143	13,4	0,0225
102	607	3,45	0,00569	3,7	0,00611	4,21	0,00693	5,61	0,00925	6,82	0,0112	8,48	0,014	13,2	0,0217
104	619	3,5	0,00565	3,85	0,00623	4,36	0,00705	5,61	0,00907	7	0,0113	8,66	0,014	13,3	0,0216
106	631	3,56	0,00564	3,96	0,00627	4,49	0,00712	5,75	0,00912	7,11	0,0113	8,77	0,0139	13,5	0,0215
108	643	3,81	0,00593	3,95	0,00614	4,47	0,00696	5,98	0,00929	7,21	0,0112	8,68	0,0135	13,5	0,021

110	655	3,91	0,00597	4,06	0,0062	4,55	0,00694	6,13	0,00936	7,33	0,0112	8,78	0,0134	13,2	0,0201
112	667	4,07	0,0061	4,16	0,00624	4,71	0,00706	6,32	0,00947	7,61	0,0114	8,92	0,0134	13,5	0,0202
114	679	3,98	0,00586	4,42	0,00651	4,94	0,00728	6,26	0,00921	7,6	0,0112	9,1	0,0134	13,8	0,0203
116	691	4,14	0,00599	4,48	0,00648	5,02	0,00726	6,36	0,0092	7,8	0,0113	9,1	0,0132	13,7	0,0198
118	703	4,32	0,00614	4,57	0,0065	5,07	0,00721	6,7	0,00952	7,82	0,0111	9,11	0,0129	13,8	0,0196
120	716	4,45	0,00621	4,73	0,00661	5,27	0,00736	6,74	0,00941	8,06	0,0113	9,21	0,0129	13,6	0,019
122	728	4,57	0,00628	4,73	0,0065	5,29	0,00728	7,06	0,00971	8,09	0,0111	9,31	0,0128	13,8	0,019
124	740	4,71	0,00637	4,84	0,00654	5,42	0,00732	7,18	0,00971	8,21	0,0111	9,53	0,0129	13,9	0,0188
126	752	4,71	0,00626	5,12	0,00681	5,68	0,00756	7,19	0,00956	8,51	0,0113	9,62	0,0128	13,9	0,0185
128	764	4,9	0,00641	5,11	0,00669	5,71	0,00747	7,56	0,0099	8,45	0,0111	9,92	0,013	13,8	0,018
130	776	4,95	0,00637	5,25	0,00676	5,93	0,00764	7,47	0,00963	8,74	0,0113	9,93	0,0128	13,9	0,018
132	788	5,06	0,00642	5,33	0,00677	5,95	0,00755	7,7	0,00977	8,73	0,0111	9,93	0,0126	14	0,0178
134	800	5,21	0,00651	5,49	0,00686	6,17	0,0077	7,71	0,00963	9,02	0,0113	10,2	0,0128	14,1	0,0176
136	812	5,38	0,00662	5,48	0,00674	6,28	0,00772	7,8	0,0096	9,27	0,0114	10,3	0,0126	14	0,0173
138	825	5,28	0,00641	5,49	0,00665	6,12	0,00742	8,05	0,00977	9,33	0,0113	10,1	0,0122	13,9	0,0169
140	837	5,62	0,00671	5,76	0,00688	6,42	0,00767	8,22	0,00982	9,51	0,0114	10,4	0,0124	13,9	0,0167
142	849	5,66	0,00667	5,91	0,00696	6,59	0,00776	8,32	0,0098	9,5	0,0112	10,3	0,0122	14,1	0,0166
144	861	5,73	0,00666	6,06	0,00704	6,8	0,0079	8,31	0,00965	9,62	0,0112	10,6	0,0123	14,4	0,0168
146	873	6	0,00687	6,09	0,00697	6,76	0,00774	8,64	0,00989	9,68	0,0111	10,8	0,0124	14,1	0,0162
148	885	6,02	0,0068	6,3	0,00712	6,84	0,00773	8,73	0,00986	9,8	0,0111	10,8	0,0122	14,1	0,0159
150	897	6,25	0,00697	6,29	0,00702	6,95	0,00775	8,88	0,0099	10,1	0,0113	11,1	0,0124	14,1	0,0157
152	909	6,39	0,00703	6,48	0,00713	7,21	0,00793	8,99	0,00989	10,3	0,0114	11,1	0,0122	14,2	0,0157
154	921	6,42	0,00697	6,53	0,00709	7,37	0,008	9,18	0,00997	10,4	0,0113	11,3	0,0123	14,5	0,0158
156	934	6,38	0,00683	6,6	0,00707	7,5	0,00803	9,27	0,00993	10,7	0,0114	11,4	0,0122	14,6	0,0156
158	946	6,72	0,00711	6,65	0,00703	7,6	0,00804	9,47	0,01	10,8	0,0114	11,6	0,0123	14,8	0,0156
160	958	6,64	0,00693	6,88	0,00718	7,82	0,00816	9,41	0,00983	10,9	0,0114	11,6	0,0121	15	0,0157
162	970	6,75	0,00696	7,34	0,00757	7,92	0,00817	9,59	0,00989	11,1	0,0114	11,9	0,0123	15	0,0155
164	982	7,17	0,0073	7,32	0,00746	7,95	0,0081	9,88	0,0101	11,2	0,0114	11,9	0,0122	15,1	0,0154
166	994	7,1	0,00714	7,51	0,00755	8,11	0,00816	9,71	0,00977	11,5	0,0116	12	0,0121	15,1	0,0152
168	1 010	7,2	0,00715	7,6	0,00755	8,17	0,00812	10	0,00998	11,6	0,0116	12,2	0,0121	15,3	0,0152
170	1 020	7,42	0,00729	7,49	0,00735	8,38	0,00822	10,3	0,0101	11,6	0,0114	12,4	0,0122	15,1	0,0149
172	1 030	7,48	0,00726	7,7	0,00747	8,54	0,00829	10,3	0,01	11,8	0,0114	12,4	0,0121	15,5	0,0151
174	1 040	7,53	0,00723	7,76	0,00745	8,73	0,00837	10,5	0,01	12	0,0116	12,7	0,0122	15,7	0,0151
176	1 050	7,83	0,00742	7,83	0,00742	8,88	0,00842	10,8	0,0102	12,2	0,0115	12,9	0,0123	16	0,0152

178	1 070	8,02	0,00752	7,85	0,00736	8,94	0,00838	11	0,0103	12,4	0,0117	13,1	0,0123	15,9	0,0149
180	1 080	8,16	0,00756	7,94	0,00736	9,05	0,00839	11	0,0102	12,7	0,0117	13,5	0,0125	16,4	0,0152
182	1 090	8,14	0,00746	8,27	0,00758	9,28	0,0085	11,2	0,0102	12,9	0,0118	13,5	0,0123	16,5	0,0151
184	1 100	8,65	0,00785	8,34	0,00756	9,42	0,00854	11,3	0,0103	13	0,0118	13,7	0,0124	16,8	0,0152
186	1 120	8,38	0,00751	8,47	0,0076	9,6	0,00861	11,4	0,0102	13,1	0,0117	13,7	0,0122	16,8	0,0151
188	1 130	8,55	0,00758	8,67	0,00769	9,74	0,00864	11,5	0,0102	13,2	0,0117	13,9	0,0123	17	0,0151
190	1 140	8,89	0,0078	8,87	0,00778	9,79	0,00859	11,9	0,0104	13,5	0,0118	14,3	0,0125	17	0,015
192	1 150	9,09	0,00789	9,01	0,00783	10	0,00869	12	0,0104	13,5	0,0117	14,3	0,0124	17,3	0,015
194	1 160	9,05	0,00778	9,14	0,00785	10,3	0,00884	12,1	0,0104	13,6	0,0117	14,5	0,0125	17,5	0,015
196	1 180	9,05	0,00769	9,34	0,00795	10,4	0,00886	12,1	0,0103	13,9	0,0118	14,6	0,0124	17,6	0,015
198	1 190	9,54	0,00803	9,42	0,00793	10,5	0,00887	12,4	0,0104	14	0,0118	15	0,0126	17,7	0,0149
200	1 200	9,65	0,00804	9,51	0,00793	10,6	0,00879	12,6	0,0105	14	0,0117	15,2	0,0127	17,6	0,0147

Time	Shear Rate	Shear Stress	Viscosity	Shear Stress	Viscosity	Shear Stress	Viscosity	Shear Stress	Viscosity	Shear Stress	Viscosity	Shear Stress	Viscosity	Shear Stress	Viscosity
[s]	[1/s]	[Pa]	[Pa·s]	[Pa]	[Pa·s]	[Pa]	[Pa·s]	[Pa]	[Pa·s]	[Pa]	[Pa·s]	[Pa]	[Pa·s]	[Pa]	[Pa·s]
Number of Intervals:		*CNC-ATT-WDFs (6 wt %) 0.0 % 70°C F.W.*	*CNC-ATT-WDFs (6 wt %) 0.0 % 70°C F.W.*	*CNC-ATT-WDFs (6 wt %) 0.4 % 70°C F.W.*	*CNC-ATT-WDFs (6 wt %) 0.4 % 70°C F.W.*	*CNC-ATT-WDFs (6 wt %) 0.8 % 70°C F.W.*	*CNC-ATT-WDFs (6 wt %) 0.8 % 70°C F.W.*	*CNC-ATT-WDFs (6 wt %) 1.2 % 70°C F.W.*	*CNC-ATT-WDFs (6 wt %) 1.2 % 70°C F.W.*	*CNC-ATT-WDFs (6 wt %) 1.6 % 70°C F.W.*	*CNC-ATT-WDFs (6 wt %) 1.6 % 70°C F.W.*	*CNC-ATT-WDFs (6 wt %) 2.0 % 70°C F.W.*	*CNC-ATT-WDFs (6 wt %) 2.0 % 70°C F.W.*	*CNC-ATT-WDFs (6 wt %) 2.4 % 70°C F.W.*	*CNC-ATT-WDFs (6 wt %) 2.4 % 70°C F.W.*
2	0,999	-0,986	-0,985	-0,642	-0,642	-0,559	-0,559	0,211	0,211	0,685	0,684	0,578	0,577	1,74	1,74
4	13,1	-0,809	-0,0617	-0,345	-0,0263	-0,116	-0,00887	0,302	0,023	1,09	0,0834	1,83	0,139	4,15	0,317
6	25,2	-0,615	-0,0244	-0,391	-0,0155	-0,23	-0,00911	0,473	0,0187	1,32	0,0523	2,56	0,102	5,29	0,21
8	37,3	-0,512	-0,0137	-0,346	-0,00927	-0,245	-0,00655	0,502	0,0134	1,53	0,0409	2,94	0,0786	6,11	0,164
10	49,4	-0,414	-0,00836	-0,314	-0,00635	-0,139	-0,00281	0,578	0,0117	1,53	0,031	2,97	0,06	6,36	0,129
12	61,6	-0,468	-0,00761	-0,313	-0,00508	0,0128	2,08E-4	0,686	0,0112	1,6	0,0259	3,01	0,0488	6,43	0,105
14	73,7	-0,411	-0,00559	-0,299	-0,00407	0,0369	5,01E-4	0,724	0,00983	1,67	0,0226	3,16	0,0428	6,73	0,0913
16	85,8	-0,283	-0,00329	-0,299	-0,00349	-0,00214	-2,49E-5	0,808	0,00942	1,84	0,0214	3,27	0,0382	6,66	0,0777
18	97,9	-0,283	-0,00289	-0,309	-0,00316	0,0642	6,55E-4	0,875	0,00894	1,97	0,0202	3,27	0,0334	6,9	0,0705
20	110	-0,293	-0,00266	-0,315	-0,00286	0,0809	7,36E-4	0,982	0,00893	2,1	0,0191	3,35	0,0305	7,07	0,0643
22	122	-0,258	-0,00211	-0,25	-0,00204	0,132	0,00108	1,07	0,00875	2,19	0,0179	3,58	0,0293	7,09	0,0581
24	134	-0,125	-9,28E-4	-0,153	-0,00114	0,209	0,00156	1,13	0,00842	2,23	0,0166	3,71	0,0276	7,46	0,0556
26	146	-0,0663	-4,53E-4	-0,153	-0,00104	0,267	0,00182	1,19	0,00814	2,34	0,016	3,75	0,0256	7,63	0,0521
28	158	0,00562	3,55E-5	-0,0203	-1,28E-4	0,329	0,00208	1,29	0,00812	2,46	0,0156	3,95	0,0249	7,86	0,0496
30	171	0,00789	4,63E-5	-0,0155	-9,1E-5	0,361	0,00212	1,36	0,008	2,54	0,0149	3,92	0,023	8,11	0,0476
32	183	0,0932	5,1E-4	0,114	6,26E-4	0,36	0,00197	1,4	0,00768	2,63	0,0144	4,13	0,0226	8,05	0,0441
34	195	0,142	7,29E-4	0,204	0,00105	0,404	0,00208	1,43	0,00735	2,72	0,014	4,19	0,0215	8,18	0,042
36	207	0,187	9,05E-4	0,199	9,61E-4	0,505	0,00244	1,54	0,00744	2,83	0,0137	4,42	0,0214	8,45	0,0408
38	219	0,251	0,00115	0,305	0,00139	0,521	0,00238	1,59	0,00725	2,94	0,0134	4,4	0,0201	8,56	0,0391

40	231	0,256	0,00111	0,301	0,0013	0,613	0,00265	1,66	0,0072	2,98	0,0129	4,41	0,0191	8,75	0,0378
42	243	0,273	0,00112	0,336	0,00138	0,658	0,00271	1,68	0,00691	3,09	0,0127	4,6	0,0189	8,93	0,0367
44	255	0,377	0,00147	0,447	0,00175	0,627	0,00245	1,77	0,00693	3,15	0,0123	4,57	0,0179	9,02	0,0353
46	267	0,403	0,00151	0,532	0,00199	0,719	0,00269	1,75	0,00654	3,25	0,0121	4,82	0,018	9,1	0,034
48	280	0,514	0,00184	0,63	0,00225	0,749	0,00268	1,87	0,00671	3,3	0,0118	4,9	0,0175	9,24	0,033
50	292	0,549	0,00188	0,604	0,00207	0,934	0,0032	1,86	0,00637	3,28	0,0113	5,12	0,0175	9,3	0,0319
52	304	0,65	0,00214	0,744	0,00245	0,946	0,00311	1,98	0,0065	3,38	0,0111	5,12	0,0169	9,58	0,0316
54	316	0,683	0,00216	0,824	0,00261	1,07	0,00339	2,01	0,00637	3,5	0,0111	5,26	0,0167	9,91	0,0314
56	328	0,846	0,00258	0,919	0,0028	1,09	0,00331	2,12	0,00645	3,48	0,0106	5,39	0,0164	9,98	0,0304
58	340	0,87	0,00256	1,05	0,00309	1,21	0,00356	2,15	0,00631	3,63	0,0107	5,32	0,0156	10	0,0295
60	352	0,947	0,00269	1,15	0,00328	1,31	0,00371	2,16	0,00612	3,68	0,0105	5,34	0,0152	9,97	0,0283
62	364	1,14	0,00314	1,17	0,00322	1,4	0,00384	2,32	0,00638	3,63	0,00997	5,56	0,0153	10,7	0,0293
64	376	1,13	0,00301	1,3	0,00344	1,54	0,00409	2,34	0,00623	3,8	0,0101	5,52	0,0147	10,6	0,0282
66	389	1,23	0,00316	1,33	0,00342	1,64	0,00422	2,48	0,00638	3,81	0,00981	5,7	0,0147	10,7	0,0276
68	401	1,27	0,00318	1,43	0,00357	1,81	0,00453	2,49	0,00621	3,99	0,00997	5,58	0,0139	10,6	0,0264
70	413	1,49	0,0036	1,58	0,00383	1,79	0,00433	2,72	0,00659	4,04	0,0098	5,75	0,0139	10,7	0,026
72	425	1,54	0,00362	1,73	0,00408	1,85	0,00436	2,83	0,00665	4,22	0,00994	5,82	0,0137	10,8	0,0253
74	437	1,65	0,00377	1,71	0,00392	1,99	0,00456	2,92	0,00668	4,14	0,00947	5,94	0,0136	11	0,0251
76	449	1,61	0,00358	1,8	0,00401	2,2	0,0049	2,84	0,00632	4,35	0,00968	5,89	0,0131	11	0,0245
78	461	2,02	0,00437	1,67	0,00363	2,01	0,00436	3,2	0,00694	4,6	0,00998	5,96	0,0129	11	0,0237
80	473	1,97	0,00415	2,01	0,00425	2,3	0,00487	3,15	0,00666	4,44	0,00938	6,12	0,0129	11,1	0,0236
82	485	1,89	0,0039	2,03	0,00418	2,5	0,00515	3,11	0,00641	4,51	0,00928	6,03	0,0124	11,2	0,0231
84	498	2,08	0,00419	2,05	0,00412	2,58	0,00518	3,29	0,00662	4,49	0,00902	6,3	0,0127	11,4	0,0229
86	510	2,09	0,0041	2,15	0,00422	2,7	0,00529	3,3	0,00647	4,6	0,00902	6,25	0,0123	11,6	0,0227
88	522	2,24	0,0043	2,45	0,00469	2,65	0,00507	3,45	0,00662	4,91	0,00941	6,2	0,0119	11,4	0,0218
90	534	2,3	0,0043	2,39	0,00449	2,82	0,00528	3,57	0,00669	4,86	0,00911	6,31	0,0118	11,5	0,0215
92	546	2,46	0,00451	2,53	0,00464	2,89	0,00529	3,75	0,00686	4,99	0,00914	6,4	0,0117	11,6	0,0212
94	558	2,49	0,00446	2,5	0,00449	3,06	0,00549	3,85	0,00689	4,99	0,00894	6,46	0,0116	11,6	0,0207
96	570	2,75	0,00482	2,79	0,00489	2,99	0,00525	4,11	0,00721	5,11	0,00897	6,63	0,0116	11,6	0,0203
98	582	2,84	0,00487	2,92	0,00501	3,11	0,00534	4,19	0,00719	5,26	0,00903	6,71	0,0115	11,7	0,0201
100	594	2,82	0,00475	2,82	0,00474	3,36	0,00565	4,27	0,00718	5,21	0,00876	6,93	0,0117	11,6	0,0196
102	607	2,94	0,00485	3,08	0,00508	3,39	0,00559	4,32	0,00712	5,43	0,00896	6,78	0,0112	11,7	0,0193
104	619	3,03	0,0049	3,08	0,00498	3,53	0,00571	4,35	0,00703	5,48	0,00886	6,92	0,0112	11,8	0,019
106	631	3,04	0,00483	3,14	0,00498	3,68	0,00583	4,54	0,00719	5,57	0,00883	7,07	0,0112	11,6	0,0184

108	643	3,27	0,00509	3,43	0,00533	3,62	0,00563	4,75	0,00739	5,79	0,00901	7,13	0,0111	11,7	0,0183
110	655	3,29	0,00502	3,55	0,00542	3,78	0,00578	4,78	0,0073	5,84	0,00892	7,09	0,0108	11,8	0,018
112	667	3,49	0,00523	3,66	0,00548	3,82	0,00573	4,96	0,00744	5,81	0,0087	7,12	0,0107	11,8	0,0176
114	679	3,43	0,00506	3,5	0,00515	4,15	0,00612	4,81	0,00708	5,86	0,00863	7,37	0,0109	11,9	0,0176
116	691	3,59	0,00519	3,69	0,00534	4,15	0,00601	5,02	0,00726	6,02	0,00871	7,44	0,0108	12	0,0174
118	703	3,66	0,0052	3,85	0,00547	4,26	0,00605	5,11	0,00726	6,19	0,0088	7,35	0,0105	12,1	0,0172
120	716	3,87	0,0054	3,89	0,00543	4,35	0,00608	5,42	0,00757	6,08	0,0085	7,52	0,0105	12,3	0,0172
122	728	3,98	0,00548	4,14	0,00569	4,35	0,00598	5,47	0,00752	6,56	0,00901	7,5	0,0103	12,3	0,017
124	740	4,1	0,00554	4,24	0,00574	4,44	0,006	5,64	0,00763	6,61	0,00893	7,63	0,0103	12	0,0163
126	752	4,06	0,0054	4,1	0,00546	4,73	0,00629	5,86	0,00779	6,65	0,00885	7,94	0,0106	12,7	0,0169
128	764	4,28	0,0056	4,35	0,0057	4,75	0,00622	5,85	0,00766	6,88	0,009	7,95	0,0104	12,5	0,0164
130	776	4,31	0,00556	4,41	0,00569	4,94	0,00637	5,84	0,00753	7,04	0,00907	8,08	0,0104	12,6	0,0162
132	788	4,37	0,00554	4,48	0,00569	5,06	0,00642	5,89	0,00747	7,18	0,00911	8,11	0,0103	12,6	0,016
134	800	4,59	0,00573	4,45	0,00555	5,16	0,00644	6,1	0,00762	7,27	0,00908	8,48	0,0106	12,6	0,0158
136	812	4,85	0,00596	4,69	0,00577	5,19	0,00639	6,35	0,00781	7,37	0,00907	8,62	0,0106	12,8	0,0158
138	825	4,53	0,00549	4,58	0,00555	5,44	0,0066	6,36	0,00772	7,55	0,00916	8,59	0,0104	13	0,0157
140	837	4,99	0,00597	4,95	0,00591	5,34	0,00638	6,61	0,0079	7,69	0,0092	8,64	0,0103	12,7	0,0152
142	849	4,98	0,00586	5,01	0,0059	5,52	0,0065	6,64	0,00782	7,81	0,0092	8,8	0,0104	12,7	0,015
144	861	5,04	0,00585	5,06	0,00587	5,71	0,00664	6,7	0,00778	7,92	0,0092	8,98	0,0104	13	0,0151
146	873	5,3	0,00607	5,32	0,00609	5,68	0,0065	6,87	0,00787	8,24	0,00944	8,97	0,0103	12,9	0,0147
148	885	5,15	0,00581	5,31	0,006	5,92	0,00669	6,79	0,00767	8,36	0,00944	9,01	0,0102	12,8	0,0145
150	897	5,38	0,006	5,51	0,00614	5,92	0,00659	7,06	0,00787	8,51	0,00949	9,32	0,0104	13,1	0,0146
152	909	5,46	0,006	5,41	0,00595	6,07	0,00667	7,08	0,00778	8,34	0,00917	9,45	0,0104	13	0,0143
154	921	5,63	0,00611	5,61	0,00609	6,07	0,00659	7,23	0,00784	8,53	0,00926	9,48	0,0103	13,2	0,0143
156	934	5,61	0,00601	5,56	0,00595	6,23	0,00668	7,23	0,00775	8,8	0,00943	9,68	0,0104	13	0,0139
158	946	5,84	0,00618	5,8	0,00613	6,31	0,00667	7,37	0,00779	8,97	0,00948	9,73	0,0103	13,1	0,0139
160	958	5,74	0,00599	5,66	0,0059	6,55	0,00684	7,3	0,00762	8,9	0,0093	9,89	0,0103	13,2	0,0138
162	970	5,83	0,00601	5,73	0,0059	6,68	0,00688	7,41	0,00764	9,02	0,0093	10	0,0103	13,3	0,0137
164	982	6,07	0,00618	6,11	0,00622	6,62	0,00675	7,45	0,00759	9,29	0,00946	10,1	0,0103	13	0,0133
166	994	6,33	0,00637	6,08	0,00612	6,76	0,0068	7,77	0,00781	9,34	0,00939	10,3	0,0104	13,7	0,0137
168	1 010	6,37	0,00633	6,2	0,00616	6,8	0,00675	7,86	0,00781	9,61	0,00955	10,5	0,0105	13,6	0,0136
170	1 020	6,42	0,00631	6,5	0,00639	6,83	0,00671	8,16	0,00802	9,67	0,0095	10,6	0,0105	13,8	0,0135
172	1 030	6,41	0,00622	6,35	0,00616	7,17	0,00695	8,11	0,00787	9,75	0,00946	10,7	0,0104	14	0,0136
174	1 040	6,62	0,00635	6,43	0,00616	7,22	0,00693	8,26	0,00792	9,85	0,00945	11	0,0105	14	0,0134

176	1 050	6,65	0,0063	6,66	0,00632	7,45	0,00706	8,29	0,00786	10,2	0,00963	10,9	0,0103	14,2	0,0135
178	1 070	7,04	0,0066	6,94	0,00651	7,35	0,00689	8,64	0,0081	10,3	0,00961	11,4	0,0107	14,2	0,0133
180	1 080	7,2	0,00667	6,95	0,00644	7,52	0,00697	8,66	0,00803	10,4	0,00963	11,2	0,0104	14,5	0,0134
182	1 090	7,04	0,00645	7,05	0,00647	7,6	0,00696	8,75	0,00802	10,6	0,00972	11,4	0,0104	14,6	0,0134
184	1 100	7,41	0,00672	7,37	0,00668	7,6	0,00689	8,83	0,00801	10,8	0,00979	11,6	0,0105	14,9	0,0135
186	1 120	7,27	0,00652	7,34	0,00659	7,89	0,00708	8,79	0,00788	11	0,00986	11,6	0,0104	14,8	0,0133
188	1 130	7,57	0,00672	7,33	0,0065	8,09	0,00717	8,97	0,00796	11	0,00977	11,9	0,0105	15	0,0133
190	1 140	7,87	0,00691	7,69	0,00675	7,98	0,007	9,35	0,00821	10,9	0,00956	12,1	0,0107	15	0,0131
192	1 150	7,88	0,00684	7,7	0,00669	8,3	0,00721	9,34	0,00811	11,1	0,00962	12,4	0,0107	15,1	0,0131
194	1 160	8,19	0,00704	7,89	0,00678	8,44	0,00725	9,55	0,00821	11,1	0,00953	12,4	0,0107	15,4	0,0132
196	1 180	8,11	0,0069	7,92	0,00674	8,65	0,00736	9,58	0,00815	11,4	0,00972	12,5	0,0106	15,5	0,0132
198	1 190	8,51	0,00716	8,15	0,00686	8,59	0,00723	9,99	0,00841	11,3	0,00953	12,9	0,0109	15,7	0,0132
200	1 200	8,65	0,00721	8,38	0,00698	8,67	0,00723	10,1	0,00839	11,9	0,0099	13,1	0,011	15,8	0,0132

Time	Shear Rate	Shear Stress	Viscosity	Shear Stress	Viscosity	Shear Stress	Viscosity	Shear Stress	Viscosity	Shear Stress	Viscosity	Shear Stress	Viscosity	Shear Stress	Viscosity
[s]	[1/s]	[Pa]	[Pa·s]	[Pa]	[Pa·s]	[Pa]	[Pa·s]	[Pa]	[Pa·s]	[Pa]	[Pa·s]	[Pa]	[Pa·s]	[Pa]	[Pa·s]
Number of Intervals:		*CNC-ATT-WDFs (6 wt %) 0.0 % 80°C F.W.*	*CNC-ATT-WDFs (6 wt %) 0.0 % 80°C F.W.*	*CNC-ATT-WDFs (6 wt %) 0.4 % 80°C F.W.*	*CNC-ATT-WDFs (6 wt %) 0.4 % 80°C F.W.*	*CNC-ATT-WDFs (6 wt %) 0.8 % 80°C F.W.*	*CNC-ATT-WDFs (6 wt %) 0.8 % 80°C F.W.*	*CNC-ATT-WDFs (6 wt %) 1.2 % 80°C F.W.*	*CNC-ATT-WDFs (6 wt %) 1.2 % 80°C F.W.*	*CNC-ATT-WDFs (6 wt %) 1.6 % 80°C F.W.*	*CNC-ATT-WDFs (6 wt %) 1.6 % 80°C F.W.*	*CNC-ATT-WDFs (6 wt %) 2.0 % 80°C F.W.*	*CNC-ATT-WDFs (6 wt %) 2.0 % 80°C F.W.*	*CNC-ATT-WDFs (6 wt %) 2.4 % 80°C F.W.*	*CNC-ATT-WDFs (6 wt %) 2.4 % 80°C F.W.*
2	0,999	-0,481	-0,481	-0,561	-0,56	-0,285	-0,286	0,156	0,156	0,361	0,36	0,538	0,538	2,35	2,35
4	13,1	-0,457	-0,0349	-0,325	-0,0248	0,0439	0,00334	0,565	0,0431	1,51	0,115	1,95	0,149	4,27	0,326
6	25,2	-0,394	-0,0156	-0,304	-0,0121	0,0712	0,00282	0,763	0,0303	1,8	0,0713	2,51	0,0995	5,6	0,222
8	37,3	-0,425	-0,0114	-0,25	-0,0067	0,221	0,00593	0,678	0,0181	1,87	0,0502	2,86	0,0767	6,52	0,175
10	49,4	-0,483	-0,00976	-0,316	-0,00639	0,172	0,00348	0,719	0,0145	1,99	0,0402	2,92	0,059	6,88	0,139
12	61,6	-0,532	-0,00864	-0,282	-0,00458	0,218	0,00354	0,875	0,0142	1,96	0,0319	2,93	0,0475	6,79	0,11
14	73,7	-0,492	-0,00667	-0,298	-0,00405	0,126	0,00171	0,836	0,0114	1,9	0,0258	3,05	0,0414	6,62	0,0899
16	85,8	-0,448	-0,00523	-0,211	-0,00246	0,18	0,0021	0,894	0,0104	2	0,0233	3,05	0,0355	6,79	0,0791
18	97,9	-0,445	-0,00455	-0,234	-0,00239	0,206	0,00211	0,945	0,00965	2,1	0,0215	3,2	0,0327	7,01	0,0716
20	110	-0,391	-0,00355	-0,236	-0,00214	0,182	0,00166	0,926	0,00842	2,24	0,0204	3,29	0,0299	7,24	0,0658
22	122	-0,254	-0,00208	-0,198	-0,00162	0,238	0,00195	0,984	0,00805	2,27	0,0186	3,34	0,0274	7,34	0,0601
24	134	-0,29	-0,00216	-0,11	-8,17E-4	0,306	0,00228	1,08	0,00808	2,3	0,0171	3,4	0,0253	7,38	0,055
26	146	-0,236	-0,00161	-0,117	-8,01E-4	0,326	0,00223	1,11	0,00756	2,38	0,0163	3,65	0,0249	7,62	0,0521
28	158	-0,154	-9,71E-4	-0,121	-7,65E-4	0,338	0,00213	1,14	0,00722	2,5	0,0158	3,76	0,0237	7,89	0,0498
30	171	-0,167	-9,8E-4	-0,0883	-5,18E-4	0,378	0,00221	1,21	0,00711	2,65	0,0156	3,76	0,022	7,99	0,0469
32	183	-0,112	-6,15E-4	0,00603	3,3E-5	0,438	0,0024	1,24	0,00677	2,7	0,0148	3,83	0,021	8,3	0,0454
34	195	-0,0329	-1,69E-4	0,0578	2,97E-4	0,545	0,0028	1,26	0,00646	2,77	0,0142	3,92	0,0201	8,33	0,0427
36	207	-0,0366	-1,77E-4	0,0796	3,85E-4	0,534	0,00258	1,29	0,00626	2,82	0,0136	4,15	0,0201	8,36	0,0404

38	219	0,034	1,55E-4	0,177	8,1E-4	0,593	0,00271	1,35	0,00616	2,95	0,0135	4,2	0,0192	8,41	0,0384
40	231	0,0671	2,9E-4	0,191	8,25E-4	0,631	0,00273	1,42	0,00613	2,99	0,0129	4,36	0,0189	8,79	0,038
42	243	0,103	4,25E-4	0,268	0,0011	1,04	0,00428	1,43	0,00587	3,03	0,0125	4,36	0,0179	8,94	0,0368
44	255	0,151	5,91E-4	0,36	0,00141	1,42	0,00555	1,49	0,00585	3,09	0,0121	4,54	0,0178	8,87	0,0348
46	267	0,244	9,13E-4	0,309	0,00115	0,585	0,00219	1,5	0,00561	3,17	0,0118	4,68	0,0175	8,97	0,0335
48	280	0,279	9,98E-4	0,411	0,00147	0,66	0,00236	1,53	0,00549	3,22	0,0115	4,67	0,0167	9,1	0,0326
50	292	0,292	0,001	0,432	0,00148	0,64	0,0022	1,61	0,00553	3,13	0,0107	4,65	0,0159	9,24	0,0317
52	304	0,376	0,00124	0,52	0,00171	0,742	0,00244	1,66	0,00547	3,24	0,0107	4,81	0,0158	9,47	0,0312
54	316	0,476	0,00151	0,555	0,00176	0,819	0,00259	1,7	0,00539	3,28	0,0104	4,83	0,0153	9,31	0,0295
56	328	0,521	0,00159	0,688	0,0021	0,908	0,00277	1,85	0,00564	3,32	0,0101	4,81	0,0147	9,5	0,029
58	340	0,676	0,00199	0,713	0,0021	1	0,00295	1,81	0,00533	3,55	0,0104	5,02	0,0148	9,71	0,0286
60	352	0,742	0,00211	0,795	0,00226	1,1	0,00311	1,91	0,00542	3,58	0,0102	5,09	0,0144	9,69	0,0275
62	364	0,747	0,00205	0,971	0,00266	1,17	0,0032	2,11	0,00578	3,53	0,00968	5,06	0,0139	9,58	0,0263
64	376	0,892	0,00237	0,974	0,00259	1,27	0,00336	2,04	0,00542	3,66	0,00972	5,26	0,014	9,9	0,0263
66	389	0,934	0,0024	1,07	0,00277	1,35	0,00347	2,15	0,00554	3,7	0,00951	5,23	0,0135	9,96	0,0256
68	401	1,01	0,00252	1,12	0,0028	1,39	0,00346	2,27	0,00566	3,81	0,0095	5,32	0,0133	10,2	0,0254
70	413	1,07	0,0026	1,32	0,00321	1,56	0,00378	2,37	0,00575	3,77	0,00914	5,26	0,0127	10	0,0243
72	425	1,15	0,00272	1,36	0,00321	1,64	0,00387	2,48	0,00584	3,93	0,00924	5,52	0,013	10,3	0,0242
74	437	1,16	0,00265	1,49	0,0034	1,68	0,00384	2,59	0,00593	3,89	0,00889	5,51	0,0126	10,5	0,0239
76	449	1,33	0,00297	1,44	0,0032	1,74	0,00387	2,56	0,0057	4,11	0,00916	5,67	0,0126	10,6	0,0236
78	461	1,17	0,00255	1,7	0,00368	2,03	0,0044	2,61	0,00566	3,89	0,00844	5,86	0,0127	10,4	0,0226
80	473	1,44	0,00304	1,68	0,00354	1,95	0,00412	2,82	0,00596	4,18	0,00882	5,73	0,0121	10,8	0,0228
82	485	1,56	0,00321	1,65	0,00339	1,97	0,00405	2,79	0,00575	4,36	0,00899	5,94	0,0122	10,9	0,0224
84	498	1,55	0,00311	1,79	0,00359	1,98	0,00398	2,98	0,00598	4,27	0,00858	5,97	0,012	10,8	0,0217
86	510	1,66	0,00326	1,82	0,00358	2,08	0,00409	2,98	0,00585	4,51	0,00885	6,15	0,0121	11	0,0217
88	522	1,83	0,0035	1,96	0,00375	2,33	0,00447	3,08	0,0059	4,71	0,00902	6,3	0,0121	10,8	0,0207
90	534	1,83	0,00342	2,02	0,00378	2,35	0,0044	3,16	0,00592	4,69	0,00879	6,12	0,0115	11,1	0,0207
92	546	1,89	0,00347	2,15	0,00395	2,5	0,00457	3,35	0,00613	4,71	0,00863	6,17	0,0113	10,9	0,0199
94	558	1,94	0,00348	2,17	0,00388	2,5	0,00448	3,36	0,00603	4,78	0,00856	6,32	0,0113	10,8	0,0194
96	570	2,01	0,00352	2,38	0,00417	2,74	0,00481	3,63	0,00636	4,88	0,00857	6,2	0,0109	11,1	0,0195
98	582	2,11	0,00362	2,45	0,00421	2,86	0,0049	3,71	0,00636	4,95	0,0085	6,3	0,0108	11,1	0,019
100	594	2,16	0,00363	2,51	0,00423	2,8	0,00471	3,79	0,00638	4,87	0,00819	6,43	0,0108	11,1	0,0187
102	607	2,35	0,00388	2,56	0,00422	3,03	0,00499	3,79	0,00624	5,12	0,00845	6,74	0,0111	11,2	0,0184
104	619	2,45	0,00395	2,65	0,00428	3,08	0,00498	3,86	0,00625	5,12	0,00827	6,64	0,0107	11,4	0,0185

106	631	2,56	0,00405	2,7	0,00428	3,05	0,00483	4,02	0,00637	5,11	0,0081	6,63	0,0105	11,5	0,0182
108	643	2,6	0,00405	2,91	0,00452	3,28	0,0051	4,2	0,00654	5,24	0,00815	6,67	0,0104	11,2	0,0175
110	655	2,76	0,00422	2,88	0,0044	3,39	0,00517	4,25	0,00649	5,48	0,00837	6,76	0,0103	11,3	0,0172
112	667	2,76	0,00414	3,05	0,00457	3,49	0,00523	4,44	0,00666	5,53	0,00829	6,74	0,0101	11,6	0,0173
114	679	2,91	0,00428	3,04	0,00447	3,44	0,00506	4,44	0,00653	5,43	0,008	6,98	0,0103	11,8	0,0174
116	691	2,98	0,00431	3,21	0,00464	3,62	0,00524	4,5	0,0065	5,63	0,00814	7,12	0,0103	11,7	0,017
118	703	3,12	0,00444	3,29	0,00468	3,78	0,00538	4,64	0,00659	5,76	0,00819	6,98	0,00992	11,6	0,0165
120	716	3,12	0,00436	3,45	0,00483	3,82	0,00534	4,79	0,0067	5,81	0,00812	7,05	0,00985	11,7	0,0163
122	728	3,27	0,0045	3,52	0,00483	4,07	0,00559	4,95	0,0068	6,16	0,00846	7,24	0,00995	11,4	0,0156
124	740	3,39	0,00458	3,65	0,00493	4,17	0,00564	5,01	0,00678	6,22	0,00841	7,34	0,00992	11,3	0,0153
126	752	3,41	0,00453	3,72	0,00495	4,08	0,00543	5,07	0,00675	6,18	0,00821	7,53	0,01	11,8	0,0157
128	764	3,59	0,0047	3,79	0,00497	4,28	0,00561	5,22	0,00683	6,44	0,00843	7,65	0,01	12	0,0157
130	776	3,68	0,00475	3,85	0,00496	4,31	0,00555	5,42	0,00698	6,57	0,00846	7,7	0,00992	12	0,0155
132	788	3,89	0,00494	3,89	0,00493	4,44	0,00563	5,5	0,00698	6,7	0,0085	7,99	0,0101	12,2	0,0155
134	800	3,79	0,00474	4,07	0,00509	4,44	0,00555	5,53	0,00691	6,73	0,00841	7,89	0,00986	12	0,015
136	812	3,93	0,00484	4,21	0,00519	4,61	0,00568	5,79	0,00712	6,78	0,00834	7,94	0,00977	12,2	0,015
138	825	4,04	0,0049	4,15	0,00503	4,61	0,00559	5,75	0,00698	7,03	0,00853	8,39	0,0102	12,1	0,0147
140	837	4,27	0,00511	4,34	0,00518	4,89	0,00584	6,03	0,0072	7,22	0,00862	8,18	0,00978	12,1	0,0145
142	849	4,39	0,00517	4,4	0,00518	4,92	0,00579	6,05	0,00712	7,36	0,00867	8,21	0,00967	12,1	0,0143
144	861	4,48	0,0052	4,46	0,00518	4,98	0,00578	6,06	0,00704	7,46	0,00866	8,4	0,00975	12,3	0,0143
146	873	4,59	0,00526	4,66	0,00533	5,21	0,00597	6,27	0,00719	7,65	0,00876	8,61	0,00986	12,3	0,014
148	885	4,85	0,00548	4,62	0,00522	5,33	0,00602	6,23	0,00704	7,79	0,0088	8,8	0,00994	12,4	0,0141
150	897	4,87	0,00543	4,77	0,00532	5,47	0,0061	6,48	0,00722	7,84	0,00874	8,97	0,01	12,5	0,014
152	909	4,77	0,00525	4,96	0,00545	5,36	0,00589	6,62	0,00728	7,69	0,00845	9,01	0,00991	12,5	0,0137
154	921	4,92	0,00534	5	0,00543	5,55	0,00602	6,75	0,00733	8	0,00868	9,23	0,01	12,6	0,0137
156	934	4,99	0,00535	5,07	0,00543	5,57	0,00597	6,77	0,00725	8,14	0,00872	9,29	0,00995	12,7	0,0136
158	946	5,1	0,00539	5,15	0,00545	5,74	0,00607	6,92	0,00732	8,32	0,0088	9,39	0,00993	12,7	0,0134
160	958	5,01	0,00523	5,12	0,00535	5,72	0,00597	6,87	0,00717	8,33	0,00869	9,78	0,0102	12,8	0,0134
162	970	5,16	0,00532	5,21	0,00537	5,78	0,00596	7,07	0,00729	8,46	0,00873	9,65	0,00995	13,1	0,0135
164	982	5,29	0,00539	5,32	0,00541	6,05	0,00616	7,1	0,00723	8,69	0,00885	9,93	0,0101	13	0,0133
166	994	5,42	0,00545	5,45	0,00548	6	0,00603	7,29	0,00733	8,76	0,00881	9,95	0,01	13	0,0131
168	1 010	5,53	0,0055	5,55	0,00551	6,15	0,00611	7,44	0,00739	8,77	0,00872	9,94	0,00988	13,1	0,013
170	1 020	5,56	0,00546	5,72	0,00561	6,34	0,00622	7,61	0,00747	9	0,00884	10,1	0,00994	13,4	0,0131
172	1 030	5,75	0,00558	5,63	0,00546	6,36	0,00617	7,56	0,00733	9,22	0,00895	10,5	0,0102	13,4	0,013

174	1 040	5,71	0,00547	5,9	0,00566	6,38	0,00612	7,72	0,0074	9,28	0,0089	10,4	0,00996	13,8	0,0132
176	1 050	6,1	0,00579	5,89	0,00558	6,59	0,00624	7,84	0,00743	9,44	0,00895	10,7	0,0101	13,8	0,0131
178	1 070	6,19	0,00581	6,22	0,00583	6,81	0,00639	8,18	0,00766	9,41	0,00882	10,7	0,01	13,6	0,0127
180	1 080	6,34	0,00588	6,29	0,00583	6,9	0,0064	8,26	0,00766	9,63	0,00893	10,8	0,01	13,9	0,0128
182	1 090	6,41	0,00588	6,34	0,00581	6,98	0,00639	8,4	0,0077	9,69	0,00888	11	0,0101	14,1	0,013
184	1 100	6,64	0,00602	6,42	0,00582	7,19	0,00652	8,56	0,00776	9,72	0,00881	11,1	0,01	14,2	0,0129
186	1 120	6,79	0,00608	6,42	0,00575	7,25	0,0065	8,58	0,00769	9,93	0,0089	11,4	0,0103	14,4	0,0129
188	1 130	6,87	0,00609	6,54	0,0058	7,4	0,00657	8,72	0,00773	10,2	0,00904	11,5	0,0102	14,5	0,0129
190	1 140	7,03	0,00617	6,83	0,006	7,55	0,00663	9,08	0,00797	10,3	0,00907	11,6	0,0102	14,5	0,0128
192	1 150	7,2	0,00625	6,98	0,00606	7,62	0,00662	9,12	0,00792	10,4	0,00899	11,6	0,0101	14,9	0,013
194	1 160	7,23	0,00621	7,16	0,00615	7,72	0,00663	9,36	0,00804	10,4	0,00897	11,9	0,0102	15,1	0,0129
196	1 180	7,35	0,00625	7,21	0,00613	7,85	0,00667	9,36	0,00796	10,5	0,00892	12,1	0,0103	15,2	0,0129
198	1 190	7,41	0,00624	7,42	0,00624	7,96	0,0067	9,71	0,00817	10,6	0,0089	12,2	0,0103	15,2	0,0128
200	1 200	7,7	0,00642	7,56	0,0063	8,18	0,00682	9,84	0,0082	11	0,00917	12,3	0,0103	15,3	0,0128

RHEOLOGICAL DATA OF CNC/SEP-WDFs (FW)

Time	Shear Rate	Shear Stress	Viscosity	Shear Stress	Viscosity	Shear Stress	Viscosity	Shear Stress	Viscosity	Shear Stress	Viscosity	Shear Stress	Viscosity	Shear Stress	Viscosity
[s]	[1/s]	[Pa]	[Pa·s]	[Pa]	[Pa·s]	[Pa]	[Pa·s]	[Pa]	[Pa·s]	[Pa]	[Pa·s]	[Pa]	[Pa·s]	[Pa]	[Pa·s]
Number of Intervals:		*CNC-SEP-WDFs (6 wt %) 0.0 % 20°C*	*CNC-SEP-WDFs (6 wt %) 0.0 % 20°C*	*CNC-SEP-WDFs (6 wt %) 0,4 % 20°C*	*CNC-SEP-WDFs (6 wt %) 0.4 % 20°C*	*CNC-SEP-WDFs (6 wt %) 0.8 % 20°C*	*CNC-SEP-WDFs (6 wt %) 0.8 % 20°C*	*CNC-SEP-WDFs (6 wt %) 1,2 % 20°C*	*CNC-SEP-WDFs (6 wt %) 1,2 % 20°C*	*CNC-SEP-WDFs (6 wt %) 1,6 % 20°C*	*CNC-SEP-WDFs (6 wt %) 1,6 % 20°C*	*CNC-SEP-WDFs (6 wt %) 2.0 % 20°C*	*CNC-SEP-WDFs (6 wt %) 2.0 % 20°C*	*CNC-SEP-WDFs (6 wt %) 2,4 % 20°C*	*CNC-SEP-WDFs (6 wt %) 2,4 % 20°C*
2	0,999	2,51	2,51	-0,116	-0,116	-0,217	-0,217	-0,553	-0,553	0,157	0,157	2,36	2,36	5,5	5,51
4	13,1	3,03	0,231	0,547	0,0417	0,758	0,0578	0,919	0,0701	2,99	0,228	7,09	0,541	14,2	1,08
6	25,2	2,97	0,118	0,715	0,0284	0,932	0,037	1,39	0,0553	3,82	0,152	8,59	0,341	16,8	0,665
8	37,3	2,99	0,0802	0,889	0,0238	0,882	0,0236	1,6	0,043	4,02	0,108	9,41	0,252	17,4	0,467
10	49,4	3,26	0,066	1,09	0,022	0,958	0,0194	1,74	0,0352	4,04	0,0817	9,49	0,192	17,8	0,361
12	61,6	3,41	0,0554	1,19	0,0194	1,05	0,0171	1,91	0,031	4,13	0,0672	9,49	0,154	18	0,292
14	73,7	3,5	0,0476	1,33	0,0181	1,17	0,0158	2,1	0,0285	4,34	0,0589	9,65	0,131	17,7	0,24
16	85,8	3,71	0,0433	1,48	0,0173	1,23	0,0144	2,28	0,0265	4,5	0,0525	9,71	0,113	18,3	0,213
18	97,9	3,89	0,0397	1,63	0,0167	1,38	0,0141	2,51	0,0256	4,78	0,0489	10,1	0,103	18,7	0,191
20	110	4,04	0,0368	1,79	0,0163	1,47	0,0134	2,68	0,0244	5,01	0,0455	10,5	0,095	19	0,173
22	122	4,28	0,035	1,92	0,0157	1,61	0,0132	2,82	0,0231	5,39	0,0441	10,5	0,0863	19,8	0,162
24	134	4,36	0,0325	2,02	0,0151	1,75	0,013	2,98	0,0222	5,73	0,0427	10,9	0,0815	20,2	0,15
26	146	4,53	0,031	2,15	0,0147	1,88	0,0129	3,15	0,0215	5,98	0,0408	11,1	0,0759	20,5	0,14
28	158	4,74	0,0299	2,28	0,0144	1,97	0,0124	3,32	0,0209	6,24	0,0394	11,4	0,072	20,9	0,132
30	171	4,95	0,029	2,4	0,014	2,08	0,0122	3,45	0,0202	6,41	0,0376	11,9	0,0699	21,8	0,128
32	183	5,12	0,028	2,49	0,0136	2,22	0,0122	3,58	0,0196	6,72	0,0368	12,1	0,0663	22,5	0,123
34	195	5,3	0,0272	2,6	0,0133	2,35	0,012	3,74	0,0192	6,92	0,0355	12,6	0,0647	22,9	0,118
36	207	5,54	0,0268	2,71	0,0131	2,43	0,0117	3,87	0,0187	7,14	0,0345	12,8	0,0618	23,3	0,113
38	219	5,76	0,0263	2,87	0,0131	2,56	0,0117	4,01	0,0183	7,37	0,0336	12,9	0,0591	23,8	0,108
40	231	6,03	0,0261	3,01	0,013	2,65	0,0114	4,18	0,0181	7,5	0,0324	13,3	0,0575	24,6	0,107
42	243	6,28	0,0258	3,14	0,0129	2,77	0,0114	4,32	0,0178	7,77	0,032	13,5	0,0554	25,2	0,104
44	255	6,44	0,0252	3,23	0,0126	2,91	0,0114	4,42	0,0173	7,96	0,0312	13,7	0,0537	24,7	0,0969
46	267	6,73	0,0252	3,37	0,0126	2,95	0,011	4,59	0,0172	8,09	0,0302	14,3	0,0534	25,3	0,0945
48	280	6,94	0,0248	3,48	0,0124	3,07	0,011	4,67	0,0167	8,3	0,0297	14,4	0,0514	25,7	0,0918
50	292	7,22	0,0248	3,64	0,0125	3,1	0,0106	4,77	0,0164	8,45	0,029	14,7	0,0504	26,2	0,09
52	304	7,44	0,0245	3,78	0,0124	3,23	0,0106	4,93	0,0162	8,56	0,0282	14,7	0,0484	26,3	0,0867
54	316	7,81	0,0247	3,9	0,0123	3,32	0,0105	5,04	0,016	8,78	0,0278	15	0,0475	26,5	0,084
56	328	8,02	0,0245	3,98	0,0121	3,45	0,0105	5,13	0,0156	8,84	0,027	15,4	0,047	27,4	0,0836
58	340	8,35	0,0246	4,13	0,0122	3,54	0,0104	5,3	0,0156	8,82	0,0259	15,4	0,0452	27,1	0,0797
60	352	8,65	0,0246	4,24	0,012	3,69	0,0105	5,48	0,0156	8,96	0,0254	15,4	0,0438	27,8	0,0789
62	364	8,99	0,0247	4,32	0,0119	3,77	0,0103	5,48	0,0151	9,19	0,0252	15,7	0,0431	27,9	0,0766
64	376	9,36	0,0249	4,49	0,0119	3,92	0,0104	5,71	0,0152	9,16	0,0243	16	0,0426	28,5	0,0757
66	389	9,72	0,025	4,6	0,0118	4	0,0103	5,85	0,0151	9,37	0,0241	16,1	0,0414	29	0,0745
68	401	10,1	0,0252	4,75	0,0118	4,1	0,0102	5,97	0,0149	9,5	0,0237	16,3	0,0406	29,3	0,073
70	413	10,4	0,0251	4,81	0,0117	4,34	0,0105	6,08	0,0147	9,71	0,0235	16,5	0,04	30,1	0,0729
72	425	10,7	0,0252	4,96	0,0117	4,5	0,0106	6,24	0,0147	9,77	0,023	16,7	0,0394	30	0,0706
74	437	11,1	0,0255	5,04	0,0115	4,53	0,0104	6,34	0,0145	9,96	0,0228	16,8	0,0385	30,2	0,069
76	449	11,6	0,0258	5,28	0,0118	4,62	0,0103	6,6	0,0147	9,84	0,0219	16,8	0,0374	30,8	0,0686
78	461	11,7	0,0255	5,42	0,0118	4,47	0,0097	6,52	0,0141	9,91	0,0215	16,8	0,0364	30,7	0,0665
80	473	12,4	0,0263	5,42	0,0115	4,77	0,0101	6,74	0,0142	10,1	0,0213	17	0,036	31,2	0,0659
82	485	12,9	0,0266	5,63	0,0116	4,84	0,00997	6,84	0,0141	10,2	0,021	17	0,035	31,6	0,0651
84	498	13,4	0,0269	5,65	0,0114	4,88	0,00981	6,83	0,0137	10,3	0,0206	17	0,0341	32	0,0643

86	510	13,9	0,0272	5,8	0,0114	5	0,0098 1	6,96	0,0136	10,3	0,0202	17	0,0333	31,8	0,0625
88	522	14,3	0,0274	5,92	0,0113	5,24	0,01	7,17	0,0137	10,4	0,0199	17,1	0,0328	32	0,0613
90	534	14,8	0,0278	6,04	0,0113	5,24	0,0098 1	7,26	0,0136	10,5	0,0196	17,1	0,032	32,4	0,0607
92	546	15,3	0,0281	6,12	0,0112	5,36	0,0098 2	7,37	0,0135	10,6	0,0194	17,3	0,0317	32,5	0,0596
94	558	15,9	0,0285	6,25	0,0112	5,4	0,0096 8	7,49	0,0134	10,7	0,0192	17,5	0,0314	32,7	0,0585
96	570	16,4	0,0287	6,29	0,011	5,59	0,0098	7,6	0,0133	10,8	0,0189	17,7	0,0311	32,4	0,0569
98	582	17	0,0291	6,39	0,011	5,71	0,0098	7,74	0,0133	10,9	0,0188	17,8	0,0306	33	0,0567
100	594	17,7	0,0297	6,49	0,0109	5,69	0,0095 7	7,9	0,0133	11	0,0185	17,6	0,0296	32,7	0,055
102	607	18,3	0,0301	6,64	0,0109	5,89	0,0097 1	8,13	0,0134	11	0,0181	17,9	0,0295	32,6	0,0537
104	619	18,9	0,0306	6,77	0,0109	5,96	0,0096 3	8,25	0,0133	11,1	0,0179	18,1	0,0292	32,9	0,0531
106	631	19,7	0,0312	6,86	0,0109	6,04	0,0095 7	8,42	0,0134	11,3	0,0179	18	0,0285	33,1	0,0525
108	643	20,2	0,0315	6,91	0,0108	6,21	0,0096 6	8,53	0,0133	11,4	0,0177	18,2	0,0283	33,1	0,0514
110	655	21	0,032	7,09	0,0108	6,43	0,0098 1	8,78	0,0134	11,4	0,0175	18,3	0,028	33,1	0,0506
112	667	21,7	0,0325	7,11	0,0107	6,52	0,0097 7	8,87	0,0133	11,6	0,0174	18,3	0,0274	33,2	0,0498
114	679	22,6	0,0333	7,29	0,0107	6,59	0,0097	9	0,0133	11,7	0,0173	18	0,0264	33,3	0,049
116	691	23,4	0,0338	7,36	0,0106	6,86	0,0099 2	9,2	0,0133	12	0,0173	18	0,026	33,5	0,0484
118	703	24,2	0,0344	7,51	0,0107	7,16	0,0102	9,34	0,0133	12	0,0171	18,2	0,0259	33,1	0,0471
120	716	25,1	0,0351	7,57	0,0106	7,34	0,0103	9,39	0,0131	12,2	0,0171	18,7	0,0261	33,5	0,0468
122	728	25,9	0,0356	7,69	0,0106	7,73	0,0106	9,52	0,0131	12,3	0,017	18,6	0,0256	34,3	0,0472
124	740	26,8	0,0362	7,86	0,0106	7,91	0,0107	9,74	0,0132	12,5	0,0169	18,5	0,025	34	0,0459
126	752	27,9	0,0371	7,99	0,0106	7,95	0,0106	9,75	0,013	12,8	0,0171	18,6	0,0247	34,5	0,0459
128	764	28,7	0,0376	8,21	0,0107	8,22	0,0108	9,98	0,0131	12,9	0,0169	18,6	0,0244	34,2	0,0448
130	776	29,8	0,0384	8,37	0,0108	8,42	0,0109	10,1	0,0131	13	0,0168	18,7	0,0241	34,5	0,0445
132	788	30,7	0,039	8,6	0,0109	8,59	0,0109	10,3	0,0131	13,2	0,0167	18,4	0,0234	34,2	0,0434
134	800	31,9	0,0398	8,86	0,0111	8,67	0,0108	10,2	0,0128	13,4	0,0168	18,7	0,0234	34,3	0,0428
136	812	32,9	0,0404	9,17	0,0113	8,88	0,0109	10,3	0,0127	13,6	0,0167	18,9	0,0232	34,2	0,0421
138	825	33,8	0,041	9,56	0,0116	9,17	0,0111	10,7	0,0129	13,6	0,0166	18,5	0,0225	34,3	0,0416
140	837	34,9	0,0417	9,66	0,0115	9,37	0,0112	10,7	0,0128	13,8	0,0165	19,2	0,0229	34,5	0,0413
142	849	36	0,0424	9,84	0,0116	9,55	0,0113	10,8	0,0127	14	0,0165	19,3	0,0227	34,2	0,0402
144	861	37,1	0,0431	10,2	0,0118	9,71	0,0113	11	0,0128	14,1	0,0164	18,8	0,0219	34,1	0,0397
146	873	38,1	0,0436	10,4	0,0119	9,97	0,0114	11,1	0,0127	14,3	0,0164	18,8	0,0216	33,6	0,0385
148	885	39,2	0,0443	10,7	0,0121	10,2	0,0115	11,3	0,0127	14,3	0,0162	18,8	0,0212	34	0,0384
150	897	40,2	0,0448	10,7	0,012	10,4	0,0116	11,3	0,0126	14,6	0,0163	18,8	0,0209	33,9	0,0378
152	909	41,4	0,0456	10,9	0,012	10,4	0,0114	11,4	0,0125	14,9	0,0164	18,8	0,0206	34	0,0373
154	921	42,4	0,046	11,1	0,0121	10,6	0,0115	11,6	0,0126	14,9	0,0162	19,3	0,0209	33,5	0,0364
156	934	43,5	0,0466	11,4	0,0122	10,8	0,0115	11,8	0,0126	15	0,0161	19,3	0,0207	33,9	0,0363
158	946	44,5	0,0471	11,6	0,0123	11,1	0,0117	12	0,0127	15,1	0,016	19,6	0,0207	33,4	0,0353
160	958	45,7	0,0477	11,8	0,0123	11,2	0,0117	12,2	0,0127	15,4	0,016	19,5	0,0204	33,6	0,0351
162	970	46,7	0,0482	12	0,0123	11,4	0,0117	12,3	0,0127	15,7	0,0162	19,7	0,0203	33,7	0,0348
164	982	47,6	0,0484	12,1	0,0124	11,6	0,0118	12,6	0,0128	15,4	0,0157	19,9	0,0202	33	0,0336
166	994	48,7	0,049	12,2	0,0123	11,7	0,0117	12,8	0,0129	15,7	0,0158	20,2	0,0203	32,9	0,0331
168	1 01 0	49,6	0,0493	12,5	0,0124	11,9	0,0119	13	0,013	15,9	0,0158	20,2	0,0201	32,8	0,0326
170	1 02 0	50,5	0,0496	12,7	0,0125	12,2	0,012	13,1	0,0129	16	0,0157	20	0,0196	33,1	0,0325
172	1 03 0	51,6	0,0501	13	0,0126	12,3	0,0119	13,5	0,0131	16,2	0,0157	20,1	0,0195	33	0,032
174	1 04 0	52,5	0,0504	13,2	0,0126	12,5	0,012	13,5	0,013	16,3	0,0156	20,4	0,0196	33,2	0,0318
176	1 05 0	53,4	0,0506	13,5	0,0128	12,8	0,0121	13,8	0,0131	16,5	0,0156	20,5	0,0194	33,1	0,0314
178	1 07 0	54,2	0,0508	13,5	0,0127	13,1	0,0123	14	0,0132	16,8	0,0157	20,8	0,0195	32,7	0,0307
180	1 08 0	55,1	0,051	13,7	0,0127	13,3	0,0123	14,3	0,0132	16,7	0,0155	21,1	0,0196	32,7	0,0303

182	1 090	55,9	0,0513	13,9	0,0127	13,5	0,0123	14,5	0,0133	16,9	0,0155	20,6	0,0189	32,7	0,03
184	1 100	56,6	0,0513	14	0,0127	13,7	0,0124	14,6	0,0133	16,8	0,0152	21,2	0,0192	32,3	0,0293
186	1 120	57,6	0,0516	14,3	0,0129	13,9	0,0124	15	0,0135	17	0,0153	21,2	0,019	32,6	0,0292
188	1 130	58,3	0,0517	14,7	0,0131	14,1	0,0125	15,2	0,0135	17,1	0,0152	21,4	0,019	32,4	0,0287
190	1 140	58,9	0,0517	14,7	0,0129	14,4	0,0126	15,4	0,0135	17,3	0,0152	21,6	0,0189	32,6	0,0286
192	1 150	59,7	0,0519	15,2	0,0132	14,5	0,0126	15,6	0,0136	17,5	0,0152	21,5	0,0187	32,8	0,0285
194	1 160	60,4	0,0519	15,2	0,0131	14,8	0,0127	15,7	0,0135	17,7	0,0152	21,7	0,0186	32,6	0,0281
196	1 180	61,1	0,052	15,6	0,0133	14,7	0,0125	16,1	0,0137	17,8	0,0151	21,8	0,0185	33	0,028
198	1 190	61,7	0,0519	15,8	0,0133	15,1	0,0127	16,2	0,0136	17,8	0,015	22,2	0,0187	32,9	0,0277
200	1 200	62,2	0,0518	16,1	0,0134	15,3	0,0128	16,5	0,0137	18,3	0,0152	22,4	0,0186	33	0,0275

Time	Shear Rate	Shear Stress	Viscosity	Shear Stress	Viscosity	Shear Stress	Viscosity	Shear Stress	Viscosity	Shear Stress	Viscosity	Shear Stress	Viscosity	Shear Stress	Viscosity
[s]	[1/s]	[Pa]	[Pa·s]	[Pa]	[Pa·s]	[Pa]	[Pa·s]	[Pa]	[Pa·s]	[Pa]	[Pa·s]	[Pa]	[Pa·s]	[Pa]	[Pa·s]
Number of Intervals:		*CNC-SEP-WDFs (6 wt %) 0.0 % 30 C*	*CNC-SEP-WDFs (6 wt %) 0.0 % 30 C*	*CNC-SEP-WDFs (6 wt %) 042 % 30 C*	*CNC-SEP-WDFs (6 wt %) 0.4 % 30 C*	*CNC-SEP-WDFs (6 wt %) 0.8 % 30 C*	*CNC-SEP-WDFs (6 wt %) 0.8 % 30 C*	*CNC-SEP-WDFs (6 wt %) 1,2 % 30 C*	*CNC-SEP-WDFs (6 wt %) 1,2 % 30 C*	*CNC-SEP-WDFs (6 wt %) 1,6 % 30 C*	*CNC-SEP-WDFs (6 wt %) 1,6 % 30 C*	*CNC-SEP-WDFs (6 wt %) 2.0 % 30 C*	*CNC-SEP-WDFs (6 wt %) 2.0 % 30 C*	*CNC-SEP-WDFs (6 wt %) 2,4 % 30 C*	*CNC-SEP-WDFs (6 wt %) 2,4 % 30 C*
2	0,999	5,8	1,72	1,72	-0,909	-0,91	-0,161	-0,161	0,068	0,068	0,846	0,847	3,82	3,82	28,7
4	13,1	0,524	2,58	0,197	0,32	0,0244	0,566	0,0432	2,19	0,167	4,63	0,353	11,2	0,857	41,4
6	25,2	0,287	2,77	0,11	0,778	0,0308	1,18	0,0467	3,15	0,125	6,18	0,245	13,6	0,541	45
8	37,3	0,2	2,84	0,0761	1,16	0,031	1,46	0,0391	3,38	0,0905	6,89	0,185	14,8	0,397	46,9
10	49,4	0,157	2,84	0,0574	1,48	0,0299	1,64	0,0333	3,47	0,0702	7,27	0,147	14,9	0,302	49,1
12	61,6	0,131	2,92	0,0474	1,68	0,0273	1,85	0,03	3,56	0,0579	7,78	0,126	15,4	0,25	50,6
14	73,7	0,114	3,06	0,0416	1,81	0,0246	2	0,0272	3,79	0,0514	8,1	0,11	15,4	0,209	52,2
16	85,8	0,103	3,2	0,0373	2,15	0,025	2,2	0,0256	4,06	0,0473	8,63	0,101	15,7	0,183	53,1
18	97,9	0,0934	3,32	0,0339	2,26	0,0231	2,43	0,0248	4,26	0,0436	8,97	0,0917	16,1	0,165	54,2
20	110	0,0864	3,42	0,0311	2,4	0,0219	2,61	0,0237	4,53	0,0412	9,25	0,0841	16,7	0,152	56,2
22	122	0,0812	3,53	0,0289	2,62	0,0214	2,85	0,0233	4,82	0,0394	9,85	0,0807	16,9	0,138	58
24	134	0,0765	3,69	0,0275	2,72	0,0203	3	0,0223	5	0,0373	10,3	0,0766	17,3	0,129	59
26	146	0,0729	3,79	0,0259	2,92	0,02	3,12	0,0213	5,24	0,0358	10,4	0,0708	17,8	0,121	59,7
28	158	0,0702	3,94	0,0248	3,03	0,0191	3,38	0,0213	5,51	0,0348	10,6	0,0668	18,4	0,116	60,4
30	171	0,0677	4,04	0,0237	3,25	0,0191	3,46	0,0203	5,72	0,0336	11,1	0,0649	19	0,111	61,2
32	183	0,0658	4,22	0,0231	3,35	0,0183	3,57	0,0195	6,01	0,0329	11,2	0,0613	19,3	0,106	61,9
34	195	0,064	4,33	0,0222	3,48	0,0179	3,76	0,0193	6,2	0,0318	11,7	0,0598	19,8	0,101	61,7
36	207	0,0626	4,46	0,0215	3,65	0,0177	3,88	0,0187	6,4	0,0309	12	0,058	19,9	0,0961	63,1
38	219	0,0613	4,53	0,0207	3,81	0,0174	4,07	0,0186	6,56	0,03	12,4	0,0568	20,5	0,0937	64,6
40	231	0,0602	4,65	0,0201	3,9	0,0169	4,2	0,0182	6,74	0,0292	12,6	0,0547	21,1	0,0913	65,1
42	243	0,0593	4,74	0,0195	4,04	0,0166	4,31	0,0177	6,86	0,0282	12,8	0,0525	21,4	0,0879	65,2
44	255	0,0587	4,88	0,0191	4,2	0,0164	4,5	0,0176	7,08	0,0277	13,1	0,0513	21,6	0,0846	66
46	267	0,0578	4,93	0,0184	4,33	0,0162	4,62	0,0173	7,21	0,0269	13,5	0,0503	21,9	0,0819	67,3
48	280	0,0573	5,1	0,0182	4,41	0,0158	4,74	0,0169	7,44	0,0266	13,7	0,0489	22,4	0,0801	69,2
50	292	0,0568	5,19	0,0178	4,49	0,0154	4,81	0,0165	7,53	0,0258	13,9	0,0478	23,3	0,0798	69,7
52	304	0,0565	5,31	0,0175	4,59	0,0151	4,92	0,0162	7,63	0,0251	14	0,046	23,5	0,0774	69,5

54	316	0,0564	5,39	0,0171	4,75	0,015	5,06	0,016	7,75	0,0245	14,1	0,0445	23,8	0,0755	71,4
56	328	0,0565	5,58	0,017	4,82	0,0147	5,28	0,0161	7,87	0,024	14,2	0,0434	24	0,0732	73,5
58	340	0,0564	5,68	0,0167	5,02	0,0148	5,5	0,0162	7,89	0,0232	14,3	0,042	24,4	0,0716	72,4
60	352	0,0564	5,8	0,0165	5,16	0,0146	5,64	0,016	7,97	0,0226	14,7	0,0416	24,5	0,0695	74,2
62	364	0,0569	5,99	0,0165	5,18	0,0142	5,59	0,0154	8,23	0,0226	14,9	0,0408	24,5	0,0673	73,7
64	376	0,057	6,09	0,0162	5,39	0,0143	5,78	0,0154	8,29	0,022	15	0,0398	24,9	0,0662	75,3
66	389	0,0574	6,27	0,0161	5,46	0,0141	5,84	0,015	8,48	0,0218	15,3	0,0394	25,4	0,0652	75,6
68	401	0,0576	6,35	0,0159	5,61	0,014	5,99	0,0149	8,56	0,0214	15,6	0,0388	25,5	0,0636	75,2
70	413	0,0582	6,56	0,0159	5,63	0,0136	6,06	0,0147	8,71	0,0211	15,9	0,0385	25,8	0,0625	76,4
72	425	0,0586	6,66	0,0157	5,77	0,0136	6,23	0,0147	8,83	0,0208	15,9	0,0374	26	0,0613	75,9
74	437	0,0592	6,82	0,0156	5,84	0,0134	6,29	0,0144	8,98	0,0205	15,7	0,0359	26,2	0,0599	77,7
76	449	0,0595	6,85	0,0153	6,07	0,0135	6,48	0,0144	8,98	0,02	15,7	0,0349	26,4	0,0588	76,9
78	461	0,06	6,8	0,0147	6,37	0,0138	6,74	0,0146	9,4	0,0204	15,6	0,0338	26,6	0,0576	78,5
80	473	0,0609	7,16	0,0151	6,19	0,0131	6,62	0,014	9,22	0,0195	16,1	0,034	26,7	0,0564	78,4
82	485	0,0614	7,18	0,0148	6,4	0,0132	6,79	0,014	9,27	0,0191	16	0,033	26,7	0,055	79,9
84	498	0,0623	7,34	0,0148	6,42	0,0129	6,82	0,0137	9,43	0,019	16,2	0,0326	27,4	0,0551	79,9
86	510	0,0629	7,4	0,0145	6,57	0,0129	6,98	0,0137	9,46	0,0186	15,9	0,0312	27,3	0,0535	80,8
88	522	0,0637	7,56	0,0145	6,69	0,0128	7,22	0,0138	9,54	0,0183	16,1	0,0308	27,1	0,052	80,4
90	534	0,0645	7,65	0,0143	6,8	0,0127	7,26	0,0136	9,67	0,0181	16,5	0,0308	27,4	0,0514	81,7
92	546	0,0655	7,81	0,0143	6,88	0,0126	7,41	0,0136	9,83	0,018	16,6	0,0303	27,1	0,0497	81
94	558	0,0663	7,88	0,0141	6,98	0,0125	7,45	0,0134	9,92	0,0178	16,5	0,0296	27,5	0,0492	84,3
96	570	0,0673	8,12	0,0142	7	0,0123	7,63	0,0134	10,1	0,0178	16,7	0,0292	27,5	0,0483	84
98	582	0,068	8,26	0,0142	7,12	0,0122	7,76	0,0133	10,3	0,0176	16,8	0,0288	27,6	0,0474	84,4
100	594	0,0689	8,26	0,0139	7,23	0,0122	7,84	0,0132	10,4	0,0174	16,9	0,0284	28,1	0,0473	83,7
102	607	0,0697	8,39	0,0138	7,42	0,0122	8,05	0,0133	10,4	0,0171	16,9	0,0279	28	0,0461	84,7
104	619	0,0705	8,48	0,0137	7,49	0,0121	8,17	0,0132	10,6	0,0171	16,9	0,0274	27,9	0,045	84,6
106	631	0,0712	8,55	0,0136	7,62	0,0121	8,31	0,0132	10,6	0,0169	17	0,0269	28,1	0,0445	85,6
108	643	0,0721	8,76	0,0136	7,61	0,0118	8,5	0,0132	10,9	0,0169	17,2	0,0267	28,2	0,0438	85,7
110	655	0,0728	8,8	0,0134	7,81	0,0119	8,69	0,0133	10,9	0,0167	17	0,0259	28,4	0,0434	85,8
112	667	0,0737	8,98	0,0135	7,81	0,0117	8,8	0,0132	11,2	0,0168	17,3	0,0259	28,6	0,0428	85,4
114	679	0,0742	8,94	0,0132	8	0,0118	8,88	0,0131	11,2	0,0165	17,5	0,0257	28,5	0,0419	87,9
116	691	0,075	9,14	0,0132	8,05	0,0116	9,04	0,0131	11,4	0,0165	17,4	0,0251	28,4	0,0411	87,9
118	703	0,0754	9,23	0,0131	8,22	0,0117	9,27	0,0132	11,5	0,0164	17,6	0,025	28,4	0,0404	87,3
120	716	0,0759	9,39	0,0131	8,34	0,0116	9,3	0,013	11,8	0,0165	17,4	0,0244	28,6	0,04	86,7

122	728	0,0765	9,52	0,0131	8,53	0,0117	9,6	0,0132	11,9	0,0163	17,6	0,0242	28,5	0,0391	89,6
124	740	0,0769	9,65	0,013	8,68	0,0117	9,67	0,0131	12	0,0162	17,8	0,024	28,8	0,0389	88,4
126	752	0,0773	9,68	0,0129	8,8	0,0117	9,64	0,0128	12,2	0,0163	17,4	0,0231	29	0,0386	90,1
128	764	0,0776	9,83	0,0129	8,94	0,0117	9,84	0,0129	12,4	0,0162	17,4	0,0228	28,9	0,0378	88,4
130	776	0,0778	9,89	0,0127	9,07	0,0117	9,91	0,0128	12,5	0,0161	17,7	0,0228	28,7	0,037	89,3
132	788	0,0781	10	0,0127	9,31	0,0118	10,2	0,0129	12,6	0,0159	17,7	0,0224	28,7	0,0364	91,2
134	800	0,0783	10,1	0,0127	9,33	0,0117	10	0,0125	12,8	0,016	17,8	0,0222	29	0,0362	91,2
136	812	0,0785	10,3	0,0127	9,58	0,0118	10,2	0,0126	12,9	0,0158	17,8	0,0219	28,5	0,035	92
138	825	0,0782	10,3	0,0125	9,96	0,0121	10,4	0,0126	12,9	0,0156	17,6	0,0214	28,9	0,0351	92,2
140	837	0,0785	10,6	0,0126	10,1	0,0121	10,8	0,0129	13,3	0,0159	17,8	0,0213	28,6	0,0342	91
142	849	0,0784	10,6	0,0125	10,4	0,0122	10,8	0,0127	13,3	0,0157	17,9	0,0211	28,6	0,0337	92,1
144	861	0,0783	10,7	0,0125	10,6	0,0123	10,9	0,0127	13,4	0,0155	18,1	0,021	28,6	0,0332	90,6
146	873	0,0783	11,3	0,0129	10,7	0,0122	11,3	0,0129	13,6	0,0156	18,2	0,0208	28,3	0,0325	89,8
148	885	0,078	11,5	0,013	11	0,0124	11,4	0,0129	13,6	0,0154	17,9	0,0202	28,5	0,0322	92
150	897	0,0778	11,9	0,0133	11,1	0,0124	11,6	0,0129	13,8	0,0154	18,4	0,0205	28,5	0,0317	90,5
152	909	0,0778	12,2	0,0134	11,3	0,0124	11,5	0,0126	14,1	0,0155	18,5	0,0203	29,2	0,0321	90,9
154	921	0,0775	12,5	0,0135	11,5	0,0125	11,7	0,0127	14,2	0,0154	18,5	0,0201	28,2	0,0306	89,8
156	934	0,0772	12,6	0,0135	11,8	0,0126	11,8	0,0126	14,2	0,0152	18,4	0,0197	28,9	0,0309	92
158	946	0,0769	12,8	0,0136	11,9	0,0126	12,1	0,0128	14,4	0,0152	18,7	0,0198	28,4	0,03	91,3
160	958	0,0765	12,9	0,0135	12,2	0,0127	12,2	0,0128	14,2	0,0148	18,6	0,0194	28,4	0,0296	91,6
162	970	0,0762	13,2	0,0136	12,4	0,0127	12,4	0,0128	14,3	0,0148	18,8	0,0194	28,5	0,0294	89,7
164	982	0,0758	13,5	0,0137	12,5	0,0128	12,7	0,0129	14,7	0,015	18,8	0,0192	28,1	0,0286	89,9
166	994	0,0755	13,7	0,0138	12,6	0,0127	12,8	0,0129	14,7	0,0148	19,1	0,0192	28,4	0,0286	88,4
168	1 010	0,0752	13,9	0,0138	12,8	0,0128	13	0,013	15,1	0,015	19	0,0189	28	0,0278	89,5
170	1 020	0,0749	14,2	0,014	13	0,0127	13,3	0,0131	15,3	0,015	19,1	0,0188	28,1	0,0276	90,1
172	1 030	0,0744	14,2	0,0138	13,4	0,013	13,4	0,013	15,3	0,0149	19,5	0,0189	28,1	0,0273	90,5
174	1 040	0,0741	14,6	0,014	13,6	0,013	13,6	0,013	15,6	0,0149	19,7	0,0189	28,1	0,0269	89,6
176	1 050	0,0735	14,8	0,014	13,9	0,0131	14	0,0133	15,7	0,0149	19,7	0,0187	28,2	0,0268	90,4
178	1 070	0,0732	15,1	0,0142	13,9	0,013	14,1	0,0132	15,8	0,0148	20	0,0188	27,7	0,026	90,4
180	1 080	0,0728	15,3	0,0142	14,2	0,0131	14,3	0,0133	15,9	0,0148	20	0,0186	28,3	0,0262	91,3
182	1 090	0,0724	15,5	0,0142	14,4	0,0132	14,6	0,0134	16,1	0,0148	20,3	0,0186	28,3	0,026	89,9
184	1 100	0,072	15,7	0,0143	14,6	0,0133	14,8	0,0135	16	0,0145	20,2	0,0183	28,3	0,0257	89,5
186	1 120	0,0714	15,9	0,0143	14,9	0,0134	15	0,0134	16,1	0,0145	20,3	0,0182	28,4	0,0254	89,4
188	1 130	0,071	16,2	0,0144	15,2	0,0135	15,3	0,0135	16,7	0,0148	20,2	0,0179	28,8	0,0255	90,7

190	1 140	0,0707	16,5	0,0145	15,2	0,0133	15,5	0,0136	17,3	0,0152	20,8	0,0182	29	0,0255	90,1
192	1 150	0,0701	16,8	0,0146	15,3	0,0133	15,7	0,0136	17,4	0,0151	20,5	0,0178	28,9	0,0251	90
194	1 160	0,0696	16,9	0,0145	15,6	0,0134	16	0,0137	17,7	0,0152	20,8	0,0179	29,6	0,0255	90
196	1 180	0,0692	17,4	0,0148	15,9	0,0135	16	0,0136	17,8	0,0151	21	0,0179	29,5	0,0251	91
198	1 190	0,0689	17,6	0,0149	15,8	0,0133	16,3	0,0138	18,3	0,0154	21,1	0,0178	29,3	0,0247	92,3
200	1 200	0,0684	17,8	0,0149	16,2	0,0135	16,5	0,0138	18,4	0,0154	21,7	0,0181	29,4	0,0245	91,3

Time	Shear Rate	Shear Stress	Viscosity	Shear Stress	Viscosity	Shear Stress	Viscosity	Shear Stress	Viscosity	Shear Stress	Viscosity	Shear Stress	Viscosity	Shear Stress	Viscosity
[s]	[1/s]	[Pa]	[Pa·s]	[Pa]	[Pa·s]	[Pa]	[Pa·s]	[Pa]	[Pa·s]	[Pa]	[Pa·s]	[Pa]	[Pa·s]	[Pa]	[Pa·s]
Number of Intervals:		*CNC-SEP-WDFs (6 wt %) 0.0 % 40° C*	*CNC-SEP-WDFs (6 wt %) 0.0 % 40° C*	*CNC-SEP-WDFs (6 wt %) 0,4 % 40° C*	*CNC-SEP-WDFs (6 wt %) 0.4 % 40° C*	*CNC-SEP-WDFs (6 wt %) 0.8 % 40° C*	*CNC-SEP-WDFs (6 wt %) 0.8 % 40° C*	*CNC-SEP-WDFs (6 wt %) 1,2 % 40° C*	*CNC-SEP-WDFs (6 wt %) 1,2 % 40° C*	*CNC-SEP-WDFs (6 wt %) 1,6 % 40° C*	*CNC-SEP-WDFs (6 wt %) 1,6 % 40° C*	*CNC-SEP-WDFs (6 wt %) 2.0 % 40° C*	*CNC-SEP-WDFs (6 wt %) 2.0 % 40° C*	*CNC-SEP-WDFs (6 wt %) 2,4 % 40° C*	*CNC-SEP-WDFs (6 wt %) 2,4 % 40° C*
2	0,999	13,5	13,4	2,32	2,32	-0,457	-0,457	-0,706	-0,707	0,098	0,0981	1,52	1,53	5,19	5,2
4	13,1	16,1	1,23	3,17	0,242	0,361	0,0276	0,274	0,0209	2,03	0,155	3,81	0,291	8,95	0,683
6	25,2	16,8	0,665	3,14	0,124	0,677	0,0269	0,906	0,0359	2,86	0,113	5,04	0,2	10,6	0,42
8	37,3	17,1	0,458	3,04	0,0813	0,917	0,0246	0,998	0,0267	3,12	0,0835	6,07	0,162	11,8	0,316
10	49,4	17,7	0,358	2,97	0,0601	1,12	0,0226	1,19	0,024	3,21	0,0649	6,58	0,133	12,5	0,253
12	61,6	18,4	0,3	3,09	0,0502	1,22	0,0199	1,42	0,0231	3,26	0,053	7,07	0,115	13,3	0,217
14	73,7	19,1	0,26	3,06	0,0416	1,4	0,019	1,52	0,0206	3,45	0,0469	7,49	0,102	13,7	0,186
16	85,8	19,8	0,231	3,12	0,0364	1,51	0,0176	1,71	0,0199	3,64	0,0424	7,75	0,0903	14,3	0,167
18	97,9	20,6	0,21	3,22	0,0329	1,7	0,0174	1,84	0,0188	3,98	0,0407	7,91	0,0809	14,8	0,152
20	110	21,3	0,194	3,3	0,03	1,81	0,0165	1,97	0,0179	4,07	0,037	8,16	0,0742	15,2	0,138
22	122	22,1	0,181	3,37	0,0276	1,97	0,0161	2,09	0,0172	4,38	0,0358	8,53	0,0698	15,9	0,13
24	134	22,7	0,169	3,41	0,0254	2,12	0,0158	2,28	0,017	4,63	0,0345	8,81	0,0657	16,2	0,121
26	146	23,5	0,16	3,59	0,0245	2,21	0,0151	2,42	0,0165	4,88	0,0333	9,3	0,0635	16,8	0,115
28	158	24,3	0,153	3,64	0,023	2,31	0,0146	2,58	0,0163	5,05	0,0319	9,32	0,0588	17,2	0,108
30	171	25,1	0,147	3,75	0,022	2,39	0,014	2,66	0,0156	5,19	0,0304	9,83	0,0576	17,4	0,102
32	183	25,9	0,142	3,82	0,0209	2,48	0,0136	2,83	0,0155	5,54	0,0303	10,3	0,0565	17,9	0,0977
34	195	26,7	0,137	3,89	0,02	2,65	0,0136	2,97	0,0153	5,68	0,0292	10,4	0,0534	18,1	0,0931
36	207	27,5	0,133	4,02	0,0194	2,73	0,0132	3,09	0,0149	5,72	0,0276	10,5	0,0506	18,5	0,0896
38	219	28,4	0,13	4,12	0,0188	2,87	0,0131	3,24	0,0148	5,97	0,0273	10,9	0,0497	18,9	0,0864
40	231	29,3	0,127	4,23	0,0183	2,92	0,0127	3,34	0,0145	6,14	0,0266	11,2	0,0485	19,4	0,0839
42	243	30,2	0,124	4,29	0,0177	3	0,0123	3,42	0,0141	6,27	0,0258	11,3	0,0464	19,8	0,0813
44	255	31,1	0,122	4,35	0,017	3,12	0,0122	3,57	0,014	6,39	0,025	11,6	0,0452	19,9	0,0778
46	267	32,1	0,12	4,46	0,0167	3,24	0,0121	3,68	0,0138	6,5	0,0243	11,7	0,0438	20,1	0,0753
48	280	33	0,118	4,52	0,0162	3,31	0,0118	3,83	0,0137	6,63	0,0237	11,9	0,0427	20,7	0,0742
50	292	34,1	0,117	4,66	0,016	3,36	0,0115	3,89	0,0133	6,69	0,023	12,2	0,0417	20,8	0,0715
52	304	35,1	0,115	4,73	0,0156	3,44	0,0113	4,02	0,0132	6,81	0,0224	12,6	0,0415	20,8	0,0685
54	316	36,1	0,114	4,87	0,0154	3,58	0,0113	4,1	0,013	6,95	0,022	12,8	0,0406	21,6	0,0685
56	328	37,1	0,113	4,92	0,015	3,6	0,011	4,28	0,0131	7,08	0,0216	12,9	0,0393	21,5	0,0656
58	340	38,3	0,113	5,05	0,0149	3,77	0,0111	4,35	0,0128	7,19	0,0211	13,1	0,0386	21,6	0,0636
60	352	39,3	0,112	5,18	0,0147	3,91	0,0111	4,52	0,0128	7,22	0,0205	13,1	0,0372	21,8	0,0619
62	364	40,4	0,111	5,25	0,0144	3,91	0,0107	4,7	0,0129	7,35	0,0202	13,4	0,0368	22,4	0,0614
64	376	41,5	0,11	5,42	0,0144	4,08	0,0108	4,81	0,0128	7,47	0,0198	13,4	0,0355	22,6	0,0601
66	389	42,6	0,11	5,56	0,0143	4,17	0,0107	4,93	0,0127	7,62	0,0196	13,6	0,035	23,2	0,0596
68	401	43,8	0,109	5,69	0,0142	4,26	0,0106	5	0,0125	7,68	0,0192	13,9	0,0347	22,9	0,0571
70	413	44,9	0,109	5,7	0,0138	4,35	0,0105	5,22	0,0126	7,94	0,0192	14,1	0,0343	23,3	0,0565
72	425	46,1	0,108	5,8	0,0137	4,49	0,0106	5,24	0,0123	7,94	0,0187	14,1	0,0331	23,7	0,0557
74	437	47,3	0,108	5,92	0,0136	4,52	0,0103	5,35	0,0122	8,02	0,0184	14,5	0,0333	23,7	0,0543
76	449	48,6	0,108	6,1	0,0136	4,7	0,0105	5,37	0,012	8,06	0,018	14,5	0,0322	24,1	0,0536
78	461	50	0,108	6,41	0,0139	4,94	0,0107	5,72	0,0124	8,47	0,0184	14,7	0,0319	23,7	0,0513
80	473	51	0,108	6,26	0,0132	4,88	0,0103	5,64	0,0119	8,32	0,0176	14,6	0,0308	24,1	0,0509
82	485	52,3	0,108	6,45	0,0133	5,01	0,0103	5,64	0,0116	8,3	0,0171	14,9	0,0308	24,5	0,0504
84	498	53,6	0,108	6,53	0,0131	5,02	0,0101	5,77	0,0116	8,41	0,0169	15	0,0302	24,3	0,0489
86	510	54,8	0,108	6,66	0,0131	5,16	0,0101	5,86	0,0115	8,47	0,0166	15	0,0294	24,5	0,0481
88	522	56	0,107	6,66	0,0128	5,35	0,0103	6,1	0,0117	8,7	0,0167	14,8	0,0284	24,9	0,0476
90	534	57,2	0,107	6,81	0,0128	5,4	0,0101	6,15	0,0115	8,79	0,0165	14,7	0,0275	24,7	0,0462
92	546	58,4	0,107	6,87	0,0126	5,47	0,01	6,32	0,0116	8,91	0,0163	14,9	0,0272	24,8	0,0455
94	558	59,7	0,107	7,01	0,0126	5,53	0,00991	6,42	0,0115	8,95	0,016	15,1	0,027	24,9	0,0447

96	570	60,8	0,107	6,99	0,0123	5,63	0,00987	6,64	0,0117	9,15	0,016	15,1	0,0264	25,3	0,0443
98	582	61,9	0,106	7,08	0,0122	5,75	0,00987	6,8	0,0117	9,34	0,016	15,2	0,026	25,4	0,0436
100	594	63,2	0,106	7,25	0,0122	5,73	0,00965	6,81	0,0115	9,33	0,0157	15,1	0,0254	25,3	0,0425
102	607	64,3	0,106	7,34	0,0121	5,96	0,00983	6,91	0,0114	9,52	0,0157	15,2	0,025	24,9	0,0411
104	619	65,4	0,106	7,46	0,0121	6,05	0,00978	7,06	0,0114	9,58	0,0155	15,1	0,0244	25	0,0404
106	631	66,6	0,106	7,59	0,012	6,16	0,00976	7,1	0,0113	9,69	0,0154	15,2	0,0241	25,2	0,0399
108	643	67,4	0,105	7,59	0,0118	6,28	0,00976	7,38	0,0115	9,86	0,0153	15,4	0,024	25,1	0,0391
110	655	68,5	0,105	7,72	0,0118	6,41	0,00979	7,47	0,0114	10	0,0153	15,4	0,0236	25,4	0,0388
112	667	69,4	0,104	7,75	0,0116	6,47	0,00969	7,67	0,0115	10,2	0,0152	15,4	0,0231	25,9	0,0388
114	679	70,3	0,104	8,08	0,0119	6,53	0,00961	7,67	0,0113	10,2	0,015	15,5	0,0229	25,7	0,0378
116	691	71,2	0,103	8,07	0,0117	6,63	0,00959	7,81	0,0113	10,5	0,0151	15,6	0,0225	26,2	0,038
118	703	72,2	0,103	8,17	0,0116	6,92	0,00984	8,03	0,0114	10,5	0,0149	15,5	0,022	25,8	0,0367
120	716	73	0,102	8,25	0,0115	6,91	0,00966	8,16	0,0114	10,8	0,0151	15,5	0,0217	26	0,0363
122	728	73,8	0,101	8,27	0,0114	7,19	0,00988	8,25	0,0113	10,9	0,015	15,4	0,0212	26,3	0,0361
124	740	74,8	0,101	8,35	0,0113	7,43	0,01	8,37	0,0113	11,2	0,0151	15,6	0,021	26,3	0,0355
126	752	75,5	0,1	8,58	0,0114	7,5	0,00997	8,36	0,0111	11,1	0,0148	15,8	0,021	26,7	0,0355
128	764	76	0,0995	8,62	0,0113	7,69	0,0101	8,6	0,0113	11,3	0,0148	15,8	0,0207	26,8	0,0351
130	776	76,9	0,0991	8,78	0,0113	7,86	0,0101	8,6	0,0111	11,5	0,0148	16,2	0,0209	26,6	0,0342
132	788	77,6	0,0985	8,86	0,0112	8,1	0,0103	8,87	0,0113	11,6	0,0147	15,7	0,0199	26,4	0,0334
134	800	78,2	0,0977	8,91	0,0111	8,14	0,0102	8,99	0,0112	11,7	0,0146	16,2	0,0203	26,4	0,033
136	812	78,8	0,097	9,09	0,0112	8,33	0,0103	9,18	0,0113	12	0,0148	16,2	0,0199	26,2	0,0322
138	825	79,5	0,0964	9,56	0,0116	8,49	0,0103	9,21	0,0112	12	0,0146	16,2	0,0197	26,2	0,0318
140	837	80	0,0956	9,52	0,0114	8,81	0,0105	9,34	0,0112	12,3	0,0147	16,2	0,0194	26,2	0,0313
142	849	80,7	0,0951	9,77	0,0115	8,9	0,0105	9,47	0,0112	12,5	0,0147	16,2	0,019	26,3	0,031
144	861	81,5	0,0946	10,1	0,0118	9,08	0,0105	9,55	0,0111	12,4	0,0145	16,3	0,0189	25,9	0,0301
146	873	81,9	0,0938	10,2	0,0117	9,28	0,0106	9,87	0,0113	12,7	0,0146	16,4	0,0188	26	0,0298
148	885	82,3	0,093	10,6	0,012	9,51	0,0107	9,89	0,0112	12,7	0,0143	16,2	0,0183	26,1	0,0295
150	897	82,5	0,092	10,7	0,0119	9,68	0,0108	10,2	0,0114	12,9	0,0144	16,6	0,0185	25,9	0,0288
152	909	83,1	0,0914	10,9	0,012	9,7	0,0107	10,3	0,0113	13,1	0,0144	16,7	0,0183	25,6	0,0281
154	921	83,4	0,0905	11,1	0,0121	10	0,0109	10,5	0,0114	13,1	0,0142	16,6	0,018	25,8	0,028
156	934	83,8	0,0898	11,4	0,0122	9,99	0,0107	10,7	0,0114	13,2	0,0141	16,8	0,018	25,9	0,0277
158	946	84,2	0,0891	11,5	0,0122	10,3	0,0109	10,9	0,0115	13,2	0,014	16,9	0,0178	26,1	0,0276
160	958	84,9	0,0886	11,9	0,0124	10,3	0,0107	10,9	0,0114	13,1	0,0137	17,2	0,018	25,5	0,0266
162	970	85,3	0,088	12	0,0123	10,5	0,0108	11,1	0,0114	13,3	0,0137	17,4	0,018	25,2	0,026
164	982	85,6	0,0872	12	0,0123	10,8	0,011	11,4	0,0116	13,5	0,0137	17,4	0,0177	25,2	0,0256
166	994	85,9	0,0865	12,3	0,0124	10,8	0,0109	11,5	0,0116	13,5	0,0136	17,6	0,0177	25,2	0,0254
168	1 010	86,3	0,0857	12,4	0,0124	11	0,0109	11,7	0,0116	13,8	0,0137	18,1	0,018	25,7	0,0255
170	1 020	86,6	0,085	12,6	0,0124	11,2	0,011	11,9	0,0117	14	0,0138	17,8	0,0175	25,8	0,0254
172	1 030	86,7	0,0842	12,9	0,0125	11,4	0,0111	11,9	0,0116	14	0,0136	17,8	0,0173	26	0,0252
174	1 040	86,4	0,0829	13,1	0,0126	11,6	0,0111	12,2	0,0117	14,1	0,0135	18,2	0,0175	25,5	0,0245
176	1 050	86,8	0,0823	13,3	0,0126	12	0,0113	12,4	0,0118	14,2	0,0135	18,1	0,0172	25,7	0,0244
178	1 070	86,9	0,0815	13,3	0,0125	11,9	0,0112	12,7	0,0119	14,7	0,0137	18,5	0,0173	25,6	0,024
180	1 080	87,4	0,081	13,7	0,0127	12,1	0,0112	12,8	0,0119	14,6	0,0135	18,8	0,0174	26	0,0241
182	1 090	87,8	0,0805	13,9	0,0128	12,4	0,0114	13	0,0119	14,7	0,0135	18,7	0,0171	26,4	0,0242

184	1 100	88	0,0798	14,2	0,0128	12,5	0,0114	13,3	0,0121	15	0,0136	18,6	0,0169	26,2	0,0237
186	1 120	88,5	0,0794	14,5	0,013	13	0,0116	13,3	0,012	15,2	0,0137	19,1	0,0172	26,6	0,0238
188	1 130	88,8	0,0788	14,6	0,0129	13	0,0115	13,4	0,0119	15,7	0,0139	18,8	0,0167	26,4	0,0234
190	1 140	88,9	0,078	14,8	0,013	13,1	0,0115	13,9	0,0122	16,1	0,0141	19,2	0,0169	26,6	0,0233
192	1 150	89,3	0,0776	15,1	0,0131	13,4	0,0116	13,9	0,012	16,2	0,0141	19,2	0,0167	26,5	0,023
194	1 160	89,6	0,077	15,3	0,0131	13,6	0,0116	14,2	0,0122	16,4	0,0141	19,4	0,0167	27,1	0,0233
196	1 180	89,6	0,0762	15,9	0,0135	13,8	0,0117	14,3	0,0122	16,6	0,0141	19,7	0,0167	26,7	0,0227
198	1 190	89,5	0,0753	15,9	0,0134	14	0,0118	14,6	0,0123	17,2	0,0145	19,6	0,0165	27	0,0227
200	1 200	89,8	0,0748	16,1	0,0134	14,1	0,0117	15	0,0125	17,3	0,0144	19,9	0,0166	27,2	0,0227

Time	Shear Rate	Shear Stress	Viscosity	Shear Stress	Viscosity	Shear Stress	Viscosity	Shear Stress	Viscosity	Shear Stress	Viscosity	Shear Stress	Viscosity	Shear Stress	Viscosity
[s]	[1/s]	[Pa]	[Pa·s]	[Pa]	[Pa·s]	[Pa]	[Pa·s]	[Pa]	[Pa·s]	[Pa]	[Pa·s]	[Pa]	[Pa·s]	[Pa]	[Pa·s]
Number of Intervals:		*CNC-SEP-WDFs (6 wt %) 0.0 % 50°C*	*CNC-SEP-WDFs (6 wt %) 0.0 % 50°C*	*CNC-SEP-WDFs (6 wt %) 0,4 % 50°C*	*CNC-SEP-WDFs (6 wt %) 0.4 % 50°C*	*CNC-SEP-WDFs (6 wt %) 0.8 % 50°C*	*CNC-SEP-WDFs (6 wt %) 0.8 % 50°C*	*CNC-SEP-WDFs (6 wt %) 1,2 % 50°C*	*CNC-SEP-WDFs (6 wt %) 1,2 % 50°C*	*CNC-SEP-WDFs (6 wt %) 1,6 % 50°C*	*CNC-SEP-WDFs (6 wt %) 1,6 % 50°C*	*CNC-SEP-WDFs (6 wt %) 2.0 % 50°C*	*CNC-SEP-WDFs (6 wt %) 2.0 % 50°C*	*CNC-SEP-WDFs (6 wt %) 2,4 % 50°C*	*CNC-SEP-WDFs (6 wt %) 2,4 % 50°C*
2	0,999	17,9	17,8	4,08	4,08	0,0947	0,0946	-0,561	-0,56	1,91E-4	1,91E-4	1,11	1,11	3,84	3,85
4	13,1	25,4	1,94	4,51	0,344	1,09	0,0833	0,242	0,0185	1,73	0,132	5,13	0,391	6,82	0,52
6	25,2	26,3	1,04	4,36	0,173	1,6	0,0636	0,66	0,0262	2,55	0,101	6,47	0,257	8,36	0,331
8	37,3	27,4	0,735	4,45	0,119	2,16	0,0579	0,958	0,0257	2,85	0,0763	7,03	0,188	9,29	0,249
10	49,4	28,7	0,581	4,34	0,0879	2,25	0,0455	1,05	0,0213	2,93	0,0593	7,23	0,146	10,1	0,205
12	61,6	29,9	0,486	4,34	0,0706	1,85	0,03	1,13	0,0184	3,05	0,0495	7,34	0,119	10,8	0,176
14	73,7	31	0,42	4,37	0,0593	2,2	0,0298	1,28	0,0174	3,24	0,044	7,33	0,0995	11,5	0,156
16	85,8	32,1	0,374	4,39	0,0512	2,2	0,0257	1,52	0,0177	3,43	0,04	7,79	0,0908	11,9	0,139
18	97,9	33,2	0,339	4,42	0,0452	2,1	0,0215	1,66	0,017	3,67	0,0375	7,9	0,0807	12,4	0,127
20	110	34,2	0,311	4,45	0,0405	2,42	0,022	1,76	0,016	3,86	0,0351	8,21	0,0746	12,9	0,117
22	122	35,2	0,288	4,52	0,0371	2,57	0,0211	1,84	0,0151	4,08	0,0334	8,47	0,0694	13,3	0,109
24	134	36,2	0,269	4,66	0,0347	2,46	0,0183	2	0,0149	4,33	0,0323	8,54	0,0636	13,8	0,102
26	146	37,1	0,253	4,72	0,0322	2,6	0,0178	2,26	0,0155	4,54	0,031	8,85	0,0605	14,3	0,0979
28	158	38	0,24	4,83	0,0305	2,88	0,0182	2,38	0,015	4,71	0,0297	9,19	0,058	14,8	0,0931
30	171	39	0,229	4,87	0,0286	3,22	0,0189	2,44	0,0143	4,87	0,0285	9,69	0,0568	15,4	0,0903
32	183	40	0,219	5	0,0274	3,39	0,0185	2,53	0,0139	5,01	0,0274	9,88	0,0541	16	0,0875
34	195	41	0,21	5,11	0,0263	3,45	0,0177	2,73	0,014	5,2	0,0267	10,1	0,0517	16,7	0,0857
36	207	42	0,203	5,16	0,025	3,36	0,0162	2,86	0,0138	5,36	0,0259	10,3	0,05	16,7	0,0806
38	219	42,9	0,196	5,25	0,024	3,57	0,0163	2,98	0,0136	5,56	0,0254	10,6	0,0483	17,3	0,079
40	231	43,9	0,19	5,35	0,0231	3,62	0,0156	3,14	0,0136	5,72	0,0247	10,8	0,0469	17,6	0,0763
42	243	44,8	0,184	5,38	0,0221	3,74	0,0154	3,26	0,0134	5,83	0,024	11	0,0454	18	0,0742
44	255	45,8	0,179	5,51	0,0216	3,95	0,0155	3,35	0,0131	5,99	0,0235	11,2	0,0437	18,5	0,0724
46	267	46,8	0,175	5,61	0,021	3,92	0,0146	3,49	0,0131	6,08	0,0227	11,2	0,042	18,9	0,0707
48	280	47,8	0,171	5,7	0,0204	4,01	0,0143	3,57	0,0128	6,27	0,0224	11,4	0,0407	18,7	0,0669
50	292	48,9	0,168	5,71	0,0196	4,05	0,0139	3,7	0,0127	6,29	0,0216	11,7	0,04	19,2	0,0659
52	304	49,9	0,164	5,86	0,0193	4,07	0,0134	3,8	0,0125	6,49	0,0214	11,9	0,0393	19,7	0,0649
54	316	50,9	0,161	5,98	0,0189	4,2	0,0133	3,92	0,0124	6,49	0,0205	11,9	0,0378	19,9	0,063
56	328	52	0,159	6,11	0,0186	4,32	0,0132	4	0,0122	6,68	0,0204	12	0,0366	20,1	0,0613
58	340	53	0,156	6,24	0,0183	4,55	0,0134	4,15	0,0122	6,79	0,02	12,3	0,0363	20,5	0,0604
60	352	54	0,153	6,35	0,018	4,65	0,0132	4,27	0,0121	6,9	0,0196	12,6	0,0359	20,5	0,0582
62	364	55,2	0,151	6,41	0,0176	4,67	0,0128	4,36	0,012	7,03	0,0193	12,7	0,035	20,9	0,0574
64	376	56,2	0,149	6,54	0,0174	4,87	0,0129	4,54	0,0121	7,1	0,0189	12,8	0,034	21,1	0,056
66	389	57,2	0,147	6,62	0,017	4,95	0,0127	4,69	0,0121	7,2	0,0185	12,9	0,0332	21,2	0,0545
68	401	58,2	0,145	6,74	0,0168	5,07	0,0126	4,82	0,012	7,26	0,0181	13,1	0,0328	21,3	0,0533
70	413	59,1	0,143	6,92	0,0168	5,16	0,0125	4,89	0,0118	7,44	0,018	13	0,0315	21,4	0,0519
72	425	60	0,141	7,02	0,0165	5,31	0,0125	5,01	0,0118	7,59	0,0179	13	0,0306	21,8	0,0512
74	437	61,1	0,14	7,06	0,0162	5,34	0,0122	5,16	0,0118	7,64	0,0175	13,2	0,0302	21,9	0,0501
76	449	61,9	0,138	7,14	0,0159	5,57	0,0124	5,37	0,012	7,69	0,0171	13,3	0,0295	22,1	0,0491
78	461	63,2	0,137	7,62	0,0165	5,37	0,0116	5,71	0,0124	7,78	0,0169	13,4	0,029	21,9	0,0476
80	473	63,7	0,135	7,39	0,0156	5,68	0,012	5,55	0,0117	7,93	0,0168	13,4	0,0284	22,7	0,0479
82	485	64,5	0,133	7,45	0,0154	5,86	0,0121	5,76	0,0119	7,98	0,0164	13,4	0,0277	22,7	0,0468
84	498	65,5	0,132	7,52	0,0151	5,86	0,0118	5,85	0,0117	8,07	0,0162	13,5	0,0271	22,8	0,0459
86	510	66,3	0,13	7,62	0,015	6	0,0118	5,97	0,0117	8,15	0,016	13,8	0,0272	23,1	0,0453
88	522	67,1	0,129	7,92	0,0152	6,17	0,0118	6,06	0,0116	8,41	0,0161	13,8	0,0264	23,1	0,0442
90	534	68	0,127	7,9	0,0148	6,23	0,0117	6,24	0,0117	8,37	0,0157	13,8	0,0258	23,1	0,0433
92	546	68,9	0,126	8,02	0,0147	6,32	0,0116	6,3	0,0115	8,58	0,0157	13,8	0,0252	23,2	0,0425
94	558	69,7	0,125	8,03	0,0144	6,38	0,0114	6,49	0,0116	8,61	0,0154	13,7	0,0246	23,4	0,0419
96	570	70,5	0,124	8,2	0,0144	6,48	0,0114	6,5	0,0114	8,87	0,0156	13,9	0,0243	23,9	0,0419
98	582	71,3	0,122	8,32	0,0143	6,58	0,0113	6,63	0,0114	9,05	0,0155	13,7	0,0236	24	0,0412
100	594	72,2	0,121	8,28	0,0139	6,6	0,0111	6,85	0,0115	9	0,0151	14	0,0236	24	0,0403

102	607	72,8	0,12	8,49	0,014	6,8	0,0112	7,02	0,0116	9,18	0,0151	13,8	0,0228	24,1	0,0397
104	619	73,6	0,119	8,52	0,0138	6,89	0,0111	7,22	0,0117	9,33	0,0151	14	0,0227	24,4	0,0394
106	631	74,4	0,118	8,57	0,0136	7,01	0,0111	7,38	0,0117	9,35	0,0148	14	0,0223	24,1	0,0382
108	643	75	0,117	8,8	0,0137	7,24	0,0113	7,43	0,0116	9,59	0,0149	14	0,0218	24,3	0,0378
110	655	75,7	0,116	8,91	0,0136	7,51	0,0115	7,63	0,0117	9,8	0,015	14,1	0,0216	23,9	0,0364
112	667	76,4	0,115	8,99	0,0135	7,58	0,0114	7,66	0,0115	9,89	0,0148	14,1	0,0211	24	0,036
114	679	77,1	0,114	8,91	0,0131	7,62	0,0112	7,97	0,0117	9,92	0,0146	14,4	0,0213	24	0,0353
116	691	77,7	0,112	9,06	0,0131	7,79	0,0113	7,99	0,0116	10	0,0145	14,2	0,0206	24	0,0347
118	703	78,2	0,111	9,19	0,0131	8	0,0114	8,11	0,0115	10,3	0,0147	14,6	0,0207	24	0,0342
120	716	78,9	0,11	9,26	0,0129	8,08	0,0113	8,2	0,0115	10,4	0,0146	14,5	0,0203	24,2	0,0338
122	728	79,4	0,109	9,49	0,013	8,31	0,0114	8,26	0,0114	10,7	0,0147	14,8	0,0203	24,3	0,0333
124	740	79,9	0,108	9,59	0,013	8,54	0,0115	8,3	0,0112	10,8	0,0146	14,8	0,02	24,3	0,0328
126	752	80,5	0,107	9,51	0,0126	8,58	0,0114	8,58	0,0114	10,8	0,0143	14,9	0,0198	24,4	0,0325
128	764	81	0,106	9,7	0,0127	8,83	0,0116	8,61	0,0113	10,9	0,0143	14,8	0,0194	24,2	0,0316
130	776	81,5	0,105	9,74	0,0126	9,01	0,0116	8,82	0,0114	11	0,0141	14,8	0,019	24,3	0,0313
132	788	81,9	0,104	9,85	0,0125	9,31	0,0118	8,99	0,0114	11,2	0,0142	14,9	0,0189	24,3	0,0308
134	800	82,5	0,103	9,86	0,0123	9,42	0,0118	9,1	0,0114	11,2	0,014	15,3	0,0191	24,2	0,0302
136	812	82,9	0,102	10	0,0124	9,58	0,0118	9,09	0,0112	11,4	0,014	15,4	0,0189	24,5	0,0301
138	825	83,2	0,101	10,2	0,0124	9,98	0,0121	9,53	0,0116	11,5	0,0139	15,6	0,019	24	0,0291
140	837	83,7	0,1	10,4	0,0124	10	0,012	9,55	0,0114	11,9	0,0142	15,3	0,0183	24,3	0,029
142	849	84,1	0,099	10,6	0,0125	10,2	0,012	9,7	0,0114	12	0,0141	15,5	0,0182	24,2	0,0285
144	861	84,4	0,098	10,7	0,0124	10,5	0,0121	9,92	0,0115	12	0,0139	15,8	0,0184	23,8	0,0276
146	873	84,7	0,097	11,2	0,0128	10,6	0,0122	10	0,0115	12,2	0,014	15,7	0,018	24,2	0,0277
148	885	84,9	0,096	11,3	0,0128	11	0,0124	10,2	0,0116	12,3	0,0139	15,7	0,0178	23,7	0,0268
150	897	85,3	0,0951	11,6	0,013	11,1	0,0124	10,4	0,0116	12,5	0,0139	16,1	0,018	23,9	0,0266
152	909	85,8	0,0944	11,7	0,0128	11,2	0,0123	10,6	0,0117	12,3	0,0136	16,2	0,0178	24,3	0,0268
154	921	86,1	0,0934	12	0,013	11,4	0,0124	10,8	0,0118	12,7	0,0138	16,2	0,0176	24,2	0,0262
156	934	86,4	0,0926	12,1	0,013	11,7	0,0125	11	0,0118	12,8	0,0137	16,5	0,0177	24	0,0257
158	946	86,7	0,0917	12,4	0,0132	11,9	0,0125	11,1	0,0118	13,1	0,0138	16,3	0,0173	23,6	0,025
160	958	87	0,0909	12,6	0,0131	12,1	0,0126	11,4	0,0119	12,9	0,0135	16,8	0,0175	23,6	0,0247
162	970	87,3	0,09	12,8	0,0132	12,3	0,0126	11,7	0,012	13	0,0134	16,7	0,0172	23,2	0,0239
164	982	87,5	0,0891	13,1	0,0134	12,3	0,0126	11,7	0,0119	13,3	0,0136	16,7	0,017	23,7	0,0242
166	994	88	0,0885	13,3	0,0133	12,4	0,0125	11,8	0,0118	13,3	0,0134	17	0,0171	23,7	0,0238
168	1 010	88,2	0,0877	13,4	0,0133	12,8	0,0127	12	0,0119	13,5	0,0134	17,2	0,0171	23,4	0,0232
170	1 020	88,5	0,0869	13,7	0,0134	12,7	0,0125	12,1	0,0119	13,7	0,0134	17	0,0167	23,6	0,0232
172	1 030	88,7	0,0861	13,7	0,0133	13,1	0,0127	12,4	0,0121	13,4	0,013	17,4	0,0169	23,9	0,0232
174	1 040	89,1	0,0855	13,8	0,0132	13,1	0,0125	12,7	0,0122	13,5	0,013	17,6	0,0169	23,7	0,0227
176	1 050	89,2	0,0846	14,4	0,0136	12,9	0,0122	13	0,0123	13,8	0,0131	17,8	0,0169	23,8	0,0226
178	1 070	89,5	0,0839	14,5	0,0135	12,9	0,0121	12,9	0,0121	14,2	0,0133	17,6	0,0165	24,1	0,0226
180	1 080	89,7	0,0832	14,7	0,0136	13	0,0121	13,2	0,0123	14,6	0,0135	17,7	0,0164	24,5	0,0227
182	1 090	90	0,0825	14,9	0,0136	13,2	0,0121	13,4	0,0123	14,9	0,0137	18,1	0,0166	24,3	0,0223
184	1 100	90,2	0,0818	15	0,0136	13,3	0,0121	13,6	0,0123	15,3	0,0139	18,2	0,0165	24,4	0,0221
186	1 120	90,4	0,0811	15,2	0,0136	13,7	0,0123	14,1	0,0126	15,4	0,0138	18,4	0,0165	24,5	0,0219
188	1 130	90,6	0,0804	15,6	0,0139	13,9	0,0123	14,1	0,0125	15,6	0,0139	18,5	0,0164	24,6	0,0218
190	1 140	90,9	0,0798	15,7	0,0138	13,9	0,0122	14,2	0,0125	16	0,014	18,6	0,0163	24,9	0,0219
192	1 150	91,1	0,0791	15,8	0,0138	14,3	0,0124	14,4	0,0125	16	0,0139	18,7	0,0162	24,6	0,0213
194	1 160	91,3	0,0784	16,5	0,0142	14,3	0,0123	14,7	0,0126	16,4	0,0141	18,9	0,0163	25,2	0,0216
196	1 180	91,5	0,0778	16,6	0,0141	14,5	0,0123	14,9	0,0126	16,6	0,0141	18,8	0,0159	25,2	0,0214
198	1 190	91,7	0,0772	16,7	0,0141	14,6	0,0123	14,9	0,0125	16,8	0,0141	19	0,016	25,3	0,0213
200	1 200	91,9	0,0766	17,3	0,0144	14,6	0,0122	15,2	0,0127	17,1	0,0143	19,3	0,0161	25,7	0,0214

Time	Shear Rate	Shear Stress	Viscosity	Shear Stress	Viscosity	Shear Stress	Viscosity	Shear Stress	Viscosity	Shear Stress	Viscosity	Shear Stress	Viscosity	Shear Stress	Viscosity
[s]	[1/s]	[Pa]	[Pa·s]	[Pa]	[Pa·s]	[Pa]	[Pa·s]	[Pa]	[Pa·s]	[Pa]	[Pa·s]	[Pa]	[Pa·s]	[Pa]	[Pa·s]
Number of Intervals:		*CNC-SEP-WDFs (6 wt %) 0.0 % 60°C*	*CNC-SEP-WDFs (6 wt %) 0.0 % 60°C*	*CNC-SEP-WDFs (6 wt %) 0,4 % 60°C*	*CNC-SEP-WDFs (6 wt %) 0.4 % 60°C*	*CNC-SEP-WDFs (6 wt %) 0.8 % 60°C*	*CNC-SEP-WDFs (6 wt %) 0.8 % 60°C*	*CNC-SEP-WDFs (6 wt %) 1,2 % 60°C*	*CNC-SEP-WDFs (6 wt %) 1,2 % 60°C*	*CNC-SEP-WDFs (6 wt %) 1,6 % 60°C*	*CNC-SEP-WDFs (6 wt %) 1,6 % 60°C*	*CNC-SEP-WDFs (6 wt %) 2.0 % 60°C*	*CNC-SEP-WDFs (6 wt %) 2.0 % 60°C*	*CNC-SEP-WDFs (6 wt %) 2,4 % 60°C*	*CNC-SEP-WDFs (6 wt %) 2,4 % 60°C*
2	0,999	20,2	20,1	4,94	4,94	-0,413	-0,413	-0,564	-0,564	-0,0568	-0,0567	0,927	0,927	0,947	0,948
4	13,1	31,9	2,43	5,38	0,411	0,572	0,0436	0,401	0,0306	1,11	0,085	5	0,381	3,67	0,28
6	25,2	34,5	1,37	5,3	0,21	0,774	0,0307	0,724	0,0287	1,55	0,0616	6,48	0,257	5,05	0,2
8	37,3	36,1	0,966	5,12	0,137	0,906	0,0243	0,85	0,0228	1,85	0,0496	6,7	0,18	5,97	0,16
10	49,4	37,7	0,762	5,11	0,103	1,16	0,0235	1,11	0,0225	2,03	0,0411	6,92	0,14	6,82	0,138
12	61,6	39,2	0,637	5,1	0,0828	1,28	0,0208	1,35	0,0219	2,24	0,0364	6,81	0,111	7,52	0,122
14	73,7	40,6	0,551	5,09	0,0691	1,4	0,019	1,42	0,0193	2,51	0,0341	7,07	0,096	8,17	0,111
16	85,8	41,9	0,489	5,16	0,0601	1,54	0,018	1,56	0,0181	2,79	0,0326	7,3	0,0851	8,82	0,103
18	97,9	43	0,44	5,08	0,0519	1,56	0,0159	1,72	0,0176	3	0,0306	7,45	0,0762	9,4	0,096
20	110	44,2	0,402	5,16	0,0469	1,8	0,0163	1,85	0,0168	3,16	0,0287	7,65	0,0695	9,95	0,0905
22	122	45,4	0,371	5,19	0,0425	1,89	0,0154	2,06	0,0169	3,34	0,0273	7,88	0,0645	10,4	0,0849
24	134	46,5	0,346	5,23	0,039	1,94	0,0145	2,16	0,0161	3,53	0,0263	8,05	0,06	10,6	0,0791
26	146	47,5	0,325	5,29	0,0362	2,07	0,0142	2,33	0,0159	3,7	0,0253	8,24	0,0563	11	0,075
28	158	48,5	0,306	5,31	0,0335	2,26	0,0142	2,49	0,0157	3,92	0,0248	8,6	0,0543	11,8	0,0743
30	171	49,5	0,29	5,37	0,0315	2,35	0,0138	2,62	0,0154	4,07	0,0239	8,86	0,052	11,9	0,0699
32	183	50,5	0,277	5,39	0,0295	2,45	0,0134	2,81	0,0154	4,27	0,0234	9,02	0,0494	12,6	0,0692
34	195	51,5	0,264	5,41	0,0278	2,51	0,0129	2,91	0,0149	4,48	0,023	9,27	0,0476	12,9	0,0661
36	207	52,4	0,253	5,47	0,0264	2,65	0,0128	2,99	0,0145	4,6	0,0223	9,36	0,0452	13,3	0,0641
38	219	53,3	0,243	5,52	0,0252	2,69	0,0123	3,11	0,0142	4,79	0,0219	9,66	0,0441	13,5	0,0615
40	231	54,2	0,235	5,56	0,0241	2,83	0,0122	3,2	0,0139	4,98	0,0216	10	0,0433	13,9	0,0603
42	243	55,1	0,227	5,61	0,0231	2,95	0,0121	3,28	0,0135	5,03	0,0207	10	0,0412	14,6	0,0599
44	255	56	0,219	5,6	0,0219	2,94	0,0115	3,43	0,0134	5,18	0,0203	10,2	0,0399	14,9	0,0582
46	267	56,9	0,213	5,67	0,0212	3,06	0,0114	3,53	0,0132	5,26	0,0197	10,4	0,039	15,1	0,0566
48	280	57,8	0,207	5,69	0,0204	3,08	0,011	3,62	0,013	5,4	0,0193	10,7	0,0383	15,1	0,0542
50	292	58,7	0,201	5,8	0,0199	3,3	0,0113	3,65	0,0125	5,44	0,0187	10,7	0,0367	15,8	0,054
52	304	59,5	0,196	5,83	0,0192	3,32	0,0109	3,77	0,0124	5,59	0,0184	10,9	0,0359	16	0,0527
54	316	60,4	0,191	5,9	0,0187	3,41	0,0108	3,87	0,0123	5,68	0,018	11	0,0349	16,3	0,0516
56	328	61,3	0,187	5,92	0,0181	3,51	0,0107	3,96	0,0121	5,75	0,0175	11,2	0,034	16,9	0,0515
58	340	62	0,182	6,04	0,0177	3,54	0,0104	4,1	0,0121	5,84	0,0172	11,4	0,0335	17,1	0,0502
60	352	62,9	0,179	6,1	0,0173	3,62	0,0103	4,2	0,0119	5,95	0,0169	11,5	0,0327	17,1	0,0486
62	364	63,8	0,175	6,15	0,0169	3,81	0,0104	4,25	0,0117	6,09	0,0167	11,6	0,032	17,5	0,048
64	376	64,6	0,172	6,28	0,0167	3,9	0,0103	4,41	0,0117	6,17	0,0164	11,9	0,0315	17,7	0,0471
66	389	65,4	0,168	6,37	0,0164	4,03	0,0104	4,45	0,0114	6,3	0,0162	11,9	0,0305	18,2	0,0469
68	401	66,2	0,165	6,47	0,0161	4,12	0,0103	4,58	0,0114	6,34	0,0158	11,9	0,0298	18,6	0,0463
70	413	66,9	0,162	6,43	0,0156	4,15	0,0101	4,74	0,0115	6,54	0,0159	12,2	0,0296	18,5	0,0447
72	425	67,6	0,159	6,48	0,0153	4,2	0,00988	4,87	0,0115	6,61	0,0156	12,4	0,0291	18,8	0,0443
74	437	68,4	0,157	6,58	0,0151	4,41	0,0101	4,82	0,011	6,69	0,0153	12,4	0,0284	18,8	0,043
76	449	68,9	0,153	6,75	0,015	4,48	0,00997	5	0,0111	6,72	0,015	12,4	0,0277	19,2	0,0429
78	461	69,4	0,15	6,97	0,0151	4,67	0,0101	5,21	0,0113	6,84	0,0148	12,4	0,0268	19,6	0,0425
80	473	70,3	0,148	6,83	0,0144	4,69	0,00991	5,15	0,0109	6,93	0,0146	12,6	0,0265	19,5	0,0412
82	485	70,8	0,146	6,99	0,0144	4,81	0,0099	5,28	0,0109	6,91	0,0142	12,4	0,0255	19,8	0,0407
84	498	71,5	0,144	7,05	0,0142	5,01	0,0101	5,27	0,0106	7,05	0,0142	12,5	0,0251	19,9	0,04
86	510	72,1	0,141	7,15	0,014	5,07	0,00995	5,4	0,0106	7,1	0,0139	12,4	0,0243	20,1	0,0395

88	522	72,6	0,139	7,1	0,0136	4,92	0,00943	5,62	0,0108	7,26	0,0139	12,7	0,0244	20	0,0384
90	534	73,2	0,137	7,24	0,0136	4,95	0,00927	5,66	0,0106	7,32	0,0137	12,6	0,0237	20,6	0,0385
92	546	73,7	0,135	7,27	0,0133	5,03	0,00922	5,81	0,0106	7,42	0,0136	12,7	0,0232	20,5	0,0376
94	558	74,3	0,133	7,39	0,0132	5,18	0,00927	5,82	0,0104	7,49	0,0134	12,5	0,0224	20,6	0,0369
96	570	74,8	0,131	7,32	0,0128	5,13	0,009	6	0,0105	7,74	0,0136	12,9	0,0227	20,6	0,0361
98	582	75,4	0,129	7,39	0,0127	5,2	0,00892	6,13	0,0105	7,83	0,0135	13,1	0,0225	21,1	0,0363
100	594	76	0,128	7,58	0,0128	5,4	0,00908	6,14	0,0103	7,91	0,0133	13	0,0219	21	0,0353
102	607	76,4	0,126	7,62	0,0126	5,4	0,0089	6,38	0,0105	8,01	0,0132	12,9	0,0213	21,4	0,0353
104	619	77	0,124	7,73	0,0125	5,54	0,00895	6,49	0,0105	8,12	0,0131	12,8	0,0207	21,3	0,0344
106	631	77,4	0,123	7,85	0,0124	5,68	0,00901	6,54	0,0104	8,19	0,013	12,7	0,0202	21,5	0,034
108	643	78	0,121	7,76	0,0121	5,63	0,00876	6,75	0,0105	8,5	0,0132	12,9	0,0201	21,5	0,0335
110	655	78,3	0,12	7,87	0,012	5,74	0,00876	6,9	0,0105	8,5	0,013	12,8	0,0195	21,6	0,033
112	667	78,9	0,118	7,88	0,0118	5,92	0,00888	6,96	0,0104	8,7	0,013	12,7	0,019	21,9	0,0328
114	679	79,3	0,117	8,14	0,012	6,16	0,00907	6,9	0,0102	8,78	0,0129	12,8	0,0188	22	0,0325
116	691	79,8	0,115	8,12	0,0118	6,27	0,00906	7,03	0,0102	8,96	0,013	12,8	0,0185	21,7	0,0314
118	703	80,2	0,114	8,2	0,0117	6,4	0,00909	7,28	0,0104	9,07	0,0129	13	0,0185	21,7	0,0308
120	716	80,7	0,113	8,29	0,0116	6,6	0,00923	7,26	0,0101	9,25	0,0129	13,1	0,0183	21,8	0,0305
122	728	81	0,111	8,26	0,0113	6,63	0,00912	7,44	0,0102	9,35	0,0129	13,2	0,0182	21,7	0,0298
124	740	81,4	0,11	8,36	0,0113	6,85	0,00926	7,64	0,0103	9,51	0,0129	13,3	0,018	21,7	0,0294
126	752	81,9	0,109	8,62	0,0115	7,15	0,00951	7,5	0,00998	9,53	0,0127	13,2	0,0175	21,8	0,029
128	764	82,2	0,108	8,67	0,0114	7,24	0,00947	7,76	0,0102	9,62	0,0126	13,2	0,0172	21,5	0,0282
130	776	82,6	0,106	8,75	0,0113	7,46	0,00962	7,84	0,0101	9,75	0,0126	13,2	0,017	21,8	0,0281
132	788	82,8	0,105	8,86	0,0112	7,57	0,00961	8,19	0,0104	9,81	0,0124	13,4	0,017	21,9	0,0277
134	800	83,3	0,104	8,9	0,0111	7,85	0,00981	8,23	0,0103	9,92	0,0124	13,5	0,0168	22,1	0,0276
136	812	83,8	0,103	8,89	0,0109	7,95	0,00979	8,33	0,0102	10	0,0123	13,8	0,017	21,9	0,0269
138	825	84,1	0,102	9,14	0,0111	8,2	0,00995	8,41	0,0102	9,99	0,0121	13,6	0,0166	22	0,0267
140	837	84,2	0,101	9,26	0,0111	8,19	0,00979	8,57	0,0102	10,3	0,0123	14	0,0168	21,9	0,0262
142	849	84,5	0,0996	9,46	0,0111	8,35	0,00984	8,67	0,0102	10,3	0,0121	14,1	0,0166	21,8	0,0257
144	861	84,8	0,0986	9,82	0,0114	8,48	0,00985	8,87	0,0103	10,3	0,012	14,3	0,0166	21,8	0,0254
146	873	85,1	0,0975	9,96	0,0114	8,54	0,00978	9,12	0,0104	10,6	0,0122	14,4	0,0165	21,7	0,0249
148	885	85,3	0,0963	10,3	0,0116	8,59	0,0097	9,33	0,0105	10,6	0,012	14,3	0,0162	21,3	0,0241
150	897	85,6	0,0954	10,3	0,0115	8,69	0,00969	9,54	0,0106	10,9	0,0122	14,3	0,016	21,2	0,0236
152	909	86	0,0945	10,7	0,0117	9,12	0,01	9,52	0,0105	11	0,0121	14,5	0,016	21,2	0,0233
154	921	86,1	0,0935	10,8	0,0117	9,12	0,00989	9,73	0,0106	11,1	0,012	14,7	0,016	21,4	0,0232
156	934	86,4	0,0925	10,9	0,0117	9,38	0,01	9,83	0,0105	11,1	0,0119	15	0,016	21,3	0,0228
158	946	86,6	0,0916	11,1	0,0117	9,32	0,00985	10	0,0106	11,3	0,0119	15	0,0159	21,5	0,0227
160	958	86,8	0,0906	11,5	0,012	9,69	0,0101	10,1	0,0105	11,3	0,0118	15,1	0,0157	21,7	0,0226

162	970	87	0,0897	11,7	0,012	9,77	0,0101	10,2	0,0105	11,4	0,0117	15	0,0155	21,7	0,0224
164	982	87,2	0,0888	11,6	0,0118	9,75	0,00993	10,5	0,0107	11,4	0,0116	15,5	0,0158	21,6	0,022
166	994	87,5	0,088	12	0,012	10,2	0,0103	10,6	0,0106	11,5	0,0116	15,4	0,0154	21,7	0,0218
168	1 010	87,6	0,0871	12,2	0,0122	10,3	0,0102	10,8	0,0107	12	0,0119	15,6	0,0155	21,9	0,0217
170	1 020	87,8	0,0862	12,4	0,0121	10,4	0,0102	11	0,0108	12,3	0,0121	15,8	0,0155	22,1	0,0217
172	1 030	87,9	0,0853	12,6	0,0122	10,6	0,0103	11	0,0107	12,3	0,012	15,6	0,0152	22,1	0,0215
174	1 040	88,1	0,0845	12,8	0,0122	10,8	0,0104	11,2	0,0107	12,6	0,0121	15,6	0,0149	22,4	0,0215
176	1 050	88,2	0,0836	13	0,0123	11	0,0104	11,6	0,011	12,8	0,0121	16,1	0,0153	22,5	0,0214
178	1 070	88,5	0,0829	12,9	0,0121	11,1	0,0104	11,5	0,0108	13,2	0,0124	16,2	0,0152	22,2	0,0208
180	1 080	88,6	0,0821	13,3	0,0123	11,3	0,0105	11,9	0,011	13,4	0,0124	16,4	0,0152	22,5	0,0209
182	1 090	88,8	0,0814	13,5	0,0124	11,6	0,0106	11,9	0,0109	13,5	0,0123	16,4	0,015	23	0,0211
184	1 100	88,9	0,0806	13,7	0,0124	11,5	0,0104	12,3	0,0112	13,7	0,0125	16,6	0,0151	22,7	0,0206
186	1 120	89	0,0798	14	0,0126	11,8	0,0106	12,4	0,0111	13,8	0,0124	16,5	0,0148	22,9	0,0205
188	1 130	89,2	0,0791	14,1	0,0125	11,9	0,0105	12,5	0,0111	14,1	0,0125	16,8	0,0149	22,8	0,0202
190	1 140	89,5	0,0786	14,2	0,0125	12,1	0,0106	12,7	0,0111	14,5	0,0127	17	0,0149	22,8	0,02
192	1 150	89,6	0,0778	14,3	0,0124	12,3	0,0107	12,8	0,0112	14,6	0,0127	17	0,0148	23,2	0,0201
194	1 160	89,9	0,0772	14,7	0,0126	12,6	0,0108	13,1	0,0113	14,8	0,0127	17	0,0146	22,9	0,0197
196	1 180	90	0,0765	15,1	0,0128	12,8	0,0109	13,1	0,0111	15	0,0128	17,3	0,0147	23,3	0,0198
198	1 190	90,3	0,076	15,3	0,0129	13,1	0,0111	13,5	0,0114	15,3	0,0129	17,7	0,0149	23,6	0,0199
200	1 200	90,4	0,0753	15,3	0,0128	13,1	0,0109	13,8	0,0115	15,5	0,0129	18,2	0,0151	23,4	0,0195

Time	Shear Rate	Shear Stress	Viscosity	Shear Stress	Viscosity	Shear Stress	Viscosity	Shear Stress	Viscosity	Shear Stress	Viscosity	Shear Stress	Viscosity	Shear Stress	Viscosity
[s]	[1/s]	[Pa]	[Pa·s]	[Pa]	[Pa·s]	[Pa]	[Pa·s]	[Pa]	[Pa·s]	[Pa]	[Pa·s]	[Pa]	[Pa·s]	[Pa]	[Pa·s]
Number of Intervals:		*CNC-SEP-WDFs (6 wt %) 0.0 % 70°C*	*CNC-SEP-WDFs (6 wt %) 0.0 % 70°C*	*CNC-SEP-WDFs (6 wt %) 0,4 % 70°C*	*CNC-SEP-WDFs (6 wt %) 0.4 % 70°C*	*CNC-SEP-WDFs (6 wt %) 0.8 % 70°C*	*CNC-SEP-WDFs (6 wt %) 0.8 % 70°C*	*CNC-SEP-WDFs (6 wt %) 1,2 % 70°C*	*CNC-SEP-WDFs (6 wt %) 1,2 % 70°C*	*CNC-SEP-WDFs (6 wt %) 1,6 % 70°C*	*CNC-SEP-WDFs (6 wt %) 1,6 % 70°C*	*CNC-SEP-WDFs (6 wt %) 2.0 % 70°C*	*CNC-SEP-WDFs (6 wt %) 2.0 % 70°C*	*CNC-SEP-WDFs (6 wt %) 2,4 % 70°C*	*CNC-SEP-WDFs (6 wt %) 2,4 % 70°C*
2	0,999	33,1	32,9	7,53	7,52	-0,054	-0,0541	-0,758	-0,759	-0,0796	-0,0797	1,23	1,23	3,28	3,28
4	13,1	38	2,89	6,38	0,486	1,18	0,0898	0,05 46	0,0041 6	1,36	0,104	3,02	0,23	6,77	0,516
6	25,2	39,5	1,56	6,16	0,244	1,33	0,0528	0,635	0,0252	2,15	0,0851	3,94	0,156	8,14	0,323
8	37,3	40,5	1,08	6,15	0,165	1,43	0,0382	1,1	0,0295	2,43	0,0651	4,51	0,121	9,16	0,245
10	49,4	42	0,849	6,16	0,125	1,57	0,0318	1,28	0,0258	2,61	0,0529	4,82	0,0974	9,77	0,198
12	61,6	43,6	0,709	6,07	0,0985	1,69	0,0275	1,36	0,0221	2,73	0,0444	5,27	0,0856	10,2	0,166
14	73,7	45	0,611	6,07	0,0823	1,81	0,0246	1,58	0,0214	2,9	0,0393	5,48	0,0744	10,6	0,144
16	85,8	46,4	0,541	6,03	0,0703	1,84	0,0215	1,63	0,019	3,07	0,0358	5,84	0,0681	11,1	0,13
18	97,9	47,6	0,486	5,99	0,0612	1,98	0,0202	1,74	0,0178	3,22	0,0329	6,17	0,063	11,6	0,118
20	110	48,7	0,443	6,07	0,0552	2,04	0,0186	1,89	0,0172	3,37	0,0307	6,46	0,0587	12,1	0,11
22	122	49,8	0,408	6,12	0,0501	2,13	0,0175	2,01	0,0165	3,55	0,029	6,63	0,0543	12,6	0,103
24	134	50,8	0,379	6,19	0,0461	2,24	0,0167	2,04	0,0152	3,71	0,0277	6,94	0,0517	12,8	0,0955
26	146	51,8	0,354	6,25	0,0427	2,36	0,0162	2,06	0,0141	3,9	0,0267	7,36	0,0503	13,4	0,0918
28	158	52,7	0,333	6,27	0,0395	2,47	0,0156	2,19	0,0138	4,04	0,0255	7,61	0,0481	13,8	0,0869
30	171	53,6	0,314	6,31	0,037	2,56	0,015	2,3	0,0135	4,12	0,0242	7,87	0,0461	14	0,0823
32	183	54,5	0,298	6,44	0,0353	2,57	0,0141	2,41	0,0132	4,28	0,0234	8,18	0,0448	14,4	0,0789
34	195	55,4	0,284	6,44	0,0331	2,67	0,0137	2,43	0,0125	4,45	0,0228	8,3	0,0426	14,7	0,0756
36	207	56,2	0,272	6,5	0,0314	2,68	0,0129	2,58	0,0125	4,55	0,022	8,39	0,0406	15	0,0724
38	219	57,1	0,261	6,49	0,0296	2,78	0,0127	2,66	0,0122	4,76	0,0217	8,68	0,0396	15,3	0,0698
40	231	57,9	0,25	6,49	0,0281	2,85	0,0123	2,79	0,0121	4,88	0,0211	8,85	0,0383	15,6	0,0676
42	243	58,6	0,241	6,54	0,0269	2,94	0,0121	2,93	0,0121	4,92	0,0202	9,11	0,0374	16,1	0,066
44	255	59,4	0,233	6,55	0,0257	3,01	0,0118	2,98	0,0117	5,1	0,02	9,18	0,036	16,2	0,0635
46	267	60,2	0,225	6,56	0,0245	3,11	0,0116	3,03	0,0113	5,2	0,0194	9,4	0,0352	16,3	0,0609
48	280	61	0,218	6,61	0,0237	3,13	0,0112	3,1	0,0111	5,25	0,0188	9,62	0,0344	16,5	0,0589
50	292	61,6	0,211	6,69	0,0229	3,18	0,0109	3,27	0,0112	5,32	0,0182	9,65	0,0331	16,8	0,0574
52	304	62,4	0,205	6,69	0,022	3,26	0,0107	3,28	0,0108	5,41	0,0178	10,1	0,0331	16,9	0,0557
54	316	63,1	0,2	6,7	0,0212	3,35	0,0106	3,33	0,0105	5,53	0,0175	10,1	0,0319	17,2	0,0546
56	328	63,8	0,195	6,77	0,0206	3,39	0,0103	3,42	0,0104	5,57	0,017	10,3	0,0313	17,6	0,0537
58	340	64,6	0,19	6,69	0,0197	3,54	0,0104	3,55	0,0104	5,79	0,017	10,4	0,0306	17,9	0,0526
60	352	65,3	0,185	6,74	0,0191	3,63	0,0103	3,64	0,0103	5,91	0,0168	10,6	0,03	17,9	0,051
62	364	66	0,181	6,92	0,019	3,61	0,0099 2	3,75	0,0103	5,92	0,0162	10,6	0,0292	18,2	0,05
64	376	66,8	0,177	6,92	0,0184	3,79	0,0101	3,83	0,0102	6,12	0,0163	10,8	0,0286	18,4	0,0489
66	389	67,4	0,173	7,03	0,0181	3,87	0,0099 5	3,95	0,0102	6,22	0,016	10,9	0,0279	18,5	0,0476
68	401	68	0,17	7,07	0,0177	3,94	0,0098 2	4,08	0,0102	6,27	0,0157	11	0,0274	18,7	0,0467
70	413	68,6	0,166	7,14	0,0173	3,96	0,0095 9	4,09	0,0099	6,38	0,0155	11,2	0,0271	18,9	0,0458
72	425	69,2	0,163	7,14	0,0168	4,1	0,0096 6	4,14	0,0097 5	6,52	0,0154	11,3	0,0266	19	0,0448
74	437	69,7	0,159	7,3	0,0167	4,14	0,0094 7	4,33	0,0099 2	6,54	0,015	11,3	0,0258	19,1	0,0437
76	449	70,3	0,157	7,24	0,0161	4,31	0,0095 9	4,46	0,0099 4	6,7	0,0149	11,3	0,0251	19	0,0423
78	461	70,6	0,153	7,53	0,0163	4,54	0,0098 5	4,43	0,0096 1	6,87	0,0149	11,2	0,0242	19,4	0,0422
80	473	71,4	0,151	7,44	0,0157	4,37	0,0092 4	4,61	0,0097 5	6,88	0,0145	11,5	0,0243	19,3	0,0407

82	485	72	0,148	7,39	0,0152	4,51	0,00929	4,71	0,0097	7,02	0,0145	11,4	0,0234	19,3	0,0397
84	498	72,4	0,145	7,55	0,0152	4,45	0,00895	4,82	0,0097	6,93	0,0139	11,5	0,0231	19,4	0,0391
86	510	72,9	0,143	7,56	0,0148	4,57	0,00896	4,93	0,00968	7,08	0,0139	11,6	0,0227	19,4	0,038
88	522	73,6	0,141	7,58	0,0145	4,69	0,00898	4,9	0,00939	7,19	0,0138	11,6	0,0223	19,5	0,0374
90	534	74	0,139	7,65	0,0143	4,71	0,00882	5,06	0,00947	7,22	0,0135	11,6	0,0218	19,5	0,0365
92	546	74,5	0,136	7,75	0,0142	4,77	0,00873	5,13	0,0094	7,29	0,0134	11,7	0,0214	19,5	0,0357
94	558	74,9	0,134	7,82	0,014	4,81	0,00861	5,34	0,00956	7,3	0,0131	11,7	0,021	19,6	0,0351
96	570	75,3	0,132	7,91	0,0139	4,83	0,00848	5,33	0,00934	7,45	0,0131	11,8	0,0208	19,7	0,0346
98	582	75,8	0,13	7,95	0,0137	4,93	0,00847	5,45	0,00935	7,52	0,0129	11,9	0,0204	19,7	0,0338
100	594	76,1	0,128	8,04	0,0135	4,98	0,00837	5,71	0,00961	7,6	0,0128	11,8	0,0198	19,7	0,0331
102	607	76,6	0,126	7,99	0,0132	5,22	0,0086	5,68	0,00937	7,77	0,0128	11,9	0,0195	19,7	0,0325
104	619	77	0,124	8,08	0,0131	5,34	0,00863	5,85	0,00945	7,86	0,0127	11,9	0,0192	19,9	0,0322
106	631	77,4	0,123	8,11	0,0129	5,41	0,00857	5,93	0,0094	7,95	0,0126	11,8	0,0187	19,8	0,0314
108	643	77,8	0,121	8,23	0,0128	5,5	0,00855	5,86	0,00912	8,09	0,0126	12	0,0187	19,8	0,0307
110	655	78,3	0,12	8,17	0,0125	5,64	0,00861	5,9	0,00901	8,25	0,0126	12,1	0,0184	19,7	0,03
112	667	78,6	0,118	8,33	0,0125	5,79	0,00868	5,99	0,00897	8,32	0,0125	12,2	0,0183	19,6	0,0294
114	679	78,8	0,116	8,37	0,0123	5,9	0,00869	6,27	0,00923	8,38	0,0123	12	0,0177	19,5	0,0288
116	691	79,2	0,115	8,52	0,0123	6,14	0,00888	6,32	0,00914	8,48	0,0123	11,9	0,0172	19,6	0,0283
118	703	79,6	0,113	8,52	0,0121	6,43	0,00914	6,44	0,00916	8,7	0,0124	11,8	0,0168	19,5	0,0278
120	716	79,8	0,112	8,66	0,0121	6,48	0,00905	6,64	0,00927	8,66	0,0121	12	0,0168	19,9	0,0279
122	728	80,3	0,11	8,65	0,0119	6,71	0,00922	6,69	0,0092	8,92	0,0123	12	0,0166	19,6	0,027
124	740	80,6	0,109	8,73	0,0118	6,86	0,00927	6,83	0,00924	9	0,0122	12,3	0,0167	19,8	0,0267
126	752	80,8	0,107	8,83	0,0117	6,9	0,00918	7,13	0,00948	9,01	0,012	12,3	0,0164	19,7	0,0262
128	764	81,2	0,106	8,86	0,0116	7,26	0,0095	7,11	0,00931	9,17	0,012	12,4	0,0163	19,7	0,0258
130	776	81,5	0,105	8,89	0,0115	7,4	0,00954	7,29	0,0094	9,32	0,012	12,4	0,016	19,7	0,0253
132	788	81,8	0,104	8,9	0,0113	7,58	0,00962	7,34	0,00931	9,53	0,0121	12,6	0,016	19,7	0,025
134	800	82	0,102	9,12	0,0114	7,64	0,00954	7,6	0,00949	9,42	0,0118	12,7	0,0159	19,8	0,0248
136	812	82,2	0,101	9,23	0,0114	7,7	0,00947	7,6	0,00935	9,48	0,0117	12,8	0,0158	19,9	0,0245
138	825	82,6	0,1	9,17	0,0111	7,88	0,00955	7,75	0,0094	9,62	0,0117	12,8	0,0155	19,8	0,024
140	837	82,9	0,0991	9,23	0,011	8,24	0,00985	7,96	0,00951	9,86	0,0118	13	0,0155	19,7	0,0236
142	849	83,2	0,098	9,58	0,0113	8,3	0,00978	8,12	0,00957	10,1	0,0119	13,1	0,0154	19,7	0,0232
144	861	83,4	0,0969	9,71	0,0113	8,37	0,00973	8,36	0,00971	10,2	0,0118	13,2	0,0153	19,7	0,0229
146	873	83,7	0,0959	9,84	0,0113	8,62	0,00987	8,33	0,00954	10,2	0,0117	13,3	0,0153	19,6	0,0225
148	885	83,9	0,0948	10	0,0113	8,8	0,00995	8,54	0,00965	10,3	0,0117	13,2	0,0149	19,5	0,0221

150	897	84,1	0,0938	10,2	0,0114	8,88	0,0099	8,61	0,00959	10,7	0,0119	13,4	0,015	19,5	0,0217
152	909	84,1	0,0925	10,7	0,0117	9,01	0,00991	8,83	0,00971	10,5	0,0115	13,6	0,0149	19,4	0,0213
154	921	84,4	0,0916	10,7	0,0116	9,25	0,01	8,95	0,00971	10,7	0,0116	13,6	0,0148	19,7	0,0214
156	934	84,6	0,0906	10,8	0,0116	9,46	0,0101	9,17	0,00982	10,9	0,0117	14	0,015	19,6	0,021
158	946	84,8	0,0896	11	0,0116	9,56	0,0101	9,23	0,00976	10,9	0,0115	13,7	0,0145	19,3	0,0204
160	958	84,8	0,0885	11,1	0,0116	9,64	0,0101	9,47	0,00989	11	0,0115	14	0,0147	19,6	0,0205
162	970	85	0,0876	11,4	0,0117	9,85	0,0102	9,72	0,01	11	0,0113	14,1	0,0146	19,9	0,0205
164	982	85,3	0,0868	11,4	0,0116	9,91	0,0101	9,71	0,00989	11,2	0,0114	14,3	0,0146	19,7	0,0201
166	994	85,3	0,0858	11,7	0,0118	9,95	0,01	9,83	0,00989	11	0,011	14,3	0,0144	20	0,0201
168	1 010	85,5	0,085	11,8	0,0117	10,1	0,0101	10,1	0,01	11,1	0,011	14,6	0,0145	19,9	0,0197
170	1 020	85,7	0,0841	12,1	0,0119	10,2	0,01	10,1	0,00995	11,5	0,0113	14,6	0,0143	20	0,0197
172	1 030	85,8	0,0833	12,1	0,0117	10,6	0,0102	10,4	0,0101	11,9	0,0116	14,7	0,0142	20,1	0,0195
174	1 040	85,9	0,0824	12,4	0,0119	10,6	0,0101	10,6	0,0101	12,2	0,0117	15	0,0144	20,1	0,0193
176	1 050	86,2	0,0817	12,4	0,0117	10,9	0,0104	10,7	0,0101	12,4	0,0117	15	0,0142	20,4	0,0194
178	1 070	86,2	0,0808	12,8	0,012	10,8	0,0101	10,8	0,0101	12,5	0,0117	15,3	0,0143	20,7	0,0194
180	1 080	86,4	0,0801	12,9	0,012	10,9	0,0101	11	0,0102	12,8	0,0118	15,3	0,0142	20,4	0,0189
182	1 090	86,5	0,0793	12,8	0,0117	11,1	0,0101	11,1	0,0101	13	0,0119	15,4	0,0141	20,6	0,0189
184	1 100	86,7	0,0786	13,2	0,012	11,4	0,0103	11,2	0,0101	13,2	0,012	15,6	0,0141	20,7	0,0188
186	1 120	86,8	0,0778	13,3	0,0119	11,7	0,0105	11,6	0,0104	13,4	0,012	15,1	0,0136	20,8	0,0186
188	1 130	87	0,0771	13,6	0,012	11,9	0,0106	11,8	0,0104	13,7	0,0121	15,3	0,0136	21,1	0,0187
190	1 140	86,9	0,0763	14,1	0,0124	11,9	0,0104	11,8	0,0103	13,7	0,012	15,8	0,0139	21,2	0,0186
192	1 150	87,1	0,0757	14	0,0122	12,1	0,0105	12	0,0104	13,9	0,0121	16	0,0139	21,3	0,0185
194	1 160	87,2	0,0749	14,5	0,0125	12,3	0,0106	12,2	0,0105	14,1	0,0121	16,3	0,014	21,3	0,0183
196	1 180	87,3	0,0742	14,3	0,0122	12,4	0,0106	12,5	0,0106	14,3	0,0122	16,6	0,0141	21,4	0,0182
198	1 190	87,3	0,0735	14,9	0,0126	12,5	0,0105	12,6	0,0106	14,4	0,0121	16,9	0,0143	21,6	0,0182
200	1 200	87,4	0,0729	15,2	0,0126	12,9	0,0108	12,7	0,0106	14,7	0,0122	17,2	0,0143	21,8	0,0181

Time	Shear Rate	Shear Stress	Viscosity	Shear Stress	Viscosity	Shear Stress	Viscosity	Shear Stress	Viscosity	Shear Stress	Viscosity	Shear Stress	Viscosity	Shear Stress	Viscosity
[s]	[1/s]	[Pa]	[Pa·s]	[Pa]	[Pa·s]	[Pa]	[Pa·s]	[Pa]	[Pa·s]	[Pa]	[Pa·s]	[Pa]	[Pa·s]	[Pa]	[Pa·s]
Number of Intervals:		*CNC-SEP-WDFs (6 wt %) 0.0 % 80°C*	*CNC-SEP-WDFs (6 wt %) 0.0 % 80°C*	*CNC-SEP-WDFs (6 wt %) 0.4 % 80°C*	*CNC-SEP-WDFs (6 wt %) 0.4 % 80°C*	*CNC-SEP-WDFs (6 wt %) 0.8 % 80°C*	*CNC-SEP-WDFs (6 wt %) 0.8 % 80°C*	*CNC-SEP-WDFs (6 wt %) 1,2 % 80°C*	*CNC-SEP-WDFs (6 wt %) 1,2 % 80°C*	*CNC-SEP-WDFs (6 wt %) 1,6 % 80°C*	*CNC-SEP-WDFs (6 wt %) 1,6 % 80°C*	*CNC-SEP-WDFs (6 wt %) 2,0 % 80°C*	*CNC-SEP-WDFs (6 wt %) 2.0 % 80°C*	*CNC-SEP-WDFs (6 wt %) 2,4 % 80°C*	*CNC-SEP-WDFs (6 wt %) 2,4 % 80°C*
2	0,999	38,5	38,2	11,6	11,6	2,16	2,15	0,258	0,258	0,569	0,569	1,71	1,71	4,1	4,11
4	13,1	47,7	3,64	11,4	0,868	3,19	0,243	1,15	0,0876	2,48	0,189	5,55	0,423	9,77	0,745
6	25,2	49,4	1,96	11,2	0,446	3,1	0,123	1,59	0,063	3,29	0,13	6,93	0,275	11,6	0,461
8	37,3	52,2	1,4	11,3	0,303	3,1	0,0829	1,82	0,0486	3,74	0,1	7,41	0,198	12,5	0,335
10	49,4	54	1,09	11,4	0,231	3,04	0,0614	1,98	0,04	3,9	0,0788	7,34	0,148	12,3	0,248
12	61,6	55,7	0,904	11,5	0,187	2,93	0,0475	2,04	0,0332	3,99	0,0648	7,57	0,123	12,4	0,201
14	73,7	57,1	0,775	11,6	0,158	2,93	0,0398	2,15	0,0292	4,15	0,0563	7,67	0,104	12,6	0,172
16	85,8	58,6	0,683	11,8	0,137	2,92	0,034	2,28	0,0266	4,29	0,05	7,83	0,0913	12,8	0,149
18	97,9	60,3	0,616	11,9	0,122	2,94	0,03	2,35	0,024	4,5	0,046	8,04	0,0822	13,1	0,134
20	110	61,8	0,562	12	0,109	2,99	0,0271	2,52	0,0229	4,71	0,0428	8,2	0,0745	13,4	0,122
22	122	63	0,516	12,1	0,0992	3,01	0,0246	2,63	0,0216	4,8	0,0393	8,44	0,0691	13,8	0,113
24	134	64,3	0,479	12,2	0,091	3,05	0,0227	2,78	0,0207	4,99	0,0371	8,58	0,0639	14,1	0,105
26	146	65,4	0,447	12,3	0,0838	3,12	0,0213	2,88	0,0197	5,08	0,0347	8,69	0,0594	14,3	0,098
28	158	66,5	0,42	12,4	0,0783	3,19	0,0201	3,04	0,0192	5,26	0,0332	8,93	0,0563	14,6	0,0924
30	171	67,6	0,396	12,5	0,0735	3,23	0,0189	3,16	0,0185	5,38	0,0316	9,11	0,0534	14,8	0,0867
32	183	68,6	0,376	12,6	0,0691	3,28	0,0179	3,27	0,0179	5,54	0,0303	9,27	0,0508	15,1	0,0825
34	195	69,6	0,357	12,7	0,0654	3,36	0,0173	3,34	0,0172	5,7	0,0293	9,45	0,0485	15,4	0,0792
36	207	70,6	0,341	12,9	0,0624	3,42	0,0165	3,45	0,0167	5,72	0,0276	9,67	0,0468	15,7	0,0757
38	219	71,5	0,327	13	0,0593	3,46	0,0158	3,46	0,0158	5,86	0,0268	9,78	0,0446	15,9	0,0724
40	231	72,4	0,313	13,1	0,0566	3,5	0,0151	3,52	0,0152	5,93	0,0257	9,91	0,0429	16	0,0691
42	243	73,2	0,301	13,2	0,0543	3,56	0,0146	3,62	0,0149	6,06	0,0249	10,1	0,0416	16,2	0,0668
44	255	74,2	0,291	13,3	0,0519	3,64	0,0143	3,68	0,0144	6,24	0,0245	10,1	0,0396	16,6	0,0648
46	267	74,9	0,28	13,4	0,0502	3,62	0,0136	3,73	0,0139	6,33	0,0237	10,3	0,0385	16,8	0,0627
48	280	75,8	0,271	13,5	0,0483	3,71	0,0133	3,83	0,0137	6,45	0,0231	10,5	0,0374	16,9	0,0605
50	292	76,6	0,262	13,6	0,0467	3,77	0,0129	3,93	0,0135	6,5	0,0223	10,7	0,0367	17	0,0583
52	304	77,3	0,254	13,7	0,0452	3,85	0,0127	4,02	0,0132	6,57	0,0216	10,8	0,0355	17,3	0,0569
54	316	78	0,247	13,9	0,0439	3,9	0,0123	4,06	0,0129	6,67	0,0211	10,8	0,0343	17,5	0,0554
56	328	78,7	0,24	13,9	0,0425	4,04	0,0123	4,21	0,0128	6,81	0,0208	11	0,0337	17,7	0,0541
58	340	79,3	0,233	14,1	0,0415	4,05	0,0119	4,21	0,0124	6,88	0,0202	11	0,0325	18	0,0528
60	352	80	0,227	14,2	0,0403	4,13	0,0117	4,32	0,0123	6,99	0,0198	11,2	0,0317	18	0,0511
62	364	80,7	0,222	14,3	0,0391	4,3	0,0118	4,53	0,0124	7,1	0,0195	11,3	0,031	18,2	0,0499
64	376	81,3	0,216	14,4	0,0383	4,34	0,0115	4,56	0,0121	7,2	0,0191	11,3	0,0301	18,5	0,0492
66	389	82	0,211	14,5	0,0373	4,47	0,0115	4,68	0,012	7,24	0,0186	11,4	0,0294	18,5	0,0477
68	401	82,7	0,206	14,6	0,0364	4,53	0,0113	4,74	0,0118	7,3	0,0182	11,6	0,029	18,5	0,0462
70	413	83,4	0,202	14,6	0,0354	4,67	0,0113	4,86	0,0118	7,47	0,0181	11,6	0,0281	18,8	0,0455
72	425	83,9	0,198	14,7	0,0345	4,68	0,011	4,89	0,0115	7,59	0,0179	11,6	0,0274	18,9	0,0444
74	437	84,5	0,193	14,8	0,0338	4,79	0,011	5,04	0,0115	7,58	0,0174	11,7	0,0268	19	0,0435
76	449	84,9	0,189	14,9	0,0332	4,77	0,0106	5,03	0,0112	7,64	0,017	11,8	0,0262	19	0,0423
78	461	85,8	0,186	14,7	0,0318	4,54	0,00984	4,84	0,0105	7,73	0,0168	11,7	0,0254	18,8	0,0408
80	473	85,9	0,182	15	0,0318	4,96	0,0105	5,26	0,0111	7,82	0,0165	11,9	0,0252	19,2	0,0405
82	485	86,3	0,178	15,2	0,0312	4,93	0,0102	5,28	0,0109	7,81	0,0161	12	0,0247	19,2	0,0396
84	498	86,8	0,174	15,2	0,0306	5,07	0,0102	5,49	0,011	7,85	0,0158	12,1	0,0244	19,3	0,0389
86	510	87,2	0,171	15,3	0,0301	5,1	0,01	5,52	0,0108	7,94	0,0156	12,2	0,0239	19,4	0,038
88	522	87,6	0,168	15,3	0,0293	5,19	0,00995	5,55	0,0106	8,15	0,0156	12	0,0231	19,5	0,0374
90	534	88,1	0,165	15,4	0,0288	5,25	0,00983	5,66	0,0106	8,14	0,0153	12,2	0,0228	19,4	0,0363
92	546	88,5	0,162	15,4	0,0283	5,36	0,00982	5,74	0,0105	8,28	0,0152	12,1	0,0222	19,3	0,0354
94	558	89	0,159	15,5	0,0278	5,45	0,00976	5,86	0,0105	8,27	0,0148	12,1	0,0218	19,4	0,0348
96	570	89,5	0,157	15,5	0,0271	5,59	0,0098	5,96	0,0105	8,52	0,0149	12,1	0,0212	19,5	0,0342

98	582	89,8	0,154	15,5	0,0267	5,69	0,00976	6	0,0103	8,61	0,0148	12,1	0,0208	19,6	0,0337
100	594	90,2	0,152	15,7	0,0264	5,74	0,00966	6,16	0,0104	8,54	0,0144	12,4	0,0209	19,5	0,0329
102	607	90,6	0,149	15,7	0,0259	5,74	0,00946	6,14	0,0101	8,72	0,0144	12,3	0,0202	19,5	0,0321
104	619	90,9	0,147	15,8	0,0256	5,79	0,00936	6,28	0,0102	8,75	0,0141	12,6	0,0203	19,4	0,0314
106	631	91,2	0,145	15,9	0,0252	5,88	0,00933	6,41	0,0102	8,77	0,0139	12,6	0,0199	19,5	0,0309
108	643	91,6	0,142	15,9	0,0247	6,03	0,00938	6,54	0,0102	9,03	0,014	12,3	0,0192	19,6	0,0305
110	655	91,9	0,14	16	0,0244	6,07	0,00927	6,52	0,00995	9,11	0,0139	12,5	0,019	19,6	0,0299
112	667	92,3	0,138	16	0,024	6,26	0,00938	6,69	0,01	9,24	0,0139	12,4	0,0186	19,8	0,0296
114	679	92,5	0,136	16,2	0,0238	6,36	0,00936	6,85	0,0101	9,16	0,0135	12,7	0,0188	19,5	0,0287
116	691	92,9	0,134	16,2	0,0234	6,48	0,00937	6,88	0,00996	9,38	0,0136	12,6	0,0183	19,8	0,0286
118	703	93,1	0,132	16,3	0,0231	6,61	0,00939	6,93	0,00986	9,46	0,0135	12,6	0,018	19,6	0,0279
120	716	93,5	0,131	16,3	0,0228	6,91	0,00965	7,07	0,00987	9,63	0,0135	12,7	0,0178	19,6	0,0274
122	728	93,8	0,129	16,3	0,0224	7	0,00962	7,07	0,00972	9,82	0,0135	12,6	0,0173	19,9	0,0273
124	740	94,1	0,127	16,4	0,0221	7,2	0,00973	7,26	0,00981	9,96	0,0135	12,7	0,0172	19,8	0,0268
126	752	94,3	0,125	16,4	0,0219	7,45	0,00991	7,58	0,0101	9,89	0,0132	12,9	0,0171	19,6	0,0261
128	764	94,6	0,124	16,5	0,0216	7,55	0,00988	7,6	0,00994	10,1	0,0132	12,8	0,0168	19,7	0,0257
130	776	94,8	0,122	16,6	0,0214	7,76	0,00999	7,75	0,00999	10,2	0,0131	12,9	0,0166	19,8	0,0255
132	788	95	0,121	16,7	0,0212	7,88	0,01	7,76	0,00984	10,2	0,013	13	0,0165	19,6	0,0249
134	800	95,4	0,119	16,8	0,021	8,08	0,0101	8,15	0,0102	10,3	0,0129	13,3	0,0166	19,7	0,0246
136	812	95,7	0,118	16,8	0,0207	8,28	0,0102	8,36	0,0103	10,5	0,013	13,4	0,0165	19,8	0,0244
138	825	96	0,116	17	0,0206	8,13	0,00986	8,38	0,0102	10,4	0,0126	13,6	0,0165	19,5	0,0237
140	837	96,1	0,115	16,9	0,0202	8,47	0,0101	8,5	0,0102	10,6	0,0126	13,4	0,016	19,6	0,0235
142	849	96,3	0,113	17	0,0201	8,62	0,0102	8,68	0,0102	10,8	0,0127	13,7	0,0162	19,6	0,023
144	861	96,5	0,112	17,1	0,0199	8,79	0,0102	8,83	0,0103	10,8	0,0126	13,9	0,0162	19,4	0,0226
146	873	96,7	0,111	17	0,0195	8,97	0,0103	8,96	0,0103	10,9	0,0124	13,8	0,0158	19,6	0,0225
148	885	96,8	0,109	17,1	0,0194	9	0,0102	8,94	0,0101	11,1	0,0125	13,9	0,0157	19,4	0,022
150	897	97,1	0,108	17,1	0,0191	9,24	0,0103	9,09	0,0101	11,2	0,0125	13,9	0,0155	19,5	0,0217
152	909	97,4	0,107	17,2	0,019	9,3	0,0102	9,45	0,0104	11,3	0,0124	14,3	0,0157	19,6	0,0216
154	921	97,5	0,106	17,3	0,0188	9,53	0,0103	9,55	0,0104	11,4	0,0123	14,3	0,0155	19,7	0,0214
156	934	97,6	0,105	17,4	0,0186	9,6	0,0103	9,68	0,0104	11,4	0,0122	14,5	0,0155	19,5	0,0209
158	946	97,7	0,103	17,4	0,0184	9,68	0,0102	9,78	0,0103	11,4	0,012	14,4	0,0152	19,7	0,0208
160	958	97,8	0,102	17,6	0,0183	9,78	0,0102	10	0,0104	11,5	0,012	14,6	0,0153	19,8	0,0207
162	970	98	0,101	17,6	0,0182	9,93	0,0102	10,1	0,0104	11,5	0,0119	14,7	0,0151	19,7	0,0204
164	982	98,2	0,1	17,6	0,0179	10,1	0,0103	10,2	0,0104	12	0,0122	14,5	0,0148	19,9	0,0202
166	994	98,4	0,099	17,6	0,0177	10,2	0,0103	10,3	0,0104	11,8	0,0119	14,6	0,0147	19,9	0,02
168	1 010	98,5	0,0979	17,6	0,0175	10,4	0,0104	10,5	0,0104	11,8	0,0117	14,7	0,0146	20	0,0198
170	1 020	98,6	0,0969	17,6	0,0173	10,6	0,0104	10,6	0,0104	11,9	0,0117	14,7	0,0144	20	0,0197
172	1 030	98,7	0,0958	17,8	0,0173	10,7	0,0104	10,8	0,0105	12	0,0117	14,9	0,0144	19,9	0,0193
174	1 040	98,9	0,0948	17,9	0,0171	10,9	0,0105	11	0,0105	11,8	0,0113	15,1	0,0145	20,1	0,0193
176	1 050	99	0,0938	18	0,017	11,1	0,0106	11,1	0,0105	12,4	0,0117	15,2	0,0144	20	0,019
178	1 070	99,2	0,093	17,9	0,0167	11,5	0,0108	11,3	0,0106	13	0,0121	15,2	0,0142	20,4	0,0191
180	1 080	99,4	0,0921	18	0,0167	11,5	0,0107	11,5	0,0106	13,1	0,0122	15,4	0,0143	20,8	0,0192

182	1 090	99,5	0,0912	18,1	0,0166	11,7	0,0108	11,6	0,0106	13,2	0,0121	15,6	0,0143	20,5	0,0188
184	1 100	99,7	0,0904	18,1	0,0164	11,9	0,0108	11,7	0,0106	13,4	0,0122	15,3	0,0139	20,7	0,0187
186	1 120	99,7	0,0894	18,3	0,0164	11,9	0,0107	12	0,0107	13,5	0,0121	15,6	0,014	20,7	0,0185
188	1 130	99,8	0,0885	18,4	0,0164	12,1	0,0107	12,1	0,0107	13,7	0,0121	15,6	0,0138	20,8	0,0185
190	1 140	100	0,0879	18,6	0,0163	12,3	0,0108	12,4	0,0109	14	0,0123	15,5	0,0136	21,2	0,0186
192	1 150	100	0,087	18,9	0,0164	12,6	0,0109	12,6	0,0109	14,3	0,0124	16	0,0139	21,1	0,0184
194	1 160	100	0,0862	19,1	0,0164	12,7	0,0109	12,8	0,011	14,4	0,0124	16,4	0,0141	21,4	0,0184
196	1 180	100	0,0854	19,3	0,0164	12,8	0,0109	12,9	0,011	14,5	0,0123	16,8	0,0143	21,3	0,0181
198	1 190	101	0,0847	19,3	0,0162	13,3	0,0112	13,3	0,0112	14,9	0,0125	17,1	0,0144	21,5	0,0181
200	1 200	101	0,084	19,3	0,0161	13,2	0,011	13,3	0,0111	15	0,0125	17,3	0,0144	21,7	0,0181

RHEOLOGICAL DATA OF CNC/BT-WDFs (SW)

Time	Shear Rate	Shear Stress	Viscosity	Shear Stress	Viscosity	Shear Stress	Viscosity	Shear Stress	Viscosity	Shear Stress	Viscosity	Shear Stress	Viscosity	Shear Stress	Viscosity
[s]	[1/s]	[Pa]	[Pa·s]	[Pa]	[Pa·s]	[Pa]	[Pa·s]	[Pa]	[Pa·s]	[Pa]	[Pa·s]	[Pa]	[Pa·s]	[Pa]	[Pa·s]
Number of Intervals:		*CNC-BT-WDFs (6 wt %) 0.0 % 20°C S.W.*	*CNC-BT-WDFs (6 wt %) 0.0 % 20°C S.W.*	*CNC-BT-WDFs (6 wt %) 0.4 % 20°C S.W.*	*CNC-BT-WDFs (6 wt %) 0.4 % 20°C S.W.*	*CNC-BT-WDFs (6 wt %) 0.8 % 20°C S.W.*	*CNC-BT-WDFs (6 wt %) 0.8 % 20°C S.W.*	*CNC-BT-WDFs (6 wt %) 1.2 % 20°C S.W.*	*CNC-BT-WDFs (6 wt %) 1.2 % 20°C S.W.*	*CNC-BT-WDFs (6 wt %) 1.6 % 20°C S.W.*	*CNC-BT-WDFs (6 wt %) 1.6 % 20°C S.W.*	*CNC-BT-WDFs (6 wt %) 2.0 % 20°C S.W.*	*CNC-BT-WDFs (6 wt %) 2.0 % 20°C S.W.*	*CNC-BT-WDFs (6 wt %) 2.4 % 20°C S.W.*	*CNC-BT-WDFs (6 wt %) 2.4 % 20°C S.W.*
2	0,999	-1,06	-1,07	-0,711	-0,711	-0,877	-0,876	-0,743	-0,743	0,0285	0,0285	0,224	0,224	0,421	0,422
4	13,1	-0,509	-0,0388	-0,478	-0,0365	-0,357	-0,0272	-0,327	-0,0249	0,296	0,0226	1,87	0,142	2,02	0,154
6	25,2	-0,336	-0,0133	-0,262	-0,0104	-0,354	-0,014	0,00781	3,1E-4	0,314	0,0125	2,42	0,096	2,37	0,0942
8	37,3	-0,474	-0,0127	-0,256	-0,00686	-0,258	-0,0069	-0,0237	-6,34E-4	0,594	0,0159	2,51	0,0673	2,51	0,0672
10	49,4	-0,374	-0,00756	-0,287	-0,0058	-0,301	-0,00608	0,152	0,00307	0,781	0,0158	2,75	0,0557	2,63	0,0532
12	61,6	-0,306	-0,00497	-0,341	-0,00554	-0,303	-0,00493	0,129	0,0021	0,874	0,0142	2,86	0,0464	2,8	0,0456
14	73,7	-0,309	-0,00419	-0,297	-0,00403	-0,263	-0,00357	0,188	0,00255	0,866	0,0118	3,19	0,0433	2,87	0,039
16	85,8	-0,298	-0,00348	-0,292	-0,00341	-0,227	-0,00264	0,415	0,00483	0,976	0,0114	3,36	0,0392	3,05	0,0356
18	97,9	-0,312	-0,00318	-0,269	-0,00275	-0,197	-0,00201	0,446	0,00456	1,08	0,0111	3,54	0,0362	3,21	0,0328
20	110	-0,256	-0,00232	-0,258	-0,00234	-0,141	-0,00128	0,431	0,00392	1,2	0,0109	3,7	0,0336	3,38	0,0308
22	122	-0,282	-0,00231	-0,198	-0,00162	-0,101	-8,31E-4	0,505	0,00413	1,17	0,00954	3,86	0,0316	3,57	0,0292
24	134	-0,248	-0,00185	-0,197	-0,00147	-0,072	-5,36E-4	0,572	0,00426	1	0,00748	4,06	0,0303	3,78	0,0282
26	146	-0,167	-0,00114	-0,161	-0,0011	-0,0677	-4,63E-4	0,639	0,00436	1,27	0,00869	4,28	0,0292	3,8	0,026
28	158	-0,157	-9,92E-4	-0,103	-6,5E-4	-0,0257	-1,62E-4	0,759	0,00479	1,23	0,00778	4,37	0,0276	3,94	0,0249
30	171	0,00335	1,96E-5	-0,101	-5,92E-4	-0,00433	-2,54E-5	0,787	0,00462	1,34	0,00784	4,5	0,0264	3,99	0,0234
32	183	0,0503	2,76E-4	-0,143	-7,84E-4	0,118	6,45E-4	0,941	0,00515	1,37	0,00749	4,72	0,0258	4,17	0,0228

34	195	0,0913	4,68E-4	-0,0732	-3,76E-4	0,0943	4,84E-4	1,07	0,00552	1,66	0,00855	4,83	0,0248	4,24	0,0218
36	207	0,106	5,11E-4	0,0645	3,12E-4	0,178	8,59E-4	1,15	0,00558	1,66	0,00803	4,96	0,024	4,3	0,0208
38	219	0,139	6,33E-4	0,15	6,83E-4	0,168	7,67E-4	1,38	0,0063	1,33	0,00607	5,03	0,023	4,4	0,0201
40	231	0,212	9,16E-4	0,237	0,00103	0,206	8,9E-4	0,896	0,00388	1,36	0,00587	5,09	0,022	4,51	0,0195
42	243	0,286	0,00117	0,327	0,00135	0,252	0,00104	0,862	0,00354	1,47	0,00602	5,19	0,0213	4,59	0,0189
44	255	0,406	0,00159	0,309	0,00121	0,279	0,00109	0,956	0,00374	1,5	0,00589	5,31	0,0208	4,65	0,0182
46	267	0,478	0,00179	0,44	0,00165	0,322	0,0012	1,03	0,00384	1,31	0,0049	5,35	0,02	4,69	0,0175
48	280	0,586	0,0021	0,47	0,00168	0,409	0,00146	1,11	0,00396	1,35	0,00483	5,44	0,0195	4,78	0,0171
50	292	0,628	0,00215	0,577	0,00198	0,516	0,00177	1,15	0,00396	1,48	0,00508	5,49	0,0188	4,72	0,0162
52	304	0,722	0,00238	0,634	0,00209	0,597	0,00196	1,23	0,00404	1,49	0,00492	5,55	0,0183	4,87	0,016
54	316	0,786	0,00249	0,745	0,00236	0,643	0,00203	1,28	0,00405	1,54	0,00487	5,63	0,0178	4,83	0,0153
56	328	0,879	0,00268	0,789	0,0024	0,75	0,00229	1,46	0,00444	1,7	0,00518	5,65	0,0172	5,01	0,0153
58	340	0,954	0,00281	0,975	0,00287	0,781	0,0023	1,52	0,00446	1,74	0,00512	5,71	0,0168	5,04	0,0148
60	352	1,08	0,00308	1,07	0,00303	0,89	0,00253	1,59	0,00451	1,81	0,00513	5,75	0,0163	5,21	0,0148
62	364	1,16	0,00319	1,15	0,00315	1,12	0,00307	1,78	0,00488	1,96	0,00539	5,84	0,016	5,19	0,0142
64	376	1,24	0,0033	1,32	0,00351	1,17	0,0031	1,81	0,00481	1,99	0,00529	5,87	0,0156	5,15	0,0137
66	389	1,37	0,00352	1,4	0,0036	1,34	0,00344	1,91	0,00492	2,13	0,00548	5,97	0,0154	5,23	0,0134
68	401	1,43	0,00356	1,54	0,00385	1,38	0,00345	1,94	0,00485	2,24	0,00558	5,89	0,0147	5,25	0,0131
70	413	1,6	0,00388	1,53	0,0037	1,54	0,00374	2,11	0,00511	2,34	0,00566	6,05	0,0147	5,47	0,0132
72	425	1,72	0,00406	1,63	0,00385	1,6	0,00378	2,19	0,00516	2,37	0,00559	6,1	0,0144	5,48	0,0129
74	437	1,77	0,00405	1,78	0,00408	1,77	0,00404	2,26	0,00518	2,54	0,00582	6,14	0,0141	5,45	0,0125
76	449	1,82	0,00404	1,98	0,00441	1,76	0,00391	2,26	0,00503	2,51	0,00559	6,07	0,0135	5,51	0,0123
78	461	1,94	0,00421	2,22	0,00481	2,06	0,00447	2,67	0,00579	2,49	0,0054	7,24	0,0157	5,33	0,0115
80	473	2	0,00422	2,15	0,00455	2,07	0,00438	2,55	0,00538	2,67	0,00564	6,31	0,0133	5,98	0,0126
82	485	2,03	0,00418	2,32	0,00479	2,12	0,00437	2,53	0,00522	2,74	0,00565	6,27	0,0129	6,19	0,0128
84	498	2,14	0,0043	2,41	0,00485	2,3	0,00462	2,73	0,00548	2,94	0,0059	6,34	0,0127	5,99	0,012
86	510	2,18	0,00429	2,54	0,00499	2,35	0,00461	2,82	0,00554	3	0,00589	6,36	0,0125	5,81	0,0114
88	522	2,34	0,00448	2,55	0,00489	2,4	0,00459	2,92	0,0056	3,02	0,00578	6,47	0,0124	5,94	0,0114
90	534	2,39	0,00447	2,7	0,00506	2,53	0,00473	3,08	0,00578	3,21	0,006	6,49	0,0121	6,02	0,0113
92	546	2,5	0,00458	2,77	0,00508	2,68	0,00491	3,23	0,00592	3,27	0,00599	6,62	0,0121	6,13	0,0112
94	558	2,44	0,00436	2,91	0,00522	2,83	0,00508	3,28	0,00587	3,44	0,00616	6,67	0,0119	6,2	0,0111
96	570	2,58	0,00453	2,89	0,00507	2,95	0,00517	3,49	0,00611	3,55	0,00623	6,88	0,0121	6,76	0,0119
98	582	2,68	0,00461	3,02	0,00518	3,06	0,00526	3,55	0,00609	3,59	0,00617	6,99	0,012	6,9	0,0119

100	594	2,68	0,0045	3,21	0,0054	3,23	0,00544	3,59	0,00604	3,81	0,0064	6,99	0,0118	6,66	0,0112
102	607	2,81	0,00463	3,2	0,00527	3,24	0,00535	3,72	0,00614	3,83	0,00632	7,11	0,0117	6,57	0,0108
104	619	2,89	0,00467	3,28	0,0053	3,43	0,00554	3,86	0,00623	3,94	0,00636	7,16	0,0116	6,67	0,0108
106	631	2,94	0,00466	3,45	0,00548	3,52	0,00558	3,9	0,00618	4,06	0,00644	7,23	0,0115	6,72	0,0107
108	643	3,1	0,00482	3,39	0,00527	3,67	0,0057	4,15	0,00645	4,03	0,00626	7,45	0,0116	6,97	0,0108
110	655	3,09	0,00471	3,57	0,00545	3,63	0,00555	4,22	0,00644	4,11	0,00627	7,54	0,0115	7,04	0,0107
112	667	3,24	0,00485	3,65	0,00547	3,79	0,00568	4,38	0,00657	4,27	0,0064	7,71	0,0116	7,19	0,0108
114	679	3,15	0,00464	3,89	0,00572	3,91	0,00576	4,45	0,00656	4,47	0,00658	7,68	0,0113	7,19	0,0106
116	691	3,42	0,00494	3,91	0,00565	4,05	0,00586	4,67	0,00676	4,42	0,00639	7,89	0,0114	7,35	0,0106
118	703	3,53	0,00502	4	0,00568	4,11	0,00585	4,71	0,00669	4,52	0,00643	7,98	0,0113	7,55	0,0107
120	716	3,59	0,00502	4,11	0,00575	4,36	0,0061	4,95	0,00692	4,59	0,00641	8,13	0,0114	7,61	0,0106
122	728	3,74	0,00514	4,14	0,0057	4,33	0,00595	5,02	0,0069	4,58	0,00629	8,26	0,0114	7,73	0,0106
124	740	3,83	0,00517	4,27	0,00577	4,51	0,00609	5,23	0,00707	4,72	0,00638	8,36	0,0113	7,79	0,0105
126	752	3,77	0,00501	4,47	0,00595	4,78	0,00636	5,34	0,0071	5,04	0,0067	8,38	0,0112	7,78	0,0104
128	764	3,91	0,00511	4,54	0,00595	4,81	0,00629	5,5	0,0072	5,02	0,00658	8,54	0,0112	7,88	0,0103
130	776	3,87	0,00499	4,72	0,00608	4,97	0,0064	5,6	0,00722	5,21	0,00671	8,57	0,011	7,98	0,0103
132	788	4,17	0,00529	4,86	0,00616	4,99	0,00633	5,72	0,00725	5,23	0,00663	8,7	0,011	7,82	0,00992
134	800	4,21	0,00526	5	0,00625	5,27	0,00659	5,83	0,00728	5,41	0,00676	8,85	0,0111	7,97	0,00996
136	812	4,27	0,00525	4,96	0,00611	5,44	0,0067	6,08	0,00749	5,56	0,00684	9,03	0,0111	8,04	0,0099
138	825	4,59	0,00557	5,24	0,00636	5,53	0,0067	5,98	0,00725	5,62	0,00682	9,01	0,0109	7,9	0,00958
140	837	4,82	0,00576	5,15	0,00615	5,53	0,00661	6,34	0,00757	5,71	0,00683	9,06	0,0108	8,32	0,00994
142	849	4,78	0,00563	5,32	0,00627	5,68	0,0067	6,45	0,0076	5,92	0,00697	9,1	0,0107	8,35	0,00984
144	861	4,74	0,00551	5,48	0,00636	5,78	0,00672	6,56	0,00761	6,11	0,0071	9,27	0,0108	8,55	0,00993
146	873	5	0,00573	5,43	0,00622	5,88	0,00673	6,84	0,00784	6,11	0,007	9,42	0,0108	8,95	0,0103
148	885	4,98	0,00563	5,66	0,00639	5,92	0,00668	6,87	0,00776	6,33	0,00715	9,46	0,0107	9,03	0,0102
150	897	5,18	0,00577	5,7	0,00635	6,06	0,00675	7,1	0,00792	6,43	0,00717	9,72	0,0108	9,34	0,0104
152	909	5,22	0,00574	5,81	0,00638	6,3	0,00693	7,22	0,00795	6,82	0,0075	9,97	0,011	9,47	0,0104
154	921	5,4	0,00587	5,95	0,00646	6,19	0,00671	7,4	0,00803	6,96	0,00755	10,1	0,011	9,67	0,0105
156	934	5,39	0,00577	6,13	0,00657	6,3	0,00675	7,47	0,008	7,11	0,00762	10,4	0,0112	9,75	0,0104
158	946	5,55	0,00586	6,27	0,00663	6,33	0,00669	7,7	0,00814	7,13	0,00754	10,6	0,0112	10	0,0106
160	958	5,47	0,00571	6,49	0,00678	6,38	0,00667	7,74	0,00808	7,38	0,00771	10,7	0,0112	9,98	0,0104
162	970	5,61	0,00579	6,55	0,00676	6,52	0,00673	7,87	0,00811	7,56	0,00779	10,9	0,0112	10,2	0,0106
164	982	5,92	0,00602	6,61	0,00673	6,58	0,0067	8,09	0,00824	7,52	0,00766	11,2	0,0114	10,6	0,0108
166	994	6	0,00603	6,73	0,00677	6,82	0,00686	8,26	0,00831	7,84	0,00789	11,4	0,0114	10,6	0,0107

168	1 010	6,1	0,00607	6,79	0,00675	6,87	0,00683	8,41	0,00836	7,96	0,00791	11,6	0,0115	10,8	0,0108
170	1 020	6,26	0,00614	6,77	0,00665	7,04	0,00691	8,68	0,00852	8,04	0,0079	11,8	0,0116	11,1	0,0109
172	1 030	6,26	0,00607	7,11	0,0069	7,1	0,00689	8,67	0,00841	8,22	0,00798	11,9	0,0115	11,1	0,0108
174	1 040	6,45	0,00619	7,27	0,00697	7,35	0,00705	8,88	0,00852	8,51	0,00816	12,1	0,0116	11,3	0,0109
176	1 050	6,57	0,00623	7,37	0,00698	7,34	0,00696	9,01	0,00854	8,54	0,0081	12,2	0,0116	11,5	0,0109
178	1 070	6,88	0,00645	7,38	0,00692	7,59	0,00712	9,34	0,00876	8,71	0,00817	12,7	0,0119	11,8	0,0111
180	1 080	7,03	0,00652	7,71	0,00715	7,7	0,00714	9,47	0,00878	8,86	0,00822	12,7	0,0118	11,9	0,0111
182	1 090	7,1	0,00651	7,86	0,00721	7,85	0,0072	9,62	0,00881	9,06	0,00831	12,9	0,0119	12,2	0,0112
184	1 100	7,35	0,00667	7,88	0,00714	7,95	0,0072	9,84	0,00892	9,14	0,00828	13,2	0,012	12,5	0,0113
186	1 120	7,37	0,00661	8,2	0,00735	8,05	0,00722	9,85	0,00883	9,34	0,00838	13,2	0,0119	12,6	0,0113
188	1 130	7,56	0,00671	8,3	0,00736	8,18	0,00726	10	0,00891	9,49	0,00842	13,4	0,0119	12,7	0,0113
190	1 140	7,82	0,00687	8,36	0,00734	8,53	0,00749	10,4	0,00911	9,7	0,00851	13,8	0,0121	13	0,0114
192	1 150	7,87	0,00684	8,57	0,00744	8,57	0,00744	10,4	0,00905	9,86	0,00856	14	0,0121	13,2	0,0115
194	1 160	8,04	0,00691	8,74	0,00751	8,79	0,00755	10,6	0,00907	10,1	0,00866	14,2	0,0122	13,5	0,0116
196	1 180	8,12	0,00691	8,94	0,00761	8,95	0,00761	10,7	0,0091	10,3	0,00872	14,4	0,0123	13,5	0,0115
198	1 190	8,48	0,00714	8,93	0,00752	9,14	0,00769	10,9	0,00917	10,4	0,00879	14,7	0,0124	13,8	0,0116
200	1 200	8,62	0,00718	9	0,0075	9,29	0,00774	10,9	0,00906	10,5	0,00878	14,9	0,0124	13,9	0,0116

Time	Shear Rate	Shear Stress	Viscosity	Shear Stress	Viscosity	Shear Stress	Viscosity	Shear Stress	Viscosity	Shear Stress	Viscosity	Shear Stress	Viscosity	Shear Stress	Viscosity
[s]	[1/s]	[Pa]	[Pa·s]	[Pa]	[Pa·s]	[Pa]	[Pa·s]	[Pa]	[Pa·s]	[Pa]	[Pa·s]	[Pa]	[Pa·s]	[Pa]	[Pa·s]
Number of Intervals:		*CNC-BT-WDFs (6 wt %) 0.0 % 30°C S.W.*	*CNC-BT-WDFs (6 wt %) 0.0 % 30°C S.W.*	*CNC-BT-WDFs (6 wt %) 0.4 % 30°C S.W.*	*CNC-BT-WDFs (6 wt %) 0.4 % 30°C S.W.*	*CNC-BT-WDFs (6 wt %) 0.8 % 30°C S.W.*	*CNC-BT-WDFs (6 wt %) 0.8 % 30°C S.W.*	*CNC-BT-WDFs (6 wt %) 1.2 % 30°C S.W.*	*CNC-BT-WDFs (6 wt %) 1.2 % 30°C S.W.*	*CNC-BT-WDFs (6 wt %) 1.6 % 30°C S.W.*	*CNC-BT-WDFs (6 wt %) 1.6 % 30°C S.W.*	*CNC-BT-WDFs (6 wt %) 2.0 % 30°C S.W.*	*CNC-BT-WDFs (6 wt %) 2.0 % 30°C S.W.*	*CNC-BT-WDFs (6 wt %) 2.4 % 30°C S.W.*	*CNC-BT-WDFs (6 wt %) 2.4 % 30°C S.W.*
2	0,999	-0,756	-0,757	-0,705	-0,704	-0,723	-0,722	-0,612	-0,612	-0,249	-0,249	0,268	0,268	-0,0924	-0,0922
4	13,1	-0,441	-0,0336	-0,405	-0,0309	-0,33	-0,0252	-0,253	-0,0193	0,183	0,0139	1,79	0,137	1,49	0,114
6	25,2	-0,449	-0,0178	-0,426	-0,0169	-0,291	-0,0115	-0,074	-0,00293	0,501	0,0199	2,3	0,091	1,75	0,0694
8	37,3	-0,406	-0,0109	-0,469	-0,0126	-0,274	-0,00733	0,00403	1,08E-4	0,528	0,0142	2,52	0,0676	1,86	0,0498
10	49,4	-0,408	-0,00824	-0,467	-0,00945	-0,397	-0,00803	-0,0128	-2,58E-4	0,487	0,00984	2,68	0,0542	1,96	0,0397
12	61,6	-0,528	-0,00858	-0,508	-0,00825	-0,382	-0,0062	0,114	0,00186	0,682	0,0111	2,94	0,0478	2,13	0,0345
14	73,7	-0,519	-0,00705	-0,481	-0,00653	-0,445	-0,00605	0,0604	8,2E-4	0,529	0,00718	3,12	0,0424	2,26	0,0307
16	85,8	-0,548	-0,00639	-0,489	-0,00571	-0,415	-0,00484	0,102	0,00119	0,591	0,00689	3,19	0,0372	2,4	0,028
18	97,9	-0,564	-0,00576	-0,445	-0,00454	-0,384	-0,00392	0,17	0,00173	0,835	0,00853	3,37	0,0344	2,54	0,0259
20	110	-0,519	-0,00472	-0,433	-0,00394	-0,322	-0,00293	0,182	0,00165	0,854	0,00777	3,55	0,0323	2,68	0,0243
22	122	-0,564	-0,00462	-0,366	-0,003	-0,273	-0,00223	0,198	0,00162	0,978	0,00801	3,72	0,0305	2,83	0,0232
24	134	-0,543	-0,00405	-0,377	-0,00281	-0,235	-0,00175	0,296	0,00221	0,924	0,00689	3,92	0,0292	2,96	0,0221
26	146	-0,464	-0,00317	-0,33	-0,00226	-0,179	-0,00123	0,337	0,0023	1,07	0,00729	4,07	0,0278	3,08	0,021
28	158	-0,401	-0,00253	-0,292	-0,00184	-0,124	-7,83E-4	0,412	0,0026	1,14	0,00721	4,27	0,0269	3,19	0,0201
30	171	-0,363	-0,00213	-0,256	-0,0015	-0,0739	-4,34E-4	0,469	0,00275	1,28	0,00751	4,44	0,026	3,36	0,0197
32	183	-0,355	-0,00195	-0,196	-0,00107	-0,0824	-4,51E-4	0,638	0,00349	1,31	0,00716	4,59	0,0251	3,41	0,0186
34	195	-0,305	-0,00157	-0,148	-7,62E-4	-0,0582	-2,99E-4	0,685	0,00351	1,46	0,00749	4,74	0,0243	3,53	0,0181
36	207	-0,201	-9,7E-4	-0,0855	-4,13E-4	0,036	1,74E-4	0,72	0,00348	1,61	0,0078	4,86	0,0235	3,67	0,0177

38	219	-0,199	-9,08E-4	-0,0821	-3,75E-4	0,0588	2,69E-4	0,872	0,00398	1,63	0,00745	5,04	0,023	3,77	0,0172
40	231	-0,149	-6,43E-4	-0,0294	-1,27E-4	0,0903	3,91E-4	0,9	0,00389	1,71	0,00739	5,12	0,0222	3,9	0,0169
42	243	-0,0902	-3,71E-4	0,0229	9,41E-5	0,118	4,85E-4	0,949	0,0039	1,77	0,00726	5,22	0,0215	4	0,0165
44	255	-0,0964	-3,78E-4	0,0343	1,34E-4	0,114	4,48E-4	1,09	0,00428	1,81	0,00709	5,3	0,0208	4,03	0,0158
46	267	-0,0576	-2,15E-4	0,162	6,06E-4	0,177	6,61E-4	1,1	0,00411	1,85	0,00692	5,46	0,0204	4,17	0,0156
48	280	-0,00656	-2,35E-5	0,228	8,17E-4	0,257	9,19E-4	1,23	0,00441	2,06	0,00737	5,48	0,0196	4,2	0,015
50	292	0,0906	3,11E-4	0,307	0,00105	0,418	0,00143	1,27	0,00437	2,12	0,00726	5,47	0,0188	4,33	0,0148
52	304	0,113	3,73E-4	0,368	0,00121	0,442	0,00146	1,39	0,00459	2,13	0,007	5,54	0,0182	4,37	0,0144
54	316	0,134	4,25E-4	0,471	0,00149	0,512	0,00162	1,49	0,0047	2,2	0,00697	5,65	0,0179	4,48	0,0142
56	328	0,221	6,73E-4	0,486	0,00148	0,589	0,0018	1,57	0,0048	2,38	0,00727	5,73	0,0175	4,49	0,0137
58	340	0,213	6,25E-4	0,588	0,00173	0,615	0,00181	1,61	0,00474	2,53	0,00745	5,84	0,0172	4,63	0,0136
60	352	0,285	8,09E-4	0,685	0,00194	0,66	0,00187	1,7	0,00483	2,17	0,00615	5,94	0,0169	4,68	0,0133
62	364	0,447	0,00123	0,579	0,00159	0,835	0,00229	1,81	0,00497	2,36	0,00648	5,95	0,0163	4,75	0,013
64	376	0,502	0,00133	0,696	0,00185	0,896	0,00238	1,93	0,00511	2,44	0,00648	6,12	0,0163	4,91	0,013
66	389	0,617	0,00159	0,744	0,00191	0,992	0,00255	2	0,00514	2,57	0,0066	6,13	0,0158	4,98	0,0128
68	401	0,713	0,00178	0,872	0,00218	1,09	0,00272	2,08	0,00519	2,63	0,00656	6,24	0,0156	5,05	0,0126
70	413	0,757	0,00183	0,873	0,00211	1,09	0,00264	2,25	0,00546	2,71	0,00657	6,28	0,0152	5,03	0,0122
72	425	0,791	0,00186	0,974	0,00229	1,13	0,00266	2,41	0,00568	2,75	0,00647	6,41	0,0151	5,1	0,012
74	437	0,951	0,00218	1,04	0,00239	1,29	0,00295	2,45	0,0056	2,94	0,00672	6,36	0,0145	5,21	0,0119
76	449	0,978	0,00218	1,23	0,00274	1,35	0,003	2,53	0,00563	2,96	0,00659	6,5	0,0145	5,4	0,012
78	461	1,27	0,00275	1,31	0,00283	1,31	0,00285	2,97	0,00643	2,76	0,00598	6,26	0,0136	5,57	0,0121
80	473	1,13	0,00238	1,35	0,00286	1,54	0,00325	2,75	0,00582	3,19	0,00674	6,54	0,0138	5,47	0,0116
82	485	1,18	0,00243	1,52	0,00313	1,64	0,00337	2,87	0,00591	3,18	0,00655	6,65	0,0137	5,62	0,0116
84	498	1,34	0,00269	1,55	0,00311	1,79	0,0036	2,97	0,00596	3,39	0,00681	6,62	0,0133	5,62	0,0113
86	510	1,4	0,00275	1,7	0,00334	1,85	0,00363	3,07	0,00601	3,49	0,00684	6,68	0,0131	5,79	0,0114
88	522	1,36	0,00261	1,74	0,00333	1,79	0,00343	3,34	0,0064	3,5	0,0067	6,81	0,013	5,81	0,0111
90	534	1,55	0,00291	1,86	0,00348	1,95	0,00365	3,4	0,00636	3,66	0,00686	6,84	0,0128	5,96	0,0112
92	546	1,61	0,00295	1,93	0,00353	2,04	0,00373	3,56	0,00652	3,76	0,00689	6,98	0,0128	6,02	0,011
94	558	1,75	0,00314	2,04	0,00366	2,15	0,00385	3,62	0,00649	3,85	0,0069	6,99	0,0125	6,17	0,0111
96	570	1,74	0,00304	2,02	0,00354	2,17	0,0038	3,82	0,0067	3,99	0,00699	7,13	0,0125	6,14	0,0108
98	582	1,75	0,003	2,1	0,00361	2,25	0,00386	3,91	0,00672	4,07	0,007	7,26	0,0125	6,27	0,0108

100	594	1,99	0,00334	2,24	0,00377	2,48	0,00416	3,86	0,0065	4,24	0,00714	7,33	0,0123	6,42	0,0108
102	607	1,88	0,0031	2,37	0,0039	2,47	0,00407	3,99	0,00658	4,3	0,00709	7,68	0,0127	6,55	0,0108
104	619	1,92	0,0031	2,49	0,00402	2,61	0,00421	4,13	0,00667	4,48	0,00723	7,77	0,0126	6,73	0,0109
106	631	2,06	0,00326	2,61	0,00414	2,74	0,00435	4,22	0,00669	4,6	0,00729	7,86	0,0125	6,85	0,0109
108	643	2,04	0,00317	2,54	0,00395	2,74	0,00427	4,5	0,007	4,7	0,0073	8	0,0124	6,87	0,0107
110	655	2,01	0,00306	2,7	0,00412	2,83	0,00432	4,62	0,00705	4,71	0,00719	8,19	0,0125	6,99	0,0107
112	667	2,06	0,00308	2,7	0,00405	2,92	0,00438	4,73	0,00708	4,84	0,00726	8,22	0,0123	7,04	0,0105
114	679	2,25	0,00331	2,9	0,00427	3,19	0,0047	4,68	0,00688	5,03	0,0074	8,24	0,0121	7,33	0,0108
116	691	2,26	0,00327	2,91	0,0042	3,29	0,00476	4,88	0,00706	5,06	0,00732	8,4	0,0121	7,39	0,0107
118	703	2,3	0,00327	3	0,00427	3,35	0,00476	5,02	0,00713	5,12	0,00728	8,6	0,0122	7,54	0,0107
120	716	2,51	0,0035	3,06	0,00428	3,54	0,00495	5,08	0,00709	5,39	0,00753	8,69	0,0121	7,55	0,0106
122	728	2,59	0,00356	3,09	0,00424	3,48	0,00478	5,32	0,00731	5,4	0,00742	8,89	0,0122	7,57	0,0104
124	740	2,74	0,00371	3,2	0,00432	3,61	0,00487	5,48	0,0074	5,51	0,00745	8,9	0,012	7,66	0,0104
126	752	3,04	0,00404	3,31	0,0044	3,9	0,00518	5,48	0,00729	5,76	0,00766	8,96	0,0119	8	0,0106
128	764	2,94	0,00385	3,4	0,00446	3,88	0,00508	5,73	0,0075	5,66	0,00741	9,18	0,012	7,99	0,0105
130	776	2,91	0,00375	3,54	0,00456	4,05	0,00522	5,83	0,00752	5,79	0,00746	9,33	0,012	8,14	0,0105
132	788	2,9	0,00368	3,66	0,00465	4,09	0,00519	5,99	0,0076	5,85	0,00742	9,4	0,0119	8,24	0,0105
134	800	3,36	0,0042	3,72	0,00465	4,33	0,00541	6,09	0,00761	6,16	0,0077	9,53	0,0119	8,29	0,0104
136	812	3,42	0,00421	3,76	0,00463	4,39	0,00541	6,26	0,0077	6,28	0,00773	9,56	0,0118	8,2	0,0101
138	825	3,41	0,00414	3,89	0,00472	4,66	0,00565	6,31	0,00765	6,25	0,00759	9,73	0,0118	8,55	0,0104
140	837	3,39	0,00405	3,99	0,00476	4,54	0,00542	6,58	0,00787	6,48	0,00774	9,67	0,0116	8,56	0,0102
142	849	3,67	0,00432	4,14	0,00488	4,7	0,00553	6,68	0,00788	6,59	0,00777	9,77	0,0115	8,75	0,0103
144	861	3,89	0,00452	4,29	0,00498	4,88	0,00567	6,78	0,00788	6,76	0,00786	9,9	0,0115	8,9	0,0103
146	873	3,85	0,00441	4,28	0,0049	4,81	0,00551	7,02	0,00804	6,9	0,0079	10	0,0115	8,98	0,0103
148	885	3,86	0,00436	4,58	0,00517	4,98	0,00562	7,05	0,00796	6,91	0,00781	10,4	0,0117	9,43	0,0107
150	897	3,94	0,00439	4,6	0,00513	5,08	0,00566	7,26	0,00809	7,08	0,00789	10,7	0,0119	9,69	0,0108
152	909	4,18	0,0046	4,65	0,00512	5,34	0,00587	7,35	0,00808	7,4	0,00814	10,7	0,0118	9,72	0,0107
154	921	4,21	0,00457	4,7	0,0051	5,4	0,00586	7,52	0,00816	7,47	0,0081	11	0,0119	9,93	0,0108
156	934	4,3	0,00461	4,82	0,00516	5,53	0,00592	7,6	0,00814	7,61	0,00815	11,1	0,0119	10,1	0,0108
158	946	4,4	0,00465	4,89	0,00517	5,54	0,00585	7,81	0,00826	7,7	0,00815	11,3	0,012	10,2	0,0108
160	958	4,45	0,00465	5,15	0,00538	5,8	0,00606	7,82	0,00817	7,89	0,00824	11,5	0,012	10,5	0,011
162	970	4,58	0,00472	5,24	0,0054	5,94	0,00613	7,93	0,00818	8,01	0,00826	11,7	0,012	10,7	0,011
164	982	4,61	0,0047	5,26	0,00536	5,88	0,00599	8,23	0,00838	8,08	0,00823	12	0,0122	10,7	0,0109
166	994	4,83	0,00486	5,37	0,0054	6,17	0,0062	8,34	0,00839	8,43	0,00848	12,1	0,0122	11	0,011

168	1 010	4,92	0,00489	5,5	0,00546	6,21	0,00617	8,5	0,00845	8,44	0,00838	12,2	0,0122	11,1	0,011
170	1 020	5,11	0,00502	5,57	0,00547	6,26	0,00615	8,73	0,00857	8,59	0,00844	12,4	0,0121	11,3	0,0111
172	1 030	5,16	0,00501	5,83	0,00566	6,39	0,00621	8,75	0,00849	8,76	0,0085	12,8	0,0124	11,6	0,0113
174	1 040	5,33	0,00511	5,98	0,00574	6,64	0,00637	8,88	0,00852	8,99	0,00862	12,9	0,0124	11,8	0,0113
176	1 050	5,34	0,00507	6,14	0,00582	6,56	0,00622	9,06	0,00859	9,04	0,00857	13,1	0,0125	12,1	0,0114
178	1 070	5,58	0,00523	6,12	0,00574	6,69	0,00627	9,36	0,00877	9,33	0,00874	13,3	0,0125	12,1	0,0113
180	1 080	5,73	0,00531	6,37	0,00591	6,84	0,00634	9,48	0,00879	9,44	0,00875	13,6	0,0126	12,3	0,0114
182	1 090	5,81	0,00533	6,44	0,0059	7,03	0,00644	9,6	0,0088	9,63	0,00883	13,7	0,0126	12,6	0,0116
184	1 100	5,89	0,00534	6,61	0,00599	7,03	0,00637	9,85	0,00893	9,73	0,00882	14	0,0127	12,7	0,0116
186	1 120	5,93	0,00532	6,86	0,00615	7,21	0,00646	9,91	0,00888	9,87	0,00885	14,3	0,0128	13	0,0117
188	1 130	6	0,00532	6,86	0,00608	7,22	0,0064	10,1	0,00898	10	0,00891	14,5	0,0129	13,1	0,0117
190	1 140	6,31	0,00554	6,78	0,00595	7,33	0,00643	10,4	0,00909	10,4	0,00912	14,7	0,0129	13,4	0,0117
192	1 150	6,37	0,00553	6,98	0,00606	7,41	0,00644	10,4	0,00906	10,5	0,00909	14,8	0,0129	13,6	0,0118
194	1 160	6,62	0,00569	7,11	0,00611	7,56	0,0065	10,6	0,00911	10,7	0,0092	15,1	0,0129	13,8	0,0118
196	1 180	6,77	0,00576	7,29	0,0062	7,74	0,00658	10,7	0,00912	10,9	0,00925	15,2	0,0129	14	0,0119
198	1 190	7	0,0059	7,28	0,00613	7,83	0,00659	11	0,00927	11,1	0,00932	15,4	0,013	14	0,0118
200	1 200	7,08	0,0059	7,5	0,00625	7,88	0,00657	11,2	0,00933	11,2	0,00935	15,5	0,0129	14,3	0,0119

Time	Shear Rate	Shear Stress	Viscosity	Shear Stress	Viscosity	Shear Stress	Viscosity	Shear Stress	Viscosity	Shear Stress	Viscosity	Shear Stress	Viscosity	Shear Stress	Viscosity
[s]	[1/s]	[Pa]	[Pa·s]	[Pa]	[Pa·s]	[Pa]	[Pa·s]	[Pa]	[Pa·s]	[Pa]	[Pa·s]	[Pa]	[Pa·s]	[Pa]	[Pa·s]
Number of Intervals:		*CNC-BT-WDFs (6 wt %) 0.0 % 40°C S.W.*	*CNC-BT-WDFs (6 wt %) 0.0 % 40°C S.W.*	*CNC-BT-WDFs (6 wt %) 0.4 % 40°C S.W.*	*CNC-BT-WDFs (6 wt %) 0.4 % 40°C S.W.*	*CNC-BT-WDFs (6 wt %) 0.8 % 40°C S.W.*	*CNC-BT-WDFs (6 wt %) 0.8 % 40°C S.W.*	*CNC-BT-WDFs (6 wt %) 1.2 % 40°C S.W.*	*CNC-BT-WDFs (6 wt %) 1.2 % 40°C S.W.*	*CNC-BT-WDFs (6 wt %) 1.6 % 40°C S.W.*	*CNC-BT-WDFs (6 wt %) 1.6 % 40°C S.W.*	*CNC-BT-WDFs (6 wt %) 2.0 % 40°C S.W.*	*CNC-BT-WDFs (6 wt %) 2.0 % 40°C S.W.*	*CNC-BT-WDFs (6 wt %) 2.4 % 40°C S.W.*	*CNC-BT-WDFs (6 wt %) 2.4 % 40°C S.W.*
2	0,999	-1,26	-1,26	-0,453	-0,453	-0,627	-0,626	-1,02	-1,02	-0,0513	-0,0512	0,863	0,862	0,751	0,751
4	13,1	-0,814	-0,0621	-0,428	-0,0326	-0,43	-0,0328	-0,469	-0,0358	0,658	0,0502	1,9	0,145	2,3	0,175
6	25,2	-0,589	-0,0233	-0,508	-0,0201	-0,469	-0,0186	-0,274	-0,0109	0,92	0,0365	2,35	0,0932	2,72	0,108
8	37,3	-0,447	-0,012	-0,45	-0,0121	-0,433	-0,0116	-0,126	-0,00336	0,987	0,0264	2,63	0,0705	2,81	0,0752
10	49,4	-0,454	-0,00919	-0,466	-0,00943	-0,4	-0,00809	-0,0407	-8,23E-4	1,1	0,0223	2,71	0,0549	2,94	0,0594
12	61,6	-0,511	-0,0083	-0,376	-0,0061	-0,4	-0,0065	-0,0386	-6,27E-4	1,27	0,0207	2,83	0,046	3,13	0,0509
14	73,7	-0,382	-0,00519	-0,354	-0,0048	-0,372	-0,00505	0,00406	5,51E-5	1,41	0,0192	3,01	0,0408	3,27	0,0444
16	85,8	-0,451	-0,00525	-0,311	-0,00362	-0,358	-0,00418	0,0532	6,2E-4	1,56	0,0182	3,12	0,0363	3,37	0,0393
18	97,9	-0,431	-0,0044	-0,357	-0,00365	-0,335	-0,00342	0,0665	6,8E-4	1,59	0,0162	3,23	0,033	3,53	0,0361
20	110	-0,367	-0,00334	-0,32	-0,00291	-0,296	-0,00269	0,108	9,85E-4	1,71	0,0156	3,37	0,0307	3,77	0,0343
22	122	-0,343	-0,0028	-0,25	-0,00205	-0,304	-0,00249	0,0858	7,02E-4	1,78	0,0146	3,54	0,029	3,88	0,0318
24	134	-0,264	-0,00196	-0,281	-0,0021	-0,23	-0,00171	0,138	0,00103	1,86	0,0139	3,64	0,0271	3,97	0,0296
26	146	-0,209	-0,00143	-0,197	-0,00134	-0,198	-0,00135	0,209	0,00143	1,97	0,0135	3,81	0,026	4,17	0,0285
28	158	-0,133	-8,41E-4	-0,258	-0,00163	-0,17	-0,00107	0,264	0,00167	2,06	0,013	3,92	0,0248	4,25	0,0268
30	171	-0,0573	-3,36E-4	-0,163	-9,55E-4	-0,0837	-4,91E-4	0,325	0,00191	2,09	0,0122	4,04	0,0237	4,49	0,0263
32	183	-0,00707	-3,87E-5	-0,15	-8,21E-4	-0,0618	-3,38E-4	0,358	0,00196	2,07	0,0114	4,24	0,0232	4,52	0,0247
34	195	0,0281	1,44E-4	-0,113	-5,78E-4	0,0339	1,74E-4	0,389	0,002	2,13	0,0109	4,32	0,0222	4,77	0,0245
36	207	0,0713	3,45E-4	-0,00912	-4,41E-5	0,0332	1,6E-4	0,47	0,00227	2,24	0,0108	4,44	0,0215	4,88	0,0236

38	219	0,104	4,73E-4	0,0938	4,28E-4	0,129	5,88E-4	0,458	0,00209	2,28	0,0104	4,57	0,0209	5,03	0,023
40	231	0,195	8,42E-4	0,178	7,7E-4	0,163	7,06E-4	0,518	0,00224	2,31	0,00998	4,65	0,0201	5,12	0,0222
42	243	0,258	0,00106	0,289	0,00119	0,221	9,1E-4	0,596	0,00245	2,35	0,00965	4,73	0,0194	5,18	0,0213
44	255	0,328	0,00129	0,322	0,00126	0,349	0,00137	0,655	0,00256	2,33	0,00913	4,92	0,0193	5,26	0,0206
46	267	0,35	0,00131	0,428	0,0016	0,445	0,00166	0,694	0,00259	2,41	0,009	5	0,0187	5,34	0,02
48	280	0,43	0,00154	0,461	0,00165	0,532	0,0019	0,795	0,00284	2,46	0,00881	5,1	0,0182	5,35	0,0191
50	292	0,523	0,00179	0,532	0,00183	0,55	0,00189	0,932	0,0032	2,57	0,0088	5,14	0,0176	5,36	0,0184
52	304	0,576	0,0019	0,587	0,00193	0,662	0,00218	0,996	0,00328	2,57	0,00847	5,22	0,0172	5,43	0,0179
54	316	0,631	0,002	0,71	0,00225	0,753	0,00239	1,06	0,00337	2,64	0,00837	5,19	0,0164	5,49	0,0174
56	328	0,745	0,00227	0,693	0,00211	0,812	0,00248	1,18	0,00359	2,65	0,00809	5,26	0,016	5,47	0,0167
58	340	0,717	0,00211	0,866	0,00255	0,958	0,00282	1,2	0,00352	2,7	0,00795	5,3	0,0156	5,58	0,0164
60	352	0,79	0,00224	0,89	0,00253	1,06	0,00302	1,23	0,00351	2,77	0,00787	5,4	0,0153	5,65	0,016
62	364	0,991	0,00272	0,925	0,00254	1,08	0,00297	1,42	0,00391	2,84	0,0078	5,37	0,0147	5,66	0,0155
64	376	1,04	0,00276	1,08	0,00287	1,21	0,00322	1,44	0,00382	2,94	0,00781	5,46	0,0145	5,8	0,0154
66	389	1,18	0,00305	1,18	0,00304	1,29	0,00333	1,54	0,00395	3,06	0,00787	5,47	0,0141	5,88	0,0151
68	401	1,26	0,00314	1,3	0,00324	1,36	0,0034	1,65	0,00413	3,19	0,00795	5,51	0,0138	5,9	0,0147
70	413	1,4	0,00339	1,3	0,00315	1,48	0,00359	1,77	0,00428	3,18	0,00769	5,66	0,0137	5,91	0,0143
72	425	1,42	0,00334	1,4	0,00329	1,6	0,00376	1,85	0,00436	3,3	0,00776	5,69	0,0134	5,98	0,0141
74	437	1,61	0,00369	1,45	0,00332	1,62	0,00371	2,09	0,00478	3,47	0,00795	5,73	0,0131	5,95	0,0136
76	449	1,6	0,00356	1,69	0,00377	1,79	0,00399	2,12	0,00472	3,6	0,00802	5,71	0,0127	6,17	0,0137
78	461	1,66	0,00359	1,57	0,0034	1,94	0,0042	1,96	0,00425	3,52	0,00763	5,55	0,012	6,4	0,0139
80	473	1,85	0,00392	1,86	0,00393	1,96	0,00414	2,37	0,00501	3,77	0,00797	5,84	0,0123	6,34	0,0134
82	485	1,85	0,00382	1,99	0,00409	2,12	0,00437	2,46	0,00507	3,92	0,00808	5,86	0,0121	6,46	0,0133
84	498	2,02	0,00407	2,01	0,00403	2,12	0,00426	2,68	0,00539	4,01	0,00806	5,86	0,0118	6,51	0,0131
86	510	2,04	0,00401	2,12	0,00416	2,24	0,0044	2,7	0,00531	4,14	0,00811	5,91	0,0116	6,53	0,0128
88	522	2,07	0,00398	2,19	0,00419	2,49	0,00478	2,69	0,00516	4,15	0,00795	6,17	0,0118	6,67	0,0128
90	534	2,2	0,00413	2,29	0,00428	2,5	0,00468	2,85	0,00533	4,25	0,00795	6,2	0,0116	6,73	0,0126
92	546	2,33	0,00427	2,33	0,00427	2,61	0,00478	2,95	0,00541	4,35	0,00796	6,28	0,0115	6,74	0,0123
94	558	2,42	0,00434	2,46	0,0044	2,62	0,0047	3,06	0,00548	4,56	0,00817	6,31	0,0113	6,77	0,0121
96	570	2,51	0,00441	2,45	0,0043	2,84	0,00499	3,13	0,00549	4,51	0,00791	6,52	0,0114	6,81	0,0119
98	582	2,58	0,00443	2,55	0,00438	2,95	0,00507	3,25	0,00558	4,58	0,00787	6,64	0,0114	6,95	0,0119
100	594	2,69	0,00453	2,69	0,00453	2,93	0,00492	3,48	0,00586	4,75	0,00799	6,59	0,0111	7,02	0,0118
102	607	2,61	0,00431	2,8	0,00462	3,17	0,00523	3,46	0,0057	4,82	0,00795	6,86	0,0113	7,24	0,0119
104	619	2,71	0,00438	2,94	0,00475	3,27	0,00528	3,66	0,00591	4,86	0,00785	6,9	0,0112	7,39	0,0119

106	631	2,73	0,00432	3,05	0,00484	3,31	0,00525	3,82	0,00605	5,05	0,00801	6,92	0,011	7,49	0,0119
108	643	2,85	0,00443	3,04	0,00472	3,49	0,00543	3,87	0,00603	5,04	0,00783	7,15	0,0111	7,62	0,0118
110	655	2,87	0,00438	3,22	0,00492	3,72	0,00567	3,93	0,006	5,02	0,00766	7,27	0,0111	7,79	0,0119
112	667	3,03	0,00454	3,2	0,00479	3,74	0,0056	4,09	0,00613	5,1	0,00765	7,39	0,0111	7,86	0,0118
114	679	3,04	0,00447	3,4	0,005	3,74	0,0055	4,34	0,00639	5,32	0,00783	7,29	0,0107	7,96	0,0117
116	691	3,17	0,00458	3,44	0,00498	3,91	0,00565	4,44	0,00642	5,35	0,00773	7,51	0,0109	8,06	0,0117
118	703	3,27	0,00466	3,56	0,00506	4,07	0,00578	4,53	0,00644	5,41	0,0077	7,61	0,0108	8,18	0,0116
120	716	3,46	0,00484	3,59	0,00502	4,08	0,0057	4,75	0,00664	5,65	0,00789	7,68	0,0107	8,26	0,0115
122	728	3,53	0,00486	3,64	0,005	4,38	0,00602	4,76	0,00655	5,7	0,00784	7,93	0,0109	8,42	0,0116
124	740	3,82	0,00516	3,72	0,00503	4,47	0,00605	4,94	0,00668	5,84	0,00789	8,07	0,0109	8,52	0,0115
126	752	3,96	0,00527	3,95	0,00526	4,44	0,00591	5,24	0,00696	6,19	0,00823	7,95	0,0106	8,8	0,0117
128	764	3,95	0,00517	4,01	0,00525	4,64	0,00607	5,25	0,00688	6,18	0,00809	8,15	0,0107	8,91	0,0117
130	776	4,01	0,00517	4,19	0,00539	4,66	0,006	5,4	0,00695	6,44	0,00829	8,24	0,0106	8,95	0,0115
132	788	4,03	0,00511	4,32	0,00548	4,85	0,00616	5,46	0,00692	6,48	0,00822	8,31	0,0105	9,16	0,0116
134	800	4,31	0,00539	4,39	0,00548	4,78	0,00598	5,77	0,00721	6,7	0,00837	8,2	0,0102	9,08	0,0113
136	812	4,43	0,00546	4,38	0,00539	4,95	0,00609	5,89	0,00725	6,87	0,00846	8,42	0,0104	9,13	0,0112
138	825	4,48	0,00543	4,73	0,00574	5,07	0,00615	6,09	0,00739	6,98	0,00846	8,35	0,0101	9,32	0,0113
140	837	4,53	0,00541	4,64	0,00555	5,32	0,00636	6,06	0,00724	7,06	0,00844	8,63	0,0103	9,41	0,0112
142	849	4,49	0,00529	4,79	0,00564	5,41	0,00638	6,23	0,00734	7,24	0,00853	8,82	0,0104	9,52	0,0112
144	861	4,55	0,00528	4,98	0,00579	5,53	0,00642	6,39	0,00742	7,42	0,00862	8,96	0,0104	9,54	0,0111
146	873	4,73	0,00541	4,97	0,0057	5,77	0,00661	6,44	0,00738	7,3	0,00836	9,27	0,0106	9,61	0,011
148	885	4,7	0,00531	5,17	0,00584	5,88	0,00664	6,55	0,0074	7,62	0,00861	9,41	0,0106	9,8	0,0111
150	897	4,84	0,0054	5,21	0,0058	6	0,00669	6,65	0,00741	7,57	0,00844	9,59	0,0107	9,8	0,0109
152	909	5,14	0,00566	5,26	0,00579	5,88	0,00646	6,98	0,00768	7,9	0,00868	9,54	0,0105	9,76	0,0107
154	921	5,15	0,00559	5,43	0,00589	5,99	0,0065	6,88	0,00747	8,02	0,0087	9,8	0,0106	10	0,0109
156	934	5,24	0,00561	5,58	0,00598	6,1	0,00653	6,85	0,00734	8,18	0,00876	9,92	0,0106	10,3	0,011
158	946	5,34	0,00564	5,61	0,00594	6,24	0,0066	6,92	0,00732	8,34	0,00881	10,2	0,0108	10,5	0,0111
160	958	5,46	0,0057	5,86	0,00612	6,15	0,00642	7,06	0,00737	8,49	0,00886	10,2	0,0107	10,8	0,0113
162	970	5,62	0,0058	5,97	0,00616	6,25	0,00645	7,22	0,00745	8,64	0,00891	10,3	0,0107	11	0,0113
164	982	5,61	0,00571	6,04	0,00615	6,55	0,00667	7,21	0,00734	8,41	0,00856	10,7	0,0109	11	0,0113
166	994	5,86	0,0059	6,1	0,00614	6,51	0,00655	7,48	0,00753	8,6	0,00866	10,8	0,0109	11,3	0,0113
168	1 010	5,92	0,00588	6,21	0,00617	6,65	0,00661	7,52	0,00747	8,98	0,00892	11,1	0,011	11,4	0,0114
170	1 020	6,06	0,00595	6,23	0,00612	6,78	0,00666	7,7	0,00756	8,95	0,00879	11,1	0,0109	11,6	0,0114
172	1 030	6,12	0,00594	6,57	0,00638	6,72	0,00653	7,84	0,0076	9,17	0,0089	11,3	0,011	12	0,0116

174	1 040	6,4	0,00613	6,66	0,00639	6,79	0,00652	8,06	0,00773	9,47	0,00908	11,5	0,0111	12,1	0,0116
176	1 050	6,45	0,00611	6,87	0,00652	7,14	0,00677	8,04	0,00762	9,62	0,00912	11,8	0,0112	12,4	0,0117
178	1 070	6,82	0,00639	6,79	0,00636	7,31	0,00685	8,31	0,00779	9,62	0,00901	12,1	0,0114	12,5	0,0117
180	1 080	7,01	0,0065	7,03	0,00651	7,38	0,00684	8,44	0,00782	9,74	0,00902	12,4	0,0115	12,8	0,0119
182	1 090	7,19	0,00659	7,21	0,00661	7,32	0,00671	8,57	0,00786	10	0,00917	12,4	0,0114	13	0,0119
184	1 100	7,28	0,0066	7,3	0,00662	7,61	0,0069	8,63	0,00782	10,1	0,00915	12,7	0,0115	13,1	0,0119
186	1 120	7,34	0,00658	7,56	0,00678	7,65	0,00686	8,85	0,00794	10,2	0,00919	12,9	0,0115	13,4	0,012
188	1 130	7,39	0,00656	7,69	0,00682	7,87	0,00698	8,97	0,00796	10,3	0,00917	13	0,0116	13,7	0,0122
190	1 140	7,69	0,00675	7,63	0,00669	8,02	0,00703	9,17	0,00804	10,5	0,00919	13,3	0,0117	13,6	0,0119
192	1 150	7,74	0,00672	7,91	0,00687	8,14	0,00707	9,35	0,00812	10,6	0,00923	13,5	0,0117	13,9	0,0121
194	1 160	8,06	0,00693	7,97	0,00685	8,19	0,00704	9,55	0,00821	10,9	0,00937	13,6	0,0117	14,1	0,0121
196	1 180	8,1	0,00689	8,23	0,007	8,27	0,00704	9,71	0,00826	11,1	0,00948	13,8	0,0117	14,4	0,0122
198	1 190	8,42	0,00709	8,22	0,00692	8,44	0,0071	9,98	0,0084	11,3	0,0095	14,1	0,0118	14,4	0,0121
200	1 200	8,55	0,00713	8,37	0,00698	8,66	0,00722	10,1	0,00842	11,5	0,00955	14,3	0,0119	14,7	0,0122

Time	Shear Rate	Shear Stress	Viscosity	Shear Stress	Viscosity	Shear Stress	Viscosity	Shear Stress	Viscosity	Shear Stress	Viscosity	Shear Stress	Viscosity	Shear Stress	Viscosity
[s]	[1/s]	[Pa]	[Pa·s]	[Pa]	[Pa·s]	[Pa]	[Pa·s]	[Pa]	[Pa·s]	[Pa]	[Pa·s]	[Pa]	[Pa·s]	[Pa]	[Pa·s]
Number of Intervals:		*CNC-BT-WDFs (6 wt %) 0.0 % 50°C S.W.*	*CNC-BT-WDFs (6 wt %) 0.0 % 50°C S.W.*	*CNC-BT-WDFs (6 wt %) 0.4 % 50°C S.W.*	*CNC-BT-WDFs (6 wt %) 0.4 % 50°C S.W.*	*CNC-BT-WDFs (6 wt %) 0.8 % 50°C S.W.*	*CNC-BT-WDFs (6 wt %) 0.8 % 50°C S.W.*	*CNC-BT-WDFs (6 wt %) 1.2 % 50°C S.W.*	*CNC-BT-WDFs (6 wt %) 1.2 % 50°C S.W.*	*CNC-BT-WDFs (6 wt %) 1.6 % 50°C S.W.*	*CNC-BT-WDFs (6 wt %) 1.6 % 50°C S.W.*	*CNC-BT-WDFs (6 wt %) 2.0 % 50°C S.W.*	*CNC-BT-WDFs (6 wt %) 2.0 % 50°C S.W.*	*CNC-BT-WDFs (6 wt %) 2.4 % 50°C S.W.*	*CNC-BT-WDFs (6 wt %) 2.4 % 50°C S.W.*
2	0,999	-0,759	-0,758	-0,649	-0,649	-0,486	-0,486	-0,776	-0,776	-0,403	-0,403	0,469	0,469	0,755	0,755
4	13,1	-0,432	-0,033	-0,306	-0,0234	-0,275	-0,021	-0,308	-0,0235	0,429	0,0327	2,01	0,153	2,29	0,175
6	25,2	-0,491	-0,0195	-0,409	-0,0162	-0,252	-0,01	-0,0852	-0,00338	0,808	0,032	2,43	0,0964	2,77	0,11
8	37,3	-0,5	-0,0134	-0,46	-0,0123	-0,285	-0,00762	0,0521	0,00139	0,789	0,0211	2,58	0,0692	2,85	0,0763
10	49,4	-0,453	-0,00917	-0,467	-0,00944	-0,232	-0,00469	0,107	0,00217	0,91	0,0184	2,78	0,0561	2,96	0,0599
12	61,6	-0,469	-0,00762	-0,434	-0,00704	-0,288	-0,00467	0,13	0,00212	0,992	0,0161	2,86	0,0465	3,09	0,0502
14	73,7	-0,459	-0,00624	-0,468	-0,00635	-0,314	-0,00427	0,152	0,00207	0,989	0,0134	2,95	0,0401	3,11	0,0422
16	85,8	-0,409	-0,00477	-0,451	-0,00526	-0,249	-0,0029	0,217	0,00253	1,09	0,0127	3,07	0,0358	3,27	0,0381
18	97,9	-0,398	-0,00406	-0,423	-0,00432	-0,232	-0,00237	0,239	0,00244	1,26	0,0128	3,15	0,0321	3,38	0,0346
20	110	-0,419	-0,00381	-0,387	-0,00352	-0,183	-0,00166	0,211	0,00192	1,4	0,0127	3,24	0,0295	3,56	0,0324
22	122	-0,381	-0,00312	-0,375	-0,00307	-0,154	-0,00126	0,242	0,00198	1,45	0,0119	3,4	0,0279	3,7	0,0303
24	134	-0,404	-0,00301	-0,442	-0,0033	-0,141	-0,00105	0,303	0,00226	1,46	0,0108	3,54	0,0264	3,8	0,0283
26	146	-0,324	-0,00221	-0,379	-0,00259	-0,0986	-6,74E-4	0,313	0,00214	1,55	0,0106	3,72	0,0254	4,03	0,0275
28	158	-0,33	-0,00209	-0,322	-0,00203	-0,062	-3,91E-4	0,363	0,00229	1,68	0,0106	3,87	0,0244	4,13	0,026
30	171	-0,294	-0,00173	-0,311	-0,00182	-0,0363	-2,13E-4	0,433	0,00254	1,8	0,0105	3,98	0,0233	4,35	0,0255
32	183	-0,298	-0,00163	-0,238	-0,0013	-0,0181	-9,92E-5	0,453	0,00248	1,83	0,01	4,11	0,0225	4,4	0,0241
34	195	-0,272	-0,0014	-0,177	-9,07E-4	-0,00336	-1,73E-5	0,485	0,00249	1,88	0,00967	4,21	0,0216	4,55	0,0233

36	207	-0,202	-9,75E-4	-0,166	-8,03E-4	0,107	5,18E-4	0,508	0,00246	1,93	0,00935	4,32	0,0209	4,61	0,0223
38	219	-0,166	-7,59E-4	-0,00734	-3,35E-5	0,107	4,91E-4	0,568	0,00259	1,98	0,00905	4,51	0,0206	4,77	0,0218
40	231	-0,12	-5,2E-4	0,0972	4,21E-4	0,235	0,00102	0,604	0,00262	2	0,00867	4,61	0,0199	4,91	0,0212
42	243	-0,0586	-2,41E-4	0,127	5,21E-4	0,254	0,00105	0,682	0,00281	2,02	0,00831	4,7	0,0193	4,96	0,0204
44	255	-0,0568	-2,23E-4	0,146	5,7E-4	0,254	9,94E-4	0,686	0,00268	2,02	0,00793	4,83	0,0189	5,03	0,0197
46	267	0,0151	5,66E-5	0,256	9,57E-4	0,316	0,00118	0,759	0,00284	2,12	0,00792	4,89	0,0183	5,19	0,0194
48	280	0,0368	1,32E-4	0,259	9,27E-4	0,409	0,00146	0,878	0,00314	2,13	0,00763	4,95	0,0177	5,22	0,0187
50	292	0,126	4,31E-4	0,324	0,00111	0,465	0,0016	1,06	0,00363	2,14	0,00733	4,98	0,0171	5,25	0,018
52	304	0,138	4,54E-4	0,368	0,00121	0,494	0,00162	0,997	0,00328	2,24	0,00736	5,05	0,0166	5,27	0,0174
54	316	0,231	7,31E-4	0,442	0,0014	0,58	0,00184	1,03	0,00326	2,3	0,00729	5,08	0,0161	5,33	0,0169
56	328	0,245	7,47E-4	0,469	0,00143	0,603	0,00184	1,05	0,0032	2,37	0,00721	5,11	0,0156	5,38	0,0164
58	340	0,357	0,00105	0,656	0,00193	0,671	0,00197	1,09	0,00322	2,47	0,00727	5,18	0,0152	5,48	0,0161
60	352	0,417	0,00118	0,693	0,00197	0,731	0,00208	1,16	0,00329	2,52	0,00717	5,25	0,0149	5,55	0,0157
62	364	0,461	0,00127	0,716	0,00197	0,829	0,00228	1,35	0,0037	2,55	0,007	5,15	0,0141	5,49	0,0151
64	376	0,585	0,00155	0,87	0,00231	0,887	0,00236	1,35	0,00357	2,71	0,00719	5,26	0,014	5,6	0,0149
66	389	0,659	0,0017	0,924	0,00238	1,01	0,00259	1,45	0,00373	2,78	0,00716	5,28	0,0136	5,64	0,0145
68	401	0,75	0,00187	0,994	0,00248	1,11	0,00276	1,55	0,00388	2,85	0,00712	5,25	0,0131	5,63	0,0141
70	413	0,701	0,0017	0,941	0,00228	1,08	0,00263	1,59	0,00385	2,86	0,00693	5,36	0,013	5,62	0,0136
72	425	0,767	0,0018	1,03	0,00242	1,13	0,00267	1,63	0,00385	3,02	0,0071	5,45	0,0128	5,66	0,0133
74	437	0,851	0,00195	1,07	0,00244	1,28	0,00293	1,84	0,00422	3,02	0,00692	5,32	0,0122	5,64	0,0129
76	449	1,02	0,00227	1,27	0,00282	1,37	0,00305	1,85	0,00411	3,22	0,00716	5,42	0,0121	5,81	0,0129
78	461	0,849	0,00184	1,5	0,00325	1,67	0,00363	1,82	0,00395	3,42	0,00741	5,64	0,0122	5,88	0,0127
80	473	1,07	0,00225	1,34	0,00284	1,54	0,00325	2,1	0,00445	3,31	0,00699	5,45	0,0115	5,8	0,0123
82	485	1,24	0,00255	1,51	0,0031	1,66	0,00343	2,23	0,0046	3,5	0,00721	5,45	0,0112	5,93	0,0122
84	498	1,31	0,00263	1,52	0,00306	1,78	0,00358	2,38	0,00479	3,54	0,00712	5,39	0,0108	5,88	0,0118
86	510	1,34	0,00263	1,63	0,00321	1,87	0,00367	2,39	0,00468	3,67	0,0072	5,4	0,0106	6	0,0118
88	522	1,32	0,00252	1,69	0,00324	1,81	0,00347	2,4	0,00461	3,74	0,00716	5,6	0,0107	6,09	0,0117
90	534	1,42	0,00265	1,81	0,00339	1,99	0,00373	2,58	0,00484	3,89	0,00729	5,62	0,0105	6,07	0,0114
92	546	1,41	0,00258	1,85	0,00338	2,05	0,00375	2,65	0,00485	3,89	0,00712	5,67	0,0104	6,02	0,011
94	558	1,54	0,00276	1,95	0,0035	2,21	0,00395	2,82	0,00506	3,99	0,00714	5,72	0,0102	6,07	0,0109
96	570	1,49	0,00261	1,89	0,00332	2,22	0,0039	2,86	0,00502	4,02	0,00705	5,91	0,0104	6,09	0,0107
98	582	1,54	0,00265	1,98	0,00341	2,29	0,00393	2,95	0,00507	4,12	0,00707	5,97	0,0103	6,16	0,0106

100	594	1,76	0,0029 7	2,1	0,0035 3	2,5	0,0042	3,22	0,0054 2	4,16	0,007	6,03	0,0101	6,33	0,0106
102	607	1,84	0,0030 3	2,21	0,0036 5	2,57	0,0042 3	3,18	0,0052 5	4,24	0,0069 8	6,22	0,0103	6,5	0,0107
104	619	1,93	0,0031 2	2,31	0,0037 3	2,64	0,0042 6	3,35	0,0054 2	4,39	0,0070 9	6,32	0,0102	6,59	0,0107
106	631	2,02	0,0032 1	2,42	0,0038 4	2,8	0,0044 4	3,51	0,0055 7	4,38	0,0069 4	6,32	0,01	6,71	0,0106
108	643	1,97	0,0030 7	2,42	0,0037 6	2,8	0,0043 5	3,5	0,0054 5	4,34	0,0067 5	6,46	0,01	6,73	0,0105
110	655	2,16	0,0032 9	2,6	0,0039 6	2,82	0,0043 1	3,53	0,0053 8	4,57	0,0069 8	6,63	0,0101	6,99	0,0107
112	667	2,15	0,0032 2	2,57	0,0038 5	2,91	0,0043 6	3,52	0,0052 7	4,53	0,0068	6,67	0,01	6,96	0,0104
114	679	2,38	0,0035	2,79	0,0041	3,13	0,0046 1	3,75	0,0055 2	4,78	0,0070 3	6,67	0,0098 2	7,08	0,0104
116	691	2,38	0,0034 4	2,79	0,0040 4	3,09	0,0044 7	3,88	0,0056 2	4,88	0,0070 7	6,72	0,0097 2	7,18	0,0104
118	703	2,48	0,0035 2	2,9	0,0041 2	3,08	0,0043 8	4	0,0056 8	5,02	0,0071 3	6,97	0,0099 1	7,27	0,0103
120	716	2,57	0,0035 9	2,99	0,0041 8	3,23	0,0045 1	4,21	0,0058 8	5,13	0,0071 6	6,92	0,0096 7	7,27	0,0102
122	728	2,57	0,0035 3	3,02	0,0041 6	3,23	0,0044 4	4,16	0,0057 1	5,3	0,0072 8	7,2	0,0099	7,44	0,0102
124	740	2,72	0,0036 8	3,12	0,0042 1	3,33	0,0045 1	4,32	0,0058 4	5,32	0,0071 8	7,33	0,0099 1	7,55	0,0102
126	752	2,91	0,0038 6	3,25	0,0043 3	3,61	0,0048 1	4,55	0,0060 6	5,42	0,0072 1	7,16	0,0095 3	7,58	0,0101
128	764	2,98	0,0039 1	3,32	0,0043 5	3,56	0,0046 6	4,51	0,0059	5,59	0,0073 1	7,32	0,0095 8	7,81	0,0102
130	776	3,14	0,0040 5	3,45	0,0044 4	3,72	0,0048	4,64	0,0059 8	5,63	0,0072 5	7,32	0,0094 4	7,98	0,0103
132	788	3,25	0,0041 3	3,59	0,0045 5	3,8	0,0048 2	4,74	0,0060 2	5,95	0,0075 4	7,51	0,0095 2	8,03	0,0102
134	800	3,32	0,0041 5	3,57	0,0044 6	3,96	0,0049 4	4,99	0,0062 4	5,93	0,0074 1	7,38	0,0092 3	7,93	0,0099 1
136	812	3,33	0,0040 9	3,61	0,0044 4	4,02	0,0049 5	5,11	0,0062 8	6	0,0073 9	7,55	0,0093	7,96	0,0098
138	825	3,63	0,0044	3,83	0,0046 5	4,23	0,0051 2	5,15	0,0062 5	6,14	0,0074 4	7,63	0,0092 5	8,2	0,0099 4
140	837	3,56	0,0042 6	3,87	0,0046 3	4,13	0,0049 4	5,25	0,0062 8	6,3	0,0075 3	7,98	0,0095 3	8,22	0,0098 3
142	849	3,72	0,0043 8	4,03	0,0047 5	4,3	0,0050 7	5,48	0,0064 6	6,46	0,0076 1	8,19	0,0096 5	8,32	0,0098 1
144	861	3,88	0,0045	4,2	0,0048 7	4,46	0,0051 9	5,68	0,0065 9	6,67	0,0077 5	8,26	0,0096	8,35	0,0097
146	873	3,86	0,0044 2	4,12	0,0047 2	4,41	0,0050 5	5,5	0,0063	6,77	0,0077 5	8,56	0,0098 1	8,47	0,0097
148	885	4,12	0,0046 5	4,36	0,0049 3	4,59	0,0051 8	5,54	0,0062 6	7,16	0,0080 8	8,75	0,0098 8	8,74	0,0098 7
150	897	4,07	0,0045 4	4,44	0,0049 5	4,61	0,0051 3	5,63	0,0062 7	7,12	0,0079 4	8,93	0,0099 5	8,9	0,0099 2
152	909	4,08	0,0044 9	4,58	0,0050 4	4,8	0,0052 8	5,91	0,0065	7,2	0,0079 2	8,82	0,0097	9	0,0099
154	921	4,18	0,0045 4	4,63	0,0050 2	4,67	0,0050 7	5,64	0,0061 2	7,14	0,0077 5	9,1	0,0098 8	9,25	0,01
156	934	4,29	0,0046	4,72	0,0050 6	4,85	0,0052	5,78	0,0061 9	7,49	0,0080 3	9,2	0,0098 6	9,4	0,0101
158	946	4,35	0,0046	4,8	0,0050 7	4,88	0,0051 6	5,79	0,0061 2	7,67	0,0081 1	9,46	0,01	9,52	0,0101
160	958	4,62	0,0048 2	4,99	0,0052 1	5,1	0,0053 3	6,07	0,0063 3	7,5	0,0078 4	9,43	0,0098 4	9,77	0,0102
162	970	4,75	0,0048 9	5,07	0,0052 3	5,18	0,0053 4	6,08	0,0062 7	7,7	0,0079 4	9,75	0,01	9,86	0,0102
164	982	4,67	0,0047 6	5,13	0,0052 3	5,06	0,0051 5	6,09	0,0062	7,86	0,0080 1	9,97	0,0102	10,1	0,0103
166	994	4,86	0,0048 9	5,12	0,0051 5	5,24	0,0052 7	6,33	0,0063 6	7,84	0,0078 9	10	0,0101	10,1	0,0102

168	1 010	4,93	0,0049	5,19	0,00516	5,29	0,00526	6,16	0,00613	7,94	0,00789	10,2	0,0101	10,4	0,0103
170	1 020	5,1	0,005	5,25	0,00516	5,34	0,00525	6,22	0,0061	8,16	0,00801	10,4	0,0102	10,5	0,0103
172	1 030	5,39	0,00524	5,46	0,0053	5,62	0,00545	6,47	0,00628	8,49	0,00824	10,5	0,0102	10,8	0,0105
174	1 040	5,51	0,00528	5,59	0,00537	5,77	0,00553	6,67	0,0064	8,52	0,00817	10,7	0,0102	10,9	0,0104
176	1 050	5,66	0,00537	5,75	0,00545	5,86	0,00555	6,72	0,00637	8,64	0,00819	11	0,0104	11,2	0,0106
178	1 070	5,56	0,00521	5,65	0,00529	5,89	0,00552	6,83	0,0064	8,67	0,00813	11,3	0,0106	11,2	0,0105
180	1 080	5,78	0,00536	5,89	0,00546	6,03	0,00559	6,97	0,00646	8,87	0,00822	11,4	0,0106	11,6	0,0107
182	1 090	5,97	0,00547	6	0,0055	6,13	0,00562	7,21	0,00661	9,01	0,00826	11,5	0,0105	11,7	0,0107
184	1 100	6,03	0,00547	6,05	0,00548	6,12	0,00555	7,27	0,00659	9,21	0,00835	11,9	0,0108	11,8	0,0107
186	1 120	6,27	0,00562	6,26	0,00561	6,32	0,00567	7,37	0,00661	9,49	0,00851	12,1	0,0108	12,3	0,011
188	1 130	6,24	0,00554	6,44	0,00571	6,42	0,0057	7,52	0,00667	9,59	0,00851	12,1	0,0107	12,4	0,011
190	1 140	6,37	0,00559	6,35	0,00557	6,49	0,0057	7,66	0,00672	9,58	0,00841	12,3	0,0108	12,6	0,011
192	1 150	6,5	0,00565	6,71	0,00583	6,78	0,00589	7,85	0,00681	10	0,0087	12,5	0,0109	12,7	0,011
194	1 160	6,75	0,0058	6,97	0,00599	6,92	0,00595	8,07	0,00693	10,1	0,0087	12,7	0,0109	12,9	0,0111
196	1 180	6,81	0,00579	7,11	0,00605	7,09	0,00603	8,17	0,00695	10,1	0,00855	12,8	0,0108	13,2	0,0112
198	1 190	6,93	0,00584	7,05	0,00593	7,1	0,00597	8,28	0,00697	10,3	0,00864	12,9	0,0109	13,1	0,011
200	1 200	6,98	0,00581	7,05	0,00587	7,17	0,00598	8,38	0,00699	10,4	0,0087	13,2	0,011	13,3	0,0111

Time	Shear Rate	Shear Stress	Viscosity	Shear Stress	Viscosity	Shear Stress	Viscosity	Shear Stress	Viscosity	Shear Stress	Viscosity	Shear Stress	Viscosity	Shear Stress	Viscosity
[s]	[1/s]	[Pa]	[Pa·s]	[Pa]	[Pa·s]	[Pa]	[Pa·s]	[Pa]	[Pa·s]	[Pa]	[Pa·s]	[Pa]	[Pa·s]	[Pa]	[Pa·s]
Number of Intervals:		*CNC-BT-WDFs (6 wt %) 0.0 % 60°C S.W.*	*CNC-BT-WDFs (6 wt %) 0.0 % 60°C S.W.*	*CNC-BT-WDFs (6 wt %) 0.4 % 60°C S.W.*	*CNC-BT-WDFs (6 wt %) 0.4 % 60°C S.W.*	*CNC-BT-WDFs (6 wt %) 0.8 % 60°C S.W.*	*CNC-BT-WDFs (6 wt %) 0.8 % 60°C S.W.*	*CNC-BT-WDFs (6 wt %) 1.2 % 60°C S.W.*	*CNC-BT-WDFs (6 wt %) 1.2 % 60°C S.W.*	*CNC-BT-WDFs (6 wt %) 1.6 % 60°C S.W.*	*CNC-BT-WDFs (6 wt %) 1.6 % 60°C S.W.*	*CNC-BT-WDFs (6 wt %) 2.0 % 60°C S.W.*	*CNC-BT-WDFs (6 wt %) 2.0 % 60°C S.W.*	*CNC-BT-WDFs (6 wt %) 2.4 % 60°C S.W.*	*CNC-BT-WDFs (6 wt %) 2.4 % 60°C S.W.*
2	0,999	-1,26	-1,26	-0,407	-0,407	-0,32	-0,32	-1,16	-1,16	-0,0684	-0,0684	0,487	0,487	0,0716	0,0715
4	13,1	-0,606	-0,0462	-0,331	-0,0252	-0,298	-0,0227	-0,341	-0,026	0,544	0,0415	2,23	0,17	2,86	0,218
6	25,2	-0,519	-0,0206	-0,448	-0,0177	-0,235	-0,00932	-0,231	-0,00917	0,747	0,0296	2,52	0,1	3	0,119
8	37,3	-0,42	-0,0112	-0,374	-0,01	-0,272	-0,00727	-0,0305	-8,16E-4	0,806	0,0216	2,65	0,071	3,23	0,0866
10	49,4	-0,399	-0,00806	-0,377	-0,00762	-0,281	-0,00568	-0,135	-0,00273	0,962	0,0194	2,72	0,0551	3,32	0,0672
12	61,6	-0,375	-0,0061	-0,37	-0,00602	-0,298	-0,00484	-0,0724	-0,00118	0,992	0,0161	2,87	0,0465	3,34	0,0543
14	73,7	-0,361	-0,00489	-0,383	-0,00519	-0,276	-0,00374	0,0211	2,86E-4	1,11	0,015	3,05	0,0414	3,52	0,0477
16	85,8	-0,331	-0,00386	-0,353	-0,00412	-0,221	-0,00258	0,0934	0,00109	1,22	0,0143	3,13	0,0365	3,66	0,0427
18	97,9	-0,238	-0,00243	-0,266	-0,00272	-0,2	-0,00204	0,116	0,00118	1,32	0,0135	3,3	0,0337	3,76	0,0384
20	110	-0,192	-0,00174	-0,23	-0,00209	-0,152	-0,00138	0,107	9,71E-4	1,46	0,0132	3,41	0,031	3,78	0,0343
22	122	-0,136	-0,00112	-0,188	-0,00154	-0,114	-9,32E-4	0,156	0,00128	1,53	0,0125	3,54	0,029	3,96	0,0324
24	134	-0,132	-9,82E-4	-0,272	-0,00203	-0,0806	-6E-4	0,345	0,00257	1,57	0,0117	3,65	0,0272	4,17	0,0311
26	146	-0,0303	-2,07E-4	-0,195	-0,00133	-0,0722	-4,93E-4	0,305	0,00208	1,69	0,0116	3,86	0,0263	4,25	0,0291
28	158	-0,0384	-2,42E-4	-0,0979	-6,18E-4	-0,0507	-3,2E-4	0,388	0,00245	1,77	0,0112	3,96	0,025	4,45	0,0281
30	171	0,0872	5,11E-4	-0,00635	-3,72E-5	0,00922	5,41E-5	0,391	0,00229	1,86	0,0109	4,04	0,0237	4,49	0,0263
32	183	0,0447	2,45E-4	-0,00527	-2,89E-5	0,0578	3,16E-4	0,462	0,00253	1,91	0,0105	4,11	0,0225	4,65	0,0255
34	195	0,102	5,22E-4	0,0234	1,2E-4	0,149	7,63E-4	0,529	0,00272	1,95	0,01	4,21	0,0216	4,76	0,0244
36	207	0,177	8,54E-4	0,226	0,00109	0,16	7,72E-4	0,511	0,00247	2,04	0,00985	4,35	0,021	4,82	0,0233

38	219	0,2	9,15E-4	0,218	9,94E-4	0,222	0,00101	0,58	0,00265	2,04	0,0093	4,51	0,0206	5,02	0,0229
40	231	0,291	0,00126	0,293	0,00127	0,307	0,00133	0,618	0,00267	2,09	0,00906	4,54	0,0196	5,13	0,0222
42	243	0,376	0,00155	0,382	0,00157	0,358	0,00147	0,653	0,00269	2,16	0,0089	4,71	0,0194	5,19	0,0213
44	255	0,363	0,00142	0,465	0,00182	0,446	0,00175	0,776	0,00304	2,19	0,0086	4,76	0,0186	5,4	0,0212
46	267	0,46	0,00172	0,552	0,00207	0,445	0,00167	0,816	0,00305	2,19	0,00821	4,88	0,0183	5,46	0,0204
48	280	0,482	0,00172	0,572	0,00204	0,576	0,00206	0,902	0,00323	2,29	0,00819	4,94	0,0177	5,57	0,0199
50	292	0,598	0,00205	0,724	0,00248	0,612	0,0021	0,923	0,00317	2,36	0,0081	5,05	0,0173	5,58	0,0191
52	304	0,602	0,00198	0,736	0,00242	0,714	0,00235	1,03	0,00339	2,42	0,00795	5,07	0,0167	5,69	0,0187
54	316	0,708	0,00224	0,759	0,0024	0,764	0,00242	1,12	0,00356	2,45	0,00774	5,13	0,0162	5,79	0,0183
56	328	0,705	0,00215	0,82	0,0025	0,908	0,00277	1,25	0,00381	2,55	0,00779	5,14	0,0157	5,87	0,0179
58	340	0,816	0,0024	0,911	0,00268	0,89	0,00262	1,3	0,00382	2,56	0,00753	5,25	0,0154	5,95	0,0175
60	352	0,89	0,00253	0,993	0,00282	0,994	0,00282	1,38	0,00393	2,65	0,00753	5,24	0,0149	6,03	0,0171
62	364	0,991	0,00272	1,09	0,00299	1,18	0,00324	1,56	0,00428	2,82	0,00775	5,21	0,0143	6,08	0,0167
64	376	1,11	0,00296	1,21	0,00322	1,2	0,00319	1,54	0,00409	2,87	0,00763	5,34	0,0142	6,1	0,0162
66	389	1,21	0,00311	1,29	0,00333	1,35	0,00347	1,67	0,0043	2,98	0,00767	5,4	0,0139	6,16	0,0159
68	401	1,33	0,00331	1,39	0,00348	1,32	0,00331	1,68	0,0042	3,13	0,00782	5,53	0,0138	6,14	0,0153
70	413	1,32	0,00319	1,36	0,0033	1,51	0,00365	1,87	0,00454	3,21	0,00777	5,38	0,013	6,3	0,0153
72	425	1,39	0,00328	1,42	0,00333	1,51	0,00356	1,99	0,00467	3,24	0,00763	5,41	0,0127	6,34	0,0149
74	437	1,49	0,0034	1,54	0,00352	1,61	0,00368	2,05	0,00469	3,4	0,00778	5,46	0,0125	6,37	0,0146
76	449	1,58	0,00352	1,69	0,00377	1,56	0,00347	2,07	0,00461	3,4	0,00758	5,52	0,0123	6,38	0,0142
78	461	1,88	0,00408	1,63	0,00353	1,64	0,00356	2,45	0,00532	3,58	0,00777	5,38	0,0117	6,25	0,0135
80	473	1,55	0,00328	1,86	0,00393	1,81	0,00383	2,32	0,0049	3,66	0,00773	5,56	0,0118	6,57	0,0139
82	485	1,67	0,00345	2,02	0,00416	1,77	0,00364	2,33	0,00479	3,66	0,00754	5,76	0,0119	6,59	0,0136
84	498	1,74	0,00349	2,14	0,00431	1,91	0,00384	2,47	0,00497	3,83	0,00771	5,78	0,0116	6,53	0,0131
86	510	1,8	0,00353	2,25	0,00442	1,95	0,00384	2,5	0,00491	3,99	0,00783	5,9	0,0116	6,57	0,0129
88	522	1,72	0,0033	2,18	0,00417	2,12	0,00407	2,72	0,00521	4,01	0,00768	5,78	0,0111	6,81	0,013
90	534	1,89	0,00354	2,36	0,00442	2,21	0,00413	2,79	0,00523	4,11	0,00769	5,94	0,0111	6,79	0,0127
92	546	1,9	0,00347	2,41	0,00441	2,34	0,00429	2,91	0,00532	4,21	0,00771	5,97	0,0109	6,91	0,0127
94	558	2,01	0,0036	2,56	0,00459	2,4	0,0043	2,9	0,0052	4,39	0,00787	6,12	0,011	6,88	0,0123
96	570	1,97	0,00346	2,48	0,00435	2,61	0,00457	3,11	0,00545	4,4	0,00772	6,07	0,0106	7,12	0,0125
98	582	2,03	0,00348	2,54	0,00436	2,67	0,00459	3,23	0,00555	4,42	0,00759	6,13	0,0105	7,16	0,0123
100	594	2,23	0,00375	2,79	0,0047	2,74	0,00461	3,23	0,00544	4,64	0,00781	6,24	0,0105	7,13	0,012
102	607	2,23	0,00367	2,78	0,00459	2,79	0,00459	3,39	0,00559	4,58	0,00756	6,39	0,0105	7,28	0,012
104	619	2,52	0,00407	2,97	0,00481	2,88	0,00466	3,41	0,00551	4,65	0,00751	6,52	0,0105	7,34	0,0119

106	631	2,71	0,0043	3,11	0,00492	2,93	0,00464	3,49	0,00554	4,84	0,00767	6,72	0,0107	7,33	0,0116
108	643	2,68	0,00417	3,05	0,00474	3,13	0,00486	3,74	0,00581	4,97	0,00773	6,61	0,0103	7,56	0,0118
110	655	2,81	0,00429	3,1	0,00474	3,2	0,00489	3,84	0,00586	4,94	0,00754	6,83	0,0104	7,64	0,0117
112	667	2,84	0,00425	3,17	0,00476	3,36	0,00504	4	0,00599	5,1	0,00764	6,87	0,0103	7,82	0,0117
114	679	3,16	0,00466	3,45	0,00508	3,26	0,00479	3,94	0,00581	5,38	0,00793	7,07	0,0104	7,74	0,0114
116	691	3,17	0,00459	3,48	0,00504	3,4	0,00492	4,14	0,00599	5,51	0,00797	7,21	0,0104	7,9	0,0114
118	703	3,21	0,00456	3,54	0,00504	3,46	0,00492	4,29	0,0061	5,63	0,00801	7,28	0,0103	8,08	0,0115
120	716	3,34	0,00466	3,66	0,00512	3,64	0,00509	4,46	0,00623	5,83	0,00815	7,32	0,0102	8,15	0,0114
122	728	3,34	0,00458	3,63	0,00498	3,81	0,00524	4,71	0,00647	5,89	0,00809	7,34	0,0101	8,36	0,0115
124	740	3,42	0,00462	3,72	0,00504	3,96	0,00536	4,87	0,00659	5,96	0,00806	7,39	0,00999	8,46	0,0114
126	752	3,66	0,00487	4,01	0,00533	4,04	0,00537	4,8	0,00638	6,36	0,00845	7,54	0,01	8,37	0,0111
128	764	3,77	0,00493	4	0,00524	4,13	0,00541	5	0,00654	6,31	0,00826	7,64	0,01	8,65	0,0113
130	776	3,89	0,00501	4,17	0,00537	4,18	0,00539	5,04	0,0065	6,49	0,00836	7,74	0,00998	8,72	0,0112
132	788	4,02	0,0051	4,27	0,00541	4,24	0,00538	5,17	0,00656	6,49	0,00824	7,85	0,00995	8,95	0,0113
134	800	4,16	0,00519	4,49	0,00562	4,39	0,00548	5,33	0,00666	6,97	0,00871	7,9	0,00987	9	0,0112
136	812	4,23	0,00521	4,59	0,00565	4,51	0,00555	5,5	0,00677	7,14	0,00878	8,03	0,00988	9,18	0,0113
138	825	4,4	0,00534	4,74	0,00575	4,45	0,0054	5,45	0,00661	7,12	0,00864	8,19	0,00994	9,04	0,011
140	837	4,37	0,00523	4,57	0,00546	4,64	0,00555	5,77	0,00689	7,1	0,00849	8,39	0,01	9,34	0,0112
142	849	4,55	0,00536	4,68	0,00552	4,62	0,00544	5,85	0,00689	7,37	0,00869	8,64	0,0102	9,31	0,011
144	861	4,69	0,00545	4,84	0,00562	4,58	0,00532	5,9	0,00685	7,47	0,00868	8,89	0,0103	9,2	0,0107
146	873	4,62	0,00529	4,77	0,00546	4,8	0,00549	6,08	0,00697	7,57	0,00868	8,89	0,0102	9,44	0,0108
148	885	4,78	0,0054	4,9	0,00554	4,72	0,00533	6,05	0,00683	7,56	0,00854	9,29	0,0105	9,4	0,0106
150	897	4,82	0,00537	4,95	0,00552	4,85	0,00541	6,29	0,00701	7,75	0,00864	9,22	0,0103	9,71	0,0108
152	909	5,05	0,00555	5,15	0,00566	5,05	0,00556	6,35	0,00699	8,04	0,00884	9,33	0,0103	9,9	0,0109
154	921	5,08	0,00551	5,24	0,00568	5,12	0,00556	6,46	0,00701	8,11	0,00881	9,6	0,0104	10,2	0,011
156	934	5,32	0,00569	5,38	0,00577	5,14	0,00551	6,54	0,007	8,34	0,00893	9,77	0,0105	10,3	0,011
158	946	5,32	0,00563	5,4	0,00571	5,29	0,0056	6,8	0,0072	8,25	0,00873	9,91	0,0105	10,5	0,0111
160	958	5,52	0,00577	5,72	0,00597	5,2	0,00543	6,68	0,00697	8,6	0,00898	10,2	0,0106	10,5	0,011
162	970	5,63	0,0058	5,84	0,00602	5,3	0,00546	6,78	0,00699	8,78	0,00905	10,4	0,0107	10,7	0,011
164	982	5,62	0,00573	5,75	0,00585	5,53	0,00563	7,1	0,00723	8,55	0,00871	10,3	0,0105	11,2	0,0114
166	994	5,89	0,00593	5,96	0,00599	5,56	0,0056	7,17	0,00721	8,85	0,0089	10,5	0,0106	11,1	0,0112
168	1 010	5,84	0,0058	6,11	0,00607	5,69	0,00565	7,33	0,00728	9	0,00895	10,6	0,0106	11,3	0,0112
170	1 020	5,93	0,00582	6,16	0,00605	5,88	0,00577	7,48	0,00734	9,43	0,00926	10,8	0,0106	11,6	0,0114
172	1 030	6,18	0,00599	6,43	0,00624	5,81	0,00564	7,43	0,00721	9,5	0,00922	11,3	0,0109	11,6	0,0113

174	1 040	6,36	0,0061	6,59	0,00632	5,97	0,00573	7,58	0,00727	9,75	0,00935	11,4	0,0109	11,8	0,0113
176	1 050	6,43	0,0061	6,7	0,00636	6,02	0,00571	7,7	0,0073	9,7	0,0092	11,6	0,011	11,9	0,0113
178	1 070	6,43	0,00603	6,54	0,00613	6,38	0,00598	8,08	0,00757	9,98	0,00935	11,6	0,0109	12,5	0,0117
180	1 080	6,68	0,0062	6,72	0,00623	6,43	0,00596	8,18	0,00758	10,2	0,00942	11,9	0,011	12,5	0,0116
182	1 090	6,88	0,0063	6,92	0,00634	6,5	0,00596	8,22	0,00753	10,3	0,00944	12	0,011	12,6	0,0116
184	1 100	6,86	0,00622	6,87	0,00623	6,69	0,00606	8,31	0,00753	10,4	0,00944	12,1	0,011	12,9	0,0117
186	1 120	7,03	0,00631	7,28	0,00653	6,73	0,00604	8,35	0,00749	10,3	0,00926	12,6	0,0113	12,9	0,0116
188	1 130	7,28	0,00645	7,45	0,00661	6,85	0,00607	8,45	0,0075	10,5	0,00932	12,6	0,0112	13,2	0,0117
190	1 140	7,27	0,00638	7,54	0,00662	7,2	0,00632	8,66	0,0076	10,9	0,00953	12,7	0,0111	13,5	0,0119
192	1 150	7,44	0,00646	7,69	0,00668	7,21	0,00626	8,7	0,00756	10,9	0,0095	13	0,0113	13,7	0,0119
194	1 160	7,65	0,00657	7,77	0,00668	7,41	0,00637	8,86	0,00761	11,2	0,00959	13,1	0,0112	14	0,012
196	1 180	7,75	0,00659	7,97	0,00678	7,43	0,00632	8,87	0,00754	11,4	0,00969	13,4	0,0114	14,1	0,012
198	1 190	7,88	0,00663	7,87	0,00663	7,79	0,00656	9,25	0,00778	11,6	0,00979	13,3	0,0112	14,4	0,0121
200	1 200	7,94	0,00662	8,01	0,00668	7,95	0,00662	9,43	0,00786	11,8	0,00982	13,5	0,0113	14,6	0,0122

Time	Shear Rate	Shear Stress	Viscosity	Shear Stress	Viscosity	Shear Stress	Viscosity	Shear Stress	Viscosity	Shear Stress	Viscosity	Shear Stress	Viscosity	Shear Stress	Viscosity
[s]	[1/s]	[Pa]	[Pa·s]	[Pa]	[Pa·s]	[Pa]	[Pa·s]	[Pa]	[Pa·s]	[Pa]	[Pa·s]	[Pa]	[Pa·s]	[Pa]	[Pa·s]
Number of Intervals:		*CNC-BT-WDFs (6 wt %) 0.0 % 70°C S.W.*	*CNC-BT-WDFs (6 wt %) 0.0 % 70°C S.W.*	*CNC-BT-WDFs (6 wt %) 0.4 % 70°C S.W.*	*CNC-BT-WDFs (6 wt %) 0.4 % 70°C S.W.*	*CNC-BT-WDFs (6 wt %) 0.8 % 70°C S.W.*	*CNC-BT-WDFs (6 wt %) 0.8 % 70°C S.W.*	*CNC-BT-WDFs (6 wt %) 1.2 % 70°C S.W.*	*CNC-BT-WDFs (6 wt %) 1.2 % 70°C S.W.*	*CNC-BT-WDFs (6 wt %) 1.6 % 70°C S.W.*	*CNC-BT-WDFs (6 wt %) 1.6 % 70°C S.W.*	*CNC-BT-WDFs (6 wt %) 2.0 % 70°C S.W.*	*CNC-BT-WDFs (6 wt %) 2.0 % 70°C S.W.*	*CNC-BT-WDFs (6 wt %) 2.4 % 70°C S.W.*	*CNC-BT-WDFs (6 wt %) 2.4 % 70°C S.W.*
2	0,999	-0,672	-0,672	-0,598	-0,599	-0,419	-0,419	-0,481	-0,482	0,324	0,323	0,918	0,917	1,06	1,06
4	13,1	-0,564	-0,043	-0,406	-0,0309	-0,424	-0,0323	-0,0172	-0,00131	0,922	0,0703	2,03	0,155	2,72	0,208
6	25,2	-0,391	-0,0155	-0,451	-0,0179	-0,451	-0,0179	0,237	0,00939	0,97	0,0385	2,46	0,0974	3,19	0,126
8	37,3	-0,387	-0,0104	-0,482	-0,0129	-0,457	-0,0122	0,264	0,00708	1,09	0,0291	2,7	0,0722	3,37	0,0903
10	49,4	-0,472	-0,00954	-0,45	-0,00909	-0,38	-0,00768	0,288	0,00582	1,04	0,021	2,84	0,0573	3,5	0,0708
12	61,6	-0,323	-0,00524	-0,435	-0,00707	-0,455	-0,00739	0,265	0,0043	1,22	0,0199	3,13	0,0508	3,73	0,0606
14	73,7	-0,472	-0,00641	-0,457	-0,0062	-0,429	-0,00582	0,265	0,00359	1,29	0,0175	3,39	0,046	4,02	0,0545
16	85,8	-0,335	-0,00391	-0,444	-0,00517	-0,393	-0,00458	0,359	0,00418	1,36	0,0158	3,74	0,0436	4,12	0,0481
18	97,9	-0,264	-0,00269	-0,41	-0,00419	-0,386	-0,00394	0,398	0,00407	1,48	0,0151	4,15	0,0424	4,02	0,0411
20	110	-0,243	-0,00221	-0,395	-0,00359	-0,356	-0,00324	0,463	0,00421	1,55	0,0141	4,38	0,0398	4,05	0,0368
22	122	-0,171	-0,0014	-0,363	-0,00297	-0,347	-0,00284	0,546	0,00447	1,69	0,0138	4,62	0,0378	4,18	0,0343
24	134	-0,118	-8,8E-4	-0,302	-0,00225	-0,271	-0,00202	0,592	0,00441	1,92	0,0143	4,73	0,0352	4,28	0,0319
26	146	-0,0596	-4,07E-4	-0,186	-0,00127	-0,269	-0,00184	0,608	0,00416	1,84	0,0126	4,88	0,0333	4,34	0,0296
28	158	-0,0325	-2,05E-4	-0,144	-9,09E-4	-0,195	-0,00123	0,636	0,00401	1,87	0,0118	4,97	0,0313	4,48	0,0283
30	171	0,0103	6,06E-5	-0,0983	-5,77E-4	-0,183	-0,00107	0,677	0,00397	1,88	0,011	5,08	0,0298	4,52	0,0265
32	183	-0,00614	-3,36E-5	-0,0939	-5,14E-4	-0,0834	-4,56E-4	0,718	0,00393	2,04	0,0111	5,29	0,0289	4,75	0,026
34	195	0,063	3,24E-4	-0,0308	-1,58E-4	0,00776	3,99E-5	0,805	0,00413	1,87	0,00962	5,5	0,0282	4,8	0,0246

36	207	0,11	5,31E-4	0,0373	1,8E-4	-0,0108	-5,2E-5	0,802	0,00388	1,87	0,00903	5,61	0,0271	4,88	0,0236
38	219	0,189	8,63E-4	0,128	5,82E-4	0,0563	2,57E-4	0,861	0,00393	1,96	0,00896	5,73	0,0261	5	0,0228
40	231	0,251	0,00109	0,203	8,8E-4	0,124	5,39E-4	0,949	0,0041	2,01	0,00868	5,84	0,0253	5,04	0,0218
42	243	0,311	0,00128	0,262	0,00108	0,215	8,85E-4	1,04	0,00427	2,03	0,00834	5,89	0,0242	5,14	0,0212
44	255	0,385	0,00151	0,296	0,00116	0,278	0,00109	1,02	0,00398	2,15	0,00843	6,06	0,0237	5,23	0,0205
46	267	0,499	0,00186	0,415	0,00155	0,337	0,00126	1,1	0,0041	2,15	0,00805	6,15	0,023	5,32	0,0199
48	280	0,532	0,0019	0,469	0,00168	0,468	0,00167	1,43	0,00511	2,22	0,00793	6,32	0,0226	5,43	0,0194
50	292	0,521	0,00179	0,531	0,00182	0,478	0,00164	1,02	0,00348	2,21	0,00756	6,35	0,0218	5,49	0,0188
52	304	0,632	0,00208	0,6	0,00197	0,561	0,00185	1,07	0,00351	2,25	0,00741	6,43	0,0212	5,56	0,0183
54	316	0,717	0,00227	0,693	0,00219	0,61	0,00193	1,1	0,00348	2,31	0,00732	6,49	0,0206	5,59	0,0177
56	328	0,746	0,00227	0,719	0,00219	0,749	0,00228	1,18	0,00361	2,4	0,00733	6,58	0,0201	5,69	0,0173
58	340	0,898	0,00264	0,878	0,00258	0,796	0,00234	1,25	0,00368	2,45	0,00721	6,73	0,0198	5,67	0,0167
60	352	0,981	0,00278	0,945	0,00268	0,852	0,00242	1,38	0,00393	2,57	0,00729	6,84	0,0194	5,77	0,0164
62	364	0,968	0,00266	0,962	0,00264	1	0,00276	1,5	0,00411	2,63	0,00722	6,84	0,0188	5,88	0,0161
64	376	1,14	0,00303	1,13	0,003	1,03	0,00273	1,46	0,00387	2,7	0,00718	6,97	0,0185	5,89	0,0156
66	389	1,19	0,00307	1,18	0,00304	1,11	0,00287	1,56	0,00401	2,82	0,00726	7,04	0,0181	5,99	0,0154
68	401	1,23	0,00306	1,3	0,00325	1,16	0,00289	1,61	0,00402	2,79	0,00697	7,14	0,0178	6,08	0,0152
70	413	1,29	0,00311	1,29	0,00311	1,37	0,00332	1,75	0,00424	2,99	0,00724	7,14	0,0173	6,19	0,015
72	425	1,43	0,00336	1,41	0,00332	1,45	0,00342	1,85	0,00436	3,14	0,00739	7,21	0,017	6,21	0,0146
74	437	1,38	0,00316	1,47	0,00336	1,55	0,00354	1,99	0,00455	3,2	0,00733	7,14	0,0163	6,24	0,0143
76	449	1,58	0,00351	1,68	0,00375	1,54	0,00344	1,95	0,00435	3,21	0,00714	7,28	0,0162	6,17	0,0137
78	461	1,82	0,00395	2	0,00433	1,44	0,00313	2,34	0,00507	3,59	0,00779	7,2	0,0156	6,41	0,0139
80	473	1,64	0,00346	1,82	0,00384	1,8	0,0038	2,24	0,00474	3,49	0,00738	7,36	0,0156	6,3	0,0133
82	485	1,8	0,00372	1,96	0,00404	1,79	0,00368	2,18	0,00449	3,5	0,0072	7,38	0,0152	6,24	0,0128
84	498	1,78	0,00357	1,96	0,00395	1,97	0,00395	2,41	0,00484	3,54	0,00711	7,28	0,0146	6,28	0,0126
86	510	1,96	0,00384	2,07	0,00407	1,97	0,00386	2,38	0,00467	3,65	0,00715	7,35	0,0144	6,33	0,0124
88	522	2,11	0,00405	2,1	0,00402	2,12	0,00407	2,49	0,00476	3,81	0,00729	7,46	0,0143	6,4	0,0123
90	534	2,12	0,00397	2,24	0,00419	2,2	0,00412	2,55	0,00477	3,89	0,00729	7,4	0,0139	6,41	0,012
92	546	2,16	0,00396	2,25	0,00412	2,33	0,00427	2,71	0,00497	4,02	0,00735	7,42	0,0136	6,55	0,012
94	558	2,26	0,00406	2,39	0,00428	2,38	0,00427	2,78	0,00498	3,96	0,0071	7,41	0,0133	6,5	0,0116
96	570	2,37	0,00416	2,36	0,00413	2,6	0,00456	2,97	0,00522	4,2	0,00736	7,43	0,013	6,72	0,0118
98	582	2,49	0,00427	2,49	0,00427	2,68	0,0046	3,07	0,00527	4,26	0,00732	7,47	0,0128	6,78	0,0116
100	594	2,51	0,00422	2,61	0,00439	2,73	0,00459	3,14	0,00528	4,17	0,00702	7,44	0,0125	6,76	0,0114

102	607	2,75	0,0045 3	2,81	0,0046 3	2,79	0,0046	3,23	0,0053 2	4,38	0,0072 2	7,63	0,0126	6,9	0,0114
104	619	2,81	0,0045 4	2,92	0,0047 2	2,89	0,0046 7	3,34	0,0054	4,39	0,0070 9	7,66	0,0124	7,28	0,0118
106	631	2,85	0,0045 1	3,05	0,0048 4	2,93	0,0046 4	3,43	0,0054 4	4,43	0,0070 2	7,66	0,0121	7,01	0,0111
108	643	2,89	0,0044 9	3,04	0,0047 2	3,13	0,0048 6	3,65	0,0056 7	4,7	0,0073 2	7,7	0,012	7,23	0,0112
110	655	3,11	0,0047 5	3,2	0,0048 9	3,19	0,0048 7	3,65	0,0055 7	4,86	0,0074 2	7,94	0,0121	7,31	0,0112
112	667	3,13	0,0046 9	3,14	0,0047 1	3,32	0,0049 7	3,86	0,0057 9	4,98	0,0074 7	7,94	0,0119	7,44	0,0111
114	679	3,13	0,0046 1	3,36	0,0049 4	3,3	0,0048 6	3,85	0,0056 7	4,94	0,0072 8	7,94	0,0117	7,39	0,0109
116	691	3,26	0,0047 2	3,38	0,0048 9	3,46	0,005	4,03	0,0058 3	5,12	0,0074	8	0,0116	7,58	0,011
118	703	3,42	0,0048 6	3,52	0,005	3,53	0,0050 2	4,11	0,0058 4	5,27	0,0074 9	8,14	0,0116	7,72	0,011
120	716	3,4	0,0047 5	3,54	0,0049 4	3,71	0,0051 8	4,33	0,0060 5	5,41	0,0075 6	8,19	0,0115	7,73	0,0108
122	728	3,66	0,0050 2	3,58	0,0049 2	3,81	0,0052 3	4,42	0,0060 8	5,66	0,0077 8	8,48	0,0116	7,93	0,0109
124	740	3,81	0,0051 4	3,63	0,0049 1	3,92	0,0053	4,58	0,0062	5,72	0,0077 3	8,5	0,0115	8,02	0,0108
126	752	3,79	0,0050 4	3,84	0,0051	3,92	0,0052 1	4,64	0,0061 8	5,6	0,0074 4	8,53	0,0113	8,05	0,0107
128	764	3,99	0,0052 2	3,86	0,0050 6	3,96	0,0051 8	4,76	0,0062 4	5,89	0,0077 2	8,65	0,0113	8,17	0,0107
130	776	4,11	0,0053	4,02	0,0051 7	4,03	0,0051 9	4,87	0,0062 8	5,97	0,0076 9	8,81	0,0114	8,15	0,0105
132	788	4,33	0,0054 9	4,15	0,0052 7	4,12	0,0052 3	4,93	0,0062 6	6,08	0,0077 1	8,88	0,0113	8,34	0,0106
134	800	4,3	0,0053 8	4,2	0,0052 5	4,25	0,0053 1	5,17	0,0064 5	6,13	0,0076 5	8,85	0,0111	8,46	0,0106
136	812	4,33	0,0053 3	4,11	0,0050 5	4,5	0,0055 3	5,34	0,0065 7	6,3	0,0077 5	8,95	0,011	8,57	0,0106
138	825	4,54	0,0055 1	4,3	0,0052 1	4,47	0,0054 2	5,21	0,0063 2	6,38	0,0077 4	9,12	0,0111	8,58	0,0104
140	837	4,74	0,0056 7	4,35	0,0052	4,65	0,0055 6	5,39	0,0064 5	6,6	0,0078 9	9,2	0,011	8,77	0,0105
142	849	4,81	0,0056 7	4,5	0,0053	4,73	0,0055 8	5,43	0,0064	6,9	0,0081 3	9,28	0,0109	8,8	0,0104
144	861	4,96	0,0057 6	4,62	0,0053 7	4,78	0,0055 6	5,5	0,0063 9	6,86	0,0079 7	9,4	0,0109	8,95	0,0104
146	873	5,02	0,0057 5	4,71	0,0054	5	0,0057 2	5,62	0,0064 4	7,08	0,0081	9,7	0,0111	9,15	0,0105
148	885	5,27	0,0059 5	4,92	0,0055 6	5	0,0056 5	5,57	0,0063	7,09	0,0080 1	9,81	0,0111	9,23	0,0104
150	897	5,34	0,0059 5	4,98	0,0055 5	5,19	0,0057 8	5,75	0,0064 1	7,3	0,0081 3	9,97	0,0111	9,57	0,0107
152	909	5,3	0,0058 3	4,98	0,0054 8	5,31	0,0058 4	6	0,0066	7,4	0,0081 4	9,81	0,0108	9,72	0,0107
154	921	5,42	0,0058 8	5,12	0,0055 6	5,39	0,0058 5	6,04	0,0065 6	7,48	0,0081 2	10	0,0109	9,96	0,0108
156	934	5,58	0,0059 7	5,21	0,0055 8	5,4	0,0057 9	6,14	0,0065 8	7,65	0,0081 9	10,3	0,011	10	0,0108
158	946	5,74	0,0060 7	5,38	0,0056 9	5,57	0,0058 9	6,26	0,0066 2	7,79	0,0082 4	10,6	0,0112	10,3	0,0109
160	958	5,88	0,0061 4	5,46	0,0057	5,54	0,0057 8	6,3	0,0065 8	7,78	0,0081 2	10,6	0,0111	10,3	0,0107
162	970	5,92	0,0061 1	5,61	0,0057 9	5,67	0,0058 5	6,49	0,0066 9	8,05	0,0083	10,9	0,0112	10,4	0,0107
164	982	6,18	0,0063	5,7	0,0058 1	5,86	0,0059 6	6,59	0,0067 2	8,26	0,0084 1	11,2	0,0115	10,8	0,011
166	994	6,15	0,0061 8	5,67	0,0057 1	5,98	0,0060 2	6,77	0,0068 1	8,24	0,0082 9	11,3	0,0113	10,9	0,011
168	1 01 0	6,33	0,0062 9	5,82	0,0057 8	6,13	0,0060 9	6,9	0,0068 6	8,32	0,0082 7	11,4	0,0114	11	0,011

170	1 020	6,36	0,00625	5,9	0,00579	6,38	0,00627	7,07	0,00694	8,57	0,00841	11,6	0,0114	11,2	0,011
172	1 030	6,68	0,00648	6,2	0,00602	6,33	0,00615	7,06	0,00686	8,56	0,0083	11,9	0,0115	11,3	0,011
174	1 040	6,54	0,00627	6,24	0,00598	6,45	0,00618	7,26	0,00696	8,71	0,00835	11,9	0,0114	11,4	0,011
176	1 050	7,02	0,00666	6,47	0,00613	6,61	0,00627	7,31	0,00694	8,93	0,00847	12,2	0,0116	11,6	0,011
178	1 070	7,11	0,00666	6,47	0,00606	6,96	0,00653	7,65	0,00717	9,1	0,00853	12,3	0,0116	12	0,0113
180	1 080	7,21	0,00669	6,67	0,00618	6,97	0,00646	7,71	0,00715	9,44	0,00875	12,5	0,0116	12,3	0,0114
182	1 090	7,37	0,00676	6,84	0,00627	7,13	0,00653	7,83	0,00718	9,46	0,00867	12,7	0,0116	12,3	0,0113
184	1 100	7,41	0,00672	6,93	0,00628	7,25	0,00657	8,01	0,00726	9,94	0,00901	13	0,0118	12,5	0,0113
186	1 120	7,77	0,00697	7,11	0,00638	7,29	0,00654	8,06	0,00723	9,94	0,00892	13,1	0,0118	12,7	0,0114
188	1 130	7,89	0,00699	7,22	0,00641	7,44	0,0066	8,23	0,0073	10	0,00891	13,5	0,0119	12,9	0,0114
190	1 140	7,71	0,00676	7,21	0,00632	7,79	0,00684	8,54	0,0075	10,2	0,00896	13,4	0,0118	13,2	0,0116
192	1 150	7,99	0,00694	7,57	0,00657	7,78	0,00675	8,57	0,00744	10,3	0,00897	13,8	0,012	13,3	0,0115
194	1 160	8,08	0,00694	7,73	0,00664	7,98	0,00686	8,78	0,00755	10,5	0,00902	14	0,012	13,6	0,0117
196	1 180	8,17	0,00695	7,85	0,00667	8,05	0,00684	8,85	0,00752	10,7	0,00906	14,1	0,012	13,7	0,0116
198	1 190	8,33	0,00701	7,99	0,00673	8,37	0,00705	9,19	0,00774	10,8	0,00912	14,3	0,012	13,9	0,0117
200	1 200	8,73	0,00728	8,15	0,00679	8,5	0,00708	9,37	0,00781	11,1	0,00926	14,6	0,0121	14,3	0,0119

Time	Shear Rate	Shear Stress	Viscosity	Shear Stress	Viscosity	Shear Stress	Viscosity	Shear Stress	Viscosity	Shear Stress	Viscosity	Shear Stress	Viscosity	Shear Stress	Viscosity
[s]	[1/s]	[Pa]	[Pa·s]	[Pa]	[Pa·s]	[Pa]	[Pa·s]	[Pa]	[Pa·s]	[Pa]	[Pa·s]	[Pa]	[Pa·s]	[Pa]	[Pa·s]
Number of Intervals:		CNC-BT-WDFs (6 wt %) 0.0 % 80°C S.W.	CNC-BT-WDFs (6 wt %) 0.0 % 80°C S.W.	CNC-BT-WDFs (6 wt %) 0.4 % 80°C S.W.	CNC-BT-WDFs (6 wt %) 0.4 % 80°C S.W.	CNC-BT-WDFs (6 wt %) 0.8 % 80°C S.W.	CNC-BT-WDFs (6 wt %) 0.8 % 80°C S.W.	CNC-BT-WDFs (6 wt %) 1.2 % 80°C S.W.	CNC-BT-WDFs (6 wt %) 1.2 % 80°C S.W.	CNC-BT-WDFs (6 wt %) 1.6 % 80°C S.W.	CNC-BT-WDFs (6 wt %) 1.6 % 80°C S.W.	CNC-BT-WDFs (6 wt %) 2.0 % 80°C S.W.	CNC-BT-WDFs (6 wt %) 2.0 % 80°C S.W.	CNC-BT-WDFs (6 wt %) 2.4 % 80°C S.W.	CNC-BT-WDFs (6 wt %) 2.4 % 80°C S.W.
2	0,999	-1,02	-1,02	-0,762	-0,763	-0,751	-0,75	-0,347	-0,347	0,262	0,262	0,573	0,573	0,548	0,548
4	13,1	-0,419	-0,032	-0,414	-0,0315	-0,15	-0,0114	0,127	0,00971	0,952	0,0726	3,09	0,236	3,47	0,265
6	25,2	-0,378	-0,015	-0,397	-0,0157	-0,135	-0,00533	0,143	0,00566	1,21	0,0478	3,26	0,129	3,87	0,154
8	37,3	-0,413	-0,0111	-0,407	-0,0109	-0,147	-0,00393	0,197	0,00528	1,25	0,0335	3,67	0,0982	3,74	0,1
10	49,4	-0,405	-0,00818	-0,441	-0,00891	-0,243	-0,00491	0,191	0,00386	1,27	0,0257	3,48	0,0703	3,82	0,0772
12	61,6	-0,419	-0,00681	-0,384	-0,00625	-0,211	-0,00344	0,155	0,00252	1,33	0,0215	3,48	0,0566	3,93	0,0638
14	73,7	-0,41	-0,00557	-0,368	-0,005	-0,211	-0,00286	0,231	0,00314	1,42	0,0193	3,57	0,0485	4,05	0,0549
16	85,8	-0,369	-0,0043	-0,39	-0,00455	-0,185	-0,00216	0,223	0,0026	1,54	0,0179	3,73	0,0435	4,3	0,0501
18	97,9	-0,279	-0,00285	-0,374	-0,00382	-0,154	-0,00157	0,306	0,00312	1,62	0,0166	3,97	0,0406	4,46	0,0455
20	110	-0,237	-0,00215	-0,392	-0,00357	-0,133	-0,00121	0,39	0,00354	1,63	0,0148	4,11	0,0373	4,61	0,0419
22	122	-0,264	-0,00216	-0,362	-0,00296	-0,122	-9,95E-4	0,485	0,00397	1,76	0,0144	4,28	0,0351	4,74	0,0388
24	134	-0,14	-0,00105	-0,245	-0,00183	-0,0237	-1,77E-4	0,595	0,00443	1,86	0,0139	4,36	0,0325	4,92	0,0367
26	146	-0,078	-5,33E-4	-0,169	-0,00115	-0,0191	-1,3E-4	0,504	0,00344	1,93	0,0132	4,51	0,0308	5,05	0,0345
28	158	-0,0353	-2,23E-4	-0,0889	-5,61E-4	0,0277	1,75E-4	0,657	0,00414	2	0,0126	4,64	0,0293	5,15	0,0325
30	171	0,0123	7,21E-5	-0,0548	-3,21E-4	0,0544	3,19E-4	0,664	0,00389	2,05	0,012	4,8	0,0282	5,23	0,0306
32	183	0,0851	4,66E-4	0,0272	1,49E-4	0,158	8,62E-4	0,705	0,00386	2,18	0,0119	4,86	0,0266	5,35	0,0293
34	195	0,145	7,46E-4	0,0859	4,41E-4	0,252	0,00129	0,739	0,0038	2,21	0,0113	4,96	0,0255	5,47	0,0281
36	207	0,143	6,92E-4	0,13	6,31E-4	0,299	0,00145	0,775	0,00375	2,26	0,0109	5,1	0,0246	5,51	0,0266

38	219	0,206	9,39E-4	0,207	9,46E-4	0,393	0,0018	0,83	0,00379	2,31	0,0106	5,13	0,0234	5,67	0,0259
40	231	0,244	0,00106	0,235	0,00102	0,453	0,00196	0,852	0,00369	2,36	0,0102	5,3	0,0229	5,76	0,0249
42	243	0,28	0,00115	0,291	0,0012	0,51	0,0021	0,869	0,00357	2,41	0,00991	5,37	0,0221	5,86	0,0241
44	255	0,377	0,00148	0,384	0,0015	0,7	0,00274	0,971	0,0038	2,5	0,0098	5,43	0,0213	5,98	0,0234
46	267	0,414	0,00155	0,423	0,00158	0,708	0,00265	1,01	0,00379	2,5	0,00936	5,51	0,0206	6,1	0,0228
48	280	0,538	0,00192	0,504	0,0018	0,791	0,00283	1,07	0,00381	2,59	0,00925	5,61	0,0201	6,22	0,0222
50	292	0,562	0,00193	0,499	0,00171	0,618	0,00212	1,05	0,00359	2,56	0,00878	5,77	0,0198	6,23	0,0214
52	304	0,667	0,00219	0,595	0,00196	0,704	0,00232	1,13	0,00373	2,6	0,00856	5,85	0,0193	6,32	0,0208
54	316	0,716	0,00227	0,7	0,00221	0,74	0,00234	1,22	0,00385	2,64	0,00836	5,88	0,0186	6,38	0,0202
56	328	0,83	0,00253	0,772	0,00235	0,838	0,00255	1,3	0,00398	2,74	0,00834	5,98	0,0182	6,47	0,0197
58	340	0,851	0,0025	0,918	0,0027	0,911	0,00268	1,42	0,00418	2,79	0,0082	6	0,0177	6,62	0,0195
60	352	0,964	0,00274	1	0,00285	1,02	0,00289	1,54	0,00437	2,8	0,00795	6,09	0,0173	6,71	0,019
62	364	1,04	0,00285	1,01	0,00278	1,12	0,00309	1,56	0,00429	2,94	0,00806	6,25	0,0171	6,68	0,0183
64	376	1,07	0,00284	1,14	0,00302	1,16	0,00308	1,65	0,00437	2,93	0,00778	6,22	0,0165	6,83	0,0181
66	389	1,2	0,00308	1,24	0,00319	1,21	0,00311	1,7	0,00437	3,01	0,00774	6,31	0,0162	6,91	0,0178
68	401	1,21	0,00302	1,27	0,00317	1,29	0,00322	1,77	0,00441	3,14	0,00783	6,37	0,0159	6,87	0,0171
70	413	1,37	0,00333	1,41	0,00342	1,46	0,00354	1,91	0,00462	3,3	0,00799	6,44	0,0156	7	0,017
72	425	1,5	0,00354	1,51	0,00356	1,56	0,00367	1,97	0,00464	3,36	0,00792	6,43	0,0151	7,04	0,0166
74	437	1,59	0,00363	1,51	0,00345	1,62	0,0037	1,93	0,00442	3,42	0,00782	6,53	0,0149	7,04	0,0161
76	449	1,53	0,00341	1,61	0,00359	1,63	0,00364	2,01	0,00447	3,42	0,00761	6,47	0,0144	7,22	0,0161
78	461	1,79	0,00388	1,59	0,00344	1,79	0,00389	2,04	0,00441	3,71	0,00804	6,81	0,0148	7	0,0152
80	473	1,75	0,00371	1,75	0,00369	1,86	0,00392	2,21	0,00467	3,63	0,00768	6,58	0,0139	7,3	0,0154
82	485	1,72	0,00355	1,77	0,00366	1,86	0,00383	2,28	0,0047	3,62	0,00746	6,49	0,0134	7,38	0,0152
84	498	1,81	0,00364	1,77	0,00356	1,94	0,00391	2,3	0,00463	3,73	0,0075	6,65	0,0134	7,31	0,0147
86	510	1,83	0,0036	1,86	0,00365	2	0,00393	2,4	0,00471	3,76	0,00737	6,58	0,0129	7,29	0,0143
88	522	2,01	0,00386	2,09	0,004	2,27	0,00435	2,64	0,00505	3,94	0,00755	6,6	0,0127	7,61	0,0146
90	534	2,03	0,00381	2,08	0,0039	2,25	0,00421	2,64	0,00495	4,03	0,00755	6,72	0,0126	7,54	0,0141
92	546	2,17	0,00398	2,2	0,00403	2,39	0,00439	2,74	0,00501	4,13	0,00756	6,79	0,0124	7,62	0,014
94	558	2,19	0,00392	2,22	0,00397	2,4	0,00429	2,78	0,00498	4,19	0,00751	6,85	0,0123	7,54	0,0135
96	570	2,4	0,00421	2,42	0,00425	2,64	0,00463	3,02	0,00529	4,43	0,00776	6,81	0,0119	7,58	0,0133
98	582	2,49	0,00427	2,55	0,00438	2,76	0,00474	3,11	0,00535	4,44	0,00762	6,87	0,0118	7,65	0,0131
100	594	2,47	0,00415	2,48	0,00417	2,76	0,00464	3,1	0,00521	4,44	0,00748	7,06	0,0119	7,61	0,0128
102	607	2,63	0,00433	2,71	0,00447	2,9	0,00477	3,28	0,0054	4,59	0,00757	6,95	0,0115	7,67	0,0126
104	619	2,7	0,00437	2,76	0,00446	2,95	0,00476	3,37	0,00544	4,64	0,0075	7,11	0,0115	7,57	0,0122

106	631	2,84	0,0045	2,81	0,00446	2,98	0,00472	3,33	0,00529	4,68	0,00742	7,26	0,0115	7,57	0,012
108	643	3,05	0,00475	2,96	0,00461	3,25	0,00506	3,53	0,00549	4,94	0,00769	7,2	0,0112	7,71	0,012
110	655	3,11	0,00475	3,14	0,00479	3,31	0,00505	3,64	0,00556	4,99	0,00761	7,14	0,0109	7,89	0,0121
112	667	3,23	0,00485	3,21	0,00481	3,44	0,00515	3,71	0,00557	5,11	0,00765	7,35	0,011	7,82	0,0117
114	679	3,12	0,0046	3,15	0,00463	3,35	0,00494	3,62	0,00533	5,06	0,00744	7,56	0,0111	7,7	0,0113
116	691	3,28	0,00475	3,26	0,00471	3,51	0,00508	3,81	0,00551	5,33	0,00771	7,53	0,0109	7,84	0,0113
118	703	3,38	0,0048	3,41	0,00484	3,63	0,00517	3,95	0,00561	5,45	0,00774	7,62	0,0108	7,9	0,0112
120	716	3,46	0,00483	3,44	0,00481	3,74	0,00523	3,96	0,00553	5,64	0,00789	7,84	0,011	7,91	0,0111
122	728	3,69	0,00506	3,7	0,00508	3,88	0,00534	4,24	0,00583	5,77	0,00793	7,8	0,0107	8,22	0,0113
124	740	3,78	0,00512	3,77	0,0051	3,96	0,00535	4,39	0,00593	5,91	0,00798	7,84	0,0106	8,29	0,0112
126	752	3,73	0,00496	3,71	0,00493	3,86	0,00514	4,31	0,00573	5,95	0,00791	8,03	0,0107	8,23	0,011
128	764	3,93	0,00515	3,92	0,00514	4,11	0,00538	4,58	0,006	6,11	0,008	8	0,0105	8,56	0,0112
130	776	3,97	0,00512	3,98	0,00513	4,17	0,00538	4,64	0,00598	6,19	0,00798	8,06	0,0104	8,6	0,0111
132	788	4,07	0,00517	4,15	0,00527	4,26	0,00541	4,86	0,00617	6,23	0,00791	8,11	0,0103	8,88	0,0113
134	800	4,17	0,00522	4,1	0,00512	4,32	0,0054	4,82	0,00602	6,49	0,00811	8,34	0,0104	8,88	0,0111
136	812	4,3	0,0053	4,26	0,00524	4,47	0,0055	5,04	0,00621	6,72	0,00827	8,4	0,0103	9,13	0,0112
138	825	4,26	0,00517	4,26	0,00517	4,4	0,00534	5,03	0,0061	6,62	0,00802	8,6	0,0104	9,36	0,0114
140	837	4,53	0,00541	4,56	0,00545	4,76	0,00569	5,34	0,00639	6,91	0,00826	8,57	0,0102	9,53	0,0114
142	849	4,67	0,0055	4,62	0,00545	4,8	0,00566	5,43	0,00639	7,1	0,00837	8,78	0,0103	9,5	0,0112
144	861	4,75	0,00552	4,67	0,00543	4,84	0,00563	5,56	0,00646	7,14	0,00829	9,06	0,0105	9,41	0,0109
146	873	4,86	0,00557	4,89	0,0056	5,11	0,00586	5,78	0,00662	7,38	0,00846	9,15	0,0105	9,77	0,0112
148	885	4,89	0,00552	4,96	0,00561	5,12	0,00579	5,89	0,00666	7,28	0,00823	9,26	0,0105	9,9	0,0112
150	897	5,12	0,00571	5,11	0,0057	5,3	0,00591	6,02	0,00671	7,42	0,00827	9,32	0,0104	10,1	0,0112
152	909	5,16	0,00568	5,04	0,00554	5,28	0,00581	5,95	0,00654	7,61	0,00837	9,75	0,0107	9,95	0,0109
154	921	5,36	0,00582	5,25	0,0057	5,47	0,00594	6,18	0,0067	7,82	0,00849	9,83	0,0107	10,2	0,0111
156	934	5,33	0,00571	5,29	0,00567	5,5	0,0059	6,23	0,00667	7,82	0,00837	9,99	0,0107	10,3	0,011
158	946	5,54	0,00586	5,48	0,0058	5,67	0,006	6,48	0,00685	8,21	0,00868	10,1	0,0107	10,4	0,011
160	958	5,41	0,00565	5,51	0,00575	5,59	0,00583	6,46	0,00674	8,31	0,00868	10,3	0,0108	10,5	0,011
162	970	5,48	0,00565	5,62	0,0058	5,69	0,00587	6,57	0,00677	8,33	0,00859	10,6	0,0109	10,8	0,0111
164	982	5,81	0,00591	5,82	0,00593	6	0,00611	6,86	0,00699	8,32	0,00848	10,5	0,0107	11,1	0,0113
166	994	5,84	0,00588	5,78	0,00581	6,05	0,00608	6,82	0,00686	8,52	0,00857	10,7	0,0108	11,1	0,0111
168	1 010	6,07	0,00603	5,92	0,00588	6,17	0,00613	7	0,00695	8,6	0,00855	10,9	0,0108	11,3	0,0112
170	1 020	6,2	0,00609	6,09	0,00598	6,33	0,00621	7,14	0,00701	8,84	0,00868	11,1	0,0109	11,6	0,0114
172	1 030	6,18	0,006	6,14	0,00596	6,33	0,00614	7,32	0,0071	9,07	0,0088	11,2	0,0109	11,6	0,0113

174	1 040	6,32	0,00606	6,23	0,00598	6,41	0,00615	7,38	0,00708	9,12	0,00875	11,6	0,0111	11,7	0,0113
176	1 050	6,49	0,00615	6,46	0,00613	6,61	0,00627	7,65	0,00725	9,13	0,00865	11,6	0,011	11,9	0,0113
178	1 070	6,76	0,00634	6,61	0,0062	6,89	0,00646	7,72	0,00724	9,5	0,00891	11,9	0,0111	12,2	0,0114
180	1 080	6,79	0,00629	6,71	0,00622	6,96	0,00645	7,93	0,00735	9,59	0,00889	12,1	0,0112	12,4	0,0115
182	1 090	6,9	0,00632	6,82	0,00625	7,07	0,00648	8,03	0,00736	9,65	0,00885	12,2	0,0112	12,5	0,0115
184	1 100	7,16	0,00649	7,19	0,00652	7,3	0,00662	8,15	0,00739	9,91	0,00898	12,4	0,0112	12,8	0,0116
186	1 120	7,25	0,0065	7,27	0,00652	7,33	0,00658	8,22	0,00737	9,84	0,00882	12,5	0,0112	13	0,0116
188	1 130	7,52	0,00667	7,32	0,00649	7,45	0,00661	8,39	0,00745	10,1	0,009	12,7	0,0112	13,3	0,0118
190	1 140	7,55	0,00663	7,38	0,00648	7,67	0,00673	8,56	0,00751	10,5	0,0092	13	0,0115	13,3	0,0117
192	1 150	7,65	0,00664	7,47	0,00648	7,74	0,00672	8,68	0,00754	10,4	0,00901	13,2	0,0114	13,6	0,0118
194	1 160	7,82	0,00672	7,6	0,00653	7,89	0,00678	8,83	0,00758	10,6	0,00913	13,4	0,0115	13,6	0,0117
196	1 180	7,93	0,00674	7,71	0,00655	7,9	0,00672	8,9	0,00757	10,7	0,00907	13,5	0,0115	13,6	0,0116
198	1 190	8,19	0,0069	7,77	0,00654	8,21	0,00691	9,08	0,00764	11,1	0,00931	13,9	0,0117	13,8	0,0116
200	1 200	8,4	0,007	8,09	0,00674	8,34	0,00695	9,24	0,0077	11,3	0,00943	13,9	0,0116	14,1	0,0117

RHEOLOGICAL DATA OF CNC/ATT-WDFs (SW)

Time	Shear Rate	Shear Stress	Viscosity	Shear Stress	Viscosity	Shear Stress	Viscosity	Shear Stress	Viscosity	Shear Stress	Viscosity	Shear Stress	Viscosity	Shear Stress	Viscosity
[s]	[1/s]	[Pa]	[Pa·s]	[Pa]	[Pa·s]	[Pa]	[Pa·s]	[Pa]	[Pa·s]	[Pa]	[Pa·s]	[Pa]	[Pa·s]	[Pa]	[Pa·s]
Number of Intervals:		*CNC-ATT-WDFs (6 wt %) 0.0 % 20°C S.W.*	*CNC-ATT-WDFs (6 wt %) 0.0 % 20°C S.W.*	*CNC-ATT-WDFs (6 wt %) 0.4 % 20°C S.W.*	*CNC-ATT-WDFs (6 wt %) 0.4 % 20°C S.W.*	*CNC-ATT-WDFs (6 wt %) 0.8 % 20°C S.W.*	*CNC-ATT-WDFs (6 wt %) 0.8 % 20°C S.W.*	*CNC-ATT-WDFs (6 wt %) 1,2 % 20°C S.W.*	*CNC-ATT-WDFs (6 wt %) 1,2 % 20°C S.W.*	*CNC-ATT-WDFs (6 wt %) 1,6 % 20°C S.W.*	*CNC-ATT-WDFs (6 wt %) 1,6 % 20°C S.W.*	*CNC-ATT-WDFs (6 wt %) 2.0 % 20°C S.W.*	*CNC-ATT-WDFs (6 wt %) 2.0 % 20°C S.W.*	*CNC-ATT-WDFs (6 wt %) 2.4 % 20°C S.W.*	*CNC-ATT-WDFs (6 wt %) 2.4 % 20°C S.W.*
2	0,999	-0,985	-0,985	-1,35	-1,35	-0,598	-0,599	2,86	2,86	1,92	1,92	2,26	2,26	8,04	8,03
4	13,1	-0,416	-0,0317	-0,175	-0,0134	0,616	0,047	3,92	0,299	2,96	0,226	3,83	0,292	12,9	0,981
6	25,2	-0,497	-0,0197	0,0376	0,00149	0,834	0,0331	4,37	0,173	3,34	0,132	4,52	0,179	14,1	0,559
8	37,3	-0,45	-0,0121	0,291	0,00781	0,91	0,0244	4,5	0,121	3,58	0,0958	4,96	0,133	14,9	0,398
10	49,4	-0,355	-0,00718	0,293	0,00593	1,03	0,0208	4,65	0,0941	3,77	0,0763	5,46	0,111	15,6	0,315
12	61,6	-0,429	-0,00698	0,333	0,00541	1,14	0,0185	4,89	0,0794	4,11	0,0667	5,9	0,0959	16,2	0,264
14	73,7	-0,385	-0,00523	0,448	0,00608	1,17	0,0159	5,13	0,0696	4,29	0,0582	6,35	0,0862	16,7	0,226
16	85,8	-0,366	-0,00427	0,409	0,00477	1,34	0,0156	5,31	0,062	4,68	0,0546	6,54	0,0762	17,1	0,199
18	97,9	-0,367	-0,00375	0,417	0,00426	1,35	0,0138	5,61	0,0573	4,97	0,0508	6,96	0,0711	17,5	0,179
20	110	-0,346	-0,00315	0,565	0,00513	1,38	0,0126	5,87	0,0533	5,21	0,0474	7,33	0,0666	18	0,163
22	122	-0,233	-0,00191	0,608	0,00498	1,59	0,0131	5,99	0,0491	5,44	0,0445	7,63	0,0625	18,6	0,152
24	134	-0,192	-0,00143	0,702	0,00523	1,69	0,0126	6,15	0,0458	5,7	0,0425	7,95	0,0593	19,2	0,143
26	146	-0,134	-9,14E-4	0,792	0,00541	1,79	0,0122	6,38	0,0436	5,93	0,0405	8,09	0,0553	19,8	0,136
28	158	-0,04	-2,53E-4	1,04	0,00656	2,03	0,0128	6,57	0,0415	6,24	0,0393	8,4	0,053	20,4	0,129
30	171	0,0977	5,73E-4	1,13	0,00663	2,09	0,0123	6,76	0,0397	6,45	0,0378	8,66	0,0508	20,9	0,123
32	183	0,161	8,79E-4	1,22	0,00668	2,2	0,012	6,95	0,038	6,7	0,0367	8,83	0,0483	21,5	0,118
34	195	0,251	0,00129	1,39	0,00713	2,23	0,0114	7,1	0,0364	6,88	0,0353	9,1	0,0467	22,2	0,114
36	207	0,359	0,00173	1,51	0,00732	2,15	0,0104	7,34	0,0355	7,01	0,0339	9,51	0,046	22,7	0,11

38	219	0,366	0,00167	1,45	0,00661	2,21	0,0101	7,42	0,0339	7,24	0,0331	9,78	0,0447	23,2	0,106
40	231	0,46	0,00199	1,45	0,00629	2,25	0,00975	7,61	0,0329	7,4	0,032	9,98	0,0432	23,5	0,102
42	243	0,516	0,00212	1,44	0,00593	2,31	0,00948	7,78	0,032	7,56	0,0311	10,1	0,0414	23,9	0,0984
44	255	0,557	0,00218	1,55	0,00608	2,48	0,0097	7,9	0,0309	7,78	0,0305	10,4	0,0407	24,4	0,0956
46	267	0,691	0,00258	1,57	0,00587	2,52	0,00941	8,02	0,03	7,96	0,0298	10,7	0,0402	24,7	0,0922
48	280	0,751	0,00269	1,68	0,00599	2,67	0,00954	8,19	0,0293	8,09	0,0289	11	0,0392	25,1	0,0897
50	292	0,896	0,00307	1,82	0,00623	2,73	0,00935	8,41	0,0288	8,18	0,028	11,2	0,0385	25,4	0,087
52	304	0,939	0,00309	1,93	0,00635	2,9	0,00954	8,51	0,028	8,31	0,0274	11,5	0,0377	25,9	0,0852
54	316	1,1	0,00349	2,01	0,00637	2,94	0,0093	8,62	0,0273	8,43	0,0267	11,7	0,037	26,2	0,0829
56	328	1,16	0,00354	2,16	0,00657	3,07	0,00937	8,81	0,0269	8,59	0,0262	11,8	0,0359	26,6	0,0811
58	340	1,34	0,00393	2,22	0,00652	3,16	0,00929	8,86	0,0261	8,71	0,0256	12	0,0354	26,9	0,079
60	352	1,45	0,00412	2,35	0,00668	3,27	0,00928	8,96	0,0254	8,96	0,0254	12,3	0,0348	27,3	0,0774
62	364	1,52	0,00416	2,57	0,00705	3,4	0,00933	9,15	0,0251	9,08	0,0249	12,5	0,0342	27,6	0,0759
64	376	1,69	0,0045	2,63	0,00698	3,48	0,00924	9,26	0,0246	9,23	0,0245	12,7	0,0336	28	0,0743
66	389	1,81	0,00465	2,83	0,00729	3,57	0,00919	9,44	0,0243	9,35	0,0241	12,9	0,0331	28,3	0,0728
68	401	1,96	0,0049	2,89	0,00722	3,62	0,00904	9,57	0,0239	9,42	0,0235	13,1	0,0328	28,6	0,0714
70	413	1,96	0,00476	3,09	0,00749	3,8	0,0092	9,68	0,0234	9,68	0,0234	13,3	0,0321	28,9	0,07
72	425	2,09	0,00492	3,25	0,00766	3,94	0,00928	9,74	0,0229	9,81	0,0231	13,5	0,0318	29,2	0,0687
74	437	2,22	0,00507	3,46	0,00791	4,07	0,00931	9,95	0,0228	9,82	0,0225	13,6	0,0312	29,5	0,0674
76	449	2,44	0,00542	3,47	0,00773	4,09	0,00911	9,95	0,0221	9,9	0,022	13,7	0,0306	29,6	0,0659
78	461	2,65	0,00574	3,9	0,00846	4,45	0,00965	9,88	0,0214	10,2	0,0222	14,1	0,0305	30,3	0,0656
80	473	2,61	0,00552	3,85	0,00812	4,48	0,00947	10,3	0,0217	10,1	0,0213	14	0,0295	30,3	0,064
82	485	2,82	0,00581	3,89	0,00802	4,51	0,00929	10,3	0,0213	10,1	0,0209	14,1	0,029	30,4	0,0626
84	498	2,89	0,00581	4,11	0,00825	4,7	0,00944	10,5	0,0211	10,1	0,0204	14	0,0282	30,8	0,0619
86	510	2,99	0,00588	4,17	0,00818	4,78	0,00938	10,6	0,0208	10,3	0,0202	14	0,0275	30,9	0,0605
88	522	3	0,00576	4,21	0,00807	5,09	0,00975	10,6	0,0203	10,5	0,0201	14,3	0,0274	31	0,0595
90	534	3,16	0,00592	4,37	0,00819	5,13	0,00961	10,7	0,0201	10,4	0,0195	14,3	0,0267	31,4	0,0588
92	546	3,24	0,00593	4,56	0,00835	5,37	0,00984	10,9	0,0199	10,6	0,0193	14,3	0,0262	31,6	0,0579
94	558	3,4	0,00609	4,75	0,00851	5,43	0,00973	11	0,0197	10,5	0,0188	14,3	0,0256	31,7	0,0568
96	570	3,4	0,00596	4,87	0,00854	5,72	0,01	11	0,0194	10,7	0,0188	14,4	0,0253	32	0,0561
98	582	3,52	0,00604	4,96	0,00851	5,85	0,0101	11,1	0,0191	10,8	0,0185	14,4	0,0247	32,1	0,0552
100	594	3,7	0,00622	5,11	0,0086	5,92	0,00997	11,4	0,0192	10,7	0,018	14,4	0,0242	32,4	0,0545
102	607	3,82	0,0063	5,22	0,00861	6,03	0,00995	11,3	0,0187	10,8	0,0178	14,5	0,0239	32,5	0,0536
104	619	3,96	0,0064	5,38	0,0087	6,14	0,00992	11,5	0,0185	10,8	0,0175	14,5	0,0234	32,7	0,0528

106	631	4,1	0,0065	5,47	0,00868	6,25	0,00991	11,6	0,0184	10,7	0,017	14,5	0,023	32,8	0,0521
108	643	4,08	0,00635	5,69	0,00884	6,59	0,0102	11,7	0,0182	10,9	0,0169	14,5	0,0225	32,9	0,0511
110	655	4,26	0,0065	5,79	0,00883	6,72	0,0103	11,7	0,0178	11	0,0168	14,6	0,0222	33	0,0503
112	667	4,31	0,00646	6,01	0,00901	6,89	0,0103	11,8	0,0177	11	0,0165	14,5	0,0217	33,2	0,0497
114	679	4,59	0,00676	6,12	0,00901	6,96	0,0103	12	0,0177	11	0,0161	14,4	0,0213	33,3	0,049
116	691	4,59	0,00664	6,34	0,00916	7,06	0,0102	12,1	0,0175	11,2	0,0161	14,5	0,021	33,5	0,0484
118	703	4,64	0,0066	6,39	0,00909	7,19	0,0102	12,1	0,0172	11,3	0,0161	14,5	0,0206	33,4	0,0475
120	716	4,55	0,00636	6,71	0,00937	7,46	0,0104	12,3	0,0172	11,3	0,0158	14,5	0,0203	33,7	0,047
122	728	4,68	0,00643	6,73	0,00925	7,62	0,0105	12,3	0,0169	11,4	0,0157	14,7	0,0202	33,7	0,0463
124	740	4,77	0,00645	6,92	0,00936	7,77	0,0105	12,4	0,0168	11,6	0,0157	14,7	0,0198	33,7	0,0456
126	752	4,91	0,00653	7,16	0,00952	7,77	0,0103	12,6	0,0167	11,6	0,0154	14,5	0,0193	33,9	0,0451
128	764	5,09	0,00666	7,2	0,00943	7,95	0,0104	12,7	0,0166	11,8	0,0155	14,8	0,0194	34	0,0444
130	776	5,22	0,00673	7,33	0,00944	8,02	0,0103	12,9	0,0166	11,9	0,0153	14,7	0,019	33,9	0,0437
132	788	5,31	0,00674	7,48	0,00949	8,2	0,0104	12,9	0,0164	12,1	0,0154	15	0,019	33,9	0,043
134	800	5,3	0,00662	7,75	0,00968	8,34	0,0104	13,2	0,0165	12,1	0,0151	14,7	0,0184	34,1	0,0426
136	812	5,3	0,00652	7,9	0,00973	8,48	0,0104	13,3	0,0164	12,3	0,0152	15	0,0184	34,1	0,042
138	825	5,93	0,0072	8,09	0,00981	8,53	0,0103	13,4	0,0162	12,6	0,0153	15,1	0,0183	34,2	0,0415
140	837	5,98	0,00715	8,13	0,00972	8,78	0,0105	13,5	0,0161	12,7	0,0152	15,3	0,0183	34	0,0406
142	849	6,14	0,00724	8,26	0,00973	8,89	0,0105	13,6	0,016	12,9	0,0152	15,3	0,018	34,1	0,0401
144	861	6,23	0,00723	8,39	0,00975	8,76	0,0102	13,7	0,0159	13	0,0151	15,4	0,0179	34,1	0,0396
146	873	6,16	0,00706	8,57	0,00982	9,09	0,0104	13,8	0,0158	13,2	0,0152	15,6	0,0179	34,1	0,039
148	885	6,52	0,00737	8,63	0,00975	9,19	0,0104	13,9	0,0157	13,4	0,0151	15,7	0,0178	34	0,0385
150	897	6,58	0,00734	8,86	0,00987	9,58	0,0107	14	0,0156	13,5	0,015	16	0,0178	34	0,0379
152	909	6,71	0,00738	9,15	0,0101	9,58	0,0105	14,4	0,0158	13,5	0,0148	16,1	0,0177	34,2	0,0376
154	921	6,77	0,00734	9,22	0,01	9,79	0,0106	14,3	0,0155	13,8	0,0149	16,3	0,0176	34,1	0,037
156	934	6,94	0,00743	9,37	0,01	9,95	0,0107	14,4	0,0154	14	0,015	16,4	0,0176	34,1	0,0365
158	946	7,04	0,00745	9,53	0,0101	10,2	0,0108	14,5	0,0153	14,3	0,0151	16,4	0,0174	33,9	0,0359
160	958	7,25	0,00757	9,63	0,0101	10,2	0,0107	14,5	0,0151	14,1	0,0147	16,5	0,0172	34,1	0,0356
162	970	7,35	0,00758	9,73	0,01	10,5	0,0108	14,7	0,0152	14,2	0,0146	16,6	0,0171	34,1	0,0351
164	982	7,3	0,00743	9,93	0,0101	10,8	0,011	14,8	0,0151	14,5	0,0148	16,9	0,0172	33,9	0,0345
166	994	7,49	0,00753	10,1	0,0102	10,9	0,011	15	0,015	14,6	0,0147	16,9	0,017	34,1	0,0343
168	1 010	7,58	0,00753	10,3	0,0102	11,2	0,0111	15	0,0149	14,6	0,0145	17,1	0,017	34	0,0338
170	1 020	7,69	0,00755	10,5	0,0103	11,4	0,0112	15,1	0,0149	14,9	0,0146	17,1	0,0168	34,1	0,0334
172	1 030	8,01	0,00778	10,6	0,0102	11,5	0,0111	15,2	0,0148	15,1	0,0146	17,4	0,0169	34	0,033

174	1 040	8,27	0,00793	10,7	0,0103	11,6	0,0111	15,5	0,0149	15,5	0,0148	17,5	0,0168	33,9	0,0325
176	1 050	8,39	0,00795	10,9	0,0103	11,8	0,0112	15,8	0,015	15,9	0,015	17,5	0,0166	33,8	0,0321
178	1 070	8,32	0,0078	11,2	0,0105	12,2	0,0114	16,4	0,0154	16,2	0,0152	17,9	0,0168	33,9	0,0318
180	1 080	8,62	0,00799	11,3	0,0105	12,4	0,0115	16,6	0,0154	16,3	0,0151	18,1	0,0167	33,8	0,0313
182	1 090	8,67	0,00795	11,5	0,0105	12,5	0,0115	16,9	0,0155	16,5	0,0152	18,1	0,0166	34	0,0312
184	1 100	8,88	0,00805	11,6	0,0106	12,8	0,0116	17,1	0,0155	16,8	0,0152	18,6	0,0169	34	0,0308
186	1 120	9,04	0,00811	11,7	0,0105	12,8	0,0115	17,3	0,0155	17,1	0,0153	18,7	0,0168	34	0,0305
188	1 130	9,25	0,00821	11,9	0,0105	13	0,0116	17,5	0,0155	17,2	0,0153	18,8	0,0167	34	0,0302
190	1 140	9,18	0,00806	12,2	0,0107	13,5	0,0118	17,8	0,0156	17,6	0,0154	19	0,0166	34,1	0,03
192	1 150	9,51	0,00826	12	0,0104	13,5	0,0118	18	0,0156	17,8	0,0155	19,2	0,0167	34,1	0,0296
194	1 160	9,61	0,00825	12,2	0,0105	13,8	0,0118	18,2	0,0157	18,1	0,0155	19,5	0,0167	34,1	0,0293
196	1 180	9,93	0,00845	12,3	0,0105	13,9	0,0118	18,3	0,0156	18	0,0154	19,7	0,0168	34,2	0,0291
198	1 190	9,93	0,00836	12,6	0,0106	14,3	0,012	18,7	0,0157	18,5	0,0156	20	0,0168	34,2	0,0288
200	1 200	10,1	0,00838	12,7	0,0106	14,5	0,0121	18,9	0,0157	18,7	0,0156	20,4	0,017	34,2	0,0285

Time	Shear Rate	Shear Stress	Viscosity	Shear Stress	Viscosity	Shear Stress	Viscosity	Shear Stress	Viscosity	Shear Stress	Viscosity	Shear Stress	Viscosity	Shear Stress	Viscosity
[s]	[1/s]	[Pa]	[Pa·s]	[Pa]	[Pa·s]	[Pa]	[Pa·s]	[Pa]	[Pa·s]	[Pa]	[Pa·s]	[Pa]	[Pa·s]	[Pa]	[Pa·s]
Number of Intervals:		*CNC-ATT-WDFs (6 wt %) 0.0 % 30°C S.W.*	*CNC-ATT-WDFs (6 wt %) 0.0 % 30°C S.W.*	*CNC-ATT-WDFs (6 wt %) 0.4 % 30°C S.W.*	*CNC-ATT-WDFs (6 wt %) 0.4 % 30°C S.W.*	*CNC-ATT-WDFs (6 wt %) 0.8 % 30°C S.W.*	*CNC-ATT-WDFs (6 wt %) 0.8 % 30°C S.W.*	*CNC-ATT-WDFs (6 wt %) 1,2 % 30°C S.W.*	*CNC-ATT-WDFs (6 wt %) 1,2 % 30°C S.W.*	*CNC-ATT-WDFs (6 wt %) 1,6 % 30°C S.W.*	*CNC-ATT-WDFs (6 wt %) 1,6 % 30°C S.W.*	*CNC-ATT-WDFs (6 wt %) 2.0 % 30°C S.W.*	*CNC-ATT-WDFs (6 wt %) 2.0 % 30°C S.W.*	*CNC-ATT-WDFs (6 wt %) 2,4 % 30°C S.W.*	*CNC-ATT-WDFs (6 wt %) 2,4 % 30°C S.W.*
2	0,999	-1,31	-1,31	-0,607	-0,607	-0,0273	-0,0273	3,02	3,02	0,94	0,941	1,15	1,15	9,13	9,14
4	13,1	-0,661	-0,0504	0,00708	5,4E-4	0,584	0,0445	3,95	0,301	4,34	0,331	3,54	0,27	12,3	0,937
6	25,2	-0,313	-0,0124	0,241	0,00957	0,779	0,0309	4,17	0,165	4,36	0,173	4,21	0,167	12,8	0,509
8	37,3	-0,262	-0,00702	0,227	0,00608	0,712	0,0191	4,32	0,116	5,17	0,138	4,5	0,12	13,6	0,365
10	49,4	-0,344	-0,00696	0,208	0,0042	0,821	0,0166	4,49	0,0908	5,29	0,107	4,86	0,0982	14,1	0,285
12	61,6	-0,293	-0,00476	0,21	0,00342	0,976	0,0159	4,57	0,0742	4,86	0,0789	5,3	0,0861	14,3	0,232
14	73,7	-0,305	-0,00414	0,229	0,00311	0,949	0,0129	4,69	0,0637	5,06	0,0687	5,85	0,0794	14,5	0,197
16	85,8	-0,342	-0,00399	0,331	0,00386	1,05	0,0122	4,86	0,0567	5,21	0,0608	6,12	0,0714	15	0,174
18	97,9	-0,295	-0,00301	0,33	0,00337	1,15	0,0117	5	0,0511	5,23	0,0534	6,42	0,0655	15,4	0,157
20	110	-0,326	-0,00296	0,372	0,00338	1,23	0,0112	5,14	0,0467	5,57	0,0506	6,75	0,0614	15,8	0,144
22	122	-0,315	-0,00258	0,414	0,00339	1,27	0,0104	5,31	0,0435	5,77	0,0472	7,02	0,0574	16,3	0,134
24	134	-0,202	-0,0015	0,448	0,00334	1,37	0,0102	5,44	0,0406	6,05	0,0451	7,21	0,0537	16,8	0,125
26	146	-0,147	-0,001	0,503	0,00343	1,45	0,00993	5,61	0,0383	6,25	0,0427	7,46	0,051	17,3	0,118
28	158	-0,074	-4,67E-4	0,546	0,00345	1,53	0,00964	5,83	0,0368	6,4	0,0404	7,84	0,0495	18	0,113
30	171	-0,0204	-1,2E-4	0,571	0,00335	1,57	0,00921	5,99	0,0351	6,48	0,038	7,97	0,0468	18,6	0,109
32	183	0,0874	4,79E-4	0,64	0,0035	1,66	0,00907	6,13	0,0336	6,66	0,0365	8,27	0,0453	19,3	0,106
34	195	0,18	9,22E-4	0,675	0,00347	1,7	0,00875	6,31	0,0324	6,87	0,0353	8,5	0,0437	19,8	0,101
36	207	0,207	0,001	0,686	0,00332	1,73	0,00835	6,48	0,0313	7	0,0338	8,91	0,0431	20,1	0,0974
38	219	0,309	0,00141	0,762	0,00348	1,74	0,00797	6,61	0,0302	7,28	0,0332	8,93	0,0408	20,7	0,0944

40	231	0,374	0,00162	0,817	0,00353	1,83	0,0079	6,71	0,029	7,37	0,0319	9,02	0,039	21,1	0,0911
42	243	0,411	0,00169	0,864	0,00355	1,89	0,00777	6,86	0,0282	7,46	0,0307	9,39	0,0386	21,6	0,0886
44	255	0,525	0,00206	0,955	0,00374	1,88	0,00736	6,9	0,027	7,68	0,0301	9,39	0,0368	22	0,086
46	267	0,567	0,00212	0,956	0,00358	1,92	0,00716	7,09	0,0265	7,85	0,0294	9,61	0,0359	22,5	0,084
48	280	0,689	0,00247	1,08	0,00385	2	0,00715	7,17	0,0257	7,99	0,0286	9,91	0,0354	22,8	0,0816
50	292	0,733	0,00251	1,18	0,00406	2,13	0,00729	7,34	0,0252	8,02	0,0275	10,2	0,0348	23,1	0,0792
52	304	0,862	0,00284	1,28	0,00423	2,26	0,00745	7,45	0,0245	8,28	0,0273	10,3	0,034	23,4	0,0769
54	316	0,94	0,00297	1,36	0,00431	2,27	0,00718	7,65	0,0242	8,4	0,0266	10,7	0,034	23,7	0,075
56	328	1,08	0,00328	1,5	0,00458	2,38	0,00727	7,69	0,0234	8,59	0,0262	10,9	0,0333	24,1	0,0734
58	340	1,16	0,00341	1,52	0,00448	2,44	0,00717	7,8	0,0229	8,71	0,0256	11,2	0,0328	24,5	0,072
60	352	1,29	0,00365	1,66	0,00471	2,53	0,00719	7,93	0,0225	8,86	0,0251	11,4	0,0325	24,8	0,0703
62	364	1,42	0,00389	1,9	0,00521	2,72	0,00746	8	0,022	8,98	0,0246	11,7	0,032	24,8	0,0681
64	376	1,52	0,00405	1,91	0,00507	2,79	0,00742	8,16	0,0217	9,04	0,024	12	0,0319	25,2	0,0669
66	389	1,6	0,00411	2,09	0,00538	2,91	0,00748	8,28	0,0213	9,2	0,0237	12,2	0,0315	25,5	0,0657
68	401	1,69	0,00422	2,19	0,00545	3,04	0,0076	8,4	0,021	9,23	0,023	12,3	0,0308	25,7	0,064
70	413	1,91	0,00463	2,37	0,00573	3,17	0,00768	8,41	0,0204	9,34	0,0226	12,2	0,0297	26	0,063
72	425	2,02	0,00475	2,51	0,0059	3,28	0,00772	8,54	0,0201	9,41	0,0221	12,4	0,0293	26,2	0,0616
74	437	2,11	0,00482	2,68	0,00613	3,4	0,00778	8,64	0,0198	9,46	0,0217	12,7	0,029	26,3	0,0603
76	449	2,14	0,00477	2,67	0,00594	3,43	0,00765	8,83	0,0197	9,45	0,021	12,9	0,0287	26,6	0,0592
78	461	2,02	0,00438	3,03	0,00658	3,3	0,00715	8,82	0,0191	9,29	0,0201	13,4	0,029	26,5	0,0574
80	473	2,38	0,00502	2,95	0,00624	3,69	0,0078	8,94	0,0189	9,67	0,0204	13	0,0274	27	0,0571
82	485	2,39	0,00493	2,97	0,00612	3,77	0,00777	9,1	0,0187	9,62	0,0198	13,1	0,0271	27,2	0,0561
84	498	2,52	0,00506	3,1	0,00624	4,07	0,00819	9,14	0,0184	9,72	0,0195	13	0,0262	27,4	0,055
86	510	2,6	0,00511	3,17	0,00622	4,08	0,008	9,25	0,0181	9,72	0,0191	13,3	0,0261	27,5	0,0539
88	522	2,85	0,00546	3,31	0,00635	4,07	0,0078	9,28	0,0178	9,86	0,0189	13,2	0,0253	27,8	0,0532
90	534	2,88	0,0054	3,43	0,00643	4,23	0,00792	9,39	0,0176	9,74	0,0182	13,3	0,025	27,9	0,0523
92	546	3,05	0,00558	3,61	0,00661	4,35	0,00797	9,44	0,0173	9,81	0,018	13,4	0,0245	28	0,0513
94	558	3,08	0,00552	3,63	0,00651	4,57	0,00818	9,54	0,0171	9,78	0,0175	13,3	0,0238	28,1	0,0503
96	570	3,27	0,00573	3,79	0,00664	4,7	0,00824	9,49	0,0166	9,97	0,0175	13,2	0,0231	28,2	0,0495
98	582	3,37	0,00579	3,93	0,00674	4,74	0,00813	9,54	0,0164	10,1	0,0173	13,2	0,0226	28,4	0,0488
100	594	3,35	0,00564	4,09	0,00688	4,9	0,00825	9,72	0,0163	10,1	0,017	13,4	0,0225	28,6	0,0481
102	607	3,4	0,00561	4,15	0,00685	4,86	0,00801	9,8	0,0162	10,1	0,0167	13,4	0,022	28,9	0,0477
104	619	3,45	0,00558	4,31	0,00697	5,1	0,00825	9,92	0,016	10,2	0,0166	13,4	0,0217	29,1	0,047
106	631	3,54	0,00561	4,45	0,00706	5,3	0,0084	10	0,0159	10,3	0,0163	13,4	0,0213	29,2	0,0463

108	643	3,84	0,00598	4,63	0,00721	5,34	0,00831	9,96	0,0155	10,5	0,0164	13,2	0,0205	29,3	0,0456
110	655	3,89	0,00594	4,67	0,00714	5,45	0,00832	10,1	0,0154	10,5	0,016	13,3	0,0204	29,5	0,045
112	667	3,98	0,00596	4,82	0,00722	5,66	0,00849	10,1	0,0151	10,6	0,0159	13,3	0,0199	29,5	0,0443
114	679	3,85	0,00566	4,91	0,00723	5,87	0,00864	10,3	0,0151	10,6	0,0157	13,4	0,0197	29,6	0,0436
116	691	4,02	0,00582	5,1	0,00737	5,94	0,00859	10,3	0,015	10,8	0,0156	13,4	0,0194	29,7	0,043
118	703	4,03	0,00572	5,18	0,00736	6,03	0,00857	10,4	0,0148	11	0,0156	13,5	0,0192	29,9	0,0425
120	716	4,1	0,00573	5,35	0,00748	6,21	0,00868	10,4	0,0146	11,1	0,0155	13,7	0,0191	29,9	0,0418
122	728	4,27	0,00587	5,54	0,00762	6,25	0,00859	10,6	0,0145	11,2	0,0154	13,6	0,0187	30	0,0412
124	740	4,44	0,006	5,66	0,00765	6,41	0,00866	10,6	0,0144	11,5	0,0155	13,6	0,0183	30	0,0406
126	752	4,51	0,006	5,79	0,0077	6,58	0,00875	10,8	0,0143	11,5	0,0152	13,7	0,0183	30,1	0,04
128	764	4,62	0,00605	5,93	0,00777	6,63	0,00867	10,9	0,0142	11,6	0,0152	14	0,0183	30,3	0,0396
130	776	4,74	0,00611	6,04	0,00778	6,81	0,00877	11	0,0142	11,7	0,0151	13,9	0,0179	30,3	0,0391
132	788	5,1	0,00647	6,14	0,00779	6,87	0,00872	11,2	0,0142	11,9	0,0151	13,8	0,0175	30,3	0,0385
134	800	5,21	0,00651	6,39	0,00798	7,1	0,00887	11,3	0,0141	12	0,015	14	0,0175	30,3	0,0378
136	812	5,37	0,00661	6,56	0,00808	7,3	0,00899	11,3	0,0139	12,4	0,0152	13,9	0,0171	30,1	0,0371
138	825	5,5	0,00667	6,65	0,00806	7,07	0,00858	11,5	0,0139	12,5	0,0151	14,2	0,0172	30,4	0,0369
140	837	5,69	0,0068	6,76	0,00808	7,28	0,0087	11,6	0,0139	12,5	0,015	14,1	0,0169	30,2	0,0361
142	849	5,65	0,00665	6,85	0,00807	7,43	0,00875	11,8	0,0138	12,7	0,0149	14,3	0,0168	30,2	0,0356
144	861	5,75	0,00668	6,93	0,00805	7,6	0,00882	11,9	0,0139	12,8	0,0149	14,3	0,0166	30,4	0,0353
146	873	6,04	0,00691	7,17	0,00822	7,73	0,00885	12	0,0137	13	0,0149	14,4	0,0164	30,3	0,0347
148	885	6,17	0,00697	7,1	0,00802	7,77	0,00878	12,2	0,0138	13	0,0147	14,7	0,0166	30,3	0,0343
150	897	6,28	0,007	7,3	0,00813	7,81	0,00871	12,2	0,0136	13,1	0,0146	14,8	0,0165	30,4	0,0338
152	909	6,23	0,00685	7,52	0,00827	8,03	0,00883	12,2	0,0135	13,1	0,0144	15	0,0165	30,3	0,0333
154	921	6,41	0,00696	7,62	0,00827	8,11	0,0088	12,3	0,0134	13,2	0,0143	15	0,0163	30,2	0,0328
156	934	6,42	0,00688	7,69	0,00824	8,28	0,00887	12,5	0,0134	13,4	0,0143	15,3	0,0164	30,4	0,0325
158	946	6,62	0,007	7,89	0,00834	8,35	0,00883	12,6	0,0133	13,7	0,0145	15,2	0,0161	30,3	0,032
160	958	6,61	0,0069	7,92	0,00827	8,63	0,00901	12,7	0,0133	13,8	0,0144	15,4	0,0161	30,5	0,0318
162	970	6,71	0,00691	8,04	0,00829	8,77	0,00904	13	0,0134	13,8	0,0143	15,4	0,0159	30,5	0,0314
164	982	6,98	0,00711	8,16	0,00831	8,76	0,00892	13,1	0,0133	14,1	0,0144	15,4	0,0157	30,5	0,031
166	994	6,96	0,007	8,31	0,00836	9,1	0,00915	13,3	0,0133	14,2	0,0142	15,7	0,0158	30,5	0,0307
168	1 010	7,11	0,00707	8,46	0,00841	9,2	0,00915	13,4	0,0133	14,3	0,0142	15,6	0,0155	30,5	0,0303
170	1 020	7,31	0,00717	8,65	0,0085	9,34	0,00917	13,7	0,0135	14,7	0,0144	15,8	0,0155	30,5	0,03
172	1 030	7,32	0,0071	8,64	0,00839	9,5	0,00922	14,2	0,0137	14,8	0,0144	16,2	0,0157	30,7	0,0298
174	1 040	7,47	0,00716	8,81	0,00845	9,83	0,00943	14,4	0,0139	15,1	0,0145	16,3	0,0157	30,6	0,0294

176	1 050	7,67	0,00727	8,93	0,00847	9,9	0,00939	14,7	0,0139	15,4	0,0146	16,4	0,0156	30,7	0,0291
178	1 070	7,97	0,00747	9,25	0,00867	10	0,00939	14,7	0,0138	15,7	0,0147	16,7	0,0157	30,5	0,0285
180	1 080	8,07	0,00748	9,33	0,00865	10,2	0,00945	15	0,0139	16,1	0,0149	17	0,0158	30,6	0,0284
182	1 090	8,14	0,00746	9,22	0,00845	10,4	0,00953	15,2	0,014	16,2	0,0149	17,3	0,0159	30,7	0,0281
184	1 100	8,37	0,00759	9,43	0,00855	10,5	0,00948	15,4	0,014	16,5	0,015	17,5	0,0159	30,7	0,0278
186	1 120	8,35	0,00748	9,48	0,0085	10,7	0,00955	15,8	0,0142	16,6	0,0149	17,9	0,0161	30,7	0,0276
188	1 130	8,5	0,00754	9,65	0,00856	10,9	0,00965	16	0,0142	16,9	0,015	18	0,016	30,8	0,0274
190	1 140	8,83	0,00775	10	0,00881	11	0,00967	16	0,0141	17,2	0,0151	18,1	0,0159	30,6	0,0269
192	1 150	8,9	0,00773	10,1	0,00877	11,2	0,00973	16,3	0,0142	17,4	0,0151	18,3	0,0159	30,8	0,0268
194	1 160	9,11	0,00783	10,3	0,00884	11,4	0,00982	16,5	0,0142	17,6	0,0151	18,6	0,016	30,8	0,0265
196	1 180	9,25	0,00787	10,4	0,00885	11,6	0,0099	16,8	0,0143	17,9	0,0152	18,9	0,0161	30,9	0,0262
198	1 190	9,53	0,00802	10,6	0,00888	11,8	0,00992	16,7	0,0141	18,1	0,0153	19,1	0,0161	30,8	0,026
200	1 200	9,65	0,00805	10,7	0,00893	11,9	0,0099	17,1	0,0142	18,4	0,0153	19,3	0,0161	30,8	0,0257

Time	Shear Rate	Shear Stress	Viscosity	Shear Stress	Viscosity	Shear Stress	Viscosity	Shear Stress	Viscosity	Shear Stress	Viscosity	Shear Stress	Viscosity	Shear Stress	Viscosity
[s]	[1/s]	[Pa]	[Pa·s]	[Pa]	[Pa·s]	[Pa]	[Pa·s]	[Pa]	[Pa·s]	[Pa]	[Pa·s]	[Pa]	[Pa·s]	[Pa]	[Pa·s]
Number of Intervals:		*CNC-ATT-WDFs (6 wt %) 0.0 % 40°C S.W.*	*CNC-ATT-WDFs (6 wt %) 0.0 % 40°C S.W.*	*CNC-ATT-WDFs (6 wt %) 0.4 % 40°C S.W.*	*CNC-ATT-WDFs (6 wt %) 0.4 % 40°C S.W.*	*CNC-ATT-WDFs (6 wt %) 0.8 % 40°C S.W.*	*CNC-ATT-WDFs (6 wt %) 0.8 % 40°C S.W.*	*CNC-ATT-WDFs (6 wt %) 1.2 % 40°C S.W.*	*CNC-ATT-WDFs (6 wt %) 1.2 % 40°C S.W.*	*CNC-ATT-WDFs (6 wt %) 1,6 % 40°C S.W.*	*CNC-ATT-WDFs (6 wt %) 1,6 % 40°C S.W.*	*CNC-ATT-WDFs (6 wt %) 2.0 % 40°C S.W.*	*CNC-ATT-WDFs (6 wt %) 2.0 % 40°C S.W.*	*CNC-ATT-WDFs (6 wt %) 2.4 % 40°C S.W.*	*CNC-ATT-WDFs (6 wt %) 2.4 % 40°C S.W.*
2	0,999	-0,49	-0,491	-0,0726	-0,0727	-0,396	-0,397	1,88	1,88	2,04	2,04	1,61	1,61	4,57	4,57
4	13,1	-0,456	-0,0348	0,0959	0,00731	0,576	0,0439	3,67	0,28	3,11	0,237	3,63	0,277	11	0,837
6	25,2	-0,414	-0,0164	0,325	0,0129	0,827	0,0328	3,84	0,152	3,72	0,148	4,38	0,174	11,7	0,465
8	37,3	-0,37	-0,00992	0,303	0,00812	0,678	0,0182	3,92	0,105	4,02	0,108	5,19	0,139	12,2	0,326
10	49,4	-0,436	-0,00881	0,338	0,00683	0,753	0,0152	3,97	0,0802	4,47	0,0904	5,1	0,103	12,6	0,255
12	61,6	-0,399	-0,00648	0,305	0,00496	0,865	0,0141	4,14	0,0673	3,9	0,0633	5,46	0,0887	13,1	0,214
14	73,7	-0,407	-0,00553	0,332	0,00451	1,05	0,0143	4,21	0,0572	4,11	0,0557	5,67	0,0769	13,4	0,182
16	85,8	-0,335	-0,00391	0,368	0,00429	1,01	0,0117	4,27	0,0497	4,08	0,0476	5,87	0,0684	13,8	0,161
18	97,9	-0,287	-0,00293	0,358	0,00366	1,08	0,011	4,42	0,0452	4,18	0,0427	6,07	0,062	14,1	0,144
20	110	-0,24	-0,00219	0,447	0,00407	1,06	0,00961	4,57	0,0415	4,4	0,04	6,27	0,057	14,5	0,132
22	122	-0,178	-0,00146	0,485	0,00397	1,19	0,00976	4,74	0,0388	4,63	0,0379	6,48	0,0531	14,9	0,122
24	134	-0,157	-0,00117	0,475	0,00354	1,22	0,00906	4,88	0,0364	4,8	0,0358	6,73	0,0502	15,6	0,116
26	146	-0,128	-8,77E-4	0,548	0,00375	1,27	0,00868	5,07	0,0346	4,95	0,0338	6,96	0,0476	16,2	0,11
28	158	-0,0469	-2,96E-4	0,641	0,00405	1,36	0,00858	5,11	0,0323	5,15	0,0325	7,32	0,0462	16,7	0,105
30	171	0,0131	7,68E-5	0,716	0,0042	1,38	0,00809	5,27	0,0309	5,27	0,0309	7,29	0,0427	17,4	0,102
32	183	0,0966	5,29E-4	0,706	0,00387	1,49	0,00814	5,36	0,0293	5,37	0,0294	7,46	0,0408	18,1	0,0989
34	195	0,151	7,76E-4	0,761	0,00391	1,49	0,00763	5,49	0,0282	5,57	0,0286	7,47	0,0383	18,5	0,0949
36	207	0,239	0,00116	0,834	0,00403	1,51	0,00731	5,64	0,0273	5,85	0,0283	7,9	0,0382	19,3	0,0933
38	219	0,279	0,00127	0,801	0,00366	1,57	0,00719	5,78	0,0264	5,87	0,0268	8,11	0,037	19,5	0,089
40	231	0,358	0,00155	0,79	0,00342	1,62	0,00701	5,88	0,0254	6,03	0,0261	8,23	0,0356	19,9	0,086

42	243	0,389	0,0016	0,846	0,00348	1,65	0,00678	5,99	0,0246	6,11	0,0251	8,36	0,0344	20,2	0,0832
44	255	0,476	0,00186	0,83	0,00325	1,72	0,00675	6,07	0,0238	6,11	0,0239	8,55	0,0335	20,6	0,0806
46	267	0,525	0,00196	0,91	0,0034	1,82	0,00681	6,22	0,0233	6,24	0,0233	8,67	0,0324	21	0,0784
48	280	0,666	0,00238	0,966	0,00346	1,9	0,00679	6,34	0,0227	6,37	0,0228	8,87	0,0317	21,4	0,0766
50	292	0,753	0,00258	1,14	0,00391	1,91	0,00656	6,45	0,0221	6,52	0,0223	8,96	0,0307	21,6	0,0742
52	304	0,865	0,00285	1,21	0,00398	2,04	0,00671	6,56	0,0216	6,56	0,0216	9,18	0,0302	22	0,0723
54	316	0,926	0,00293	1,25	0,00396	2,11	0,00669	6,71	0,0212	6,69	0,0212	9,39	0,0297	22,2	0,0703
56	328	1,09	0,00334	1,33	0,00407	2,2	0,00672	6,76	0,0206	6,82	0,0208	9,64	0,0294	22,5	0,0686
58	340	1,14	0,00334	1,42	0,00419	2,34	0,00687	6,94	0,0204	6,9	0,0203	9,85	0,0289	22,7	0,0668
60	352	1,24	0,00351	1,54	0,00439	2,41	0,00685	7,04	0,02	6,96	0,0198	10	0,0284	22,9	0,0649
62	364	1,45	0,00397	1,71	0,0047	2,47	0,00678	7,1	0,0195	7,11	0,0195	10,2	0,0279	23,3	0,0639
64	376	1,51	0,00402	1,88	0,00499	2,55	0,00677	7,25	0,0193	7,17	0,019	10,4	0,0275	23,5	0,0624
66	389	1,65	0,00424	2,04	0,00524	2,77	0,00714	7,33	0,0189	7,24	0,0186	10,5	0,0271	23,7	0,061
68	401	1,7	0,00424	2,15	0,00535	2,82	0,00704	7,46	0,0186	7,36	0,0184	10,6	0,0265	24	0,06
70	413	1,89	0,00457	2,16	0,00523	2,94	0,00712	7,45	0,018	7,38	0,0179	10,7	0,026	24,3	0,0589
72	425	1,99	0,00468	2,23	0,00525	3,07	0,00724	7,53	0,0177	7,4	0,0174	10,8	0,0254	24,4	0,0574
74	437	2,11	0,00484	2,35	0,00538	3,1	0,00708	7,57	0,0173	7,56	0,0173	10,9	0,0249	24,8	0,0568
76	449	2,11	0,0047	2,51	0,00558	3,27	0,00729	7,74	0,0172	7,6	0,0169	11	0,0246	24,8	0,0551
78	461	1,98	0,0043	2,63	0,0057	3,49	0,00756	7,65	0,0166	7,83	0,017	10,7	0,0231	24,8	0,0539
80	473	2,39	0,00506	2,73	0,00576	3,39	0,00716	7,84	0,0166	7,72	0,0163	11	0,0233	25,3	0,0535
82	485	2,38	0,00491	2,86	0,0059	3,46	0,00713	7,98	0,0164	7,73	0,0159	10,9	0,0225	25,4	0,0523
84	498	2,47	0,00497	3,01	0,00605	3,48	0,007	7,98	0,016	7,84	0,0158	10,9	0,022	25,5	0,0513
86	510	2,57	0,00505	3,16	0,0062	3,58	0,00703	8,09	0,0159	7,92	0,0155	11	0,0215	25,8	0,0506
88	522	2,66	0,0051	3,12	0,00599	3,78	0,00725	8,16	0,0156	7,9	0,0151	11,2	0,0214	25,9	0,0496
90	534	2,78	0,00521	3,31	0,0062	3,89	0,00728	8,23	0,0154	8,03	0,015	11,1	0,0208	26,2	0,049
92	546	2,91	0,00534	3,36	0,00615	4,06	0,00743	8,32	0,0152	8,14	0,0149	11,3	0,0207	26,3	0,0482
94	558	2,98	0,00534	3,49	0,00626	4,14	0,00741	8,36	0,015	8,26	0,0148	11,3	0,0202	26,6	0,0476
96	570	3,11	0,00545	3,5	0,00614	4,34	0,00762	8,37	0,0147	8,2	0,0144	11,4	0,0201	26,7	0,0469
98	582	3,2	0,0055	3,63	0,00624	4,45	0,00764	8,45	0,0145	8,32	0,0143	11,4	0,0197	26,9	0,0462
100	594	3,38	0,00568	3,94	0,00663	4,52	0,0076	8,58	0,0144	8,51	0,0143	11,3	0,019	27	0,0455
102	607	3,41	0,00562	3,99	0,00659	4,69	0,00773	8,75	0,0144	8,45	0,0139	11,5	0,0189	27,1	0,0447
104	619	3,47	0,00561	4,16	0,00673	4,77	0,00771	8,83	0,0143	8,55	0,0138	11,3	0,0183	27,3	0,0441
106	631	3,51	0,00556	4,36	0,00691	4,87	0,00772	8,93	0,0142	8,63	0,0137	11,2	0,0178	27,5	0,0436
108	643	3,67	0,00571	4,29	0,00668	5,14	0,00799	8,96	0,0139	8,67	0,0135	11,5	0,0178	27,6	0,0429

110	655	3,65	0,00558	4,43	0,00677	5,24	0,008	9,09	0,0139	8,71	0,0133	11,5	0,0176	27,7	0,0422
112	667	3,83	0,00575	4,57	0,00685	5,33	0,00799	9,09	0,0136	8,82	0,0132	11,5	0,0172	27,8	0,0417
114	679	3,96	0,00583	4,87	0,00718	5,33	0,00785	9,28	0,0137	9,02	0,0133	11,4	0,0167	27,8	0,0409
116	691	4,09	0,00591	4,93	0,00713	5,55	0,00802	9,31	0,0135	9,05	0,0131	11,4	0,0164	27,9	0,0403
118	703	4,11	0,00584	5,01	0,00712	5,65	0,00804	9,43	0,0134	9,16	0,013	11,5	0,0164	27,8	0,0396
120	716	4,28	0,00598	5,17	0,00722	5,67	0,00792	9,48	0,0133	9,25	0,0129	11,5	0,0161	28	0,0391
122	728	4,35	0,00598	5,22	0,00718	5,87	0,00807	9,62	0,0132	9,26	0,0127	11,8	0,0162	28,1	0,0386
124	740	4,56	0,00616	5,36	0,00725	6,04	0,00816	9,7	0,0131	9,46	0,0128	11,7	0,0158	28,1	0,038
126	752	4,7	0,00625	5,64	0,0075	6,07	0,00808	9,86	0,0131	9,75	0,013	11,6	0,0155	28,1	0,0374
128	764	4,85	0,00634	5,63	0,00737	6,24	0,00817	9,96	0,013	9,71	0,0127	11,8	0,0154	28,2	0,0369
130	776	4,91	0,00633	5,86	0,00755	6,31	0,00813	10,1	0,013	9,94	0,0128	11,7	0,0151	28,1	0,0362
132	788	5	0,00635	5,96	0,00756	6,45	0,00818	10,3	0,013	10	0,0127	11,9	0,0151	28,2	0,0357
134	800	5,12	0,00639	6,17	0,00771	6,5	0,00812	10,3	0,0129	10,2	0,0128	11,8	0,0147	28,2	0,0353
136	812	5,34	0,00657	6,25	0,00769	6,62	0,00815	10,4	0,0127	10,3	0,0127	11,9	0,0147	28,4	0,0349
138	825	5,18	0,00629	6,55	0,00794	6,71	0,00814	10,5	0,0127	10,6	0,0129	12	0,0145	28,2	0,0341
140	837	5,49	0,00657	6,38	0,00763	7,08	0,00846	10,7	0,0128	10,3	0,0123	12,2	0,0146	28,4	0,034
142	849	5,57	0,00656	6,6	0,00778	7,09	0,00835	10,9	0,0128	10,4	0,0123	12,3	0,0145	28,4	0,0335
144	861	5,65	0,00656	6,76	0,00785	7,01	0,00814	11	0,0128	10,5	0,0122	12,3	0,0143	28,3	0,0329
146	873	5,81	0,00666	6,75	0,00773	7,23	0,00828	10,9	0,0125	10,6	0,0121	12,7	0,0145	28,4	0,0325
148	885	5,81	0,00656	6,91	0,00781	7,47	0,00843	11,1	0,0126	10,7	0,012	12,7	0,0144	28,3	0,032
150	897	5,97	0,00665	6,98	0,00778	7,57	0,00844	11,3	0,0126	10,7	0,0119	12,9	0,0143	28,4	0,0316
152	909	6,23	0,00685	7,15	0,00786	7,56	0,00832	11,2	0,0123	11	0,0121	12,7	0,014	28,3	0,0312
154	921	6,28	0,00682	7,25	0,00786	7,78	0,00844	11,3	0,0123	11	0,012	13	0,0141	28,5	0,0309
156	934	6,41	0,00687	7,28	0,0078	7,83	0,00839	11,6	0,0124	11,4	0,0122	13	0,014	28,3	0,0303
158	946	6,52	0,00689	7,29	0,00771	8,09	0,00855	11,8	0,0124	11,6	0,0122	13,2	0,014	28,3	0,0299
160	958	6,62	0,00692	7,55	0,00788	8,2	0,00856	12	0,0125	11,9	0,0124	13,1	0,0137	28,2	0,0295
162	970	6,8	0,00701	7,73	0,00797	8,33	0,00859	12,2	0,0126	12,1	0,0125	13,4	0,0138	28,2	0,0291
164	982	6,9	0,00703	7,67	0,00781	8,6	0,00876	12,4	0,0126	12,1	0,0123	13,5	0,0137	28,2	0,0287
166	994	7,09	0,00713	7,99	0,00803	8,63	0,00868	12,7	0,0128	12,4	0,0125	13,5	0,0136	28,2	0,0284
168	1 010	7,25	0,00721	7,96	0,00791	8,81	0,00876	12,8	0,0127	12,5	0,0125	13,7	0,0137	28,1	0,0279
170	1 020	7,37	0,00724	8,09	0,00794	8,97	0,00881	13	0,0127	12,8	0,0126	14	0,0138	28,2	0,0277
172	1 030	7,4	0,00718	8,27	0,00803	9,11	0,00884	13,3	0,0129	13,1	0,0127	14,1	0,0137	28,1	0,0273
174	1 040	7,61	0,0073	8,52	0,00817	9,22	0,00885	13,5	0,0129	13,3	0,0128	14,3	0,0137	28,2	0,027
176	1 050	7,61	0,00721	8,66	0,00821	9,48	0,00899	13,6	0,0129	13,5	0,0128	14,5	0,0138	28,2	0,0267

178	1 070	8,01	0,00751	8,62	0,00808	9,66	0,00905	13,8	0,0129	13,6	0,0127	15	0,014	28,3	0,0265
180	1 080	8,05	0,00746	8,78	0,00813	9,83	0,00911	14	0,0129	13,9	0,0128	15,1	0,014	28,2	0,0261
182	1 090	8,19	0,0075	8,87	0,00813	9,91	0,00908	14,3	0,0131	14	0,0129	15,3	0,014	28,2	0,0259
184	1 100	8,46	0,00767	8,86	0,00803	10,2	0,00924	14,4	0,013	14,2	0,0128	15,6	0,0142	28,2	0,0256
186	1 120	8,44	0,00757	9,16	0,00822	10,2	0,00918	14,6	0,0131	14,6	0,0131	15,8	0,0142	28,2	0,0253
188	1 130	8,57	0,0076	9,29	0,00824	10,5	0,00927	14,9	0,0132	14,7	0,0131	16,1	0,0143	28,3	0,0251
190	1 140	8,92	0,00783	9,34	0,0082	10,7	0,00935	14,9	0,0131	14,9	0,0131	16,4	0,0144	28,5	0,025
192	1 150	8,99	0,00781	9,58	0,00832	10,8	0,00941	15,2	0,0132	15,2	0,0132	16,6	0,0144	28,3	0,0246
194	1 160	9,25	0,00795	9,68	0,00832	10,9	0,00938	15,4	0,0132	15,3	0,0132	16,8	0,0144	28,3	0,0243
196	1 180	9,38	0,00797	9,91	0,00843	11	0,00939	15,8	0,0134	15,6	0,0132	17	0,0144	28,4	0,0241
198	1 190	9,64	0,00811	9,92	0,00835	11,3	0,00948	15,7	0,0132	15,8	0,0133	17	0,0143	28,6	0,0241
200	1 200	9,84	0,0082	10,1	0,00843	11,5	0,00957	16	0,0133	15,9	0,0133	17,3	0,0144	28,5	0,0238

Time	Shear Rate	Shear Stress	Viscosity	Shear Stress	Viscosity	Shear Stress	Viscosity	Shear Stress	Viscosity	Shear Stress	Viscosity	Shear Stress	Viscosity	Shear Stress	Viscosity
[s]	[1/s]	[Pa]	[Pa·s]	[Pa]	[Pa·s]	[Pa]	[Pa·s]	[Pa]	[Pa·s]	[Pa]	[Pa·s]	[Pa]	[Pa·s]	[Pa]	[Pa·s]
Number of Intervals:		*CNC-ATT-WDFs (6 wt %) 0.0 % 50°C S.W.*	*CNC-ATT-WDFs (6 wt %) 0.0 % 50°C S.W.*	*CNC-ATT-WDFs (6 wt %) 0.4 % 50°C S.W.*	*CNC-ATT-WDFs (6 wt %) 0.4 % 50°C S.W.*	*CNC-ATT-WDFs (6 wt %) 0.8 % 50°C S.W.*	*CNC-ATT-WDFs (6 wt %) 0.8 % 50°C S.W.*	*CNC-ATT-WDFs (6 wt %) 1.2 % 50°C S.W.*	*CNC-ATT-WDFs (6 wt %) 1.2 % 50°C S.W.*	*CNC-ATT-WDFs (6 wt %) 1.6 % 50°C S.W.*	*CNC-ATT-WDFs (6 wt %) 1.6 % 50°C S.W.*	*CNC-ATT-WDFs (6 wt %) 2.0 % 50°C S.W.*	*CNC-ATT-WDFs (6 wt %) 2.0 % 50°C S.W.*	*CNC-ATT-WDFs (6 wt %) 2.4 % 50°C S.W.*	*CNC-ATT-WDFs (6 wt %) 2.4 % 50°C S.W.*
2	0,999	-1,01	-1,01	-0,15	-0,15	-0,0259	-0,0259	2,2	2,19	1,99	1,99	2,3	2,3	7,02	6,97
4	13,1	-0,518	-0,0395	-0,118	-0,00902	0,59	0,045	4,18	0,319	3,36	0,256	4,22	0,322	10,2	0,779
6	25,2	-0,467	-0,0185	-0,1	-0,00397	0,655	0,026	4,24	0,168	3,17	0,126	4,42	0,175	10,6	0,421
8	37,3	-0,478	-0,0128	-0,0509	-0,00136	0,789	0,0211	4,19	0,112	3,55	0,095	4,34	0,116	11,5	0,307
10	49,4	-0,459	-0,00928	0,0292	5,9E-4	0,825	0,0167	4,08	0,0825	4,75	0,0961	4,48	0,0906	12,2	0,246
12	61,6	-0,446	-0,00724	0,0377	6,12E-4	0,861	0,014	4,3	0,0699	3,85	0,0626	4,81	0,0781	12,8	0,208
14	73,7	-0,386	-0,00524	0,0601	8,16E-4	0,896	0,0122	4,31	0,0585	3,68	0,05	5,18	0,0703	13,2	0,179
16	85,8	-0,44	-0,00513	0,0908	0,00106	0,932	0,0109	4,34	0,0506	4,16	0,0485	5,39	0,0629	13,5	0,158
18	97,9	-0,433	-0,00442	0,158	0,00161	0,967	0,00988	4,52	0,0462	3,89	0,0397	5,73	0,0585	14,2	0,145
20	110	-0,335	-0,00305	0,149	0,00136	1,01	0,00921	4,69	0,0426	4,18	0,038	5,95	0,0541	14,6	0,133
22	122	-0,236	-0,00193	0,189	0,00155	1,08	0,00887	4,86	0,0398	4,41	0,0361	5,88	0,0481	15	0,123
24	134	-0,157	-0,00117	0,214	0,00159	1,14	0,0085	5,02	0,0374	4,64	0,0346	6,23	0,0464	15,4	0,115
26	146	-0,155	-0,00106	0,252	0,00172	1,19	0,00812	5,16	0,0353	4,85	0,0332	6,37	0,0435	15,8	0,108
28	158	-0,118	-7,44E-4	0,279	0,00176	1,27	0,00803	5,19	0,0328	4,99	0,0315	6,68	0,0421	16,7	0,105
30	171	-0,0775	-4,54E-4	0,344	0,00202	1,22	0,00716	5,29	0,031	5,22	0,0306	6,79	0,0398	17,3	0,101
32	183	-0,029	-1,59E-4	0,371	0,00203	1,27	0,00695	5,37	0,0294	5,35	0,0293	7,09	0,0388	17,9	0,098
34	195	0,0224	1,15E-4	0,394	0,00202	1,31	0,00674	5,48	0,0281	5,5	0,0282	7,04	0,0362	18,6	0,0954
36	207	0,0654	3,16E-4	0,388	0,00188	1,32	0,00638	5,58	0,027	5,69	0,0275	7,18	0,0347	18,9	0,0914

38	219	0,164	7,5E-4	0,484	0,00221	1,38	0,00631	5,72	0,0261	5,83	0,0266	7,44	0,034	19,3	0,0881
40	231	0,18	7,81E-4	0,537	0,00232	1,43	0,00617	5,81	0,0251	5,93	0,0256	7,52	0,0326	19,7	0,0852
42	243	0,234	9,62E-4	0,61	0,00251	1,42	0,00583	5,9	0,0243	6,06	0,0249	7,83	0,0322	20,1	0,0825
44	255	0,318	0,00125	0,684	0,00268	1,5	0,00587	5,98	0,0234	6,28	0,0246	8,03	0,0314	20,3	0,0793
46	267	0,363	0,00136	0,741	0,00277	1,56	0,00583	6,1	0,0228	6,22	0,0232	8,28	0,0309	20,7	0,0772
48	280	0,426	0,00152	0,779	0,00279	1,59	0,00569	6,18	0,0221	6,38	0,0228	8,41	0,0301	21	0,075
50	292	0,422	0,00145	0,84	0,00288	1,56	0,00533	6,27	0,0215	6,49	0,0223	8,63	0,0296	21,4	0,0733
52	304	0,537	0,00177	0,894	0,00294	1,64	0,0054	6,33	0,0208	6,61	0,0218	8,67	0,0285	21,7	0,0713
54	316	0,628	0,00199	0,988	0,00313	1,72	0,00543	6,45	0,0204	6,72	0,0213	8,86	0,028	22	0,0696
56	328	0,717	0,00219	1,06	0,00322	1,81	0,00553	6,54	0,0199	6,88	0,021	8,99	0,0274	22,4	0,0681
58	340	0,843	0,00248	1,24	0,00366	1,95	0,00575	6,79	0,02	7,06	0,0207	9,16	0,0269	22,6	0,0666
60	352	0,928	0,00263	1,35	0,00383	2,09	0,00593	6,8	0,0193	7,05	0,02	9,3	0,0264	22,9	0,0649
62	364	0,95	0,00261	1,44	0,00395	2,18	0,00598	6,89	0,0189	7,2	0,0198	9,51	0,0261	23,2	0,0636
64	376	1,09	0,00289	1,62	0,00431	2,28	0,00605	6,99	0,0186	7,2	0,0191	9,71	0,0258	23,3	0,0619
66	389	1,19	0,00307	1,68	0,00433	2,39	0,00616	7,09	0,0183	7,35	0,0189	9,82	0,0253	23,6	0,0607
68	401	1,23	0,00308	1,77	0,00442	2,4	0,00599	7,16	0,0179	7,45	0,0186	9,77	0,0244	23,7	0,0591
70	413	1,39	0,00336	1,83	0,00443	2,56	0,00619	7,14	0,0173	7,52	0,0182	9,9	0,024	24	0,0581
72	425	1,51	0,00355	1,94	0,00456	2,65	0,00624	7,27	0,0171	7,53	0,0177	10,1	0,0238	24,2	0,0569
74	437	1,51	0,00346	1,96	0,0045	2,69	0,00616	7,32	0,0167	7,64	0,0175	10	0,023	24,3	0,0557
76	449	1,67	0,00371	2,17	0,00483	2,8	0,00623	7,47	0,0166	7,69	0,0171	10,3	0,0229	24,4	0,0544
78	461	1,6	0,00347	2,41	0,00523	2,54	0,00551	7,56	0,0164	8,08	0,0175	9,98	0,0216	24,6	0,0534
80	473	1,8	0,00381	2,24	0,00473	2,87	0,00607	7,62	0,0161	7,77	0,0164	10,3	0,0219	24,8	0,0524
82	485	1,86	0,00384	2,4	0,00494	2,94	0,00606	7,83	0,0161	7,81	0,0161	10,3	0,0213	24,8	0,0511
84	498	1,87	0,00376	2,45	0,00493	2,91	0,00586	7,84	0,0158	7,99	0,0161	10,2	0,0206	24,9	0,05
86	510	1,93	0,00379	2,51	0,00493	3,06	0,00601	7,93	0,0156	8,2	0,0161	10,3	0,0203	25,1	0,0493
88	522	2,15	0,00412	2,72	0,00522	3,29	0,00631	8,06	0,0154	8,1	0,0155	10,6	0,0203	25,2	0,0483
90	534	2,13	0,00399	2,78	0,00521	3,38	0,00632	8,07	0,0151	8,24	0,0154	10,5	0,0197	25,3	0,0475
92	546	2,25	0,00412	2,92	0,00534	3,51	0,00642	8,17	0,015	8,29	0,0152	10,7	0,0196	25,6	0,0469
94	558	2,24	0,00402	2,97	0,00532	3,59	0,00643	8,15	0,0146	8,44	0,0151	10,6	0,0189	25,7	0,046
96	570	2,42	0,00425	3,04	0,00532	3,77	0,00661	8,2	0,0144	8,43	0,0148	10,7	0,0188	26	0,0456
98	582	2,51	0,00431	3,19	0,00548	3,9	0,0067	8,25	0,0142	8,46	0,0145	10,9	0,0187	26,1	0,0448
100	594	2,47	0,00416	3,17	0,00534	3,9	0,00656	8,27	0,0139	8,64	0,0145	10,8	0,0181	26,1	0,0439
102	607	2,68	0,00442	3,4	0,00561	4,11	0,00678	8,4	0,0139	8,52	0,014	11,1	0,0182	26,3	0,0433
104	619	2,82	0,00456	3,53	0,0057	4,18	0,00676	8,47	0,0137	8,66	0,014	11	0,0177	26,4	0,0427

106	631	2,89	0,0045 7	3,61	0,0057 3	4,25	0,0067 4	8,54	0,0135	8,71	0,0138	11,1	0,0175	26,4	0,0419
108	643	3,05	0,0047 4	3,67	0,0057	4,42	0,0068 8	8,62	0,0134	8,78	0,0137	11,1	0,0172	26,6	0,0414
110	655	3,18	0,0048 5	3,84	0,0058 6	4,54	0,0069 3	8,77	0,0134	8,88	0,0136	11,3	0,0173	26,5	0,0405
112	667	3,2	0,0047 9	3,86	0,0057 9	4,69	0,0070 3	8,73	0,0131	8,9	0,0133	11,3	0,0169	26,8	0,0401
114	679	3,18	0,0046 8	3,97	0,0058 5	4,59	0,0067 5	8,85	0,013	9,15	0,0135	11,2	0,0164	26,7	0,0393
116	691	3,34	0,0048 3	4,07	0,0058 9	4,7	0,0068	8,97	0,013	9,24	0,0134	11,3	0,0163	26,8	0,0387
118	703	3,44	0,0049	4,23	0,0060 1	4,8	0,0068 2	9,1	0,0129	9,32	0,0132	11,3	0,0161	26,8	0,0381
120	716	3,49	0,0048 7	4,26	0,0059 5	4,93	0,0068 8	9,13	0,0128	9,35	0,0131	11,2	0,0157	26,9	0,0376
122	728	3,75	0,0051 5	4,47	0,0061 4	5,19	0,0071 3	9,33	0,0128	9,35	0,0128	11,4	0,0156	27	0,0372
124	740	3,87	0,0052 3	4,54	0,0061 4	5,37	0,0072 5	9,39	0,0127	9,44	0,0128	11,4	0,0154	27	0,0366
126	752	3,82	0,0050 8	4,59	0,0061 1	5,25	0,0069 8	9,49	0,0126	9,86	0,0131	11,2	0,0149	27	0,0359
128	764	4	0,0052 4	4,79	0,0062 6	5,46	0,0071 4	9,59	0,0126	9,84	0,0129	11,5	0,015	27,1	0,0355
130	776	4,09	0,0052 7	4,91	0,0063 2	5,51	0,0071	9,75	0,0126	10	0,0129	11,6	0,0149	27,1	0,035
132	788	4,2	0,0053 3	5,07	0,0064 3	5,71	0,0072 5	9,89	0,0126	10,1	0,0128	11,6	0,0148	27,2	0,0345
134	800	4,18	0,0052 2	5,05	0,0063 1	5,74	0,0071 7	9,87	0,0123	10,3	0,0129	11,6	0,0145	27,3	0,0341
136	812	4,31	0,0053 1	5,15	0,0063 3	5,74	0,0070 7	9,99	0,0123	10,4	0,0128	11,6	0,0143	27,4	0,0337
138	825	4,43	0,0053 8	5,19	0,0063	5,99	0,0072 6	10,3	0,0125	10,3	0,0125	11,8	0,0143	27,4	0,0332
140	837	4,72	0,0056 4	5,49	0,0065 7	6,29	0,0075 2	10,3	0,0123	10,4	0,0125	12	0,0143	27,4	0,0328
142	849	4,78	0,0056 3	5,62	0,0066 2	6,45	0,0076	10,4	0,0123	10,4	0,0123	12,1	0,0142	27,4	0,0323
144	861	4,86	0,0056 5	5,71	0,0066 3	6,48	0,0075 3	10,6	0,0123	10,7	0,0125	12,3	0,0143	27,4	0,0318
146	873	5,06	0,0057 9	5,78	0,0066 2	6,72	0,0076 9	10,6	0,0121	10,7	0,0122	12,5	0,0143	27,5	0,0315
148	885	5,13	0,0057 9	6,01	0,0067 9	6,81	0,0076 9	10,6	0,012	10,9	0,0123	12,6	0,0142	27,4	0,031
150	897	5,29	0,0059	6,04	0,0067 3	7,02	0,0078 3	10,7	0,0119	11,1	0,0123	12,8	0,0142	27,4	0,0305
152	909	5,26	0,0057 8	6,03	0,0066 3	7,02	0,0077 2	10,7	0,0117	11,6	0,0128	12,7	0,014	27,4	0,0301
154	921	5,47	0,0059 4	6,2	0,0067 3	7,21	0,0078 3	10,8	0,0117	11,7	0,0127	12,9	0,0141	27,3	0,0296
156	934	5,61	0,0060 1	6,31	0,0067 6	7,3	0,0078 1	10,8	0,0116	11,9	0,0127	12,9	0,0138	27,2	0,0291
158	946	5,8	0,0061 3	6,41	0,0067 8	7,49	0,0079 2	11,1	0,0118	12,2	0,0128	12,9	0,0136	27,3	0,0288
160	958	5,77	0,0060 2	6,46	0,0067 5	7,43	0,0077 6	11,2	0,0117	12,4	0,013	13	0,0136	27,1	0,0283
162	970	5,86	0,0060 4	6,49	0,0066 9	7,53	0,0077 7	11,5	0,0118	12,5	0,0129	13,3	0,0137	27	0,0279
164	982	6,17	0,0062 8	6,6	0,0067 3	7,85	0,0079 9	11,6	0,0118	12,5	0,0127	13,3	0,0135	27	0,0275
166	994	6,13	0,0061 6	6,57	0,0066	7,83	0,0078 8	11,8	0,0119	13	0,0131	13,4	0,0135	27,1	0,0272
168	1 01 0	6,24	0,0062	6,7	0,0066 6	8,05	0,008	12,1	0,012	13	0,0129	13,6	0,0135	27,1	0,0269
170	1 02 0	6,45	0,0063 3	6,81	0,0066 9	8,21	0,0080 6	12,3	0,0121	13,3	0,013	13,9	0,0136	27,2	0,0267
172	1 03 0	6,56	0,0063 7	7,05	0,0068 4	8,28	0,0080 3	12,6	0,0122	13,5	0,0131	14,3	0,0138	27,1	0,0263

174	1 040	6,63	0,00636	7,08	0,00679	8,37	0,00803	12,6	0,0121	13,7	0,0131	14,3	0,0138	27	0,0259
176	1 050	6,86	0,00651	7,41	0,00702	8,58	0,00813	13	0,0123	13,8	0,0131	14,7	0,0139	26,9	0,0255
178	1 070	7,07	0,00663	7,41	0,00695	8,86	0,00831	13	0,0122	14	0,0131	14,8	0,0139	27,2	0,0255
180	1 080	7,17	0,00664	7,55	0,007	9	0,00834	13,2	0,0122	14,3	0,0132	15	0,0139	27	0,0251
182	1 090	7,33	0,00672	7,69	0,00705	9,09	0,00833	13,5	0,0124	14,5	0,0133	15,1	0,0138	27	0,0247
184	1 100	7,44	0,00674	7,81	0,00708	9,36	0,00849	13,6	0,0124	14,6	0,0132	15,6	0,0142	27,1	0,0246
186	1 120	7,45	0,00668	8,04	0,00721	9,38	0,00841	13,9	0,0125	14,7	0,0132	15,8	0,0141	27	0,0243
188	1 130	7,67	0,00681	8,2	0,00728	9,47	0,0084	14,1	0,0125	15,1	0,0134	16	0,0142	27	0,024
190	1 140	7,81	0,00686	8,21	0,0072	9,71	0,00852	14,1	0,0124	15,2	0,0134	16,2	0,0142	27,2	0,0239
192	1 150	8,02	0,00696	8,49	0,00738	9,62	0,00835	14,4	0,0125	15,5	0,0135	16,4	0,0142	27,2	0,0236
194	1 160	8	0,00687	8,61	0,0074	9,75	0,00838	14,6	0,0125	15,7	0,0135	16,6	0,0143	27,2	0,0233
196	1 180	8,32	0,00708	8,67	0,00738	9,83	0,00836	14,8	0,0126	16	0,0136	16,8	0,0143	27,1	0,0231
198	1 190	8,38	0,00706	8,84	0,00745	10,1	0,00847	14,8	0,0124	16	0,0135	16,9	0,0142	27,5	0,0231
200	1 200	8,62	0,00718	8,97	0,00748	10,3	0,00854	15	0,0125	16,3	0,0136	17,1	0,0143	27,6	0,023

Time	Shear Rate	Shear Stress	Viscosity	Shear Stress	Viscosity	Shear Stress	Viscosity	Shear Stress	Viscosity	Shear Stress	Viscosity	Shear Stress	Viscosity	Shear Stress	Viscosity
[s]	[1/s]	[Pa]	[Pa·s]	[Pa]	[Pa·s]	[Pa]	[Pa·s]	[Pa]	[Pa·s]	[Pa]	[Pa·s]	[Pa]	[Pa·s]	[Pa]	[Pa·s]
Number of Intervals:		*CNC-ATT-WDFs (6 wt %) 0.0 % 60°C S.W.*	*CNC-ATT-WDFs (6 wt %) 0.0 % 60°C S.W.*	*CNC-ATT-WDFs (6 wt %) 0.4 % 60°C S.W.*	*CNC-ATT-WDFs (6 wt %) 0.4 % 60°C S.W.*	*CNC-ATT-WDFs (6 wt %) 0.8 % 60°C S.W.*	*CNC-ATT-WDFs (6 wt %) 0.8 % 60°C S.W.*	*CNC-ATT-WDFs (6 wt %) 1.2 % 60°C S.W.*	*CNC-ATT-WDFs (6 wt %) 1.2 % 60°C S.W.*	*CNC-ATT-WDFs (6 wt %) 1.6 % 60°C S.W.*	*CNC-ATT-WDFs (6 wt %) 1.6 % 60°C S.W.*	*CNC-ATT-WDFs (6 wt %) 2.0 % 60°C S.W.*	*CNC-ATT-WDFs (6 wt %) 2.0 % 60°C S.W.*	*CNC-ATT-WDFs (6 wt %) 2.4 % 60°C S.W.*	*CNC-ATT-WDFs (6 wt %) 2.4 % 60°C S.W.*
2	0,999	-0,91	-0,91	-0,25	-0,249	0,00565	0,00565	1,52	1,52	1,91	1,91	2,15	2,14	5,75	5,76
4	13,1	-0,686	-0,0523	-0,0306	-0,00234	0,618	0,0471	3,22	0,246	2,58	0,197	4,11	0,313	14,3	1,09
6	25,2	-0,697	-0,0276	0,0121	4,8E-4	0,737	0,0292	3,74	0,148	2,78	0,11	4,5	0,178	13,7	0,544
8	37,3	-0,527	-0,0141	0,0793	0,00212	0,792	0,0212	3,77	0,101	2,96	0,0792	5,37	0,144	14	0,375
10	49,4	-0,472	-0,00955	0,111	0,00225	0,857	0,0173	3,85	0,0779	3,08	0,0624	5,95	0,12	15,4	0,311
12	61,6	-0,465	-0,00756	0,0188	3,06E-4	0,859	0,014	3,93	0,0638	3,33	0,0541	5,47	0,0889	16	0,26
14	73,7	-0,446	-0,00605	0,0461	6,25E-4	0,869	0,0118	4,07	0,0553	3,56	0,0483	5,63	0,0764	15,9	0,216
16	85,8	-0,449	-0,00523	8,68E-4	1,01E-5	0,907	0,0106	4,19	0,0488	3,79	0,0442	5,63	0,0656	15,6	0,182
18	97,9	-0,446	-0,00456	0,0158	1,62E-4	0,951	0,00971	4,28	0,0437	4,02	0,041	5,73	0,0585	15,8	0,161
20	110	-0,346	-0,00315	0,0977	8,88E-4	0,97	0,00881	4,42	0,0402	4,32	0,0393	5,75	0,0523	16,3	0,148
22	122	-0,271	-0,00222	0,215	0,00176	0,981	0,00803	4,63	0,0379	4,65	0,0381	6	0,0491	17	0,139
24	134	-0,289	-0,00215	0,225	0,00167	1,14	0,00848	4,87	0,0363	4,68	0,0349	6,18	0,0461	18	0,134
26	146	-0,269	-0,00184	0,208	0,00142	1,16	0,0079	4,99	0,0341	4,89	0,0334	6,31	0,0431	18,6	0,127
28	158	-0,166	-0,00105	0,322	0,00203	1,25	0,00791	5,14	0,0324	5,11	0,0322	6,57	0,0414	18,5	0,116
30	171	-0,146	-8,54E-4	0,252	0,00148	1,25	0,00732	5,28	0,031	5,2	0,0305	6,52	0,0382	18,3	0,108
32	183	-0,0779	-4,27E-4	0,3	0,00164	1,35	0,0074	5,45	0,0299	5,27	0,0288	6,65	0,0364	18	0,0986
34	195	-0,0664	-3,41E-4	0,368	0,00189	1,4	0,00717	5,55	0,0285	5,32	0,0273	7	0,0359	18,1	0,093
36	207	-0,0208	-1E-4	0,406	0,00196	1,42	0,00688	5,59	0,027	5,52	0,0267	7,07	0,0342	17,9	0,0865

38	219	0,0843	3,85E-4	0,426	0,00195	1,5	0,00683	5,64	0,0258	5,63	0,0257	7,3	0,0333	18,3	0,0836
40	231	0,143	6,21E-4	0,504	0,00218	1,51	0,00655	5,73	0,0248	5,71	0,0247	7,48	0,0323	18,6	0,0803
42	243	0,241	9,92E-4	0,552	0,00227	1,51	0,0062	5,82	0,0239	5,79	0,0238	7,7	0,0317	18,9	0,0779
44	255	0,287	0,00112	0,62	0,00243	1,55	0,00608	5,95	0,0233	5,95	0,0233	7,91	0,031	19,2	0,0752
46	267	0,357	0,00134	0,669	0,0025	1,58	0,0059	6,01	0,0225	5,98	0,0224	8	0,0299	19,9	0,0745
48	280	0,38	0,00136	0,761	0,00272	1,66	0,00596	6,1	0,0218	6,06	0,0217	8,07	0,0289	20,2	0,0724
50	292	0,447	0,00153	0,853	0,00293	1,65	0,00565	6,12	0,021	6,06	0,0208	8,19	0,0281	20,9	0,0715
52	304	0,504	0,00166	0,916	0,00302	1,74	0,00573	6,17	0,0203	6,21	0,0204	8,42	0,0277	21,5	0,0708
54	316	0,603	0,00191	0,986	0,00312	1,75	0,00554	6,26	0,0198	6,26	0,0198	8,49	0,0269	22	0,0696
56	328	0,651	0,00199	1,13	0,00343	1,86	0,00568	6,39	0,0195	6,41	0,0195	8,74	0,0266	22,2	0,0678
58	340	0,86	0,00253	1,18	0,00348	1,86	0,00548	6,45	0,019	6,46	0,019	8,74	0,0257	22,5	0,066
60	352	0,976	0,00277	1,28	0,00362	1,95	0,00553	6,53	0,0185	6,63	0,0188	8,9	0,0253	22,7	0,0645
62	364	0,954	0,00262	1,48	0,00406	2,12	0,00581	6,65	0,0182	6,63	0,0182	8,87	0,0244	23	0,0632
64	376	1,13	0,00301	1,52	0,00404	2,11	0,0056	6,69	0,0178	6,72	0,0179	9,17	0,0244	23,4	0,0622
66	389	1,18	0,00304	1,63	0,00418	2,22	0,0057	6,83	0,0176	6,81	0,0175	9,38	0,0241	23,8	0,0613
68	401	1,3	0,00325	1,7	0,00424	2,28	0,00568	6,86	0,0171	6,82	0,017	9,49	0,0237	23,9	0,0597
70	413	1,28	0,00309	1,86	0,00451	2,41	0,00584	6,99	0,0169	6,89	0,0167	9,57	0,0232	24,1	0,0583
72	425	1,36	0,00319	1,94	0,00457	2,52	0,00592	7,08	0,0167	7,02	0,0165	9,71	0,0229	24,2	0,0571
74	437	1,42	0,00325	2,08	0,00475	2,64	0,00605	7,1	0,0162	6,96	0,0159	9,79	0,0224	24,4	0,0559
76	449	1,59	0,00354	2,06	0,0046	2,62	0,00584	7,11	0,0158	7,01	0,0156	9,9	0,022	24,8	0,0552
78	461	1,86	0,00403	2,41	0,00523	2,49	0,00539	7,38	0,016	7,32	0,0159	10,1	0,0219	24,7	0,0535
80	473	1,64	0,00347	2,3	0,00485	2,92	0,00617	7,29	0,0154	7,13	0,0151	9,85	0,0208	25,2	0,0533
82	485	1,82	0,00374	2,34	0,00482	2,95	0,00607	7,28	0,015	7,12	0,0147	9,94	0,0205	25,4	0,0524
84	498	1,82	0,00366	2,45	0,00492	3,08	0,00619	7,36	0,0148	7,17	0,0144	9,82	0,0197	25,5	0,0512
86	510	1,94	0,00381	2,48	0,00487	3,14	0,00616	7,4	0,0145	7,24	0,0142	9,92	0,0195	25,6	0,0502
88	522	2,02	0,00387	2,63	0,00505	3,29	0,00631	7,58	0,0145	7,44	0,0143	10,1	0,0193	25,7	0,0492
90	534	2,15	0,00402	2,73	0,00512	3,52	0,00659	7,57	0,0142	7,36	0,0138	9,91	0,0186	25,7	0,0482
92	546	2,26	0,00413	2,86	0,00524	3,65	0,00668	7,72	0,0141	7,39	0,0135	10	0,0183	25,8	0,0472
94	558	2,36	0,00423	2,98	0,00535	3,72	0,00667	7,74	0,0139	7,36	0,0132	9,89	0,0177	25,9	0,0464
96	570	2,37	0,00415	3,2	0,00561	3,9	0,00684	7,97	0,014	7,49	0,0131	10	0,0176	25,9	0,0455
98	582	2,46	0,00422	3,31	0,00568	3,98	0,00683	8,02	0,0138	7,62	0,0131	9,97	0,0171	26	0,0446
100	594	2,54	0,00427	3,39	0,00571	4,07	0,00684	8,02	0,0135	7,57	0,0127	9,8	0,0165	26,1	0,0439
102	607	2,7	0,00445	3,47	0,00572	4,16	0,00685	8,1	0,0134	7,7	0,0127	9,89	0,0163	26,4	0,0435
104	619	2,81	0,00454	3,6	0,00581	4,22	0,00682	8,15	0,0132	7,73	0,0125	9,83	0,0159	26,5	0,0429

106	631	2,92	0,00464	3,67	0,00581	4,29	0,0068	8,15	0,0129	7,73	0,0122	9,97	0,0158	26,6	0,0422
108	643	2,94	0,00457	3,88	0,00604	4,5	0,007	8,35	0,013	7,89	0,0123	9,97	0,0155	26,6	0,0413
110	655	3,16	0,00482	3,9	0,00596	4,53	0,00691	8,48	0,0129	8,03	0,0123	10,1	0,0154	26,8	0,0409
112	667	3,16	0,00473	4,1	0,00614	4,66	0,00698	8,57	0,0128	8,17	0,0122	10	0,015	26,6	0,0399
114	679	3,33	0,0049	4,08	0,00601	4,7	0,00692	8,5	0,0125	7,96	0,0117	10,1	0,0148	26,7	0,0393
116	691	3,39	0,00491	4,25	0,00615	4,89	0,00708	8,63	0,0125	8,25	0,0119	10,1	0,0146	26,8	0,0388
118	703	3,55	0,00504	4,33	0,00616	4,99	0,00709	8,71	0,0124	8,28	0,0118	10,1	0,0144	26,9	0,0383
120	716	3,62	0,00505	4,47	0,00625	5,1	0,00713	8,85	0,0124	8,36	0,0117	10,1	0,0142	26,9	0,0375
122	728	3,65	0,00502	4,59	0,00631	5,3	0,00729	8,97	0,0123	8,61	0,0118	10,2	0,014	27,1	0,0373
124	740	3,81	0,00515	4,69	0,00634	5,38	0,00727	9,17	0,0124	8,74	0,0118	10,2	0,0138	27,2	0,0368
126	752	3,89	0,00517	4,68	0,00623	5,34	0,0071	9,21	0,0122	8,62	0,0115	10,1	0,0135	27,3	0,0363
128	764	4,03	0,00527	4,78	0,00625	5,55	0,00726	9,43	0,0123	8,88	0,0116	10,3	0,0135	27,5	0,036
130	776	4,14	0,00533	4,86	0,00626	5,63	0,00726	9,48	0,0122	8,87	0,0114	10,3	0,0132	27,6	0,0355
132	788	4,3	0,00545	4,91	0,00623	5,68	0,0072	9,49	0,012	8,98	0,0114	10,5	0,0133	27,5	0,0349
134	800	4,32	0,0054	5,08	0,00635	5,87	0,00733	9,64	0,012	8,98	0,0112	10,3	0,0129	27,5	0,0343
136	812	4,38	0,00539	5,26	0,00647	5,99	0,00738	9,81	0,0121	9,24	0,0114	10,4	0,0128	27,3	0,0336
138	825	4,71	0,00571	5,14	0,00623	5,94	0,0072	9,7	0,0118	9,32	0,0113	10,5	0,0127	27,5	0,0334
140	837	4,64	0,00555	5,48	0,00655	6,18	0,00739	9,98	0,0119	9,57	0,0114	10,7	0,0128	27,6	0,033
142	849	4,78	0,00564	5,52	0,0065	6,18	0,00729	10,1	0,0119	9,61	0,0113	10,8	0,0127	27,8	0,0327
144	861	4,89	0,00568	5,65	0,00656	6,28	0,00729	10,2	0,0119	9,64	0,0112	10,9	0,0127	27,8	0,0322
146	873	4,96	0,00568	5,79	0,00664	6,5	0,00744	10,3	0,0118	9,8	0,0112	10,8	0,0124	27,9	0,0319
148	885	5,2	0,00588	5,8	0,00655	6,51	0,00736	10,2	0,0115	9,89	0,0112	10,9	0,0123	27,9	0,0316
150	897	5,25	0,00585	6	0,00669	6,7	0,00746	10,5	0,0116	9,84	0,011	11	0,0122	27,9	0,0311
152	909	5,19	0,00571	6,13	0,00674	6,88	0,00757	10,5	0,0115	9,88	0,0109	10,9	0,012	27,8	0,0305
154	921	5,42	0,00588	6,15	0,00668	6,97	0,00757	10,5	0,0114	10,2	0,0111	11	0,012	27,8	0,0302
156	934	5,57	0,00596	6,09	0,00652	7	0,0075	10,7	0,0114	10,3	0,0111	11,1	0,0119	27,7	0,0297
158	946	5,72	0,00605	6,21	0,00657	7,16	0,00758	10,9	0,0115	10,6	0,0112	11,4	0,012	27,8	0,0294
160	958	5,9	0,00616	6,18	0,00646	7,16	0,00747	10,9	0,0114	10,7	0,0112	11,6	0,0121	27,8	0,029
162	970	5,98	0,00617	6,25	0,00644	7,29	0,00751	11	0,0113	10,9	0,0113	11,8	0,0122	27,7	0,0286
164	982	6,03	0,00614	6,48	0,0066	7,44	0,00758	11,3	0,0115	11,2	0,0114	12	0,0123	27,5	0,0281
166	994	6,06	0,0061	6,57	0,00661	7,6	0,00765	11,6	0,0117	11,2	0,0113	12,1	0,0121	27,5	0,0277
168	1 010	6,18	0,00614	6,69	0,00665	7,72	0,00768	11,8	0,0117	11,4	0,0113	12,3	0,0123	27,5	0,0273
170	1 020	6,24	0,00613	6,88	0,00676	7,96	0,00782	12,2	0,012	11,7	0,0115	12,6	0,0124	27,5	0,027
172	1 030	6,53	0,00633	6,81	0,00661	7,95	0,00771	12,2	0,0118	11,8	0,0114	12,7	0,0123	27,7	0,0269

174	1 040	6,66	0,00639	6,89	0,00661	8,17	0,00784	12,4	0,0119	12	0,0115	12,8	0,0123	27,7	0,0265
176	1 050	6,82	0,00647	7,06	0,00669	8,23	0,00781	12,5	0,0119	12,3	0,0116	13,1	0,0124	27,6	0,0261
178	1 070	6,88	0,00645	7,33	0,00687	8,55	0,00801	12,8	0,012	12,5	0,0117	13,3	0,0124	27,5	0,0258
180	1 080	6,98	0,00647	7,43	0,00688	8,63	0,008	12,9	0,012	12,6	0,0117	13,4	0,0124	27,5	0,0254
182	1 090	7,26	0,00665	7,52	0,00689	8,77	0,00804	13,2	0,0121	12,7	0,0117	13,6	0,0125	27,5	0,0252
184	1 100	7,39	0,0067	7,69	0,00698	8,84	0,00801	13,4	0,0122	13	0,0118	13,9	0,0126	27,4	0,0248
186	1 120	7,43	0,00667	7,74	0,00694	8,85	0,00793	13,5	0,0121	13,1	0,0117	14,2	0,0128	27,6	0,0247
188	1 130	7,55	0,0067	7,89	0,007	9,01	0,00799	13,7	0,0122	13,4	0,0119	14,5	0,0128	27,6	0,0245
190	1 140	7,72	0,00677	8,21	0,00721	9,37	0,00822	14	0,0123	13,6	0,0119	14,5	0,0128	27,4	0,024
192	1 150	7,84	0,00681	8,27	0,00718	9,38	0,00814	14,1	0,0122	13,7	0,0119	14,6	0,0126	27,4	0,0238
194	1 160	7,86	0,00675	8,43	0,00725	9,59	0,00824	14,3	0,0122	13,9	0,0119	14,8	0,0127	27,6	0,0237
196	1 180	8,11	0,0069	8,5	0,00723	9,66	0,00822	14,3	0,0122	14	0,0119	15,1	0,0128	27,6	0,0234
198	1 190	7,96	0,0067	8,8	0,00741	10	0,00843	14,8	0,0125	14,2	0,012	15,1	0,0127	27,5	0,0231
200	1 200	8,25	0,00688	8,97	0,00748	10,2	0,00846	14,9	0,0125	14,6	0,0122	15,3	0,0128	27,5	0,0229

Time	Shear Rate	Shear Stress	Viscosity	Shear Stress	Viscosity	Shear Stress	Viscosity	Shear Stress	Viscosity	Shear Stress	Viscosity	Shear Stress	Viscosity	Shear Stress	Viscosity
[s]	[1/s]	[Pa]	[Pa·s]	[Pa]	[Pa·s]	[Pa]	[Pa·s]	[Pa]	[Pa·s]	[Pa]	[Pa·s]	[Pa]	[Pa·s]	[Pa]	[Pa·s]
Number of Intervals:		*CNC-ATT-WDFs (6 wt %) 0.0 % 70°C S.W.*	*CNC-ATT-WDFs (6 wt %) 0.0 % 70°C S.W.*	*CNC-ATT-WDFs (6 wt %) 0.4 % 70°C S.W.*	*CNC-ATT-WDFs (6 wt %) 0.4 % 70°C S.W.*	*CNC-ATT-WDFs (6 wt %) 0.8 % 70°C S.W.*	*CNC-ATT-WDFs (6 wt %) 0.8 % 70°C S.W.*	*CNC-ATT-WDFs (6 wt %) 1.2 % 70°C S.W.*	*CNC-ATT-WDFs (6 wt %) 1.2 % 70°C S.W.*	*CNC-ATT-WDFs (6 wt %) 1.6 % 70°C S.W.*	*CNC-ATT-WDFs (6 wt %) 1.6 % 70°C S.W.*	*CNC-ATT-WDFs (6 wt %) 2.0 % 70°C S.W.*	*CNC-ATT-WDFs (6 wt %) 2.0 % 70°C S.W.*	*CNC-ATT-WDFs (6 wt %) 2.4 % 70°C S.W.*	*CNC-ATT-WDFs (6 wt %) 2.4 % 70°C S.W.*
2	0,999	-0,421	-0,421	-0,784	-0,783	-0,384	-0,384	2,44	2,43	1,54	1,54	1,27	1,27	6,48	6,46
4	13,1	-0,671	-0,0512	0,352	0,0269	0,653	0,0498	3,51	0,268	2,58	0,197	3,87	0,295	11,2	0,854
6	25,2	-0,765	-0,0303	0,232	0,00921	0,638	0,0253	3,76	0,149	2,84	0,113	4,46	0,177	11,4	0,451
8	37,3	-0,489	-0,0131	0,162	0,00434	0,584	0,0157	3,71	0,0993	2,82	0,0755	5,24	0,14	12,1	0,325
10	49,4	-0,473	-0,00956	0,0886	0,00179	0,681	0,0138	3,86	0,0781	3,02	0,0612	5,98	0,121	12,4	0,251
12	61,6	-0,49	-0,00796	0,238	0,00386	0,791	0,0128	3,89	0,0631	3,21	0,0522	5,35	0,0869	13	0,212
14	73,7	-0,413	-0,00561	0,118	0,00161	0,79	0,0107	4,15	0,0563	3,38	0,0458	5,32	0,0722	13,7	0,185
16	85,8	-0,376	-0,00439	0,191	0,00223	0,876	0,0102	4,33	0,0505	3,58	0,0417	5,43	0,0633	13,8	0,161
18	97,9	-0,351	-0,00359	0,235	0,0024	0,948	0,00968	4,49	0,0459	3,76	0,0384	5,69	0,0581	14,1	0,144
20	110	-0,318	-0,00289	0,296	0,00269	0,951	0,00865	4,74	0,0431	4,09	0,0371	5,93	0,0539	14,5	0,132
22	122	-0,302	-0,00247	0,36	0,00295	0,985	0,00807	4,98	0,0408	4,25	0,0348	6,03	0,0494	15,2	0,125
24	134	-0,233	-0,00174	0,374	0,00279	1,05	0,00783	5,12	0,0382	4,46	0,0332	6,22	0,0464	16,1	0,12
26	146	-0,213	-0,00146	0,492	0,00336	1,18	0,00807	5,3	0,0362	4,65	0,0317	6,39	0,0437	16,6	0,113
28	158	-0,107	-6,75E-4	0,485	0,00306	1,17	0,00738	5,39	0,034	4,71	0,0297	6,71	0,0423	17,3	0,109
30	171	-0,0797	-4,67E-4	0,568	0,00333	1,23	0,00718	5,43	0,0318	4,83	0,0283	6,68	0,0391	17,2	0,101
32	183	0,0182	9,95E-5	0,577	0,00316	1,22	0,0067	5,58	0,0306	4,93	0,027	6,83	0,0374	17,6	0,0964
34	195	0,0995	5,11E-4	0,624	0,0032	1,29	0,00661	5,65	0,029	5,13	0,0264	7,15	0,0367	17,7	0,091
36	207	0,0833	4,03E-4	0,693	0,00335	1,37	0,00662	5,88	0,0284	5,3	0,0256	7,37	0,0356	17,9	0,0865
38	219	0,18	8,2E-4	0,722	0,0033	1,4	0,00638	5,99	0,0274	5,36	0,0245	7,52	0,0343	18,1	0,0827

40	231	0,215	9,32E-4	0,679	0,00294	1,44	0,00625	6,06	0,0262	5,33	0,0231	7,5	0,0324	18,5	0,0801
42	243	0,228	9,38E-4	0,79	0,00325	1,51	0,0062	6,13	0,0252	5,49	0,0226	7,78	0,032	19,2	0,0789
44	255	0,313	0,00123	0,775	0,00303	1,53	0,00599	6,22	0,0244	5,6	0,0219	7,76	0,0304	19,4	0,0759
46	267	0,38	0,00142	0,823	0,00308	1,55	0,00579	6,34	0,0237	5,68	0,0212	7,93	0,0297	19,7	0,0735
48	280	0,49	0,00175	0,847	0,00303	1,6	0,00572	6,37	0,0228	5,71	0,0204	8,06	0,0288	20	0,0717
50	292	0,484	0,00166	1,03	0,00352	1,72	0,00591	6,48	0,0222	5,76	0,0198	8,25	0,0283	20,4	0,0698
52	304	0,601	0,00198	1,11	0,00367	1,78	0,00586	6,54	0,0215	5,86	0,0193	8,26	0,0272	20,5	0,0674
54	316	0,702	0,00222	1,26	0,00399	1,77	0,00559	6,66	0,0211	5,95	0,0188	8,44	0,0267	20,7	0,0656
56	328	0,801	0,00244	1,34	0,00409	1,82	0,00554	6,69	0,0204	6,05	0,0184	8,55	0,0261	21,4	0,0653
58	340	0,884	0,0026	1,49	0,00438	1,89	0,00556	6,82	0,02	6,09	0,0179	8,6	0,0253	21,7	0,0637
60	352	0,981	0,00279	1,6	0,00453	1,95	0,00553	6,9	0,0196	6,15	0,0175	8,72	0,0247	21,9	0,0621
62	364	1,08	0,00297	1,76	0,00484	2,11	0,00578	6,96	0,0191	6,31	0,0173	8,87	0,0243	22,3	0,0612
64	376	1,17	0,00311	1,95	0,00517	2,21	0,00586	7,13	0,0189	6,34	0,0168	9,09	0,0242	22,2	0,0589
66	389	1,31	0,00337	2,19	0,00564	2,32	0,00598	7,24	0,0186	6,39	0,0165	9,24	0,0238	22,4	0,0575
68	401	1,31	0,00327	2,03	0,00507	2,45	0,00611	7,35	0,0183	6,34	0,0158	9,37	0,0234	22,6	0,0564
70	413	1,49	0,0036	2,1	0,00509	2,51	0,00609	7,3	0,0177	6,36	0,0154	9,35	0,0227	22,8	0,0552
72	425	1,6	0,00376	1,98	0,00465	2,52	0,00593	7,37	0,0173	6,36	0,015	9,34	0,022	23	0,0542
74	437	1,65	0,00378	2,11	0,00484	2,71	0,00619	7,44	0,017	6,54	0,015	9,51	0,0218	23,3	0,0533
76	449	1,69	0,00376	2,26	0,00504	2,72	0,00605	7,63	0,017	6,51	0,0145	9,53	0,0212	23,4	0,0521
78	461	1,43	0,0031	2,66	0,00577	3,11	0,00675	7,42	0,0161	6,85	0,0149	9,83	0,0213	23,5	0,051
80	473	1,93	0,00407	2,4	0,00507	2,98	0,0063	7,71	0,0163	6,69	0,0141	9,83	0,0208	23,8	0,0503
82	485	1,93	0,00397	2,57	0,0053	3,05	0,00628	7,88	0,0162	6,66	0,0137	9,76	0,0201	23,8	0,0491
84	498	2,03	0,00408	2,68	0,00538	3,19	0,00641	7,89	0,0159	6,79	0,0137	9,8	0,0197	24	0,0483
86	510	2,09	0,00409	2,79	0,00548	3,27	0,00641	8,04	0,0158	6,82	0,0134	9,78	0,0192	24,1	0,0473
88	522	2,3	0,00441	2,79	0,00534	3,29	0,0063	8,05	0,0154	6,82	0,0131	9,91	0,019	24,3	0,0466
90	534	2,32	0,00435	2,96	0,00555	3,51	0,00658	8,12	0,0152	6,91	0,0129	9,8	0,0184	24,4	0,0456
92	546	2,46	0,0045	3	0,0055	3,62	0,00663	8,13	0,0149	6,99	0,0128	9,88	0,0181	24,6	0,045
94	558	2,47	0,00442	3,17	0,00568	3,75	0,00672	8,23	0,0147	7,08	0,0127	9,98	0,0179	24,5	0,0439
96	570	2,75	0,00483	3,15	0,00553	3,82	0,00669	8,17	0,0143	7,15	0,0125	9,71	0,017	24,9	0,0436
98	582	2,86	0,0049	3,22	0,00553	3,85	0,0066	8,22	0,0141	7,25	0,0124	9,69	0,0166	24,9	0,0428
100	594	2,85	0,00479	3,47	0,00583	4,13	0,00694	8,37	0,0141	7,32	0,0123	9,91	0,0167	24,9	0,0419
102	607	2,99	0,00493	3,49	0,00575	4,1	0,00676	8,41	0,0139	7,31	0,012	9,79	0,0161	25	0,0412
104	619	3,06	0,00495	3,65	0,0059	4,25	0,00687	8,49	0,0137	7,41	0,012	9,99	0,0162	25	0,0404
106	631	3,1	0,00491	3,79	0,00601	4,42	0,00701	8,59	0,0136	7,5	0,0119	10,2	0,0161	25	0,0397

108	643	3,35	0,0052	3,79	0,0059	4,5	0,007	8,52	0,0133	7,59	0,0118	10	0,0156	25,3	0,0393
110	655	3,4	0,0051	3,88	0,0059	4,41	0,0067	8,71	0,0133	7,7	0,0118	10	0,0153	25,4	0,0388
112	667	3,56	0,0053	3,98	0,0059	4,59	0,0068	8,71	0,0131	7,79	0,0117	10,2	0,0152	25,6	0,0384
114	679	3,45	0,0050	4,26	0,0062	4,73	0,0069	8,9	0,0131	7,8	0,0115	10,2	0,015	25,4	0,0373
116	691	3,63	0,0052	4,27	0,0061	4,74	0,0068	8,93	0,0129	7,9	0,0114	10,2	0,0147	25,6	0,037
118	703	3,76	0,0053	4,39	0,0062	4,8	0,0068	9,06	0,0129	7,96	0,0113	10,2	0,0145	25,6	0,0364
120	716	3,85	0,0053	4,52	0,0063	5	0,0069	9,12	0,0127	8,18	0,0114	10,4	0,0145	25,7	0,0359
122	728	4,09	0,0056	4,54	0,0062	5	0,0068	9,14	0,0126	8,19	0,0113	10,3	0,0141	25,9	0,0356
124	740	4,21	0,0056	4,59	0,0062	5,15	0,0069	9,3	0,0126	8,36	0,0113	10,3	0,0139	25,9	0,035
126	752	4,17	0,0055	4,89	0,0065	5,39	0,0071	9,53	0,0127	8,52	0,0113	10,5	0,0139	25,8	0,0344
128	764	4,36	0,0057	4,97	0,0065	5,47	0,0071	9,57	0,0125	8,57	0,0112	10,4	0,0136	25,8	0,0338
130	776	4,42	0,0056	5,13	0,0066	5,78	0,0074	9,71	0,0125	8,62	0,0111	10,4	0,0134	25,8	0,0333
132	788	4,59	0,0058	5,14	0,0065	5,81	0,0073	9,81	0,0124	8,73	0,0111	10,5	0,0133	25,9	0,0329
134	800	4,6	0,0057	5,29	0,0066	6,08	0,0075	9,89	0,0124	8,98	0,0112	10,6	0,0133	26	0,0324
136	812	4,81	0,0059	5,35	0,0065	6,14	0,0075	9,91	0,0122	9,14	0,0113	10,7	0,0131	26	0,032
138	825	4,89	0,0059	5,41	0,0065	6,42	0,0077	10,2	0,0123	9,27	0,0112	10,7	0,013	25,9	0,0314
140	837	5,13	0,0061	5,42	0,0064	6,23	0,0074	10,2	0,0122	9,24	0,011	10,8	0,0129	26,2	0,0313
142	849	5,14	0,0060	5,6	0,0066	6,31	0,0074	10,4	0,0122	9,43	0,0111	10,8	0,0127	26,1	0,0307
144	861	5,15	0,0059	5,8	0,0067	6,49	0,0075	10,5	0,0123	9,46	0,011	10,9	0,0127	26,2	0,0304
146	873	5,41	0,0062	5,75	0,0065	6,54	0,0074	10,5	0,012	9,49	0,0109	10,9	0,0125	26,3	0,0302
148	885	5,45	0,0061	5,94	0,0067	6,58	0,0074	10,6	0,012	9,5	0,0107	11,1	0,0125	26,2	0,0296
150	897	5,64	0,0062	5,97	0,0066	6,67	0,0074	10,6	0,0118	9,65	0,0108	11	0,0123	26,2	0,0292
152	909	5,6	0,0061	6,14	0,0067	6,98	0,0076	10,6	0,0117	10,1	0,0111	11,2	0,0123	26,2	0,0288
154	921	5,75	0,0062	6,23	0,0067	6,99	0,0075	10,8	0,0117	10,3	0,0112	11,3	0,0123	26,4	0,0286
156	934	5,84	0,0062	6,43	0,0068	7,13	0,0076	10,9	0,0117	10,4	0,0111	11,4	0,0122	26,3	0,0282
158	946	6,03	0,0063	6,43	0,0068	7,19	0,0076	10,9	0,0116	10,4	0,011	11,4	0,012	26,3	0,0278
160	958	6	0,0062	6,7	0,007	7,43	0,0077	11,2	0,0117	10,6	0,0111	11,5	0,012	26,1	0,0273
162	970	6,14	0,0063	6,8	0,0070	7,59	0,0078	11,4	0,0117	10,9	0,0112	11,7	0,012	26,1	0,0269
164	982	6,33	0,0064	6,7	0,0068	7,52	0,0076	11,4	0,0116	11	0,0112	11,8	0,012	26,2	0,0267
166	994	6,32	0,0063	6,86	0,0069	7,76	0,0078	11,7	0,0118	11,2	0,0113	12,1	0,0121	26,3	0,0265
168	1 010	6,48	0,0064	6,92	0,0068	7,84	0,0077	12,2	0,0121	11,4	0,0114	12,1	0,0121	26,3	0,0261
170	1 020	6,62	0,0065	7	0,0068	7,96	0,0078	12,2	0,012	11,6	0,0114	12,4	0,0122	26,4	0,026
172	1 030	6,77	0,0065	7,24	0,0070	8,1	0,0078	12,6	0,0122	11,6	0,0113	12,6	0,0122	26,4	0,0256
174	1 040	6,89	0,0066	7,42	0,0071	8,31	0,0079	12,7	0,0122	11,9	0,0114	12,8	0,0123	26,4	0,0253

176	1 050	7,11	0,00674	7,49	0,0071	8,31	0,00788	13	0,0123	12,1	0,0115	13,1	0,0124	26,3	0,025
178	1 070	7,32	0,00686	7,56	0,00708	8,39	0,00787	13	0,0122	12,4	0,0116	13,2	0,0124	26,6	0,025
180	1 080	7,43	0,00689	7,72	0,00716	8,6	0,00797	13,3	0,0123	12,5	0,0116	13,4	0,0124	26,5	0,0245
182	1 090	7,53	0,00691	7,91	0,00725	8,77	0,00804	13,5	0,0124	12,6	0,0116	13,5	0,0124	26,4	0,0242
184	1 100	7,62	0,00691	7,94	0,0072	8,8	0,00797	13,7	0,0125	12,7	0,0116	13,7	0,0124	26,6	0,0241
186	1 120	7,88	0,00707	8,14	0,0073	8,98	0,00805	14,1	0,0126	12,8	0,0115	13,9	0,0124	26,4	0,0236
188	1 130	7,86	0,00697	8,23	0,0073	9,09	0,00806	14,1	0,0125	13,1	0,0116	14,1	0,0125	26,5	0,0235
190	1 140	8,04	0,00706	8,33	0,00731	9,26	0,00813	14,1	0,0123	13,5	0,0119	14,1	0,0124	26,6	0,0234
192	1 150	8,34	0,00724	8,54	0,00742	9,49	0,00824	14,3	0,0124	13,5	0,0117	14,5	0,0126	26,5	0,023
194	1 160	8,25	0,00709	8,54	0,00734	9,74	0,00837	14,4	0,0124	13,8	0,0118	14,7	0,0126	26,5	0,0227
196	1 180	8,51	0,00723	8,78	0,00747	9,94	0,00845	14,6	0,0125	14	0,0119	14,9	0,0126	26,4	0,0224
198	1 190	8,66	0,00729	8,79	0,0074	10,1	0,00849	14,6	0,0123	14,1	0,0119	15,1	0,0128	26,6	0,0224
200	1 200	8,73	0,00727	8,9	0,00742	10,2	0,00851	14,9	0,0124	14,3	0,0119	15,3	0,0128	26,6	0,0222

Time	Shear Rate	Shear Stress	Viscosity	Shear Stress	Viscosity	Shear Stress	Viscosity	Shear Stress	Viscosity	Shear Stress	Viscosity	Shear Stress	Viscosity	Shear Stress	Viscosity
[s]	[1/s]	[Pa]	[Pa·s]	[Pa]	[Pa·s]	[Pa]	[Pa·s]	[Pa]	[Pa·s]	[Pa]	[Pa·s]	[Pa]	[Pa·s]	[Pa]	[Pa·s]
Number of Intervals:		CNC-ATT-WDFs (6 wt %) 0.0 % 80°C S.W.	CNC-ATT-WDFs (6 wt %) 0.0 % 80°C S.W.	CNC-ATT-WDFs (6 wt %) 0.4 % 80°C S.W.	CNC-ATT-WDFs (6 wt %) 0.4 % 80°C S.W.	CNC-ATT-WDFs (6 wt %) 0.8 % 80°C S.W.	CNC-ATT-WDFs (6 wt %) 0.8 % 80°C S.W.	CNC-ATT-WDFs (6 wt %) 1.2 % 80°C S.W.	CNC-ATT-WDFs (6 wt %) 1.2 % 80°C S.W.	CNC-ATT-WDFs (6 wt %) 1.6 % 80°C S.W.	CNC-ATT-WDFs (6 wt %) 1.6 % 80°C S.W.	CNC-ATT-WDFs (6 wt %) 2.0 % 80°C S.W.	CNC-ATT-WDFs (6 wt %) 2.0 % 80°C S.W.	CNC-ATT-WDFs (6 wt %) 2.4 % 80°C S.W.	CNC-ATT-WDFs (6 wt %) 2.4 % 80°C S.W.
2	0,999	-0,428	-0,428	-0,305	-0,304	0,43	0,43	2,75	2,74	2,35	2,34	2,68	2,68	7,7	7,74
4	13,1	-0,477	-0,0364	0,0495	0,00378	0,666	0,0508	4	0,305	2,75	0,209	4,2	0,32	11,8	0,9
6	25,2	-0,384	-0,0152	-0,0268	-0,00106	0,751	0,0298	4,53	0,179	2,71	0,107	4,82	0,191	12,3	0,488
8	37,3	-0,426	-0,0114	-0,0397	-0,00106	0,729	0,0195	4,75	0,127	2,96	0,0794	5,64	0,151	12,6	0,337
10	49,4	-0,417	-0,00843	0,0525	0,00106	0,747	0,0151	4,96	0,1	3,11	0,0628	6,31	0,128	13,7	0,277
12	61,6	-0,475	-0,00772	-0,0436	-7,08E-4	0,736	0,012	5,01	0,0814	3,34	0,0543	5,61	0,0911	14,7	0,238
14	73,7	-0,477	-0,00647	-0,0272	-3,69E-4	0,718	0,00975	4,37	0,0593	3,61	0,049	5,43	0,0736	15,8	0,215
16	85,8	-0,426	-0,00497	-0,00676	-7,88E-5	0,825	0,00961	4,41	0,0515	3,94	0,0459	5,57	0,0649	16,9	0,197
18	97,9	-0,428	-0,00437	-0,0204	-2,09E-4	0,802	0,0082	4,57	0,0467	4,34	0,0443	5,88	0,0601	18,3	0,187
20	110	-0,404	-0,00368	0,0121	1,1E-4	0,817	0,00743	4,72	0,043	4,42	0,0402	5,94	0,054	18,3	0,166
22	122	-0,367	-0,003	0,0807	6,61E-4	0,777	0,00636	4,94	0,0405	4,56	0,0373	6,05	0,0495	16	0,131
24	134	-0,392	-0,00292	-0,0418	-3,12E-4	0,849	0,00633	5,01	0,0373	4,79	0,0357	6,11	0,0455	16,7	0,124
26	146	-0,354	-0,00242	-0,0196	-1,34E-4	0,9	0,00615	5,17	0,0354	5,12	0,035	6,26	0,0428	17,7	0,121
28	158	-0,272	-0,00172	0,0413	2,61E-4	0,952	0,00601	5,29	0,0334	5,19	0,0327	6,32	0,0399	18,2	0,115
30	171	-0,289	-0,00169	0,051	2,99E-4	0,98	0,00574	5,41	0,0317	5,19	0,0304	6,63	0,0389	18,4	0,108
32	183	-0,239	-0,00131	0,0701	3,84E-4	1,04	0,00567	5,44	0,0298	5,2	0,0285	6,73	0,0369	18,9	0,103
34	195	-0,221	-0,00113	0,114	5,88E-4	1,07	0,0055	5,53	0,0284	5,34	0,0274	6,88	0,0353	19,2	0,0985
36	207	-0,113	-5,44E-4	0,145	7,03E-4	1,01	0,00487	5,63	0,0272	5,49	0,0265	7,03	0,034	19,4	0,0937

38	219	-0,12	-5,48E-4	0,163	7,45E-4	1,06	0,00484	5,73	0,0261	5,51	0,0252	7,15	0,0326	19,7	0,0901
40	231	-0,0486	-2,1E-4	0,2	8,64E-4	1,1	0,00478	5,8	0,0251	5,67	0,0245	7,43	0,0322	20	0,0866
42	243	0,00473	1,94E-5	0,286	0,00118	1,16	0,00477	5,92	0,0243	5,78	0,0237	7,64	0,0314	20,1	0,0826
44	255	0,0107	4,2E-5	0,316	0,00124	1,25	0,0049	5,93	0,0232	5,92	0,0232	7,66	0,03	20,1	0,0787
46	267	-0,00286	-1,07E-5	0,441	0,00165	1,22	0,00456	5,98	0,0224	5,93	0,0222	7,86	0,0294	20,5	0,0765
48	280	0,0721	2,58E-4	0,431	0,00154	1,33	0,00477	6,02	0,0215	5,96	0,0213	7,99	0,0286	20,9	0,0746
50	292	0,167	5,73E-4	0,563	0,00193	1,31	0,00451	6,06	0,0208	6,12	0,021	8,16	0,028	21,2	0,0726
52	304	0,213	7,01E-4	0,593	0,00195	1,36	0,00447	6,17	0,0203	6,1	0,0201	8,33	0,0274	21,4	0,0706
54	316	0,245	7,74E-4	0,701	0,00222	1,42	0,00451	6,24	0,0197	6,12	0,0194	8,53	0,027	21,8	0,0689
56	328	0,378	0,00115	0,722	0,0022	1,54	0,0047	6,28	0,0192	6,26	0,0191	8,45	0,0258	22,6	0,0688
58	340	0,348	0,00102	0,876	0,00257	1,55	0,00455	6,46	0,019	6,21	0,0183	8,66	0,0255	22,2	0,0653
60	352	0,418	0,00119	0,967	0,00275	1,56	0,00444	6,56	0,0186	6,32	0,0179	8,76	0,0249	22,6	0,0643
62	364	0,627	0,00172	1,01	0,00278	1,78	0,00487	6,57	0,018	6,48	0,0178	9,02	0,0248	22,9	0,0628
64	376	0,622	0,00165	1,16	0,00307	1,82	0,00482	6,73	0,0179	6,51	0,0173	9,03	0,024	22,9	0,0609
66	389	0,716	0,00184	1,27	0,00327	1,92	0,00494	6,75	0,0174	6,5	0,0167	9,29	0,0239	23,5	0,0605
68	401	0,787	0,00196	1,34	0,00335	1,92	0,0048	6,83	0,0171	6,63	0,0165	9,2	0,023	23,7	0,059
70	413	0,878	0,00213	1,29	0,00314	2,1	0,0051	6,79	0,0164	6,69	0,0162	9,43	0,0228	23,9	0,058
72	425	0,909	0,00214	1,38	0,00324	2,14	0,00504	6,87	0,0162	6,61	0,0156	9,53	0,0224	24,5	0,0575
74	437	1,08	0,00247	1,47	0,00335	2,24	0,00513	6,88	0,0157	6,77	0,0155	9,56	0,0219	24,3	0,0556
76	449	1,02	0,00227	1,69	0,00376	2,19	0,00488	7,1	0,0158	6,71	0,0149	9,56	0,0213	24,8	0,0552
78	461	1,38	0,00299	1,99	0,00431	2,55	0,00553	7,33	0,0159	7,04	0,0153	9,77	0,0212	25,3	0,0549
80	473	1,26	0,00267	1,76	0,00373	2,49	0,00526	7,1	0,015	6,92	0,0146	9,82	0,0207	25,4	0,0537
82	485	1,24	0,00255	1,99	0,00409	2,44	0,00503	7,3	0,015	6,88	0,0142	9,85	0,0203	25,6	0,0527
84	498	1,43	0,00288	2	0,00401	2,63	0,00529	7,25	0,0146	7,07	0,0142	9,87	0,0198	26	0,0523
86	510	1,44	0,00283	2,13	0,00418	2,68	0,00527	7,37	0,0145	7,01	0,0138	9,86	0,0194	26,4	0,0518
88	522	1,47	0,00283	2,07	0,00396	2,77	0,00531	7,43	0,0142	7,04	0,0135	9,95	0,0191	26,4	0,0505
90	534	1,58	0,00296	2,2	0,00412	2,85	0,00535	7,47	0,014	7,06	0,0132	9,89	0,0185	26,6	0,0497
92	546	1,71	0,00313	2,24	0,00411	3,02	0,00552	7,47	0,0137	7,03	0,0129	10,2	0,0186	26,9	0,0492
94	558	1,81	0,00325	2,46	0,0044	3,08	0,00552	7,54	0,0135	7,15	0,0128	10,1	0,018	27	0,0484
96	570	1,9	0,00333	2,4	0,0042	3,3	0,00578	7,45	0,0131	7,14	0,0125	10,3	0,018	27,1	0,0475
98	582	1,99	0,00341	2,49	0,00427	3,4	0,00583	7,52	0,0129	7,13	0,0122	10,3	0,0178	27,1	0,0465
100	594	2,12	0,00357	2,66	0,00448	3,4	0,00572	7,56	0,0127	7,26	0,0122	10,2	0,0171	27,1	0,0456

102	607	2,09	0,0034	2,78	0,0045	3,45	0,0057	7,7	0,0127	7,22	0,0119	10,1	0,0166	27,1	0,0447
104	619	2,21	0,0035	2,87	0,0046	3,59	0,0058	7,75	0,0125	7,31	0,0118	10,1	0,0163	27,2	0,0439
106	631	2,31	0,0036	3,01	0,0047	3,57	0,0056	7,81	0,0124	7,28	0,0115	10	0,0159	27,3	0,0433
108	643	2,37	0,0036	2,93	0,0045	3,84	0,0059	7,8	0,0121	7,38	0,0115	10,2	0,0158	27,1	0,0422
110	655	2,36	0,0036	3,07	0,0046	3,79	0,0057	8,03	0,0123	7,44	0,0114	10,2	0,0155	27,2	0,0416
112	667	2,55	0,0038	3,13	0,0046	4,06	0,0060	8	0,012	7,55	0,0113	10,2	0,0152	27,1	0,0407
114	679	2,67	0,0039	3,36	0,0049	4	0,0058	8,14	0,012	7,68	0,0113	9,96	0,0147	27,5	0,0404
116	691	2,74	0,0039	3,35	0,0048	4,14	0,0059	8,15	0,0118	7,66	0,0111	10,2	0,0147	27,4	0,0397
118	703	2,8	0,0039	3,46	0,0049	4,2	0,0059	8,29	0,0118	7,79	0,0111	10,1	0,0144	27,5	0,0391
120	716	2,99	0,0041	3,49	0,0048	4,36	0,0061	8,25	0,0115	7,9	0,011	10,1	0,0141	27,6	0,0385
122	728	3,01	0,0041	3,47	0,0047	4,49	0,0061	8,37	0,0115	7,89	0,0108	10,3	0,0141	27,6	0,038
124	740	3,12	0,0042	3,55	0,0048	4,55	0,0061	8,44	0,0114	7,98	0,0108	10,4	0,014	27,6	0,0374
126	752	3,26	0,0043	3,78	0,0050	4,58	0,0061	8,58	0,0114	8,21	0,0109	10,2	0,0136	27,7	0,0369
128	764	3,31	0,0043	3,8	0,0049	4,71	0,0061	8,69	0,0114	8,18	0,0107	10,3	0,0135	27,7	0,0362
130	776	3,35	0,0043	3,99	0,0051	4,76	0,0061	8,81	0,0114	8,35	0,0108	10,4	0,0134	27,7	0,0357
132	788	3,39	0,0043	4,11	0,0052	4,83	0,0061	9,04	0,0115	8,4	0,0107	10,4	0,0132	27,6	0,035
134	800	3,64	0,0045	4,23	0,0052	4,97	0,0062	8,97	0,0112	8,68	0,0108	10,5	0,0131	27,7	0,0346
136	812	3,84	0,0047	4,23	0,0052	5,19	0,0063	9,06	0,0111	8,69	0,0107	10,6	0,013	27,7	0,0341
138	825	3,89	0,0047	4,46	0,0054	5,09	0,0061	9,31	0,0113	8,62	0,0105	10,4	0,0126	27,8	0,0337
140	837	3,91	0,0046	4,4	0,0052	5,29	0,0063	9,37	0,0112	8,75	0,0105	10,7	0,0128	27,6	0,033
142	849	4,06	0,0047	4,59	0,0054	5,29	0,0062	9,47	0,0112	8,81	0,0104	10,8	0,0127	27,6	0,0325
144	861	4,24	0,0049	4,73	0,0055	5,34	0,0062	9,56	0,0111	8,99	0,0104	10,9	0,0126	27,5	0,032
146	873	4,23	0,0048	4,74	0,0054	5,66	0,0064	9,62	0,011	8,99	0,0103	10,9	0,0125	27,4	0,0314
148	885	4,25	0,0048	4,96	0,0056	5,76	0,0065	9,84	0,0111	9,07	0,0102	10,8	0,0121	27,4	0,031
150	897	4,29	0,0047	4,9	0,0054	5,91	0,0065	9,98	0,0111	9,19	0,0102	10,8	0,012	27,5	0,0307
152	909	4,58	0,0050	4,99	0,0054	6,11	0,0067	9,92	0,0109	9,58	0,0105	10,9	0,012	27,8	0,0306
154	921	4,64	0,0050	5,08	0,0055	6,21	0,0067	10,1	0,011	9,71	0,0105	11	0,012	27,6	0,03
156	934	4,6	0,0049	5,24	0,0056	6,27	0,0067	10,2	0,011	9,9	0,0106	10,9	0,0117	27,8	0,0297
158	946	4,75	0,0050	5,25	0,0055	6,42	0,0067	10,3	0,0109	10,1	0,0106	11,1	0,0117	27,6	0,0292
160	958	4,97	0,0051	5,5	0,0057	6,42	0,0067	10,3	0,0108	10,3	0,0107	11	0,0115	27,7	0,0289
162	970	5,03	0,0051	5,65	0,0058	6,51	0,0067	10,6	0,0109	10,3	0,0107	11	0,0113	27,7	0,0286
164	982	4,98	0,0050	5,63	0,0057	6,69	0,0068	10,7	0,0109	10,4	0,0106	11,2	0,0114	27,6	0,0281
166	994	5,35	0,0053	5,77	0,0058	6,87	0,0069	10,9	0,011	10,7	0,0108	11,5	0,0116	27,7	0,0279
168	1 010	5,34	0,0053	5,85	0,0058	6,94	0,0068	11,2	0,0111	10,9	0,0108	11,6	0,0115	27,7	0,0276

170	1 020	5,48	0,00538	5,88	0,00578	7,13	0,00701	11,4	0,0111	11	0,0108	11,8	0,0116	27,6	0,0271
172	1 030	5,37	0,00521	6,19	0,00601	7,08	0,00687	11,7	0,0113	11,1	0,0108	12	0,0116	27,8	0,027
174	1 040	5,76	0,00553	6,3	0,00605	7,33	0,00703	11,7	0,0113	11,4	0,011	12,1	0,0116	27,9	0,0267
176	1 050	5,68	0,00539	6,34	0,00601	7,36	0,00698	12	0,0114	11,4	0,0108	12,4	0,0118	27,8	0,0263
178	1 070	5,93	0,00556	6,29	0,0059	7,7	0,00722	12	0,0113	11,7	0,0109	12,6	0,0118	27,9	0,0262
180	1 080	6,06	0,00561	6,48	0,00601	7,78	0,00721	12,2	0,0113	11,8	0,0109	12,9	0,0119	27,8	0,0257
182	1 090	6,19	0,00567	6,68	0,00612	7,85	0,0072	12,4	0,0114	11,9	0,0109	13	0,0119	27,9	0,0255
184	1 100	6,15	0,00558	6,64	0,00602	8,09	0,00733	12,6	0,0114	12,1	0,011	13,3	0,0121	27,6	0,025
186	1 120	6,21	0,00557	6,98	0,00626	8,06	0,00723	12,9	0,0116	12,4	0,0111	13,2	0,0118	27,6	0,0248
188	1 130	6,46	0,00573	7,1	0,0063	8,18	0,00725	13,1	0,0116	12,5	0,0111	13,3	0,0118	27,7	0,0245
190	1 140	6,54	0,00574	7,03	0,00617	8,57	0,00752	13	0,0115	12,7	0,0112	13,7	0,012	27,6	0,0242
192	1 150	6,8	0,0059	7,28	0,00632	8,57	0,00744	13,3	0,0116	12,9	0,0112	13,8	0,012	27,6	0,0239
194	1 160	6,84	0,00588	7,34	0,00631	8,79	0,00755	13,5	0,0116	13,1	0,0113	14,1	0,0121	27,7	0,0238
196	1 180	7,19	0,00611	7,55	0,00642	8,82	0,0075	13,7	0,0116	13,4	0,0114	14,1	0,012	27,7	0,0235
198	1 190	7,17	0,00604	7,5	0,00632	9,14	0,00769	13,7	0,0116	13,4	0,0113	14,6	0,0123	27,6	0,0232
200	1 200	7,37	0,00614	7,57	0,00631	9,35	0,0078	13,9	0,0116	13,6	0,0113	14,7	0,0123	27,4	0,0228

RHEOLOGICAL DATA OF CNC/SEP-WDFs (SW)

Time	Shear Rate	Shear Stress	Viscosity	Shear Stress	Viscosity	Shear Stress	Viscosity	Shear Stress	Viscosity	Shear Stress	Viscosity	Shear Stress	Viscosity	Shear Stress	Viscosity
[s]	[1/s]	[Pa]	[Pa·s]	[Pa]	[Pa·s]	[Pa]	[Pa·s]	[Pa]	[Pa·s]	[Pa]	[Pa·s]	[Pa]	[Pa·s]	[Pa]	[Pa·s]
Number of Intervals:		*CNC-SEP-WDFs (6 wt %) 0.0 % 20°C S.W.*	*CNC-SEP-WDFs (6 wt %) 0.0 % 20°C S.W.*	*CNC-SEP-WDFs (6 wt %) 0.4 % 20°C S.W.*	*CNC-SEP-WDFs (6 wt %) 0.4 % 20°C S.W.*	*CNC-SEP-WDFs (6 wt %) 0.8 % 20°C S.W.*	*CNC-SEP-WDFs (6 wt %) 0.8 % 20°C S.W.*	*CNC-SEP-WDFs (6 wt %) 1.2 % 20°C S.W.*	*CNC-SEP-WDFs (6 wt %) 1.2 % 20°C S.W.*	*CNC-SEP-WDFs (6 wt %) 1.6 % 20°C S.W.*	*CNC-SEP-WDFs (6 wt %) 1.6 % 20°C S.W.*	*CNC-SEP-WDFs (6 wt %) 2.0 % 20°C S.W.*	*CNC-SEP-WDFs (6 wt %) 2.0 % 20°C S.W.*	*CNC-SEP-WDFs (6 wt %) 2.4 % 20°C S.W.*	*CNC-SEP-WDFs (6 wt %) 2.4 % 20°C S.W.*
2	0,999	5,74	5,73	30,5	30,8	38,3	38,2	35,7	35,7	40,4	40,3	50,7	50,6	47,8	47,6
4	13,1	8,54	0,651	43,7	3,33	57,7	4,41	50,3	3,84	52,1	3,97	61,8	4,72	73,5	5,62
6	25,2	9,32	0,37	50,2	1,99	59,6	2,36	56,4	2,24	58	2,3	72	4,18	94,7	3,74
8	37,3	10,1	0,27	56,2	1,5	60,5	1,62	62,9	1,69	66,4	1,78	84	3,14	95,3	2,95
10	49,4	10,6	0,214	61	1,23	63,6	1,29	67,9	1,37	68,5	1,39	95	2,21	96,1	2,09
12	61,6	11	0,179	64,8	1,05	67	1,09	72,8	1,18	74,4	1,21	101	1,65	97,5	1,86
14	73,7	11,5	0,156	68,1	0,924	70,5	0,956	75,4	1,02	77,1	1,05	105	1,43	101,2	1,39
16	85,8	12,1	0,141	70,9	0,826	74,6	0,87	78,2	0,912	79,5	0,927	108	1,26	103	1,34
18	97,9	12,6	0,129	73,2	0,748	75,6	0,772	80,9	0,826	81,9	0,837	105	1,07	106	1,15
20	110	13,2	0,12	75,4	0,685	77,8	0,707	83,4	0,758	84	0,764	108	0,982	108	0,978
22	122	13,7	0,112	77,4	0,634	85,8	0,703	85,9	0,703	86,1	0,705	108	0,883	110	0,903
24	134	14,3	0,107	79,3	0,59	82,3	0,613	87,7	0,654	88,1	0,656	111	0,824	116	0,868
26	146	15	0,102	80,9	0,553	83,2	0,569	89,7	0,613	89,7	0,613	110	0,75	117	0,799
28	158	15,7	0,0988	82,4	0,52	84,8	0,535	90,9	0,574	91,1	0,575	112	0,707	121	0,767
30	171	16,3	0,0959	83,9	0,492	85,9	0,504	92,9	0,545	92,7	0,543	114	0,666	121	0,709
32	183	17,1	0,0933	85,2	0,467	87,5	0,479	94	0,515	94	0,514	114	0,627	122	0,671
34	195	17,8	0,0913	86,6	0,445	88,7	0,455	96,1	0,494	95,1	0,488	113	0,582	124	0,639
36	207	18,5	0,0892	87,9	0,425	89,9	0,435	97,1	0,469	96,1	0,465	115	0,555	123	0,594
38	219	19,3	0,0881	89,1	0,407	91,2	0,416	97,3	0,444	97,1	0,443	113	0,517	127	0,582
40	231	20,1	0,0868	90,2	0,39	92,3	0,4	99,3	0,43	98,1	0,424	115	0,497	125	0,541
42	243	20,8	0,0856	91,4	0,376	93,4	0,384	100	0,412	98,9	0,407	116	0,478	127	0,523
44	255	21,7	0,085	92,5	0,362	94,5	0,37	101	0,395	100	0,392	118	0,462	129	0,506
46	267	22,6	0,0845	93,5	0,35	95,5	0,357	102	0,38	101	0,377	118	0,441	128	0,478
48	280	23,5	0,0842	94,5	0,338	96,6	0,345	103	0,368	102	0,365	122	0,436	132	0,473
50	292	24,5	0,0839	95,4	0,327	97,5	0,334	104	0,356	104	0,355	123	0,422	131	0,45
52	304	25,5	0,084	96,4	0,317	98,5	0,324	105	0,344	104	0,344	124	0,41	136	0,447
54	316	26,6	0,0843	97,3	0,308	99,4	0,315	105	0,334	105	0,333	122	0,388	131	0,414
56	328	27,8	0,0847	98,3	0,3	100	0,306	106	0,324	107	0,325	123	0,375	132	0,402
58	340	29,1	0,0854	99,1	0,292	101	0,298	107	0,315	107	0,315	122	0,36	132	0,387
60	352	30,3	0,0862	100	0,284	102	0,29	108	0,306	108	0,308	124	0,351	132	0,375
62	364	31,6	0,0868	101	0,277	103	0,283	108	0,298	109	0,299	126	0,345	133	0,366
64	376	33,1	0,0878	102	0,27	104	0,276	109	0,288	109	0,29	124	0,331	133	0,354
66	389	34,5	0,0888	103	0,264	105	0,269	109	0,281	110	0,283	125	0,321	133	0,343
68	401	36	0,0899	103	0,258	105	0,263	110	0,275	111	0,277	128	0,319	135	0,336
70	413	37,6	0,0911	104	0,252	106	0,257	111	0,268	111	0,27	129	0,312	135	0,327
72	425	39,3	0,0924	105	0,247	107	0,251	112	0,263	111	0,262	129	0,303	136	0,32
74	437	40,9	0,0936	106	0,242	108	0,246	112	0,257	112	0,257	129	0,296	137	0,313
76	449	42,7	0,095	106	0,236	108	0,241	113	0,251	112	0,25	129	0,288	136	0,303
78	461	44,1	0,0957	107	0,232	109	0,237	113	0,246	114	0,247	130	0,281	137	0,297
80	473	46,2	0,0976	107	0,227	110	0,231	114	0,24	114	0,24	131	0,276	138	0,292
82	485	48,1	0,099	108	0,222	110	0,227	114	0,235	114	0,235	130	0,268	139	0,287
84	498	49,9	0,1	108	0,218	111	0,223	115	0,231	115	0,231	131	0,264	140	0,282
86	510	51,8	0,102	109	0,214	111	0,218	116	0,227	115	0,226	132	0,258	140	0,274
88	522	53,8	0,103	110	0,21	112	0,215	116	0,223	116	0,223	132	0,253	140	0,267
90	534	55,7	0,104	110	0,206	113	0,211	117	0,218	116	0,218	132	0,248	140	0,262
92	546	57,5	0,105	111	0,203	113	0,207	117	0,215	117	0,214	133	0,244	141	0,258
94	558	59,4	0,106	111	0,199	114	0,204	118	0,211	118	0,212	134	0,239	141	0,252

96	570	61,3	0,108	112	0,196	114	0,2	118	0,207	119	0,208	135	0,236	142	0,249
98	582	63,2	0,109	112	0,192	115	0,197	119	0,204	119	0,204	135	0,232	142	0,244
100	594	65	0,109	113	0,189	115	0,194	119	0,201	119	0,2	136	0,228	142	0,24
102	607	66,9	0,11	113	0,186	115	0,19	120	0,198	119	0,197	135	0,223	143	0,235
104	619	68,7	0,111	114	0,184	116	0,187	120	0,195	120	0,194	136	0,22	143	0,231
106	631	70,5	0,112	114	0,181	116	0,184	121	0,191	120	0,191	136	0,216	143	0,227
108	643	72,3	0,112	114	0,178	117	0,182	121	0,188	120	0,187	136	0,212	144	0,224
110	655	74,1	0,113	115	0,175	117	0,179	122	0,186	121	0,185	137	0,209	145	0,221
112	667	75,6	0,113	115	0,173	118	0,176	122	0,182	122	0,183	137	0,205	145	0,217
114	679	77,1	0,114	116	0,17	118	0,174	122	0,18	122	0,18	138	0,203	145	0,214
116	691	78,7	0,114	116	0,168	118	0,171	123	0,177	122	0,177	138	0,199	147	0,212
118	703	80,3	0,114	116	0,165	119	0,169	123	0,174	122	0,174	138	0,196	147	0,208
120	716	81,6	0,114	117	0,163	119	0,167	123	0,172	123	0,172	139	0,194	147	0,205
122	728	83,2	0,114	117	0,161	120	0,164	123	0,169	123	0,169	139	0,191	149	0,204
124	740	84,5	0,114	118	0,159	120	0,162	124	0,167	124	0,168	140	0,189	149	0,201
126	752	85,7	0,114	118	0,157	120	0,16	124	0,165	124	0,165	140	0,186	149	0,198
128	764	87,1	0,114	118	0,155	121	0,158	124	0,163	125	0,163	140	0,183	148	0,194
130	776	88,3	0,114	119	0,153	121	0,156	125	0,16	125	0,161	140	0,181	149	0,192
132	788	89,6	0,114	119	0,151	121	0,154	125	0,159	125	0,159	141	0,179	149	0,189
134	800	90,6	0,113	119	0,149	122	0,152	125	0,156	126	0,157	141	0,176	149	0,187
136	812	91,8	0,113	119	0,147	122	0,15	126	0,154	126	0,155	141	0,174	151	0,185
138	825	92,9	0,113	120	0,145	122	0,148	126	0,152	126	0,153	141	0,171	149	0,181
140	837	94,1	0,112	120	0,143	123	0,146	126	0,15	127	0,151	141	0,169	150	0,179
142	849	95,2	0,112	120	0,142	123	0,145	126	0,148	127	0,149	143	0,169	150	0,177
144	861	96,2	0,112	121	0,14	123	0,143	126	0,147	127	0,148	145	0,169	150	0,174
146	873	97,3	0,111	121	0,139	123	0,141	127	0,145	128	0,146	145	0,166	151	0,172
148	885	98,4	0,111	121	0,137	124	0,14	127	0,143	128	0,144	144	0,163	151	0,17
150	897	99,4	0,111	121	0,135	124	0,138	127	0,141	128	0,142	143	0,16	151	0,168
152	909	100	0,11	122	0,134	124	0,137	127	0,14	128	0,141	144	0,158	151	0,166
154	921	101	0,11	122	0,132	124	0,135	127	0,138	128	0,139	144	0,157	152	0,165
156	934	102	0,109	122	0,131	125	0,134	127	0,136	128	0,138	144	0,154	152	0,163
158	946	103	0,109	123	0,13	125	0,132	128	0,135	129	0,136	144	0,152	152	0,161
160	958	104	0,108	123	0,128	125	0,13	128	0,133	129	0,134	144	0,151	152	0,159
162	970	105	0,108	123	0,127	125	0,129	128	0,132	129	0,133	144	0,149	153	0,157
164	982	106	0,108	123	0,126	126	0,128	128	0,13	129	0,131	145	0,147	154	0,156
166	994	106	0,107	123	0,124	126	0,127	128	0,129	129	0,13	145	0,145	153	0,154
168	1 010	107	0,107	124	0,123	126	0,125	128	0,127	129	0,129	145	0,144	153	0,152
170	1 020	108	0,106	124	0,122	126	0,124	128	0,126	130	0,127	146	0,143	153	0,151
172	1 030	109	0,106	124	0,12	126	0,123	128	0,125	130	0,126	146	0,141	154	0,149
174	1 040	110	0,105	124	0,119	127	0,121	128	0,123	130	0,125	145	0,139	153	0,147
176	1 050	110	0,105	125	0,118	127	0,12	129	0,122	130	0,124	145	0,138	154	0,146
178	1 070	111	0,104	125	0,117	127	0,119	129	0,121	131	0,122	146	0,136	154	0,144
180	1 080	112	0,104	125	0,116	127	0,118	129	0,119	131	0,121	146	0,136	154	0,143
182	1 090	112	0,103	125	0,115	127	0,117	129	0,118	131	0,12	146	0,134	154	0,141
184	1 100	113	0,103	126	0,114	128	0,116	129	0,117	131	0,119	146	0,133	154	0,14
186	1 120	114	0,102	126	0,113	128	0,115	129	0,116	131	0,118	147	0,132	154	0,138
188	1 130	115	0,102	126	0,112	128	0,114	129	0,115	132	0,117	147	0,13	155	0,137
190	1 140	115	0,101	126	0,111	128	0,113	130	0,114	132	0,116	147	0,129	155	0,136
192	1 150	116	0,101	126	0,11	128	0,112	130	0,112	132	0,115	147	0,127	155	0,134
194	1 160	116	0,1	126	0,109	129	0,111	130	0,111	132	0,114	146	0,126	155	0,133
196	1 180	117	0,0996	126	0,107	129	0,11	130	0,11	131	0,111	147	0,125	155	0,132

198	1 190	118	0,099	127	0,107	129	0,109	130	0,109	131	0,11	149	0,126	155	0,131
200	1 200	118	0,0987	127	0,106	129	0,108	130	0,108	131	0,109	148	0,123	156	0,13

Time	Shear Rate	Shear Stress	Viscosity	Shear Stress	Viscosity	Shear Stress	Viscosity	Shear Stress	Viscosity	Shear Stress	Viscosity	Shear Stress	Viscosity	Shear Stress	Viscosity
[s]	[1/s]	[Pa]	[Pa·s]	[Pa]	[Pa·s]	[Pa]	[Pa·s]	[Pa]	[Pa·s]	[Pa]	[Pa·s]	[Pa]	[Pa·s]	[Pa]	[Pa·s]
Number of Intervals:		*CNC-SEP-WDFs (6 wt %) 0.0 % 30°C S.W.*	*CNC-SEP-WDFs (6 wt %) 0.0 % 30°C S.W.*	*CNC-SEP-WDFs (6 wt %) 0.4 % 30°C S.W.*	*CNC-SEP-WDFs (6 wt %) 0.4 % 30°C S.W.*	*CNC-SEP-WDFs (6 wt %) 0.8 % 30°C S.W.*	*CNC-SEP-WDFs (6 wt %) 0.8 % 30°C S.W.*	*CNC-SEP-WDFs (6 wt %) 1.2 % 30°C S.W.*	*CNC-SEP-WDFs (6 wt %) 1.2 % 30°C S.W.*	*CNC-SEP-WDFs (6 wt %) 1.6 % 30°C S.W.*	*CNC-SEP-WDFs (6 wt %) 1.6 % 30°C S.W.*	*CNC-SEP-WDFs (6 wt %) 2.0 % 30°C S.W.*	*CNC-SEP-WDFs (6 wt %) 2.0 % 30°C S.W.*	*CNC-SEP-WDFs (6 wt %) 2.4 % 30°C S.W.*	*CNC-SEP-WDFs (6 wt %) 2.4 % 30°C S.W.*
2	0,999	10,7	10,7	33,3	33,2	46	46,2	41,2	41,1	96,1	96	56,5	56,9	98	98,9
4	13,1	16,8	1,28	43,3	3,3	56	4,27	53,9	4,11	96,2	7,32	83,6	6,37	133	10,1
6	25,2	18,8	0,744	50,4	2	83,2	3,29	61,4	2,43	115	4,58	91,5	3,63	118	4,69
8	37,3	20,6	0,551	56,6	1,52	91,5	2,45	68	1,82	110	2,95	87,7	2,35	119	3,18
10	49,4	22	0,444	61,5	1,24	91,1	1,84	70,8	1,43	121	2,44	92,8	1,88	127	2,57
12	61,6	23,3	0,379	65,5	1,06	88,7	1,44	78,6	1,28	116	1,89	94,6	1,54	131	2,12
14	73,7	24,5	0,333	68,7	0,932	94,5	1,28	78,8	1,07	120	1,62	96,4	1,31	134	1,81
16	85,8	25,9	0,302	71,4	0,833	94,5	1,1	84,2	0,981	122	1,42	99	1,15	134	1,57
18	97,9	27,2	0,278	73,8	0,754	94,8	0,968	85	0,868	122	1,24	103	1,05	140	1,43
20	110	28,5	0,259	75,8	0,689	97,1	0,882	86,5	0,786	129	1,18	105	0,956	141	1,29
22	122	29,8	0,244	77,7	0,636	98,4	0,805	89,1	0,73	129	1,05	106	0,871	143	1,17
24	134	31,3	0,233	79,5	0,592	106	0,793	92	0,685	124	0,923	108	0,803	141	1,05
26	146	32,8	0,224	81,1	0,554	107	0,73	93,3	0,638	127	0,869	108	0,739	145	0,988
28	158	34,4	0,217	82,6	0,521	112	0,709	95	0,6	127	0,804	110	0,691	148	0,932
30	171	35,9	0,211	84	0,493	119	0,695	94,4	0,554	131	0,771	108	0,634	149	0,872
32	183	37,6	0,206	85,3	0,467	120	0,657	95,7	0,524	129	0,708	110	0,604	134	0,735
34	195	39,4	0,202	86,5	0,444	122	0,626	97,3	0,5	129	0,662	113	0,582	136	0,699
36	207	41,2	0,199	87,7	0,424	117	0,566	98,6	0,477	134	0,649	112	0,544	136	0,657
38	219	43,1	0,197	88,8	0,406	113	0,515	98,2	0,448	131	0,599	113	0,516	140	0,638
40	231	45,1	0,195	89,9	0,389	113	0,49	99,9	0,432	133	0,577	115	0,499	140	0,607
42	243	47,1	0,193	90,9	0,374	114	0,468	100	0,413	136	0,557	118	0,485	141	0,578
44	255	49	0,192	91,8	0,36	113	0,441	101	0,397	132	0,518	120	0,472	142	0,557
46	267	51,1	0,191	92,9	0,347	112	0,418	102	0,383	134	0,501	119	0,444	147	0,551
48	280	53,1	0,19	93,7	0,335	112	0,402	104	0,371	133	0,476	122	0,436	148	0,528
50	292	55,2	0,189	94,7	0,325	115	0,395	104	0,355	136	0,467	119	0,409	147	0,505
52	304	57,2	0,188	95,5	0,315	115	0,378	105	0,346	137	0,45	119	0,393	148	0,487
54	316	59,2	0,188	96,4	0,305	115	0,363	105	0,333	137	0,435	118	0,374	150	0,474
56	328	61,3	0,187	97,2	0,296	115	0,351	106	0,324	137	0,419	118	0,359	151	0,461
58	340	63,4	0,186	98	0,288	114	0,336	107	0,315	137	0,404	118	0,347	155	0,455
60	352	65,4	0,186	98,8	0,28	115	0,325	108	0,306	137	0,39	118	0,336	155	0,44
62	364	67,4	0,185	99,5	0,273	118	0,323	108	0,297	138	0,38	122	0,334	156	0,428
64	376	69,2	0,184	100	0,266	116	0,308	109	0,289	139	0,369	124	0,33	158	0,419
66	389	71,1	0,183	101	0,26	117	0,301	109	0,28	140	0,361	120	0,31	158	0,408
68	401	73	0,182	102	0,254	118	0,295	110	0,274	142	0,355	119	0,298	159	0,396
70	413	74,8	0,181	102	0,248	119	0,288	111	0,268	142	0,343	120	0,291	156	0,379
72	425	76,7	0,18	103	0,242	119	0,279	111	0,262	143	0,336	121	0,284	158	0,371
74	437	78,6	0,18	103	0,237	120	0,274	111	0,255	144	0,329	121	0,277	158	0,363
76	449	80,4	0,179	104	0,232	119	0,265	112	0,249	144	0,321	121	0,269	161	0,359
78	461	82	0,178	105	0,227	120	0,26	113	0,244	144	0,312	121	0,263	163	0,352
80	473	83,9	0,177	105	0,222	120	0,254	113	0,239	141	0,298	121	0,256	164	0,346
82	485	85,6	0,176	106	0,218	120	0,247	113	0,234	142	0,293	122	0,251	163	0,335
84	498	87,2	0,175	106	0,214	121	0,242	114	0,229	144	0,289	125	0,25	163	0,329
86	510	88,8	0,174	107	0,21	121	0,237	115	0,225	147	0,288	128	0,25	162	0,317
88	522	90,1	0,173	107	0,206	120	0,229	115	0,22	147	0,281	127	0,244	162	0,311
90	534	91,7	0,172	108	0,202	121	0,227	115	0,216	148	0,276	128	0,24	160	0,3
92	546	93	0,17	108	0,198	121	0,222	116	0,213	147	0,268	128	0,234	162	0,297
94	558	94,4	0,169	109	0,195	121	0,217	117	0,209	148	0,266	124	0,223	167	0,298
96	570	95,6	0,168	109	0,191	121	0,213	117	0,205	144	0,252	125	0,22	169	0,296
98	582	96,9	0,166	110	0,188	122	0,209	117	0,202	143	0,246	127	0,218	170	0,291
100	594	98,3	0,165	110	0,185	122	0,205	118	0,198	145	0,244	129	0,216	172	0,289
102	607	99,3	0,164	110	0,182	122	0,201	118	0,195	146	0,24	128	0,211	174	0,287
104	619	101	0,163	111	0,179	122	0,198	119	0,192	148	0,239	129	0,208	179	0,289

106	631	102	0,161	111	0,176	122	0,194	119	0,189	149	0,236	129	0,204	179	0,283
108	643	103	0,16	112	0,174	122	0,19	119	0,186	149	0,231	130	0,202	179	0,278
110	655	104	0,158	112	0,171	122	0,187	120	0,183	149	0,227	131	0,2	176	0,268
112	667	105	0,157	112	0,168	123	0,184	120	0,18	148	0,222	131	0,196	175	0,263
114	679	106	0,156	113	0,166	123	0,182	121	0,178	149	0,219	131	0,192	174	0,256
116	691	107	0,154	113	0,163	124	0,179	121	0,175	150	0,218	131	0,189	174	0,252
118	703	107	0,153	113	0,161	123	0,175	121	0,173	151	0,214	132	0,187	172	0,245
120	716	108	0,151	114	0,159	124	0,173	122	0,17	150	0,21	132	0,185	174	0,243
122	728	109	0,15	114	0,156	124	0,17	122	0,168	148	0,204	131	0,18	175	0,24
124	740	110	0,148	114	0,154	124	0,168	122	0,165	151	0,204	132	0,178	175	0,237
126	752	111	0,147	115	0,152	124	0,165	123	0,163	151	0,2	132	0,175	175	0,233
128	764	111	0,145	115	0,15	125	0,163	123	0,161	151	0,198	132	0,173	174	0,227
130	776	112	0,144	115	0,148	125	0,161	123	0,159	150	0,194	132	0,17	176	0,227
132	788	113	0,143	115	0,146	125	0,158	124	0,157	151	0,192	132	0,167	176	0,223
134	800	113	0,142	116	0,145	126	0,157	124	0,155	153	0,192	132	0,165	176	0,22
136	812	114	0,14	116	0,143	126	0,155	124	0,153	152	0,188	133	0,164	178	0,22
138	825	114	0,139	116	0,141	126	0,153	124	0,151	148	0,18	133	0,162	179	0,217
140	837	115	0,137	116	0,139	126	0,15	125	0,149	149	0,179	134	0,16	181	0,216
142	849	116	0,136	117	0,137	126	0,148	125	0,147	147	0,174	133	0,157	182	0,214
144	861	116	0,135	117	0,136	126	0,146	125	0,146	147	0,171	134	0,156	181	0,21
146	873	117	0,134	117	0,134	126	0,144	126	0,144	149	0,171	134	0,153	183	0,209
148	885	117	0,132	117	0,133	126	0,142	126	0,142	150	0,17	134	0,151	182	0,206
150	897	118	0,131	117	0,131	126	0,141	126	0,14	149	0,166	133	0,148	184	0,205
152	909	118	0,13	118	0,13	127	0,139	126	0,139	150	0,165	133	0,146	180	0,198
154	921	119	0,129	118	0,128	127	0,137	127	0,137	151	0,163	134	0,145	184	0,199
156	934	119	0,128	118	0,127	127	0,136	127	0,136	150	0,161	134	0,143	181	0,194
158	946	120	0,126	118	0,125	126	0,134	127	0,134	150	0,158	133	0,141	182	0,193
160	958	120	0,126	119	0,124	126	0,132	127	0,133	152	0,159	134	0,14	187	0,195
162	970	121	0,124	119	0,123	126	0,13	127	0,131	152	0,157	134	0,138	187	0,193
164	982	121	0,123	119	0,121	127	0,129	127	0,13	150	0,153	136	0,138	189	0,192
166	994	121	0,122	119	0,12	127	0,128	128	0,128	151	0,152	136	0,137	189	0,19
168	1 010	122	0,121	119	0,119	127	0,126	128	0,127	154	0,153	134	0,133	191	0,189
170	1 020	122	0,12	120	0,117	127	0,125	128	0,126	154	0,152	134	0,132	191	0,187
172	1 030	123	0,119	120	0,116	127	0,124	128	0,124	153	0,148	134	0,13	187	0,181
174	1 040	123	0,118	120	0,115	127	0,122	128	0,123	153	0,147	134	0,129	189	0,181
176	1 050	123	0,117	120	0,114	128	0,121	128	0,122	152	0,144	135	0,128	184	0,175
178	1 070	124	0,116	120	0,113	128	0,12	129	0,12	153	0,144	135	0,126	185	0,173
180	1 080	124	0,115	121	0,112	128	0,119	129	0,119	151	0,14	134	0,125	186	0,172
182	1 090	124	0,114	121	0,111	128	0,118	129	0,118	150	0,138	135	0,124	190	0,174
184	1 100	125	0,113	121	0,11	128	0,116	129	0,117	153	0,138	137	0,124	190	0,172
186	1 120	125	0,112	121	0,109	128	0,115	129	0,116	150	0,134	134	0,121	189	0,17
188	1 130	125	0,111	121	0,108	129	0,114	129	0,115	149	0,132	135	0,119	182	0,161
190	1 140	126	0,11	121	0,106	129	0,113	129	0,113	148	0,13	135	0,118	177	0,156
192	1 150	126	0,109	122	0,106	129	0,112	129	0,112	146	0,127	138	0,12	177	0,153
194	1 160	126	0,108	122	0,105	129	0,111	129	0,111	145	0,124	139	0,119	176	0,152
196	1 180	127	0,108	122	0,104	129	0,11	130	0,11	145	0,123	136	0,116	169	0,144
198	1 190	127	0,107	122	0,103	130	0,109	130	0,109	145	0,122	138	0,116	171	0,144
200	1 200	127	0,106	122	0,102	130	0,108	130	0,108	145	0,12	139	0,116	172	0,143

Time	Shear Rate	Shear Stress	Viscosity	Shear Stress	Viscosity	Shear Stress	Viscosity	Shear Stress	Viscosity	Shear Stress	Viscosity	Shear Stress	Viscosity	Shear Stress	Viscosity
[s]	[1/s]	[Pa]	[Pa·s]	[Pa]	[Pa·s]	[Pa]	[Pa·s]	[Pa]	[Pa·s]	[Pa]	[Pa·s]	[Pa]	[Pa·s]	[Pa]	[Pa·s]
Number of Intervals:		*CNC-SEP-WDFs (6 wt %) 0.0 % 40°C S.W.*	*CNC-SEP-WDFs (6 wt %) 0.0 % 40°C S.W.*	*CNC-SEP-WDFs (6 wt %) 0.4 % 40°C S.W.*	*CNC-SEP-WDFs (6 wt %) 0.4 % 40°C S.W.*	*CNC-SEP-WDFs (6 wt %) 0.8 % 40°C S.W.*	*CNC-SEP-WDFs (6 wt %) 0.8 % 40°C S.W.*	*CNC-SEP-WDFs (6 wt %) 1.2 % 40°C S.W.*	*CNC-SEP-WDFs (6 wt %) 1.2 % 40°C S.W.*	*CNC-SEP-WDFs (6 wt %) 1.6 % 40°C S.W.*	*CNC-SEP-WDFs (6 wt %) 1.6 % 40°C S.W.*	*CNC-SEP-WDFs (6 wt %) 2.0 % 40°C S.W.*	*CNC-SEP-WDFs (6 wt %) 2.0 % 40°C S.W.*	*CNC-SEP-WDFs (6 wt %) 2.4 % 40°C S.W.*	*CNC-SEP-WDFs (6 wt %) 2.4 % 40°C S.W.*
2	0,999	22,3	22,4	35,5	35,5	40,7	40,5	50,1	50	55,7	55,9	79,9	79,7	97,4	97,1
4	13,1	28,8	2,19	46	3,51	53,2	4,06	63,5	4,84	69,4	5,29	85	9	90,1	6,86
6	25,2	32,9	1,3	53	2,1	63,5	2,52	70,7	2,8	84,9	3,36	89,1	3,53	110	6,35
8	37,3	36,2	0,969	59,4	1,59	67,9	1,82	77,2	2,07	88,3	2,37	102	2,96	118	4,04
10	49,4	39	0,788	62,9	1,27	70,2	1,42	80,6	1,63	89,3	1,81	108	2,18	121	2,93
12	61,6	41,3	0,671	66,8	1,09	73,1	1,19	84,2	1,37	88	1,43	111	1,94	127	2,06
14	73,7	43,4	0,589	70	0,95	78,7	1,07	87,2	1,18	91,3	1,24	117	1,59	136	1,85
16	85,8	45,4	0,529	72	0,839	78,8	0,919	89,8	1,05	93,5	1,09	116	1,35	137	1,69
18	97,9	47,2	0,483	74,2	0,758	81,2	0,829	92	0,94	93,2	0,952	120	1,23	138	1,41
20	110	49,2	0,447	76,6	0,697	84,4	0,767	94,1	0,855	95,3	0,866	119	1,09	138	1,33
22	122	51	0,417	78	0,639	83,9	0,687	95,7	0,784	96,4	0,789	119	0,974	139	1,2
24	134	52,8	0,393	79,4	0,591	85,3	0,635	98,3	0,732	97,6	0,727	123	0,917	140	1,07
26	146	54,6	0,373	80,8	0,552	86,7	0,592	99,2	0,678	98,5	0,673	122	0,833	141	0,981
28	158	56,4	0,356	82,2	0,519	88,2	0,556	101	0,639	101	0,636	123	0,775	142	0,899
30	171	58,2	0,341	83,6	0,49	89,3	0,524	102	0,597	102	0,598	122	0,716	143	0,84
32	183	60	0,328	84,7	0,464	90,4	0,495	104	0,569	104	0,569	123	0,674	144	0,788
34	195	61,7	0,317	85,5	0,439	92,5	0,475	105	0,537	104	0,536	124	0,634	145	0,743
36	207	63,4	0,306	86,6	0,418	92,7	0,448	106	0,512	105	0,508	123	0,594	148	0,715
38	219	65	0,297	87,7	0,401	93,4	0,426	107	0,491	104	0,477	125	0,571	143	0,654
40	231	66,7	0,288	88,8	0,384	95	0,411	109	0,47	105	0,456	125	0,543	146	0,615
42	243	68,2	0,281	90	0,37	95,2	0,391	109	0,446	107	0,44	127	0,521	145	0,594
44	255	69,7	0,273	90,7	0,355	96,3	0,377	110	0,431	107	0,417	128	0,502	145	0,567
46	267	71,3	0,266	91,1	0,34	97	0,363	110	0,413	108	0,402	129	0,483	145	0,543
48	280	72,7	0,26	91,8	0,328	97,5	0,349	112	0,399	107	0,384	126	0,451	142	0,508
50	292	74,1	0,254	92,6	0,317	98	0,336	111	0,38	109	0,375	126	0,431	144	0,494
52	304	75,5	0,248	93,2	0,307	99,2	0,326	112	0,368	111	0,366	126	0,416	141	0,465
54	316	76,7	0,243	93,9	0,297	99,3	0,314	112	0,355	113	0,357	128	0,405	141	0,445
56	328	77,8	0,237	95,4	0,291	101	0,307	112	0,342	116	0,352	128	0,391	143	0,436
58	340	79	0,232	95,9	0,282	101	0,297	113	0,331	110	0,324	129	0,379	145	0,425
60	352	80,1	0,227	96	0,273	101	0,287	113	0,321	112	0,317	129	0,365	144	0,409
62	364	81,1	0,222	96,9	0,266	102	0,281	114	0,312	113	0,311	128	0,352	142	0,389
64	376	82,1	0,218	96,9	0,257	102	0,272	114	0,303	113	0,3	129	0,344	140	0,373
66	389	83,1	0,214	97,8	0,252	103	0,266	114	0,295	116	0,298	128	0,33	143	0,368
68	401	84	0,21	98,1	0,245	104	0,259	115	0,287	112	0,28	130	0,324	143	0,357
70	413	84,8	0,205	98,2	0,238	104	0,253	115	0,28	112	0,271	129	0,313	142	0,343
72	425	85,7	0,202	98,6	0,232	105	0,246	116	0,272	112	0,263	129	0,305	141	0,332
74	437	86,5	0,198	99,1	0,227	106	0,242	116	0,265	113	0,258	130	0,298	146	0,333
76	449	87,4	0,195	99,7	0,222	107	0,239	117	0,26	113	0,251	129	0,288	143	0,318
78	461	88,3	0,192	99,9	0,217	107	0,232	116	0,252	114	0,246	130	0,281	142	0,309
80	473	88,9	0,188	101	0,212	107	0,227	117	0,246	114	0,241	129	0,273	143	0,302
82	485	89,7	0,185	101	0,208	106	0,218	117	0,241	115	0,236	129	0,266	143	0,294
84	498	90,3	0,181	101	0,204	106	0,214	117	0,236	114	0,23	128	0,258	145	0,291
86	510	91	0,179	102	0,2	107	0,209	118	0,231	115	0,225	129	0,253	145	0,284
88	522	91,6	0,176	102	0,196	107	0,205	118	0,227	115	0,22	130	0,249	144	0,275
90	534	92,3	0,173	103	0,192	108	0,201	119	0,223	116	0,216	130	0,243	145	0,272
92	546	92,9	0,17	103	0,189	108	0,197	119	0,218	117	0,214	130	0,239	144	0,265
94	558	93,5	0,168	103	0,185	108	0,194	119	0,214	118	0,211	129	0,231	145	0,26
96	570	94	0,165	104	0,182	108	0,19	120	0,21	117	0,205	131	0,23	145	0,254
98	582	94,6	0,162	104	0,179	109	0,187	120	0,206	117	0,201	131	0,225	145	0,249
100	594	95,2	0,16	104	0,176	109	0,184	120	0,202	118	0,198	131	0,221	146	0,245
102	607	95,7	0,158	105	0,173	110	0,181	121	0,199	118	0,195	132	0,217	145	0,239
104	619	96,3	0,156	105	0,17	110	0,177	121	0,196	119	0,192	131	0,212	147	0,237

106	631	96,8	0,153	106	0,167	110	0,175	121	0,192	119	0,188	133	0,211	146	0,231
108	643	97,2	0,151	106	0,165	110	0,172	121	0,189	119	0,185	133	0,207	145	0,226
110	655	97,8	0,149	106	0,162	111	0,169	122	0,186	120	0,183	133	0,202	145	0,221
112	667	98,2	0,147	106	0,159	111	0,166	122	0,183	120	0,18	132	0,198	145	0,217
114	679	98,8	0,145	107	0,157	111	0,164	122	0,18	120	0,177	133	0,196	145	0,214
116	691	99,2	0,144	107	0,155	111	0,161	123	0,178	120	0,174	134	0,193	146	0,211
118	703	99,7	0,142	107	0,153	112	0,159	126	0,179	120	0,171	133	0,189	146	0,207
120	716	100	0,14	108	0,15	112	0,156	124	0,174	123	0,172	133	0,186	146	0,204
122	728	101	0,138	108	0,148	112	0,154	124	0,17	121	0,166	133	0,183	146	0,201
124	740	101	0,136	108	0,146	112	0,152	124	0,168	121	0,163	134	0,181	146	0,198
126	752	101	0,135	108	0,144	113	0,15	125	0,166	121	0,161	134	0,178	147	0,195
128	764	102	0,133	108	0,142	113	0,148	125	0,164	121	0,158	134	0,176	147	0,192
130	776	102	0,132	109	0,14	113	0,146	125	0,161	121	0,156	135	0,173	147	0,189
132	788	103	0,13	109	0,138	113	0,144	125	0,159	123	0,156	135	0,171	147	0,186
134	800	103	0,129	109	0,136	114	0,142	125	0,157	124	0,155	135	0,169	148	0,185
136	812	103	0,127	109	0,135	114	0,14	127	0,156	121	0,149	135	0,166	149	0,183
138	825	104	0,126	109	0,133	114	0,138	126	0,153	122	0,148	135	0,164	148	0,18
140	837	104	0,124	110	0,131	114	0,136	126	0,151	124	0,148	135	0,161	149	0,178
142	849	104	0,123	110	0,129	114	0,135	126	0,149	122	0,143	135	0,159	148	0,175
144	861	105	0,121	110	0,128	115	0,133	127	0,147	123	0,143	136	0,158	151	0,175
146	873	105	0,12	110	0,126	115	0,131	127	0,145	124	0,142	136	0,156	148	0,17
148	885	105	0,119	110	0,125	115	0,13	127	0,144	123	0,138	136	0,154	148	0,167
150	897	105	0,117	111	0,123	115	0,128	127	0,142	122	0,136	136	0,152	148	0,165
152	909	106	0,116	111	0,122	115	0,127	127	0,14	123	0,135	136	0,149	149	0,164
154	921	106	0,115	111	0,12	115	0,125	128	0,139	123	0,133	136	0,148	149	0,161
156	934	106	0,114	111	0,119	116	0,124	128	0,137	123	0,131	137	0,147	149	0,16
158	946	106	0,112	111	0,118	116	0,122	128	0,136	123	0,13	137	0,145	150	0,159
160	958	107	0,111	111	0,116	116	0,121	129	0,134	124	0,129	137	0,143	149	0,156
162	970	107	0,11	112	0,115	116	0,12	129	0,133	123	0,127	136	0,14	150	0,154
164	982	107	0,109	112	0,114	116	0,118	129	0,131	123	0,126	135	0,137	150	0,153
166	994	107	0,108	112	0,112	116	0,117	129	0,13	124	0,124	135	0,136	151	0,152
168	1 010	108	0,107	112	0,111	116	0,115	129	0,128	124	0,123	135	0,134	150	0,149
170	1 020	108	0,106	112	0,11	116	0,114	130	0,127	124	0,122	135	0,132	150	0,148
172	1 030	108	0,105	112	0,109	116	0,113	130	0,126	123	0,12	135	0,131	150	0,146
174	1 040	108	0,104	113	0,108	117	0,112	130	0,125	124	0,119	135	0,129	150	0,144
176	1 050	108	0,103	113	0,107	117	0,111	130	0,123	125	0,118	135	0,128	150	0,143
178	1 070	109	0,102	113	0,106	117	0,11	129	0,121	124	0,117	135	0,127	151	0,141
180	1 080	109	0,101	113	0,105	117	0,108	130	0,12	125	0,116	136	0,126	151	0,14
182	1 090	109	0,0999	113	0,104	117	0,107	130	0,119	125	0,114	136	0,124	151	0,138
184	1 100	109	0,0989	113	0,103	117	0,106	129	0,117	126	0,114	136	0,123	151	0,137
186	1 120	109	0,0981	113	0,102	117	0,105	131	0,118	125	0,112	135	0,121	151	0,135
188	1 130	110	0,0973	113	0,101	118	0,104	131	0,116	125	0,111	136	0,12	151	0,134
190	1 140	110	0,0962	113	0,0996	118	0,103	132	0,116	125	0,11	136	0,12	151	0,132
192	1 150	110	0,0954	114	0,0987	118	0,102	130	0,113	125	0,108	137	0,119	151	0,131
194	1 160	110	0,0945	114	0,0978	118	0,101	129	0,111	125	0,107	137	0,117	152	0,13
196	1 180	110	0,0937	114	0,0969	118	0,1	133	0,113	125	0,106	136	0,115	152	0,129
198	1 190	110	0,0928	114	0,0959	118	0,0993	134	0,113	126	0,106	138	0,116	151	0,127
200	1 200	110	0,0919	114	0,095	118	0,0984	134	0,112	125	0,104	138	0,115	151	0,126

Time	Shear Rate	Shear Stress	Viscosity	Shear Stress	Viscosity	Shear Stress	Viscosity	Shear Stress	Viscosity	Shear Stress	Viscosity	Shear Stress	Viscosity	Shear Stress	Viscosity
[s]	[1/s]	[Pa]	[Pa·s]	[Pa]	[Pa·s]	[Pa]	[Pa·s]	[Pa]	[Pa·s]	[Pa]	[Pa·s]	[Pa]	[Pa·s]	[Pa]	[Pa·s]
Number of Intervals:		*CNC-SEP-WDFs (6 wt %) 0.0 % 50°C S.W.*	*CNC-SEP-WDFs (6 wt %) 0.0 % 50°C S.W.*	*CNC-SEP-WDFs (6 wt %) 0.4 % 50°C S.W.*	*CNC-SEP-WDFs (6 wt %) 0.4 % 50°C S.W.*	*CNC-SEP-WDFs (6 wt %) 0.8 % 50°C S.W.*	*CNC-SEP-WDFs (6 wt %) 0.8 % 50°C S.W.*	*CNC-SEP-WDFs (6 wt %) 1.2 % 50°C S.W.*	*CNC-SEP-WDFs (6 wt %) 1.2 % 50°C S.W.*	*CNC-SEP-WDFs (6 wt %) 1.6 % 50°C S.W.*	*CNC-SEP-WDFs (6 wt %) 1.6 % 50°C S.W.*	*CNC-SEP-WDFs (6 wt %) 2.0 % 50°C S.W.*	*CNC-SEP-WDFs (6 wt %) 2.0 % 50°C S.W.*	*CNC-SEP-WDFs (6 wt %) 2.4 % 50°C S.W.*	*CNC-SEP-WDFs (6 wt %) 2.4 % 50°C S.W.*
2	0,999	36,3	36,2	35,7	35,9	37,8	38,1	64,3	64,6	59,6	59,5	65,6	65,5	65,1	65,6
4	13,1	41,1	3,13	48,4	3,69	53,1	4,05	71,1	5,42	81,3	6,21	74,4	5,68	93,6	7,14
6	25,2	46,7	1,85	53,5	2,12	58,3	2,31	91,7	3,64	75,5	2,99	95,2	3,77	99,8	3,95
8	37,3	50,9	1,36	59,7	1,6	63,5	1,7	96,3	2,58	84,7	2,26	102	2,72	102	2,73
10	49,4	54,7	1,11	65,7	1,33	67,9	1,37	99,2	2,01	86,8	1,76	101	2,05	97,7	1,97
12	61,6	57,8	0,939	67,7	1,1	71,3	1,16	96,4	1,57	96,5	1,57	102	1,66	103	1,68
14	73,7	60,3	0,819	71,6	0,972	74	1	102	1,39	97,5	1,32	105	1,43	108	1,47
16	85,8	62,6	0,73	73,6	0,858	76,3	0,89	105	1,22	98,9	1,15	108	1,26	110	1,28
18	97,9	64,7	0,661	75,6	0,772	78,4	0,801	106	1,09	102	1,04	108	1,11	112	1,14
20	110	66,7	0,606	77,5	0,704	80,4	0,731	109	0,991	100	0,912	111	1,01	114	1,03
22	122	68,5	0,561	79,4	0,65	81,9	0,671	111	0,908	103	0,843	113	0,926	116	0,947
24	134	70,2	0,523	81,1	0,604	83,5	0,622	111	0,826	105	0,782	116	0,866	121	0,901
26	146	71,9	0,491	82,1	0,561	85	0,581	112	0,767	105	0,718	116	0,791	124	0,846
28	158	73,4	0,463	83,6	0,527	86,3	0,545	114	0,716	106	0,671	117	0,737	124	0,781
30	171	74,9	0,439	84,7	0,497	87,6	0,514	115	0,671	107	0,63	117	0,686	127	0,742
32	183	76,4	0,418	85,9	0,47	88,7	0,486	117	0,638	108	0,593	117	0,641	125	0,686
34	195	77,8	0,399	87	0,447	89,8	0,461	120	0,614	110	0,564	111	0,572	125	0,643
36	207	79,1	0,382	88,1	0,426	90,9	0,439	120	0,582	110	0,531	112	0,539	127	0,615
38	219	80,3	0,367	89	0,407	91,9	0,419	119	0,542	112	0,514	113	0,517	128	0,585
40	231	81,5	0,353	89,8	0,389	92,9	0,402	119	0,514	112	0,484	111	0,482	126	0,547
42	243	82,6	0,34	90,8	0,373	93,8	0,386	121	0,498	112	0,46	113	0,463	128	0,524
44	255	83,7	0,328	91,4	0,358	94,4	0,37	122	0,478	114	0,445	113	0,441	130	0,51
46	267	84,7	0,317	92,3	0,345	95	0,355	123	0,46	115	0,429	113	0,424	129	0,481
48	280	85,8	0,307	93	0,333	95,8	0,343	121	0,433	115	0,413	114	0,407	133	0,477
50	292	86,8	0,298	93,6	0,321	96,7	0,332	123	0,422	114	0,39	114	0,391	129	0,441
52	304	87,8	0,289	94,3	0,311	97,5	0,321	122	0,402	115	0,38	115	0,377	129	0,425
54	316	88,8	0,281	95	0,301	97,9	0,31	124	0,391	117	0,369	115	0,364	130	0,411
56	328	89,8	0,274	95,5	0,291	98,4	0,3	123	0,376	117	0,358	116	0,352	131	0,4
58	340	90,6	0,267	96,2	0,283	98,9	0,291	125	0,367	118	0,348	116	0,341	132	0,388
60	352	91,5	0,26	96,9	0,275	99,4	0,282	125	0,355	120	0,34	117	0,332	133	0,377
62	364	92,3	0,253	97,4	0,267	100	0,275	126	0,346	119	0,326	117	0,322	132	0,362
64	376	93	0,247	98	0,26	101	0,267	127	0,337	120	0,318	118	0,313	132	0,351
66	389	93,7	0,241	98,5	0,254	101	0,26	130	0,333	120	0,309	118	0,303	133	0,342
68	401	94,4	0,236	99,2	0,248	102	0,253	129	0,321	121	0,301	118	0,294	133	0,333
70	413	95,2	0,231	99,7	0,242	102	0,247	128	0,309	121	0,294	119	0,287	133	0,323
72	425	95,8	0,226	100	0,236	102	0,241	128	0,301	122	0,287	119	0,281	134	0,314
74	437	96,5	0,221	101	0,23	103	0,235	128	0,293	122	0,278	120	0,275	134	0,307
76	449	97	0,216	101	0,226	103	0,23	128	0,285	124	0,276	120	0,267	135	0,3
78	461	98	0,212	102	0,22	104	0,226	128	0,278	124	0,268	120	0,261	134	0,291
80	473	98,3	0,208	102	0,216	104	0,22	129	0,273	123	0,259	121	0,256	135	0,286
82	485	98,8	0,204	103	0,212	105	0,216	129	0,265	123	0,254	122	0,25	135	0,278
84	498	99,4	0,2	103	0,207	105	0,212	129	0,26	124	0,248	122	0,245	137	0,274
86	510	99,9	0,196	104	0,203	106	0,207	130	0,255	124	0,243	123	0,241	136	0,267
88	522	100	0,193	104	0,199	106	0,203	130	0,248	125	0,24	123	0,235	136	0,261
90	534	101	0,189	104	0,195	106	0,199	131	0,245	123	0,23	123	0,231	136	0,255
92	546	101	0,186	105	0,192	107	0,196	130	0,239	122	0,223	124	0,226	137	0,25
94	558	102	0,183	105	0,188	107	0,193	131	0,235	122	0,219	124	0,222	137	0,246
96	570	102	0,18	105	0,185	108	0,189	131	0,229	122	0,215	124	0,218	138	0,242
98	582	103	0,177	106	0,181	108	0,186	131	0,225	123	0,212	125	0,214	139	0,238
100	594	103	0,174	106	0,178	109	0,183	132	0,221	123	0,207	125	0,211	138	0,233
102	607	104	0,171	106	0,175	109	0,18	132	0,217	123	0,203	126	0,207	138	0,227
104	619	104	0,168	107	0,173	109	0,177	132	0,214	123	0,199	127	0,205	138	0,223

106	631	105	0,166	107	0,17	110	0,174	133	0,211	123	0,195	126	0,2	138	0,219
108	643	105	0,163	107	0,167	110	0,171	133	0,207	123	0,192	127	0,198	139	0,216
110	655	105	0,161	108	0,165	110	0,168	135	0,206	123	0,188	127	0,194	139	0,212
112	667	106	0,159	108	0,162	110	0,165	134	0,2	123	0,185	128	0,191	139	0,208
114	679	106	0,156	108	0,159	110	0,163	134	0,198	124	0,182	128	0,188	139	0,204
116	691	107	0,154	109	0,157	111	0,16	134	0,194	124	0,179	128	0,185	140	0,202
118	703	107	0,152	109	0,155	111	0,157	135	0,191	124	0,177	128	0,183	140	0,199
120	716	107	0,15	109	0,153	111	0,155	135	0,188	124	0,173	129	0,18	140	0,196
122	728	108	0,148	109	0,15	111	0,153	135	0,186	124	0,171	129	0,177	141	0,194
124	740	108	0,146	110	0,148	111	0,15	135	0,182	124	0,167	130	0,175	141	0,191
126	752	108	0,144	110	0,146	112	0,149	136	0,181	123	0,164	130	0,173	141	0,188
128	764	109	0,142	110	0,144	112	0,146	135	0,177	124	0,162	130	0,17	142	0,186
130	776	109	0,14	111	0,142	112	0,144	135	0,175	124	0,16	130	0,167	143	0,184
132	788	109	0,138	111	0,14	112	0,142	136	0,172	124	0,158	130	0,165	143	0,181
134	800	109	0,137	111	0,138	113	0,141	136	0,17	125	0,156	131	0,163	143	0,179
136	812	110	0,135	111	0,136	113	0,139	137	0,168	125	0,154	132	0,162	143	0,176
138	825	110	0,133	111	0,135	113	0,137	137	0,166	126	0,152	131	0,159	143	0,174
140	837	110	0,132	111	0,133	113	0,135	137	0,164	125	0,15	131	0,157	144	0,172
142	849	111	0,13	112	0,132	113	0,133	137	0,161	125	0,148	132	0,155	144	0,17
144	861	111	0,129	112	0,13	113	0,132	137	0,16	126	0,146	132	0,153	145	0,168
146	873	111	0,127	112	0,128	114	0,13	138	0,158	126	0,144	132	0,151	145	0,166
148	885	111	0,126	112	0,127	114	0,128	138	0,155	126	0,143	132	0,149	145	0,164
150	897	112	0,124	112	0,125	114	0,127	138	0,154	126	0,14	132	0,147	145	0,162
152	909	112	0,123	112	0,124	114	0,125	138	0,152	126	0,138	133	0,146	146	0,161
154	921	112	0,122	113	0,122	114	0,124	138	0,15	126	0,137	133	0,144	146	0,158
156	934	112	0,12	113	0,121	114	0,122	138	0,148	126	0,135	133	0,142	146	0,157
158	946	112	0,119	113	0,12	114	0,121	138	0,146	126	0,133	133	0,14	146	0,155
160	958	112	0,117	113	0,118	115	0,12	139	0,145	126	0,131	134	0,14	146	0,152
162	970	113	0,116	113	0,117	115	0,118	139	0,143	126	0,13	135	0,139	146	0,151
164	982	113	0,115	114	0,116	115	0,117	139	0,142	126	0,128	135	0,137	147	0,15
166	994	113	0,114	114	0,114	115	0,116	139	0,14	126	0,126	135	0,136	147	0,148
168	1 010	113	0,113	114	0,113	115	0,114	139	0,138	126	0,125	135	0,134	146	0,145
170	1 020	114	0,112	114	0,112	115	0,113	139	0,137	126	0,123	135	0,132	147	0,144
172	1 030	114	0,11	114	0,111	115	0,112	140	0,135	126	0,122	135	0,131	147	0,143
174	1 040	114	0,109	114	0,11	116	0,111	140	0,134	126	0,121	134	0,129	148	0,142
176	1 050	114	0,108	115	0,109	116	0,11	140	0,133	126	0,12	134	0,127	148	0,14
178	1 070	114	0,107	115	0,107	116	0,108	140	0,131	126	0,118	135	0,126	147	0,138
180	1 080	115	0,106	115	0,106	116	0,107	140	0,13	126	0,117	135	0,125	147	0,136
182	1 090	115	0,105	115	0,105	116	0,106	140	0,128	126	0,116	135	0,124	147	0,134
184	1 100	115	0,104	115	0,104	116	0,105	140	0,127	127	0,115	135	0,122	147	0,133
186	1 120	115	0,103	115	0,103	116	0,104	141	0,126	127	0,114	135	0,121	147	0,132
188	1 130	115	0,102	115	0,102	116	0,103	141	0,125	127	0,112	135	0,12	147	0,13
190	1 140	116	0,101	115	0,101	116	0,102	142	0,125	127	0,111	135	0,119	147	0,129
192	1 150	116	0,1	115	0,0998	117	0,101	143	0,124	127	0,11	136	0,118	147	0,128
194	1 160	116	0,0995	115	0,0988	117	0,1	143	0,123	127	0,109	136	0,117	147	0,127
196	1 180	116	0,0986	115	0,0979	117	0,0994	142	0,121	127	0,108	137	0,116	147	0,125
198	1 190	116	0,0978	115	0,0969	117	0,0984	142	0,12	127	0,107	137	0,115	148	0,124
200	1 200	116	0,0969	115	0,096	117	0,0974	142	0,119	127	0,106	137	0,114	148	0,123

Time	Shear Rate	Shear Stress	Viscosity	Shear Stress	Viscosity	Shear Stress	Viscosity	Shear Stress	Viscosity	Shear Stress	Viscosity	Shear Stress	Viscosity	Shear Stress	Viscosity
[s]	[1/s]	[Pa]	[Pa·s]	[Pa]	[Pa·s]	[Pa]	[Pa·s]	[Pa]	[Pa·s]	[Pa]	[Pa·s]	[Pa]	[Pa·s]	[Pa]	[Pa·s]
Number of Intervals:		*CNC-SEP-WDFs (6 wt %) 0.0 % 60°C S.W.*	*CNC-SEP-WDFs (6 wt %) 0.0 % 60°C S.W.*	*CNC-SEP-WDFs (6 wt %) 0.4 % 60°C S.W.*	*CNC-SEP-WDFs (6 wt %) 0.4 % 60°C S.W.*	*CNC-SEP-WDFs (6 wt %) 0.8 % 60°C S.W.*	*CNC-SEP-WDFs (6 wt %) 0.8 % 60°C S.W.*	*CNC-SEP-WDFs (6 wt %) 1.2 % 60°C S.W.*	*CNC-SEP-WDFs (6 wt %) 1.2 % 60°C S.W.*	*CNC-SEP-WDFs (6 wt %) 1.6 % 60°C S.W.*	*CNC-SEP-WDFs (6 wt %) 1.6 % 60°C S.W.*	*CNC-SEP-WDFs (6 wt %) 2.0 % 60°C S.W.*	*CNC-SEP-WDFs (6 wt %) 2.0 % 60°C S.W.*	*CNC-SEP-WDFs (6 wt %) 2.4 % 60°C S.W.*	*CNC-SEP-WDFs (6 wt %) 2.4 % 60°C S.W.*
2	0,999	30,3	30,4	49,1	49,4	51,4	51,5	58,2	58	57,4	57,2	67,9	67,5	52,9	52,6
4	13,1	41,5	3,17	64,2	4,9	79,4	6,07	70,6	5,38	68,6	5,23	84,2	6,42	76,7	5,85
6	25,2	47,5	1,88	70,2	2,78	75,8	3	78	3,09	76,3	3,02	85,9	3,41	82	3,25
8	37,3	52	1,39	75,7	2,03	83,8	2,24	85,1	2,28	80,7	2,16	88,8	2,38	81,4	2,18
10	49,4	55,4	1,12	79,7	1,61	85,1	1,72	88,5	1,79	84,8	1,72	93,4	1,89	84,2	1,7
12	61,6	58,2	0,946	83	1,35	93,3	1,52	90,4	1,47	88,8	1,44	96,1	1,56	86,7	1,41
14	73,7	60,6	0,823	85,8	1,16	93,7	1,27	94,9	1,29	92,3	1,25	101	1,37	92,8	1,26
16	85,8	62,9	0,733	88,2	1,03	94,2	1,1	96,9	1,13	94,6	1,1	104	1,21	98,1	1,14
18	97,9	64,9	0,663	90,2	0,921	97,3	0,995	99,7	1,02	97	0,991	106	1,09	104	1,06
20	110	66,7	0,606	91,8	0,835	96,2	0,875	103	0,937	99,1	0,901	108	0,983	108	0,983
22	122	68,4	0,56	93,5	0,766	97,7	0,801	106	0,866	101	0,824	110	0,9	113	0,923
24	134	70	0,521	94,9	0,707	100	0,747	107	0,798	102	0,76	111	0,825	115	0,86
26	146	71,5	0,489	96,2	0,658	101	0,692	108	0,74	104	0,707	112	0,766	118	0,808
28	158	72,9	0,46	97,6	0,616	102	0,645	110	0,696	105	0,662	114	0,718	120	0,759
30	171	74,2	0,435	98,8	0,579	102	0,6	112	0,654	107	0,626	115	0,672	122	0,715
32	183	75,5	0,413	100	0,548	104	0,568	112	0,613	108	0,589	115	0,629	123	0,676
34	195	76,7	0,394	101	0,52	105	0,541	113	0,579	109	0,56	117	0,599	127	0,65
36	207	77,8	0,376	102	0,494	105	0,505	115	0,554	109	0,529	117	0,567	129	0,621
38	219	79	0,361	103	0,472	107	0,49	115	0,525	111	0,505	118	0,54	130	0,592
40	231	80,1	0,346	104	0,451	107	0,465	116	0,503	112	0,485	119	0,514	130	0,564
42	243	81,1	0,333	105	0,432	109	0,448	117	0,481	113	0,463	119	0,489	131	0,54
44	255	82	0,321	106	0,416	111	0,434	118	0,461	113	0,442	120	0,469	133	0,521
46	267	83	0,31	107	0,4	112	0,42	119	0,445	114	0,424	120	0,45	134	0,502
48	280	83,9	0,3	108	0,386	112	0,4	120	0,429	114	0,408	121	0,433	135	0,482
50	292	84,8	0,291	109	0,373	111	0,382	121	0,415	115	0,393	122	0,418	136	0,467
52	304	85,7	0,282	110	0,361	112	0,37	122	0,4	116	0,381	123	0,404	139	0,458
54	316	86,5	0,274	110	0,349	113	0,359	122	0,386	116	0,366	123	0,39	139	0,439
56	328	87,3	0,266	111	0,339	114	0,347	122	0,373	116	0,354	124	0,378	140	0,428
58	340	88,3	0,259	112	0,329	116	0,34	123	0,361	117	0,343	125	0,369	141	0,414
60	352	89	0,253	112	0,319	115	0,327	123	0,351	117	0,333	125	0,355	142	0,404
62	364	89,6	0,246	113	0,31	114	0,312	124	0,34	118	0,323	126	0,345	143	0,391
64	376	90,4	0,24	114	0,302	114	0,303	125	0,332	118	0,315	126	0,335	143	0,381
66	389	91	0,234	114	0,294	118	0,303	125	0,323	119	0,306	127	0,326	145	0,374
68	401	91,6	0,229	115	0,286	117	0,293	126	0,314	119	0,298	127	0,318	146	0,365
70	413	92,2	0,223	115	0,279	119	0,288	126	0,306	120	0,29	127	0,308	146	0,354
72	425	92,8	0,218	116	0,272	118	0,277	127	0,299	120	0,282	128	0,301	146	0,343
74	437	93,3	0,213	116	0,265	119	0,272	128	0,292	121	0,277	128	0,292	147	0,336
76	449	94	0,209	116	0,259	120	0,267	128	0,285	121	0,269	128	0,285	147	0,326
78	461	94,8	0,206	117	0,253	117	0,253	128	0,279	122	0,263	129	0,279	149	0,322
80	473	95,1	0,201	117	0,247	121	0,255	129	0,273	122	0,257	129	0,272	151	0,319
82	485	95,7	0,197	117	0,241	120	0,248	130	0,268	122	0,252	129	0,266	151	0,312
84	498	96,1	0,193	118	0,236	120	0,24	130	0,262	123	0,246	130	0,261	155	0,311
86	510	96,6	0,19	118	0,231	123	0,242	131	0,257	123	0,241	130	0,255	154	0,302
88	522	97,2	0,186	118	0,227	124	0,237	131	0,252	122	0,235	130	0,249	150	0,288
90	534	97,7	0,183	119	0,222	124	0,231	132	0,247	123	0,23	130	0,244	150	0,281
92	546	98,1	0,18	119	0,218	117	0,214	132	0,242	123	0,226	131	0,239	150	0,275
94	558	98,5	0,177	119	0,213	121	0,216	133	0,238	124	0,222	132	0,236	151	0,27
96	570	99	0,174	119	0,209	118	0,206	134	0,234	124	0,218	132	0,231	152	0,267
98	582	99,5	0,171	120	0,206	120	0,206	134	0,23	124	0,213	132	0,227	153	0,262
100	594	99,8	0,168	120	0,202	122	0,206	135	0,227	125	0,21	133	0,223	152	0,255
102	607	100	0,165	121	0,199	121	0,199	135	0,223	125	0,206	133	0,219	152	0,25
104	619	101	0,163	121	0,195	123	0,199	136	0,219	126	0,203	134	0,216	153	0,247

106	631	101	0,16	121	0,192	125	0,198	136	0,216	125	0,199	134	0,212	152	0,241
108	643	101	0,158	121	0,189	124	0,192	137	0,213	126	0,196	134	0,209	153	0,237
110	655	102	0,156	122	0,186	123	0,187	137	0,21	126	0,193	135	0,206	153	0,233
112	667	102	0,153	122	0,183	123	0,184	138	0,207	127	0,19	134	0,201	154	0,23
114	679	102	0,151	122	0,18	124	0,183	139	0,204	127	0,187	134	0,197	154	0,226
116	691	103	0,149	123	0,177	125	0,18	139	0,2	127	0,184	135	0,195	154	0,223
118	703	103	0,147	123	0,174	125	0,177	139	0,198	127	0,181	135	0,192	154	0,219
120	716	103	0,144	123	0,172	125	0,174	140	0,195	127	0,178	136	0,191	154	0,216
122	728	104	0,143	123	0,17	122	0,168	140	0,192	127	0,175	136	0,187	155	0,213
124	740	104	0,141	124	0,167	122	0,165	140	0,189	127	0,172	136	0,184	156	0,21
126	752	104	0,139	124	0,165	122	0,163	140	0,186	128	0,17	136	0,181	156	0,208
128	764	105	0,137	124	0,162	122	0,16	141	0,184	128	0,167	137	0,179	156	0,204
130	776	105	0,135	124	0,16	123	0,159	141	0,182	128	0,165	137	0,176	156	0,201
132	788	105	0,134	125	0,158	123	0,156	141	0,179	128	0,163	137	0,174	157	0,199
134	800	106	0,132	125	0,156	122	0,153	142	0,177	129	0,161	137	0,172	157	0,196
136	812	106	0,13	125	0,154	124	0,152	142	0,175	129	0,159	138	0,17	157	0,194
138	825	106	0,129	125	0,152	124	0,15	143	0,173	129	0,157	138	0,167	158	0,191
140	837	106	0,127	125	0,15	124	0,148	143	0,171	130	0,155	138	0,166	158	0,188
142	849	107	0,126	126	0,148	124	0,146	143	0,168	130	0,153	138	0,163	158	0,186
144	861	107	0,124	126	0,146	124	0,144	143	0,166	130	0,151	139	0,161	157	0,182
146	873	107	0,123	126	0,144	123	0,141	143	0,164	130	0,149	139	0,159	157	0,18
148	885	108	0,121	126	0,143	123	0,139	144	0,162	130	0,147	139	0,157	157	0,178
150	897	108	0,12	126	0,141	123	0,137	144	0,16	131	0,145	139	0,155	158	0,176
152	909	108	0,119	126	0,139	122	0,134	144	0,158	131	0,144	140	0,154	158	0,173
154	921	108	0,117	127	0,137	123	0,133	144	0,157	131	0,142	141	0,153	158	0,171
156	934	108	0,116	127	0,136	123	0,132	145	0,155	131	0,14	140	0,15	158	0,169
158	946	109	0,115	127	0,134	123	0,13	145	0,153	131	0,139	140	0,148	158	0,167
160	958	109	0,113	127	0,132	123	0,129	145	0,151	131	0,137	140	0,147	158	0,165
162	970	109	0,112	127	0,131	124	0,128	145	0,149	131	0,135	140	0,144	158	0,163
164	982	109	0,111	127	0,13	124	0,127	145	0,148	131	0,134	139	0,142	159	0,162
166	994	109	0,11	128	0,128	125	0,126	145	0,146	132	0,132	139	0,14	159	0,16
168	1 010	109	0,109	128	0,127	124	0,123	145	0,145	131	0,13	139	0,138	159	0,158
170	1 020	110	0,108	128	0,126	123	0,121	146	0,143	132	0,129	140	0,137	159	0,156
172	1 030	110	0,107	128	0,124	123	0,12	146	0,142	131	0,128	140	0,136	159	0,154
174	1 040	110	0,106	128	0,123	123	0,118	146	0,14	131	0,126	140	0,135	159	0,153
176	1 050	110	0,105	128	0,122	123	0,117	146	0,139	132	0,125	141	0,133	159	0,151
178	1 070	111	0,104	129	0,12	123	0,116	146	0,137	132	0,124	140	0,131	159	0,149
180	1 080	111	0,103	129	0,119	123	0,114	146	0,136	132	0,123	140	0,13	160	0,148
182	1 090	111	0,102	129	0,118	123	0,113	147	0,134	133	0,122	140	0,129	159	0,146
184	1 100	111	0,101	129	0,117	124	0,113	146	0,133	133	0,121	140	0,127	160	0,145
186	1 120	111	0,0999	129	0,116	124	0,111	147	0,132	133	0,119	140	0,126	160	0,144
188	1 130	112	0,0989	129	0,115	124	0,11	147	0,13	133	0,118	141	0,125	160	0,142
190	1 140	111	0,0978	129	0,114	124	0,109	147	0,129	133	0,117	140	0,123	160	0,141
192	1 150	112	0,0971	130	0,112	124	0,108	147	0,128	134	0,116	141	0,122	161	0,14
194	1 160	112	0,0961	130	0,111	124	0,107	147	0,127	134	0,115	141	0,121	161	0,138
196	1 180	112	0,0953	130	0,11	124	0,106	148	0,126	134	0,114	141	0,12	161	0,137
198	1 190	112	0,0944	130	0,109	124	0,105	148	0,125	134	0,113	141	0,119	161	0,135
200	1 200	112	0,0936	130	0,108	124	0,104	148	0,123	134	0,112	140	0,117	161	0,134

Time	Shear Rate	Shear Stress	Viscosity	Shear Stress	Viscosity	Shear Stress	Viscosity	Shear Stress	Viscosity	Shear Stress	Viscosity	Shear Stress	Viscosity	Shear Stress	Viscosity
[s]	[1/s]	[Pa]	[Pa·s]	[Pa]	[Pa·s]	[Pa]	[Pa·s]	[Pa]	[Pa·s]	[Pa]	[Pa·s]	[Pa]	[Pa·s]	[Pa]	[Pa·s]
Number of Intervals:		CNC-SEP-WDFs (6 wt %) 0.0 % 70°C S.W.	CNC-SEP-WDFs (6 wt %) 0.0 % 70°C S.W.	CNC-SEP-WDFs (6 wt %) 0.4 % 70°C S.W.	CNC-SEP-WDFs (6 wt %) 0.4 .2 % 70°C S.W.	CNC-SEP-WDFs (6 wt %) 0.8 % 70°C S.W.	CNC-SEP-WDFs (6 wt %) 0.8 % 70°C S.W.	CNC-SEP-WDFs (6 wt %) 1.2 % 70°C S.W.	CNC-SEP-WDFs (6 wt %) 1.2 % 70°C S.W.	CNC-SEP-WDFs (6 wt %) 1.6 % 70°C S.W.	CNC-SEP-WDFs (6 wt %) 1.6 % 70°C S.W.	CNC-SEP-WDFs (6 wt %) 2.0 % 70°C S.W.	CNC-SEP-WDFs (6 wt %) 2.0 % 70°C S.W.	CNC-SEP-WDFs (6 wt %) 2.4 % 70°C S.W.	CNC-SEP-WDFs (6 wt %) 0.0 % 70°C S.W.
2	0,999	30,3	30,2	48,8	49,1	69	68,8	62,2	62,6	56,6	56,8	69,1	68,9	86,4	87
4	13,1	39,4	3	63,3	4,83	81,2	6,18	77,9	5,94	81	6,18	74,4	5,67	101	7,71
6	25,2	44,8	1,78	70,4	2,79	77,1	3,06	82,2	3,26	96,6	3,83	87,8	3,48	97	3,84
8	37,3	49,2	1,32	72,7	1,95	82,8	2,22	86,2	2,31	97,5	2,61	90,2	2,42	91,6	2,45
10	49,4	52,9	1,07	76,2	1,54	85,9	1,74	89,8	1,82	102	2,06	93,6	1,89	89,3	1,8
12	61,6	59,1	0,96	80,8	1,31	89,1	1,45	92,8	1,51	104	1,7	95,4	1,55	90,4	1,47
14	73,7	61,8	0,838	81,8	1,11	88	1,19	96,7	1,31	109	1,48	101	1,37	93	1,26
16	85,8	64	0,746	84,3	0,983	94,3	1,1	98,1	1,14	110	1,28	105	1,23	97,3	1,13
18	97,9	66,2	0,676	85,7	0,875	93,1	0,951	100	1,02	112	1,16	108	1,1	103	1,05
20	110	68	0,618	87,7	0,797	96,3	0,875	103	0,933	113	1,1	112	1,02	109	0,987
22	122	69,5	0,57	88,4	0,724	95,8	0,785	105	0,858	113	0,929	114	0,932	115	0,938
24	134	71	0,529	89,8	0,669	96,6	0,72	106	0,786	114	0,853	115	0,858	119	0,89
26	146	72,4	0,494	91,2	0,623	97,3	0,665	107	0,733	116	0,791	117	0,798	124	0,844
28	158	73,6	0,465	92,8	0,586	98,9	0,624	108	0,682	117	0,737	117	0,738	127	0,802
30	171	74,8	0,439	93,3	0,547	101	0,59	110	0,643	118	0,691	119	0,695	130	0,764
32	183	76	0,416	94,8	0,519	103	0,564	111	0,608	119	0,653	121	0,66	132	0,725
34	195	77,1	0,396	95,7	0,491	103	0,529	112	0,574	121	0,619	122	0,628	135	0,691
36	207	78	0,377	96,5	0,467	104	0,502	113	0,546	121	0,586	124	0,599	136	0,656
38	219	79	0,361	97,5	0,445	105	0,479	114	0,519	122	0,559	124	0,568	138	0,628
40	231	79,9	0,346	98,5	0,426	105	0,454	114	0,493	124	0,536	126	0,544	139	0,603
42	243	80,8	0,332	99,1	0,407	106	0,434	115	0,472	125	0,513	127	0,52	142	0,583
44	255	81,7	0,32	100	0,393	107	0,419	115	0,452	125	0,489	127	0,498	144	0,565
46	267	82,6	0,309	101	0,378	108	0,402	116	0,434	126	0,471	128	0,48	146	0,544
48	280	83,4	0,298	102	0,364	109	0,389	117	0,418	127	0,455	130	0,465	146	0,522
50	292	84,1	0,288	102	0,351	109	0,375	118	0,404	128	0,438	131	0,448	146	0,501
52	304	84,9	0,279	103	0,339	109	0,36	119	0,391	129	0,425	131	0,432	148	0,486
54	316	85,6	0,271	104	0,328	110	0,349	119	0,378	130	0,412	132	0,417	152	0,481
56	328	86,4	0,263	105	0,32	111	0,338	120	0,366	132	0,401	135	0,412	154	0,468
58	340	87,1	0,256	106	0,311	111	0,327	121	0,355	132	0,387	133	0,392	154	0,454
60	352	87,7	0,249	106	0,3	112	0,317	121	0,344	132	0,374	133	0,377	153	0,435
62	364	88,3	0,242	107	0,292	112	0,308	122	0,334	132	0,362	132	0,363	153	0,419
64	376	88,9	0,236	107	0,285	113	0,301	122	0,325	132	0,351	134	0,355	153	0,408
66	389	89,5	0,23	108	0,278	114	0,292	123	0,317	133	0,343	135	0,347	154	0,397
68	401	90	0,225	108	0,271	114	0,284	124	0,309	133	0,333	135	0,337	154	0,385
70	413	90,6	0,22	109	0,265	115	0,278	124	0,301	134	0,325	135	0,328	155	0,376
72	425	91,2	0,215	110	0,26	115	0,27	125	0,294	134	0,316	134	0,316	156	0,367
74	437	91,7	0,21	111	0,254	115	0,264	125	0,287	135	0,308	135	0,309	156	0,358
76	449	92,2	0,205	111	0,248	116	0,258	126	0,28	135	0,3	136	0,302	157	0,35
78	461	92,5	0,201	112	0,242	117	0,253	126	0,273	135	0,293	136	0,294	157	0,34
80	473	93,3	0,197	112	0,237	117	0,248	127	0,269	136	0,287	137	0,289	159	0,335
82	485	93,8	0,193	113	0,232	118	0,242	128	0,263	137	0,282	137	0,282	160	0,329
84	498	94,3	0,19	113	0,226	118	0,237	128	0,257	137	0,276	139	0,279	159	0,321
86	510	94,8	0,186	113	0,222	117	0,23	129	0,253	138	0,27	139	0,272	160	0,313
88	522	95,3	0,183	114	0,218	118	0,226	129	0,247	138	0,264	138	0,265	161	0,308
90	534	95,7	0,179	114	0,213	118	0,221	129	0,242	138	0,259	139	0,26	160	0,3
92	546	96,2	0,176	115	0,21	119	0,217	130	0,238	139	0,254	139	0,255	161	0,294
94	558	96,5	0,173	115	0,206	119	0,213	131	0,234	139	0,249	140	0,25	161	0,289
96	570	97,1	0,17	116	0,203	120	0,21	131	0,23	140	0,246	140	0,246	162	0,284
98	582	97,5	0,167	116	0,199	120	0,206	132	0,226	141	0,241	141	0,242	162	0,279
100	594	97,8	0,164	116	0,195	120	0,203	132	0,223	141	0,238	142	0,238	163	0,274
102	607	98,2	0,162	117	0,192	121	0,2	133	0,219	141	0,233	142	0,233	162	0,268

104	619	98,5	0,159	117	0,189	121	0,196	133	0,216	142	0,229	142	0,229	163	0,263
106	631	98,8	0,157	117	0,186	122	0,193	134	0,212	143	0,226	143	0,226	163	0,259
108	643	99,3	0,155	118	0,183	122	0,189	135	0,209	143	0,223	143	0,223	164	0,255
110	655	99,7	0,152	118	0,181	122	0,187	135	0,206	144	0,22	144	0,219	165	0,253
112	667	100	0,15	119	0,178	123	0,184	135	0,203	144	0,216	144	0,216	165	0,247
114	679	100	0,147	119	0,175	123	0,181	136	0,2	144	0,213	145	0,213	166	0,244
116	691	101	0,145	119	0,172	124	0,179	136	0,197	145	0,21	144	0,209	166	0,24
118	703	101	0,143	119	0,17	124	0,176	137	0,194	145	0,207	144	0,205	166	0,236
120	716	101	0,141	120	0,168	124	0,173	137	0,192	147	0,205	144	0,202	166	0,232
122	728	102	0,14	120	0,165	124	0,17	138	0,189	146	0,201	145	0,2	167	0,229
124	740	102	0,138	121	0,163	124	0,167	138	0,186	146	0,198	145	0,196	167	0,225
126	752	102	0,136	121	0,16	124	0,165	139	0,184	146	0,194	146	0,195	168	0,224
128	764	102	0,134	121	0,159	123	0,162	139	0,181	147	0,192	147	0,192	169	0,221
130	776	103	0,132	121	0,156	124	0,159	139	0,179	147	0,19	147	0,19	168	0,216
132	788	103	0,131	122	0,155	124	0,157	140	0,177	148	0,187	148	0,187	168	0,213
134	800	103	0,129	122	0,152	124	0,155	140	0,175	147	0,184	147	0,183	168	0,21
136	812	103	0,127	122	0,15	125	0,154	140	0,173	147	0,181	147	0,181	168	0,207
138	825	104	0,126	123	0,149	125	0,152	141	0,171	148	0,18	147	0,178	169	0,205
140	837	104	0,124	123	0,147	125	0,149	141	0,169	149	0,178	147	0,176	169	0,202
142	849	104	0,123	123	0,145	125	0,147	142	0,167	150	0,176	147	0,173	170	0,2
144	861	104	0,121	123	0,143	125	0,145	142	0,165	150	0,174	149	0,173	171	0,198
146	873	105	0,12	124	0,142	125	0,143	142	0,163	149	0,171	147	0,169	171	0,195
148	885	105	0,119	124	0,14	125	0,142	142	0,161	149	0,169	148	0,168	171	0,193
150	897	105	0,117	125	0,139	126	0,14	143	0,159	150	0,167	148	0,164	171	0,19
152	909	105	0,116	125	0,137	126	0,139	143	0,157	149	0,164	148	0,163	172	0,189
154	921	106	0,115	125	0,136	126	0,137	143	0,155	150	0,162	148	0,161	172	0,186
156	934	106	0,114	125	0,134	126	0,135	143	0,153	150	0,161	148	0,159	171	0,184
158	946	106	0,112	125	0,133	126	0,134	143	0,151	150	0,159	148	0,157	171	0,181
160	958	106	0,111	126	0,131	126	0,132	143	0,149	151	0,158	150	0,156	172	0,18
162	970	107	0,11	126	0,13	126	0,13	143	0,148	151	0,156	149	0,154	172	0,177
164	982	107	0,109	126	0,129	127	0,129	143	0,146	152	0,154	149	0,152	172	0,176
166	994	107	0,108	126	0,127	127	0,127	144	0,144	151	0,152	149	0,15	172	0,173
168	1 010	107	0,107	127	0,126	127	0,126	144	0,143	151	0,15	149	0,148	173	0,172
170	1 020	108	0,106	127	0,125	127	0,125	144	0,142	151	0,149	150	0,147	173	0,17
172	1 030	108	0,104	127	0,123	127	0,123	144	0,14	151	0,147	150	0,145	173	0,168
174	1 040	108	0,103	127	0,122	127	0,122	145	0,139	151	0,145	150	0,144	173	0,166
176	1 050	108	0,102	127	0,121	127	0,121	145	0,137	152	0,144	150	0,142	173	0,164
178	1 070	108	0,102	128	0,12	128	0,12	145	0,136	152	0,142	150	0,141	173	0,163
180	1 080	109	0,101	128	0,118	128	0,118	145	0,135	152	0,141	150	0,139	173	0,161
182	1 090	109	0,0996	128	0,117	128	0,117	146	0,134	152	0,139	152	0,139	174	0,16
184	1 100	109	0,0988	128	0,116	128	0,116	146	0,132	152	0,138	151	0,137	174	0,157
186	1 120	109	0,0979	128	0,115	128	0,115	146	0,131	152	0,136	151	0,136	174	0,156
188	1 130	109	0,0969	129	0,114	128	0,114	146	0,13	153	0,135	151	0,134	174	0,155
190	1 140	110	0,0962	129	0,113	128	0,113	146	0,128	153	0,134	151	0,133	174	0,153
192	1 150	110	0,0953	129	0,112	128	0,112	146	0,127	153	0,133	151	0,131	174	0,151
194	1 160	110	0,0945	129	0,111	128	0,11	146	0,126	153	0,131	152	0,13	175	0,15
196	1 180	110	0,0936	129	0,11	129	0,109	146	0,124	153	0,13	152	0,129	175	0,149
198	1 190	110	0,0929	129	0,109	129	0,108	146	0,123	153	0,129	152	0,128	175	0,147
200	1 200	111	0,0922	129	0,108	129	0,107	147	0,122	153	0,127	152	0,127	175	0,145

Time	Shear Rate	Shear Stress	Viscosity	Shear Stress	Viscosity	Shear Stress	Viscosity	Shear Stress	Viscosity	Shear Stress	Viscosity	Shear Stress	Viscosity	Shear Stress	Viscosity
[s]	[1/s]	[Pa]	[Pa·s]	[Pa]	[Pa·s]	[Pa]	[Pa·s]	[Pa]	[Pa·s]	[Pa]	[Pa·s]	[Pa]	[Pa·s]	[Pa]	[Pa·s]
Number of Intervals:		*CNC-SEP-WDFs (6 wt %) 0.0 % 80°C S.W.*	*CNC-SEP-WDFs (6 wt %) 0.0 % 80°C S.W.*	*CNC-SEP-WDFs (6 wt %) 0.4 % 80°C S.W.*	*CNC-SEP-WDFs (6 wt %) 0.4 % 80°C S.W.*	*CNC-SEP-WDFs (6 wt %) 0.8 % 80°C S.W.*	*CNC-SEP-WDFs (6 wt %) 0.8 % 80°C S.W.*	*CNC-SEP-WDFs (6 wt %) 1.2 % 80°C S.W.*	*CNC-SEP-WDFs (6 wt %) 1.2 % 80°C S.W.*	*CNC-SEP-WDFs (6 wt %) 1.6 % 80°C S.W.*	*CNC-SEP-WDFs (6 wt %) 1.6 % 80°C S.W.*	*CNC-SEP-WDFs (6 wt %) 2.0 % 80°C S.W.*	*CNC-SEP-WDFs (6 wt %) 2.0 % 80°C S.W.*	*CNC-SEP-WDFs (6 wt %) 2.4 % 80°C S.W.*	*CNC-SEP-WDFs (6 wt %) 2.4 % 80°C S.W.*
2	0,999	42	41,8	50,4	50,8	49,6	49,9	66,5	66,2	75,9	75,8	59,3	59,1	69,7	69,6
4	13,1	49,4	3,77	71,7	5,48	64,4	4,91	76,9	5,86	92,7	7,06	71,1	5,42	81	6,18
6	25,2	55,7	2,21	74,1	2,93	67,3	2,67	84,3	3,34	96,5	3,82	78,5	3,11	91,6	3,63
8	37,3	60,4	1,62	80,1	2,14	71,3	1,91	89,2	2,39	100	2,68	80,7	2,16	103	2,77
10	49,4	64,5	1,3	80,7	1,63	77,3	1,56	94	1,9	109	2,2	83,2	1,68	99	2
12	61,6	67,7	1,1	85,1	1,38	78,3	1,27	97	1,58	110	1,78	86,1	1,4	93,4	1,52
14	73,7	70,3	0,954	88,9	1,21	83,1	1,13	104	1,41	115	1,55	91,9	1,25	96,4	1,31
16	85,8	72,4	0,844	83,2	0,97	83,1	0,969	109	1,27	120	1,4	97,7	1,14	97,1	1,13
18	97,9	74,2	0,758	87,2	0,891	84,5	0,863	110	1,12	125	1,28	103	1,05	99,2	1,01
20	110	75,9	0,69	85,4	0,776	87,2	0,793	113	1,02	127	1,15	106	0,96	106	0,96
22	122	77,5	0,634	86,6	0,709	89,7	0,735	117	0,955	127	1,04	109	0,891	111	0,905
24	134	78,8	0,587	89,6	0,667	90,9	0,677	118	0,882	129	0,963	111	0,826	119	0,886
26	146	80,2	0,548	91,3	0,624	92,9	0,635	120	0,821	130	0,888	112	0,768	123	0,839
28	158	81,5	0,514	92,3	0,582	93,8	0,592	121	0,764	132	0,83	114	0,721	130	0,823
30	171	82,7	0,485	93,2	0,546	94,7	0,555	121	0,712	133	0,779	115	0,677	134	0,787
32	183	83,9	0,459	94,5	0,517	95	0,52	124	0,679	134	0,735	118	0,644	137	0,747
34	195	85	0,436	95,5	0,49	96	0,493	126	0,645	135	0,695	119	0,611	141	0,722
36	207	86,1	0,416	96,3	0,466	97,6	0,472	127	0,612	137	0,661	120	0,581	144	0,698
38	219	87	0,397	97,4	0,445	99,2	0,453	128	0,583	137	0,628	121	0,553	150	0,685
40	231	88	0,381	98,2	0,425	99,7	0,431	128	0,554	139	0,6	122	0,528	152	0,658
42	243	89	0,366	98,7	0,406	99,7	0,41	129	0,529	140	0,576	123	0,505	153	0,631
44	255	89,9	0,352	99,7	0,39	100	0,393	129	0,504	141	0,552	124	0,485	155	0,608
46	267	90,8	0,34	101	0,376	101	0,377	129	0,483	141	0,528	125	0,466	157	0,587
48	280	91,7	0,328	101	0,361	101	0,363	129	0,462	142	0,508	125	0,449	159	0,567
50	292	92,6	0,318	102	0,349	102	0,351	130	0,447	142	0,487	126	0,432	161	0,551
52	304	93,5	0,308	102	0,337	103	0,339	132	0,435	143	0,47	127	0,418	162	0,533
54	316	94,4	0,299	103	0,328	103	0,327	132	0,419	144	0,455	127	0,401	164	0,519
56	328	95,3	0,291	104	0,317	104	0,318	132	0,403	144	0,44	128	0,392	165	0,502
58	340	96,1	0,283	105	0,308	105	0,308	132	0,389	145	0,427	129	0,381	165	0,484
60	352	96,9	0,275	105	0,299	105	0,299	132	0,376	145	0,412	130	0,369	167	0,475
62	364	97,6	0,268	105	0,289	106	0,29	132	0,363	146	0,401	131	0,359	168	0,461
64	376	98,3	0,261	106	0,282	106	0,283	133	0,354	147	0,39	132	0,35	169	0,45
66	389	99,1	0,255	107	0,275	107	0,275	133	0,342	148	0,38	131	0,337	171	0,44
68	401	99,7	0,249	107	0,268	108	0,269	133	0,331	148	0,37	132	0,329	173	0,431
70	413	100	0,243	108	0,261	108	0,263	133	0,323	149	0,361	130	0,314	172	0,417
72	425	101	0,237	109	0,256	109	0,256	133	0,314	149	0,351	131	0,308	173	0,406
74	437	102	0,233	109	0,249	109	0,25	134	0,306	150	0,342	132	0,301	173	0,397
76	449	102	0,228	110	0,244	109	0,244	134	0,299	150	0,335	134	0,297	173	0,386
78	461	103	0,223	110	0,239	110	0,239	134	0,29	150	0,326	134	0,291	174	0,378
80	473	104	0,219	111	0,234	111	0,234	135	0,285	151	0,32	136	0,287	175	0,37
82	485	104	0,214	112	0,23	111	0,228	136	0,28	152	0,314	136	0,281	176	0,362
84	498	105	0,211	112	0,225	111	0,224	136	0,273	153	0,308	134	0,269	176	0,354
86	510	105	0,207	112	0,22	112	0,22	137	0,268	153	0,301	133	0,261	177	0,347
88	522	106	0,203	113	0,216	112	0,215	137	0,263	154	0,295	135	0,259	178	0,341
90	534	106	0,199	113	0,212	113	0,212	139	0,26	154	0,288	136	0,254	178	0,334
92	546	107	0,196	114	0,208	113	0,208	139	0,255	155	0,283	137	0,251	179	0,327
94	558	107	0,193	114	0,204	114	0,204	140	0,251	155	0,278	138	0,247	179	0,321
96	570	108	0,189	114	0,2	114	0,201	141	0,247	156	0,273	138	0,242	180	0,316
98	582	108	0,186	115	0,197	115	0,197	141	0,242	156	0,268	138	0,237	181	0,311
100	594	109	0,183	115	0,194	116	0,195	141	0,237	156	0,263	138	0,232	181	0,305
102	607	109	0,18	116	0,191	116	0,191	142	0,234	157	0,259	139	0,23	183	0,301
104	619	110	0,177	116	0,187	117	0,188	142	0,23	158	0,255	137	0,221	184	0,297

106	631	110	0,174	116	0,184	117	0,186	142	0,226	158	0,251	137	0,218	183	0,291
108	643	110	0,172	116	0,181	118	0,183	144	0,223	159	0,247	137	0,214	183	0,284
110	655	111	0,169	117	0,179	118	0,18	143	0,219	160	0,244	139	0,212	182	0,278
112	667	111	0,167	117	0,176	118	0,177	144	0,215	160	0,24	138	0,207	183	0,274
114	679	112	0,164	118	0,173	119	0,175	145	0,213	161	0,237	141	0,207	184	0,271
116	691	112	0,162	118	0,171	119	0,173	144	0,209	161	0,233	141	0,204	186	0,269
118	703	112	0,159	119	0,169	120	0,17	145	0,206	162	0,23	141	0,2	186	0,265
120	716	113	0,157	119	0,166	120	0,168	145	0,203	162	0,226	142	0,198	187	0,262
122	728	113	0,155	119	0,164	121	0,166	146	0,2	162	0,222	141	0,194	187	0,258
124	740	113	0,153	120	0,162	121	0,163	147	0,198	163	0,22	142	0,192	187	0,253
126	752	114	0,151	120	0,159	121	0,16	146	0,195	163	0,217	140	0,187	188	0,25
128	764	114	0,149	120	0,157	121	0,158	146	0,192	163	0,213	140	0,184	189	0,247
130	776	114	0,147	120	0,155	121	0,156	147	0,19	163	0,21	141	0,182	189	0,243
132	788	115	0,145	121	0,153	122	0,154	147	0,187	163	0,207	142	0,18	189	0,24
134	800	115	0,144	121	0,151	122	0,153	148	0,185	163	0,204	141	0,176	189	0,237
136	812	115	0,142	121	0,149	122	0,15	148	0,182	164	0,201	141	0,174	190	0,234
138	825	116	0,14	122	0,148	122	0,148	148	0,18	164	0,199	141	0,171	190	0,231
140	837	116	0,138	122	0,146	123	0,147	148	0,177	163	0,195	140	0,168	190	0,227
142	849	116	0,137	122	0,144	123	0,145	149	0,176	164	0,193	141	0,167	191	0,225
144	861	116	0,135	123	0,143	123	0,143	149	0,173	164	0,191	143	0,166	191	0,222
146	873	117	0,134	123	0,141	124	0,142	149	0,17	165	0,189	143	0,164	191	0,219
148	885	117	0,132	124	0,14	124	0,14	149	0,169	164	0,186	143	0,162	191	0,215
150	897	117	0,131	124	0,138	124	0,138	150	0,167	165	0,183	143	0,16	191	0,213
152	909	118	0,129	124	0,136	124	0,137	150	0,165	165	0,181	144	0,158	192	0,211
154	921	118	0,128	124	0,135	125	0,135	150	0,163	166	0,18	144	0,157	191	0,208
156	934	118	0,127	125	0,134	125	0,134	151	0,161	166	0,178	144	0,154	191	0,205
158	946	118	0,125	125	0,132	125	0,132	151	0,16	166	0,176	144	0,152	192	0,203
160	958	119	0,124	125	0,131	125	0,131	151	0,158	167	0,174	144	0,151	191	0,2
162	970	119	0,123	125	0,129	126	0,13	151	0,156	167	0,172	145	0,149	192	0,198
164	982	119	0,121	126	0,128	126	0,128	151	0,154	167	0,17	145	0,148	193	0,196
166	994	119	0,12	126	0,127	126	0,127	151	0,152	167	0,168	145	0,146	193	0,194
168	1 010	120	0,119	126	0,125	126	0,126	151	0,15	167	0,166	145	0,144	193	0,192
170	1 020	120	0,118	126	0,124	127	0,124	151	0,149	167	0,164	145	0,142	192	0,189
172	1 030	120	0,117	127	0,123	127	0,123	152	0,148	167	0,162	146	0,141	194	0,188
174	1 040	121	0,116	127	0,122	127	0,122	153	0,147	168	0,161	146	0,14	194	0,186
176	1 050	121	0,114	127	0,121	127	0,121	154	0,146	168	0,159	147	0,139	194	0,184
178	1 070	121	0,114	128	0,12	128	0,12	153	0,144	167	0,157	145	0,136	195	0,183
180	1 080	121	0,112	128	0,119	128	0,119	153	0,142	167	0,155	146	0,135	196	0,181
182	1 090	121	0,111	128	0,118	129	0,118	154	0,141	168	0,154	146	0,134	196	0,18
184	1 100	122	0,11	129	0,117	128	0,116	153	0,138	168	0,152	147	0,133	195	0,177
186	1 120	122	0,109	129	0,116	129	0,115	154	0,138	168	0,15	147	0,132	196	0,176
188	1 130	122	0,109	129	0,115	129	0,114	155	0,137	168	0,149	146	0,13	197	0,174
190	1 140	123	0,108	130	0,114	129	0,113	154	0,135	168	0,147	146	0,128	198	0,174
192	1 150	123	0,107	130	0,113	129	0,112	155	0,135	169	0,147	147	0,127	197	0,171
194	1 160	123	0,106	130	0,112	130	0,112	155	0,133	170	0,146	146	0,126	198	0,17
196	1 180	123	0,105	130	0,111	130	0,111	156	0,133	169	0,144	147	0,125	199	0,169
198	1 190	124	0,104	131	0,11	130	0,11	157	0,132	169	0,143	147	0,124	199	0,168
200	1 200	124	0,103	131	0,109	130	0,109	155	0,129	169	0,141	148	0,123	198	0,165

INDEX B: FLUID LOSS DATA

Time	**Fluid loss**	**Fluid loss**	**Fluid loss**	**Fluid loss**	**Fluid loss**	**Fluid loss**	**Fluid loss**	**Fluid loss**	**Fluid loss**	**Fluid loss**	**Fluid loss**	**Fluid loss**	**Fluid loss**	**Pressure**	**Fluid loss (30 min)**	**Fluid loss (30 min)**	**Fluid loss (30 min)**	
[min]	**[ml]**	**[ml]**	**[ml]**	**[ml]**	**[ml]**	**[ml]**	**[ml]**	**[ml]**	**[ml]**	**[ml]**	**[ml]**	**[ml]**	**[ml]**	**KPa**	**[ml]**	**[ml]**	**[ml]**	
	CNC-BT-WDFs (0.8 wt %) 22°C 150 KPa	***CNC-BT-WDFs FW (0.8 wt %) 22°C 250 KPa***	***CNC-BT-WDFs FW(0.8 wt %) 22°C 350 KPa***	***CNC-BT-WDFs FW(0.8 wt %) 22°C 450 KPa***	***CNC-BT-WDFs (1.0 wt %) 22°C 150 KPa***	***CNC-BT-WDFs FW(1.0 wt %) 22°C 250 KPa***	***CNC-BT-WDFs FW (1.0 wt %) 22°C 350 KPa***	***CNC-BT-WDFs FW(1.0 wt %) 22°C 450 KPa***	***CNC-BT-WDFs FW(1.2 wt %) 22°C 150 KPa***	***CNC-BT-WDFs FW (1.2 wt %) 22°C 250 KPa***	***CNC-BT-WDFs FW(1.2 wt %) 22°C 350 KPa***	***CNC-BT-WDFs FW(1.2 wt %) 22°C 450 KPa***			***CNC-BT-WDFs FW(0.8 wt %) 22°C***	***CNC-BT-WDFs FW(1.0 wt %) 22°C***	***CNC-BT-WDFs FW(1.2 wt %) 22°C***	
0	0	0	0	0	0	0	0	0	0	0	0	0	0	150	4	4,8	3,6	
7,5	0,4	1,8	1,85	1,36	1,6	2,2	2,62	1,35	0,22	1,8	2,18	1,2	250	6,8	5,6	6,1		
15	1,65	3,6	3,58	2,62	2,8	3,45	4,1	2,5	1,45	3,38	3,8	2,2	350	6,42	6,4	6,22		
20	2,55	4,6	4,45	3,6	3,5	4,252	4,91	3,06	2,18	4,2	4,7	2,8	450	5,2	4,2	4		
30		6,8	6,42	5,2	4,8	5,6	6,4	4,2	3,6	6,1	6,22	4	--					
Time	**Fluid loss**	**Fluid loss**	**Fluid loss**	**Fluid loss**	**Fluid loss**	**Fluid loss**	**Temperature**	**Fluid loss (30 min)**	**Fluid loss (30 min)**	**Time**	**Fluid loss**	**Fluid loss**	**Fluid loss**	**Fluid loss**	**Fluid loss**			
[min]	**[ml]**	**[ml]**	**[ml]**	**[ml]**	**[ml]**	**[ml]**	**[°C]**	**[ml]**	**[ml]**	**[min]**	**[ml]**	**[ml]**	**[ml]**	**[ml]**	**[ml]**			
	CNC-BT-WDFs FW (1.0 wt %) 30°C 450 KPa	***CNC-BT-WDFs FW (1.0 wt %) 40°C 450 KPa***	***CNC-BT-WDFs FW (1.0 wt %) 50°C 450 KPa***	***CNC-BT-WDFs FW (1.2 wt %) 30°C 450 KPa***	***CNC-BT-WDFs FW (1.2 wt %) 40°C 450 KPa***	***CNC-BT-WDFs FW (1.2 wt %) 50°C 450 KPa***		***CNC-BT-WDFs FW (1.0 wt %) 450 KPa***	***CNC-BT-WDFs FW (1.2 wt %) 450 KPa***		***CNC-BT-WDFs FW (1.0 wt %) 20°C 150 KPa***	***CNC-BT-WDFs FW (1.0 wt %) 20°C 250 KPa***	***CNC-BT-WDFs FW (1.0 wt %) 20°C 350 KPa***	***CNC-BT-WDFs FW (1.0 wt %) 20°C 450 KPa***	***CNC-BT-WDFs FW (1.0 wt %) 80°C 450 KPa***			
0	0	0	0	0	0	0	20	4,2	4	0	0	0	0	0	0			
1	0,1	0,4	0,42	0	0,4	0,27	30	11,62	9,8	7,5	1,6	2,2	2,62	1,35	3			
7,5	3,65	3,35	4,25	2,2	3,6	3,2	40	10,68	10,56	15	2,8	3,45	4,1	2,5	5,6			
15	6,8	6,45	7,38	5,05	6,25	6,1	50	11	9,8	20	3,5	4,252	4,91	3,06	6,9			
20	8,65	8	9	6,82	7,78	7,2	60	10,6	--	30	4,8	5,6	6,4	4,2	9,2			
30	11,62	10,68	11	9,8	10,56	9,8	70	10,1	--									
--	--	--	--	--	--	--	80	9,2	--									
Time	**Fluid loss**	**Fluid loss**	**Fluid loss**	**Fluid loss**	**Fluid loss**	**Fluid loss**	**Fluid loss**	**Fluid loss**	**Fluid loss**	**Fluid loss**	**Fluid loss**	**Fluid loss**	**Fluid loss**	**Fluid loss**	**Fluid loss**	**Fluid loss**	**Fluid loss**	**Fluid loss**
[min]	**[ml]**	**[ml]**	**[ml]**	**[ml]**	**[ml]**	**[ml]**	**[ml]**	**[ml]**	**[ml]**	**[ml]**	**[ml]**	**[ml]**	**[ml]**	**[ml]**	**[ml]**	**[ml]**	**[ml]**	**[ml]**

	CNC-BT-WDFs FW (1.0 wt %) 20°C 450 KPa	CNC-BT-WDFs FW (1.0 wt %) 30°C 450 KPa	CNC-BT-WDFs FW (1.0 wt %) 40°C 450 KPa	CNC-BT-WDFs FW (1.0 wt %) 50°C 450 KPa	CNC-BT-WDFs FW (1.0 wt %) 60°C 450 KPa	CNC-BT-WDFs FW (1.0 wt %) 70°C 450 KPa	CNC-BT-WDFs FW (1.0 wt %) 80°C 450 KPa	CNC-BT-WDFs FW (0,0 wt %) 80°C 450 KPa	CNC-BT-WDFs FW (0,2 wt %) 80°C 450 KPa	CNC-BT-WDFs FW (0,4 wt %) 80°C 450 KPa	CNC-BT-WDFs FW (0,6 wt %) 80°C 450 KPa	CNC-BT-WDFs FW (0,8 wt %) 80°C 450 KPa	CNC-BT-WDFs FW (1,0 wt %) 80°C 450 KPa	CNC-BT-WDFs FW (1.2 wt %) 80°C 450 KPa	CNC-SEP-WDFs FW (1.2 wt %) 30°C 450 KPa	CNC-SEP-WDFs FW (1.2 wt %) 40°C 450 KPa	CNC-SEP--WDFs FW (1.2 wt %)80°C 450 KPa
0	0	0	0	0	0	0	0	0	0	0	0	0	0	0	0	0	0
1	0,01	0,1	0,4	0,42	0,2	0,6	0,2	0	0,3	0,4	0,6	0	0	0,05	0	0	0
7,5	1,35	3,65	3,35	4,25	3,3	4,2	3	3,84	4,25	4	4,5	3,45	3,8	3,25	2,4	2,4	3,5
15	2,5	6,8	6,45	7,38	6,4	6,6	5,6	7,6	8,1	7,6	8,5	7,4	8,05	6,67	6,2	6	7,8
20	3,06	8,65	8	9	8,8	7,95	6,9	9,8	10,45	9,82	10,8	9,57	10,45	8,7	8,68	8,4	10,6
30	4,2	11,62	10,68	11	10,6	10,1	9,2	13,4	15,1	13,4	15,78	12,8	13,7	12	13,4	13,8	16
Time	**Fluid loss**	**Fluid loss**	**Fluid loss**	**Fluid loss**	**Fluid loss**	**Fluid loss**	**Time**	**Fluid loss**	**Fluid loss**	**Fluid loss**	**Fluid loss**	**Fluid loss**	**Fluid loss**	**Fluid loss**			
[min]	**[ml]**	**[ml]**	**[ml]**	**[ml]**	**[ml]**	**[ml]**	**[min]**	**[ml]**	**[ml]**	**[ml]**	**[ml]**	**[ml]**	**[ml]**	**[ml]**			
	CNC-ATT-WDFs FW (0.0 wt %) 20°C 450 KPa	**CNC-ATT-WDFs FW (0.8 wt %) 20°C 450 KPa**	**CNC-ATT-WDFs FW (1.0 wt %) 20°C 450 KPa**	**CNC-ATT-WDFs FW (1.2 wt %) 20°C 450 KPa**	**CNC-ATT-WDFs FW (1.0 wt %) 80°C 450 KPa**	**CNC-ATT-WDFs FW (1.2 wt %) 80°C 450 KPa**		**CNC-SEP-WDFs FW (1.2 wt %) 20°C 450 KPa**	**CNC-SEP-WDFs FW (1.2 wt %) 30°C 450 KPa**	**CNC-SEP-WDFs FW (1.2 wt %) 40°C 450 KPa**	**CNC-SEP-WDFs FW (1.2 wt %) 50°C 450 KPa**	**CNC-SEP-WDFs FW (1.2 wt %) 60°C 450 KPa**	**CNC-SEP-WDFs FW (1.2 wt %) 70°C 450 KPa**	**CNC-SEP-WDFs FW (1.2 wt %) 80°C 450 KPa**			
0	0	0	0	0	0	0	0		0	0	0	0	0	0			
1	1	1	0	0	0	0	1		0	0	0	0	0	0			
7,5	2,6	3,2	2,2	3	3,4	3,6	7,5		2,4	2,4	3	3,2	3,5	4			
15	6,8	7,2	6,2	6,84	7,7	7,92	15		6,2	6	7,4	7,7	7,8	8,6			
20	9,3	9,8	8,86	9,2	105	10,6	20		8,68	8,4	10,2	10,4	10,6	11,4			
30	14,8	14,85	14	14,2	13,6	16,2	30		13,4	13,8	14,8	15,8	16	17,2			
Time	**Fluid loss**	**Fluid loss**	**Fluid loss**	**Fluid loss**	**Fluid loss**	**Fluid loss**	**Fluid loss**	**Time**	**Fluid loss**	**Fluid loss**	**Fluid loss**	**Fluid loss**	**Fluid loss**	**Fluid loss**	**Fluid loss**	**Fluid loss**	
[min]	**[ml]**	**[ml]**	**[ml]**	**[ml]**	**[ml]**	**[ml]**	**[ml]**	**[min]**	**[ml]**	**[ml]**	**[ml]**	**[ml]**	**[ml]**	**[ml]**	**[ml]**	**[ml]**	
	CNC-SEP-WDFs FW (1.2 wt %) 20°C 450 KPa	**CNC-SEP-WDFs FW (1.2 wt %) 30°C 450 KPa**	**CNC-SEP-WDFs FW (1.2 wt %) 40°C 450 KPa**	**CNC-SEP-WDFs FW (1.2 wt %) 50°C 450 KPa**	**CNC-SEP-WDFs FW (1.2 wt %) 60°C 450 KPa**	**CNC-SEP-WDFs FW (1.2 wt %) 70°C 450 KPa**	**CNC-SEP-WDFs FW (1.2 wt %) 80°C 450 KPa**		**CNC-BT-WDFs SW (1.2 wt %) 20°C 450 KPa**	**CNC-BT-WDFs SW (1.2 wt %) 30°C 450 KPa**	**CNC-BT-WDFs SW (1.2 wt %) 40°C 450 KPa**	**CNC-BT-WDFs SW (1.2 wt %) 50°C 450 KPa**	**CNC-BT-WDFs SW (1.2 wt %) 60°C 450 KPa**	**CNC-BT-WDFs SW (1.2 wt %) 70°C 450 KPa**	**CNC-BT-WDFs SW (1.2 wt %) 80°C 450 KPa**			
0		0	0	0	0	0	0	0		0	0	0	0	0	0		
1		0	0	0	0	0	0	1		0,1	0,1	0,1	0	0,2	0		
7,5		2,4	2,4	3	3,2	3,5	4	7,5		2,2	3,4	2,9	3	4,2	4,05		
15		6,2	6	7,4	7,7	7,8	8,6	15		6	7,4	7,2	7,4	9	8,1		
20		8,68	8,4	10,2	10,4	10,6	11,4	20		8,7	10,1	10	10,15	11,8	11		
30		13,4	13,8	14,8	15,8	16	17,2	30		13,9	15,5	15,5	15,8	16,4	16,7		
Time	**Fluid loss**	**Fluid loss**	**Fluid loss**	**Fluid loss**	**Fluid loss**	**Fluid loss**	**Fluid loss**	**Time**	**Fluid loss**	**Fluid loss**	**Fluid loss**	**Fluid loss**	**Fluid loss**	**Fluid loss**	**Fluid loss**	**Fluid loss**	
[min]	**[ml]**	**[ml]**	**[ml]**	**[ml]**	**[ml]**	**[ml]**	**[ml]**	**[min]**	**[ml]**	**[ml]**	**[ml]**	**[ml]**	**[ml]**	**[ml]**	**[ml]**	**[ml]**	

	CNC-ATT-WDFs SW(1.2 wt %) 20°C 450 KPa	***CNC-ATT-WDFs SW (1.2 wt %) 30°C 450 KPa***	***CNC-ATT-WDFs SW (1.2 wt %) 40°C 450 KPa***	***CNC-ATT-WDFs SW (1.2 wt %) 50°C 450 KPa***	***CNC-ATT-WDFs SW (1.2 wt %) 60°C 450 KPa***	***CNC-ATT-WDFs SW (1.2 wt %) 70°C 450 KPa***	***CNC-ATT-WDFs SW (1.2 wt %) 80°C 450 KPa***		***CNC-SEP-WDFs SW (1.2 wt %) 20°C 450 KPa***	***CNC-SEP-WDFs SW (1.2 wt %) 30°C 450 KPa***	***CNC-SEP-WDFs SW (1.2 wt %) 40°C 450 KPa***	***CNC-SEP-WDFs SW (1.2 wt %) 50°C 450 KPa***	***CNC-SEP-WDFs SW (1.2 wt %) 60°C 450 KPa***	***CNC-SEP-WDFs SW (1.2 wt %) 70°C 450 KPa***	***CNC-SEP-WDFs S W(1.2 wt %) 80°C 450 KPa***		
0		0	0	0	0	0	0	0		0	0	0	0	0	0	
1		0	0	0	0	0	0	1		0	0	0	0	0	0	
7,5		2,5	2,7	2,2	3,9	4	3,8	7,5		1,8	2,65	2,95	2,6	2,7	3,6	
15		6,4	6,75	6,35	8,2	8,5	8,2	15		5,77	6,7	7	6,95	7,2	8	
20		8,9	9,4	8,95	10,8	11,2	11,1	20		8,18	9,2	9,75	9,7	9,8	10,7	
30		14	14,6	14,4	16,6	16,95	16,8	30		13	14,4	14,8	15	15,2	16,1	

INDEX C: AGING TIME DATA

Time	Shear Rate	Shear Stress	Viscosity	Shear Stress	Viscosity	Shear Stress	Viscosity	Shear Stress	Viscosity	Shear Stress	Viscosity	Shear Stress	Viscosity
[s]	[1/s]	[Pa]	[Pa·s]	[Pa]	[Pa·s]	[Pa]	[Pa·s]	[Pa]	[Pa·s]	[Pa]	[Pa·s]	[Pa]	[Pa·s]
		CNC-BT-WDFs (6 wt %) 1.2 wt % F.W. 25C FRESH 1	*CNC-BT-WDFs (6 wt %) 1.2 wt % F.W. 25C FRESH 1*	*CNC-ATT-WDFs (6 wt %) 1.2 wt % F.W. 25C FRESH 1*	*CNC-ATT-WDFs (6 wt %) 1.2 wt % F.W. 25C FRESH 1*	*CNC-SEP-WDFs (6 wt %) 1.2 wt % F.W. 25C FRESH 1*	*CNC-SEP-WDFs (6 wt %) 1.2 wt % F.W. 25C FRESH 1*	*CNC-BT-WDFs (6 wt %) 1.2 wt % F.W. 80C FRESH 1*	*CNC-BT-WDFs (6 wt %) 1.2 wt % F.W. 80C FRESH 1*	*CNC-ATT-WDFs (6 wt %) 1.2 wt % F.W. 80C FRESH 1*	*CNC-ATT-WDFs (6 wt %) 1.2 wt % F.W. 80C FRESH 1*	*CNC-SEP-WDFs (6 wt %) 1.2 wt % F.W. 80C FRESH 1*	*CNC-SEP-WDFs (6 wt %) 1.2 wt % F.W. 80C FRESH 1*
2	1	9,36	9,35	2,7	2,7	15,2	15,1	20,2	20,2	5,82	5,84	31,9	31,4
4	13,1	18,1	1,38	6,57	0,501	30,9	2,36	28,5	2,18	11,3	0,866	39,5	3,01
6	25,2	21,7	0,861	8,31	0,329	35,4	1,4	28,1	1,11	12,3	0,489	31,7	1,25
8	37,3	23,1	0,618	10,9	0,292	37,3	1	28,4	0,762	13,1	0,352	28,6	0,765
10	49,4	23,6	0,476	12,9	0,26	37,8	0,765	28,2	0,571	15,2	0,307	28,5	0,577
12	61,6	24,2	0,393	12,4	0,202	37,9	0,616	27,4	0,446	16,4	0,266	30,2	0,491
14	73,7	25,1	0,341	11,5	0,156	38,7	0,525	27,6	0,375	17,3	0,234	33	0,448
16	85,8	26	0,304	11,3	0,132	39,5	0,461	27,8	0,324	12,7	0,148	36,6	0,427
18	97,9	26,7	0,273	11,9	0,121	40,5	0,413	28,1	0,287	10,9	0,112	40,9	0,418
20	110	27,4	0,249	12,3	0,112	41,1	0,374	28,2	0,256	10,7	0,0974	43,5	0,396
22	122	27,9	0,228	12,5	0,102	42	0,344	28,5	0,233	10,4	0,0855	40,6	0,332
24	134	28,6	0,213	12,9	0,096	43	0,321	28,5	0,213	10,7	0,0793	41,5	0,309
26	146	29	0,198	13,4	0,0916	44,1	0,301	28,9	0,197	10,5	0,072	42,6	0,291
28	158	29,6	0,187	13,1	0,0827	45,3	0,286	29	0,183	11,5	0,0727	44,1	0,279
30	171	30,2	0,177	13,6	0,0796	46,3	0,272	29,3	0,172	11,2	0,0659	45	0,264
32	183	30,8	0,168	13,6	0,0746	47,3	0,259	29,4	0,161	11,1	0,0609	46,4	0,254
34	195	31,5	0,162	13	0,0667	48,3	0,248	29,6	0,152	11,3	0,0578	47,4	0,243
36	207	31,7	0,153	13,8	0,0669	49,3	0,238	29,8	0,144	11	0,0532	48,8	0,236
38	219	32,2	0,147	14,2	0,0648	50,1	0,229	30	0,137	11,3	0,0518	49,8	0,227
40	231	32,7	0,141	14,6	0,0632	51	0,221	30,3	0,131	11,5	0,0496	50,6	0,219
42	243	32,9	0,135	15,2	0,0624	51,9	0,213	30,4	0,125	11,9	0,049	51,6	0,212
44	255	33,5	0,131	15,2	0,0594	52,7	0,206	30,6	0,12	11,9	0,0468	52,4	0,205
46	267	34	0,127	15,4	0,0575	53,6	0,2	30,7	0,115	11,8	0,0442	53,9	0,201
48	280	34,5	0,123	15,2	0,0544	54,3	0,194	30,9	0,111	12,2	0,0437	55	0,197
50	292	34,7	0,119	15,4	0,0529	55	0,189	31,2	0,107	12,7	0,0437	56,3	0,193
52	304	35,1	0,116	15,7	0,0516	55,8	0,184	31,3	0,103	12,9	0,0425	57,3	0,189
54	316	35,4	0,112	16,3	0,0515	56,6	0,179	31,4	0,0993	12,7	0,0402	58,3	0,184
56	328	35,8	0,109	16,8	0,0512	57,1	0,174	31,8	0,0969	12,9	0,0395	59,1	0,18
58	340	36,2	0,107	16,8	0,0494	57,9	0,17	31,9	0,0938	13	0,0383	60,1	0,177
60	352	36,6	0,104	17,3	0,049	58,6	0,166	32	0,0908	12,5	0,0354	60,8	0,173
62	364	37,2	0,102	17,4	0,0477	59	0,162	32,3	0,0887	12,6	0,0347	61,2	0,168
64	376	37,3	0,099	18,1	0,0481	59,7	0,159	32,5	0,0862	13,4	0,0357	61,7	0,164
66	389	37,7	0,097	18	0,0462	60,2	0,155	32,7	0,0841	13,7	0,0352	62,2	0,16
68	401	38,3	0,0955	17,8	0,0443	60,9	0,152	32,8	0,0819	13,9	0,0348	62,9	0,157
70	413	38,7	0,0938	18,2	0,0441	61,1	0,148	32,9	0,0796	14	0,0338	63	0,153
72	425	39,2	0,0923	18,5	0,0436	61,7	0,145	33	0,0777	14	0,033	63,3	0,149
74	437	39,5	0,0904	18,6	0,0425	62,2	0,142	33,2	0,076	13,9	0,0317	63,8	0,146
76	449	39,7	0,0885	18,6	0,0415	62,8	0,14	33,2	0,074	13,7	0,0306	64,1	0,143
78	461	39,7	0,0861	18,8	0,0408	63,1	0,137	33	0,0716	13,4	0,029	64,7	0,14
80	473	40,6	0,0857	19,6	0,0415	63,6	0,134	33,5	0,0707	13,4	0,0283	65,2	0,138
82	485	40,7	0,0839	19,8	0,0409	64,3	0,133	33,7	0,0694	13,7	0,0281	65,8	0,135
84	498	40,9	0,0822	20,1	0,0405	64,5	0,13	34	0,0683	14,3	0,0287	65,9	0,132
86	510	41,3	0,081	20	0,0393	65	0,128	34	0,0667	15	0,0295	66	0,129
88	522	41,8	0,08	20,3	0,0389	65,3	0,125	33,9	0,065	15,1	0,0289	65,9	0,126
90	534	42,1	0,0789	20,3	0,038	65,8	0,123	34,3	0,0642	15,4	0,0288	66,3	0,124
92	546	42,4	0,0776	20,2	0,0371	66,2	0,121	34,2	0,0627	15,3	0,0281	66,3	0,121

94	558	42,5	0,0762	20,9	0,0375	66,4	0,119	34,6	0,062	15,1	0,0271	66,7	0,119
96	570	43,1	0,0755	20,9	0,0366	66,7	0,117	34,6	0,0607	14,8	0,026	66,9	0,117
98	582	43,6	0,0749	20,6	0,0354	67,1	0,115	34,6	0,0594	14,2	0,0245	67,2	0,115
100	594	43,3	0,0728	21,1	0,0356	67,6	0,114	35,1	0,0591	15,5	0,026	67,3	0,113
102	607	43,4	0,0716	21,4	0,0352	68,1	0,112	35	0,0578	14,8	0,0244	67,3	0,111
104	619	43,8	0,0708	21,4	0,0346	68,4	0,111	35,4	0,0572	14,2	0,023	67,4	0,109
106	631	44	0,0697	21,5	0,0341	68,7	0,109	35,2	0,0558	14,6	0,0232	67,4	0,107
108	643	44,2	0,0687	21,9	0,0341	68,9	0,107	35,2	0,0547	15	0,0233	67,7	0,105
110	655	44,4	0,0677	22,1	0,0337	69,3	0,106	35,2	0,0538	14,8	0,0226	67,6	0,103
112	667	44,4	0,0666	22,1	0,0332	69,4	0,104	35,4	0,053	15	0,0225	67,6	0,101
114	679	44,5	0,0655	21,9	0,0323	69,8	0,103	35,7	0,0525	15,5	0,0228	67,9	0,0999
116	691	44,8	0,0648	21,9	0,0317	70	0,101	35,6	0,0515	15,6	0,0226	67,9	0,0983
118	703	45,1	0,064	22,1	0,0315	70	0,0995	35,7	0,0508	15,4	0,0219	68,2	0,097
120	716	45	0,0629	22,3	0,0311	70,1	0,098	36	0,0503	14,8	0,0207	68,4	0,0956
122	728	45,3	0,0623	22,1	0,0304	70,4	0,0967	35,7	0,0491	15,3	0,0211	68,3	0,0939
124	740	45,5	0,0615	22,7	0,0306	70,7	0,0955	35,9	0,0486	15,8	0,0214	68,7	0,0929
126	752	45,7	0,0607	22,6	0,03	70,9	0,0943	36	0,0479	14,3	0,019	68,6	0,0913
128	764	45,7	0,0599	22,4	0,0293	71,1	0,0931	36,2	0,0473	14,8	0,0193	68,7	0,0899
130	776	45,7	0,0589	22,5	0,0289	71,5	0,0921	36,3	0,0468	14,5	0,0187	68,5	0,0883
132	788	45,5	0,0578	22,7	0,0288	71,7	0,091	36,1	0,0458	15	0,0191	68,5	0,0869
134	800	46	0,0575	22,4	0,0279	71,7	0,0896	36,4	0,0455	15,3	0,0192	68,7	0,0858
136	812	46	0,0567	22,4	0,0275	71,7	0,0883	36,7	0,0451	15	0,0185	68,8	0,0847
138	825	45,8	0,0555	22,7	0,0276	72	0,0873	36,8	0,0446	17	0,0206	68,6	0,0832
140	837	46,1	0,0551	22,8	0,0272	71,9	0,0859	36,6	0,0438	17,5	0,021	69,2	0,0827
142	849	46,2	0,0544	22,5	0,0265	72,1	0,085	36,5	0,0429	15,3	0,0181	69,1	0,0814
144	861	46,1	0,0536	22,9	0,0266	72,4	0,084	36,7	0,0426	16,6	0,0193	69	0,0801
146	873	46,3	0,053	22,8	0,0261	72,3	0,0828	36,6	0,042	14,6	0,0168	69,1	0,0792
148	885	46	0,052	22,8	0,0258	72,5	0,0819	36,9	0,0417	15,7	0,0177	69	0,078
150	897	46,1	0,0513	22,7	0,0253	72,6	0,0809	36,7	0,0409	15,7	0,0175	69,1	0,0771
152	909	46,3	0,0509	22,8	0,0251	72,6	0,0799	37	0,0407	15,3	0,0168	69,4	0,0763
154	921	46,3	0,0502	22,5	0,0244	72,7	0,0789	36,9	0,0401	15,3	0,0166	69,3	0,0752
156	934	46,2	0,0495	22,3	0,0239	72,9	0,078	37,1	0,0397	15,4	0,0164	69,3	0,0742
158	946	46,1	0,0487	22,8	0,0241	72,8	0,077	37	0,0391	15,4	0,0163	69	0,073
160	958	46,2	0,0482	22,2	0,0232	73	0,0762	37,2	0,0388	15,8	0,0165	69,2	0,0722
162	970	46,1	0,0475	22,9	0,0236	73,2	0,0754	37	0,0381	15,7	0,0162	69,1	0,0712
164	982	46,1	0,047	22,5	0,0229	73,2	0,0746	37,1	0,0377	15,9	0,0162	68,9	0,0702
166	994	46,1	0,0463	22,5	0,0226	73,3	0,0737	37,2	0,0374	16	0,0161	69	0,0694
168	1 010	46,2	0,0459	22,4	0,0222	73,1	0,0726	37,1	0,0368	16,7	0,0166	69,2	0,0687
170	1 020	46,2	0,0454	22,1	0,0217	73,2	0,0719	37,1	0,0365	16,8	0,0165	69,2	0,068
172	1 030	45,8	0,0444	22,5	0,0218	73,6	0,0714	37,2	0,0361	16,8	0,0163	69,1	0,067
174	1 040	46	0,0441	22,5	0,0216	73,6	0,0706	37,5	0,0359	17,3	0,0166	69,1	0,0663
176	1 050	45,9	0,0435	22,4	0,0213	73,6	0,0698	37,5	0,0355	17,4	0,0165	69,1	0,0655
178	1 070	45,9	0,0431	22,5	0,0211	73,3	0,0687	37,4	0,0351	17,6	0,0165	69,5	0,0651
180	1 080	45,9	0,0426	22,3	0,0207	73,5	0,0681	37,4	0,0347	17,7	0,0164	69,6	0,0645
182	1 090	45,8	0,042	22,8	0,0209	73,6	0,0675	37,6	0,0344	18,2	0,0166	69,7	0,0639
184	1 100	45,9	0,0416	22,4	0,0203	73,7	0,0668	37,4	0,0339	18,4	0,0167	69,8	0,0633
186	1 120	45,7	0,041	22,4	0,0201	73,9	0,0663	37,6	0,0337	18,8	0,0169	69,5	0,0623
188	1 130	45,7	0,0405	21,9	0,0194	74	0,0656	37,9	0,0336	18,8	0,0167	69,7	0,0618
190	1 140	45,8	0,0402	22,5	0,0197	73,8	0,0647	37,9	0,0333	19,1	0,0168	70,1	0,0615
192	1 150	45,8	0,0398	22,5	0,0196	73,8	0,0641	38	0,033	19,2	0,0166	70,3	0,061
194	1 160	45,5	0,0391	22,6	0,0194	73,8	0,0634	38,2	0,0328	19,1	0,0164	70,4	0,0605
196	1 180	45,6	0,0388	22,4	0,0191	73,7	0,0627	38,3	0,0326	19,2	0,0163	70,3	0,0598
198	1 190	45,7	0,0384	22,4	0,0189	73,7	0,062	38,4	0,0323	19,5	0,0165	70,4	0,0593
200	1 200	45,5	0,0379	22,1	0,0184	73,5	0,0612	38,3	0,0319	19,4	0,0161	70,6	0,0588

Time	Shear Rate	Shear Stress	Viscosity	Shear Stress	Viscosity	Shear Stress	Viscosity	Shear Stress	Viscosity	Shear Stress	Viscosity	Shear Stress	Viscosity
[s]	[1/s]	[Pa]	[Pa·s]	[Pa]	[Pa·s]	[Pa]	[Pa·s]	[Pa]	[Pa·s]	[Pa]	[Pa·s]	[Pa]	[Pa·s]
		CNC-BT-WDFs (6 wt %) 1.2 wt % F.W. 25C AFTER 24 HRS 1	*CNC-BT-WDFs (6 wt %) 1.2 wt % F.W. 25C AFTER 24 HRS 1*	*CNC-ATT-WDFs (6 wt %) 1.2 wt % F.W. 25C AFTER 24 HRS 1*	*CNC-ATT-WDFs (6 wt %) 1.2 wt % F.W. 25C AFTER 24 HRS 1*	*CNC-SEP-WDFs (6 wt %) 1.2 wt % F.W. 25C AFTER 24 HRS 1*	*CNC-SEP-WDFs (6 wt %) 1.2 wt % F.W. 25C AFTER 24 HRS 1*	*CNC-BT-WDFs (6 wt %) 1.2 wt % F.W. 80C AFTER 24 HRS 1*	*CNC-BT-WDFs (6 wt %) 1.2 wt % F.W. 80C AFTER 24 HRS 1*	*CNC-ATT-WDFs (6 wt %) 1.2 wt % F.W. 80C AFTER 24 HRS NEW 1*	*CNC-ATT-WDFs (6 wt %) 1.2 wt % F.W. 80C AFTER 24 HRS NEW 1*	*CNC-SEP-WDFs (6 wt %) 1.2 wt % F.W. 80C AFTER 24 HRS 1*	*CNC-SEP-WDFs (6 wt %) 1.2 wt % F.W. 80C AFTER 24 HRS 1*
2	1	8,14	8,13	4,18	4,18	23,5	23,4	16,7	16,6	14,1	14,1	25,9	25,8
4	13,1	17,9	1,37	7,43	0,567	41,4	3,16	25,8	1,96	22,4	1,71	32,2	2,45
6	25,2	20,8	0,825	9,09	0,36	44,8	1,78	26,7	1,06	22,6	0,894	28,7	1,14
8	37,3	22,7	0,607	10,5	0,281	47,1	1,26	27,4	0,735	22	0,59	29,4	0,787
10	49,4	22,8	0,462	11,9	0,24	48,7	0,984	27,6	0,558	20,7	0,42	30,4	0,614
12	61,6	23,6	0,383	12,5	0,203	49,9	0,811	27,7	0,451	19,9	0,323	31,4	0,51
14	73,7	24,3	0,329	12,1	0,164	51,4	0,698	28,3	0,384	18,7	0,254	32,2	0,438
16	85,8	25	0,292	12	0,139	52,7	0,614	28,8	0,336	21	0,244	33,7	0,393
18	97,9	26,1	0,266	12,3	0,126	53,9	0,55	29,1	0,297	22,1	0,226	35,1	0,358
20	110	26,7	0,243	12,9	0,117	55	0,5	29,6	0,269	16,6	0,15	37	0,337
22	122	27,6	0,226	13,5	0,111	56,8	0,465	29,9	0,245	13,9	0,113	38,6	0,316
24	134	28,3	0,211	13,7	0,102	58,4	0,435	30,2	0,225	13,3	0,0995	40,7	0,303
26	146	29	0,198	14,1	0,0961	59,7	0,408	30,7	0,21	13,7	0,0938	43,1	0,295
28	158	29,7	0,187	14,3	0,0899	61,1	0,386	31,2	0,197	13,5	0,085	45,8	0,289
30	171	30,4	0,178	14,5	0,085	62,5	0,366	31,5	0,185	14,1	0,0829	49,1	0,288
32	183	31	0,169	14,4	0,0788	63,6	0,348	32	0,175	14,1	0,0771	53,4	0,292
34	195	31,9	0,164	15	0,0771	64,8	0,333	32,2	0,166	14,4	0,0738	56,2	0,288
36	207	32,4	0,157	15	0,0725	66	0,319	32,4	0,156	14,3	0,0693	59,9	0,29
38	219	33,3	0,152	15,2	0,0695	67	0,306	32,9	0,15	15,3	0,0699	61,2	0,279
40	231	33,9	0,147	14,9	0,0646	67,8	0,294	33,2	0,143	15,3	0,066	62,2	0,269
42	243	34,4	0,142	14,9	0,0614	68,9	0,283	33,5	0,138	15,7	0,0647	62,6	0,257
44	255	35	0,137	15,7	0,0614	70	0,274	33,8	0,132	15,9	0,0622	63,4	0,248
46	267	35,5	0,133	15,7	0,0586	70,8	0,265	34,1	0,127	16,2	0,0604	64,4	0,241
48	280	35,9	0,128	16	0,0571	71,6	0,256	34,4	0,123	16,3	0,0582	65,3	0,234
50	292	36,3	0,125	15,9	0,0547	72,3	0,248	34,4	0,118	16,8	0,0577	65,9	0,226
52	304	36,8	0,121	16,5	0,0543	73	0,24	34,8	0,115	17,1	0,0562	66,7	0,219
54	316	37,2	0,118	16,7	0,0528	73,6	0,233	34,9	0,111	17,1	0,0541	67,5	0,214
56	328	37,9	0,115	16,9	0,0514	74,4	0,227	35,5	0,108	17,4	0,053	68,3	0,208
58	340	38,4	0,113	17,4	0,0511	74,8	0,22	35,6	0,105	17,8	0,0524	69,2	0,203
60	352	38,7	0,11	16,8	0,0478	75,6	0,215	35,9	0,102	18,6	0,0527	69,5	0,197
62	364	39,3	0,108	16,8	0,0461	76,1	0,209	36,2	0,0993	19,1	0,0525	70	0,192
64	376	39,9	0,106	17,1	0,0454	76,7	0,204	36,4	0,0968	19,3	0,0514	70,7	0,188
66	389	39,9	0,103	17,4	0,0448	77,2	0,199	36,7	0,0944	19,5	0,0501	71,1	0,183
68	401	40,3	0,101	17,3	0,0433	77,7	0,194	36,8	0,0919	20	0,0498	71,8	0,179
70	413	41	0,0992	17,9	0,0434	78,2	0,189	37,1	0,09	20,6	0,05	72,3	0,175
72	425	41,3	0,0971	18,2	0,0429	78,6	0,185	37,4	0,088	21,6	0,0508	72,7	0,171
74	437	41,6	0,0953	18,6	0,0425	79	0,181	37,8	0,0865	21,8	0,0499	73	0,167
76	449	42	0,0935	19,6	0,0437	79,5	0,177	37,8	0,0841	21,2	0,0473	73,7	0,164
78	461	42,3	0,0918	20,3	0,044	80,1	0,174	38	0,0824	21,4	0,0463	73,9	0,16
80	473	42,5	0,0897	20,3	0,0429	80,2	0,169	38,4	0,0812	21,8	0,046	74,5	0,157
82	485	42,9	0,0884	20,6	0,0424	80,4	0,166	38,4	0,0791	21,8	0,045	74,7	0,154
84	498	43	0,0864	21,1	0,0424	80,6	0,162	38,8	0,078	22,6	0,0454	74,6	0,15
86	510	43,3	0,085	21,3	0,0418	80,9	0,159	38,8	0,0761	23,1	0,0453	75,1	0,147
88	522	43,8	0,084	21,8	0,0417	81,3	0,156	39,3	0,0754	23,9	0,0459	76,3	0,146
90	534	43,9	0,0823	22	0,0412	81,4	0,152	39,5	0,074	24,3	0,0456	76,6	0,144
92	546	44,2	0,081	21,9	0,0402	81,6	0,149	39,7	0,0726	25,6	0,0468	76,7	0,14
94	558	44,2	0,0792	21,9	0,0392	81,9	0,147	39,9	0,0714	27,9	0,05	76,4	0,137
96	570	44,5	0,078	22	0,0386	82	0,144	40	0,0701	26,4	0,0463	76,3	0,134
98	582	44,8	0,077	22,3	0,0383	82,4	0,141	40,3	0,0692	23,1	0,0397	76	0,131
100	594	44,7	0,0752	22,4	0,0377	82,5	0,139	40,4	0,0679	23,3	0,0392	76,5	0,129
102	607	45,1	0,0744	22,9	0,0378	82,7	0,136	40,7	0,0671	23,7	0,039	76,5	0,126
104	619	45,4	0,0734	22,8	0,0368	82,9	0,134	40,8	0,0659	24,2	0,0392	77,1	0,125

106	631	45,6	0,0723	23,1	0,0366	83,1	0,132	40,8	0,0647	23,4	0,0372	77,8	0,123
108	643	45,7	0,0711	23,1	0,0359	83,5	0,13	41,4	0,0643	23,5	0,0365	78	0,121
110	655	45,9	0,07	23,8	0,0363	83,7	0,128	41,2	0,0628	24,2	0,037	78,7	0,12
112	667	46,3	0,0694	24	0,036	83,8	0,126	41,6	0,0624	24,7	0,037	78,6	0,118
114	679	46,1	0,0679	23,8	0,035	83,9	0,124	41,6	0,0613	26,1	0,0384	78,6	0,116
116	691	46,3	0,067	24,2	0,035	84,1	0,122	41,8	0,0604	25,4	0,0367	79	0,114
118	703	46,7	0,0663	24	0,0341	84,3	0,12	41,9	0,0596	23,3	0,0332	79,1	0,112
120	716	46,8	0,0654	24,3	0,034	84,5	0,118	42,1	0,0588	23,4	0,0327	79,1	0,111
122	728	47,1	0,0648	24,6	0,0338	84,8	0,117	42,3	0,0581	24,9	0,0342	78,8	0,108
124	740	47	0,0635	24,7	0,0334	84,9	0,115	42,5	0,0574	23,5	0,0318	78,8	0,107
126	752	47,3	0,0629	24,5	0,0325	84,9	0,113	42,3	0,0563	24,4	0,0324	78,7	0,105
128	764	47,6	0,0624	24,7	0,0323	85	0,111	42,4	0,0555	24	0,0314	78,9	0,103
130	776	47,4	0,0611	25,1	0,0324	85,2	0,11	42,5	0,0547	24	0,031	79	0,102
132	788	48	0,0609	25,6	0,0325	85,3	0,108	42,6	0,0541	24,6	0,0312	79	0,1
134	800	47,8	0,0597	25,3	0,0316	85,3	0,107	42,7	0,0534	26	0,0324	78,6	0,0982
136	812	48	0,0591	25,7	0,0316	85,7	0,106	42,8	0,0527	25,7	0,0317	78,8	0,097
138	825	48,5	0,0588	25,3	0,0307	85,6	0,104	42,7	0,0518	26,3	0,0319	78,8	0,0956
140	837	48,7	0,0582	25,3	0,0302	85,9	0,103	43,1	0,0516	26,2	0,0313	79,1	0,0945
142	849	48,9	0,0577	25,6	0,0302	86	0,101	42,9	0,0506	26,4	0,0311	78,6	0,0926
144	861	49,2	0,0571	25,1	0,0291	86	0,0999	42,9	0,0498	26,7	0,031	78,9	0,0917
146	873	49,5	0,0568	25,1	0,0287	86,2	0,0987	43,2	0,0495	25,5	0,0292	78,9	0,0904
148	885	49,7	0,0562	25,1	0,0284	86,2	0,0974	43,3	0,0489	26,7	0,0302	79,1	0,0894
150	897	49,9	0,0556	25,3	0,0282	86,4	0,0963	43,1	0,0481	26,9	0,03	79,4	0,0885
152	909	49,5	0,0544	25,2	0,0277	86,2	0,0948	43,4	0,0477	25,5	0,0281	79,1	0,087
154	921	50	0,0542	25,6	0,0278	86,5	0,0938	43,2	0,0469	28,6	0,031	79,6	0,0864
156	934	49,9	0,0535	25,2	0,027	86,2	0,0924	43,3	0,0464	26,8	0,0287	79,3	0,085
158	946	50,3	0,0532	24,8	0,0262	86,5	0,0914	43,3	0,0457	26,7	0,0283	79,5	0,0841
160	958	50,4	0,0526	24,9	0,026	86,3	0,0902	43	0,0449	26,8	0,0279	79,2	0,0827
162	970	50,3	0,0519	24,8	0,0255	86,3	0,0889	43,1	0,0445	25,6	0,0264	79,1	0,0815
164	982	50,7	0,0516	24,8	0,0253	86,4	0,088	43,1	0,0439	24,6	0,0251	79,4	0,0808
166	994	50,6	0,0509	24,7	0,0248	86,3	0,0868	43	0,0433	23,7	0,0238	79,3	0,0798
168	1 010	51	0,0506	24,4	0,0243	86,4	0,0858	43,2	0,043	23,8	0,0236	79,2	0,0787
170	1 020	51,2	0,0503	25	0,0246	86,2	0,0847	43,3	0,0425	25,1	0,0247	78,9	0,0775
172	1 030	51,1	0,0496	24,9	0,0241	86,2	0,0837	43,3	0,042	26,3	0,0256	78,5	0,0762
174	1 040	51,2	0,0491	25	0,024	86	0,0825	43,1	0,0413	26,3	0,0252	78,1	0,0749
176	1 050	51,4	0,0488	24,7	0,0234	86,2	0,0817	43,2	0,041	26,7	0,0253	78,1	0,074
178	1 070	51,6	0,0484	25	0,0234	86,1	0,0807	43,4	0,0407	27,3	0,0256	77,8	0,0729
180	1 080	51,7	0,048	24,9	0,0231	86	0,0797	43,4	0,0403	27,6	0,0256	77,8	0,0721
182	1 090	51,8	0,0475	24,7	0,0227	85,9	0,0787	43,3	0,0397	27,7	0,0254	77,7	0,0712
184	1 100	52,1	0,0472	24,5	0,0223	85,9	0,0778	43,5	0,0395	28	0,0254	77,8	0,0705
186	1 120	52,2	0,0468	24,2	0,0217	86	0,0771	43,5	0,039	28,7	0,0257	77,5	0,0695
188	1 130	52,7	0,0467	24,4	0,0216	85,8	0,0761	43,4	0,0385	29,9	0,0265	77,3	0,0685
190	1 140	52,6	0,0462	24,8	0,0217	86,1	0,0756	43,7	0,0383	30,6	0,0268	77,2	0,0677
192	1 150	52,8	0,0459	24,3	0,0211	85,7	0,0745	43,4	0,0377	27,7	0,024	77,3	0,0671
194	1 160	52,8	0,0454	24,7	0,0212	85,6	0,0736	43,5	0,0373	28,7	0,0247	77,2	0,0664
196	1 180	53,1	0,0451	24,2	0,0206	85,5	0,0727	43,5	0,037	28,8	0,0245	77,3	0,0657
198	1 190	53,1	0,0447	24,7	0,0208	85,6	0,072	43,7	0,0368	30,7	0,0258	77,3	0,0651
200	1 200	53	0,0442	24,7	0,0206	85,5	0,0712	43,8	0,0365	30,9	0,0257	77	0,0642

Time	Shear Rate	Shear Stress	Viscosity	Shear Stress	Viscosity	Shear Stress	Viscosity	Shear Stress	Viscosity	Shear Stress	Viscosity	Shear Stress	Viscosity
[s]	[1/s]	[Pa]	[Pa·s]	[Pa]	[Pa·s]	[Pa]	[Pa·s]	[Pa]	[Pa·s]	[Pa]	[Pa·s]	[Pa]	[Pa·s]
		CNC-BT-WDFs (6 wt %) F.W 25 C 48 HRS 1	*CNC-BT-WDFs (6 wt %) F.W 25 C 48 HRS 1*	*CNC-ATT-WDFs (6 wt %) F.W 25 C 48 HRS 1*	*CNC-ATT-WDFs (6 wt %) F.W 25 C 48 HRS 1*	*CNC-SEP-WDFs (6 wt %) F.W 25 C 48 HRS 1*	*CNC-SEP-WDFs (6 wt %) F.W 25 C 48 HRS 1*	*CNC-BT-WDFs (6 wt %) F.W 80C 48 HRS 1*	*CNC-BT-WDFs (6 wt %) F.W 80C 48 HRS 1*	*CNC-ATT-WDFs (6 wt %) F.W 80C 48 HRS NEW*	*CNC-ATT-WDFs (6 wt %) F.W 80C 48 HRS NEW*	*CNC-SEP-WDFs (6 wt %) F.W 80C 48 HRS 1*	*CNC-SEP-WDFs (6 wt %) F.W 80C 48 HRS 1*
2	1	9,57	9,55	4,29	4,3	18,5	18,5	18,8	18,7	26,4	26,5	35,7	35,7
4	13,1	20,6	1,57	8,93	0,681	41,8	3,19	28,1	2,14	37,8	2,88	34,9	2,66
6	25,2	24,6	0,975	10,8	0,43	46,6	1,85	29,7	1,18	30	1,19	42,7	1,69
8	37,3	25,4	0,68	12,9	0,344	50	1,34	31	0,831	34,2	0,914	43,3	1,16
10	49,4	26,3	0,532	15,4	0,311	52,2	1,06	30,9	0,624	30,7	0,621	46,2	0,934
12	61,6	27,6	0,448	15,9	0,258	53,9	0,876	31,2	0,507	35,6	0,579	46,9	0,763
14	73,7	28,7	0,39	13,8	0,188	56	0,76	31,8	0,432	36,6	0,497	52,9	0,718
16	85,8	30	0,35	13,9	0,162	57,7	0,673	32,1	0,374	42,6	0,497	56,1	0,654
18	97,9	31	0,317	14,1	0,144	58,9	0,602	32,4	0,331	49,7	0,508	57,4	0,586
20	110	31,8	0,29	14,1	0,128	60,5	0,55	32,9	0,299	54,3	0,493	60,5	0,55
22	122	32,9	0,269	13,8	0,113	62	0,508	33,3	0,273	48,1	0,394	62,9	0,515
24	134	33,5	0,25	14,5	0,108	63,6	0,474	33,9	0,253	27,9	0,208	67,3	0,502
26	146	34,5	0,235	14,5	0,0994	64,8	0,443	34,3	0,234	24,6	0,168	62,9	0,43
28	158	35,5	0,224	15	0,0948	66,1	0,417	34,7	0,219	23,9	0,151	65,7	0,414
30	171	36,1	0,212	14,9	0,0871	67,5	0,396	35,3	0,207	23,6	0,139	66,4	0,389
32	183	36,8	0,202	15,4	0,0844	68,8	0,377	35,6	0,195	23,6	0,129	67,3	0,369
34	195	37,7	0,193	15,9	0,0819	69,9	0,359	36,1	0,185	24,2	0,124	68,9	0,354
36	207	38,2	0,185	16,4	0,0791	71,2	0,344	36,5	0,177	24	0,116	69,6	0,336
38	219	38,8	0,177	16,8	0,0765	72,1	0,329	37	0,169	23,2	0,106	69,6	0,318
40	231	39,7	0,172	16,6	0,0717	73,2	0,317	37,3	0,162	22,9	0,0989	70,5	0,305
42	243	39,9	0,164	17	0,0698	74,1	0,305	37,5	0,154	23,2	0,0954	72,6	0,298
44	255	40,6	0,159	17,1	0,0671	74,9	0,293	37,8	0,148	23	0,0901	73	0,286
46	267	41,3	0,155	18,1	0,0676	75,7	0,283	38,1	0,143	24,1	0,0901	72,9	0,273
48	280	42	0,15	18,6	0,0664	76,4	0,273	38,3	0,137	24	0,0857	74,1	0,265
50	292	42,3	0,145	18,5	0,0633	77,2	0,265	38,6	0,132	24,4	0,0837	75,8	0,26
52	304	42,6	0,14	19,2	0,0632	77,8	0,256	38,8	0,128	24,4	0,0805	76,4	0,252
54	316	43,2	0,137	19,6	0,062	78,6	0,249	39	0,124	25,1	0,0796	77,4	0,245
56	328	43,4	0,132	20	0,0611	79,3	0,242	39,5	0,12	25,8	0,0785	78,5	0,239
58	340	44,3	0,13	20	0,0589	79,9	0,235	39,8	0,117	26,1	0,0768	78,8	0,232
60	352	44,7	0,127	20,3	0,0577	80,6	0,229	40,2	0,114	25,9	0,0735	79	0,224
62	364	45,2	0,124	20	0,0548	81,2	0,223	40,5	0,111	27,1	0,0744	79,6	0,218
64	376	45,5	0,121	20,5	0,0546	81,6	0,217	40,9	0,109	27,1	0,0721	80,4	0,214
66	389	46	0,118	20	0,0516	82,1	0,211	41,1	0,106	26,2	0,0675	80,9	0,208
68	401	46,5	0,116	20,6	0,0514	82,8	0,207	41,5	0,103	26,4	0,066	82,2	0,205
70	413	46,9	0,114	20,5	0,0498	83	0,201	41,7	0,101	27,3	0,066	83	0,201
72	425	47,4	0,112	20,8	0,049	83,4	0,196	41,9	0,0987	27,5	0,0647	82,3	0,194
74	437	48	0,11	21,5	0,0493	84	0,192	42	0,0962	27,7	0,0635	83,5	0,191
76	449	48,2	0,107	21,7	0,0484	84,3	0,188	42,2	0,0939	27,1	0,0604	83,3	0,185
78	461	48,5	0,105	21,9	0,0476	84,9	0,184	42,5	0,0921	27,9	0,0604	83,3	0,181
80	473	48,9	0,103	22,3	0,0472	85,3	0,18	42,8	0,0905	27,3	0,0578	83,6	0,177
82	485	49	0,101	22	0,0453	85,6	0,176	43,3	0,0891	27,3	0,0563	83,2	0,171
84	498	49,5	0,0996	22,5	0,0453	86,1	0,173	43,5	0,0875	27,3	0,0548	83,8	0,168
86	510	50,1	0,0983	22,6	0,0443	86,5	0,17	43,5	0,0854	27,6	0,0542	84,3	0,165
88	522	50,1	0,0961	22,6	0,0433	86,6	0,166	43,9	0,0842	28,3	0,0543	84	0,161
90	534	50,6	0,0948	23,1	0,0432	87	0,163	44	0,0824	28,7	0,0537	84,3	0,158
92	546	50,7	0,0928	23,9	0,0437	87,3	0,16	44,7	0,0818	29	0,0531	84	0,154
94	558	51,1	0,0916	23,9	0,0428	87,6	0,157	44,6	0,0798	29,1	0,0522	84,5	0,151
96	570	51,4	0,0901	24,3	0,0425	87,7	0,154	44,7	0,0785	30,8	0,054	84,9	0,149
98	582	51,6	0,0886	24,3	0,0417	87,8	0,151	45,3	0,0777	29,6	0,0508	85	0,146
100	594	51,8	0,0872	24,7	0,0415	88,2	0,148	45,4	0,0764	29,2	0,0491	85,1	0,143
102	607	52,2	0,0861	24,3	0,0401	88,4	0,146	45,7	0,0753	29,5	0,0486	85,8	0,141
104	619	52,3	0,0846	25,1	0,0406	88,4	0,143	45,9	0,0742	28	0,0453	86,7	0,14

106	631	52,4	0,0831	25,7	0,0408	88,7	0,141	46,1	0,073	28,1	0,0446	87,9	0,139
108	643	53	0,0824	25,7	0,0399	88,8	0,138	46,3	0,0721	28,7	0,0446	87,4	0,136
110	655	53,1	0,081	26,1	0,0398	88,9	0,136	46,4	0,0708	28,8	0,0439	87,6	0,134
112	667	53,2	0,0798	26,2	0,0393	89	0,133	46,6	0,0698	29	0,0434	88,2	0,132
114	679	53,3	0,0785	26,6	0,0392	89,4	0,132	46,4	0,0684	29,2	0,0429	88,4	0,13
116	691	53,8	0,0778	27,1	0,0391	89,6	0,13	46,6	0,0674	29,2	0,0422	88,2	0,128
118	703	53,9	0,0767	27,2	0,0387	89,7	0,127	46,9	0,0667	30	0,0427	88,6	0,126
120	716	54,2	0,0757	27,5	0,0384	90,2	0,126	46,9	0,0655	32	0,0447	88,9	0,124
122	728	54,3	0,0746	27,8	0,0382	90,2	0,124	47,4	0,0652	34,8	0,0479	88,6	0,122
124	740	54,5	0,0736	27,4	0,0371	90,3	0,122	47,4	0,0641	32,2	0,0435	89,6	0,121
126	752	54,6	0,0727	27,9	0,0372	90,8	0,121	47,4	0,0631	30,7	0,0408	89,8	0,119
128	764	54,7	0,0716	28,1	0,0367	90,8	0,119	47,8	0,0626	30,6	0,04	90	0,118
130	776	54,9	0,0707	28,1	0,0363	91,1	0,117	47,6	0,0614	30,6	0,0394	89,8	0,116
132	788	55	0,0698	28,4	0,036	91,3	0,116	47,7	0,0605	30,8	0,039	90,7	0,115
134	800	55,3	0,0691	28,6	0,0358	91,4	0,114	47,6	0,0595	34,4	0,043	89,9	0,112
136	812	55,5	0,0683	28,7	0,0353	91,6	0,113	47,9	0,059	38,2	0,0471	90,1	0,111
138	825	55,5	0,0673	28,6	0,0346	91,8	0,111	47,6	0,0578	35,6	0,0432	90,1	0,109
140	837	55,5	0,0663	28,7	0,0343	91,8	0,11	47,8	0,0571	34,7	0,0415	90,1	0,108
142	849	55,8	0,0657	28,9	0,0341	91,8	0,108	47,9	0,0564	33,8	0,0399	90	0,106
144	861	55,8	0,0648	28,7	0,0333	92	0,107	48	0,0558	35,4	0,0411	90,3	0,105
146	873	55,8	0,0639	29,2	0,0335	92	0,105	48,2	0,0552	37,8	0,0433	90,4	0,104
148	885	55,7	0,0629	29,2	0,033	92	0,104	48	0,0543	38,5	0,0435	90,6	0,102
150	897	55,7	0,0621	28,5	0,0317	92,1	0,103	48,4	0,0539	33,6	0,0374	90,6	0,101
152	909	55,9	0,0614	28,9	0,0318	92,3	0,101	47,9	0,0527	32	0,0352	90,8	0,0999
154	921	55,8	0,0606	29	0,0315	92,1	0,0999	48,1	0,0522	33,7	0,0366	90,4	0,0981
156	934	56,1	0,0601	28,4	0,0304	92,3	0,0989	48	0,0515	34,7	0,0372	91,5	0,098
158	946	56	0,0592	28,7	0,0304	92,3	0,0976	48,2	0,051	33,9	0,0359	89,8	0,095
160	958	56,1	0,0585	28,2	0,0294	92,5	0,0966	47,9	0,05	33,5	0,035	89,3	0,0932
162	970	56,1	0,0579	28,5	0,0293	92,7	0,0956	47,9	0,0494	32,7	0,0338	89,5	0,0923
164	982	56,2	0,0572	28,7	0,0292	92,5	0,0942	48,1	0,049	34	0,0347	89,8	0,0914
166	994	56,2	0,0566	28	0,0282	92,7	0,0933	48	0,0483	32,3	0,0324	90	0,0905
168	1 010	56,3	0,056	28,1	0,0279	92,6	0,092	48,1	0,0478	32,5	0,0323	89,3	0,0888
170	1 020	56,7	0,0557	28	0,0275	92,7	0,091	48	0,0471	31,7	0,0311	89,3	0,0877
172	1 030	56,6	0,0549	27,8	0,027	92,8	0,09	47,8	0,0464	35,6	0,0345	88,9	0,0862
174	1 040	56,3	0,054	27,5	0,0264	92,9	0,0891	47,5	0,0456	36,7	0,0352	88,6	0,085
176	1 050	56,4	0,0534	27,4	0,026	92,6	0,0878	47,6	0,0452	39,7	0,0376	88,5	0,0839
178	1 070	56,7	0,0531	27,6	0,0258	92,4	0,0867	47,9	0,0449	34,7	0,0325	88,4	0,0829
180	1 080	56,4	0,0523	27,5	0,0255	92,5	0,0858	47,7	0,0442	32,5	0,0301	88	0,0816
182	1 090	56,4	0,0517	27,2	0,025	92,7	0,0849	47,4	0,0435	33,9	0,0311	87,6	0,0803
184	1 100	56,5	0,0513	27	0,0245	92,5	0,0839	47,6	0,0432	32,7	0,0296	87,3	0,0792
186	1 120	56,3	0,0505	26,8	0,024	92,3	0,0828	47,5	0,0426	32,6	0,0293	87,1	0,0781
188	1 130	56,2	0,0498	26,5	0,0235	92,3	0,0818	47,5	0,0422	36,5	0,0323	87,3	0,0774
190	1 140	56,3	0,0494	27,2	0,0239	92,2	0,0809	47,6	0,0417	35,2	0,0309	87,5	0,0768
192	1 150	56,3	0,0489	27,1	0,0236	92,3	0,0802	47,5	0,0413	33,4	0,029	86,8	0,0753
194	1 160	56,2	0,0483	27,8	0,0239	92,4	0,0794	47,5	0,0408	34,1	0,0293	86,8	0,0746
196	1 180	56,2	0,0478	27,4	0,0233	92,2	0,0784	47,3	0,0402	34,2	0,0291	86,5	0,0736
198	1 190	56,3	0,0474	27,4	0,023	92,4	0,0778	47,4	0,0399	35,7	0,03	86,3	0,0726
200	1 200	56,4	0,047	27	0,0225	92,2	0,0768	47,4	0,0395	34,9	0,0291	86,5	0,0721

Time	Shear Rate	Shear Stress	Viscosity	Shear Stress	Viscosity	Shear Stress	Viscosity	Shear Stress	Viscosity	Shear Stress	Viscosity	Shear Stress	Viscosity
[s]	[1/s]	[Pa]	[Pa·s]	[Pa]	[Pa·s]	[Pa]	[Pa·s]	[Pa]	[Pa·s]	[Pa]	[Pa·s]	[Pa]	[Pa·s]
		CNC-BT-WDFs 1.2 wt % F.W. 25C 72 HRS	*CNC-BT-WDFs 1.2 wt % F.W. 25C 72 HRS*	*CNC-ATT-WDFs 1.2 wt % F.W. 25C 72 HRS*	*CNC-ATT-WDFs 1.2 wt % F.W. 25C 72 HRS*	*CNC-SEP-WDFs 1.2 wt % F.W. 25C 72 HRS*	*CNC-SEP-WDFs 1.2 wt % F.W. 25C 72 HRS*	*CNC-BT-WDFs 1.2 wt % F.W. 80C 72 HRS*	*CNC-BT-WDFs 1.2 wt % F.W. 80C 72 HRS*	*CNC-ATT-WDFs 1.2 wt % F.W. 80 C 72 HRS NEW*	*CNC-ATT-WDFs 1.2 wt % F.W. 80 C 72 HRS NEW*	*CNC-SEP-WDFs 1.2 wt % F.W. 80 C 72 HRS NEW*	*CNC-SEP-WDFs 1.2 wt % F.W. 80 C 72 HRS NEW*
2	1	12,9	12,9	5,55	5,56	21,8	21,8	24,6	24,6	25,5	25,5	51,7	51,9
4	13,1	22,9	1,75	9,82	0,749	41,6	3,17	30,5	2,33	36	2,75	51,6	3,93
6	25,2	26,1	1,03	11,7	0,462	48,9	1,94	33,4	1,32	39,4	1,56	48,4	1,92
8	37,3	27,8	0,745	13,5	0,363	53,4	1,43	34	0,91	45,2	1,21	42,6	1,14
10	49,4	28,7	0,581	15,6	0,315	57,1	1,16	33,1	0,67	53,5	1,08	39,8	0,804
12	61,6	29,4	0,477	17,2	0,279	58	0,942	32,5	0,529	42,7	0,693	40,2	0,653
14	73,7	30,3	0,411	18,1	0,246	59,5	0,807	32,8	0,445	45,2	0,614	42,5	0,576
16	85,8	30,9	0,36	16,5	0,193	62,2	0,725	33,1	0,386	55,5	0,647	44,2	0,515
18	97,9	31,7	0,324	15,2	0,156	63,3	0,647	33,5	0,342	56,6	0,578	45,6	0,466
20	110	32,2	0,293	15,6	0,142	64,9	0,59	33,8	0,307	50,4	0,458	48	0,436
22	122	33	0,27	15,8	0,13	66,6	0,546	34,2	0,28	33	0,271	51,3	0,42
24	134	34,1	0,254	16,3	0,122	67,8	0,505	34,6	0,257	29,6	0,221	55,4	0,413
26	146	35	0,239	16,4	0,112	69,3	0,473	34,8	0,238	30,3	0,207	60,3	0,412
28	158	35,9	0,227	17,3	0,109	71	0,448	35	0,221	30	0,19	67,7	0,427
30	171	36,6	0,215	17,8	0,104	72,3	0,424	35,7	0,209	30	0,176	75,5	0,442
32	183	37,3	0,204	17,4	0,0951	73,6	0,403	35,8	0,196	30,8	0,169	74,5	0,408
34	195	37,9	0,194	17,9	0,0918	74,8	0,384	36,1	0,185	31	0,159	75,5	0,388
36	207	38,5	0,186	17,8	0,086	76,1	0,368	36,5	0,176	30,9	0,149	76,8	0,371
38	219	39,4	0,18	18,5	0,0846	77,1	0,352	36,7	0,168	31,6	0,144	78,4	0,358
40	231	40,1	0,174	18,5	0,0803	78,1	0,338	37,2	0,161	31,6	0,137	80,6	0,349
42	243	40,8	0,168	19	0,078	79	0,325	37,5	0,154	31,5	0,129	81,5	0,335
44	255	41,2	0,161	19,8	0,0775	80,1	0,314	37,9	0,148	32,2	0,126	82,9	0,325
46	267	41,9	0,157	20,5	0,0765	80,9	0,303	38,1	0,143	33,1	0,124	83,5	0,312
48	280	42,3	0,151	20,6	0,0737	81,7	0,292	38,3	0,137	33,6	0,12	85,2	0,305
50	292	42,9	0,147	20,9	0,0716	82,6	0,283	38,6	0,132	33,9	0,116	86,5	0,297
52	304	43,4	0,143	21,6	0,0709	83,3	0,274	38,8	0,128	33,7	0,111	87,4	0,288
54	316	43,9	0,139	22,1	0,0699	84	0,266	39,2	0,124	33,6	0,106	88,7	0,281
56	328	44,7	0,136	22	0,0671	84,8	0,258	39,3	0,12	33,9	0,103	89,8	0,274
58	340	45,1	0,133	22,7	0,0667	85,4	0,251	39,6	0,116	33,7	0,0991	91	0,268
60	352	45,6	0,129	22,8	0,0648	86	0,244	39,8	0,113	34,2	0,0971	91	0,258
62	364	46,1	0,126	22,5	0,0618	86,7	0,238	39,9	0,11	34,9	0,0957	91,8	0,252
64	376	46,7	0,124	22,7	0,0604	87,3	0,232	40,4	0,107	34,5	0,0916	92,3	0,245
66	389	47,2	0,121	23,1	0,0594	87,9	0,226	40,6	0,105	35,9	0,0923	93,5	0,241
68	401	47,4	0,118	23	0,0574	88,3	0,22	41	0,102	36,1	0,09	94,9	0,237
70	413	47,9	0,116	23,4	0,0568	88,9	0,215	41,1	0,0996	36	0,0872	94,7	0,229
72	425	48	0,113	23,6	0,0554	89,4	0,21	41,5	0,0977	35,9	0,0844	94,2	0,222
74	437	48,4	0,111	23,9	0,0546	90,1	0,206	41,4	0,0946	36,2	0,0828	95,2	0,218
76	449	48,7	0,108	24,1	0,0536	90,2	0,201	41,7	0,0928	37	0,0823	93,9	0,209
78	461	49,6	0,108	24,5	0,053	90,6	0,196	41,7	0,0905	37,2	0,0807	95,8	0,208
80	473	49,7	0,105	24,1	0,0508	91,2	0,193	42,2	0,0892	38,2	0,0806	95,9	0,203
82	485	49,7	0,102	23,9	0,0492	91,4	0,188	42,5	0,0877	38,9	0,0801	95,6	0,197
84	498	50,2	0,101	24,5	0,0492	91,7	0,184	42,6	0,0855	39	0,0783	96,1	0,193
86	510	50,6	0,0993	24,8	0,0486	92,1	0,181	42,7	0,0839	38,9	0,0763	96,4	0,189
88	522	51,2	0,0982	24,9	0,0478	92,3	0,177	42,9	0,0822	39,4	0,0755	95,3	0,183
90	534	51,5	0,0965	25,4	0,0475	92,6	0,173	42,8	0,0803	40,1	0,0751	95,8	0,18
92	546	52	0,0952	25,7	0,0471	93	0,17	43,1	0,079	42	0,0769	96,2	0,176
94	558	51,9	0,093	26,1	0,0467	93,3	0,167	43,4	0,0777	40,4	0,0724	95,5	0,171
96	570	52,5	0,0921	26,6	0,0466	93,7	0,164	43,7	0,0766	41,9	0,0735	97,6	0,171
98	582	52,7	0,0904	26,6	0,0456	93,9	0,161	43,8	0,0753	43,4	0,0745	98	0,168
100	594	52,6	0,0885	26,3	0,0443	94,3	0,159	44	0,074	43,7	0,0735	94,2	0,158
102	607	53,1	0,0876	27,2	0,0448	94,3	0,155	44,2	0,0728	43,6	0,072	93,9	0,155
104	619	53,5	0,0865	27,2	0,044	94,7	0,153	44,4	0,0718	42,8	0,0691	94,4	0,153

106	631	53,6	0,085	26,9	0,0427	94,8	0,15	44,7	0,0708	42,5	0,0674	94,1	0,149
108	643	54	0,0839	27,5	0,0428	95,1	0,148	44,9	0,0698	42	0,0653	95,3	0,148
110	655	54,3	0,0829	27,9	0,0426	95,1	0,145	44,8	0,0684	42,2	0,0644	94,3	0,144
112	667	54,5	0,0817	27,8	0,0416	95,3	0,143	44,9	0,0673	43,7	0,0655	93,6	0,14
114	679	54,4	0,0801	28,1	0,0413	95,7	0,141	45,2	0,0665	46	0,0677	93,7	0,138
116	691	54,6	0,079	28,3	0,0409	95,8	0,139	45,2	0,0654	48	0,0694	93,4	0,135
118	703	54,9	0,0781	28,6	0,0407	95,9	0,136	45,3	0,0645	48,9	0,0696	92,8	0,132
120	716	55,1	0,077	28,7	0,0401	96,2	0,135	45,3	0,0632	51,4	0,0718	93,2	0,13
122	728	55,6	0,0765	29	0,0398	96,5	0,133	45,5	0,0625	51,9	0,0713	93,1	0,128
124	740	55,7	0,0753	29,4	0,0398	96,7	0,131	45,6	0,0617	51,7	0,0698	93,5	0,126
126	752	55,7	0,0741	28,9	0,0385	96,9	0,129	45,9	0,061	46,4	0,0616	94,4	0,126
128	764	55,8	0,073	29,1	0,0382	97,1	0,127	46,3	0,0605	42,5	0,0557	94,7	0,124
130	776	56	0,0721	29,5	0,038	97,3	0,125	46,2	0,0596	42,9	0,0552	95,8	0,123
132	788	56,3	0,0714	29,6	0,0376	97,3	0,123	46,2	0,0587	41,8	0,053	96,2	0,122
134	800	56,3	0,0704	29,5	0,0369	97,5	0,122	46,2	0,0577	41,6	0,0519	95,3	0,119
136	812	56,5	0,0696	30,1	0,037	97,7	0,12	46,4	0,0571	42,8	0,0526	95,7	0,118
138	825	56,6	0,0686	30	0,0363	97,8	0,119	46,4	0,0563	43,2	0,0524	94,6	0,115
140	837	57,2	0,0684	30,3	0,0362	97,9	0,117	46,6	0,0556	45,4	0,0543	94,5	0,113
142	849	57,4	0,0676	30,5	0,036	97,8	0,115	46,5	0,0548	45,5	0,0536	93,8	0,11
144	861	57,5	0,0668	30,2	0,0351	98	0,114	46,3	0,0538	45,9	0,0533	95,8	0,111
146	873	58,2	0,0666	30,2	0,0346	97,8	0,112	46,8	0,0536	48,6	0,0557	98,2	0,113
148	885	58	0,0655	30,2	0,0341	97,9	0,111	46,9	0,053	49,6	0,0561	97	0,11
150	897	58,1	0,0647	30,2	0,0337	98,2	0,109	46,8	0,0522	49,5	0,0552	96,9	0,108
152	909	58,1	0,0639	29,7	0,0327	98,5	0,108	46,6	0,0512	51,1	0,0562	97,6	0,107
154	921	58,5	0,0635	30,4	0,033	98,6	0,107	46,7	0,0506	50,9	0,0552	93,9	0,102
156	934	58,5	0,0626	30,3	0,0325	98,7	0,106	46,8	0,0502	48,9	0,0524	95	0,102
158	946	58,9	0,0622	30,7	0,0325	98,7	0,104	46,9	0,0496	48,4	0,0512	96,1	0,102
160	958	58,6	0,0612	30,8	0,0322	98,8	0,103	46,8	0,0489	47,4	0,0495	97,3	0,102
162	970	58,7	0,0606	30,2	0,0311	98,7	0,102	46,8	0,0482	48,1	0,0495	95,3	0,0982
164	982	59,4	0,0605	29,8	0,0304	98,5	0,1	46,8	0,0476	46,6	0,0475	95,4	0,0971
166	994	59,6	0,0599	29,5	0,0297	98,7	0,0993	46,7	0,047	45,3	0,0455	95,7	0,0963
168	1 010	59,5	0,0592	29,1	0,0289	98,6	0,098	46,8	0,0466	47,9	0,0476	97	0,0964
170	1 020	59,7	0,0586	29,6	0,0291	98,6	0,0969	46,7	0,0459	50,9	0,05	96,8	0,0951
172	1 030	60,1	0,0583	29,5	0,0287	98,7	0,0958	47	0,0456	48,9	0,0474	96,1	0,0933
174	1 040	60	0,0576	29	0,0278	98,8	0,0948	46,8	0,0449	45,1	0,0433	95,8	0,0919
176	1 050	60,1	0,057	28,9	0,0274	98,5	0,0934	46,7	0,0443	42,9	0,0407	96,1	0,0911
178	1 070	60,3	0,0566	29,2	0,0274	98,7	0,0925	46,8	0,0439	45,1	0,0422	96	0,09
180	1 080	60,6	0,0562	29,2	0,027	98,5	0,0913	46,9	0,0434	50,4	0,0467	96	0,089
182	1 090	60,7	0,0556	28,9	0,0265	98,7	0,0905	46,9	0,0429	45,6	0,0418	95,6	0,0876
184	1 100	60,8	0,0552	28,6	0,0259	98,7	0,0895	46,8	0,0425	47,2	0,0428	95,7	0,0867
186	1 120	61	0,0547	28,4	0,0255	98,6	0,0884	47	0,0421	49,7	0,0446	95,5	0,0856
188	1 130	61,1	0,0542	28,7	0,0255	98,7	0,0875	47	0,0417	46,2	0,041	95,6	0,0848
190	1 140	61,6	0,054	28,6	0,0251	98,8	0,0868	46,8	0,041	44,6	0,0391	96,2	0,0844
192	1 150	61,7	0,0536	29,3	0,0254	98,5	0,0855	47,1	0,0409	41,9	0,0364	96,1	0,0835
194	1 160	61,6	0,053	28,9	0,0248	98,9	0,085	46,8	0,0402	43,5	0,0374	95,9	0,0824
196	1 180	61,8	0,0526	28,5	0,0243	98,8	0,084	46,9	0,0399	48,2	0,041	95,5	0,0812
198	1 190	61,9	0,0521	28,3	0,0238	98,6	0,083	46,9	0,0395	47,6	0,0401	95,5	0,0804
200	1 200	62,2	0,0519	28,8	0,024	98,7	0,0823	47	0,0391	50,7	0,0422	95,2	0,0794

Time	Shear Rate	Shear Stress	Viscosity	Shear Stress	Viscosity	Shear Stress	Viscosity	Shear Stress	Viscosity	Shear Stress	Viscosity	Shear Stress	Viscosity
[s]	[1/s]	[Pa]	[Pa·s]	[Pa]	[Pa·s]	[Pa]	[Pa·s]	[Pa]	[Pa·s]	[Pa]	[Pa·s]	[Pa]	[Pa·s]
		CNC-BT-WDFs (6 wt %) 1.2 wt % S.W. 25C FRESH 1	*CNC-BT-WDFs (6 wt %) 1.2 wt % S.W. 25C FRESH 1*	*CNC-ATT-WDFs (6 wt %) 1.2 wt % S.W. 25C FRESH 1*	*CNC-ATT-WDFs (6 wt %) 1.2 wt % S.W. 25C FRESH 1*	*CNC-SEP-WDFs (6 wt %) 1.2 wt % S.W. 25C FRESH 1*	*CNC-SEP-WDFs (6 wt %) 1.2 wt % S.W. 25C FRESH 1*	*CNC-BT-WDFs (6 wt %) 1.2 wt % S.W. 80C FRESH 1*	*CNC-BT-WDFs (6 wt %) 1.2 wt % S.W. 80C FRESH 1*	*CNC-ATT-WDFs (6 wt %) 1.2 wt % S.W. 80C FRESH 1*	*CNC-ATT-WDFs (6 wt %) 1.2 wt % S.W. 80C FRESH 1*	*CNC-SEP-WDFs (6 wt %) 1.2 wt % S.W. 80C FRESH 1*	*CNC-SEP-WDFs (6 wt %) 1.2 wt % S.W. 80C FRESH 1*
2	1	0,837	0,837	1,56	1,56	35,9	36	1,82	1,82	3,67	3,67	30,3	30,4
4	13,1	2,82	0,215	5,38	0,41	40	3,05	4,02	0,307	6,53	0,498	42,6	3,25
6	25,2	3,29	0,13	6,02	0,239	42,6	1,69	4,68	0,186	6,78	0,269	41,5	1,65
8	37,3	3,56	0,0955	6,2	0,166	44,1	1,18	4,04	0,108	6,53	0,175	41,1	1,1
10	49,4	3,38	0,0684	6,15	0,124	45,4	0,919	4,15	0,0839	5,95	0,12	40,7	0,822
12	61,6	3,73	0,0606	6,05	0,0983	47,6	0,773	4,39	0,0712	5,97	0,0969	41,7	0,677
14	73,7	4,03	0,0547	5,88	0,0798	50,2	0,681	4,99	0,0677	6,46	0,0877	43	0,584
16	85,8	4,26	0,0497	6,06	0,0706	53	0,618	5,21	0,0607	6,33	0,0737	44,1	0,515
18	97,9	4,5	0,0459	6,56	0,067	55,7	0,569	4,55	0,0465	5,76	0,0589	44,8	0,458
20	110	4,64	0,0422	7,11	0,0646	58,1	0,528	5,15	0,0468	6,17	0,0561	45,8	0,416
22	122	4,86	0,0398	6,96	0,057	60,4	0,495	5	0,0409	6,28	0,0514	46,9	0,384
24	134	5,34	0,0398	7,14	0,0532	62,5	0,466	4,64	0,0345	6,6	0,0492	48,5	0,362
26	146	5,24	0,0358	7,6	0,0519	64,5	0,441	4,64	0,0317	6,75	0,0462	50,2	0,343
28	158	5,48	0,0346	7,72	0,0487	66	0,416	4,75	0,03	6,92	0,0437	51,7	0,326
30	171	5,78	0,0339	7,86	0,0461	67,4	0,395	4,94	0,029	7,07	0,0415	53,1	0,312
32	183	5,88	0,0322	7,75	0,0424	68,8	0,377	5,14	0,0282	7,32	0,0401	54,3	0,298
34	195	5,94	0,0305	7,97	0,0409	70,1	0,36	5,21	0,0267	7,53	0,0386	55,9	0,287
36	207	6,19	0,0299	8,2	0,0396	71,3	0,344	5,49	0,0266	7,74	0,0374	57,9	0,28
38	219	6,34	0,029	8,45	0,0386	72,3	0,33	5,52	0,0252	7,73	0,0353	59	0,27
40	231	6,34	0,0274	8,84	0,0382	73,2	0,317	5,67	0,0245	7,86	0,034	60,7	0,263
42	243	6,35	0,0261	9,17	0,0377	74,1	0,305	5,61	0,0231	7,71	0,0317	62,1	0,256
44	255	6,64	0,026	9,07	0,0355	75,1	0,294	6,02	0,0236	8,02	0,0314	63,3	0,248
46	267	6,78	0,0253	9,44	0,0353	75,7	0,283	6,32	0,0236	7,98	0,0298	64,9	0,243
48	280	6,88	0,0246	9,47	0,0339	76,6	0,274	6,19	0,0221	8,02	0,0287	66	0,236
50	292	6,95	0,0238	9,62	0,033	77,3	0,265	6,08	0,0208	8,03	0,0275	67,5	0,232
52	304	7,01	0,0231	9,74	0,032	78,1	0,257	6,15	0,0202	8,03	0,0264	68,4	0,225
54	316	7,03	0,0223	10,1	0,0318	78,7	0,249	6,26	0,0198	8,29	0,0262	69,5	0,22
56	328	6,95	0,0212	10,2	0,0312	79,4	0,242	6,11	0,0186	8,42	0,0257	71	0,216
58	340	6,97	0,0205	10,3	0,0304	80,1	0,235	6,46	0,019	8,67	0,0255	71,8	0,211
60	352	7,04	0,02	10,6	0,0302	80,6	0,229	6,36	0,0181	8,78	0,0249	73	0,207
62	364	7,15	0,0196	10,6	0,0291	81,4	0,223	6,28	0,0172	9,11	0,025	74,4	0,204
64	376	7,1	0,0189	10,8	0,0288	81,8	0,217	6,38	0,0169	9,38	0,0249	75,6	0,201
66	389	7,2	0,0185	10,9	0,028	82,4	0,212	6,15	0,0158	9,48	0,0244	77,1	0,199
68	401	7,16	0,0179	11,1	0,0276	82,7	0,206	5,92	0,0148	9,44	0,0236	77,9	0,194
70	413	7,06	0,0171	11,1	0,0268	83,3	0,202	5,63	0,0136	10	0,0242	78,6	0,19
72	425	7,07	0,0166	11,1	0,0262	83,8	0,197	5,49	0,0129	10,3	0,0242	79,3	0,187
74	437	7,1	0,0162	11	0,0252	84,1	0,192	5,58	0,0128	9,99	0,0229	80	0,183
76	449	6,9	0,0154	11,3	0,0252	84,3	0,188	5,76	0,0128	10,1	0,0225	80,7	0,18
78	461	6,87	0,0143	11,4	0,0247	85,1	0,184	5,9	0,0128	10,2	0,0222	81,1	0,176
80	473	6,89	0,0142	11,1	0,023	85,5	0,176	6,09	0,0126	10,8	0,0222	82,5	0,17
82	485	6,97	0,014	11,3	0,0226	85,9	0,173	6,5	0,0131	11,1	0,0224	83,1	0,167
84	498	7,05	0,0138	11,5	0,0225	86,2	0,169	6,37	0,0125	11	0,0216	83,4	0,164
86	510	6,96	0,0133	11,4	0,0219	86,6	0,166	6,42	0,0123	11,4	0,0218	83,7	0,16
88	522	6,83	0,0128	11,5	0,0215	86,9	0,163	6,5	0,0122	11	0,0205	84,2	0,158
90	534	6,96	0,0127	11,5	0,0211	87,5	0,16	6,1	0,0112	10,2	0,0187	84,5	0,155
92	546	7,21	0,0129	11,5	0,0206	87,8	0,157	6,07	0,0109	10,5	0,0189	85,1	0,152
94	558	7,27	0,0127	11,6	0,0203	88,2	0,155	6,46	0,0113	10,7	0,0188	85	0,149
96	570	7,33	0,0126	11,5	0,0197	88,5	0,152	6,49	0,0111	10,7	0,0184	85,5	0,147
98	582	7,35	0,0124	11,5	0,0194	88,8	0,149	6,74	0,0113	11,2	0,0188	85,9	0,144
100	594	7,3	0,012	11,5	0,0189	89,1	0,147	6,81	0,0112	10,8	0,0178	86,1	0,142
102	607	7,44	0,012	11,5	0,0186	89,6	0,145	6,9	0,0112	10,2	0,0165	86,3	0,14
104	619	7,56	0,012	11,4	0,0181	89,9	0,143	6,88	0,0109	10,5	0,0167	86,9	0,138

106	631	7,54	0,0117	11,2	0,0175	90,2	0,14	6,96	0,0108	10,7	0,0166	87,2	0,136
108	643	7,71	0,0118	11,6	0,0177	90,4	0,138	7,18	0,011	10,9	0,0166	87,6	0,134
110	655	7,94	0,0119	11,4	0,0171	90,7	0,136	7,38	0,0111	10,4	0,0156	87,9	0,132
112	667	8,15	0,012	11,5	0,017	90,8	0,134	7,52	0,0111	10	0,0148	88,3	0,13
114	679	8,29	0,012	11,4	0,0165	91	0,132	7,58	0,011	10,8	0,0156	88,6	0,128
116	691	8,46	0,012	11,5	0,0164	91,4	0,13	7,58	0,0108	11	0,0156	88,8	0,126
118	703	8,62	0,012	11,3	0,0158	91,6	0,128	7,75	0,0108	9,8	0,0137	89	0,124
120	716	8,73	0,012	11,2	0,0153	91,8	0,126	7,9	0,0109	10,6	0,0145	89	0,122
122	728	8,78	0,0119	11,4	0,0155	92,1	0,125	8,08	0,0109	10,9	0,0148	89,4	0,121
124	740	9,08	0,0121	11,5	0,0153	92,4	0,123	8,18	0,0109	10	0,0133	89,9	0,12
126	752	9,2	0,012	11,6	0,0152	92,8	0,121	8,21	0,0107	10,6	0,0139	90,1	0,118
128	764	9,32	0,012	11,7	0,015	93	0,12	8,54	0,011	10,4	0,0134	90,4	0,116
130	776	9,51	0,0121	11,7	0,0148	93,4	0,118	8,72	0,0111	10,9	0,0138	90,5	0,115
132	788	9,84	0,0123	11,7	0,0146	93,6	0,117	8,52	0,0106	10,6	0,0133	90,9	0,114
134	800	10	0,0123	11,8	0,0145	93,8	0,116	8,63	0,0106	10,7	0,0132	90,9	0,112
136	812	10	0,0122	12	0,0146	93,9	0,114	8,95	0,0109	10,5	0,0128	91,4	0,111
138	825	10,1	0,0121	12,2	0,0146	94,2	0,113	8,94	0,0107	11,2	0,0134	91,2	0,109
140	837	10,2	0,012	12,3	0,0145	94,4	0,111	9,2	0,0108	12,1	0,0142	91,5	0,108
142	849	10,7	0,0124	12,6	0,0147	94,6	0,11	9,32	0,0108	11,5	0,0133	91,7	0,107
144	861	10,8	0,0124	12,4	0,0143	94,8	0,109	9,48	0,0109	11,8	0,0135	91,6	0,105
146	873	10,7	0,0121	12,8	0,0145	94,8	0,107	9,68	0,0109	12,4	0,014	91,9	0,104
148	885	11	0,0122	13	0,0145	95,1	0,106	9,87	0,011	12,2	0,0136	92	0,103
150	897	11,4	0,0125	12,9	0,0142	95,2	0,105	9,84	0,0108	12,3	0,0135	92,4	0,102
152	909	11,4	0,0123	13,2	0,0143	95,3	0,103	10,1	0,0109	12,8	0,0139	92,4	0,1
154	921	11,5	0,0123	13,4	0,0143	95,4	0,102	10,3	0,011	13	0,0139	92,6	0,0992
156	934	11,8	0,0125	13,7	0,0145	95,6	0,101	10,4	0,011	13,2	0,0139	92,6	0,0979
158	946	11,9	0,0124	13,9	0,0145	95,7	0,0999	10,8	0,0113	13,2	0,0137	92,8	0,0969
160	958	12,1	0,0124	14,2	0,0146	95,9	0,0989	10,8	0,0111	13,4	0,0138	93	0,0959
162	970	12,1	0,0123	14,3	0,0146	96	0,0978	10,7	0,0109	13,5	0,0138	93,1	0,0948
164	982	12,4	0,0125	14,4	0,0145	96,3	0,0968	10,8	0,0109	13,6	0,0137	93,3	0,0938
166	994	12,6	0,0125	14,7	0,0146	96,5	0,0959	11	0,011	13,9	0,0138	93,1	0,0926
168	1 010	12,7	0,0124	15	0,0147	96,7	0,0949	11,2	0,011	13,8	0,0136	93	0,0914
170	1 020	13	0,0126	15,2	0,0147	96,6	0,0938	11,6	0,0113	14,2	0,0138	93,3	0,0905
172	1 030	13,3	0,0128	15,4	0,0147	96,7	0,0927	11,5	0,0111	14,2	0,0136	93,3	0,0895
174	1 040	13,4	0,0127	15,5	0,0147	96,9	0,0919	11,9	0,0113	14,4	0,0137	93,3	0,0884
176	1 050	13,6	0,0128	15,5	0,0146	97,1	0,0911	11,8	0,0111	14,5	0,0136	93,2	0,0874
178	1 070	13,7	0,0127	15,9	0,0147	97,2	0,0901	12,1	0,0112	15	0,0139	93,4	0,0866
180	1 080	13,9	0,0128	16,3	0,0149	97,4	0,0893	12,5	0,0114	15,1	0,0139	93,7	0,0859
182	1 090	14,1	0,0128	16,5	0,0149	97,3	0,0882	12,6	0,0114	15,4	0,014	93,8	0,085
184	1 100	14,3	0,0128	16,8	0,0151	97,5	0,0874	12,7	0,0114	15,5	0,0139	93,9	0,0842
186	1 120	14,5	0,0129	17,1	0,0151	97,4	0,0864	12,8	0,0114	15,6	0,0139	93,9	0,0833
188	1 130	14,8	0,013	17	0,0149	97,5	0,0856	12,9	0,0113	16	0,014	93,8	0,0823
190	1 140	15	0,013	17,3	0,015	97,6	0,0847	13	0,0113	16,2	0,0141	93,9	0,0815
192	1 150	15	0,0129	17,3	0,0148	97,6	0,0839	13,3	0,0114	16,2	0,014	94	0,0807
194	1 160	15,4	0,0131	17,7	0,0151	97,6	0,083	13,5	0,0115	16,4	0,0139	94,2	0,0801
196	1 180	15,5	0,013	17,8	0,015	97,9	0,0824	13,6	0,0114	16,7	0,014	94,1	0,0792
198	1 190	15,8	0,0132	18,2	0,0152	97,8	0,0815	13,6	0,0114	16,9	0,0141	94,1	0,0784
200	1 200	0,837	0,837	1,56	1,56	35,9	36	1,82	1,82	3,67	3,67	30,3	30,4

Time	Shear Rate	Shear Stress	Viscosity	Shear Stress	Viscosity	Shear Stress	Viscosity	Shear Stress	Viscosity	Shear Stress	Viscosity	Shear Stress	Viscosity
[s]	[1/s]	[Pa]	[Pa·s]	[Pa]	[Pa·s]	[Pa]	[Pa·s]	[Pa]	[Pa·s]	[Pa]	[Pa·s]	[Pa]	[Pa·s]
		CNC-BT-WDFs (6 wt %) 1.2 wt % S.W..25C AFTER 24 HRS 1	*CNC-BT-WDFs (6 wt %) 1.2 wt % S.W..25C AFTER 24 HRS 1*	*CNC-ATT-WDFs (6 wt %) 1.2 wt % S.W. 25C AFTER 24 HRS 1*	*CNC-ATT-WDFs (6 wt %) 1.2 wt % S.W. 25C AFTER 24 HRS 1*	*CNC-SEP-WDFs (6 wt %) 1.2 wt % S.W. 25C AFTER 24 HRS 1*	*CNC-SEP-WDFs (6 wt %) 1.2 wt % S.W. 25C AFTER 24 HRS 1*	*CNC-BT-WDFs (6 wt %) 1.2 wt % S.W. 80C AFTER 24 HRS 1*	*CNC-BT-WDFs (6 wt %) 1.2 wt % S.W. 80C AFTER 24 HRS 1*	*CNC-ATT-WDFs (6 wt %) 1.2 wt % S.W. 80C AFTER 24 HRS 1*	*CNC-ATT-WDFs (6 wt %) 1.2 wt % S.W. 80C AFTER 24 HRS 1*	*CNC-SEP-WDFs (6 wt %) 1.2 wt % S.W. 80C AFTER 24 HRS 1*	*CNC-SEP-WDFs (6 wt %) 1.2 wt % S.W. 80C AFTER 24 HRS 1*
2	1	0,913	0,913	2,59	2,58	17,6	17,7	1,61	1,61	3,6	3,61	26,4	26,5
4	13,1	3,41	0,26	5,24	0,399	38,2	2,91	4,72	0,36	8,64	0,659	45,7	3,48
6	25,2	4,04	0,16	5,93	0,235	41	1,63	4,76	0,191	10,4	0,413	45,9	1,82
8	37,3	4,26	0,114	6,63	0,178	43	1,15	4,24	0,114	10,2	0,273	42,5	1,14
10	49,4	4,12	0,0834	6,95	0,141	44,9	0,909	4,06	0,0822	10,2	0,206	41,9	0,848
12	61,6	4,29	0,0697	7,32	0,119	47,2	0,767	3,93	0,0638	10,4	0,169	43	0,699
14	73,7	4,68	0,0636	7,44	0,101	49,4	0,67	4,53	0,0615	8,8	0,119	43,2	0,587
16	85,8	4,88	0,0569	7,88	0,0918	51,7	0,603	4,74	0,0553	8,08	0,0942	44	0,512
18	97,9	5,22	0,0533	8,5	0,0868	53,9	0,551	4,56	0,0466	7,72	0,0789	45,5	0,465
20	110	5,62	0,0511	8,7	0,0791	56,1	0,51	4,66	0,0424	7,99	0,0727	47,5	0,432
22	122	5,79	0,0474	9,22	0,0755	57,9	0,474	4,98	0,0408	8,17	0,0669	49,1	0,402
24	134	6,28	0,0468	9,45	0,0704	59,8	0,445	5,43	0,0405	8,7	0,0648	50,4	0,375
26	146	6,51	0,0445	9,83	0,0672	61,3	0,419	5,79	0,0396	8,9	0,0608	52,3	0,357
28	158	6,77	0,0427	9,86	0,0622	62,8	0,397	6,19	0,0391	8,99	0,0568	54,2	0,342
30	171	7,01	0,0411	10,4	0,0609	64,1	0,376	6,31	0,037	9,46	0,0555	56,2	0,33
32	183	7,15	0,0391	10,5	0,0573	65,2	0,357	6,47	0,0354	9,92	0,0543	58	0,317
34	195	7,36	0,0378	10,8	0,0552	66,3	0,34	6,52	0,0335	10,5	0,0538	59,1	0,304
36	207	7,63	0,0369	11,2	0,0544	67,4	0,326	6,62	0,032	10,2	0,0495	60,3	0,291
38	219	7,79	0,0356	11,4	0,0521	68,2	0,312	7,01	0,032	10,4	0,0476	61,8	0,282
40	231	7,74	0,0335	11,6	0,0502	69,2	0,299	7,41	0,0321	10,5	0,0453	62,8	0,272
42	243	7,98	0,0328	11,6	0,0478	69,9	0,288	7,65	0,0315	10,5	0,043	64,3	0,264
44	255	7,92	0,031	11,8	0,0462	70,6	0,277	7,62	0,0298	10,9	0,0426	65,8	0,258
46	267	8,29	0,031	12,1	0,0454	71,4	0,267	7,66	0,0286	10,9	0,0408	66,9	0,25
48	280	8,37	0,03	12,2	0,0438	72,3	0,259	7,89	0,0282	11,2	0,0399	68,1	0,244
50	292	8,41	0,0288	12,2	0,0419	72,9	0,25	8,04	0,0276	11,4	0,039	69,3	0,237
52	304	8,59	0,0283	12,5	0,0412	73,5	0,242	8,1	0,0267	11,5	0,0379	70,2	0,231
54	316	8,6	0,0272	12,9	0,0409	74,1	0,235	8,09	0,0256	11,8	0,0372	71,2	0,226
56	328	8,71	0,0265	13	0,0395	74,5	0,227	8,12	0,0247	12	0,0365	72,2	0,22
58	340	8,87	0,0261	13,5	0,0396	75	0,221	7,91	0,0233	12,2	0,0359	72,8	0,214
60	352	9	0,0255	13,8	0,039	75,6	0,215	7,96	0,0226	12,5	0,0356	73,6	0,209
62	364	9,11	0,025	13,8	0,0379	76	0,209	8,18	0,0225	12,7	0,0348	74,5	0,205
64	376	9,25	0,0246	14,3	0,0379	76,5	0,203	8,53	0,0227	12,5	0,0331	75	0,199
66	389	9,35	0,0241	14,1	0,0364	76,9	0,198	8,68	0,0223	12,6	0,0324	75,5	0,194
68	401	9,35	0,0233	14,3	0,0356	77,4	0,193	8,7	0,0217	13,2	0,0331	76,5	0,191
70	413	9,37	0,0227	14,5	0,035	77,8	0,189	8,5	0,0206	13,8	0,0333	77,7	0,188
72	425	9,34	0,022	14,7	0,0346	78,2	0,184	8,77	0,0207	13,7	0,0322	77,5	0,182
74	437	9,38	0,0215	14,8	0,0339	78,6	0,18	8,58	0,0196	13,9	0,0319	78,5	0,18
76	449	9,42	0,021	15,1	0,0336	79,1	0,176	8,45	0,0188	14,1	0,0315	79,3	0,176
78	461	9,37	0,0203	14,7	0,0319	79,2	0,172	8,39	0,0182	13,9	0,03	79,4	0,172
80	473	9,48	0,0195	15,1	0,0311	80,2	0,165	8,13	0,0167	14,9	0,0307	80,2	0,165
82	485	9,4	0,0189	15,4	0,0309	80,5	0,162	8,11	0,0163	14,9	0,0299	81,1	0,163
84	498	9,36	0,0184	15,3	0,03	80,8	0,159	8,06	0,0158	14,9	0,0293	82,6	0,162
86	510	9,49	0,0182	15,6	0,0299	81	0,155	8,86	0,017	15,2	0,0292	85,9	0,165
88	522	9,35	0,0175	15,5	0,029	81,4	0,153	9,11	0,0171	15,3	0,0287	86,4	0,162
90	534	9,21	0,0169	15,7	0,0287	81,8	0,15	9,08	0,0166	15,6	0,0285	87,1	0,16
92	546	9,2	0,0165	15,5	0,0278	82	0,147	9,01	0,0161	15,4	0,0275	87,7	0,157
94	558	9,21	0,0162	15,3	0,0268	82,2	0,144	9,27	0,0163	14,5	0,0254	88	0,154
96	570	9,33	0,016	15,4	0,0265	82,4	0,142	9,25	0,0159	14,3	0,0246	88,6	0,152
98	582	9,22	0,0155	15,3	0,0258	82,8	0,139	8,81	0,0148	14,3	0,0241	88,9	0,15
100	594	9,3	0,0153	15,6	0,0258	83,1	0,137	9,33	0,0154	15	0,0248	89	0,147

102	607	9,3	0,015	15,4	0,025	83,4	0,135	8,79	0,0142	14,8	0,0239	89,5	0,145
104	619	9,32	0,0148	15,5	0,0245	83,7	0,133	8,98	0,0142	14,5	0,023	89,9	0,143
106	631	9,5	0,0148	15,3	0,0239	83,7	0,13	9,36	0,0146	14,2	0,0221	90,3	0,141
108	643	9,51	0,0145	15,7	0,0239	84,1	0,128	9,4	0,0144	14	0,0214	90,8	0,139
110	655	9,74	0,0146	15,6	0,0234	84,3	0,126	9,03	0,0135	16	0,0241	91,2	0,137
112	667	9,67	0,0142	15,4	0,0227	84,7	0,125	9,53	0,014	14,9	0,0219	91,3	0,134
114	679	9,85	0,0142	15,2	0,022	84,9	0,123	9,84	0,0142	15,6	0,0226	91,3	0,132
116	691	9,85	0,014	15,3	0,0217	85,1	0,121	9,87	0,014	14	0,02	91,9	0,131
118	703	9,88	0,0138	15,3	0,0213	85,2	0,119	9,79	0,0137	13,6	0,0191	92,3	0,129
120	716	10,3	0,0141	15,4	0,0211	85,5	0,118	10,1	0,0138	13,7	0,0188	92,3	0,127
122	728	10,1	0,0137	15,1	0,0204	85,8	0,116	10,3	0,0139	14,5	0,0196	92,8	0,125
124	740	10,2	0,0136	14,8	0,0197	86,2	0,115	10,4	0,0138	13,8	0,0183	93,1	0,124
126	752	10,3	0,0135	15	0,0197	86,3	0,113	10,6	0,0139	14,2	0,0186	93	0,122
128	764	10,6	0,0136	15,1	0,0194	86,6	0,112	10,6	0,0137	13,9	0,018	93,2	0,12
130	776	10,8	0,0137	15,2	0,0193	86,8	0,11	10,8	0,0137	14	0,0177	93,4	0,118
132	788	10,9	0,0136	15,1	0,0188	87	0,109	10,4	0,0131	13,6	0,017	94,1	0,118
134	800	11,2	0,0138	15	0,0185	87	0,107	11	0,0135	14,1	0,0173	94,1	0,116
136	812	11,3	0,0136	15,4	0,0186	87,5	0,106	11	0,0133	13,9	0,0168	94,3	0,114
138	825	11,6	0,0139	15,3	0,0182	87,2	0,104	11,2	0,0133	14,4	0,0172	94,6	0,113
140	837	11,7	0,0138	15,3	0,018	87,4	0,103	11,3	0,0134	14,6	0,0172	94,6	0,111
142	849	11,9	0,0138	15,4	0,0179	87,5	0,102	11,5	0,0133	14,8	0,0171	94,9	0,11
144	861	12	0,0137	15,5	0,0178	87,6	0,1	11,6	0,0133	15	0,0172	95,1	0,109
146	873	12,4	0,014	15,7	0,0177	87,8	0,0992	11,8	0,0134	15	0,017	95,5	0,108
148	885	12,4	0,0139	15,6	0,0174	87,9	0,098	11,9	0,0133	15	0,0167	95,5	0,106
150	897	12,7	0,014	15,6	0,0172	88,2	0,097	12	0,0132	14,9	0,0164	95,6	0,105
152	909	12,9	0,014	16	0,0174	88,2	0,0957	12,2	0,0133	15,1	0,0164	95,6	0,104
154	921	13	0,0139	15,8	0,0169	88,4	0,0947	12	0,0129	15	0,016	96,4	0,103
156	934	13,1	0,0138	16	0,0169	88,3	0,0933	12,5	0,0132	15,2	0,0161	96,9	0,102
158	946	13,2	0,0137	16,2	0,0169	88,4	0,0923	12,4	0,013	15	0,0156	96,9	0,101
160	958	13,4	0,0138	16,2	0,0167	88,5	0,0913	12,6	0,013	14,9	0,0154	97,1	0,1
162	970	13,6	0,0139	16,5	0,0168	88,4	0,09	12,8	0,013	15,4	0,0157	97,3	0,0991
164	982	13,8	0,0139	16,5	0,0166	88,6	0,0891	13	0,013	15,4	0,0155	97,1	0,0977
166	994	14	0,0139	16,6	0,0165	88,5	0,0879	13	0,0129	15,7	0,0156	97,3	0,0967
168	1 010	14,3	0,014	16,4	0,0162	88,7	0,0871	13,2	0,0129	16	0,0157	98	0,0962
170	1 020	14,4	0,014	17	0,0165	89	0,0863	13,3	0,0129	16,2	0,0157	97,7	0,0948
172	1 030	14,6	0,014	16,9	0,0162	89	0,0854	13,5	0,0129	16,2	0,0155	98,4	0,0944
174	1 040	14,9	0,0141	17,6	0,0167	89,1	0,0844	13,9	0,0131	16,2	0,0154	98,5	0,0934
176	1 050	15,2	0,0142	17,8	0,0167	88,8	0,0832	14	0,0131	16,8	0,0157	98,9	0,0928
178	1 070	15,4	0,0143	18,2	0,0169	88,9	0,0824	14,4	0,0133	16,4	0,0152	99,2	0,0919
180	1 080	15,6	0,0143	18,4	0,0168	89,1	0,0816	14,4	0,0132	16,9	0,0155	99,2	0,0909
182	1 090	15,7	0,0143	18,7	0,0169	89,1	0,0808	14,7	0,0133	17,4	0,0158	99,4	0,0901
184	1 100	15,9	0,0143	19	0,017	89,2	0,08	14,8	0,0132	17,2	0,0154	99,3	0,0891
186	1 120	16,2	0,0144	19,2	0,017	89,2	0,0791	15,1	0,0134	17,6	0,0156	99,4	0,0882
188	1 130	16,4	0,0144	19,3	0,0169	89	0,0781	15,3	0,0134	17,8	0,0156	100	0,0879
190	1 140	16,7	0,0145	19,5	0,0169	89	0,0773	15,4	0,0134	17,8	0,0154	100	0,0871
192	1 150	16,8	0,0145	19,9	0,0171	89,1	0,0766	15,6	0,0134	18,1	0,0155	101	0,0865
194	1 160	16,9	0,0144	19,8	0,0168	89,1	0,0758	15,7	0,0133	18	0,0153	101	0,0856
196	1 180	17,4	0,0146	20	0,0168	89,2	0,0751	16	0,0135	18,4	0,0155	101	0,0851
198	1 190	17,5	0,0146	20,4	0,017	89	0,0742	16,2	0,0135	18,6	0,0155	101	0,0844
200	1 200	0,913	0,913	2,59	2,58	17,6	17,7	1,61	1,61	3,6	3,61	26,4	26,5

Time	Shear Rate	Shear Stress	Viscosity	Shear Stress	Viscosity	Shear Stress	Viscosity	Shear Stress	Viscosity	Shear Stress	Viscosity	Shear Stress	Viscosity
[s]	[1/s]	[Pa]	[Pa·s]	[Pa]	[Pa·s]	[Pa]	[Pa·s]	[Pa]	[Pa·s]	[Pa]	[Pa·s]	[Pa]	[Pa·s]
		CNC-BT-WDFs (6 wt %) S.W. 25 C 48 HRS 1	*CNC-BT-WDFs (6 wt %) S.W. 25 C 48 HRS 1*	*CNC-ATT-WDFs (6 wt %) S.W. 25 C 48 HRS 1*	*CNC-ATT-WDFs (6 wt %) S.W. 25 C 48 HRS 1*	*CNC-SEP-WDFs (6 wt %) S.W. 25 C 48 HRS 1*	*CNC-SEP-WDFs (6 wt %) S.W. 25 C 48 HRS 1*	*CNC-BT-WDFs (6 wt %) S.W. 80C 48 HRS 1*	*CNC-BT-WDFs (6 wt %) S.W. 80C 48 HRS 1*	*CNC-ATT-WDFs (6 wt %) S.W 80C 48 HRS*	*CNC-ATT-WDFs (6 wt %) S.W 80C 48 HRS*	*CNC-SEP-WDFs (6 wt %) S.W. 80C 48 HRS 1*	*CNC-SEP-WDFs (6 wt %) S.W. 80C 48 HRS 1*
2	1	0,871	0,871	3,05	3,04	10,8	10,9	2,63	2,63	9,17	9,22	24,7	24,9
4	13,1	4,09	0,312	6,07	0,463	31,4	2,39	5,32	0,406	14,6	1,12	48,7	3,71
6	25,2	4,61	0,183	7,35	0,292	36,8	1,46	5,32	0,211	14	0,556	48,3	1,92
8	37,3	4,87	0,13	7,89	0,211	39,7	1,06	4,14	0,111	12,7	0,341	45,5	1,22
10	49,4	4,89	0,0989	7,74	0,157	42,3	0,856	4,21	0,0852	12,4	0,251	44,7	0,905
12	61,6	5,14	0,0835	7,59	0,123	44,9	0,729	4,47	0,0725	12,8	0,208	44,4	0,721
14	73,7	5,08	0,0689	7,75	0,105	47,1	0,64	4,37	0,0593	11,2	0,153	44,9	0,61
16	85,8	5,37	0,0626	8,07	0,0941	49,5	0,577	4,57	0,0533	11	0,129	46,3	0,54
18	97,9	5,69	0,0581	8,15	0,0833	51,7	0,528	4,9	0,0501	10,6	0,108	48,3	0,494
20	110	6,09	0,0554	8,45	0,0768	53,7	0,488	5,18	0,0471	9,91	0,0901	49,9	0,454
22	122	6,35	0,052	8,7	0,0712	55,6	0,455	6,02	0,0493	10,1	0,083	52,1	0,427
24	134	6,73	0,0501	9,43	0,0703	57,3	0,427	6,48	0,0483	10,1	0,0756	54,5	0,406
26	146	7,18	0,0491	9,63	0,0658	58,9	0,402	6,5	0,0444	10,6	0,0724	57	0,39
28	158	7,43	0,0469	10	0,0633	60,2	0,38	7,07	0,0446	11	0,0697	58,9	0,372
30	171	7,63	0,0447	10	0,0588	61,5	0,361	7,11	0,0417	11,5	0,0674	61	0,358
32	183	7,84	0,0429	10,5	0,0575	62,5	0,342	7,22	0,0395	11,7	0,0641	62,9	0,344
34	195	7,98	0,041	10,7	0,0551	63,6	0,326	7,49	0,0385	11,6	0,0597	65,2	0,335
36	207	8,29	0,0401	11	0,0532	64,7	0,313	7,2	0,0348	11,9	0,0577	66,9	0,323
38	219	8,33	0,038	11,5	0,0526	65,5	0,299	7,47	0,0341	12,1	0,0552	68,5	0,313
40	231	8,57	0,0371	11,8	0,0513	66,3	0,287	7,88	0,0341	11,9	0,0516	69,9	0,303
42	243	8,65	0,0356	12,1	0,0497	67,1	0,276	7,72	0,0318	11,9	0,0488	71,5	0,294
44	255	8,8	0,0345	12,3	0,0482	67,9	0,266	8,5	0,0333	12,2	0,0478	73,1	0,286
46	267	8,81	0,033	12,2	0,0458	68,5	0,256	8,4	0,0314	12,3	0,0461	75,1	0,281
48	280	8,96	0,0321	12,6	0,0451	69,2	0,247	8,7	0,0311	12,5	0,0447	76,4	0,273
50	292	9,23	0,0317	12,6	0,0432	69,8	0,239	8,61	0,0295	12,9	0,0443	78	0,267
52	304	9,38	0,0309	12,9	0,0426	70,3	0,232	9,18	0,0302	13,2	0,0435	79,1	0,26
54	316	9,43	0,0299	13,2	0,0416	70,8	0,224	9,5	0,0301	13,4	0,0424	80,4	0,255
56	328	9,6	0,0293	13,5	0,0411	71,3	0,217	9,1	0,0278	13,4	0,0408	81,5	0,249
58	340	9,66	0,0284	13,5	0,0398	71,8	0,211	9,9	0,0291	13,6	0,0399	82,7	0,243
60	352	9,87	0,028	13,9	0,0395	72,3	0,205	9,93	0,0282	14,3	0,0405	83,8	0,238
62	364	9,94	0,0273	14	0,0384	72,8	0,2	9,59	0,0263	14,4	0,0395	84,8	0,233
64	376	10	0,0266	13,9	0,037	73,1	0,194	10,1	0,0267	14,9	0,0395	85,9	0,228
66	389	10,1	0,026	14,1	0,0364	73,6	0,189	9,38	0,0241	15	0,0387	86,6	0,223
68	401	10,1	0,0251	14,2	0,0354	74,1	0,185	9,35	0,0233	15,1	0,0377	87,1	0,217
70	413	10,1	0,0245	14,4	0,0349	74,3	0,18	9,91	0,024	15,3	0,037	88,2	0,214
72	425	10	0,0236	14,7	0,0345	74,8	0,176	9,83	0,0231	15,8	0,0372	89	0,209
74	437	10,3	0,0236	14,6	0,0335	75,3	0,172	9,83	0,0225	15,4	0,0353	89,6	0,205
76	449	10,2	0,0228	14,7	0,0327	75,6	0,168	9,63	0,0214	15,1	0,0336	90,4	0,201
78	461	10,5	0,0228	14,8	0,0322	75,7	0,164	9,86	0,0214	15,6	0,0339	91,3	0,198
80	473	10,5	0,0216	15,1	0,031	76,6	0,158	9,45	0,0195	16,9	0,0348	92,7	0,191
82	485	10,6	0,0212	15,3	0,0307	76,9	0,155	9,8	0,0197	17,2	0,0346	93,2	0,187
84	498	10,4	0,0205	15,1	0,0296	77,1	0,151	9,36	0,0184	17,4	0,0341	94	0,184
86	510	10,5	0,0201	15,4	0,0296	77,3	0,148	9,94	0,0191	18,4	0,0353	94,8	0,182
88	522	10,6	0,0198	15,3	0,0286	77,5	0,145	9,86	0,0185	17,8	0,0334	95,2	0,178
90	534	10,5	0,0192	15,5	0,0284	77,9	0,143	10	0,0184	16,5	0,0302	95,7	0,175
92	546	10,5	0,0188	15,5	0,0278	78,2	0,14	10	0,0179	16,4	0,0293	96,3	0,173
94	558	10,5	0,0184	15,7	0,0275	78,5	0,138	9,96	0,0175	16,6	0,029	97,2	0,17
96	570	10,4	0,0178	15,5	0,0266	78,6	0,135	10,3	0,0176	17	0,0292	97,5	0,167
98	582	10,5	0,0177	15,5	0,026	79,3	0,133	9,99	0,0168	16,8	0,0282	97,6	0,164
100	594	10,3	0,017	15,9	0,0263	79,3	0,131	10	0,0165	17,9	0,0295	98,2	0,162
102	607	10,3	0,0166	15,9	0,0258	79,7	0,129	10,3	0,0167	17,3	0,0279	98,6	0,159

104	619	10,3	0,0164	15,9	0,0253	80	0,127	10,4	0,0165	16,2	0,0256	98,8	0,157
106	631	10,3	0,016	15,9	0,0247	80,3	0,125	9,97	0,0155	16,1	0,025	99,4	0,155
108	643	10,3	0,0158	16	0,0245	80,5	0,123	10,3	0,0158	15,8	0,0242	99,9	0,152
110	655	10,3	0,0155	16	0,0239	80,8	0,121	10,3	0,0155	16,5	0,0247	100	0,15
112	667	10,6	0,0156	15,7	0,0231	81,1	0,119	10,3	0,0151	16,6	0,0245	100	0,147
114	679	10,5	0,0151	15,5	0,0225	81,2	0,117	10,8	0,0156	17,7	0,0256	101	0,145
116	691	10,3	0,0146	15,3	0,0217	81,5	0,116	10,5	0,0149	18	0,0255	101	0,143
118	703	10,6	0,0148	15,2	0,0212	81,8	0,114	10,7	0,0149	17,7	0,0248	101	0,141
120	716	10,3	0,0141	15,2	0,0209	81,8	0,112	10,8	0,0148	15,6	0,0215	102	0,14
122	728	10,5	0,0141	15,1	0,0204	82	0,111	11	0,0149	15,9	0,0215	102	0,138
124	740	10,6	0,0141	15,1	0,02	82,3	0,11	10,9	0,0146	16,7	0,0222	102	0,136
126	752	10,7	0,014	14,9	0,0195	82,4	0,108	11,4	0,0149	16,2	0,0212	102	0,134
128	764	10,9	0,014	15,1	0,0194	82,4	0,106	11,6	0,0149	15,9	0,0205	102	0,132
130	776	11	0,0139	15,1	0,0191	82,6	0,105	11,6	0,0147	16,9	0,0215	102	0,13
132	788	11,2	0,014	14,9	0,0187	82,9	0,104	11,6	0,0145	16,1	0,0201	102	0,128
134	800	11,3	0,0139	15	0,0185	83	0,102	11,9	0,0146	16,1	0,0198	103	0,127
136	812	11,4	0,0138	15	0,0182	83	0,101	11,7	0,0142	16	0,0195	103	0,125
138	825	11,7	0,0139	15,2	0,0182	83,1	0,0993	11,9	0,0142	16,1	0,0192	103	0,124
140	837	12	0,0141	15,1	0,0177	83,2	0,0981	12	0,0142	16,5	0,0194	103	0,122
142	849	12,2	0,0142	15,3	0,0178	83,3	0,0968	12,1	0,0141	15,7	0,0182	104	0,12
144	861	12,3	0,0141	15,4	0,0176	83,5	0,0956	12,3	0,0141	16,2	0,0185	104	0,119
146	873	12,5	0,0141	15,6	0,0176	83,6	0,0944	12,4	0,014	16,7	0,0189	104	0,118
148	885	12,7	0,0142	15,5	0,0173	83,4	0,093	12,5	0,014	16,8	0,0187	104	0,116
150	897	12,9	0,0142	15,5	0,017	83,5	0,0919	12,5	0,0137	16,3	0,018	104	0,115
152	909	13,2	0,0143	15,5	0,0169	83,6	0,0907	12,8	0,0139	16,5	0,0179	104	0,113
154	921	13,4	0,0144	15,4	0,0165	83,6	0,0895	12,9	0,0138	16,4	0,0175	104	0,112
156	934	13,6	0,0144	16	0,0169	83,5	0,0883	13,1	0,0139	16,5	0,0175	105	0,111
158	946	13,9	0,0145	15,9	0,0166	83,5	0,0872	12,9	0,0135	16,7	0,0174	105	0,11
160	958	14	0,0144	16,1	0,0166	83,2	0,0858	13,3	0,0137	16,6	0,0171	105	0,108
162	970	14	0,0143	16,4	0,0167	83,2	0,0847	13,7	0,0139	16,7	0,017	105	0,107
164	982	14,4	0,0145	16,5	0,0166	83,2	0,0837	13,8	0,0138	16,8	0,0169	105	0,105
166	994	14,6	0,0145	17	0,0168	83,2	0,0827	14	0,0139	17	0,0169	105	0,104
168	1 010	14,8	0,0145	17,2	0,0168	83,2	0,0817	14,3	0,014	16,9	0,0166	105	0,103
170	1 020	15	0,0146	17,2	0,0167	83	0,0806	14,3	0,0139	17	0,0165	105	0,102
172	1 030	15,4	0,0147	17,4	0,0167	83,1	0,0797	14,4	0,0138	17,5	0,0168	105	0,101
174	1 040	15,4	0,0146	17,8	0,0168	82,9	0,0786	14,6	0,0138	17,7	0,0168	105	0,1
176	1 050	15,7	0,0147	18	0,0169	83	0,0778	14,9	0,014	17,8	0,0167	106	0,0991
178	1 070	15,9	0,0147	18,4	0,017	83,1	0,077	15	0,0139	18,1	0,0168	106	0,0981
180	1 080	16,1	0,0147	18,2	0,0167	82,9	0,076	15	0,0137	18,2	0,0167	106	0,097
182	1 090	16,4	0,0148	18,8	0,017	82,9	0,0752	15,3	0,0139	18,4	0,0166	106	0,096
184	1 100	16,5	0,0148	18,9	0,017	82,9	0,0743	15,7	0,014	18,7	0,0167	106	0,0951
186	1 120	16,7	0,0149	19,1	0,0169	82,8	0,0735	16	0,0141	18,8	0,0166	106	0,0942
188	1 130	17	0,0149	19,4	0,017	83	0,0729	15,9	0,014	19	0,0167	106	0,0932
190	1 140	17,4	0,0151	19,7	0,0171	83	0,0721	16	0,0139	19,4	0,0168	106	0,0922
192	1 150	17,7	0,0152	19,9	0,0171	83,1	0,0714	16,3	0,014	19,5	0,0167	106	0,0912
194	1 160	17,8	0,0151	20,1	0,0171	83	0,0706	16,5	0,014	19,5	0,0165	106	0,0902
196	1 180	18,1	0,0152	20,4	0,0172	83	0,0699	16,8	0,0142	19,7	0,0166	106	0,0893
198	1 190	18,4	0,0153	20,7	0,0173	83	0,0692	17	0,0142	19,9	0,0166	106	0,0887
200	1 200	0,871	0,871	3,05	3,04	10,8	10,9	2,63	2,63	9,17	9,22	24,7	24,9

Time	Shear Rate	Shear Stress	Viscosity	Shear Stress	Viscosity	Shear Stress	Viscosity	Shear Stress	Viscosity	Shear Stress	Viscosity	Shear Stress	Viscosity
[s]	[1/s]	[Pa]	[Pa·s]	[Pa]	[Pa·s]	[Pa]	[Pa·s]	[Pa]	[Pa·s]	[Pa]	[Pa·s]	[Pa]	[Pa·s]
		CNC-BT-WDFs 1.2 wt % S.W 25C 72 HRS	*CNC-BT-WDFs 1.2 wt % S.W 25C 72 HRS*	*CNC-ATT-WDFs 1.2 wt % S.W 25C 72 HRS*	*CNC-ATT-WDFs 1.2 wt % S.W 25C 72 HRS*	*CNC-SEP-WDFs 1.2 wt % S.W 25C 72 HRS*	*CNC-SEP-WDFs 1.2 wt % S.W 25C 72 HRS*	*CNC-BT-WDFs 1.2 wt % S.W 80C 72 HRS*	*CNC-BT-WDFs 1.2 wt % S.W 80C 72 HRS*	*CNC-ATT-WDFs 1.2 wt % S.W 80 C 72 HRS*	*CNC-ATT-WDFs 1.2 wt % S.W 80 C 72 HRS*	*CNC-SEP-WDFs 1.2 wt % S.W 80C 72 HRS*	*CNC-SEP-WDFs 1.2 wt % S.W 80C 72 HRS*
2	1	0,998	0,997	3,47	3,46	14,3	14,3	4,5	4,51	5,73	5,74	36,6	36,8
4	13,1	4,01	0,306	6,22	0,474	34,2	2,61	7,37	0,562	10,8	0,821	51,9	3,96
6	25,2	4,68	0,186	7,37	0,292	37,8	1,5	7,35	0,291	11,8	0,468	48	1,9
8	37,3	5,05	0,135	7,87	0,211	39,9	1,07	6,88	0,184	11,2	0,3	48,9	1,31
10	49,4	5,24	0,106	7,91	0,16	42,4	0,858	6,86	0,139	11	0,222	48,4	0,979
12	61,6	5,65	0,0917	7,5	0,122	44,8	0,727	5,52	0,0897	11,2	0,183	46,6	0,757
14	73,7	5,96	0,0809	7,68	0,104	46,9	0,636	6,6	0,0896	11,8	0,16	46,5	0,631
16	85,8	6,24	0,0727	7,96	0,0928	48,9	0,57	6,64	0,0774	9,76	0,114	46,7	0,545
18	97,9	6,62	0,0676	8,1	0,0828	51	0,521	6,06	0,0619	10,3	0,105	47,4	0,484
20	110	6,88	0,0626	8,79	0,0799	53,1	0,482	6,37	0,058	10,7	0,0975	49,1	0,447
22	122	7,2	0,059	8,98	0,0736	55	0,45	6,45	0,0528	10,8	0,0884	51,7	0,423
24	134	7,71	0,0574	9,4	0,07	56,4	0,421	6,66	0,0496	10,7	0,0796	53,7	0,4
26	146	7,99	0,0546	9,75	0,0666	58,1	0,397	6,76	0,0462	10,6	0,0726	55,5	0,379
28	158	8,28	0,0523	10,2	0,0642	59,5	0,376	7,18	0,0453	10,4	0,0654	57,6	0,364
30	171	8,57	0,0503	10,4	0,0611	60,7	0,356	7,63	0,0447	10,8	0,0631	59,7	0,35
32	183	8,79	0,0481	10,6	0,0583	61,9	0,339	8,14	0,0446	11,1	0,0609	62	0,339
34	195	9,03	0,0464	10,9	0,056	63	0,323	8,46	0,0434	11,2	0,0575	64,4	0,331
36	207	9,3	0,0449	11,5	0,0557	64	0,309	8,53	0,0412	11,3	0,0547	66,8	0,323
38	219	9,36	0,0428	11,5	0,0526	64,9	0,296	8,66	0,0395	11,6	0,053	68,5	0,313
40	231	9,71	0,042	11,6	0,0503	65,7	0,284	9,23	0,0399	11,8	0,0511	70,4	0,305
42	243	9,78	0,0402	12	0,0492	66,5	0,273	9,31	0,0383	12,2	0,0502	72,3	0,297
44	255	10,1	0,0394	12,3	0,048	67,1	0,263	9,4	0,0368	12,3	0,0483	73,7	0,289
46	267	10	0,0374	12,6	0,0471	67,8	0,253	9,81	0,0367	12,7	0,0476	75,3	0,282
48	280	10,1	0,0362	12,9	0,0461	68,6	0,245	9,92	0,0355	13	0,0466	77	0,275
50	292	10,3	0,0353	13,1	0,0449	69,3	0,238	10,2	0,0349	13,1	0,045	78,5	0,269
52	304	10,6	0,0347	13,3	0,0439	69,9	0,23	10,2	0,0337	13,7	0,045	79,9	0,263
54	316	10,7	0,0339	13,4	0,0424	70,4	0,223	10,4	0,033	14,2	0,0449	81,3	0,257
56	328	10,9	0,0332	13,7	0,0418	71	0,216	10,5	0,0319	14,5	0,0441	82,8	0,253
58	340	11,1	0,0326	13,8	0,0407	71,4	0,21	10,4	0,0305	14,6	0,0431	84	0,247
60	352	11,2	0,0319	14,2	0,0402	71,8	0,204	10,8	0,0306	15,2	0,0431	85,4	0,242
62	364	11,4	0,0313	14,2	0,0391	72,3	0,198	10,7	0,0293	15,5	0,0425	86	0,236
64	376	11,6	0,0308	14,5	0,0385	72,7	0,193	9,83	0,0261	16	0,0424	86,4	0,229
66	389	11,6	0,0299	14,5	0,0373	73,2	0,188	9,61	0,0247	16	0,0411	88,2	0,227
68	401	11,5	0,0287	14,8	0,0369	73,7	0,184	9,33	0,0233	15,9	0,0397	89	0,222
70	413	11,7	0,0285	15	0,0363	74,1	0,179	9,59	0,0232	16,6	0,0402	90	0,218
72	425	11,9	0,028	15,1	0,0355	74,4	0,175	9,96	0,0234	16,5	0,0388	90,3	0,213
74	437	12,1	0,0276	15,4	0,0351	74,8	0,171	9,63	0,022	16,7	0,0381	90,4	0,207
76	449	12,1	0,0269	15,5	0,0345	75,1	0,167	9,53	0,0212	16,8	0,0373	91,7	0,204
78	461	11,9	0,0257	15,8	0,0343	75,8	0,164	10,1	0,0219	16,8	0,0364	93,5	0,203
80	473	12,2	0,0252	15,8	0,0325	76,3	0,157	9,89	0,0204	17,3	0,0357	93,5	0,193
82	485	12	0,0242	15,9	0,032	76,5	0,154	9,65	0,0194	17,6	0,0354	93,6	0,188
84	498	12	0,0236	16,1	0,0316	76,9	0,151	10,1	0,0198	17,8	0,0349	95	0,186
86	510	12,3	0,0237	16,2	0,031	77,1	0,148	9,96	0,0191	19,2	0,0369	96	0,184
88	522	12,1	0,0227	16,4	0,0306	77,4	0,145	10,5	0,0196	18,8	0,0353	97	0,182
90	534	12,3	0,0225	16,4	0,03	77,6	0,142	10,3	0,0188	19	0,0347	98,5	0,18
92	546	12,3	0,022	16,4	0,0293	77,9	0,14	10,8	0,0194	19,5	0,0349	99,2	0,178
94	558	12,5	0,0219	16,5	0,0289	78,3	0,137	10,8	0,019	19,6	0,0344	99,9	0,175
96	570	12,4	0,0214	16,7	0,0287	78,4	0,135	10,7	0,0184	18,7	0,0321	101	0,173
98	582	12,3	0,0207	16,7	0,0282	78,9	0,133	10,6	0,0178	18,6	0,0312	102	0,171
100	594	12,2	0,0202	16,7	0,0276	79	0,13	10,8	0,0177	18,8	0,0311	102	0,168
102	607	12,2	0,0196	16,5	0,0267	79,2	0,128	10,8	0,0175	19,4	0,0314	103	0,166
104	619	12	0,019	16,6	0,0263	79,3	0,126	10,7	0,0169	19,6	0,031	103	0,164

106	631	12,2	0,019	16,5	0,0257	79,5	0,124	10,5	0,0163	20,1	0,0313	104	0,161
108	643	12,2	0,0186	16,5	0,0252	79,7	0,122	10,7	0,0163	19,7	0,0301	104	0,159
110	655	12	0,018	16,6	0,0249	79,9	0,12	10,7	0,016	19,7	0,0295	105	0,157
112	667	12	0,0177	16,8	0,0247	80,2	0,118	11,1	0,0163	19,1	0,0281	106	0,156
114	679	12,1	0,0175	16,9	0,0244	80,4	0,116	11,1	0,0161	19,4	0,028	106	0,154
116	691	12,1	0,0172	16,6	0,0236	80,6	0,115	11,2	0,0159	19,5	0,0278	106	0,151
118	703	12,1	0,0169	16,7	0,0233	80,8	0,113	11	0,0153	19,3	0,027	107	0,15
120	716	12,1	0,0166	16,5	0,0227	80,8	0,111	10,7	0,0147	19,4	0,0266	107	0,148
122	728	12,3	0,0166	16,4	0,0222	81	0,109	11,1	0,015	18,2	0,0246	108	0,146
124	740	12,1	0,0161	16,2	0,0215	81,4	0,108	11,3	0,015	18,6	0,0247	108	0,144
126	752	12,3	0,0161	16,2	0,0211	81,3	0,106	10,9	0,0142	18,9	0,0247	109	0,142
128	764	12,1	0,0156	16,1	0,0207	81,6	0,105	11,4	0,0147	19,5	0,0251	109	0,141
130	776	12,4	0,0157	16,1	0,0205	81,8	0,104	11,6	0,0148	19,3	0,0245	110	0,139
132	788	12,2	0,0152	16,3	0,0204	82	0,103	11,9	0,0149	18,7	0,0234	110	0,138
134	800	12,2	0,015	16,3	0,0201	82,3	0,101	11,8	0,0146	17,9	0,022	111	0,136
136	812	12,2	0,0148	16,3	0,0198	82,4	0,0999	12,3	0,0149	18,4	0,0223	111	0,135
138	825	12,5	0,015	16	0,0192	82,3	0,0983	12,3	0,0147	18,4	0,022	111	0,133
140	837	12,5	0,0148	15,9	0,0188	82,4	0,0971	12,1	0,0143	18,9	0,0222	112	0,132
142	849	12,7	0,0148	15,8	0,0183	82,5	0,0959	12,4	0,0144	19,2	0,0223	113	0,131
144	861	12,9	0,0148	16,1	0,0185	82,6	0,0946	12,4	0,0142	19,4	0,0222	113	0,13
146	873	13,1	0,0148	16	0,0181	82,5	0,0932	12,5	0,0141	19,2	0,0217	114	0,128
148	885	13,1	0,0146	15,8	0,0176	82,6	0,092	12,5	0,014	19,3	0,0215	114	0,127
150	897	13,2	0,0145	16,1	0,0177	82,8	0,091	12,8	0,0141	19,1	0,021	114	0,125
152	909	13,3	0,0144	16,2	0,0176	82,8	0,0899	13	0,0141	19,2	0,0209	114	0,124
154	921	13,6	0,0146	16,2	0,0173	83	0,0889	13,4	0,0143	19,3	0,0207	115	0,123
156	934	13,9	0,0147	16,4	0,0173	82,9	0,0877	13,5	0,0143	19,2	0,0203	115	0,121
158	946	14,1	0,0147	16,3	0,017	83,2	0,0868	13,5	0,0141	19,5	0,0204	115	0,12
160	958	13,9	0,0144	16,2	0,0167	83,2	0,0857	13,6	0,0141	20,1	0,0207	116	0,119
162	970	14,6	0,0149	16,2	0,0165	83,1	0,0846	13,8	0,014	19,9	0,0203	116	0,118
164	982	14,6	0,0147	16,5	0,0166	83,4	0,0839	13,9	0,014	19,8	0,02	116	0,116
166	994	15	0,0149	16,7	0,0166	83,3	0,0828	14,1	0,014	20,1	0,0199	116	0,115
168	1 010	15,1	0,0148	16,9	0,0165	83,3	0,0818	14,4	0,0141	19,7	0,0193	116	0,114
170	1 020	15,3	0,0148	16,8	0,0163	83,4	0,0809	14,4	0,014	20	0,0194	116	0,113
172	1 030	15,5	0,0149	17,2	0,0165	83,7	0,0803	14,9	0,0143	19,5	0,0187	116	0,112
174	1 040	15,7	0,0149	17,4	0,0165	83,6	0,0793	14,9	0,0141	19,6	0,0185	116	0,11
176	1 050	16	0,015	18	0,0168	83,6	0,0784	14,9	0,0139	19,4	0,0182	116	0,109
178	1 070	16,4	0,0152	18,2	0,0169	83,7	0,0775	15,1	0,014	19,5	0,0181	116	0,108
180	1 080	16,3	0,015	18,2	0,0167	83,7	0,0768	15,3	0,014	19,7	0,018	117	0,107
182	1 090	17	0,0154	18,6	0,0168	83,6	0,0758	15,3	0,0139	19,3	0,0175	117	0,106
184	1 100	16,8	0,0151	18,6	0,0167	83,6	0,075	15,5	0,0139	19,5	0,0175	117	0,105
186	1 120	17,2	0,0153	19	0,0169	83,8	0,0744	15,8	0,014	20,2	0,0179	117	0,104
188	1 130	17,4	0,0153	19,4	0,017	83,5	0,0733	15,7	0,0138	20,2	0,0177	117	0,103
190	1 140	17,7	0,0154	19,4	0,0169	83,8	0,0727	16	0,0139	20,2	0,0176	117	0,102
192	1 150	17,7	0,0152	20	0,0172	83,7	0,072	16,4	0,0141	20,4	0,0176	118	0,101
194	1 160	18	0,0153	19,9	0,0169	84	0,0714	16,4	0,014	20,4	0,0174	118	0,101
196	1 180	18,4	0,0155	20,5	0,0173	84	0,0707	16,4	0,0138	20,4	0,0172	118	0,0991
198	1 190	18,8	0,0156	20,6	0,0172	83,8	0,0698	16,7	0,0139	20,7	0,0172	118	0,0985
200	1 200	0,998	0,997	3,47	3,46	14,3	14,3	4,5	4,51	5,73	5,74	36,6	36,8

INDEX D: RATE OF PENETRATION DATA

PRESSURE	ROP(BT)	ROP(BT)	ROP(BT)	ROP(BT)	ROP(ATT)	ROP(ATT)	ROP(ATT)	ROP(ATT)	ROP(SEP)	ROP(SEP)	ROP(SEP)	ROP(SEP)
MPa	mm/min	mm/min	mm/min	mm/min	mm/min	mm/min	mm/min	mm/min	mm/min	mm/min	mm/min	mm/min
	BRECCIA ROCK/ CNC-BT-WDFs 1,2 wt %	*BRECCIA ROCK/ CNC-BT-WDFs 1,2 wt %*	*BRECCIA ROCK/ CNC-BT-WDFs 1,2 wt %*	*BRECCIA ROCK(BT) MEAN*	*BRECCIA ROCK/ CNC-ATT-WDFs 2,0 wt %*	*BRECCIA ROCK/ CNC-ATT-WDFs 2,0 wt %*	*BRECCIA ROCK/ CNC-ATT-WDFs 2,0 wt %*	*BRECCIA ROCK(ATT) MEAN*	*BRECCIA ROCK/ CNC-SEP-WDFs 1,2 wt %*	*BRECCIA ROCK/ CNC-SEP-WDFs 1,2 wt %*	*BRECCIA ROCK/ CNC-SEP-WDFs 1,2 wt %*	*BRECCIA ROCK(SEP) MEAN*
1,7348	11,85	11,11	11,78	11,58	11,91	12,44	11,91	12,09	5,38	3,62	3,72	4,24
2,0812	9,21	9,14	11,64	9,997	14,03	14,02	10,48	12,84	13,89	11,85	4,29	10,01
2,4287	10,37	11,14	3,52	10,76	12,47	12,84	14,21	13,17	15,8	14,59	8,82	13,07
2,7757	10,32	10,47	10,38	10,39	8,97	10,67	12,07	10,57	14,61	10,82	13,82	13,08
3,1226	13,43	14,56	12,09	13,36	13,65	11,55	16,33	13,84	8,12	9,3	17,6	11,67
PRESSURE	**ROP(BT)**	**ROP(BT)**	**ROP(BT)**	**ROP(BT)**	**ROP(ATT)**	**ROP(ATT)**	**ROP(ATT)**	**ROP(ATT)**	**ROP(SEP)**	**ROP(SEP)**	**ROP(SEP)**	**ROP(SEP)**
MPa	**mm/min**	**mm/min**	**mm/min**	**mm/min**	**mm/min**	**mm/min**	**mm/min**	**mm/min**	**mm/min**	**mm/min**	**mm/min**	**mm/min**
	SHALE ROCK/ CNC-BT-WDFs 1,2 wt %	*SHALE ROCK/ CNC-BT-WDFs 1,2 wt %*	*SHALE ROCK/ CNC-BT-WDFs 1,2 wt %*	*SHALE ROCK(BT) MEAN*	*SHALE ROCK/ CNC-ATT-WDFs 2,0 wt %*	*SHALE ROCK/ CNC-ATT-WDFs 2,0 wt %*	*SHALE ROCK/ CNC-ATT-WDFs 2,0 wt %*	*SHALE ROCK(ATT) MEAN*	*SHALE ROCK/ CNC-SEP-WDFs 1,2 wt %*	*SHALE ROCK/ CNC-SEP-WDFs 1,2 wt %*	*SHALE ROCK/ CNC-SEP-WDFs 1,2 wt %*	*SHALE ROCK(SEP) MEAN*
1,7348	0,86	1,27	1,02	1,05	3,88	1,27	1,64	2,26	0,7	0,73	0,74	0,72
2,0812	1,05	1,19	0,13	1,12	1,15	1,17	1,3	1,21	1,75	0,91	0,75	1,14
2,4287	1,51	1,42	1,99	1,64	1,59	4,59	5,54	3,91	1	0,97	1,07	1,01
2,7757	1,52	1,17	1,77	1,49	2	6,13	1,11	3,08	1,22	1,17	1,77	1,39
3,1226	1,87	3,64	3,98	3,16	4,53	9,28	7,56	7,12	1,2	1,73	1,22	1,38
PRESSURE	**ROP(BT)**	**ROP(BT)**	**ROP(BT)**	**ROP(BT)**	**ROP(ATT)**	**ROP(ATT)**	**ROP(ATT)**	**ROP(ATT)**	**ROP(SEP)**	**ROP(SEP)**	**ROP(SEP)**	**ROP(SEP)**
MPa	**mm/min**	**mm/min**	**mm/min**	**mm/min**	**mm/min**	**mm/min**	**mm/min**	**mm/min**	**mm/min**	**mm/min**	**mm/min**	**mm/min**
	DOLO ROCK/ CNC-BT-WDFs 1,2 wt %	**DOLO ROCK/ CNC-BT-WDFs 1,2 wt %**	**DOLO ROCK/ CNC-BT-WDFs 1,2 wt %**	**DOLO ROCK(BT) MEAN**	**DOLO ROCK/ CNC-ATT-WDFs 2,0 wt %**	**DOLO ROCK/ CNC-ATT-WDFs 2,0 wt %**	**DOLO ROCK/ CNC-ATT-WDFs 2,0 wt %**	**DOLO ROCK(ATT) MEAN**	**DOLO ROCK/ CNC-SEP-WDFs 1,2 wt %**	**DOLO ROCK/ CNC-SEP-WDFs 1,2 wt %**	**DOLO ROCK/ CNC-SEP-WDFs 1,2 wt %**	**DOLO ROCK(SEP) MEAN**
1,7348	0,34	0,39	0,59	0,444	0,47	0,39	0,15	0,37	0,35	0,43	0,29	0,36
2,0812	0,44	0,7	0,59	0,58	0,58	0,22	0,38	0,39	0,37	0,55	0,34	0,42
2,4287	0,48	0,87	0,43	0,59	0,15	0,47	0,14	0,47	0,5	0,65	1,13	0,76
2,7757	0,86	1,08	0,56	0,83	0,55	0,61	0,67	0,61	1,12	0,91	1,1	1,04
3,1226	0,68	0,7	0,61	0,66	1,03	0,61	0,38	0,82	2,04	1,43	1,54	1,67
PRESSURE	**ROP(BT)**	**ROP(BT)**	**ROP(BT)**	**ROP(BT)**	**ROP(ATT)**	**ROP(ATT)**	**ROP(ATT)**	**ROP(ATT)**	**ROP(SEP)**	**ROP(SEP)**	**ROP(SEP)**	**ROP(SEP)**
MPa	**mm/min**	**mm/min**	**mm/min**	**mm/min**	**mm/min**	**mm/min**	**mm/min**	**mm/min**	**mm/min**	**mm/min**	**mm/min**	**mm/min**
	SANDSTONE ROCK/ CNC-BT-WDFs 1,2 wt %	**SANDSTONE ROCK/ CNC-BT-WDFs 1,2 wt %**	**SANDSTONE ROCK/ CNC-BT-WDFs 1,2 wt %**	**SANDSTONE ROCK(BT) MEAN**	**SANDSTONE ROCK/ CNC-ATT-WDFs 2,0 wt %**	**SANDSTONE ROCK/ CNC-ATT-WDFs 2,0 wt %**	**SANDSTONE ROCK/ CNC-ATT-WDFs 2,0 wt %**	**SANDSTONE ROCK(ATT) MEAN**	**SANDSTONE ROCK/ CNC-SEP-WDFs 1,2 wt %**	**SANDSTONE ROCK/ CNC-SEP-WDFs 1,2 wt %**	**SANDSTONE ROCK/ CNC-SEP-WDFs 1,2 wt %**	**SANDSTONE ROCK(SEP) MEAN**
1,7348	0,25	0,16	0,51	0,31	0,45	0,33	0,11	0,39	0,58	0,58	0,72	0,63

2,0812	1,58	1,19	1,45	1,41	0,46	0,46	0,42	0,45	1,02	1,05	1,06	1,04
2,4287	1,82	1,97	1,8	1,86	0,52	0,53	0,32	0,525	1,3	1,31	1,21	1,27
2,7757	1,79	1,8	2,24	1,94	0,65	0,53	0,53	0,59	1,25	1,33	1,2	1,29
3,1226	2,02	2,1	1,92	2,01	0,93	0,49	0,25	0,71	1,42	0,93	1,01	1,42

PRESSURE	ROP	ROP	ROP	ROP	ROP	ROP	ROP	ROP	ROP	ROP	ROP	ROP
MPa	mm/min	mm/min	mm/min	mm/min	mm/min	mm/min	mm/min	mm/min	mm/min	mm/min	mm/min	mm/min
	BRECCIA ROCK/ CNC-BT-WDFs 1,2 wt % SW.	BRECCIA ROCK/ CNC-BT-WDFs 1,2 wt % SW.	BRECCIA ROCK/ CNC-BT-WDFs 1,2 wt % SW.	BRECCIA ROCK(BT) MEAN	BRECCIA ROCK/ CNC-ATT-WDFs 1,2 wt % SW.	BRECCIA ROCK/ CNC-ATT-WDFs 1,2 wt % SW.	BRECCIA ROCK/ CNC-ATT-WDFs 1,2 wt % SW.	BRECCIA ROCK(ATT) MEAN	BRECCIA ROCK/ CNC-SEP-WDFs 1,2 wt % SW.	BRECCIA ROCK/ CNC-SEP-WDFs 1,2 wt % SW.	BRECCIA ROCK/ CNC-SEP-WDFs 1,2 wt % SW.	BRECCIA ROCK(SEP) MEAN
1,7348	9,31	7,66	0,54	5,83667	10,43	6,79	7,06	8,09333	8,09	9,07	2,52	6,56
2,0812	7,89	9,11	3,91	6,97	9,11	8,63	7,8	8,51333	8,96	8,48	9,06	8,83333
2,4287	10,39	8,46	9,45	9,43333	10,29	2,45	3,8	5,51333	10,35	10,35	9,05	9,91667
2,7757	3,58	9,81	11,38	8,25667	8,85	10,33	1,26	6,81333	10,9	2,88	10,51	8,09667
3,1226	11,12	9,31	5,72	8,71667	7,06	3,01	4,46	4,84333	11,71	11,01	12,14	11,62
PRESSURE	**ROP**	**ROP**	**ROP**	**ROP**	**ROP**	**ROP**	**ROP**	**ROP**	**ROP**	**ROP**	**ROP**	**ROP**
MPa	**mm/min**	**mm/min**	**mm/min**	**mm/min**	**mm/min**	**mm/min**	**mm/min**	**mm/min**	**mm/min**	**mm/min**	**mm/min**	**mm/min**
	SHALE ROCK/ CNC-BT-WDFs 1,2 wt % SW.	SHALE ROCK/ CNC-BT-WDFs 1,2 wt % SW.	SHALE ROCK/ CNC-BT-WDFs 1,2 wt % SW.	SHALE ROCK(BT) MEAN	SHALE ROCK/ CNC-ATT-WDFs 1,2 wt % SW.	SHALE ROCK/ CNC-ATT-WDFs 1,2 wt % SW.	SHALE ROCK/ CNC-ATT-WDFs 1,2 wt % SW.	SHALE ROCK(ATT) MEAN	SHALE ROCK/ CNC-SEP-WDFs 1,2 wt % SW.	SHALE ROCK/ CNC-SEP-WDFs 1,2 wt % SW.	SHALE ROCK/ CNC-SEP-WDFs 1,2 wt % SW.	SHALE ROCK(SEP) MEAN
1,7348	0,28	0,19	0,21	0,22667	0,21	0,15	0,34	0,23333	0,32	0,31	0,31	0,31333
2,0812	0,24	0,22	0,27	0,24333	0,45	0,63	0,36	0,48	0,24	0,36	0,29	0,29667
2,4287	0,31	0,31	0,49	0,37	0,44	0,19	0,2	0,27667	0,69	0,6	0,33	0,54
2,7757	0,29	0,31	0,36	0,32	0,51	0,38	0,28	0,39	0,97	0,35	1,42	0,91333
3,1226	0,46	0,59	0,53	0,52667	0,37	0,34	0,58	0,43	1,02	1,05	1,06	1,04333
PRESSURE	ROP	ROP	ROP	ROP	ROP	ROP	ROP	ROP	ROP	ROP	ROP	ROP
MPa	mm/min	mm/min	mm/min	mm/min	mm/min	mm/min	mm/min	mm/min	mm/min	mm/min	mm/min	mm/min
	DOLOROCK / CNC-BT-WDFs 1,2 wt % SW.	DOLOROCK / CNC-BT-WDFs 1,2 wt % SW.	DOLOROCK / CNC-BT-WDFs 1,2 wt % SW.	DOLOROCK(BT) MEAN	DOLOROCK / CNC-ATT-WDFs 1,2 wt % SW.	DOLOROCK / CNC-ATT-WDFs 1,2 wt % SW.	DOLOROCK / CNC-ATT-WDFs 1,2 wt % SW.	DOLOROCK(ATT) MEAN	DOLOROCK / CNC-SEP-WDFs 1,2 wt % SW.	DOLOROCK / CNC-SEP-WDFs 1,2 wt % SW.	DOLOROCK / CNC-SEP-WDFs 1,2 wt % SW.	DOLOROCK(SEP) MEAN
1,7348	0,14	0,17	0,27	0,19333	0,32	0,24	0,24	0,26667	0,35	0,14	0,16	0,21667
2,0812	0,48	0,42	0,42	0,44	0,19	0,25	0,22	0,22	0,2	0,42	0,14	0,25333
2,4287	0,34	0,51	0,27	0,37333	0,28	0,65	0,22	0,38333	0,15	0,14	0,35	0,21333
2,7757	0,21	0,36	0,36	0,31	0,32	0,53	0,45	0,43333	0,22	0,32	0,34	0,29333
3,1226	0,23	0,28	0,26	0,25667	0,45	0,28	0,47	0,4	0,52	0,4	0,39	0,43667
PRESSURE	**ROP**	**ROP**	**ROP**	**ROP**	**ROP**	**ROP**	**ROP**	**ROP**	**ROP**	**ROP**	**ROP**	**ROP**
MPa	**mm/min**	**mm/min**	**mm/min**	**mm/min**	**mm/min**	**mm/min**	**mm/min**	**mm/min**	**mm/min**	**mm/min**	**mm/min**	**mm/min**

	SANDSTONE ROCK/ CNC-BT-WDFs 1,2 wt % SW.	SANDSTONE ROCK/ CNC-BT-WDFs 1,2 wt % SW.	SANDSTONE ROCK/ CNC-BT-WDFs 1,2 wt % SW.	SANDSTONE ROCK(BT) MEAN	SANDSTONE ROCK/ CNC-ATT-WDFs 1,2 wt % SW.	SANDSTONE ROCK/ CNC-ATT-WDFs 1,2 wt % SW.	SANDSTONE ROCK/ CNC-ATT-WDFs 1,2 wt % SW.	SANDSTONE ROCK(ATT) MEAN	SANDSTONE ROCK/ CNC-SEP-WDFs 1,2 wt % SW.	SANDSTONE ROCK/ CNC-SEP-WDFs 1,2 wt % SW.	SANDSTONE ROCK/ CNC-SEP-WDFs 1,2 wt % SW.	SANDSTONE ROCK(SEP) MEAN
1,7348	0,35	0,33	0,33	0,33667	0,48	0,38	0,7	0,52	0,21	0,23	0,26	0,23333
2,0812	0,44	0,46	0,48	0,46	0,49	0,7	0,73	0,64	0,46	0,48	0,43	0,45667
2,4287	0,65	0,66	0,59	0,63333	0,76	0,71	0,6	0,69	0,43	0,37	0,26	0,35333
2,7757	0,48	0,47	0,33	0,42667	0,8	0,57	0,65	0,67333	0,6	0,75	1,04	0,79667
3,1226	0,32	0,49	0,39	0,4	0,91	0,85	0,61	0,79	0,73	1,12	1,04	0,96333